

RELEVANCE OF SIGNAL TRANSDUCTION PATHWAY MUTATIONS IN PEDIATRIC T-ALL

Lidwina Catharina Zuurbier



Relevance of Signal Transduction Pathway Mutations in Pediatric T-ALL

Copyright © 2014 Lidwina Catharina Zuurbier

Cover: represents the T-ALL puzzle that needs to be solved. The nucleotide letters encode the 5-HTTLPR polymorphism in the promoter of the *SLC6A4* gene. The protein letters encode the first part of the *SLC6A4* gene that is translated. Literature describes that people having this 5-HTTLPR long variant, are twice as happy and satisfied than people lacking this polymorphism (de Neve et al., 2011, Journal of Human Genetics).

ISBN: 978-94-6259-453-1

Layout: Blaasvis Producties

Printing: Ipskamp Drukkers

The work described in this thesis was performed at the Department of Pediatric Oncology/ Hematology of the Erasmus Medical Center – Sophia Children’s Hospital Rotterdam, The Netherlands and was funded by “Kinderen Kankervrij (KiKa)” .

The publication of this thesis was financially supported by:



RELEVANCE OF SIGNAL TRANSDUCTION PATHWAY MUTATIONS IN PEDIATRIC T-ALL

De relevantie van mutaties in signaal transductiepaden in kinderleukemie

Proefschrift

ter verkrijging van de graad van doctor
aan de Erasmus Universiteit Rotterdam
op gezag van de rector magnificus
Prof.dr. H.A.P. Pols
en volgens besluit van het College voor Promoties.

De openbare verdediging zal plaatsvinden op
woensdag 17 december 2014 om 11:30 uur

door

Lidwina Catharina Zuurbier
geboren te Niedorp



PROMOTIECOMMISSIE

Promotor: Prof.dr. R. Pieters

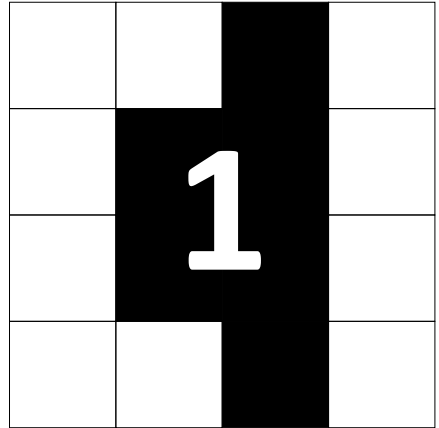
Leescommissie: Prof.dr. J.J. Cornelissen
Prof.dr. D.F.E. Huylebroeck
Prof.dr. M.L. den Boer

Co-promotor: Dr. J.P.P. Meijerink

TABLE OF CONTENTS

Chapter 1	Introduction & Aims of this thesis	9
Chapter 2	Signaling transduction pathways affected by mutations and their druggable potential in T-cell acute lymphoblastic leukemia	17
Chapter 3	<i>NOTCH1</i> and/or <i>FBXW7</i> mutations predict for initial good prednisone response but not for improved outcome in pediatric T-cell Acute Lymphoblastic Leukemia patients treated on DCOG or COALL protocols + supplementary data	47
Chapter 4	The significance of <i>PTEN</i> and <i>AKT</i> aberrations in pediatric T-cell acute lymphoblastic leukemia + supplementary data	67
Chapter 5	<i>PTEN</i> micro-deletions in T-cell acute lymphoblastic leukemia are caused by illegitimate RAG-mediated recombination events + supplementary data	95
Chapter 6	Mutually exclusive mutations in the IL7-receptor signaling pathway in T-cell acute lymphoblastic leukemia respond to combined inhibition of MEK/ERK and PI3K/AKT/mTOR pathways + supplementary data	125
Chapter 7	Immature <i>MEF2C</i> -dysregulated T-cell leukemia patients have an early T-cell precursor acute lymphoblastic leukemia gene signature and typically have non-rearranged T-cell receptors + supplementary data	151
Chapter 8	Differential activation of pathways in genetic subgroups of T-cell acute lymphoblastic leukemia + supplementary data	175
Chapter 9	Summary & Future prospective	251
	Nederlandse Samenvatting	263
Chapter 10	About the author	271
	List of publications	272
	Curriculum Vitae	274
	PhD portfolio	275
	Dankwoord	277

CHAPTER



Introduction

HEMATOPOIESIS & T-CELL DEVELOPMENT

The functions of our blood are coagulation, oxygen and nutrient transportation, toxics and waste disposal and immunity. These tasks are achieved by multiple cell types (platelets, erythrocytes and leukocytes) that continuously develop from a common ancestor (hematopoiesis); i.e. the hematopoietic stem cell (HSC). HSCs reside in the bone marrow and represent only a minor fraction of adult blood cells; 0.01-0.05%. Differentiation of HSCs into mature blood cells occurs in the bone marrow and/or secondary lymphoid organs including thymus and spleen following specific stimuli (**Figure 1**).

During hematopoiesis, HSCs first differentiate into lineage restricted immature myeloid or lymphoid precursor cells (blasts). These can then develop further into erythrocytes (red blood cells), thrombocytes (platelets), or leukocytes (white blood cells). Leukocytes include granulocytes and macrophages (i.e. the myeloid cells) and B- and T lymphocytes¹.

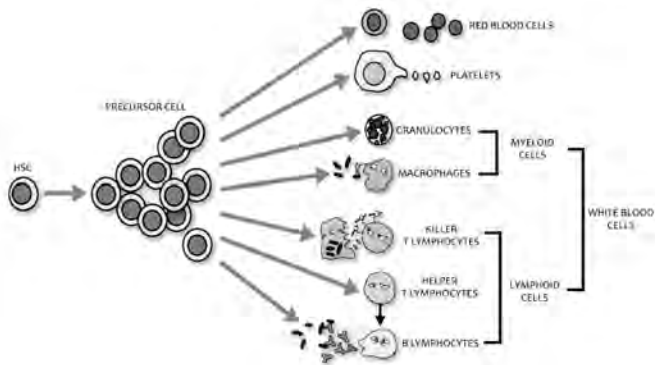


Figure 1 | **Haematopoiesis.** Differentiation HSCs into different effector blood cells. These can be subdivided into red blood cells, platelets, myeloid white blood cells or lymphoid white blood cells.

¹<http://www.rikenresearch.riken.jp>

During T lymphocyte (T-cell) maturation, HSCs first develop into early thymic progenitor (ETP) cells. These cells differentiate into either T- or B lymphocytes. Precursor (pro) T-cells rearrange the TCR gene elements by V(D)J rearrangement to form distinct $\gamma\delta$ or $\alpha\beta$ TCRs. $\alpha\beta$ TCRs are functionally tested during beta-selection, positive selection and negative selection. At these selection points, the functionality of TCRs and their ability to bind major histocompatibility complex (MHC) molecules and to recognize MHC-bound self-peptides, is verified². $\alpha\beta$ -Positive thymocytes further differentiate into mature CD4-positive T-cell helper subsets or into a CD8-positive cytotoxic T-cell subset. Both with different functions².

Different stages of T-cell development can be distinguished by specific protein markers on the cell surface. These include CD (cluster of differentiation) markers such as CD44, CD25, CD4, CD8 or CD3, c-kit and the $\alpha\beta$ or $\gamma\delta$ T-cell receptors (TCR) (**Figure 2**). This also involves the activation of specific intracellular signaling pathways and transcription factors like NOTCH1 and interaction with the microenvironment.

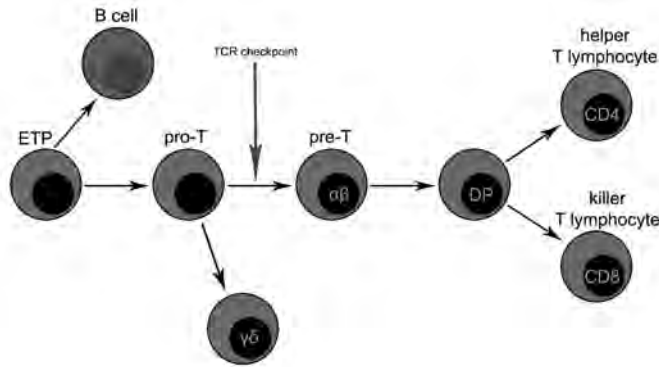


Figure 2 | T-cell development. Early thymic progenitor cells can further mature into either B cells or pro-T-cells. A pro-T-cell continues the T-cell receptor (TCR) $\gamma\delta$ -expressing or $\alpha\beta$ -expressing lineage. When the pro-T-cell succeeds the TCR checkpoint it develops into a pre-T-cell and DP (double-positive) T-cell, which expresses both CD4 and CD8 molecules. The final step involves downregulation of either CD4 or CD8, leaving a CD8 positive (killer/cytotoxic T lymphocyte) or CD4-positive (helper T lymphocyte) effector T-cell.

LEUKEMIA

Leukemia is the outgrowth of leukocytes and can either develop in a very short period of time (acute leukemia) or develop more slowly (chronic leukemia). Children most often are presented with the acute form of leukemia in which immature blasts are arrested in differentiation and expand uncontrollably. Depending on the cell lineage involved, acute leukemia is defined as acute myeloid leukemia (AML) or acute lymphoid leukemia (ALL). In case of lymphoid cells, these can be further specified in precursor B- or T-cells (B-ALL or T-ALL).

As the bone marrow of acute leukemic patients is packed with leukemic cells, the development of normal erythrocytes, thrombocytes and mature leukocytes has become repressed. This causes the majority of symptoms when the disease presents itself. Patients are pale and show signs of fatigue (lack of erythrocytes), bruise easily, have spontaneous bleedings (lack of coagulation due to low thrombocyte numbers) and are susceptible to infections and fever (shortage of mature leukocytes). Furthermore, leukemic blasts can infiltrate organs, lymph nodes and the central nervous system and can also form solid masses resulting in more severe symptoms like hepatosplenomegaly, adenopathy or stroke³.

Pediatric T-cell acute lymphoblastic leukemia (T-ALL)

The incidence of ALL in children peaks between 2 to 5 years of age. Most acute leukemias are of lymphoid origin (80%) of which the majority are B cell lineage malignancies. About 15% of ALL is caused by T-cell lineage ALL (T-ALL)³. This corresponds to 15-20 new patients each year in the Netherlands of which the majority is generally male. The survival rates of pediatric T-ALL patients have increased over the last years and according to the most recent published

DCOG ALL9 protocol, the 5yrs event-free survival for T-ALL is 72%⁴. About a quarter of T-ALL patients relapse. This relapse is in general more aggressive than the primary disease due to acquired therapy resistance, and these patients almost all ultimately die. All patients receive combinational chemotherapy including prednisone, dexamethasone, vincristine, asparaginase, daunorubicine, methotrexate, cytarabine, and mercaptopurine⁴. Until now, the only prognostic factors in pediatric T-ALL are age and white blood cell count. However, no uniform genetic aberration that is correlated to poor or good outcome has been defined for T-ALL³. Whereas *TAL1* rearrangements were associated with a good prognosis in the ALL7/8/9 cohorts⁵, this could not be confirmed by others⁶. *CALM-AF10* seems to be associated with poor prognosis. This, however, was reported by only two studies^{5,7}.

Improving survival

To improve outcome of T-ALL patients, we need to investigate disease biology that might contribute to the development of more effective (and specific) treatment. With children in early childhood, side-effects of therapy can affect developing organs resulting in negative effects later in life. To reduce side-effects we aim for personalized treatment and stratification of patients, to prevent over-treatment in patients who respond very well on relatively lighter regimens. For this, predictive biomarkers for therapy response and prognostic biomarkers for outcome (before or during therapy) are essential.

T-ALL GENETICS

T-ALL is a result of accumulated genetic defects in developing T-cells. These defects lead to aberrant gene expression and uncontrolled self-renewal of cells which have been arrested in differentiation. Abnormal expansion of cells is due to accelerated growth factor signaling and resistance to apoptosis. Genetic defects include numerical chromosomal aberrations (i.e. gain or loss of entire chromosomes), deletions of entire chromosomal arms, translocations that result in the exchange of chromosomal domains between chromosomes, inversions, single nucleotide point and missense mutations, insertion/deletion mutations or local amplifications or deletions that involve few genes.

Type A mutations

The knowledge of genetic changes occurring in T-ALL is expanding. Several genetic mutations in T-ALL that lead to the activation of specific oncogenes occur in a mutually exclusive manner and T-ALL subgroups are defined based on these mutations (type A mutations⁸). These aberrations lead to the expression of the oncogenes; *TAL1* or *TAL2*, *LMO1*, *LMO2* or *LMO3*, *TLX1* (*HOX11*), *TLX3* (*HOX11L2*), *HOXA*, *MEF2C*, *NKX2.1* or *NKX2.2*. Most are transcription factors involved in the control of gene expression regulating the development of blasts. There are still patients without any (so far detected) aberration affecting the expression of these genes (unknowns),

and the genetic background of these patients is currently under extensive investigation. Forty patients of the COALL-97 and DCOG ALL7/8/9 pediatric T-ALL cohorts which have been used for the research described in this thesis, have a type A mutation in the *TAL1*, *TAL2*, *LMO1*, *LMO2* or *LMO3* gene or genes that have a similar function (TALLMO-like). The second largest group of patients is characterized by an aberration in the *TLX3* gene (21%). The remainder of the “known” patients have *HOXA*, *TLX1*, *NKX2.1* or *NKX2.2*, and *MEF2C* abnormalities (**Figure 3**)⁸.

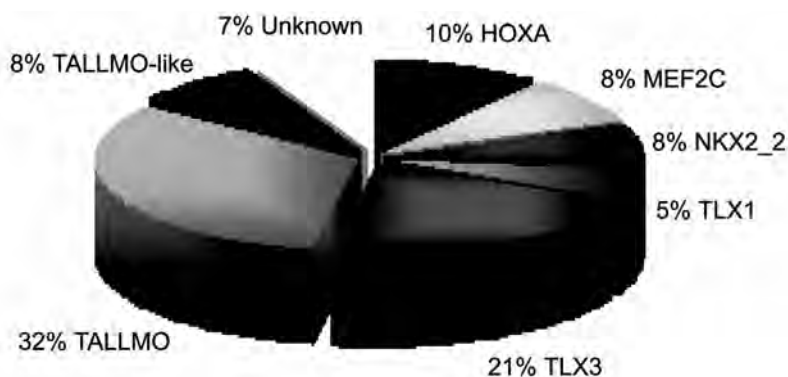


Figure 3 | Distribution of chromosomal rearrangements (type A mutations) within COALL-97 and DCOG ALL7/8/9. This includes *HOXA*, *MEF2C*-activating, *NKX2.2*, *TLX1*, *TLX3*, *TAL/LMO* or *TAL/LMO*-like aberrations. Also a minority of patients have yet unidentified type A mutations.

Type B mutations

In addition to type A mutations, T-ALL patients can have multiple type B mutations, scattered among all T-ALL subgroups. Type B mutations often occur in other cancers as well and affect genes involved in cell cycle, proliferation and apoptosis. The most prevalent type B mutation in T-ALL abolishes the cyclin-dependent kinases *CDKN2B* and/or *CDKN2A* gene expression (~80% of patients). Another type B-mutated protein frequently increased in activity and more specific for T-ALL, is the NOTCH1 receptor (~38-63% of patients). Increased NOTCH1 activity can be a result of genetic mutations in the *NOTCH1* gene itself and/or mutations in the *FBXW7* gene. These mutations affect NOTCH1 protein localization and stability. Other type B mutations involved in T-ALL affect, among others, *PTEN*, *WT1*, *RAS*, *IL7R* and *PHF6* expression⁹. Dysregulation of these genes can affect whole protein cascades (pathways) that are involved in signal transduction. Examples are the NOTCH1, PI3K/AKT, and RAS/MEK/ERK pathway which are canonical pathways that are interconnected. Hyperactivation of these pathways in T-ALL can be blocked/dampened by (specific) therapy. For example, gamma-secretase inhibitors can inhibit the activation of the NOTCH1 signaling but are, unfortunately, so far proven to be too toxic in clinical trials.

AIMS OF THIS THESIS

In this thesis, we investigated the role of type A and type B mutations and their relation to outcome and other clinical and biological parameters in pediatric T-ALL, with a focus on type B mutations. The research in this thesis has predominantly been performed using samples from 146 pediatric T-ALL patients that were treated according to the German COALL-97 cohort and the Dutch DCOG ALL7, ALL8 or ALL9 cohort.

Many reviews highlight the incidence and important role of chromosomal rearrangements (so called type A mutations⁸) in T-ALL. Since the focus of this thesis is on type B mutations, **chapter 2** gives an overview of all type B mutations known in pediatric T-ALL. This chapter focuses on specific signal transduction pathways that may be dysregulated in T-ALL as a result of type B mutations. These pathways are normally involved in cell cycle, proliferation, or apoptosis.

In **chapter 3**, we explored the incidence of various types of mutations that activate the NOTCH1 transcription factor. NOTCH1 is a transmembrane receptor that is normally activated by various proteolytic cleavages including cleavage at the intracellular domain that is executed by the γ -secretase complex upon ligand binding. Cleaved NOTCH1 (intracellular NOTCH or ICN) is translocated to the nucleus and initiates transcription. Until now, mutations in the *NOTCH1* gene itself have been described as well as inactivating mutations in other genes such as *FBXW7*, a ubiquitin ligase that normally targets intracellular NOTCH1 for ubiquitin-mediated proteolysis. Their prognostic value varies among study cohorts.

PTEN, *PI3K* and *AKT* mutations are type B mutations in pediatric T-ALL patients that have been suggested to hyperactivate the PI3K/AKT pathway and subsequent mTOR pathway. *PTEN*-inactivating mutations were initially proposed to follow NOTCH1-activating mutations as a γ -secretase inhibitor resistance mechanism¹⁰. In **chapter 4**, we examined the incidence of *PTEN*, *PI3K* and *AKT* mutations and their association with clinical and biological parameters as well as with PTEN, AKT and further downstream protein expression. In addition, we investigated a potential role of epigenetic silencing and defective RNA splicing of *PTEN* in T-ALL as well as *PTEN* promoter mutations as alternative mechanisms to inactivate PTEN.

In this thesis, research about the *PTEN* gene was extended by exploring the cause of the newly discovered *PTEN* splice-defects resulting in micro-deletions (**chapter 5**).

In **chapter 6**, we extended our screening by identifying *IL7R* (IL7 receptor), *N-RAS*, *K-RAS*, *JAK1* and *JAK3* (Janus Kinases) mutations within our cohorts and verified how these mutations co-occurred with each other and our previously identified NOTCH1-activating and *PI3K/AKT* mutations. Mutations in the IL7R α -chain have recently been identified as an additional type B mutation in ~9% of T-ALL pediatric patients, resulting in IL7-independent signaling^{11,12}. The IL7R can signal downstream through JAK-STAT, RAS-MEK-ERK or PI3K/AKT pathways. For some of the detected mutations, we determined their transformation capacity using IL3-dependent Ba/F3 cell lines and measured activated downstream signaling. In addition to this, we tested clinically relevant inhibitors for their ability to block the activation of these pathways.

In 2011, we described an immature T-ALL subtype revealed by gene expression profiling

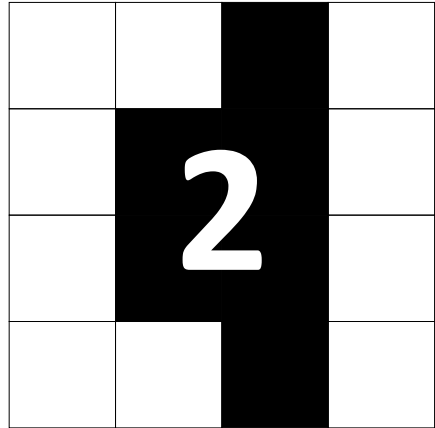
analysis, that is characterized by early T-cell developmental markers and frequent expression of myeloid markers and *MEF2C*-activating aberrations. Comparable immature T-ALL entities, i.e. early thymic progenitor ALL (ETP-ALL) or the ABD (absence of bi-allelic deletion) T-ALL subgroups were identified by others^{13,14}. In **chapter 7**, we analyzed whether features for all three entities identified would point to one and the same disease entity.

In **chapter 8**, we have performed a proteome screening using reverse-phase protein arrays (RPMAs) to identify the activation status of a set of molecules that act in signal transduction pathways. We explored differential activation of pathways between different T-ALL subgroups that are characterized by specific type A or B mutations such as NOTCH1-activating, *PTEN/AKT* or *WT1*-inactivating mutations. RPMA data was combined with global test analyses of mRNA gene expression data. The study was performed to contribute to the understanding of T-ALL biology and to diagnostic or prognostic biomarker discovery or druggable targets. The analysis of these protein arrays reveals various suggestions of important pathways that play a role in particular subgroups that should be further validated.

REFERENCES

1. Orkin SH, Zon LI. Hematopoiesis: an evolving paradigm for stem cell biology. *Cell*. 2008;132:631-644.
2. Koch U, Radtke F. Mechanisms of T cell development and transformation. *Annu Rev Cell Dev Biol*;27:539-562.
3. Pui CH, Robison LL, Look AT. Acute lymphoblastic leukaemia. *Lancet*. 2008;371:1030-1043.
4. Veerman AJ, Kamps WA, van den Berg H, et al. Dexamethasone-based therapy for childhood acute lymphoblastic leukaemia: results of the prospective Dutch Childhood Oncology Group (DCOG) protocol ALL-9 (1997-2004). *Lancet Oncol*. 2009;10:957-966.
5. van Grotel M, Meijerink JP, van Wering ER, et al. Prognostic significance of molecular-cytogenetic abnormalities in pediatric T-ALL is not explained by immunophenotypic differences. *Leukemia*. 2008;22:124-131.
6. Wang D, Zhu G, Wang N, et al. SIL-TAL1 rearrangement is related with poor outcome: a study from a Chinese institution. *PLoS One*;8:e73865.
7. Asnafi V, Radford-Weiss I, Dastugue N, et al. CALM-AF10 is a common fusion transcript in T-ALL and is specific to the TCRgammadelta lineage. *Blood*. 2003;102:1000-1006.
8. Van Vlierberghe P, Pieters R, Beverloo HB, Meijerink JP. Molecular-genetic insights in paediatric T-cell acute lymphoblastic leukaemia. *Br J Haematol*. 2008;143:153-168.
9. Van Vlierberghe P, Ferrando A. The molecular basis of T cell acute lymphoblastic leukemia. *J Clin Invest*;122:3398-3406.
10. Palomero T, Sulis ML, Cortina M, et al. Mutational loss of PTEN induces resistance to NOTCH1 inhibition in T-cell leukemia. *Nat Med*. 2007;13:1203-1210.
11. Shochat C, Tal N, Bandapalli OR, et al. Gain-of-function mutations in interleukin-7 receptor-alpha (IL7R) in childhood acute lymphoblastic leukemias. *J Exp Med*;208:901-908.
12. Zenatti PP, Ribeiro D, Li W, et al. Oncogenic IL7R gain-of-function mutations in childhood T-cell acute lymphoblastic leukemia. *Nat Genet*;43:932-939.
13. Coustan-Smith E, Mullighan CG, Onciu M, et al. Early T-cell precursor leukaemia: a subtype of very high-risk acute lymphoblastic leukaemia. *Lancet Oncol*. 2009;10:147-156.
14. Gutierrez A, Dahlberg SE, Neuberg DS, et al. Absence of biallelic TCRgamma deletion predicts early treatment failure in pediatric T-cell acute lymphoblastic leukemia. *J Clin Oncol*;28:3816-3823.

CHAPTER



Signal transduction pathways affected by mutations and their druggable potential in T-cell acute lymphoblastic leukemia

Linda Zuurbier¹, Rob Pieters^{1,2} and Jules P.P. Meijerink¹

From the ¹Department of Pediatric Oncology/Hematology, Erasmus MC Rotterdam-Sophia Children's Hospital, Rotterdam, The Netherlands; ²Princess Maxima Center for pediatric Oncology, Utrecht, The Netherlands.

Review

ABSTRACT

T-cell acute lymphoblastic leukemia (T-ALL) is genetically a very heterogeneous disease involving type A mutations reflecting T-ALL genetic subgroups and additional type B mutations. Multiple type B mutations affect a limited number of signal transduction pathways, including the IL7-JAK-STAT, RAS-MEK-ERK, PI3K-AKT and NOTCH1 signaling. The importance of these pathways for regulation of cellular proliferation and survival, regulation of DNA damage, gene transcription and translation has been demonstrated. Although some mutations have been related to the very immature early T-cell progenitor ALL, no clear and consistent relation is observed between mutations and clinical parameters in T-ALL yet. Drugs that specifically target a pathway are under development and single or combinational therapy with these therapeutics may be beneficial for patients that have hyperactivating mutations in these pathways.

Acute Lymphoblastic leukemia

Acute Lymphoblastic leukemia (ALL) is a malignant blood disease affecting one in 1500 children before the age of 18. Leukemia develops following genetic mutations leading to deregulation of various cellular processes including signal transduction pathway activities. Enhanced cellular proliferation and maintenance, arrest in differentiation and increased resistance to apoptosis transform normal cells into leukemic cells.

Genetic changes in T-cell acute lymphoblastic leukemia (T-ALL) can be classified into so called type A and type B aberrations^{1,2}. Type A mutations are mostly chromosomal rearrangements that result in a differentiation arrest and define patient subtypes. Type B abnormalities are scattered among all “type A” patient groups and frequently result in changes in activities of signal transduction pathways. An elegant study by *Clappier and colleagues (2011)* showed the importance of type B abnormalities during tumor progression³. They investigated clonal selection of genetic subclones as present in diagnosis samples of T-ALL patient biopsies using a xenograft transplantation model and found multiple leukemic subclones that harbor a different landscape of type B mutations, according to the neo-Darwinian model⁴. They suggested that specific type B mutations could be drivers of leukemic selection towards highly aggressive subclones. One example of clonal selection of leukemia subclones comprising such type B abnormalities was demonstrated and affected inactivating mutations in the *PTEN* tumor suppressor gene that was responsible for the outgrowth of a particular leukemic subclone during relapse. Only a limited number of signal transduction pathways are altered by a variety of type B abnormalities. In T-ALL, most frequent abnormalities affect the PI3K/AKT and NOTCH pathway activity and cell cycle regulators such as deletions of the *CDKN2A/2B* genes. However, aberrant activation of the T-cell receptor (TCR) signaling, RAS-MEK-ERK, IL7R-JAK-STAT and other signal transduction pathways have frequently been implicated in the development of T-ALL.

In this review, we give an overview of signal transduction pathways that are altered as a result of type B abnormalities and have a converged role in T-ALL leukemogenesis. Furthermore, we highlight drugs that may be suitable to specifically counteract the activity of affected pathways.

T-cell Receptor signaling

The T-cell receptor (TCR) has a pivotal role in the function of T-cells and provides specificity to cellular response epitopes in the context of major histocompatibility complex I or II molecules⁵. To fulfill these actions, the TCR signals through many different pathways to ultimately respond to cellular and environmental changes (**Figure 1**). This results in cytokine production, T-cell-supported B-cell responses or cellular lysis by natural-killer or cytotoxic T-cells. The TCR signaling cascade is indispensable for T-cell survival and proliferation.

Pre-TCR and TCR signal through similar downstream molecules upon activation, in which the Syk family, Src family and Tec family tyrosine kinases are involved. The TCR is non-covalently linked to the CD3 complex on the membrane. Other essential molecules present on the membrane are co-receptors like CD4, CD8 or CD28. The Src family tyrosine kinases LCK (lymphocyte-specific protein tyrosine kinase) or Fyn are constitutively bound to the cytoplasmic tails of the CD4/CD8

or CD28 molecules and can become dephosphorylated (inactivated) by CD45 (PTPRC). Upon TCR activation, LCK and Fyn phosphorylate certain ITAMs (Immune receptor tyrosine activation motifs) located on the cytoplasmic tails of CD3 and TCR. This enables the recruitment of Syk tyrosine kinases including ZAP-70 (zeta-chain associated protein kinase of 70 kDa) to the membrane, which also becomes phosphorylated by LCK/Fyn and thereby allows downstream signaling. ZAP-70 phosphorylates T-cell specific adapter proteins like LAT (linker of activated T-cells) and SLP76 (SH-2 domain containing lymphocyte protein of 76 000 MW). Misschien is hier een plaatje handig! The T-cell specific adapters form complexes with various molecules, for example Tec family kinases, and thereby link TCR molecules to various downstream routes including the PI3K/AKT pathway, the RAS-MEK-ERK pathway, and NFAT (nuclear factor of activated T-cells)⁵. The PI3K/AKT and RAS-MEK-ERK pathways will be described separately in the review. NFAT initiates transcriptional activation of cytokine genes through Jun/Fos transcription factors. For this, NFAT translocates to the nucleus upon dephosphorylation by the Calcineurin (*PPP3CC*) phosphatase, which is activated following calcium efflux from mitochondria. This calcium release is regulated by activated PLC γ (phospholipase C γ) via LAT following TCR activation. PLC γ can hydrolyze PtdIns(4,5)P $_2$ into IP $_3$ (inositol 1,4,5-triphosphate) and DAG (diacylglycerol). IP $_3$ binds to the IP $_3$ receptor on mitochondria, thereby eliciting a calcium efflux⁶.

Mutations in the TCR cascade that result in immunodeficiency are known^{7,8}. Regarding its important role, it is surprising that aberrant hyperactivation due to genetic changes within the initial TCR signaling are relatively infrequent or unknown in T-cell leukemias. Aberrations in the TCR signaling cascade found in T-cell malignancies are SYK translocations in a few T-cell lymphoma patients, in which SYK is fused to Itk⁹. Itk is a member of the Tec family kinases. Also in cutaneous T-cell lymphoma, mutations in the *PLCG1* gene were found in 19% of patients¹⁰. In T-ALL, hyperactivation of LCK as a result of translocation to the *TCRB* gene has been rarely observed in patients and is observed in the T-ALL cell line HSB2^{11,12}. Furthermore, loss-of-function mutations in the PTPRC phosphatase are occasionally found in T-ALL patients¹³.

Mutations in the initial TCR pathway are not frequently found. On the other hand, downstream TCR pathways like the RAS-MEK-ERK and PI3K/AKT pathway are often mutated (described in this review). Preliminary data of our pathway analyses indicate that the initial TCR pathway seems active in many T-ALL patient samples. Although this may be a consequence of the arrest at specific T-cell development stages for particular T-ALL subtypes, therapeutic approaches targeting this pathway might theoretically be effective for T-ALL patients like Calcineurin inhibitors such as cyclosporin A or the Src kinase inhibitors imatinib and dasatinib^{14,15}.

IL7 receptor signaling

The IL7 receptor (IL7R) signaling is essential for the development and homeostatic maintenance of T and B lymphocytes and other hematopoietic cell lineages. It is activated through IL7R-IL7 cytokine binding. The receptor is composed of two heterodimeric chains; the IL7R α chain and the IL2 common γ -chain. Both chains are shared among different cytokine receptors which interaction is influenced by the presence of cytokines: the IL7R α -TSLPR (thymic stromal

lymphopoietin receptor) dimer binds TSLP on T-cells, pre-B cells and dendritic cells and the IL7R α -IL7R γ -c dimer binds IL7 on T-cells specifically. The IL7R receptor has several downstream substrates that can activate various pathways (**Figure 1**). The major downstream cytoplasmic interactors are JAK kinases. Each JAK family member has specificity for a receptor chain¹⁶.

Hereditary recessive loss-of-function mutations in *IL7R* are correlated with SCID and a polymorphism in the *IL7R* gene promotes exon 6 skipping in multiple sclerosis patients resulting in higher soluble IL7R α levels. The same polymorphism was also associated with rheumatoid arthritis¹⁷⁻¹⁹. Gain-of-function mutations were recently found in B-ALL and in 9-12% of T-ALL patients, predominantly by in-frame insertion/deletion (INDEL) mutations but also point mutations^{13,20-23}. Most of these mutations result in the introduction of a cysteine in the juxtamembrane/transmembrane region. This results in constitutive IL7R α homodimerization and ligand independent JAK-STAT and PI3K/AKT pathway activation. *IL7R* mutations initiated tumor formation in mice and exhibited oncogenic transformation capacity in IL3-dependent Ba/F3 cells and IL7-dependent D1 thymocytes, which was abrogated when the unpaired cysteines were substituted by serine/alanine/glycine²⁴. Recently, *IL7R* mutations are also detected by next generation sequencing of children with early T-cell progenitor ALL (ETP-ALL)²⁵. This reflects leukemia with a very immature T-cell differentiation arrest with retained myeloid features. These mutations induce ETP-ALL in mice transplanted with primitive transduced thymocytes from *p19^{Arf}-/-* that can be inhibited with JAK-STAT inhibitors²⁶.

JAK-STAT signaling

The JAK (Janus kinase) family comprises four non-receptor tyrosine kinases; JAK1, JAK2, JAK3 and TYK2. They mainly signal through STATs (signal transducers and activators of transcription proteins) to activate transcription following stimulation of the TCR or other receptors (**Figure 1**). Loss-of-function mutations affecting JAK-STAT signaling can result in autosomal severe combined immune deficiency (SCID)²⁷. On the other hand, gain-of-function mutations can result in malignant transformation.

JAK family members are constitutively bound to the intracellular part of various transmembrane receptors (e.g. IL7 receptor), which do not have intrinsic catalytic activity on their own but exert their function through proteins like JAK kinases. Depending on the type of receptor, different homo- or heterodimer JAK-complexes are attached to the receptor, each resulting in specific downstream signaling events when activated²⁸. Activation occurs upon extracellular ligand-receptor binding by various cytokines, interferons or growth hormones, resulting in either dimerization of receptor subunits or conformational changes of receptors. As a result, two receptor-bound JAK molecules come in close proximity to each other, which allows trans-phosphorylation of specific amino acids within the JAK activation loop and activation of JAK. First, activated JAK proteins phosphorylate their neighboring receptor, enabling recruitment of STAT proteins to the receptor. Consequently, JAK proteins can phosphorylate STAT proteins, leading to the formation of STAT dimers or other STAT complexes. These complexes then translocate to the nucleus to initiate transcription. Activation of JAK proteins also results in the activation of

downstream RAS-MEK-ERK and PI3K/AKT pathways. STAT proteins can also become activated by other tyrosine kinases than JAK kinases. Negative regulators of the JAK-STAT pathway are various phosphatases (including CD45, PTPN2 and SHP1), PIAS (Protein inhibitor of activated STAT) and SLIM (Stat-interacting LIM) proteins and members of the SOCS family comprising CIS (cytokine-inducible SH2 protein) and SOCS (suppressor of cytokine signaling) motifs. Phosphatases can counteract the function of JAK. PIAS proteins target activated STAT that act as transcription factors in the nucleus by preventing binding to DNA and promoting STAT protein sumoylation. In addition, they can recruit transcriptional corepressors such as histon acetylases. SLIM proteins are E3 ligases and can target STAT for proteasomal degradation. SOCS proteins physically interact with JAK and thereby block JAK-STAT-binding, inhibit JAK kinase activity or induce JAK or STAT ubiquitination^{29,30}.

Various members of the JAK-STAT pathway can be affected by mutations causing malignant transformation of cells. Mutations have rarely been observed in solid tumors but more frequently in hematopoietic diseases. The *JAK2* V617F mutation is predominantly observed in myeloproliferative disorders (MPDs) and Down syndrome-associated ALL patients³¹⁻³³. Also some pediatric B-ALL patients are characterized by *JAK* mutations³⁴. Mutations in *JAK* family members have been rarely reported in pediatric T-ALL patients. Different studies report an incidence of 4-27% *JAK1* mutations in adult T-ALL patients³⁵⁻³⁷ and only 2% in pediatric T-ALL³⁶. A study that did not discriminate adult and pediatric patients identified 1 and 3 out of 42 T-ALL patients with *JAK1* or *JAK3* mutations, respectively³⁸. *JAK1* and *JAK3* mutations were also identified by whole genome sequencing of ETP-ALL children and exome screening of adult/pediatric T-ALL patients^{25,39}. Moreover, various *JAK* fusion proteins are described in leukemia, of which only *ETV6-JAK2* and *TEL-JAK2*⁴⁰ have been occasionally found in T-ALL, but are more common in B-ALL. Mutations in STAT have never been identified in cancer whereas their expression has been reported to be frequently upregulated in various tumors⁴¹⁻⁴³. Furthermore, negative regulators of the JAK-STAT pathway are known to be hypermethylated or mutated in hematological malignancies. *SOCS1*, *SHP1* and *PTPN2* deletions/mutations occur in 6-8% of T-ALL⁴⁴⁻⁴⁷. One patient with a *PTPN11* mutation has been reported³⁸. Interestingly, *PTPN2* loss results in increased phosphorylation of *JAK1* and *STAT1/5* as well as the inability to dephosphorylate the NUP214-ABL1 fusion protein⁴⁸. The JAK-STAT pathway is also one of the inhibitory targets of PTPRC (CD45), a gene that is occasionally mutated in T-ALL patients¹³, as discussed before. The prognostic significance of mutations affecting the JAK-STAT pathway in T-ALL has not been thoroughly investigated yet.

Inhibitors targeting the JAK-STAT pathway are JAK-specific kinase inhibitors. Besides general protein tyrosine kinase inhibitors like dasatinib, various specific JAK inhibitors are already in clinical trial regarding autoimmunity diseases like rheumatoid arthritis and psoriasis, immunosuppressors during kidney transplantation and myeloproliferative disorders⁴⁹⁻⁵². These drugs may also be a future option for the treatment of T-ALL patients with mutations in the JAK-STAT pathway.

The RAS-MEK-ERK pathway

RAS uses multiple factors to mediate transcription in T-cells. It has a general role in proliferation and differentiation during development of T-cells (positive selection) and peripheral lymphocyte activation by processes like cytokine production⁵³. The RAS-MEK-ERK pathway is aberrantly expressed in various tumors including T-ALL⁵⁴.

RAS is a small GTPase that is constitutively present in a silent state and anchored to the intracellular part of the cell membrane. RAS is member of the RAS superfamily that further includes related RHO, RAB, ARF, RAC and RAN family members. Three different highly homologous RAS genes are known: H-RAS (Harvey-RAS), N-RAS (Neuroblastoma-RAS), and K-RAS (Kirsten-RAS) that has two different splice forms (K-RAS4A and K-RAS4B). The N-terminals are identical, but the GTP-binding domains differ among these three RAS proteins. RAS proteins cycle between GDP-bound (inactive) and GTP-bound (active) states, a mechanism controlled by GEFs (guanine-exchanging factors) and GAPs (GTPase-activating proteins). SOS (Son of Sevenless) or GRP (T-cell specifically expressed guanine nucleotide releasing protein) are GEF's that can exchange RAS-bound GDP for GTP, thereby activating RAS. The activation of GEF's takes place via RAS-adaptor molecules, mainly following ligand-activation of extracellular transmembrane receptor, for example via LAT upon TCR or cytokine receptors (**Figure 1**). The most common RAS-adaptor molecules are Shc and Grb2 (Growth factor receptor-bound protein 2). GTP-bound RAS undergoes a conformational change that results in the dissociation and replacement of GAPs by GEFs to become fully activated, but also to specify downstream interactions. RAS can activate many downstream signaling pathways of which the MEK-ERK pathway and PI3K/AKT pathway are most often described. RAS contains intrinsic GTPase activity that can hydrolyze GTP into GDP and consequential inactivation of RAS. GTPases like NF1 (neurofibromin 1), GAP or p120GAP can accelerate this reaction. Furthermore, RAS can directly activate PI3K that activates the PI3K/AKT pathway⁵³.

Missense mutations in RAS are well known to occur in cancer including AML and B-ALL⁵⁵⁻⁵⁷. N-RAS point mutations have been identified in 4-9% of pediatric T-ALL patients⁵⁸⁻⁶⁴. H-RAS mutations are investigated but not found in pediatric T-ALL patients. K-RAS mutations are detected in two pediatric T-ALL patients studies in 2% and 9.5% of patients^{61,65}. Recently, RAS signaling mutations are found to be associated with the myeloid-like ETP ALL⁶⁶. RAS mutations have predominantly been found in codon 12 and 13 but also 61, 63, 117, 119 and 146. These mutations impair the intrinsic RAS GTPase capacity, rendering mutant RAS proteins constitutively active. These mutations may sterically hinder GTPase activity due to a consequent conformational change or a decrement in GDP nucleotide affinity. Von Lintig and colleagues (2000) determined the activity of the RAS protein in 18 T-ALL children using an enzyme-based method⁶⁷. They observed that half of the patients had an enhanced RAS activity compared to healthy subjects, but a mutation analysis had not been performed in this context. Given the fact that RAS mutations are generally detected in only a minority of pediatric T-ALL patients, increased RAS activation in these patients is most likely caused by other factors upstream of RAS, e.g. by *IL7R*, *JAK* or *NF1* mutations. Also other members of the RAS-MEK-ERK pathway are frequently mutated in cancer, but have not

been observed in T-ALL so far.

FLT3 (FMS-like tyrosine kinase 3 gene) encodes for a tyrosine kinase receptor that dimerizes upon ligand binding. Subsequent autophosphorylation initiates downstream signaling, including the RAS-MEK-ERK pathway, PI3K/AKT pathway or Src tyrosine family kinases involved in TCR signaling. Cells with *FLT3*-ITD also activate STAT5 molecules. *FLT3* is altered in one-third of AML patients by in frame ITDs (internal tandem duplications) or point mutations, resulting in a constitutive activation of the receptor. *FLT3* ITDs and point mutations are also found in ALL patients, although less frequently. In 2004, *Paietta and colleagues* reported three adult T-ALL patients that had *FLT3* ITD or point mutations. In three separate studies, 3-7% of pediatric T-ALL patients were identified with *FLT3*-ITD mutations⁶⁸⁻⁷⁰. Very recently, *FLT3* mutations were also shown to be enriched in adult early ETP- ALL⁷¹. Deletions and mutations in the *NF1* gene also result in activated RAS. We described mutations and/or deletions in *NF1* in 3% of pediatric T-ALL patients, including 2 patients that contained an *NF1* deletion thereby inactivating both *NF1* alleles⁷².

RAS mutations are associated with a poor survival in AML and *MLL*-rearranged B-ALL^{73,74}. In T-ALL, *N-RAS* mutations have been associated with a higher risk for relapse⁵⁹. Furthermore, they have been associated with relapsed T-ALL⁷⁵ as well as with the poor prognostic ETP-ALL subtype^{76,77}.

RAS specific inhibitors are still awaiting. Drugs were developed targeting the posttranslational farnesylation event of *RAS* proteins, essential to anchor *RAS* to the plasma membrane. Tipifarnib is one such a drug that showed a good response in AML and T-ALL cell lines *in vitro*⁷⁸. Although farnesyl transferase inhibitors (FTI's) are effective in clinical trial⁷⁹⁻⁸¹, the efficacy appeared not related to *RAS* mutations^{78,82} and leukemic cells often acquire an increased resistance to these compounds⁸¹. Therefore, studies focuses more on drugs targeting *RAS* downstream molecules like B-RAF or MEK1/2.

PI3K/AKT pathway

The PI3K/AKT pathway contributes to many cellular processes and can become activated through activated transmembrane receptors like the TCR (**Figure 1**). Hyperactivation of this pathway by mutations is shown to be oncogenic in various tumors⁸³⁻⁸⁵.

The PI3K/AKT pathway signals via direct interaction of the PI3K (phosphatidylinositol 3-kinase) regulatory subunit with an upstream membrane bound receptor. Apart from direct receptor binding, the PI3K/AKT pathway can be activated through the T-cell specific adapter complex or through *RAS*, which can directly bind and activate PI3K⁸⁶. Activated PI3K phosphorylates PtdIns(3,4)P₂ (PIP₂) to form PtdIns(3,4,5)P₃ (PIP₃), which activates PDK1 at the membrane. Activated PDK1 allows recruitment and phosphorylation of AKT on Ser473 and Thr308 positions, in concert with a still unknown kinase. AKT activates or inhibits various downstream processes through protein phosphorylation. Best known examples are a) the synthesis of proteins and initiation of cell growth by activation of the downstream mTOR pathway through direct inhibition of the mTOR inhibitor TSC2 b) through nuclear export of Forkhead transcription

factors that transcribe the cell cycle inhibitor p27, among others, c) stimulation of the cell cycle by delocalization of the cell cycle inhibitor p27 through direct phosphorylation or stabilization of cyclin D1 d) prevention of apoptosis by the phosphorylation and inactivation of pro-apoptotic proteins including BAD or pro-caspase 9⁸⁷. PI3K/AKT activity is counteracted by the phosphatases PTEN (phosphatase and tensin homologue deleted on chromosome 10) or SHIP1/2 (SH2-containing inositol polyphosphate 5-phosphatase), which dephosphoryates PIP₃ at the 3rd or 5th position of the inositol ring, respectively⁸⁶. PTEN also directly interacts with p53 thereby stabilizing the protein and changing its DNA binding potential, or interacts with other nuclear proteins that control DNA damage like MDM2 and Chk1⁸⁷. It has recently been shown that PTEN can be transcriptionally silenced by the HES1 repressor following activation of the NOTCH1 pathway in T-ALL cell lines. Although we could not confirm it, it has been postulated that this results in elevated AKT activity. Oncogenic loss of PTEN has also been associated with resistance to NOTCH inhibitors like gamma-secretase inhibitors⁸⁸, however as our data indicates a nearly mutual exclusive pattern of *PTEN/AKT* and NOTCH1-activation mutations we doubt the clinical relevance of this⁸⁹.

The PI3K/AKT pathway is deregulated in a broad range of cancers in which loss of PTEN function is the most prevalent cause. *PTEN* germ-line mutations result in various hereditary diseases that predispose to cancer, whereas somatic *PTEN* inactivation has been documented in various forms of cancer including glioblastoma, lung, breast, prostate, melanoma, bladder, endometrial and renal cancer, among others⁹⁰⁻⁹⁵. The *PTEN* locus is mostly inactivated through chromosomal deletions, although point-or frame shift mutations in the *PTEN* coding region or *PTEN* promoter as well as promoter hypermethylation are commonly detected⁹⁶⁻⁹⁸. Alternative to *PTEN* mutations, we found several patients with *PTEN* splice defects resulting in loss of PTEN protein^{89,99}. PTEN phosphorylates various downstream targets and several studies showed that the AKT pathway is mostly affected by PTEN loss in cancer^{88,96,100}. PTEN is a haploinsufficient tumor suppressor gene, indicating that loss of a single gene copy results in a cellular phenotype⁹⁸. Bi-allelic inactivation of *PTEN* has been associated with disease progression or an aggressive cancer phenotype^{101,102}. Our study supports the idea of PTEN acting as a haploinsufficient tumor suppressor, as we noticed a difference in PTEN expression levels between mono-allelic and bi-allelic-mutated patients, and the ongoing pressure on leukemic cells that have lost already one allele to lose or mutate the remaining wild-type allele¹⁰³⁸⁸. In pediatric T-ALL, *PTEN* mutations have been detected in 9-17% of patients^{65,104}. Smaller studies reported variable incidences between 5 and 63%^{103,105}. Besides *PTEN*, also *PI3K* and *AKT* are mutated in cancers including colorectal, gastric, breast and ovarian cancer¹⁰⁶⁻¹⁰⁸. In our study, *AKT1* mutations were present in only 2% of the patients while no *PIK3RI* and *PIK3CA* mutations were observed in contrast to earlier observations¹⁰⁹. In that study, *Gutierrez et al (2009)* determined the frequency of *PI3K*, *AKT* or *PTEN* mutations/deletions in a small cohort and found a total incidence of 48%. In addition, other mechanisms to hyperactivate the PI3K/AKT pathway are observed in T-ALL. This is a decrease in PTEN activity as a result of CK2 (casein kinase 2) overexpression or high levels of ROS¹⁰⁹.

Elevated AKT levels have been associated with poor prognosis in acute myeloid leukemia

(AML)¹¹⁰. Regarding pediatric T-ALL, five studies have correlated aberrations of the PI3K/AKT pathway with clinical outcome. In three of these studies, a correlation with long-term survival was noticed in subgroups of patients only^{104,111-113}. In one study, also NOTCH1-activating mutations were taken into account. Patients with both *PTEN* and NOTCH1-activating mutations have favorable MRD (multiple residual disease) levels (alike single NOTCH1-activating mutations) at day 78 but not day 33. Moreover these patients had improved long-term survival rates¹⁰⁴. *PTEN*/*AKT*-mutated patients of the Dutch cohorts were associated with negative long-term survival rates when NOTCH1-activating mutations were taken into account⁸⁹.

The many feedback and feed-forward loops in the PI3K/AKT pathway makes it a very complex pathway. Therefore, therapeutically targeting the PI3K/AKT pathway might be most effective when targeting molecules at multiple levels in this pathway. Various inhibitors have been developed, including PI3K inhibitors including Wortmannin and LY294002, a PDK1 inhibitor such as GSK2334470, AKT inhibitors as Triciribine, AKT-blocking agents as D-3-deoxy-phosphatidylmyoinositol analogues or Perifosine or the mTOR inhibitor Rapamycin¹¹⁴⁻¹²⁰. In T-ALL, single-agent treatment as well as targeting multiple levels of the pathway works effectively or even synergistically *in vitro*. Similar effects are achieved when combined with glucocorticoids^{116,121,122}. For example, the AKT inhibitor Triciribine induces cell cycle arrest and apoptosis in T-ALL cell lines¹²³. Also a dual inhibitor targeting both PI3K and mTOR induces cell cycle arrest and apoptosis in T-ALL cell lines and patient samples^{124,125}. In xenografts, rapamycin induces apoptosis of T-ALL¹²⁶. In addition, since the PI3K/AKT pathway might intertwine with the NOTCH pathway, it is postulated that a combination of inhibitors targeting both pathways would be effective. Indeed, rapamycin may have an additional effect when combined with NOTCH inhibitors in mice and synergism between NOTCH1 and mTOR inhibitors or PI3K inhibitors was observed in T-ALL cells *in vitro*^{127,128}.

NOTCH signaling

One of the most prevalent type B mutations in T-ALL affect genes of the NOTCH signaling pathway including *NOTCH1* and the E3-ubiquitin ligase *FBXW7* (F-BOX domain containing protein 7), resulting in a constitutively active NOTCH1 pathway. Cellular changes of active NOTCH signaling differ among tissue types, but NOTCH activation in developing T-cells affects differentiation and proliferation. NOTCH has also a prominent role in hematopoietic stem cells (HSCs) during embryonic development, adult HSC maintenance and cell fate decisions¹²⁹.

NOTCH proteins are transmembrane receptor proteins (**Figure 1**) that transmit extracellular signals towards the nucleus upon interaction with a variety of NOTCH1 ligands including jagged1, jagged2, delta1, delta3 or delta4 (Delta/Serrate/Lag-2 family) that are expressed on neighboring cells. The NOTCH receptors exist of two non-covalently bound heterodimeric parts, which are sequentially processed from a larger NOTCH molecule following a furin-cleavage (S1-cleavage) in the golgi apparatus. Activation of the receptors upon ligand-binding triggers another cleavage (S2-cleavage) by metalloproteases, that results in a conformational change of the Lin12/NOTCH repeats (LNR) and a consequential conformational change in the heterodimerization domain

that facilitates a third cleavage (S3-cleavage) by the γ -secretase complex in the cytoplasm. This results in the release of an intracellular part of the NOTCH receptor (ICN) that migrates toward the nucleus where it acts as a transcription factor. Here, it binds the DNA-binding protein CBF1 (C promoter binding factor 1) while displacing its co-repressors. The ICN transcription complex further involves proteins like MAML (mastermind-like), p300 and deltex. NOTCH has many potential transcriptional targets and the choice of gene transcription depends on the level of NOTCH activation but also on tissue type, differentiation state and type of ligand binding. Well-known NOTCH targets in T-cells are members of the *HES* (hairy enhancer of split) family, *MYC* and *PTCRA* (pre-T- α)^{129,130}. Although CBF1-binding is indispensable for NOTCH function, a non-canonical CBF1-independent NOTCH pathway is known¹³¹.

Several proteins are known to regulate the NOTCH expression levels and activity. The turnover of ICN is regulated by phosphorylation of so-called phospho-degron motifs located in the C-terminal PEST domain. Phosphorylation by CDK8 (cyclin-dependent kinase 8) is followed by subsequent ubiquitination by the E3 ubiquitin ligase FBXW7. Another cytoplasmic NOTCH inhibitor is Numb that prevents ICN to translocate to the nucleus. In turn, expression of Numb can be inhibited by Musashi¹³². Furthermore, Spen (Mint) can corepress NOTCH activity in the nucleus by binding to CBF1 and recruitment of histone deacetylases¹³³.

In humans, four different *NOTCH* genes (*NOTCH1-4*) are known. Apart from enhanced NOTCH expression in several solid tumors as breast, melanoma, medulloblastoma and ovarian cancer, aberrations in NOTCH genes or regulators are not commonly found in cancer¹³⁴⁻¹³⁸. In pediatric T-ALL, the incidence of mutations in the NOTCH pathway varies among study populations and with an average of 50% in the *NOTCH1* gene only^{2,111,139-147} and 55% in *NOTCH1* and/or *FBXW7*^{2,65,70,111,140-144,148-151}. Reduced numbers of *NOTCH1* mutations have been observed in ETP-ALL^{71,76,77}, possibly as an effect of their maturational arrest before definite T-cell commitment. In T-ALL most *NOTCH1* mutations are present in the heterodimerization (HD) domain or the proline glutamic serine threonine (PEST) domain. HD-domain mutations, but also mutations in the transmembrane (JM), result in ligand-independent exposure of the S3-cleavage site that provokes cleavage by the γ -secretase complex and release of ICN¹⁵². PEST domain mutations abrogate FBXW7-binding and NOTCH ubiquitination, prolonging the half-life of ICN. Inactivating mutations in *FBXW7* phenocopy *NOTCH1* PEST-domain mutations, and also result in increased half-life of ICN^{144,153}. As expected, mutations in the *NOTCH1* PEST domain and *FBXW7* are mutually exclusive. *NOTCH1* HD and PEST mutations *in cis* or either of these mutations in combination with *FBXW7* act synergistically in activating the NOTCH1 pathway^{144,145}. Single *NOTCH1* HD or PEST mutations are weak leukemia-initiating mutations. In contrast, combinations of *NOTCH1* HD and PEST domain mutations, or HD mutations in combination with mutant *FBXW7* or single *NOTCH1* JM mutations act as strong activating mutations¹⁴⁵. Sporadic mutations flanking the LNR or mutations located in the ANK and TAD domains have also been reported^{144,146,154}. LNR mutations result in the destabilization of the heterodimers of the HD-domain and continuously exposure of the S3-cleavage site^{152,155}. Although the exact mechanism of ANK and TAD mutations in T-ALL development is not completely understood, it is hypothesized that they interfere with

NOTCH1 protein binding. Furthermore, rare TCR-recombination driven *NOTCH1* translocations are described for T-ALL placing part of the *NOTCH1* gene under control of T-cell receptor regulatory elements¹⁵⁶⁻¹⁵⁸. Most known is the translocation in which the intracellular part of *NOTCH1* is juxtaposed to the joining segment of *TCRB* thereby producing constitutively active truncated NOTCH1 protein (TAN1)¹⁵⁶. Also, an alternative mechanism of Notch activation in leukemogenesis was discovered. Deletion of the 5' end of NOTCH1 accelerates spontaneous leukemogenesis in Ikaros-knockout mice. These mice lack the normal *NOTCH1* promoter and use an alternative *NOTCH1* promoter located in an intron upstream of the HD-domain encoding exons that drives expression of ICN¹⁵⁹. This new mechanism of NOTCH1 activation was earlier discovered in radiation-induced mouse thymic lymphomas and needs further investigation regarding T-ALL oncogenesis¹⁶⁰. Strong activating *NOTCH1* mutations are especially associated with *TLX3* rearranged T-ALL².

The prognostic relevance of NOTCH1-activating mutations in pediatric T-ALL patients is still under debate. Some studies reported favorable survival rates or treatment responses for *NOTCH1*-mutated patients while other studies reported no difference or even unfavorable survival rates or treatment response for NOTCH1-mutated patients^{2,65,111,139,140,142,143,146,147,149,151,161}. This variation can be a consequence of the heterogeneity within NOTCH1-activating mutations, reflecting different types of weak and strong mutations, which are differently distributed among cohorts. Also, little attention has been given to the types of NOTCH1-activating mutations in relation to outcomes in these studies, or their association with other type B mutations. Comparison of study results is further hampered by the fact that not every study screens for both *NOTCH1* and *FBXW7* mutations and that different treatment protocols exist among study cohorts that may result in a different treatment response.

Due to the high mutational rate of this pathway in pediatric T-ALL, therapeutic inhibition of the NOTCH pathway is particularly attractive. The NOTCH pathway can be targeted on various levels; best examined are *g*-secretase inhibitors (GSIs) that inhibit S3-cleavage of NOTCH and thereby release of ICN. GSIs were initially developed to treat Alzheimer's disease. A phase I trial with GSI MK-0752 in relapsed T-ALL and acute myeloid leukemia patients resulted in major gastrointestinal toxicity¹⁶². Nevertheless, GSIs may still be useful as *in vitro* and pre-clinical studies showed the successively use of GSI in combination therapy^{126,128}. An important finding is the resensitization to steroids of otherwise glucocorticoid-resistant T-ALL cells by GSI¹⁶³. Vice versa, steroids seem to be able to overcome gastro-toxicity effects by GSIs¹⁶³. The proteasome inhibitor bortezomib is an alternative approach to block NOTCH1 activity and looks most promising. Most likely it inhibits the NOTCH-transactivator SP1. Addition of bortezomib resulted in downregulation of ICN levels, which is probably due to dissociation of the SP1 transcription factor from the NOTCH promoter and consequential downregulation of NOTCH targets¹⁶⁴. Currently, other models that silence the NOTCH pathway have been successively studied *in vitro* and *in vivo* and are awaiting for clinical trial. Examples are antagonists targeting distinct NOTCH receptors¹⁶⁵ or MAML1¹⁶⁶ and NOTCH1 antibodies¹⁶⁷.

Cell cycle and DNA repair

Cyclins and CDKs (cyclin-dependent protein kinases) heterodimeric complexes are master regulators of cell cycle. Various different cyclin and CDK proteins are known that act at specific phases of cell cycle, and the nature of the heterodimeric complex determines the activation of particular downstream proteins. The action of cyclin-CDK complexes is blocked by various members of the INK/ARF (p15, p16, p18 and p19) and CIP/KIP (p21, p27 and p57) cell cycle inhibitor gene families¹⁶⁸. The regulation and expression of these genes are regulated by upstream signaling cascades, including the PI3K/AKT and RAS-MEK-ERK pathways. Also other kinases like ATM/ATR kinases become active upon DNA damage, together with other essential enzymes and proteins including p53. Among these are Chk1 and Chk2 proteins and the tyrosine kinase Abl1. After repair, the block in cell cycle progression is relieved by the activation of Cdc25 and the inactivation of particular kinases and proteins⁸⁷.

The chromosomal 9p21 deletion is a frequent genetic lesion in cancer and the most commonly detected abnormality in pediatric T-ALL. The deletion frequently includes the *CDKN2A* gene, encoding for p16/p14^{ARF} as well as the *CDKN2B* gene encoding for p15. The incidence of *CDKN2A/B* deletions is highly variable among study cohorts but comprises 60% of pediatric T-ALL patients on average^{20-22,58,169-188}. Inactivating mutations have also been described for *CDKN2A/B*, with frequencies between 0-13%^{175,178,180-183,186,187}. Both genes can further become inactivated by hypermethylation of their promoter regions, which occurs in less than 5% of patients for *CDKN2A* but is more prevalent for *CDKN2B*, with reported incidences of 38-47% of pediatric T-ALL patients^{58,174,186,189,190}. Another member of the INK/ARF family is *p18* and deletions are described in a single study so far with a reported incidence of 14% of pediatric T-ALL patients¹⁷³. The *p27* cell cycle inhibitor gene may comprise both mutations and deletions in 60-67% of pediatric T-ALL patients^{191,192}. Also overexpression of Cyclins itself are potential oncogenic targets in T-ALL. Rare *Cyclin D2* translocations are described in 5 patients^{193,194}.

Apart from interference with direct cell cycle molecules, outbalancing the apoptotic system or creating genetic instability by inactivation of the DNA-repair system can deregulate the cell cycle. In pediatric T-ALL, around 5% of patients have *p53*-inactivating mutations/deletions at diagnosis and it is hypothesized that *p53* aberrations are associated with relapse and poor survival rates after relapse^{58,177,195,196}. Also 5 and 10% of somatic *ATM* mutations/deletions are reported in two studies and furthermore, *ATM* germ-line mutations are suggested to be associated with T-ALL^{177,196-200}.

Other type B abnormalities

Besides mutations that deregulate specific pathways, T-ALL also carries mutations of which the oncogenic mechanism remains unclear. These include *ABL1* fusion proteins, inactivating *WT1* mutations/deletions, *Ikaros* deletions, *LEF1* mutations and *PHF6* mutations.

ABL is a predominantly nuclear protein that has been connected to regulate a variety of processes including cellular shape, motility and adhesion, cell cycle, DNA repair and apoptosis. *ABL1* fusion proteins as consequence of chromosomal rearrangements are observed in a small

percentage of pediatric T-ALL patients with *ETV6*, *EML1*, *NUP214* and *BCR* as fusion partners. The *ETV6-ABL1* and *EML1-ABL1* fusions have only been described for single pediatric T-ALL cases^{201,202}. The *NUP214-ABL1* fusion as a result of the 9q34.11-9q34.13 deletion is the most commonly observed ABL1 fusion protein in T-ALL and present in ~5% of pediatric T-ALL patients^{203,204}. BCR-ABL1 translocations are known to occur in B-ALL patients but are exceptionally rare in T-ALL²⁰⁵⁻²⁰⁸. Whereas ABL1 phosphorylates many downstream targets, based on *in vitro* and *in vivo* models, the BCR-ABL1 and ETV6-ABL1 fusion protein seem to activate RAS-MEK-ERK and PI3K/AKT pathways. For this, BCR-ABL1 has been demonstrated to bind to GRB2 (growth factor receptor-bound protein 2), which can phosphorylate the docking protein GAB2 (GRB2-associated binding protein 2) that allows recruitment of the GDP to GTP exchange factor SOS (son of seventhless) to activate membrane-bound RAS proteins. Also recruitment of the protein-tyrosine phosphatase PTPN11 (SHP2) further enhances RAS-MEK-ERK and PI3K/AKT signaling. BCR-ABL1 can also interact with the adapter molecule SHC or directly activate the RAS MAPK pathway through GRB2-binding²⁰⁹. In addition, JAK2 and STAT1 or STAT5 molecules are known phosphorylation targets of BCR-ABL1^{210,211}. Imatinib is a tyrosine kinase inhibitor that is successfully used in BCR-ABL1 patients. However, many BCR-ABL1 translocated patients develop resistance against imatinib by acquiring mutations in the imatinib binding pocket, and second generation kinase inhibitors have been developed like dasatinib, nilotinib and ponatinib²¹². Patients with other ABL1 fusion proteins are also sensitive for ABL1 kinase inhibitors but also in these patients resistance may develop²⁰¹.

WT1 (Wilms tumor 1) is another gene regularly mutated/deleted in acute myeloid leukemia but more recently also found to play a role in occasional pediatric T-ALL patients^{213,214}. Mutations are often heterozygous frame-shift mutations that result in the truncation of the WT1 transcription factor rendering it incapable to bind to DNA. In two studies *WT1* mutations were identified in 10-13% of pediatric T-ALL patients^{215,216}. The consequence of *WT1* alterations in malignant transformation is not exactly clear. *WT1* acts as a haploinsufficient tumor suppressor gene. It can probably inhibit wild-type *WT1* proteins in a dominant-negative fashion. During hematopoiesis *WT1* confers the regulation of differentiation, apoptosis and proliferation. Treatment options that specifically target *WT1* or downstream pathways have not been identified yet.

Ikaros is a DNA-binding protein and loss of this protein is important in the development of B-ALL, though the involvement of Ikaros in human T-cell leukemogenesis is rare. In contrast, loss of *IKZF1* (Ikaros gene) is frequently observed in mice developing T-cell lymphoma/leukemia. So far, around 5% of adult/pediatric T-ALL patients have been identified to carry *IKZF1* deletions²¹⁷⁻²²⁰. Ikaros aberrations were described for ~10% of T-ALL patients by next generation sequencing²⁵. The function of Ikaros in T-cells needs to be established, but a strong association is observed between NOTCH1 expression and *IKZF1* mutations in lymphoma/leukemia mice. Ikaros can bind to the same DNA-binding sites as NOTCH1 and may therefore be able to suppress NOTCH target gene expression²²¹. Furthermore, a recent study suggests that Ikaros is regulated by CK2 kinases during cell cycle in both T-ALL and B-ALL cell lines²²². Ikaros is induced by a retinoid receptor agonist in BCR-ABL1 cells which increased sensitivity to conventional tyrosine kinase inhibitor therapy²²³.

LEF1 (lymphoid enhancer-binding factor 1) is a transcription factor of the Wnt signaling. Microdeletions and inactivating mutations have been found in LEF1 in ~5%-7% of pediatric T-ALL patients²²⁴. The authors showed that *LEF1* inactivation was associated with high MYC levels. It was hypothesized that LEF1 may act in concert with NOTCH1 function to achieve high MYC levels. However, the exact role of LEF1 in T-cell leukemogenesis is not clear and needs further investigation. Very recently, mutations in the *TCF7* transcription factor are found in a small number of early T-cell progenitor ALL patients which interferes with LEF1 function and can thereby cooperate with *LEF1* mutations²²⁵. Treatment options that specifically target LEF1 or downstream pathways have not been identified yet.

Another mutated gene in T-ALL is *PHF6*. Although the function of PHF6 is unclear it is postulated that it is involved in cell cycle regulation and DNA repair. Inactivating *PHF6* mutations and deletions are detected in 16% and 38% of pediatric T-ALL patients, respectively²²⁶, and in 28% of a mixed adult/pediatric Korean cohort²⁰. In response to these findings, *Yoo et al* sequenced *PHF6* in several tumors including T-ALL and detected that 35% adult/pediatric T-ALL patients have mutations²²⁷. Later, *Wang et al* reported 19% of *PHF6* mutations in adult and 5% in pediatric T-ALL²²⁸.

Targeting epigenetic regulators

When proper transcription factors like ETV6 or RUNX1 are available, RNA polymerases are able to bind to a core sequence within the DNA promoter to initiation of RNA transcription. Ribosomal RNA represent ribosome components for mRNA translation into protein. Deadenylation is crucial in the degradation of mRNA. Transcription factors and RNA polymerases are only able to bind when the genetic material harbors an accessible configuration. This is regulated by DNA- and histone modifications. This is, for instance, exhibited by DNA methyltransferases (DNMTs) that catalyze the methyl-group transfer to the DNA, histone acetyltransferase or methyltransferase enzymes. The latter enzyme complex is represented by polycomb complexes.

Whole exome sequencing of adult and pediatric T-ALL samples revealed *CNOT3* mutations in 8% and *RPL5* and *RPL10* mutations in 10%²²⁹. *CNOT3* is part of a deadenylation complex that is involved in the shortening of the mRNA 3'poly(A) tail. Silencing of this gene in the *Drosophila* eye model results in a marked increase in tumor incidence. Loss-of-function mutations in the ribosomal protein *RPL10* result in impaired proliferation and ribosome biogenesis effects.

The DNA-methyltransferase *DNMT3* that is involved in transferring methyl-groups to cytosine residues in the DNA is frequently mutated in acute myeloid leukemia. It is recently identified by next generation sequencing to be mutated in 16-17% of adult T-ALL patients but was not identified in pediatric T-ALL^{77,230-235}. The genes *EED*, *EZH2* and *SUZ12* that encode the polycomb repression complex 2 (PRC2), which is involved in the epigenetics of the chromatin, are mutated in adult and pediatric T-ALL and predominantly in ETP-ALL patients^{25,232,236-238}. Also inactivating mutations in the transcriptional repressor *ETV6* are recently identified in adult T-ALL. In this same study, inactivating point mutations and truncating frame shift mutations in the *RUNX1* transcription factor were identified. Both mutations are also detected by next generation

sequencing of 12 ETP-ALL children and in a cohort of 77 additionally T-ALL children (*RUNX1*; 16% of T-ALL patients, *ETV6* in 33% of ETP-ALL patients). *RUNX1* regulates various genes involved in cell differentiation including the granulocyte-macrophage colony-stimulating factor. Mutant alleles of *RUNX1* and *ETV6* are suggested to act in a dominant negative fashion^{25,232,239-242}.

Demethylating agents alter the level of DNA methylation and are predominantly represented by cytidine analogs like azacitidine. Azacitidine is FDA-approved to treat patients with myelodysplastic syndromes and adult AML²⁴³. Also targeting chromatin-remodeling events to prevent DNA exposure is therapeutically proven. Treatment with histone deacetylase (HDACs) inhibitors result in retained hyperacetylated histone lysine residues and accessible chromatin. This affects the gene expression of a small number of tumor suppressor or oncogenes by activation or repression. Inhibitors Vorinostat and Romidepsin have been FDA-approved for the treatment of subcutaneous T-cell lymphoma. Various alternatives are currently in clinical trial²⁴⁴. Also RNA polymerases can be targeted by drugs like BMH-21, which was initially a p53 activator but also degrades the RNA polymerase I subunit and thereby reduces rRNA synthesis. In addition, transcriptional processes can be indirectly reduced by the interference of associated transcriptional complexes like TFIID. Interference with TFIID enables the opening of double stranded DNA and thereby transcription. One such a drug is Triptolide that is currently used in cancer treatment with positive effects²⁴⁵.

CONCLUSION

Many mutations are known that make T-ALL a very heterogeneous disease. Type B mutations in T-ALL affect a various signal transduction pathways. To a minor extent, this includes the TCR signaling pathway. More frequently, the IL7R/JAK/STAT, RAS-MEK-ERK, PI3K/AKT and NOTCH signaling pathways are affected. Also general cellular processes like cell cycle, DNA repair, transcription and translation are frequently dysregulated by mutations in T-ALL. Type B mutations are, in contrast to type A driving oncogenic events, frequently present on the near clonal or subclonal level, making them difficult targets for targeted drug strategies. Also, the multitude of different type B mutations may hamper to analyze the prognostic significance of single type B mutations in relative small patient cohorts of pediatric T-ALL patients. It may therefore be important to group genetic alterations to their common involvement in signal transduction pathways or cellular processes. This may help to recognize relevant prognostic disease subtypes that may be stratified towards a specific treatment strategy.

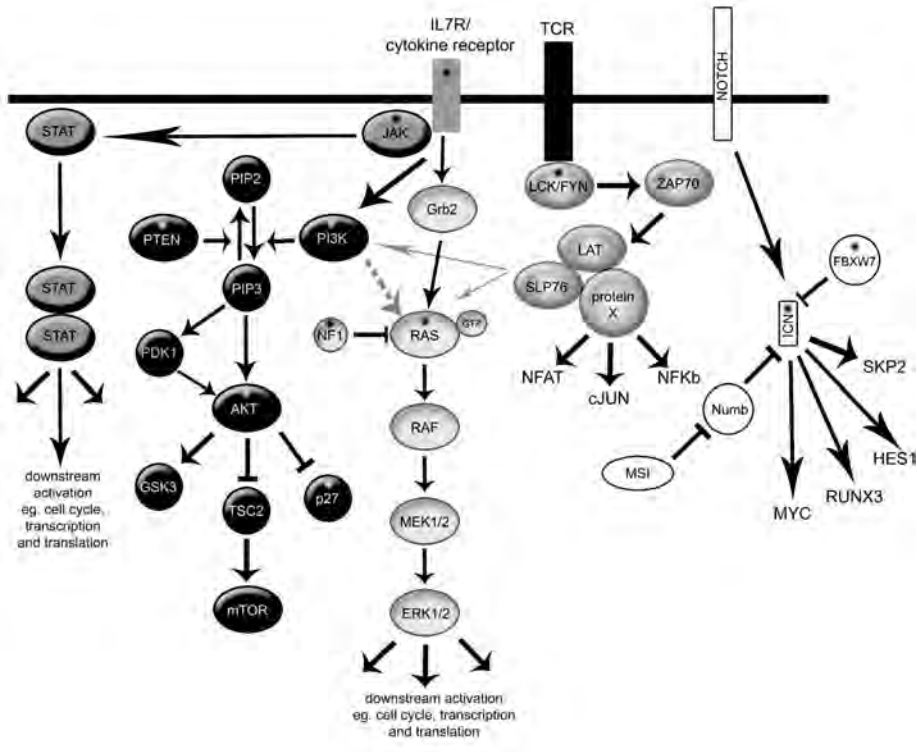


Figure 1 | **Aberrantly expressed signal transduction pathways by type B mutations in T-ALL.** This includes the TCR (T-cell receptor), IL7R, JAK-STAT, RAS-MEK-ERK, PI3K/AKT and NOTCH1 signaling. Moreover this affects cell cycle, DNA damage control and epigenetic regulation. Known mutated proteins in T-ALL are indicated by *.

2

REFERENCES

1. Van Vlierberghe P, Pieters R, Beverloo HB, Meijerink JP. Molecular-genetic insights in paediatric T-cell acute lymphoblastic leukaemia. *Br J Haematol*. 2008;143:153-168.
2. Zuurbier L, Homminga I, Calvert V, et al. NOTCH1 and/or FBXW7 mutations predict for initial good prednisone response but not for improved outcome in pediatric T-cell acute lymphoblastic leukemia patients treated on DCOG or COALL protocols. *Leukemia*. 2010;24:2014-2022.
3. Clappier E, Gerby B, Sigaux F, et al. Clonal selection in xenografted human T cell acute lymphoblastic leukemia recapitulates gain of malignancy at relapse. *J Exp Med*. 2011;208:653-661.
4. Greaves M. Cancer stem cells: back to Darwin? *Semin Cancer Biol*;20:65-70.
5. Brownlie RJ, Zamoyska R. T cell receptor signalling networks: branched, diversified and bounded. *Nat Rev Immunol*;13:257-269.
6. Macian F. NFAT proteins: key regulators of T-cell development and function. *Nat Rev Immunol*. 2005;5:472-484.
7. Morgan NV, Goddard S, Cardno TS, et al. Mutation in the TCRalpha subunit constant gene (TRAC) leads to a human immunodeficiency disorder characterized by a lack of TCRalphabeta+ T cells. *J Clin Invest*;121:695-702.
8. Elder ME, Lin D, Clever J, et al. Human severe combined immunodeficiency due to a defect in ZAP-70, a T cell tyrosine kinase. *Science*. 1994;264:1596-1599.
9. Streubel B, Vinatzer U, Willheim M, Raderer M, Chott A. Novel t(5;9)(q33;q22) fuses ITK to SYK in unspecified peripheral T-cell lymphoma. *Leukemia*. 2006;20:313-318.
10. Vaque JP, Gomez-Lopez G, Monsalvez V, et al. PLCG1 mutations in cutaneous T-cell lymphomas. *Blood*.
11. Tycko B, Smith SD, Sklar J. Chromosomal translocations joining LCK and TCRB loci in human T cell leukemia. *J Exp Med*. 1991;174:867-873.
12. Wright DD, Sefton BM, Kamps MP. Oncogenic activation of the Lck protein accompanies translocation of the LCK gene in the human HSB2 T-cell leukemia. *Mol Cell Biol*. 1994;14:2429-2437.
13. Porcu M, Kleppe M, Gianfelici V, et al. Mutation of the receptor tyrosine phosphatase PTPRC (CD45) in T-cell acute lymphoblastic leukemia. *Blood*;119:4476-4479.
14. Medyouf H, Alcalde H, Berthier C, et al. Targeting calcineurin activation as a therapeutic strategy for T-cell acute lymphoblastic leukemia. *Nat Med*. 2007;13:736-741.
15. Wang G, Yan Y, Chen X, Lin C, Li Y. SEA Antagonizes the Imatinib-Meditated Inhibitory Effects on T Cell Activation via the TCR Signaling Pathway. *Biomed Res Int*;2014:682010.
16. Ribeiro D, Melao A, Barata JT. IL-7R-mediated signaling in T-cell acute lymphoblastic leukemia. *Adv Biol Regul*;53:211-222.
17. O'Doherty C, Alloza I, Rooney M, Vandenbroeck K. IL7RA polymorphisms and chronic inflammatory arthropathies. *Tissue Antigens*. 2009;74:429-431.
18. Lundmark F, Duvefelt K, Iacobaeus E, et al. Variation in interleukin 7 receptor alpha chain (IL7R) influences risk of multiple sclerosis. *Nat Genet*. 2007;39:1108-1113.
19. Giliani S, Mori L, de Saint Basile G, et al. Interleukin-7 receptor alpha (IL-7Ralpha) deficiency: cellular and molecular bases. Analysis of clinical, immunological, and molecular features in 16 novel patients. *Immunol Rev*. 2005;203:110-126.
20. Huh HJ, Lee SH, Yoo KH, et al. Gene mutation profiles and prognostic implications in Korean patients with T-lymphoblastic leukemia. *Ann Hematol*;92:635-644.
21. Shochat C, Tal N, Bandapalli OR, et al. Gain-of-function mutations in interleukin-7 receptor-alpha (IL7R) in childhood acute lymphoblastic leukemias. *J Exp Med*;208:901-908.

22. Zenatti PP, Ribeiro D, Li W, et al. Oncogenic IL7R gain-of-function mutations in childhood T-cell acute lymphoblastic leukemia. *Nat Genet*;43:932-939.
23. Kim MS, Chung NG, Kim MS, Yoo NJ, Lee SH. Somatic mutation of IL7R exon 6 in acute leukemias and solid cancers. *Hum Pathol*;44:551-555.
24. Zenatti PP, Ribeiro D, Li W, et al. Oncogenic IL7R gain-of-function mutations in childhood T-cell acute lymphoblastic leukemia. *Nat Genet*. 2011;43:932-939.
25. Zhang J, Ding L, Holmfeldt L, et al. The genetic basis of early T-cell precursor acute lymphoblastic leukaemia. *Nature*. 2012;481:157-163.
26. Treanor LM, Zhou S, Janke L, et al. Interleukin-7 receptor mutants initiate early T cell precursor leukemia in murine thymocyte progenitors with multipotent potential. *J Exp Med*;211:701-713.
27. Macchi P, Villa A, Giliani S, et al. Mutations of Jak-3 gene in patients with autosomal severe combined immune deficiency (SCID). *Nature*. 1995;377:65-68.
28. Ghoreschi K, Laurence A, O'Shea JJ. Janus kinases in immune cell signaling. *Immunol Rev*. 2009;228:273-287.
29. Rawlings JS, Rosler KM, Harrison DA. The JAK/STAT signaling pathway. *J Cell Sci*. 2004;117:1281-1283.
30. Benekli M, Baumann H, Wetzler M. Targeting signal transducer and activator of transcription signaling pathway in leukemias. *J Clin Oncol*. 2009;27:4422-4432.
31. Bercovich D, Ganmore I, Scott LM, et al. Mutations of JAK2 in acute lymphoblastic leukaemias associated with Down's syndrome. *Lancet*. 2008;372:1484-1492.
32. Gaikwad A, Rye CL, Devidas M, et al. Prevalence and clinical correlates of JAK2 mutations in Down syndrome acute lymphoblastic leukaemia. *Br J Haematol*. 2009;144:930-932.
33. Kearney L, Gonzalez De Castro D, Yeung J, et al. Specific JAK2 mutation (JAK2R683) and multiple gene deletions in Down syndrome acute lymphoblastic leukemia. *Blood*. 2009;113:646-648.
34. Mullighan CG, Zhang J, Harvey RC, et al. JAK mutations in high-risk childhood acute lymphoblastic leukemia. *Proc Natl Acad Sci U S A*. 2009;106:9414-9418.
35. Asnafi V, Le Noir S, Lhermitte L, et al. JAK1 mutations are not frequent events in adult T-ALL: a GRAALL study. *Br J Haematol*. 2010;148:178-179.
36. Flex E, Petrangeli V, Stella L, et al. Somatic acquired JAK1 mutations in adult acute lymphoblastic leukemia. *J Exp Med*. 2008;205:751-758.
37. Jeong EG, Kim MS, Nam HK, et al. Somatic mutations of JAK1 and JAK3 in acute leukemias and solid cancers. *Clin Cancer Res*. 2008;14:3716-3721.
38. Bains T, Heinrich MC, Loriaux MM, et al. Newly described activating JAK3 mutations in T-cell acute lymphoblastic leukemia. *Leukemia*;26:2144-2146.
39. De Keersmaecker K, Atak ZK, Li N, et al. Exome sequencing identifies mutation in CNOT3 and ribosomal genes RPL5 and RPL10 in T-cell acute lymphoblastic leukemia. *Nat Genet*. 2013;45:186-190.
40. Lacronique V, Boureux A, Valle VD, et al. A TEL-JAK2 fusion protein with constitutive kinase activity in human leukemia. *Science*. 1997;278:1309-1312.
41. Lin Q, Lai R, Chirieac LR, et al. Constitutive activation of JAK3/STAT3 in colon carcinoma tumors and cell lines: inhibition of JAK3/STAT3 signaling induces apoptosis and cell cycle arrest of colon carcinoma cells. *Am J Pathol*. 2005;167:969-980.
42. Mora LB, Buettner R, Seigne J, et al. Constitutive activation of Stat3 in human prostate tumors and cell lines: direct inhibition of Stat3 signaling induces apoptosis of prostate cancer cells. *Cancer Res*. 2002;62:6659-6666.
43. Song L, Turkson J, Karras JG, Jove R, Haura EB. Activation of Stat3 by receptor tyrosine kinases and cytokines regulates survival in human non-small cell carcinoma cells. *Oncogene*. 2003;22:4150-4165.
44. Chim CS, Wong AS, Kwong YL. Epigenetic dysregulation of the Jak/STAT pathway by frequent aberrant methylation of SHP1 but not SOCS1 in acute leukaemias. *Ann Hematol*. 2004;83:527-532.

45. Reddy J, Shivapurkar N, Takahashi T, et al. Differential methylation of genes that regulate cytokine signaling in lymphoid and hematopoietic tumors. *Oncogene*. 2005;24:732-736.
46. Chen CY, Tsay W, Tang JL, et al. SOCS1 methylation in patients with newly diagnosed acute myeloid leukemia. *Genes Chromosomes Cancer*. 2003;37:300-305.
47. Kleppe M, Lahortiga I, El Chaar T, et al. Deletion of the protein tyrosine phosphatase gene PTPN2 in T-cell acute lymphoblastic leukemia. *Nat Genet*;42:530-535.
48. Kleppe M, Lahortiga I, El Chaar T, et al. Deletion of the protein tyrosine phosphatase gene PTPN2 in T-cell acute lymphoblastic leukemia. *Nat Genet*. 2010;42:530-535.
49. Fleischmann R, Cutolo M, Genovese MC, et al. Phase IIb dose-ranging study of the oral JAK inhibitor tofacitinib (CP-690,550) or adalimumab monotherapy versus placebo in patients with active rheumatoid arthritis with an inadequate response to disease-modifying antirheumatic drugs. *Arthritis Rheum*;64:617-629.
50. Punwani N, Scherle P, Flores R, et al. Preliminary clinical activity of a topical JAK1/2 inhibitor in the treatment of psoriasis. *J Am Acad Dermatol*;67:658-664.
51. Vafadari R, Quaedackers ME, Kho MM, et al. Pharmacodynamic analysis of tofacitinib and basiliximab in kidney allograft recipients. *Transplantation*;94:465-472.
52. Cervantes F, Vannucchi AM, Kiladjian JJ, et al. Three-year efficacy, safety, and survival findings from COMFORT-II, a phase 3 study comparing ruxolitinib with best available therapy for myelofibrosis. *Blood*;122:4047-4053.
53. Genot E, Cantrell DA. Ras regulation and function in lymphocytes. *Curr Opin Immunol*. 2000;12:289-294.
54. Fernandez-Medarde A, Santos E. Ras in cancer and developmental diseases. *Genes Cancer*. 2011;2:344-358.
55. Barbosa TC, Andrade FG, Lopes BA, et al. Impact of mutations in FLT3, PTPN11 and RAS genes on the overall survival of pediatric B cell precursor acute lymphoblastic leukemia in Brazil. *Leuk Lymphoma*. 2014.
56. Driessen EM, van Roon EH, Spijkers-Hagelstein JA, et al. Frequencies and prognostic impact of RAS mutations in MLL-rearranged acute lymphoblastic leukemia in infants. *Haematologica*. 2013;98:937-944.
57. Prella C, Bursen A, Dingermann T, Marschalek R. Secondary mutations in t(4;11) leukemia patients. *Leukemia*. 2013;27:1425-1427.
58. Kawamura M, Ohnishi H, Guo SX, et al. Alterations of the p53, p21, p16, p15 and RAS genes in childhood T-cell acute lymphoblastic leukemia. *Leuk Res*. 1999;23:115-126.
59. Lubbert M, Mirro J, Jr., Miller CW, et al. N-ras gene point mutations in childhood acute lymphocytic leukemia correlate with a poor prognosis. *Blood*. 1990;75:1163-1169.
60. Nakao M, Janssen JW, Seriu T, Bartram CR. Rapid and reliable detection of N-ras mutations in acute lymphoblastic leukemia by melting curve analysis using LightCycler technology. *Leukemia*. 2000;14:312-315.
61. Perentesis JP, Bhatia S, Boyle E, et al. RAS oncogene mutations and outcome of therapy for childhood acute lymphoblastic leukemia. *Leukemia*. 2004;18:685-692.
62. Rodenhuis S, Bos JL, Slater RM, et al. Absence of oncogene amplifications and occasional activation of N-ras in lymphoblastic leukemia of childhood. *Blood*. 1986;67:1698-1704.
63. Yamamoto T, Isomura M, Xu Y, et al. PTPN11, RAS and FLT3 mutations in childhood acute lymphoblastic leukemia. *Leuk Res*. 2006;30:1085-1089.
64. Yokota S, Nakao M, Horiike S, et al. Mutational analysis of the N-ras gene in acute lymphoblastic leukemia: a study of 125 Japanese pediatric cases. *Int J Hematol*. 1998;67:379-387.
65. Mansur MB, Hassan R, Barbosa TC, et al. Impact of complex NOTCH1 mutations on survival in

- paediatric T-cell leukaemia. *BMC Cancer*;12:9.
66. Zhang SY, Klein-Szanto AJ, Sauter ER, et al. Higher frequency of alterations in the p16/CDKN2 gene in squamous cell carcinoma cell lines than in primary tumors of the head and neck. *Cancer Res.* 1994;54:5050-5053.
 67. Von Lintig FC, Huvar I, Law P, et al. Ras activation in normal white blood cells and childhood acute lymphoblastic leukemia. *Clin Cancer Res.* 2000;6:1804-1810.
 68. Van Vlierberghe P, Meijerink JP, Stam RW, et al. Activating FLT3 mutations in CD4+/CD8- pediatric T-cell acute lymphoblastic leukemias. *Blood.* 2005;106:4414-4415.
 69. Mansur MB, Emerenciano M, Splendore A, et al. T-cell lymphoblastic leukemia in early childhood presents NOTCH1 mutations and MLL rearrangements. *Leuk Res.* 2010;34:483-486.
 70. Kraszewska MD, Dawidowska M, Kosmalka M, et al. BCL11B, FLT3, NOTCH1 and FBXW7 mutation status in T-cell acute lymphoblastic leukemia patients. *Blood Cells Mol Dis*;50:33-38.
 71. Neumann M, Coskun E, Fransecky L, et al. FLT3 mutations in early T-cell precursor ALL characterize a stem cell like leukemia and imply the clinical use of tyrosine kinase inhibitors. *PLoS One*;8:e53190.
 72. Balgobind BV, Van Vlierberghe P, van den Ouweland AM, et al. Leukemia-associated NF1 inactivation in patients with pediatric T-ALL and AML lacking evidence for neurofibromatosis. *Blood.* 2008;111:4322-4328.
 73. Barbosa TC, Andrade FG, Lopes BA, et al. Impact of mutations in FLT3, PTPN11 and RAS genes on the overall survival of pediatric B cell precursor acute lymphoblastic leukemia in Brazil. *Leuk Lymphoma.*
 74. Driessen EM, van Roon EH, Spijkers-Hagelstein JA, et al. Frequencies and prognostic impact of RAS mutations in MLL-rearranged acute lymphoblastic leukemia in infants. *Haematologica*;98:937-944.
 75. Tzoneva G, Perez-Garcia A, Carpenter Z, et al. Activating mutations in the NT5C2 nucleotidase gene drive chemotherapy resistance in relapsed ALL. *Nat Med*;19:368-371.
 76. Van Vlierberghe P, Ambesi-Impiombato A, Perez-Garcia A, et al. ETV6 mutations in early immature human T cell leukemias. *J Exp Med*;208:2571-2579.
 77. Zhang J, Ding L, Holmfeldt L, et al. The genetic basis of early T-cell precursor acute lymphoblastic leukaemia. *Nature*;481:157-163.
 78. Goemans BF, Zwaan CM, Harlow A, et al. In vitro profiling of the sensitivity of pediatric leukemia cells to tipifarnib: identification of T-cell ALL and FAB M5 AML as the most sensitive subsets. *Blood.* 2005;106:3532-3537.
 79. Cortes J, Albitar M, Thomas D, et al. Efficacy of the farnesyl transferase inhibitor R115777 in chronic myeloid leukemia and other hematologic malignancies. *Blood.* 2003;101:1692-1697.
 80. Feldman EJ, Cortes J, DeAngelo DJ, et al. On the use of lonafarnib in myelodysplastic syndrome and chronic myelomonocytic leukemia. *Leukemia.* 2008;22:1707-1711.
 81. Blum R, Kloog Y. Tailoring Ras-pathway--inhibitor combinations for cancer therapy. *Drug Resist Updat.* 2005;8:369-380.
 82. Kurzrock R, Kantarjian HM, Cortes JE, et al. Farnesyltransferase inhibitor R115777 in myelodysplastic syndrome: clinical and biologic activities in the phase 1 setting. *Blood.* 2003;102:4527-4534.
 83. Karakas B, Bachman KE, Park BH. Mutation of the PIK3CA oncogene in human cancers. *Br J Cancer.* 2006;94:455-459.
 84. Kim MS, Jeong EG, Yoo NJ, Lee SH. Mutational analysis of oncogenic AKT E17K mutation in common solid cancers and acute leukaemias. *Br J Cancer.* 2008;98:1533-1535.
 85. Grabiner BC, Nardi V, Birsoy K, et al. A Diverse Array of Cancer-Associated MTOR Mutations Are Hyperactivating and Can Predict Rapamycin Sensitivity. *Cancer Discov*;4:554-563.
 86. Chang F, Lee JT, Navolanic PM, et al. Involvement of PI3K/Akt pathway in cell cycle progression, apoptosis, and neoplastic transformation: a target for cancer chemotherapy. *Leukemia.* 2003;17:590-603.

87. Manning BD, Cantley LC. AKT/PKB signaling: navigating downstream. *Cell*. 2007;129:1261-1274.
88. Palomero T, Sulis ML, Cortina M, et al. Mutational loss of PTEN induces resistance to NOTCH1 inhibition in T-cell leukemia. *Nat Med*. 2007;13:1203-1210.
89. Zuurbier L, Petricoin EF, 3rd, Vuerhard MJ, et al. The significance of PTEN and AKT aberrations in pediatric T-cell acute lymphoblastic leukemia. *Haematologica*. 2012;97:1405-1413.
90. Rhei E, Kang L, Bogomolny F, et al. Mutation analysis of the putative tumor suppressor gene PTEN/MMAC1 in primary breast carcinomas. *Cancer Res*. 1997;57:3657-3659.
91. Cairns P, Okami K, Halachmi S, et al. Frequent inactivation of PTEN/MMAC1 in primary prostate cancer. *Cancer Res*. 1997;57:4997-5000.
92. Kong D, Suzuki A, Zou TT, et al. PTEN1 is frequently mutated in primary endometrial carcinomas. *Nat Genet*. 1997;17:143-144.
93. Guldberg P, thor Straten P, Birck A, et al. Disruption of the MMAC1/PTEN gene by deletion or mutation is a frequent event in malignant melanoma. *Cancer Res*. 1997;57:3660-3663.
94. Aveyard JS, Skilleter A, Habuchi T, Knowles MA. Somatic mutation of PTEN in bladder carcinoma. *Br J Cancer*. 1999;80:904-908.
95. Alimov A, Li C, Gizatullin R, et al. Somatic mutation and homozygous deletion of PTEN/MMAC1 gene of 10q23 in renal cell carcinoma. *Anticancer Res*. 1999;19:3841-3846.
96. Zhou XP, Waite KA, Pilarski R, et al. Germline PTEN promoter mutations and deletions in Cowden/Bannayan-Riley-Ruvalcaba syndrome result in aberrant PTEN protein and dysregulation of the phosphoinositol-3-kinase/Akt pathway. *Am J Hum Genet*. 2003;73:404-411.
97. Roman-Gomez J, Jimenez-Velasco A, Agirre X, et al. Lack of CpG island methylator phenotype defines a clinical subtype of T-cell acute lymphoblastic leukemia associated with good prognosis. *J Clin Oncol*. 2005;23:7043-7049.
98. Teresi RE, Zbuk KM, Pezzolesi MG, Waite KA, Eng C. Cowden syndrome-affected patients with PTEN promoter mutations demonstrate abnormal protein translation. *Am J Hum Genet*. 2007;81:756-767.
99. Mendes RD, Sarmiento LM, Cante-Barrett K, et al. PTEN micro-deletions in T-cell acute lymphoblastic leukemia are caused by illegitimate RAG-mediated recombination events. *Blood*. 2014.
100. Sansal I, Sellers WR. The biology and clinical relevance of the PTEN tumor suppressor pathway. *J Clin Oncol*. 2004;22:2954-2963.
101. Kwabi-Addo B, Giri D, Schmidt K, et al. Haploinsufficiency of the Pten tumor suppressor gene promotes prostate cancer progression. *Proc Natl Acad Sci U S A*. 2001;98:11563-11568.
102. Kwon CH, Zhao D, Chen J, et al. Pten haploinsufficiency accelerates formation of high-grade astrocytomas. *Cancer Res*. 2008;68:3286-3294.
103. Zuurbier L, Petricoin EF, 3rd, Vuerhard MJ, et al. The significance of PTEN and AKT aberrations in pediatric T-cell acute lymphoblastic leukemia. *Haematologica*;97:1405-1413.
104. Bandapalli OR, Zimmermann M, Kox C, et al. NOTCH1 activation clinically antagonizes the unfavorable effect of PTEN inactivation in BFM-treated children with precursor T-cell acute lymphoblastic leukemia. *Haematologica*;98:928-936.
105. Mendes RD, Sarmiento LM, Cante-Barrett K, et al. PTEN micro-deletions in T-cell acute lymphoblastic leukemia are caused by illegitimate RAG-mediated recombination events. *Blood*.
106. Velho S, Oliveira C, Ferreira A, et al. The prevalence of PIK3CA mutations in gastric and colon cancer. *Eur J Cancer*. 2005;41:1649-1654.
107. Wu G, Xing M, Mambo E, et al. Somatic mutation and gain of copy number of PIK3CA in human breast cancer. *Breast Cancer Res*. 2005;7:R609-616.
108. Kuo KT, Mao TL, Jones S, et al. Frequent activating mutations of PIK3CA in ovarian clear cell carcinoma. *Am J Pathol*. 2009;174:1597-1601.
109. Silva A, Jotta PY, Silveira AB, et al. Regulation of PTEN by CK2 and Notch1 in primary T-cell acute

- lymphoblastic leukemia: rationale for combined use of CK2- and gamma-secretase inhibitors. *Haematologica*;95:674-678.
110. Min YH, Eom JI, Cheong JW, et al. Constitutive phosphorylation of Akt/PKB protein in acute myeloid leukemia: its significance as a prognostic variable. *Leukemia*. 2003;17:995-997.
 111. Larson Gedman A, Chen Q, Kugel Desmoulin S, et al. The impact of NOTCH1, FBW7 and PTEN mutations on prognosis and downstream signaling in pediatric T-cell acute lymphoblastic leukemia: a report from the Children's Oncology Group. *Leukemia*. 2009;23:1417-1425.
 112. Gutierrez A, Sanda T, Grebliunaite R, et al. High frequency of PTEN, PI3K, and AKT abnormalities in T-cell acute lymphoblastic leukemia. *Blood*. 2009;114:647-650.
 113. Jotta PY, Ganazza MA, Silva A, et al. Negative prognostic impact of PTEN mutation in pediatric T-cell acute lymphoblastic leukemia. *Leukemia*;24:239-242.
 114. Wu Q, Chen Y, Cui G, Cheng Y. Wortmannin inhibits K562 leukemic cells by regulating PI3k/Akt channel in vitro. *J Huazhong Univ Sci Technolog Med Sci*. 2009;29:451-456.
 115. Medina JR. Selective 3-phosphoinositide-dependent kinase 1 (PDK1) inhibitors: dissecting the function and pharmacology of PDK1. *J Med Chem*;56:2726-2737.
 116. Evangelisti C, Ricci F, Tazzari P, et al. Preclinical testing of the Akt inhibitor triciribine in T-cell acute lymphoblastic leukemia. *J Cell Physiol*;226:822-831.
 117. Batista A, Barata JT, Raderschall E, et al. Targeting of active mTOR inhibits primary leukemia T cells and synergizes with cytotoxic drugs and signaling inhibitors. *Exp Hematol*;39:457-472 e453.
 118. Ikezoe T, Nishioka C, Bandobashi K, et al. Longitudinal inhibition of PI3K/Akt/mTOR signaling by LY294002 and rapamycin induces growth arrest of adult T-cell leukemia cells. *Leuk Res*. 2007;31:673-682.
 119. Meuillet EJ, Mahadevan D, Vankayalapati H, et al. Specific inhibition of the Akt1 pleckstrin homology domain by D-3-deoxy-phosphatidyl-myo-inositol analogues. *Mol Cancer Ther*. 2003;2:389-399.
 120. Chiarini F, Del Sole M, Mongiorgi S, et al. The novel Akt inhibitor, perifosine, induces caspase-dependent apoptosis and downregulates P-glycoprotein expression in multidrug-resistant human T-acute leukemia cells by a JNK-dependent mechanism. *Leukemia*. 2008;22:1106-1116.
 121. Chiarini F, Grimaldi C, Ricci F, et al. Activity of the novel dual phosphatidylinositol 3-kinase/mammalian target of rapamycin inhibitor NVP-BEZ235 against T-cell acute lymphoblastic leukemia. *Cancer Res*;70:8097-8107.
 122. Batista A, Barata JT, Raderschall E, et al. Targeting of active mTOR inhibits primary leukemia T cells and synergizes with cytotoxic drugs and signaling inhibitors. *Exp Hematol*. 2011;39:457-472 e453.
 123. Evangelisti C, Ricci F, Tazzari P, et al. Preclinical testing of the Akt inhibitor triciribine in T-cell acute lymphoblastic leukemia. *J Cell Physiol*. 2011;226:822-831.
 124. Chiarini F, Grimaldi C, Ricci F, et al. Activity of the novel dual phosphatidylinositol 3-kinase/mammalian target of rapamycin inhibitor NVP-BEZ235 against T-cell acute lymphoblastic leukemia. *Cancer Res*. 2010;70:8097-8107.
 125. Chiarini F, Fala F, Tazzari PL, et al. Dual Inhibition of Class IA Phosphatidylinositol 3-Kinase and Mammalian Target of Rapamycin as a New Therapeutic Option for T-Cell Acute Lymphoblastic Leukemia. *Cancer Research*. 2009;69:3520-3528.
 126. Cullion K, Draheim KM, Hermance N, et al. Targeting the Notch1 and mTOR pathways in a mouse T-ALL model. *Blood*. 2009;113:6172-6181.
 127. Chan S. Targeting the mammalian target of rapamycin (mTOR): a new approach to treating cancer. *Br J Cancer*. 2004;91:1420-1424.
 128. Sanda T, Li X, Gutierrez A, et al. Interconnecting molecular pathways in the pathogenesis and drug sensitivity of T-cell acute lymphoblastic leukemia. *Blood*. 2010;115:1735-1745.
 129. Anderson AC, Robey EA, Huang YH. Notch signaling in lymphocyte development. *Curr Opin Genet*

- Dev. 2001;11:554-560.
130. Ferrando AA. The role of NOTCH1 signaling in T-ALL. *Hematology Am Soc Hematol Educ Program*. 2009;353-361.
 131. Andersen P, Uosaki H, Shenje LT, Kwon C. Non-canonical Notch signaling: emerging role and mechanism. *Trends Cell Biol*;22:257-265.
 132. Imai T, Tokunaga A, Yoshida T, et al. The neural RNA-binding protein Musashi1 translationally regulates mammalian numb gene expression by interacting with its mRNA. *Mol Cell Biol*. 2001;21:3888-3900.
 133. Fiuza UM, Arias AM. Cell and molecular biology of Notch. *J Endocrinol*. 2007;194:459-474.
 134. Jiao X, Wood LD, Lindman M, et al. Somatic mutations in the Notch, NF-KB, PIK3CA, and Hedgehog pathways in human breast cancers. *Genes Chromosomes Cancer*;51:480-489.
 135. Clay MR, Varma S, West RB. MAST2 and NOTCH1 translocations in breast carcinoma and associated pre-invasive lesions. *Hum Pathol*;44:2837-2844.
 136. Hoek K, Rimm DL, Williams KR, et al. Expression profiling reveals novel pathways in the transformation of melanocytes to melanomas. *Cancer Res*. 2004;64:5270-5282.
 137. Xu P, Yu S, Jiang R, et al. Differential expression of Notch family members in astrocytomas and medulloblastomas. *Pathol Oncol Res*. 2009;15:703-710.
 138. Rahman MT, Nakayama K, Rahman M, et al. Notch3 overexpression as potential therapeutic target in advanced stage chemoresistant ovarian cancer. *Am J Clin Pathol*;138:535-544.
 139. Breit S, Stanulla M, Flohr T, et al. Activating NOTCH1 mutations predict favorable early treatment response and long-term outcome in childhood precursor T-cell lymphoblastic leukemia. *Blood*. 2006;108:1151-1157.
 140. Clappier E, Collette S, Grardel N, et al. NOTCH1 and FBXW7 mutations have a favorable impact on early response to treatment, but not on outcome, in children with T-cell acute lymphoblastic leukemia (T-ALL) treated on EORTC trials 58881 and 58951. *Leukemia*. 2010;24:2023-2031.
 141. Erbilgin Y, Sayitoglu M, Hatirnaz O, et al. Prognostic significance of NOTCH1 and FBXW7 mutations in pediatric T-ALL. *Dis Markers*. 2010;28:353-360.
 142. Kox C, Zimmermann M, Stanulla M, et al. The favorable effect of activating NOTCH1 receptor mutations on long-term outcome in T-ALL patients treated on the ALL-BFM 2000 protocol can be separated from FBXW7 loss of function. *Leukemia*. 2010;24:2005-2013.
 143. Park MJ, Taki T, Oda M, et al. FBXW7 and NOTCH1 mutations in childhood T cell acute lymphoblastic leukaemia and T cell non-Hodgkin lymphoma. *Br J Haematol*. 2009;145:198-206.
 144. Thompson BJ, Buonamici S, Sulis ML, et al. The SCFFBW7 ubiquitin ligase complex as a tumor suppressor in T cell leukemia. *J Exp Med*. 2007;204:1825-1835.
 145. Weng AP, Ferrando AA, Lee W, et al. Activating mutations of NOTCH1 in human T cell acute lymphoblastic leukemia. *Science*. 2004;306:269-271.
 146. Zhu YM, Zhao WL, Fu JF, et al. NOTCH1 mutations in T-cell acute lymphoblastic leukemia: prognostic significance and implication in multifactorial leukemogenesis. *Clin Cancer Res*. 2006;12:3043-3049.
 147. van Grotel M, Meijerink JP, van Wering ER, et al. Prognostic significance of molecular-cytogenetic abnormalities in pediatric T-ALL is not explained by immunophenotypic differences. *Leukemia*. 2008;22:124-131.
 148. Huh HJ, Lee SH, Yoo KH, et al. Gene mutation profiles and prognostic implications in Korean patients with T-lymphoblastic leukemia. *Ann Hematol*. 2013;92:635-644.
 149. Jenkinson S, Koo K, Mansour MR, et al. Impact of NOTCH1/FBXW7 mutations on outcome in pediatric T-cell acute lymphoblastic leukemia patients treated on the MRC UKALL 2003 trial. *Leukemia*;27:41-47.
 150. Gallo Llorente L, Luther H, Schneppenheim R, et al. Identification of novel NOTCH1 mutations: Increasing our knowledge of the NOTCH signaling pathway. *Pediatr Blood Cancer*;61:788-796.
 151. Fogelstrand L, Staffas A, Wasslavik C, et al. Prognostic implications of mutations in NOTCH1 and

- FBXW7 in childhood T-ALL treated according to the NOPHO ALL-1992 and ALL-2000 protocols. *Pediatr Blood Cancer*;61:424-430.
152. Sulis ML, Williams O, Palomero T, et al. NOTCH1 extracellular juxtamembrane expansion mutations in T-ALL. *Blood*. 2008;112:733-740.
 153. O'Neil J, Grim J, Strack P, et al. FBW7 mutations in leukemic cells mediate NOTCH pathway activation and resistance to gamma-secretase inhibitors. *J Exp Med*. 2007;204:1813-1824.
 154. Asnafi V, Buzyn A, Le Noir S, et al. NOTCH1/FBXW7 mutation identifies a large subgroup with favorable outcome in adult T-cell acute lymphoblastic leukemia (T-ALL): a Group for Research on Adult Acute Lymphoblastic Leukemia (GRAALL) study. *Blood*. 2009;113:3918-3924.
 155. Gordon WR, Roy M, Vardar-Ulu D, et al. Structure of the Notch1-negative regulatory region: implications for normal activation and pathogenic signaling in T-ALL. *Blood*. 2009;113:4381-4390.
 156. Ellisen LW, Bird J, West DC, et al. TAN-1, the human homolog of the *Drosophila* notch gene, is broken by chromosomal translocations in T lymphoblastic neoplasms. *Cell*. 1991;66:649-661.
 157. Palomero T, Barnes KC, Real PJ, et al. CUTLL1, a novel human T-cell lymphoma cell line with t(7;9) rearrangement, aberrant NOTCH1 activation and high sensitivity to gamma-secretase inhibitors. *Leukemia*. 2006;20:1279-1287.
 158. Suzuki S, Nagel S, Schneider B, et al. A second NOTCH1 chromosome rearrangement: t(9;14)(q34.3;q11.2) in T-cell neoplasia. *Leukemia*. 2009;23:1003-1006.
 159. Jeannet R, Mastio J, Macias-Garcia A, et al. Oncogenic activation of the Notch1 gene by deletion of its promoter in Ikaros-deficient T-ALL. *Blood*. 2010;116:5443-5454.
 160. Tsuji H, Ishii-Ohba H, Ukai H, Katsube T, Ogiu T. Radiation-induced deletions in the 5' end region of Notch1 lead to the formation of truncated proteins and are involved in the development of mouse thymic lymphomas. *Carcinogenesis*. 2003;24:1257-1268.
 161. Gallo Llorente L, Luther H, Schneppenheim R, et al. Identification of novel NOTCH1 mutations: Increasing our knowledge of the NOTCH signaling pathway. *Pediatr Blood Cancer*. 2014;61:788-796.
 162. DeAngelo DJ, Stone RM, Heaney ML, et al. Phase 1 clinical results with tandutinib (MLN518), a novel FLT3 antagonist, in patients with acute myelogenous leukemia or high-risk myelodysplastic syndrome: safety, pharmacokinetics, and pharmacodynamics. *Blood*. 2006;108:3674-3681.
 163. Real PJ, Ferrando AA. NOTCH inhibition and glucocorticoid therapy in T-cell acute lymphoblastic leukemia. *Leukemia*. 2009;23:1374-1377.
 164. Koyama D, Kikuchi J, Hiraoka N, et al. Proteasome inhibitors exert cytotoxicity and increase chemosensitivity via transcriptional repression of Notch1 in T-cell acute lymphoblastic leukemia. *Leukemia*.
 165. Wu Y, Cain-Hom C, Choy L, et al. Therapeutic antibody targeting of individual Notch receptors. *Nature*. 2010;464:1052-1057.
 166. Moellering RE, Cornejo M, Davis TN, et al. Direct inhibition of the NOTCH transcription factor complex. *Nature*. 2009;462:182-188.
 167. Aste-Amezaga M, Zhang N, Lineberger JE, et al. Characterization of Notch1 antibodies that inhibit signaling of both normal and mutated Notch1 receptors. *PLoS One*;5:e9094.
 168. Vermeulen K, Van Bockstaele DR, Berneman ZN. The cell cycle: a review of regulation, deregulation and therapeutic targets in cancer. *Cell Prolif*. 2003;36:131-149.
 169. Bertin R, Acquaviva C, Mirebeau D, et al. CDKN2A, CDKN2B, and MTAP gene dosage permits precise characterization of mono- and bi-allelic 9p21 deletions in childhood acute lymphoblastic leukemia. *Genes Chromosomes Cancer*. 2003;37:44-57.
 170. Diccianni MB, Batova A, Yu J, et al. Shortened survival after relapse in T-cell acute lymphoblastic leukemia patients with p16/p15 deletions. *Leuk Res*. 1997;21:549-558.
 171. Graf Einsiedel H, Taube T, Hartmann R, et al. Deletion analysis of p16(INKa) and p15(INKb) in relapsed

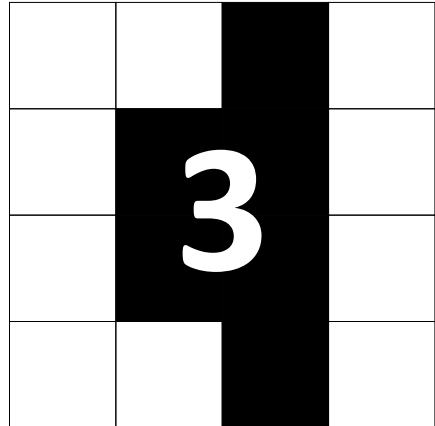
- childhood acute lymphoblastic leukemia. *Blood*. 2002;99:4629-4631.
172. Hebert J, Cayuela JM, Berkeley J, Sigaux F. Candidate tumor-suppressor genes MTS1 (p16INK4A) and MTS2 (p15INK4B) display frequent homozygous deletions in primary cells from T- but not from B-cell lineage acute lymphoblastic leukemias. *Blood*. 1994;84:4038-4044.
 173. Iolascon A, Faienza MF, Coppola B, et al. Homozygous deletions of cyclin-dependent kinase inhibitor genes, p16(INK4A) and p18, in childhood T cell lineage acute lymphoblastic leukemias. *Leukemia*. 1996;10:255-260.
 174. Irvani M, Dhat R, Price CM. Methylation of the multi tumor suppressor gene-2 (MTS2, CDKN1, p15INK4B) in childhood acute lymphoblastic leukemia. *Oncogene*. 1997;15:2609-2614.
 175. Kamb A, Gruis NA, Weaver-Feldhaus J, et al. A cell cycle regulator potentially involved in genesis of many tumor types. *Science*. 1994;264:436-440.
 176. Kees UR, Burton PR, Lu C, Baker DL. Homozygous deletion of the p16/MTS1 gene in pediatric acute lymphoblastic leukemia is associated with unfavorable clinical outcome. *Blood*. 1997;89:4161-4166.
 177. Krieger D, Moericke A, Oschlies I, et al. Frequency and clinical relevance of DNA microsatellite alterations of the CDKN2A/B, ATM and p53 gene loci: a comparison between pediatric precursor T-cell lymphoblastic lymphoma and T-cell lymphoblastic leukemia. *Haematologica*. 2010;95:158-162.
 178. Lemos JA, Defavery R, Scrideli CA, Tone LG. Analysis of p16 gene mutations and deletions in childhood acute lymphoblastic leukemias. *Sao Paulo Med J*. 2003;121:58-62.
 179. M'Soka T J, Nishioka J, Taga A, et al. Detection of methylthioadenosine phosphorylase (MTAP) and p16 gene deletion in T cell acute lymphoblastic leukemia by real-time quantitative PCR assay. *Leukemia*. 2000;14:935-940.
 180. Nakao M, Yokota S, Kaneko H, et al. Alterations of CDKN2 gene structure in childhood acute lymphoblastic leukemia: mutations of CDKN2 are observed preferentially in T lineage. *Leukemia*. 1996;10:249-254.
 181. Nobori T, Miura K, Wu DJ, et al. Deletions of the cyclin-dependent kinase-4 inhibitor gene in multiple human cancers. *Nature*. 1994;368:753-756.
 182. Ohnishi H, Kawamura M, Ida K, et al. Homozygous deletions of p16/MTS1 gene are frequent but mutations are infrequent in childhood T-cell acute lymphoblastic leukemia. *Blood*. 1995;86:1269-1275.
 183. Quesnel B, Preudhomme C, Philippe N, et al. p16 gene homozygous deletions in acute lymphoblastic leukemia. *Blood*. 1995;85:657-663.
 184. Ramakers-van Woerden NL, Pieters R, Slater RM, et al. In vitro drug resistance and prognostic impact of p16INK4A/P15INK4B deletions in childhood T-cell acute lymphoblastic leukaemia. *Br J Haematol*. 2001;112:680-690.
 185. Rubnitz JE, Behm FG, Pui CH, et al. Genetic studies of childhood acute lymphoblastic leukemia with emphasis on p16, MLL, and ETV6 gene abnormalities: results of St Jude Total Therapy Study XII. *Leukemia*. 1997;11:1201-1206.
 186. Sulong S, Moorman AV, Irving JA, et al. A comprehensive analysis of the CDKN2A gene in childhood acute lymphoblastic leukemia reveals genomic deletion, copy number neutral loss of heterozygosity, and association with specific cytogenetic subgroups. *Blood*. 2009;113:100-107.
 187. Takeuchi S, Bartram CR, Seriu T, et al. Analysis of a family of cyclin-dependent kinase inhibitors: p15/MTS2/INK4B, p16/MTS1/INK4A, and p18 genes in acute lymphoblastic leukemia of childhood. *Blood*. 1995;86:755-760.
 188. Zhou M, Gu L, Yeager AM, Findley HW. Incidence and clinical significance of CDKN2/MTS1/P16ink4A and MTS2/P15ink4B gene deletions in childhood acute lymphoblastic leukemia. *Pediatr Hematol Oncol*. 1997;14:141-150.
 189. Batova A, Diccianni MB, Yu JC, et al. Frequent and selective methylation of p15 and deletion of both

- p15 and p16 in T-cell acute lymphoblastic leukemia. *Cancer Res.* 1997;57:832-836.
190. Tsellou E, Troungos C, Moschovi M, et al. Hypermethylation of CpG islands in the promoter region of the p15INK4B gene in childhood acute leukaemia. *Eur J Cancer.* 2005;41:584-589.
 191. Komuro H, Valentine MB, Rubnitz JE, et al. p27KIP1 deletions in childhood acute lymphoblastic leukemia. *Neoplasia.* 1999;1:253-261.
 192. Markaki EA, Stiakaki E, Zafiroopoulos A, et al. Mutational analysis of the cell cycle inhibitor Kip1/p27 in childhood leukemia. *Pediatr Blood Cancer.* 2006;47:14-21.
 193. Clappier E, Cuccuini W, Cayuela JM, et al. Cyclin D2 dysregulation by chromosomal translocations to TCR loci in T-cell acute lymphoblastic leukemias. *Leukemia.* 2006;20:82-86.
 194. Karrman K, Andersson A, Bjorgvinsdottir H, et al. Dereglulation of cyclin D2 by juxtaposition with T-cell receptor alpha/delta locus in t(12;14)(p13;q11)-positive childhood T-cell acute lymphoblastic leukemia. *Eur J Haematol.* 2006;77:27-34.
 195. Hof J, Krentz S, van Schewick C, et al. Mutations and deletions of the TP53 gene predict nonresponse to treatment and poor outcome in first relapse of childhood acute lymphoblastic leukemia. *J Clin Oncol.* 2011;29:3185-3193.
 196. Liberzon E, Avigad S, Stark B, et al. Germ-line ATM gene alterations are associated with susceptibility to sporadic T-cell acute lymphoblastic leukemia in children. *Genes Chromosomes Cancer.* 2004;39:161-166.
 197. Gumy Pause F, Wacker P, Maillet P, Betts D, Sappino AP. ATM gene alterations in childhood acute lymphoblastic leukemias. *Hum Mutat.* 2003;21:554.
 198. Luo L, Lu FM, Hart S, et al. Ataxia-telangiectasia and T-cell leukemias: no evidence for somatic ATM mutation in sporadic T-ALL or for hypermethylation of the ATM-NPAT/E14 bidirectional promoter in T-PLL. *Cancer Res.* 1998;58:2293-2297.
 199. Meier M, den Boer ML, Hall AG, et al. Relation between genetic variants of the ataxia telangiectasia-mutated (ATM) gene, drug resistance, clinical outcome and predisposition to childhood T-lineage acute lymphoblastic leukaemia. *Leukemia.* 2005;19:1887-1895.
 200. Takeuchi S, Koike M, Park S, et al. The ATM gene and susceptibility to childhood T-cell acute lymphoblastic leukaemia. *British Journal of Haematology.* 1998;103:536-538.
 201. De Keersmaecker K, Graux C, Odero MD, et al. Fusion of EML1 to ABL1 in T-cell acute lymphoblastic leukemia with cryptic t(9;14)(q34;q32). *Blood.* 2005;105:4849-4852.
 202. Van Limbergen H, Beverloo HB, van Drunen E, et al. Molecular cytogenetic and clinical findings in ETV6/ABL1-positive leukemia. *Genes Chromosomes Cancer.* 2001;30:274-282.
 203. Barber KE, Martineau M, Harewood L, et al. Amplification of the ABL gene in T-cell acute lymphoblastic leukemia. *Leukemia.* 2004;18:1153-1156.
 204. Quintas-Cardama A, Tong W, Manshoury T, et al. Activity of tyrosine kinase inhibitors against human NUP214-ABL1-positive T cell malignancies. *Leukemia.* 2008;22:1117-1124.
 205. Sazawal S, Bakhshi S, Raina V, Swaroop C, Saxena R. Detection and clinical relevance of BCR-ABL fusion gene in childhood T-lineage acute lymphoblastic leukemia: a report on 4 cases. *J Pediatr Hematol Oncol.* 2009;31:850-852.
 206. Lo Nigro L, Sainati L, Mirabile E, et al. Association of cytogenetic abnormalities with detection of BCR-ABL fusion transcripts in children with T-lineage lymphoproliferative diseases (T-ALL and T-NHL). *Pediatr Blood Cancer.* 2004;42:278-280.
 207. Silva ML, Fernandez Tde S, de Souza MH, et al. M-BCR rearrangement in a case of T-cell childhood acute lymphoblastic leukemia. *Med Pediatr Oncol.* 1999;32:455-456.
 208. Tchirkov A, Bons JM, Chassagne J, et al. Molecular detection of a late-appearing BCR-ABL gene in a child with T-cell acute lymphoblastic leukemia. *Ann Hematol.* 1998;77:55-59.
 209. Pendergast AM, Quilliam LA, Cripe LD, et al. BCR-ABL-induced oncogenesis is mediated by direct

- interaction with the SH2 domain of the GRB-2 adaptor protein. *Cell*. 1993;75:175-185.
210. De Groot RP, Raaijmakers JA, Lammers JW, Jove R, Koenderman L. STAT5 activation by BCR-Abl contributes to transformation of K562 leukemia cells. *Blood*. 1999;94:1108-1112.
 211. Chakraborty S, Lin YH, Leng X, et al. Activation of Jak2 in patients with blast crisis chronic myelogenous leukemia: inhibition of Jak2 inactivates Lyn kinase. *Blood Cancer J*;3:e142.
 212. Breccia M, Alimena G. Second-Generation Tyrosine Kinase Inhibitors (Tki) as Salvage Therapy for Resistant or Intolerant Patients to Prior TKIs. *Mediterr J Hematol Infect Dis*;6:e2014003.
 213. King-Underwood L, Pritchard-Jones K. Wilms' tumor (WT1) gene mutations occur mainly in acute myeloid leukemia and may confer drug resistance. *Blood*. 1998;91:2961-2968.
 214. Van Vlierberghe P, Homminga I, Zuurbier L, et al. Cooperative genetic defects in TLX3 rearranged pediatric T-ALL. *Leukemia*. 2008;22:762-770.
 215. Tosello V, Mansour MR, Barnes K, et al. WT1 mutations in T-ALL. *Blood*. 2009;114:1038-1045.
 216. Renneville A, Kaltenbach S, Clappier E, et al. Wilms tumor 1 (WT1) gene mutations in pediatric T-cell malignancies. *Leukemia*. 2010;24:476-480.
 217. Mullighan CG, Miller CB, Radtke I, et al. BCR-ABL1 lymphoblastic leukaemia is characterized by the deletion of Ikaros. *Nature*. 2008;453:110-114.
 218. Marçais A, Jeannot R, Hernandez L, et al. Genetic inactivation of Ikaros is a rare event in human T-ALL. *Leuk Res*. 2010;34:426-429.
 219. Kuiper RP, Schoenmakers EF, van Reijmersdal SV, et al. High-resolution genomic profiling of childhood ALL reveals novel recurrent genetic lesions affecting pathways involved in lymphocyte differentiation and cell cycle progression. *Leukemia*. 2007;21:1258-1266.
 220. Maser RS, Choudhury B, Campbell PJ, et al. Chromosomally unstable mouse tumours have genomic alterations similar to diverse human cancers. *Nature*. 2007;447:966-971.
 221. Kastner P, Chan S. Role of Ikaros in T-cell acute lymphoblastic leukemia. *World J Biol Chem*. 2011;2:108-114.
 222. Simonis M, Klous P, Splinter E, et al. Nuclear organization of active and inactive chromatin domains uncovered by chromosome conformation capture-on-chip (4C). *Nat Genet*. 2006;38:1348-1354.
 223. Churchman M LJ, Payne-Turner D. High content screening identifies synthetic lethality of retinoid receptor agonist in IKZF1-mutated BCR-ABL1-positive acute lymphoblastic leukemia. *Blood*. 2013;122:172.
 224. Gutierrez A, Sanda T, Ma W, et al. Inactivation of LEF1 in T-cell acute lymphoblastic leukemia. *Blood*. 2010;115:2845-2851.
 225. Yu S, Zhou X, Steinke FC, et al. The TCF-1 and LEF-1 transcription factors have cooperative and opposing roles in T cell development and malignancy. *Immunity*;37:813-826.
 226. Van Vlierberghe P, Palomero T, Khiabani H, et al. PHF6 mutations in T-cell acute lymphoblastic leukemia. *Nat Genet*. 2010;42:338-342.
 227. Yoo NJ, Kim YR, Lee SH. Somatic mutation of PHF6 gene in T-cell acute lymphoblastic leukemia, acute myelogenous leukemia and hepatocellular carcinoma. *Acta Oncol*. 2011.
 228. Wang Q, Qiu H, Jiang H, et al. Mutation of PHF6 is associated with mutations of NOTCH1, JAK1 and rearrangement of SET-NUP214 in T-cell acute lymphoblastic leukemia. *Haematologica*. 2011.
 229. De Keersmaecker K, Atak ZK, Li N, et al. Exome sequencing identifies mutation in CNOT3 and ribosomal genes RPL5 and RPL10 in T-cell acute lymphoblastic leukemia. *Nat Genet*;45:186-190.
 230. Neumann M, Heesch S, Schlee C, et al. Whole-exome sequencing in adult ETP-ALL reveals a high rate of DNMT3A mutations. *Blood*;121:4749-4752.
 231. Grossmann V, Haferlach C, Weissmann S, et al. The molecular profile of adult T-cell acute lymphoblastic leukemia: mutations in RUNX1 and DNMT3A are associated with poor prognosis in T-ALL. *Genes Chromosomes Cancer*;52:410-422.

232. Van Vlierberghe P, Ambesi-Impiombato A, De Keersmaecker K, et al. Prognostic relevance of integrated genetic profiling in adult T-cell acute lymphoblastic leukemia. *Blood*. 2013;122:74-82.
233. Ley TJ, Ding L, Walter MJ, et al. DNMT3A mutations in acute myeloid leukemia. *N Engl J Med*;363:2424-2433.
234. Simon C, Chagraoui J, Kros J, et al. A key role for EZH2 and associated genes in mouse and human adult T-cell acute leukemia. *Genes Dev*;26:651-656.
235. Paganin M, Pigazzi M, Bresolin S, et al. DNA methyltransferase 3a hot-spot locus is not mutated in pediatric patients affected by acute myeloid or T-cell acute lymphoblastic leukemia: an Italian study. *Haematologica*. 2011;96:1886-1887.
236. Ntziachristos P, Tsirigos A, Van Vlierberghe P, et al. Genetic inactivation of the polycomb repressive complex 2 in T cell acute lymphoblastic leukemia. *Nat Med*. 2012;18:298-301.
237. Simon C, Chagraoui J, Kros J, et al. A key role for EZH2 and associated genes in mouse and human adult T-cell acute leukemia. *Genes Dev*. 2012;26:651-656.
238. Neumann M, Heesch S, Schlee C, et al. Whole-exome sequencing in adult ETP-ALL reveals a high rate of DNMT3A mutations. *Blood*. 2013;121:4749-4752.
239. Grossmann V, Haferlach C, Weissmann S, et al. The molecular profile of adult T-cell acute lymphoblastic leukemia: mutations in RUNX1 and DNMT3A are associated with poor prognosis in T-ALL. *Genes Chromosomes Cancer*. 2013;52:410-422.
240. Van Vlierberghe P, Ambesi-Impiombato A, Perez-Garcia A, et al. ETV6 mutations in early immature human T cell leukemias. *J Exp Med*. 2011;208:2571-2579.
241. Grossmann V, Kern W, Harbich S, et al. Prognostic relevance of RUNX1 mutations in T-cell acute lymphoblastic leukemia. *Haematologica*;96:1874-1877.
242. Della Gatta G, Palomero T, Perez-Garcia A, et al. Reverse engineering of TLX oncogenic transcriptional networks identifies RUNX1 as tumor suppressor in T-ALL. *Nat Med*;18:436-440.
243. Navada SC, Steinmann J, Lubbert M, Silverman LR. Clinical development of demethylating agents in hematology. *J Clin Invest*;124:40-46.
244. New M, Olzscha H, La Thangue NB. HDAC inhibitor-based therapies: can we interpret the code? *Mol Oncol*;6:637-656.
245. Villicana C, Cruz G, Zurita M. The basal transcription machinery as a target for cancer therapy. *Cancer Cell Int*;14:18.

CHAPTER



***NOTCH1* and/or *FBXW7* mutations predict for initial good prednisone response but not for improved outcome in pediatric T-cell Acute Lymphoblastic Leukemia patients treated on DCOG or COALL protocols**

Linda Zuurbier¹, Irene Homminga¹, Valerie Calvert², Mariël L. te Winkel¹, Jessica G.C.A.M. Buijs-Gladdines¹, Clarissa Kooi¹, Willem K. Smits¹, Edwin Sonneveld³, Anjo J.P. Veerman,³ Willem A. Kamps,^{3,4} Martin Horstmann^{5,6}, Emanuel F. Petricoin III^{2,7}, Rob Pieters¹, and Jules P.P. Meijerink¹

From the ¹Department of Pediatric Oncology/Hematology, Erasmus University Medical Center-Sophia Children's Hospital, Rotterdam, the Netherlands; ²Center for Applied Proteomics and Molecular Medicine, George Mason University, Manassas, VA, USA; the ³Dutch Childhood Oncology Group (DCOG), the Hague, the Netherlands; the ⁴Department of Pediatric Oncology, University of Groningen-Beatrix Children's Hospital, Groningen, the Netherlands; the ⁵German Cooperative Study Group for Childhood Acute Lymphoblastic Leukemia (COALL), Hamburg, Germany; ⁶the Research Institute Children's Cancer Center Hamburg, Clinic of Pediatric Hematology and Oncology, University Medical Center Hamburg-Eppendorf, Hamburg, Germany; ⁷NCI-FDA Clinical Proteomics Program, Food and Drug Administration, Bethesda, MD, USA.

ABSTRACT

Aberrant activation of the NOTCH1 pathway by inactivating and activating mutations in *NOTCH1* or *FBXW7* is a frequent phenomenon in T-ALL. We retrospectively investigated the relevance of *NOTCH1/FBXW7* mutations for pediatric T-ALL patients enrolled on Dutch DCOG ALL7/8 or ALL9 or the German COALL-97 protocols.

NOTCH1-activating mutations were identified in 63% of patients. *NOTCH1* mutations affected the heterodimerization, the juxtamembrane and/or the PEST domains but not the RBP-J-kappa-associated module, the ankyrin-repeats or the transactivation domain. Reverse-phase protein microarray data confirmed that *NOTCH1 and FBXW7* mutations resulted in increased intracellular NOTCH1 levels in primary T-ALL biopsies. Based on microarray expression analysis, *NOTCH1/FBXW7* mutations were associated with activation of NOTCH1 direct target genes including *HES1, DTX1, NOTCH3, PTCRA* but not *cMYC*. *NOTCH1/FBXW7* mutations were associated with *TLX3* rearrangements, but were less frequently identified in *TAL1* or *LMO2*-rearranged cases. NOTCH1-activating mutations were less frequently associated with mature T-cell developmental stage. Mutations were associated with a good initial *in vivo* prednisone response, but were not associated with a superior outcome in the DCOG and COALL cohorts.

Comparing our data with other studies, we conclude that the prognostic significance for *NOTCH1/FBXW7* mutations is not consistent and may depend on the treatment protocol given.

INTRODUCTION

T-cell acute lymphoblastic leukemia (T-ALL) accounts for approximately 10-15% of all leukemias in children. Despite improved therapy, still 30% of these cases relapse and ultimately die ^{1,2}.

Various chromosomal aberrations are known in T-ALL and some have been associated with prognosis ³⁻⁵. *NOTCH1* may be important for T-ALL pathogenesis and was initially identified as part of rare t(7;9) translocations ^{6,7}. A role for NOTCH1 is now more clear as nearly 60 percent of T-ALL cases have *NOTCH1* mutations affecting the heterodimerization (HD), the juxtamembrane domain (JM) or the proline, glutamic acid, serine, threonine rich (PEST) domains ^{8,9}. HD or JM mutations result in a ligand-independent proteolytical cleavages (reviewed in ¹⁰), resulting in the release of intracellular NOTCH1 (ICN). ICN is a transcription factor that regulates differentiation and proliferation through the activation of various target genes including *cMYC*, *HES1*, *PTCRA* ¹⁰⁻¹².

As an alternative NOTCH1 activation mechanism, inactivating mutations in the F-Box WD40 domain containing protein 7 gene (*FBXW7*) were identified in 8%-30% of T-ALL patients ¹³⁻¹⁶. *FBXW7* is part of the E3 ubiquitin ligase complex that controls the turnover of various proteins including ICN. *FBXW7* interacts with phosphodegrom domains located in the PEST domain of ICN. Therefore, inactivating mutations in *FBXW7* or loss of the phosphodegrom domains through truncating *NOTCH1* PEST mutations both result in the stabilization of ICN in the nucleus. Mutations in *FBXW7* and *NOTCH1* PEST mutations are mutually exclusive ^{13,14,16}, indicating that they seem to exert an equivalent oncogenic effect.

Mutations in *NOTCH1* or *FBXW7* may have prognostic relevance in T-ALL. Breit *et al* (2006) reported that *NOTCH1* mutant pediatric patients in the German ALL-BFM 2000 study demonstrate a good *in vivo* prednisone response and have an improved event free survival (EFS)¹⁷. In contrast, Zhu *et al* (2006) published an unfavorable outcome for *NOTCH1*-mutated adult T-ALL patients, but not for pediatric patients ¹⁸. We could not confirm a favorable prognostic effect for *NOTCH1*-mutated pediatric T-ALL patients treated on DCOG protocols ¹⁹, and this was confirmed by children treated on POG protocols for which no relation was identified between the presence of *NOTCH1* mutations and relapse ²⁰. These initial studies investigated the relevance for *NOTCH1* HD and PEST mutations ¹⁷⁻¹⁹, but did not include *NOTCH1* JM mutations or *FBXW7* mutations. We now extended our initial study by examining the prognostic effect of *NOTCH1* and *FBXW7* mutations in 141 pediatric T-ALL patients treated on Dutch DCOG or German COALL-97 protocols. The functional consequences of *NOTCH1*/*FBXW7* mutations in relation to ICN levels and activation of target genes in primary leukemia samples were investigated.

MATERIAL AND METHODS

Patient samples

This study comprised 146 primary pediatric T-ALL patients, of which 72 were treated on Dutch

Childhood Oncology Group (DCOG) protocols ALL-7/8^{21, 22} ($n=30$) or ALL-9 ($n=42$)²³. This cohort had a median follow up of 67 months, and included 51 male and 21 female patients. Because the overall disease free survival for patients treated on these DCOG protocols are comparable, these patients will be analyzed as one cohort as done before^{19,24}. Seventy of these patients were part of our previous study¹⁹. For ALL7/8 patients, *in vivo* prednisone response was monitored at day 8 following 7 days of BFM-like prednisone monotherapy and one intrathecal dose of methotrexate. A clearance to less than 1000 blasts per micro liter blood at day 8 was considered as a good initial prednisone response (GPR). Seventy-four patients were enrolled in the German Co-Operative Study Group for Childhood Acute Lymphoblastic Leukemia study (COALL-97) protocol¹⁹ with a median follow up of 52 months. This cohort included 49 male and 25 female patients. The patients' parents or legal guardians provided informed consent to use leftover diagnostic biopsies for research in accordance with the Institutional Review Board and the Declaration of Helsinki. Isolation of leukemia cells from blood or bone marrow samples has been described before²⁵ and all samples contained >90% of leukemic blasts. Clinical and immunophenotypic data were supplied by both study centers. Classification into T-cell development stages was based on EGIL criteria²⁶: pro-/pre- (CD7⁺, CD2⁺ and/or CD5⁺ and/or CD8⁺), cortical (CD1⁺) or mature T-cell stage (sCD3⁺/CD1⁻).

Genomic DNA and RNA extraction

Isolation of genomic DNA and RNA from 5×10^6 leukemic cells using the Trizol reagent (Invitrogen, Breda, The Netherlands) and copy-DNA synthesis were done as described before²⁴.

Mutational detection

NOTCH1 exons 25-34 were screened for mutations that include all relevant domains (**Table S1**). For *FBXW7*, the F-box and WD40 domains (exon 5, exons 7-11) were amplified, covering all *FBXW7* mutations as published so far. PCR reactions were done as described before¹⁹. Primers are displayed in Table 1. PCR products were sequenced using the BigDye Terminator v3.1 Cycle sequencing Kit (Applied Biosystems) on a 3130 DNA Analyzer (Applied Biosystems).

Identification of recurrent rearrangements by FISH, RQ-PCR or array-CGH

SIL-TAL, *CALM-AF10* or rearrangements of *LMO2*, *TLX1*, *TLX3*, *TAL1*, *CALM-AF10*, *SET-NUP214*, *HOXA*, or *MLL* were determined with fluorescence in-situ hybridization (FISH) as previously described^{24,27,28}. *NOTCH1* translocations were detected using bacterial artificial chromosomes (BACs) clones RP11-769N4, RP11-1008C19, RP11-83N9 and RP11-662J2 covering both sides adjacent to the *NOTCH1* locus. BACs were obtained from BAC/PAC Resource Center (Children's Hospital, Oakland, CA). Expression levels of *TLX1*, *TLX3*, *TAL1*, *LMO2* or *HOXA* or *CALM-AF10* and *SET-NUP214* fusion products were measured relative to the expression of glyceraldehyde-3-phosphate dehydrogenase (*GAPDH*) as described before^{27,28}. Array-CGH analysis was performed as previously described²⁷, on the human genome CGH Microarray 105K or 400K dual arrays (Agilent Technologies, Santa-Clara, USA), which consists of ~105,000 or ~400,000 60-mer

oligonucleotide probes that span both coding and non-coding sequences with an average spatial resolution of ~15 or 5kb, respectively. Microarray images were analyzed using feature extraction software (version 8.1, Agilent) and the data were subsequently imported into array-CGH analytics software v3.1.28 (Agilent).

Gene expression array analysis

RNA integrity testing, copy-DNA and ccRNA syntheses, hybridization and washing to Human Genome U133 plus2.0 microarrays (Affymetrix, Santa-Clara, CA, USA), extraction of probeset intensities from CEL-files and normalization with RMA or VSN methods were done as described before ²⁸. Differentially expressed genes between *NOTCH1* mutant versus wild-type T-ALL patients were determined by Wilcoxon statistics and corrected for multiple testing error ²⁹ using the Bioconductor package “Multtest” in *R*. Heatmaps based on the TOP50 most significant differentially expressed genes were performed in Dchip software ³⁰. Microarray data are available at <http://www.ncbi.nlm.nih.gov/geo/>.

Reverse-phase Protein Microarray analysis (RPMA) and western blot

Reverse-phase protein microarray construction and analysis was performed essentially as previously described ^{31,32}. To isolate proteins from 10^8 leukemic cells, lysis was performed in 20 μ L Tissue Protein Extraction Reagent (TPER, Pierce Biotechnology, Rockford, IL, USA) with 300 nM NaCl, 1 mM orthovanadate and protease inhibitors. Cells were incubated at 4°C for 20' and subsequently centrifuged at 10.000 rpm for 5' in an Eppendorf centrifuge. Supernatants were stored at -80°C prior to printing on the microarrays. Lysates were diluted to 1.0 mg/ml protein concentration and mixed 1:1 with 2x SDS Tris-glycine buffer (Invitrogen) containing 5% 2-mercaptoethanol (Sigma, Zwijndrecht, the Netherlands) (FC = 0.5 mg/ml). Lysates were spotted at a concentration of 0.5 μ g/ μ l (neat spot) and 0,125 μ g/ μ l in duplicate with 350 micron pins on glass-backed nitrocellulose coated array slides (FAST slides, Whatman plc, Kent, UK) using an Aushon Biosystems 2470 (Aushon Biosystems, Billerica, MA, USA). Printed slides were stored at -20°C or directly used. The first of each 25 slides printed were subjected to Sypro Ruby Protein Blot staining (Invitrogen) to determine total protein amount. These slides were visualized on a NovaRay CCD fluorescent scanner (Alpha Innotech. San Leandro, CA, USA). The remaining slides were used for staining with a specific antibody. Prior to this, slides were incubated with 1x Reblot (Chemicon, Temecula, CA, USA) for 15' and subsequently washed with PBS twice. This was continued with a blocking procedure for 5 hrs using 1gr I-block (Applied Biosystems) diluted in 500mL PBS with 0,5% Tween-20. Slides were stained with an automated slide stainer (Dako) according to manufacturer's instructions using the Autostainer catalyzed signal amplification (CSA) kit (Dako). In each staining run, a negative control slide was stained with the secondary antibody only for background subtraction. Briefly, endogenous biotin was blocked for 10 minutes with the biotin blocking kit (Dako), followed by application of protein block for 5 minutes; primary antibodies were diluted in antibody diluent and incubated on slides for 30 minutes and biotinylated secondary antibodies were incubated for 15 minutes. Signal amplification involved

incubation with a streptavidin-biotin-peroxidase complex provided in the CSA kit for 15 minutes, and amplification reagent (biotinyl-tyramide/hydrogen peroxide, streptavidin-peroxidase) for 15 minutes each. A signal is generated using streptavidin-conjugated IRDye680 (LI-COR Biosciences, Lincoln, NE, USA). Slides were allowed to air dry following development. Stained slides were scanned individually on the NovaRay scanner (Alpha Innotech) and files were saved in TIF format in Photoshop 7.0. All slides were subsequently analyzed with the MicroVigene v2.8.1.0 program (VigeneTech, Carlisle, MA, USA). To screen for ICN protein levels, we have used and optimized the conditions for the ICN Val1744 antiserum (Cat#2421, Cell Signaling Technology, Beverly MA, USA). Slides were scanned in a NovaRay scanner (Alpha Innotech) and analyzed with the MicroVigene v2.8.1.0 program (VigeneTech, Carlisle, MA, USA). For western blot validation²⁸, protein loading was validated by staining for Actin (Sigma, Cat#2547)

Statistics

Statistics were performed using SPSS 15.0 software. The Pearson's Chi-square test or the Fisher's exact test was used to test differences in the distribution of nominal data as indicated. Statistical significance for continuous distributed data was tested using the Mann-Whitney-U test. Differences between patient populations in event free survival (EFS) and relapse free survival (RFS) were tested by using the log-rank test. For RFS, an event is defined as relapse or non-response towards induction therapy at day 56 (COALL) or at start of consolidation therapy (DCOG). An event for EFS is defined as relapse, non-response towards induction therapy, death in remission due to toxicity or development of a secondary malignancy. Data were considered significant when $p \leq 0.05$ (two-sided).

RESULTS

***NOTCH1* and/or *FBXW7* mutations in pediatric T-ALL patients**

Bone marrow or blood DNA samples for 146 primary T-ALL patients were analyzed for *NOTCH1* (exons 25-34) and/or *FBXW7* mutations (exons 5, 7-11) and 141 samples were successfully amplified and sequenced. The locations of mutations in specific *NOTCH1* or *FBXW7* domains are shown in **Figure 1A**.

Heterozygous mutations in *NOTCH1* were detected in 79 out of 141 cases (56%) whereas 23 T-ALL patients (16%) harbored a point mutation in *FBXW7*. In total, 89 patients (63%) contained *NOTCH1* and/or *FBXW7* mutations. Thirty-five patients (39%) had a missense mutation or an in-frame insertion/deletion in the HD-domain of *NOTCH1* whereas nine (10%) and 13 (15%) patients harbored a combination of HD and PEST or *FBXW7* mutations, respectively. Seventeen patients (19%) had a single *NOTCH1* PEST mutation and ten (11%) had a single *FBXW7* mutation (**Figure 1B**). We confirmed that *NOTCH1* PEST domain mutations and *FBXW7* mutations were nearly mutual exclusive^{14,16}, but one patient carried a *FBXW7* and a *NOTCH1* PEST mutation. Five patients had a mutation in the JM domain of *NOTCH1* (5.6%) of which one also had a *NOTCH1*

HD mutation. It is not known whether these JM and HD mutations occurred in *cis* or affected different alleles.

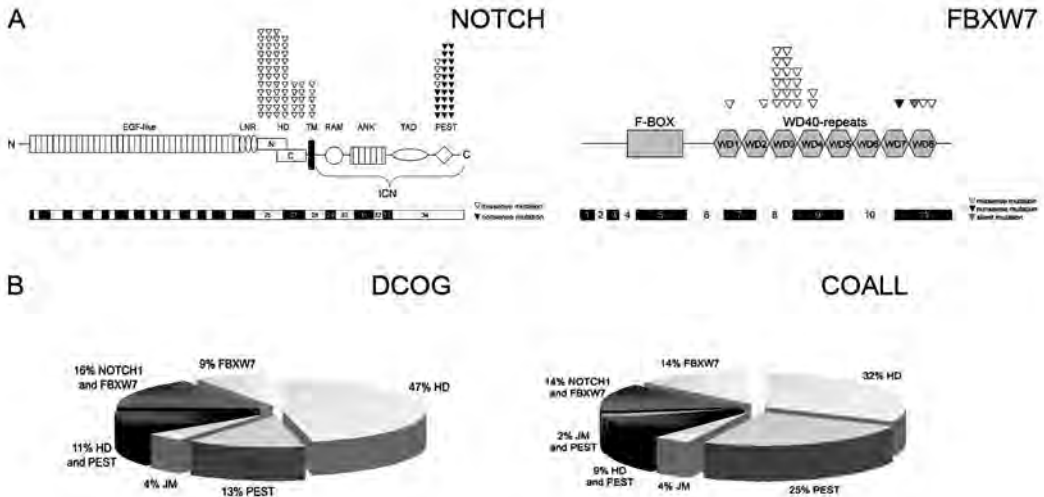


Figure 1 | NOTCH1 and FBXW7 mutations in pediatric T-ALL patients. (A) Schematic representation of identified mutations in the heterodimerization (HD), juxtamembrane (JM) and PEST domains in *NOTCH1* and in the WD40-repeats of *FBXW7*. Missense mutations are indicated by an open triangle, a silent mutation is indicated by a filled grey triangle, and nonsense mutations are indicated by a filled black triangle **(B)** The distribution of *NOTCH1* and *FBXW7* mutation types in the DCOG and COALL cohorts.

In total, 66 different *NOTCH1* mutations were found and ten HD and nine PEST mutations were not reported before to the best of our knowledge (**Figure S1**). Ten different *FBXW7* point mutations were found, five of which have not been observed before in T-ALL (**Figure S2**). These are H379L in exon 7, R465P in exon 8, and K622STOP, G687V and E693K in exon 11. The E693K mutation was previously identified in a gastric carcinoma patient ³³.

NOTCH1 and/or FBXW7 mutations activate ICN and downstream target genes in primary T-ALL samples

As published for T-ALL cell lines^{8,9,11,12,14,16}, we demonstrated by using reverse-phase protein microarrays (RPMA) that *NOTCH1* and/or *FBXW7* mutations result in enhanced levels of ICN in primary T-ALL cells. The specificity of the *NOTCH1* antibody was validated on the T-ALL cell line HPB-ALL, and ICN detection was lost upon treatment with a *g*-secretase inhibitor (**Figure 2A**). *NOTCH1* and/or *FBXW7*-mutated patients displayed about 2 fold higher ICN levels compared to wild-type patients (**Figure 2B**, $p=0.0015$). Strikingly, four wild-type patients also showed high ICN levels despite the absence of *NOTCH1* and/or *FBXW7* mutations (**Figure 2B**). Subsequent FISH and array-CGH analyses ruled out potential *NOTCH1* translocations or other chromosomal *NOTCH1* rearrangements in these four patients (data not shown).

NOTCH1/FBXW7 mutations in relation to clinical, immunophenotypic and cytogenetic parameters

We did not observe a relationship between *NOTCH1/FBXW7* mutations with gender, age or white blood cell counts (**Table 1**). For 23 patients, the *in vivo* prednisone response was known. *NOTCH1*-activated patients were correlated with a good *in vivo* prednisone response since 14 out of 16 patients with a good initial prednisone response (GPR) contained *NOTCH1* mutations, in contrast to two out of seven cases with a poor response ($p=0.01$). This observation was stronger by including *FBXW7* data where 15 out of 16 cases with a GPR had a *NOTCH1/FBXW7* mutation in contrast to only two out of seven PPR cases ($p=0.003$, **Table 1**). Classification into T-cell development stages on EGIL criteria²⁶ revealed that *NOTCH1/FBXW7* mutations were less frequently identified in mature T-ALL cases ($p=0.05$, **Table 1**). In relation to molecular cytogenetic data, *NOTCH1/FBXW7* mutations were identified in all cytogenetic T-ALL subgroups (**Table 1**). Considering *TAL1* or *LMO2* rearranged cases as a single *TAL/LMO* entity based on their identical expression profiles^{28,34}, and including an additional 19 *TALLMO*-like patients with a *TAL/LMO* signature that lack *TAL1* or *LMO2* rearrangements²⁸, *NOTCH1* mutations were less frequent. Only 25 out of 60 *TALLMO* patients (42%) had a *NOTCH1* mutation ($p=0.002$, **Table 1**). This remained significant when including *FBXW7* mutations since only 30 out of 60 cases (50%) had a *NOTCH1/FBXW7* mutation ($p=0.004$). *NOTCH1* mutations were more prevalent in *TLX3*-rearranged cases, in which 21 out of 27 cases (86%) had a *NOTCH1* mutation ($p=0.02$). This remained significant when taking *FBXW7* mutations into account ($p=0.01$).

Clinical	comparison	NOTCH1 mutation			FBXW7 mutation			NOTCH1/FBXW7 mutations		
		WT n(%)	Mut n(%)	p-value	WT n(%)	Mut n(%)	p-value	WT n(%)	Mut n(%)	p-value
Gender	Male-Female distribution			1.0			0.81			1
	Male	42 (43%)	55 (57%)		81 (84%)	16 (16%)		35 (36%)	62 (64%)	
	Female	19 (43%)	25 (57%)		36 (82%)	8 (18%)		16 (36%)	28 (64%)	
	Age (years)	7.2	7.8	0.30*	7.5	8.2	0.29*	7	7.8	0.09*
	WBC (x10e9 cells/liter)	131	119	0.69*	126	109	0.28*	134	110	0.41*
	<i>In vivo</i> prednisone response	PGR or PPR			0.01			NE		
	PGR	2	14					1	15	
	PPR	5	2					5	2	
Immunophenotypic										
Pre-T/Pro-T	Pre-T/Pro-T vs other	16 (41%)	23 (59%)	0.81	34 (87%)	5 (13%)	0.42#	13 (33%)	26 (67%)	0.68
Cortical T	Cortical T vs other	21 (36%)	37 (64%)	0.19	47 (81%)	11 (19%)	0.58	16 (28%)	42 (72%)	0.08
Mature T	Mature T vs other	21 (54%)	18 (46%)	0.18	32 (83%)	7 (17%)	0.89	20 (51%)	19 (49%)	0.05
Cytogenetics										
<i>TAL1</i>	<i>TAL1+</i> vs <i>TAL1-</i>	13 (50%)	13 (50%)	0.51	23 (88%)	3 (12%)	0.57#	13 (50%)	13 (50%)	0.12
<i>LMO2</i>	<i>LMO2+</i> vs <i>LMO2-</i>	7 (50%)	7 (50%)	0.78	11 (79%)	3 (21%)	0.71#	5 (36%)	9 (64%)	1#
<i>TALLMO</i>	<i>TAL/LMO+</i> vs <i>TAL/LMO-</i>	35 (58%)	25 (42%)	0.002	51 (85%)	9 (15%)	0.66	30 (50%)	30 (50%)	0.004
<i>TLX3</i>	<i>TLX3+</i> vs <i>TLX3-</i>	6 (22%)	21 (78%)	0.02	19 (70%)	8 (30%)	0.08	4 (15%)	23 (85%)	0.01#
<i>TLX1</i>	<i>TLX1+</i> vs <i>TLX1-</i>	3 (43%)	4 (57%)	1#	7 (100%)	0 (0%)	0.60#	3 (43%)	4 (57%)	0.70#
<i>HOXA</i>	<i>HOXA+</i> vs <i>HOXA-</i>	4 (31%)	9 (69%)	0.39#	10 (77%)	3 (23%)	0.46#	3 (23%)	10 (77%)	0.38#
others	others vs cytogenetic annotated	13 (39%)	20 (61%)	0.69	29 (88%)	4 (12%)	0.60#	11 (33%)	22 (67%)	0.84

Table 1 | Distribution of wild-type and NOTCH1 mutations within categorized subgroups of T-ALL patients. Abbreviations: Mut, mutant; PGR, prednisone good response; PPR, prednisone poor response; NE, not evaluable; T-ALL, T-cell acute lymphoblastic leukemia; WBC, white blood cell count; WT, wild-type. Only significant P-values are indicated in bold. #P-values calculated by the Fisher’s exact method; *P-values calculated by the Mann–Whitney-U method.

Prognostic relevance of NOTCH1 and/or FBXW7 mutations

We then investigated the relevance of *NOTCH1* and/or *FBXW7* mutations in relation to treatment outcome. For the DCOG cohort, mutations in *NOTCH1* and/or *FBXW7* trended towards poor treatment outcome. The 5 years event free survival (5 yrs EFS) rates for patients with *NOTCH1* mutations only compared to wild-type patients were 57±8% versus 76±8% ($p=0.08$) for the

DCOG cohort but $63\pm 8\%$ versus $64\pm 10\%$ for the COALL cohort ($p=0.99$, **Figure 3A,B**). Inclusion of *FBXW7* mutations resulted in 5 yrs EFS rates of $58\pm 7\%$ versus $74\pm 9\%$ ($p=0.16$) for the DCOG cohort and $63\pm 8\%$ versus $68\pm 10\%$ for the COALL cohort ($p=0.90$, not shown).

Events in both cohorts are summarized in **Table 2**. *NOTCH1* mutations trended towards a lower relapse free survival (RFS) in the DCOG ($p=0.068$) and COALL cohorts ($p=0.094$) with 5 years RFS of 83 ± 7 versus 62 ± 8 percent for the DCOG cohort and 89 ± 6 versus 67 ± 8 percent for the COALL cohort for wild-type and *NOTCH1*-mutated patients, respectively (**Figure 3C,D**). These trends became less evident when including *FBXW7* mutation data, with a RFS of 82 ± 8 versus 62 ± 8 percent in the DCOG cohort ($p=0.101$) and a RFS of 86 ± 7 versus 70 ± 8 percent in the COALL cohort ($p=0.23$) for wild-type or *NOTCH1*-activated patients, respectively (not shown).

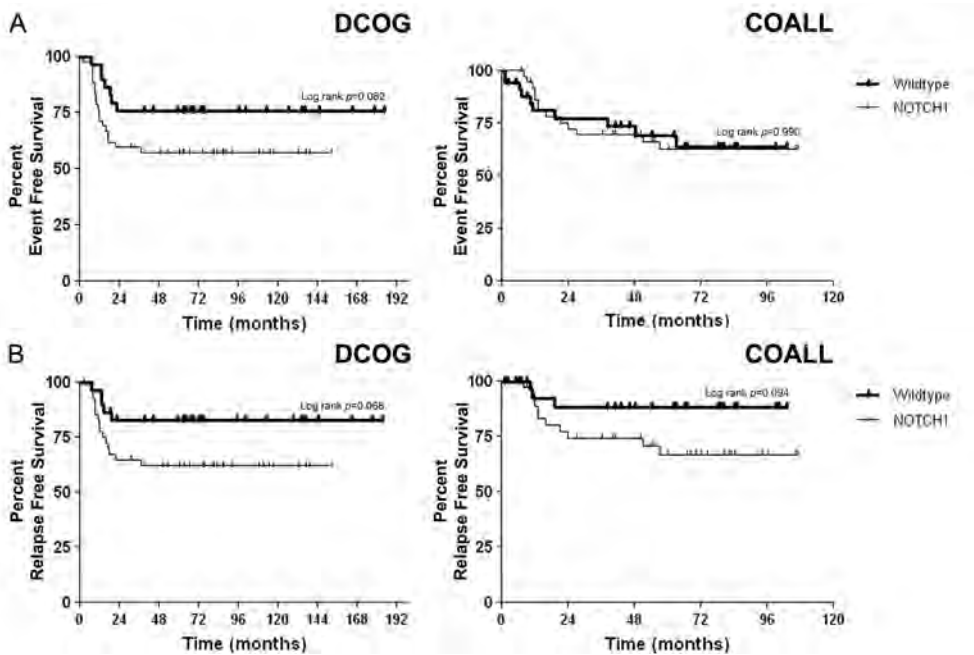


Figure 3 | NOTCH1-activating mutations have no prognostic implication in pediatric T-ALL. Event Free Survival (EFS) (**A,B**) and Relapse Free Survival (RFS) (**C,D**) for the pediatric T-ALL patients treated on DCOG protocols (**A,C**) or the COALL protocol (**B, D**). Patients carrying *NOTCH1* and/or *FBXW7* mutations and wild-type patients have been indicated.

	DCOG		COALL	
	WT	Mut	WT	Mut
	<i>n</i> =29	<i>n</i> =42	<i>n</i> =35	<i>n</i> =39
events	7	18	10	13
relapse ^a	5	15	3	11
CNS relapse	2	2	1	4
Toxic death	1	2	5	3
second malignancy	1	1	2	1

Table 2 | Events in DCOG and COALL cohorts. Abbreviations: CNS, central nervous system; DCOG, Dutch Childhood Oncology Group; COALL, Childhood Acute Lymphoblastic Leukemia study; Mut, mutant for *NOTCH1*; WT, wild-type.

^aIncludes CNS relapse.

We also investigated the effect for specific *NOTCH1* and/or *FBXW7* mutations on the activation of downstream target genes and outcome. As published by the group of Pear and co-workers, specific *NOTCH1* mutations or combinations of *NOTCH1*/*FBXW7* mutations may have strong NOTCH1-activating effects whereas others may only have modest activating effects³⁵. For this, we distinguished weak NOTCH1-activating mutations, i.e. *NOTCH1* HD or PEST mutations or *FBXW7* mutations, and strong NOTCH1-activating mutations, i.e. *NOTCH1* JM mutations or combinations of *NOTCH1* HD mutations with PEST mutations or *FBXW7* mutations. Although ICN protein levels were significantly higher for *NOTCH1* and/or *FBXW7* mutated cases versus wild-type cases, there was relation to the types of NOTCH1-activating mutations investigated (**Figure S3**). To investigate differential activation of downstream target genes between patients with weak or strong NOTCH1-activating mutations, we first calculated the most significantly and differently expressed genes (probesets) between patients with strong NOTCH1-activating mutations versus wild-type patients, which again revealed mostly bonafide NOTCH1 target genes. However, these genes were expressed at intermediate levels for patients having weak NOTCH1-activating mutations (**Figure S4**) indicating that these types of mutations indeed differ in their potential to activate downstream target genes in primary leukemic samples. Distinction between these types of mutations may also have prognostic significance as patients from the DCOG cohort with strong NOTCH1-activating mutations had a significant poor outcome relative to wild-type patients ($p=0.012$) as well as to patients carrying weak NOTCH1-activating mutations ($p=0.048$) (**Figure S5A**). However, this observation could not be substantiated for COALL-97 T-ALL patients (**Figure S5B**). We also investigated whether ICN protein levels itself had prognostic significance. As 55 out of 66 patients for which ICN protein levels were available were treated on the COALL cohort, we divided these patients into quartiles and determined their RFS and EFS rates. However, no relationship between ICN protein levels and RFS nor EFS was present ($p=0.98$ and $p=0.97$, respectively).

DISCUSSION

Activation of NOTCH1 as a consequence of activating *NOTCH1* mutations or inactivating *FBXW7* mutations is a frequent phenomenon in T-ALL⁸. We screened for *NOTCH1* and *FBXW7* mutations in 141 pediatric T-ALL patient samples and identified *NOTCH1* mutations in 56% and *FBXW7* mutations in 16% of the patients. In total, 63 percent of the patients had an aberrantly activated NOTCH1 pathway due to mutations. In line with previous studies^{14,16}, we observed that *NOTCH1* PEST domain mutations and *FBXW7* mutations occurred in a mutually exclusive fashion with the exception of one patient. This patient had a nonsense mutation in *FBXW7* in contrast to missense mutations that are normally observed in *FBXW7* mutated patients. This implies that mutant *FBXW7* but not truncated *FBXW7* proteins exert a dominant negative effect in the E3-ubiquitin ligase complex. Interestingly, Park *et al* (2009) also discovered a nonsense mutation due to a 5 bp insertion in *FBXW7* in combination with a *NOTCH1* PEST mutation in a non-Hodgkin's lymphoma

patient¹⁵.

The frequency of NOTCH1-activating mutations is in line with other studies also comprising adult T-ALL patient series^{36,37}. In adult studies, *NOTCH1* and *FBXW7* mutations were identified in 60-62% and 18-24% of the T-ALL patients, respectively. This indicates that the oncogenic role for *NOTCH1/FBXW7* during T-cell oncogenesis remains conserved over age. We did not find evidence for mutations outside the *NOTCH1* HD, JM and PEST-domains in any of the 141 pediatric T-ALL patients indicating that reported mutations in the LNR region, the RAM-, ANK-, and TAD-domains are very rare^{18,36,38}.

We found that *NOTCH1* and *FBXW7* mutations resulted in increased levels of cleaved NOTCH1 (ICN) in primary leukemia cells and was associated with the activation of NOTCH1 target genes¹⁰⁻¹², including *HES1*, *HES4*, *DTX1*, *PTCRA*, *NOTCH3*, *PTPRC*, *CR2*, *LZTFL1*, *TASP1* and *RHOA*. This confirms that the mutations manifest functionally at the protein level in patient samples. We identified ten patients that lacked *NOTCH1* and/or *FBXW7* mutations that either expressed high levels of ICN or that expressed NOTCH1 target genes. As we did not find chromosomal translocations or other types of rearrangements involving the *NOTCH1* locus, this implies that additional mutation mechanisms in *NOTCH1* or directly downstream regulatory genes must exist, that so far been left unnoticed in T-ALL. Although *cMYC* was identified as a prominent NOTCH1 target in T-ALL cell lines^{11,12}, it was not identified as target gene in primary samples. However, two cases expressed ectopic *cMYC* levels due to a t(8;14)(q24;q11) translocation which were both wild-type for *NOTCH1* and *FBXW7*, supporting a role for *MYC* as NOTCH1 target. Further research will be required to establish whether *cMYC* is generally upregulated by means of other oncogenic mechanisms in addition to activated *NOTCH1* in primary samples and therefore left undetected, or that the expression of *cMYC* is rapidly lost upon isolation of primary leukemic cells.

NOTCH1/FBXW7 mutations were identified at a lower frequency in T-ALL cases with a mature immunophenotype. This may explain the low incidence of *NOTCH1/FBXW7* mutations in the *TAL/LMO* subgroup because *TAL1* rearrangements, which are the most recurrent abnormality in this subgroup, are associated with a mature T-cell development arrest^{24,39}. This is an interesting finding and suggests that the oncogenic role of *NOTCH1* is less prominent in T-ALL cases arrested at a relative mature T-cell developmental stage. Interestingly, *NOTCH1/FBXW7* mutations were identified at a higher frequency in *TLX3*-rearranged T-ALL. The oncogenic activation of NOTCH1 thus far has been regarded as one of the earliest acquired abnormalities in a pre-leukemic progenitor cell that therefore becomes committed to the T-ALL^{10,40}. In this perspective, our data indicate that the importance of deregulated NOTCH1 as initiating event during T-cell oncogenesis depends on additional collaborating events like *TLX3* or *TAL1* rearrangements. It also suggests that the oncogenic program that is followed by T-ALL cases that eventually arrest at the mature development stage may be less dependent on NOTCH1. Whether NOTCH1-activating mutations represent truly initiating leukemic events or not needs to be established, as evidence is emerging that NOTCH1 activation in some T-ALL cases may have occurred as a secondary event which may be acquired or lost at relapse⁴¹.

In the study of Breit *et al* (2006), *NOTCH1* mutations were associated with a good initial prednisone response and a significantly lower minimal residual disease (MRD) content at day 78¹⁷. Our study supports this association with initial prednisone response for *NOTCH1/FBXW7* mutant patients. This association is also validated for patients of the EORTC-CLG study. In that study, *NOTCH1*-activating mutations were also associated with reduced minimal residual disease during therapy⁴². The association for *NOTCH1*-activating mutations with initial good prednisone response seems to be in contrast with the finding that gamma-secretase inhibitors (GSIs) can sensitize for glucocorticoids in glucocorticoid resistant cells⁴³. It may be that the *NOTCH* pathway has opposing effects in the glucocorticoid response in responsive versus resistance patients, but it now seems clear that activation of *NOTCH1* by mutations does not drive glucocorticoid resistance. Further research will be required to clarify this seeming contradiction.

NOTCH1 mutations are not associated with a superior outcome for patients treated on the BFM-like DCOG protocols or the COALL-97 protocol. The survival of *NOTCH1*-activated patients was actually lower than for wild-type patients. Separating patients carrying strong *NOTCH1*-activating mutations from those with weak *NOTCH1*-activating mutations³⁵ or patients that were wild-type, demonstrated a significant poor outcome for patients having strong *NOTCH1*-activating mutations in the DCOG cohort. This could not be reproduced for T-ALL patients treated on the German COALL-97 protocol. In the accompanying paper of Clappier and coworkers, *NOTCH1*-activating mutations did not predict improved outcome for patients treated on the BFM-derived EORTC-CLG protocols either⁴². These observations are in contrast to the findings by the BFM study group¹⁷. In the accompanying paper of Kox *et al* (2009), this finding is now validated in an extended series comprising 301 pediatric T-ALL patients treated on the ALL-BFM 2000 protocol⁴⁴. A favorable prognostic effect of *NOTCH1* and/or *FBXW7* mutations was also identified in a recent study by Park *et al* (2009), although the overall incidence of identified *NOTCH1* mutations was only 31%¹⁵. No favorable outcome of *NOTCH1* and/or *FBXW7*-mutated cases has been observed for adult T-ALL patients treated on GMALL 05/93 and 06/99 multicenter protocols⁴⁵, nor for patients treated on the MRC UKALLXII/ECOG E2993³⁷ or LALA-94³⁶ protocols. A significant association with improved outcome for *NOTCH1*-activating mutations has only been observed for adult T-ALL patients treated on the GRAALL-2003 multicenter protocol³⁶. These results indicate that the prognostic effect of *NOTCH1/FBXW7* mutations may strongly depend on the treatment protocol given.

Compared to the ALL-BFM-2000 protocol, the DCOG ALL-7/8 protocol in general showed an inferior outcome²². Although both protocols are highly related, part of the patients treated on the DCOG ALL-7/8 cohort received less chemotherapy and none of them received prophylactic cranial irradiation, except for patients with initial central-nervous system involvement. *NOTCH1*-activating mutations may provoke CNS relapse due to the activation of the *CCR7* chemokine⁴⁶. This study therefore predicts that *NOTCH1*-activating mutations would result in increased risk for CNS relapse via the *CCL19-CCR7* axis in the absence of cranial irradiation. However the numbers of CNS relapses in our cohorts were too low to substantiate this notion. Besides, neither the *CCR7* gene nor its ligand *CCL19* were identified as significantly differentially expressed

genes that were activated in *NOTCH1/FBXW7*-mutated T-ALL patients based on our microarray expression dataset (data not shown). As our patient biopsies were all obtained from peripheral blood or bone marrow samples, we cannot exclude that these genes are only upregulated in malignant blasts in the context of a neuronal environment. Cranial radiation may contribute to the differences in prognostic value for NOTCH1-activating mutations between the DCOG and ALL-BFM-2000 cohorts, but this does not apply for the COALL-97 cohort that includes cranial irradiation. Therefore, other differences among treatment protocols seem important.

In conclusion, *NOTCH1/FBXW7* mutations that activate the NOTCH1 pathway are identified in more than 60 percent of pediatric T-ALL patients and result in elevated ICN levels and activation of NOTCH1 target genes. Mutations were more often found in association with *TLX3*-rearranged T-ALL, but were less frequently identified in *TAL/LMO* T-ALL patients and T-ALL patients with a mature T-cell phenotype. *NOTCH1/FBXW7* mutations predict for an initial good prednisone response, which does not translate into a superior outcome of T-ALL on DCOG ALL-7/8, ALL-9 or COALL-97 protocols.

AUTHORSHIPS AND DISCLOSURES

L.Z. designed experiments, performed research and wrote manuscript, I.H. performed research and wrote manuscript, V.C. performed RPMA analysis, M.L.W. performed research, J.B.-G. performed *NOTCH1* and *FBXW7* mutation analysis, C.K. performed western blot analysis, W.S. prepared samples for RPMA analysis, E.S., A.J.P.V, W.K. and M.H. provided patient samples and clinical and immunophenotypic data, E.P. supervised study, and wrote manuscript, R.P. designed and supervised study and wrote manuscript, J.P.P.M. was principal investigator, designed and supervised the study, and wrote manuscript.

ACKNOWLEDGEMENTS

L.Z. and W.K.S. are financed by the Stichting Kinderen Kankervrij (KiKa; Grant no. KiKa 2007-012). I.H. is financed by the Dutch Cancer Society Dutch Cancer Society (KWF-EMCR 2006-3500) C.K. is financed by KiKa (Grant no. KiKa 2008-029). We also would like to thank the German Jose Carreras Leukemia Foundation (Grant no. SP 04/03 to M.H.).

REFERENCES

1. Pieters R, Carroll WL. Biology and treatment of acute lymphoblastic leukemia. *Pediatr Clin North Am*. 2008;55:1-20, ix.
2. Pui CH, Evans WE. Treatment of acute lymphoblastic leukemia. *N Engl J Med*. 2006;354:166-178.
3. Cave H, Suciu S, Preudhomme C, et al. Clinical significance of HOX11L2 expression linked to t(5;14) (q35;q32), of HOX11 expression, and of SIL-TAL fusion in childhood T-cell malignancies: results of EORTC studies 58881 and 58951. *Blood*. 2004;103:442-450.
4. Meijerink JP, den Boer ML, Pieters R. New genetic abnormalities and treatment response in acute lymphoblastic leukemia. *Semin Hematol*. 2009;46:16-23.
5. Van Vlierberghe P, Pieters R, Beverloo HB, Meijerink JP. Molecular-genetic insights in paediatric T-cell acute lymphoblastic leukaemia. *Br J Haematol*. 2008;143:153-168.
6. Ellisen LW, Bird J, West DC, et al. TAN-1, the human homolog of the Drosophila notch gene, is broken by chromosomal translocations in T lymphoblastic neoplasms. *Cell*. 1991;66:649-661.
7. Suzuki S, Nagel S, Schneider B, et al. A second NOTCH1 chromosome rearrangement: t(9;14) (q34.3;q11.2) in T-cell neoplasia. *Leukemia*. 2009;23:1003-1006.
8. Weng AP, Ferrando AA, Lee W, et al. Activating mutations of NOTCH1 in human T cell acute lymphoblastic leukemia. *Science*. 2004;306:269-271.
9. Sulis ML, Williams O, Palomero T, et al. NOTCH1 extracellular juxtamembrane expansion mutations in T-ALL. *Blood*. 2008;112:733-740.
10. Grabher C, von Boehmer H, Look AT. Notch 1 activation in the molecular pathogenesis of T-cell acute lymphoblastic leukaemia. *Nat Rev Cancer*. 2006;6:347-359.
11. Palomero T, Lim WK, Odom DT, et al. NOTCH1 directly regulates c-MYC and activates a feed-forward-loop transcriptional network promoting leukemic cell growth. *Proc Natl Acad Sci U S A*. 2006;103:18261-18266.
12. Weng AP, Millholland JM, Yashiro-Ohtani Y, et al. c-Myc is an important direct target of Notch1 in T-cell acute lymphoblastic leukemia/lymphoma. *Genes Dev*. 2006;20:2096-2109.
13. Malyukova A, Dohda T, von der Lehr N, et al. The tumor suppressor gene hCDC4 is frequently mutated in human T-cell acute lymphoblastic leukemia with functional consequences for Notch signaling. *Cancer Res*. 2007;67:5611-5616.
14. O'Neil J, Grim J, Strack P, et al. FBW7 mutations in leukemic cells mediate NOTCH pathway activation and resistance to gamma-secretase inhibitors. *J Exp Med*. 2007;204:1813-1824.
15. Park MJ, Taki T, Oda M, et al. FBXW7 and NOTCH1 mutations in childhood T cell acute lymphoblastic leukaemia and T cell non-Hodgkin lymphoma. *Br J Haematol*. 2009;145:198-206.
16. Thompson BJ, Buonamici S, Sulis ML, et al. The SCFFBW7 ubiquitin ligase complex as a tumor suppressor in T cell leukemia. *J Exp Med*. 2007;204:1825-1835.
17. Breit S, Stanulla M, Flohr T, et al. Activating NOTCH1 mutations predict favorable early treatment response and long-term outcome in childhood precursor T-cell lymphoblastic leukemia. *Blood*. 2006;108:1151-1157.
18. Zhu YM, Zhao WL, Fu JF, et al. NOTCH1 mutations in T-cell acute lymphoblastic leukemia: prognostic significance and implication in multifactorial leukemogenesis. *Clin Cancer Res*. 2006;12:3043-3049.
19. van Grotel M, Meijerink JP, van Wering ER, et al. Prognostic significance of molecular-cytogenetic abnormalities in pediatric T-ALL is not explained by immunophenotypic differences. *Leukemia*. 2008;22:124-131.
20. Larson Gedman A, Chen Q, Kugel Desmoulin S, et al. The impact of NOTCH1, FBW7 and PTEN mutations on prognosis and downstream signaling in pediatric T-cell acute lymphoblastic leukemia: a report from

- the Children's Oncology Group. *Leukemia*. 2009;23:1417-1425.
21. Kamps WA, Bokkerink JP, Hahlen K, et al. Intensive treatment of children with acute lymphoblastic leukemia according to ALL-BFM-86 without cranial radiotherapy: results of Dutch Childhood Leukemia Study Group Protocol ALL-7 (1988-1991). *Blood*. 1999;94:1226-1236.
 22. Kamps WA, Bokkerink JP, Hakvoort-Cammel FG, et al. BFM-oriented treatment for children with acute lymphoblastic leukemia without cranial irradiation and treatment reduction for standard risk patients: results of DCLSG protocol ALL-8 (1991-1996). *Leukemia*. 2002;16:1099-1111.
 23. Veerman AJ, Kamps WA, van den Berg H, et al. Dexamethasone-based therapy for childhood acute lymphoblastic leukaemia: results of the prospective Dutch Childhood Oncology Group (DCOG) protocol ALL-9 (1997-2004). *Lancet Oncol*. 2009;10:957-966.
 24. van Grotel M, Meijerink JP, Beverloo HB, et al. The outcome of molecular-cytogenetic subgroups in pediatric T-cell acute lymphoblastic leukemia: a retrospective study of patients treated according to DCOG or COALL protocols. *Haematologica*. 2006;91:1212-1221.
 25. Stam RW, den Boer ML, Meijerink JP, et al. Differential mRNA expression of Ara-C-metabolizing enzymes explains Ara-C sensitivity in MLL gene-rearranged infant acute lymphoblastic leukemia. *Blood*. 2003;101:1270-1276.
 26. Bene MC, Castoldi G, Knapp W, et al. Proposals for the immunological classification of acute leukemias. European Group for the Immunological Characterization of Leukemias (EGIL). *Leukemia*. 1995;9:1783-1786.
 27. Van Vlierberghe P, van Grotel M, Beverloo HB, et al. The cryptic chromosomal deletion del(11)(p12p13) as a new activation mechanism of LMO2 in pediatric T-cell acute lymphoblastic leukemia. *Blood*. 2006;108:3520-3529.
 28. Van Vlierberghe P, van Grotel M, Tchinda J, et al. The recurrent SET-NUP214 fusion as a new HOXA activation mechanism in pediatric T-cell acute lymphoblastic leukemia. *Blood*. 2008;111:4668-4680.
 29. Hochberg Y, Benjamini Y. More powerful procedures for multiple significance testing. *Stat Med*. 1990;9:811-818.
 30. Li C, Wong WH. Model-based analysis of oligonucleotide arrays: expression index computation and outlier detection. *Proc Natl Acad Sci U S A*. 2001;98:31-36.
 31. Paweletz CP, Charboneau L, Bichsel VE, et al. Reverse phase protein microarrays which capture disease progression show activation of pro-survival pathways at the cancer invasion front. *Oncogene*. 2001;20:1981-1989.
 32. Petricoin EF, 3rd, Espina V, Araujo RP, et al. Phosphoprotein pathway mapping: Akt/mammalian target of rapamycin activation is negatively associated with childhood rhabdomyosarcoma survival. *Cancer Res*. 2007;67:3431-3440.
 33. Lee JW, Soung YH, Kim HJ, et al. Mutational analysis of the hCDC4 gene in gastric carcinomas. *Eur J Cancer*. 2006;42:2369-2373.
 34. Homminga I, Jager AW, De Laat W, et al. NKX2-1 and MEF2C oncogenes delineate novel subtypes in T-Cell Acute Lymphoblastic Leukemia. 2010:submitted.
 35. Chiang MY, Xu L, Shestova O, et al. Leukemia-associated NOTCH1 alleles are weak tumor initiators but accelerate K-ras-initiated leukemia. *J Clin Invest*. 2008;118:3181-3194.
 36. Asnafi V, Buzyn A, Le Noir S, et al. NOTCH1/FBXW7 mutation identifies a large subgroup with favorable outcome in adult T-cell acute lymphoblastic leukemia (T-ALL): a Group for Research on Adult Acute Lymphoblastic Leukemia (GRAALL) study. *Blood*. 2009;113:3918-3924.
 37. Mansour MR, Sulis ML, Duke V, et al. Prognostic implications of NOTCH1 and FBXW7 mutations in adults with T-cell acute lymphoblastic leukemia treated on the MRC UKALLXII/ECOG E2993 protocol. *J Clin Oncol*. 2009;27:4352-4356.
 38. Gordon WR, Roy M, Vardar-Ulu D, et al. Structure of the Notch1-negative regulatory region:

- implications for normal activation and pathogenic signaling in T-ALL. *Blood*. 2009;113:4381-4390.
39. Asnafi V, Radford-Weiss I, Dastugue N, et al. CALM-AF10 is a common fusion transcript in T-ALL and is specific to the TCRgammadelta lineage. *Blood*. 2003;102:1000-1006.
 40. Eguchi-Ishimae M, Eguchi M, Kempski H, Greaves M. NOTCH1 mutation can be an early, prenatal genetic event in T-ALL. *Blood*. 2008;111:376-378.
 41. Mansour MR, Duke V, Feroni L, et al. Notch-1 mutations are secondary events in some patients with T-cell acute lymphoblastic leukemia. *Clin Cancer Res*. 2007;13:6964-6969.
 42. Clappier E, Collette S, Grardel N, et al. Prognostic significance of NOTCH1 and FBXW7 mutations in childhood T-cell acute leukemia: results from the EORTC Children Leukemia Group. Submitted to *Leukemia*. 2010.
 43. Real PJ, Tosello V, Palomero T, et al. Gamma-secretase inhibitors reverse glucocorticoid resistance in T cell acute lymphoblastic leukemia. *Nat Med*. 2009;15:50-58.
 44. Kox C, Zimmermann M, Stanulla M, et al. The favorable effect of activating *NOTCH1* receptor mutations on long-term outcome in T-ALL can be separated from NOTCH pathway activation by *FBXW7* loss of function. Submitted to *Leukemia*. 2010.
 45. Baldus CD, Thibaut J, Goekbuget N, et al. Prognostic implications of NOTCH1 and FBXW7 mutations in adult acute T-lymphoblastic leukemia. *Haematologica*. 2009;94:1383-1390.
 46. Buonamici S, Trimarchi T, Ruocco MG, et al. CCR7 signalling as an essential regulator of CNS infiltration in T-cell leukaemia. *Nature*. 2009;459:1000-1004.

WD40-repeats



Known *FBXW7* mutations as previous identified in the studies of Thompson *et al* (2007)[1], O'Neil *et al* (2007)[2], Malyukova *et al* (2007)[3], Park *et al* (2009)[4], Asnafi *et al* (2009)[5], Larson *et al* (2009)[6] and Mansour *et al* (2009)[7].

References

1. Thompson, B.J., et al., *The SCFFBW7 ubiquitin ligase complex as a tumor suppressor in T cell leukemia*. J Exp Med, 2007. **204**(8): p. 1825-35.
2. O'Neil, J., et al., *FBW7 mutations in leukemic cells mediate NOTCH pathway activation and resistance to gamma-secretase inhibitors*. J Exp Med, 2007. **204**(8): p. 1813-24.
3. Malyukova, A., et al., *The tumor suppressor gene hCDC4 is frequently mutated in human T-cell acute lymphoblastic leukemia with functional consequences for Notch signaling*. Cancer Res, 2007. **67**(12): p. 5611-6.
4. Park, M.J., et al., *FBXW7 and NOTCH1 mutations in childhood T cell acute lymphoblastic leukaemia and T cell non-Hodgkin lymphoma*. Br J Haematol, 2009. **145**(2): p. 198-206.
5. Asnafi, V., et al., *NOTCH1/FBXW7 mutation identifies a large subgroup with favorable outcome in adult T-cell acute lymphoblastic leukemia (T-ALL): a Group for Research on Adult Acute Lymphoblastic Leukemia (GRAALL) study*. Blood, 2009. **113**(17): p. 3918-24.
6. Larson Gedman, A., et al., *The impact of NOTCH1, FBW7 and PTEN mutations on prognosis and downstream signaling in pediatric T-cell acute lymphoblastic leukemia: a report from the Children's Oncology Group*. Leukemia, 2009. **23**(8): p. 1417-25.
7. Mansour, M.R., et al., *Prognostic implications of NOTCH1 and FBXW7 mutations in adults with T-cell acute lymphoblastic leukemia treated on the MRC UKALLXII/ECOG E2993 protocol*. J Clin Oncol, 2009. **27**(26): p. 4352-6.

Figure S2 | *FBXW7* mutations in pediatric T-ALL patients. Amino acid changes in the WD40-repeats, as a result of *FBXW7* mutations, are listed for each patient. New mutations and the reference of each known mutation are indicated.

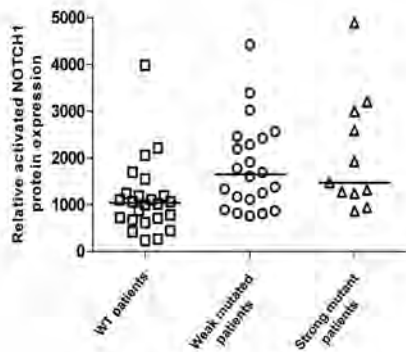


Figure S3 | ICN levels in wild-type, weak NOTCH1-activated (single HD, single PEST, single *FBXW7* mutation) and strong NOTCH1-activated (HD+PEST, HD+*FBXW7*, JM mutation) T-ALL patients analyzed with reverse-phase protein microarray.

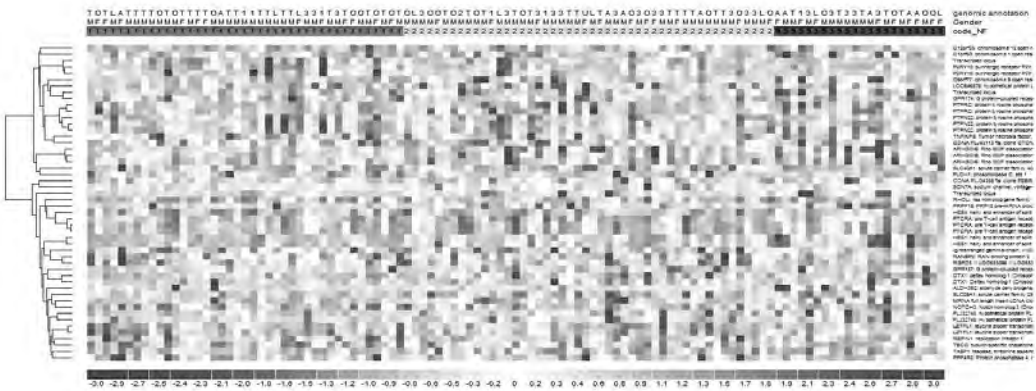


Figure S4 | Heatmap showing the TOP50 most differentially expressed genes between patients with strong NOTCH1-activating mutations versus wild-type patients. *NOTCH1* JM mutations or combinations of *NOTCH1* HD mutations with PEST mutations or *FBXW7* mutations were considered as strong NOTCH1-activating mutations. Annotations indicated are genetic rearrangements, gender and *NOTCH1*/*FBXW7* mutation status. Genetic rearrangements indicated are: T, *TAL1* or *SIL-TAL1*; L, *LMO1* or *LMO2* (includes del(11)(p12p13)); A, *HOXA*-activated (includes cases with *SET-NUP214*; *CALM-AF10* or Inv(7)(p15q34)); 1, *TLX1*; 2, *TLX2*; 3, *TLX3*; 0, Other; U, Aberration unknown. Gender is indicated F, Female or M, Male. *NOTCH1*/*FBXW7* mutation status is indicated “1” in blue box for wild-type, “2” in yellow box for patients with weak NOTCH1-activating mutations and “3” in red box for patients having strong NOTCH1-activating mutations.

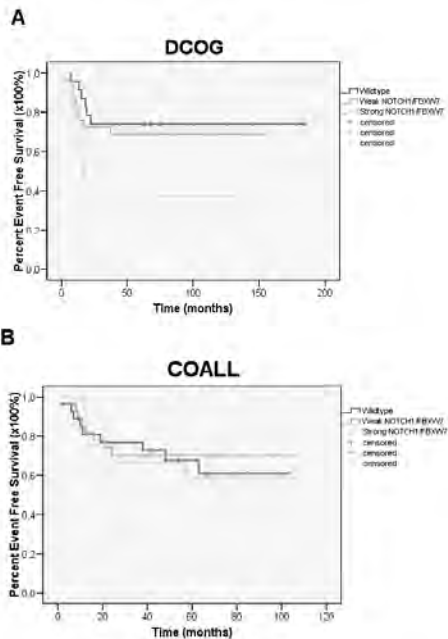
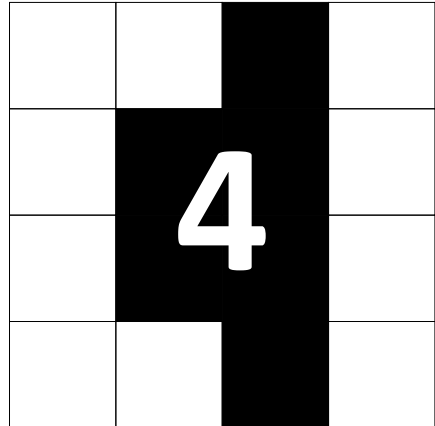


Figure S5 | The prognostic effect of *NOTCH1*/*FBXW7* mutations. Weak NOTCH1-activating mutations were considered as *NOTCH1* HD, PEST or *FBXW7* mutations, whereas strong NOTCH1-activating mutations were considered as *NOTCH1* JM mutations or *NOTCH1* HD mutations in combination with PEST or *FBXW7* mutations. **A.** For DCOG T-ALL patients, strong NOTCH1-activating mutations are significantly associated with poor outcome, with p -values of $p=0.012$ and $p=0.048$, compared to patients without *NOTCH1*/*FBXW7* mutations (wild-type) or patients with weak NOTCH1-activating mutations, respectively. **B.** No significant association with poor outcome was observed for weak or strong activated NOTCH1 T-ALL patients treated according to the COALL-97 protocol.

CHAPTER



The significance of *PTEN* and *AKT* aberrations in pediatric T-cell acute lymphoblastic leukemia

Linda Zuurbier¹, Maartje J. Vuerhard¹, Valerie Calvert², Clarissa Kooi¹, Jessica G.C.A.M. Buijs-Gladdines¹, Willem K. Smits¹, Edwin Sonneveld³, Anjo J.P. Veerman^{3,4}, Willem A. Kamps^{3,5}, Martin Horstmann^{6,7}, Emanuel F. Petricoin III^{2,8}, Rob Pieters¹ and Jules P.P. Meijerink¹

From the ¹Department of Pediatric Oncology/Hematology, Erasmus MC Rotterdam-Sophia Children's Hospital, Rotterdam, the Netherlands; ²Center for Applied Proteomics and Molecular Medicine, George Mason University, Manassas, VA, USA; the ³Dutch Childhood Oncology Group (DCOG), the Hague, the Netherlands; the ⁴Department of Pediatric Oncology/Hematology, VU University Medical Center, Amsterdam, ⁵Department of Pediatric Oncology, University of Groningen-Beatrix Children's Hospital, Groningen, the Netherlands; the ⁶German Cooperative Study Group for Childhood Acute Lymphoblastic Leukemia (COALL), Hamburg, Germany; ⁷the Research Institute Children's Cancer Center Hamburg, Clinic of Pediatric Hematology and Oncology, University Medical Center Hamburg-Eppendorf, Hamburg, Germany; ⁸NCI-FDA Clinical Proteomics Program, Food and Drug Administration, Bethesda, MD, USA.

ABSTRACT

PI3K/AKT pathway mutations are found in T-cell acute lymphoblastic leukemia, but impact and associations with other genetic aberrations is unknown. PTEN mutations have been proposed as secondary mutations that follow NOTCH1-activating mutations and that cause cellular resistance to gamma-secretase inhibitors. The impact of *PTEN*, *PI3K* and *AKT* aberrations was studied in genetically well-characterized pediatric T-cell leukemia patient cohort ($n=146$) treated on DCOG or COALL protocols. *PTEN* and AKT E17K aberrations were detected in 13% and 2% of patients, respectively. Defective *PTEN*-splicing was identified in incidental cases. Patients without PTEN protein but lacking exon-, splice-, promoter mutations or promoter hypermethylation were present. *PTEN/AKT* mutations were especially abundant in *TAL-* or *LMO*-rearranged leukemia but nearly absent in *TLX3*-rearranged patients ($p=0.03$), an association pattern that seems reciprocal to NOTCH1-activating mutations. Most *PTEN/AKT* mutant patients either lacked NOTCH1-activating mutations ($p=0.006$) or had weak NOTCH1-activating mutations ($p=0.011$), and consequently expressed low intracellular NOTCH1, cMYC and MUSASHI levels. T-cell leukemia patients without *PTEN/AKT* and NOTCH1-activating mutations fared well, with a cumulative incidence of relapse of only 8% versus 35% for *PTEN/AKT* and/or NOTCH1-activated patients ($p=0.005$). In conclusion, PI3K/AKT pathway aberrations are present in 18% of pediatric T-cell acute lymphoblastic leukemia patients. Absence of strong NOTCH1-activating mutations in these cases may explain cellular insensitivity to γ -secretase inhibitors.

INTRODUCTION

Despite improved treatment outcome, children with T-cell Acute Lymphoblastic Leukemia (T-ALL) have a higher relapse risk than children with B-lineage ALL¹. T-ALL is characterized by mutually exclusive abnormalities in *TAL1*, *LMO2*, *TLX3/HOX11L2*, *TLX1/HOX11* or *HOXA* oncogenes. Gene expression analyses supported the view that the aberrations delineate specific T-ALL subgroups²⁻⁴, in which cases with *TAL1* or *LMO2* aberrations share an identical expression profile and may be considered as a single TALLMO subgroup^{4,5}. These abnormalities are accompanied by other genetic aberrations, denoted as so-called type B mutations⁶, that are found in nearly all subgroups. These latter mutations include NOTCH1-activating mutations affecting the *NOTCH1* gene itself and/or inactivating mutations in the F-Box WD40 domain containing protein *FBXW7* gene, which is a ubiquitin ligase that apart of NOTCH1 can also target various other molecules⁷. NOTCH1-activating mutations have been observed in more than 60% of T-ALL pediatric patients⁸⁻¹⁴. We recently observed that the incidence of NOTCH1-activating mutations is higher for *TLX3*-rearranged patients while lower for *TAL*- or *LMO*-rearranged patients¹⁴. NOTCH1 is a transmembrane receptor that is activated upon ligand binding¹⁵, and these mutations result in ligand independent activation¹³. The prognostic consequences of NOTCH1-activating mutations are different in various studies^{8-12,14,16-18}.

Recurrent mutations in the phosphatase and tensin homolog (*PTEN*) gene were discovered in T-ALL patient samples following common *PTEN* deletions in the triple knockout mouse model (*Terc*, *Atm* and *Trp53*) that developed T-cell lymphomas¹⁹ as well as by a genome-wide copy number analysis in ALL samples²⁰. *PTEN* mutations were also observed in T-ALL cell lines²¹⁻²³, and analyses of T-ALL patient samples revealed *PTEN* mutations and deletions in 5% and 15%, respectively¹⁹. Palomero and coworkers found absence of *PTEN* expression in T-ALL cell lines that were resistant to γ -secretase inhibitors (GSI). Sequence analysis revealed *PTEN* mutations in 9 out of 111 primary T-ALL samples, suggesting that *PTEN* mutations that follow *NOTCH1* mutations may provoke GSI resistance²⁴. Various other studies showed a variable incidence of *PTEN* mutations and/or deletions in T-ALL patients (range 18-63%^{10,25,26}).

PTEN acts downstream of the T-cell receptor and various other pathways. It controls the PI3K/AKT pathway by dephosphorylating PtdIns(3,4,5)P₃ (PIP₃) into PtdIns(3,4)P₂ (PIP₂). PI3-kinase (PI3K) has an opposite function and phosphorylates PIP₂ into PIP₃, which allows activation of AKT via PDK1. *PTEN*-inactivating mutations result in an overactive PI3K/AKT pathway^{21,24}. Few mutations are found in *PI3K* and *AKT1* genes itself as alternative mechanisms to activate AKT²⁶. Activated AKT can act on multiple downstream targets that are involved in proliferation, cell metabolism and apoptosis^{27,28}. One major downstream target is *TSC2*, which is repressed by AKT that therefore facilitates protein synthesis through activation of mTOR.

The prognostic significance of an aberrantly activated PI3K/AKT pathway by mutations in pediatric T-ALL is fairly unknown^{10,25,26}. Also, *PTEN*, *PI3K* or *AKT1* aberrations in relation to NOTCH1-activating mutations are unclear^{10,24}. We therefore investigated the incidence of mono-allelic or bi-allelic *PTEN*-inactivating events and *PI3K* or *AKT1* aberrations in genetic subtypes of

T-ALL, their potential downstream effects, and their relationship with clinical outcome.

MATERIALS AND METHODS

Patient samples

A total of 146 primary pediatric T-ALL patients were included in this study: 72 enrolled on the Dutch Childhood Oncology Group (DCOG) protocols ALL-7/8 ($n=30$)^{29,30} or ALL-9 ($n=42$)³¹, and 74 patients enrolled on the German Co-Operative Study Group for Childhood Acute Lymphoblastic Leukemia study (COALL-97, $n=74$)¹² with median follow-up of 67 and 52 months, respectively. The patients' parents or legal guardians provided informed consent to use diagnostic patient biopsies for research in accordance with the Institutional Review Board of the ErasmusMC Rotterdam and the declaration of Helsinki. Isolation of leukemia cells was described before³², with all samples containing >90% of leukemic blasts. Clinical and immunophenotypic data were supplied by the study centers. Patients were classified into T-cell development stages based on EGIL criteria, i.e. the pro-/pre-T-cell subgroup (CD7⁺ CD2⁺ and/or CD5⁺ and/or CD8⁺, but CD1⁻ and sCD3⁻), the cortical T-cell (CD1⁺) or the mature T-cell subgroup (sCD3⁺/CD1⁺). Patients were indicated positive for an immunophenotypic marker when $\geq 25\%$ of leukemic blast stained positive for this marker.

Cell culture, γ -secretase inhibitor treatment and cell cycle analysis

T-ALL cell lines (DSMZ, Braunschweig, Germany) were cultured in RPMI-1640 supplemented with 10-20% fetal calf serum (Integro, Zaandam, the Netherlands), 100 IU/ml penicillin, 100 $\mu\text{g}/\text{ml}$ streptomycin and 0.125 $\mu\text{g}/\text{ml}$ fungizone (Invitrogen, Life Technologies, Breda, the Netherlands) at 37°C under 5% CO₂. T-ALL cell lines (JURKAT, CEM, LOUCY, SKW3, ALL SIL, HPBALL, PF382, HSB2, PEER, MOLT3, MOLT16, P12 ICHIKAWA, KARPAS45, RPMI8402, BE13, TALL1, SUPT1, KE37 and DND41) were grown under 1 μM Compound E (Enzo Life sciences (Alexis), Lausen, Switzerland) or 0.002% DMSO for 4 days, and 1×10^6 cells were harvested. Cell were fixed with 70% cold ethanol and stained with propidium iodide (Invitrogen), after trypsin (Gibco BRL, Life Technologies, Breda, the Netherlands) and RNase A (Sigma, Zwijndrecht, the Netherlands) treatment. DNA content was measured and analyzed by flow cytometry (FACSCalibur, Becton Dickson, San Jose, CA, USA).

Genomic DNA and RNA extraction

Genomic DNA and RNA were isolated from at least 5×10^6 leukemic cells using the Trizol reagent (Invitrogen) according to the manufacturer with minor modifications³². Copy-DNA synthesis of 1 μg of total RNA was performed as described before³². DNA was stored at 4°C, whereas RNA and cDNA were stored at -80°C.

Detection of mutations and splice variants

The phosphatase domain and C2-domain of *PTEN* (exons 1-9), the pleckstrin homology (PH)

domain of *AKT1* (exon 4), the SH2-domain of *PIK3CA* (p85, exon 12 and 13) and the accessory domain of *PIK3RI* (p110, exon 10) were amplified and sequenced. Primers used are described in **Table S1**. PCR reactions were performed on 50ng of DNA, 300nM of primers, 200 μ M of dNTPs, 4mM MgCl₂, 1.25U of *ampliTaq* gold (Applied Biosystems (AB), Foster City, CA, USA) in 1x PCR buffer II (Applied Biosystems) in a volume of 50 μ l. After denaturation at 94°C for 5', PCR was performed for 40 cycles at 94°C for 15'' and 60°C for 1'. Due to the GC-rich content, PCR of *PTEN* exon 1 was followed by a second asymmetric PCR for 10 cycles, using the forward or reverse primer. PCR products were purified with the Millipore Vacuum Manifold filter system (Millipore, Billerica, MA, USA) and sequenced (BigDye Terminator v3.1 Cycle sequencing Kit, AB) on an ABI PRISM 3130 DNA Analyzer (AB). Amplicons of patients that demonstrated two mutations were cloned using the TOPO-TA cloning kit (Invitrogen) to determine whether mutations occurred in *cis* or *trans*.

To examine promoter mutations, one primer set was used to amplify the promoter area. PCR-reactions were carried out as described above in the presence of 2mM MgCl₂ and 5% DMSO. Annealing temperature started at 63°C, and was lowered by 0.5°C each cycle till a final annealing temperature of 58°C. To investigate alternative *PTEN*-splicing, two primer pairs were used to amplify the complete *PTEN* transcript, using PCR conditions as described above in the presence of 2mM MgCl₂. *NOTCH1* mutations were identified as described in our previous study¹⁴.

Methylation specific PCR (MSP)

For methylation specific PCR (MSP), sodium bisulfite conversion was done using the EZ DNA methylation kit (Zymo research, Orange, CA, USA). Primers used are listed in **Table S1**. PCR was performed using 0.6U Hotstar *Taq* plus DNA polymerase (Qiagen, Venlo, the Netherlands), 1x PCR buffer, 200 μ M dNTPs, 300nM primers, 1x Q-solution, 3,5mM MgCl₂ and 100ng converted DNA in a total volume of 50 μ l. *Taq* polymerase was activated by 5' at 95°C, followed by 35 PCR cycles at 95°C for 30'', 59°C for 30'' and 72°C for 1' and a final elongation step of 10' at 72°C. *In-vitro* methylated DNA with CpG methyltransferase Sss1 and co-substrate S-adenosylmethionine (SAM, New England Biolabs, Ipswich, MA, USA) served as positive control, untreated genomic DNA served as negative control.

Fluorescence in-situ hybridization analysis (FISH) and RQ-PCR

Rearrangements of the *TLX1*, *TLX3*, *TAL1*, *LMO2* and *MLL* loci were determined with fluorescence in-situ hybridization analysis (FISH) as described before^{4,32,33}. *SET-NUP214* or *CALM-AF10* fusion products or expression levels of *SIL-TAL1*, *TLX1* or *TLX3* were detected by an RQ-PCR strategy as described^{4,32,33}. BAC clones and RQ-PCR primers/probes are summarized in **Table S2**. To identify *PTEN* deletions by FISH, bacterial artificial chromosomes (BAC) clones RP11-846G17 and/or RP11-124B18 were used. Probe RP11-265I15 covering the X-chromosomal *BEX1* gene was used as control. BACs were obtained from BAC/PAC Resource Center (Children's Hospital, Oakland, CA).

Microarray-based comparative genome hybridization (array-CGH)

Array-CGH analysis was performed on the human genome CGH Microarray 44A ($n=33$), 105K ($n=2$), and 400K ($n=78$) (Agilent Technologies, Santa-Clara, CA, USA), which consists of 60-mer oligo-nucleotide probes, that span both coding and non-coding sequences. The procedure was done as described before⁴.

Western Blot procedure

Western blot was performed as described previously⁴. Antibodies were obtained from Cell Signaling Technology (Beverly, MA, USA) for PTEN (Cat#9552), phosphorylated (S380) PTEN (Cat#9551), phosphorylated (Thr308 and S473) AKT (Cat#9275 and 9271), phosphorylated (S2448 and S2481) mTOR (Cat#2971 and 2974), phosphorylated (Thr389) p70 S6 kinase (Cat#9205), phosphorylated (S65 and T70) 4E-BP1 (Cat#9451 and 9455), phosphorylated (Y1571) TSC2 (Cat#3614), phosphorylated (S256) FOXO1 (Cat#9461), intracellular NOTCH1 (ICN) Val1744 (Cat#2421), cMYC (Cat#9402) and MUSASH1/2 (Cat#2154). To detect phosphorylated (S246) PRAS40, Cat#44-1100 from Invitrogen/Biosource was used. Total protein load was determined by staining for actin (Sigma, Cat#2547).

Reverse-phase protein microarray analysis (RPMA)

Reverse-phase protein microarray construction and analysis was performed essentially as previously described^{14,34,35}.

Statistics

Statistics was done in SPSS 15.0 software. Pearson's Chi-square or the Fisher's exact tests were performed to test significance levels for nominal data distributions, whereas the Mann-Whitney-U test was used for continuous data. Differences in cumulative incidence of relapse (CIR), relapse-free survival (RFS) and event-free survival (EFS) were tested by the log-rank test. An EFS event is defined as relapse, non-response to induction therapy, toxicity related death or development of a secondary malignancy. Data were considered significant when $p \leq 0.05$ (two-sided).

RESULTS

Inactivating PTEN aberrations in pediatric T-ALL patients

To determine the prevalence of *PTEN* mutations, all 9 coding exons were amplified and sequenced, providing data for 142 out of 146 pediatric T-ALL patients. Twenty-seven mutations were identified in 16 patients (11%), mostly representing heterozygous nonsense mutations that truncate the PTEN protein (**Figure 1A; Table S3**). Ten patients had two mutations in single exons or distributed over different exons. Re-sequencing of cloned PCR products revealed compound heterozygous insertion mutations in 8 out of 9 patients. One patient (#1959) comprised two

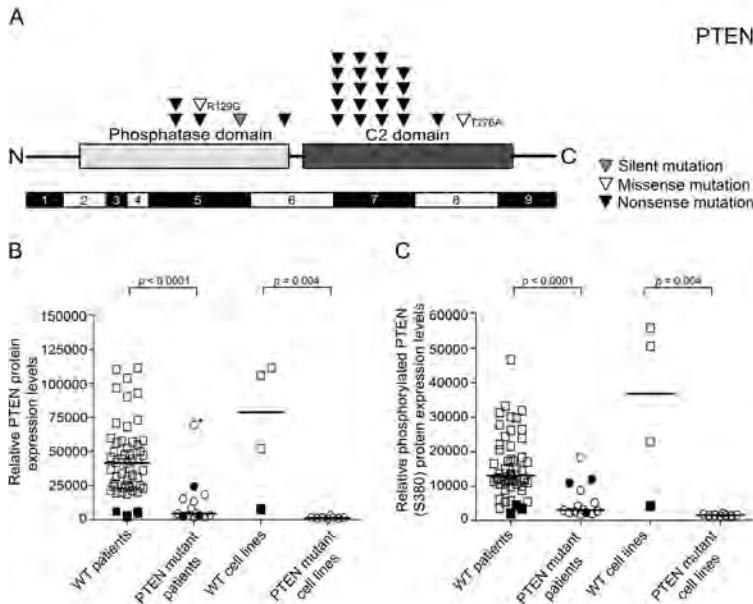


Figure 1 | PTEN aberrations result in low PTEN expression in pediatric T-ALL patients. (A) Schematic representation of identified mutations in the phosphatase- and C2-domains of the *PTEN* gene. Missense mutations are indicated by open triangles, whereas a silent mutation is presented as a filled grey triangle. Nonsense mutations due to insertions and/or deletions are indicated by a filled black triangle. **(B)** Total PTEN and **(C)** phosphorylated PTEN (S380) expression levels in wild-type and *PTEN*-mutated pediatric T-ALL patient samples and T-ALL cell lines, analyzed by reverse-phase protein microarray. Patients with a *PTEN* deletion are represented by a filled circle and patients with *PTEN* missense or nonsense mutations by an open circle. Wild-type patients that lack PTEN protein expression are indicated by a black square. Patient sample #335 is marked by an asterisk, and this patient bears a *PTEN* R129G missense mutation.

mutations that occurred in *cis*. Most deletion/insertion mutations occurred in exon 7, truncating PTEN in the C2-domain. Other mutations were detected in exon 5, 6 and 8. Two patients (#335 and #9963) had missense mutations, of which the R129G mutation was proven to inactivate phosphatase activity before³⁶.

We also detected four patients that had intron mutations located at the 3'-end in introns 1-2, 2-3 or 4-5, but amplification and sequencing of *PTEN* transcripts in these patients revealed no alternative *PTEN* splice isoforms.

High resolution array-CGH was performed on 113 out of 146 pediatric T-ALL patients, and heterozygous *PTEN* deletions were observed in three patients (#531, #8815 and #321, **Table S3; Figure S1A**). Loss of one *PTEN* allele in patient #531 explained its homozygous mutation pattern. Patient #2486 had a homozygous deletion of both *PTEN* alleles and since the deleted areas were identical, homozygosity may be due to uniparental disomy in this patient. Deletions could be validated by FISH in 3 patients except for patient #2486 due to the relatively small size of that deletion (**Figure S1B**). Array-CGH analysis also revealed subclonal deletions in two *PTEN*-mutated patients (#344 and #1959) that both carried two nonsense mutations affecting exons 5 and 7 (**Table S3; Figure S1C**). Validation by FISH demonstrated copy loss in 40% of the leukemic

blasts for patient #344, for which material was available (**Figure S1D**). Taken together, 19 of the 142 pediatric T-ALL patients (13%) harbored inactivating *PTEN* aberrations including missense and nonsense mutations as well as deletions of the entire *PTEN* locus. Bi-allelic *PTEN* inactivation was evident for 12 out of 19 patients.

PTEN protein levels in relation to the *PTEN* mutation status

Nonsense *PTEN* mutations result in loss of PTEN protein levels in T-ALL cell lines^{19,24}. Using reverse-phase protein microarray (RPMA), total PTEN protein levels as well as phosphorylated (inactivated) PTEN protein levels (S380) were quantified. *PTEN* mutant T-ALL cell lines had significantly lower PTEN and phosphorylated PTEN levels than wild-type cell lines, and validated this technique (**Figure 1B-C** $p=0.004$ and $p=0.004$, respectively). Material for RPMA analysis was available for 66 out of 146 T-ALL patient samples. Total PTEN (**Figure 1B** $p<0.0001$) as well as phosphorylated PTEN protein levels (**Figure 1C** $p<0.0001$) were significantly lower for patients bearing inactivating *PTEN* mutations. One *PTEN*-mutated patient (#335) expressed PTEN protein (**Figure 1B-C**) from the mutant allele carrying the missense R129G mutation while the second allele was lost due to a frameshift insertion in exon 5. PTEN protein levels were absent or low in all other *PTEN*-mutated patients. PTEN levels were significantly lower for bi-allelic affected patients compared to mono-allelic affected patients (**Figure S2** $p=0.04$). Some mono-allelic-mutated/deleted patients had expression levels that were comparable to bi-allelic patients, indicating that the remaining wild-type allele in these patients may be silenced through yet unknown mechanisms. In addition, three seemingly *PTEN* wild-type patient samples (#769, #8629 and #9243) and the *PTEN* wild-type cell line HPBALL lacked PTEN protein (**Figure 1B-C** black squares). Array-CGH data were not available for these patients, but large *PTEN* deletions were excluded by FISH analysis in 2 out of these 3 patients and HPBALL (data not shown).

Defective *PTEN*-splicing in pediatric T-ALL patients

We then investigated whether absence of PTEN protein in these three patients and HPBALL was due to splice defects, mutations or hypermethylation of the *PTEN* promoter region. In addition, we further investigated the seven T-ALL patients that seemed to comprise mono-allelic mutations or deletions (#9160, #9919, #9963, #2759, #2852, #321 and #8815). One out of the three seemingly *PTEN* wild-type patients (#9243) and 2 out of 7 patients with mono-allelic *PTEN* mutations (#2852 and #8815) demonstrated aberrant *PTEN*-splicing and lacked expression of the full-length *PTEN* isoform (**Figure 2; Table S3**). PCR-sequence analysis for patient #9243 confirmed defective splicing of exon 3 to exon 6, whereas intron 1-2 was defectively spliced to exon 4 in patient #2852. Patient #8815 demonstrated defective *PTEN* exon 4 to exon 6 splicing that eliminates the phosphatase domain. Miss-splicing therefore provides an additional mechanism to eliminate wild-type PTEN expression. So far, no explanation was found for defective *PTEN*-splicing as no mutations were identified in the first 20-30 intronic bases flanking acceptor/donor splice sites of affected exons. Defective splicing in the absence of full-length *PTEN* transcript was also observed in the mono-allelic *PTEN*-deleted cell line LOUCY. All 11 control T-ALL patient

samples expressed the *PTEN* wild-type isoform only (Figure 2, 7 controls are shown).

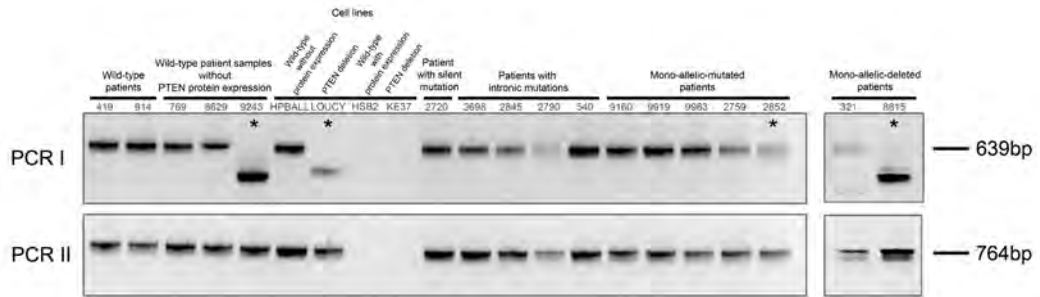


Figure 2 | Defective splicing of *PTEN* transcripts. Analysis of alternative *PTEN* splicing in two wild-type *PTEN* patients and *PTEN* expression (#419 and #914), seven *PTEN* wild-type patients and cell lines without *PTEN* expression (#768, #8628, #9243, HPBALL, LOUCY, HSB2 and KE37), patients with silent or intronic mutations (#2720, #2698, #2845, #2790 and #540) and seven patients with mono-allelic *PTEN* mutations or deletions (#9160, #9919, #9963, #2759, #2852, #321 and #8815). RT-PCR I covers wild-type and alternative *PTEN* transcripts from exon 1 through exon 6, whereas RT-PCR II covers wild-type and alternative *PTEN* transcripts from exon 6 through 9. Patients and cell lines expressing aberrant transcripts while lacking the full-length *PTEN* transcript are marked with an asterisk.

These three *PTEN* wild-type patients with reduced *PTEN* expression as well as these seven *PTEN* mono-allelic-mutated patients were also investigated for *PTEN* promoter hypermethylation as potential mechanism to silence wild-type *PTEN* alleles. For this, methylation specific PCR (MSP) was performed for the -1223 to -1032 region upstream relative to the transcriptional start site of *PTEN* (Figure S3A), in which hypermethylation has been described before in solid tumors and T-ALL³⁷⁻³⁹. However, we found no evidence for *PTEN* promoter hypermethylation (Figures S3B-C). We also did not find evidence for deletions or mutations in the *PTEN* promoter region (-1414 to -613bp) in any of these T-ALL patients.

PI3K/AKT pathway mutations in pediatric T-ALL patients

PTEN regulates the PI3K/AKT pathway, and inactivation of *PTEN* may result in constitutive activation of the AKT pathway. Rare activating mutations in *PI3K* and *AKT* have been described in T-ALL patient samples²⁶. To screen for such mutations, exons 12 and 13 of *PIK3RI* (p85 regulatory subunit) and exon 10 of *PIK3CA* (p110 catalytic subunit class IA) and exon 4 of *AKT1* were amplified and sequenced, and results were obtained for 135 out of the 146 T-ALL patients. No mutations were identified in *PIK3RI* or *PIK3CA*. Three patients (2%) had a mutation in *AKT1* changing glutamic acid into lysine at position 17 (E17K) (Table S3). This mutation has been reported before in a single T-ALL patient²⁶, and constitutively activates AKT1⁴⁰.

All *AKT1*-mutated patients lacked *PTEN* aberrations. Overall, *PTEN* mutations or *AKT1* mutations were identified in 25 out of 142 pediatric T-ALL patients (18%), and were denoted as the *PTEN/AKT* mutant patient group. This group comprised both *PTEN* wild-type patients that lacked *PTEN* protein expression (#769 and #8629). Based on our findings and literature^{19,24}, more than half of T-ALL cell lines have inactivated *PTEN* (summarized in Table S4).

Comparing the activation status of AKT and potential downstream signaling molecules in

PTEN/AKT-mutated versus wild-type patients using RPMA, we did not observe differences in phosphorylated AKT (Ser473 and Thr308) levels, nor in the phosphorylated status of downstream AKT targets including mTOR, p70 S6 kinase, 4E-BP1, TSC2, PRAS40 and FOXO1 (**Figure S4A-B**). As AKT activation has also been described to occur downstream of the NOTCH1 pathway^{24,41}, we distinguished between *PTEN/AKT*-mutant patients, NOTCH1-activated and patients lacking *PTEN/AKT* or NOTCH1/*FBXW7* mutations but did not identify significant differences in phosphorylated AKT levels nor downstream AKT targets (not shown).

***PTEN/AKT* aberrations in relation to biological, clinical and molecular-cytogenetic parameters**

PTEN/AKT mutations were not associated with gender ($p=0.97$) or white blood cell counts ($p=0.61$), but seemed associated with younger age (**Table 1** $p=0.05$).

Eight out of 25 *PTEN/AKT* patients had *TAL1* rearrangements (**Table 1 and Table S5**, $p=0.05$), whereas only 3 out of 25 *PTEN/AKT* patients had *TLX1* or *TLX3* rearrangements (1 *TLX3*- and 2 *TLX1*-rearranged patients; $p=0.003$). Similar associations were observed for *PTEN*-mutated patients only. For T-ALL clusters based on unsupervised gene expression profiling⁵, we noticed that *PTEN/AKT* mutations were predominantly present in *TAL/LMO* cluster patients albeit not significant, while the incidence of these mutations was significantly lower for the *TLX* cluster that comprise most *TLX3*- and *HOXA*-rearranged cases ($p=0.002$). No associations were observed with *PHF6* or *WT1* mutations nor with *CDKN2A/B* deletions, in line with previous findings as reported by Gutierrez et al (2009)²⁶.

Initially, *PTEN* mutations have been suggested as secondary mutations following NOTCH1-activating mutations, rendering cells insensitive to γ -secretase inhibitors²⁴. We therefore compared the distribution of *PTEN/AKT* mutations with that of NOTCH1-activating mutations. NOTCH1-activating mutations (in *NOTCH1* and/or *FBXW7*) were present in 63% of the patients¹⁴. Strikingly, patients carrying NOTCH1-activating mutations seemed to have a lower incidence of *PTEN/AKT* aberrations as only 10 out of 90 *NOTCH1/FBXW7*-mutated patients carried *PTEN/AKT* aberrations, in contrast to 15 out of 51 *NOTCH1/FBXW7* wild-type patients (**Table 1**, $p=0.006$). Remarkably, *PTEN/AKT*-mutated patients that had *NOTCH1/FBXW7* mutations especially harbored weak NOTCH1-activating mutations only (9 out of 10 cases, $p=0.011$)^{14,42}.

So NOTCH1-activating mutations and *PTEN/AKT* mutations seem hits that are associated with different molecular cytogenetic T-ALL subgroups (¹⁴, and this study). These observations were further strengthened by our RPMA analyses that showed that *PTEN/AKT* mutant patients have low expression of intracellular NOTCH1 (ICN, $p=0.003$), cMYC, as a prime NOTCH1-target gene^{24,43} ($p=0.01$) and MUSASHI1/2 (*MSI1/2*, **Figure S4C** $p=0.002$), which is a repressor of the NOTCH1 negative regulator NUMB⁴⁴. This is different in T-ALL cell lines, as 10 out of 13 *PTEN/AKT*-mutated cell lines also harbor NOTCH1-activating mutations (**Table S4**).

We then investigated whether *PTEN/AKT* mutations are associated with resistance to γ -secretase inhibitors such as previously suggested²⁴. For this purpose, we measured the G1-arrest in a large panel of T-ALL cell lines following γ -secretase inhibitor treatment. Various cell lines (JURKAT, P12Ichikawa, PF382, MOLT16 and KARPAS45) that had *PTEN*-inactivating

mutations (Table S4) were resistant to γ -secretase inhibitor treatment (Figure S5A)²⁴, but four lines with *PTEN*-inactivating aberrations (SKW3, SUPT1, LOUCY, KE37) rapidly underwent G1-arrest following treatment. So, *PTEN* loss-of-function mutations are not necessarily associated with resistance towards γ -secretase inhibitors. All *PTEN* mutant lines lacked PTEN protein expression regardless of their γ -secretase inhibitor response, with the exception of SUPT1 and RPMI8402 that had *PTEN* missense mutations (Figure S5B).

Clinical (n=142)	PTEN mutation/deletion			<i>PTEN</i> or <i>AKT1</i> mutation/deletion + patients with a low PTEN protein expression (PTEN/AKT)		
	WT	Mut	<i>p</i> -value	WT	Mut	<i>p</i> -value
Gender			0,60			0,97
Male	85	12		80	17	
Female	38	7		37	8	
Median age (range)	7.8 (1.1-17.8)	4.3 (2.2-15.9)	0.07†	7.9 (1.1-17.8)	4.9 (2.2-15.9)	0.05†
Median WBC (range)	120 (2.0-900.0)	136 (5.0-600.0)	0.33†	120 (2.0-900.0)	136 (5.0-600.0)	0.61†
Cytogenetics (n=142)	WT n(%)	Mut n(%)	<i>p</i> -value	WT n(%)	Mut n(%)	<i>p</i> -value
TAL1 + (n=26)	20 (77)	6 (23)	0,11	18 (69)	8 (31)	0,05
LMO2 + (n=14)	13 (93)	1 (7)	0,69‡	13 (93)	1 (7)	0,46‡
TLX3 + (n=28)	28 (100)	0 (0)	0.03‡	27 (96)	1 (4)	0.03‡
TLX1 + (n=7)	6 (86)	1 (14)	1‡	5 (71)	2 (29)	0,61‡
HOUX4 + (n=13)	13 (100)	0 (0)	0,22‡	13 (100)	0 (0)	0,13‡
\$MEF2C+ (n=6)	5 (83)	1 (17)	0,81‡	5 (83)	1 (17)	1‡
\$NKX2-1+ (n=6)	5 (83)	1 (17)	0,81‡	5 (83)	1 (17)	1‡
Unknown (n=42)	33 (79)	9 (21)	0,07	31 (74)	11 (25)	0,08
Gene expression clusters (n=113)	WT n(%)	Mut n(%)	<i>p</i> -value	WT n(%)	Mut n(%)	<i>p</i> -value
TAL/LMO + (n=51)	41 (80)	10 (20)	0,07	38 (75)	13 (25)	0,09
TLX + (n=28)	28 (100)	0 (0)	0.02‡	28 (100)	0 (0)	0.002‡
Proliferative + (n=19)	16 (84)	3 (16)	0,72‡	13 (68)	6 (32)	0,11
Immature/(ETP)ALL + (n=15)	13 (87)	2 (13)	1‡	13 (87)	2 (13)	0,73‡
NOTCH1/FBXW7 status (n=141)	WT n(%)	Mut n(%)	<i>p</i> -value	WT n(%)	Mut n(%)	<i>p</i> -value
wild-type (n=51)	39 (76)	12 (24)	0,008	36 (71)	15 (29)	0,006
mutant (n=90)	83 (92)	7 (8)		80 (89)	10 (11)	
wild-type (n=51)	39 (76)	12 (24)	0.02‡	36 (71)	15 (29)	0.011‡
¶ weak mutant (n=62)	56 (90)	6 (10)		53 (85)	9 (15)	
# strong mutant (n=28)	27 (96)	1 (4)		27 (96)	1 (4)	
PHF6 status (n=62)	WT n(%)	Mut n(%)	<i>p</i> -value	WT n(%)	Mut n(%)	<i>p</i> -value
wild-type	11 (100)	0 (0)	0,33‡	10 (91)	1 (9)	0,67‡
mutant	44 (86)	7 (14)		42 (82)	9 (18)	
WT1 status (n=142)	WT n(%)	Mut n(%)	<i>p</i> -value	WT n(%)	Mut n(%)	<i>p</i> -value
wild-type	16 (100)	0 (0)	0,13‡	14 (88)	2 (12)	0,74‡
mutant	107 (85)	19 (15)		103 (82)	23 (18)	
Del 9p21 status (n=112)	WT n(%)	Mut n(%)	<i>p</i> -value	WT n(%)	Mut n(%)	<i>p</i> -value
wild-type	73 (84)	14 (16)	0,52‡	72 (83)	15 (17)	0,76‡
mutant	23 (92)	2 (8)		22 (88)	3 (12)	

Table 1 | Overall clinical, immunophenotypic and molecular cytogenetic characteristics of PTEN or PTEN/AKT-mutated patients versus wild-type patients. Significant *P* values are indicated in bold; all *P* values were calculated by using Pearson's χ^2 test, unless indicated otherwise; WT: wild-type; Mut: mutant; *P*: *P* value; \square statistical analysis of the frequency of PTEN or PTEN/AKT aberrations for specific genetic T-ALL subgroups indicated compared to all other T-ALL subgroups combined; Median age indicated in years; WBC: white blood cell count; white blood cell counts are indicated as number of blasts ($\times 10^9/L$); †Mann-Whitney-U test; ‡Fisher's exact test; §Different genetic aberrations have been identified that all result in the activation of the MEF2C or NKX2-1/NKX2-2 oncogenes that define novel genetic T-ALL subtypes; ¶Weak, 113 out of 117 T-ALL patients included in the gene expression profiling study had a known PTEN and AKT mutation status. T-ALL patients were assigned to clusters based on unsupervised gene expression cluster analysis. 5 The TAL/LMO group is based on the presence of TAL1 or LMO2 rearrangements or by having a TAL/LMO expression signature; 5 ¶Weak NOTCH1 activating mutations are considered as mutations in the NOTCH1 heterodimerization (HD) domain or NOTCH1 PEST domain or in FBXW7; 39 #Strong NOTCH1 activating mutations are considered as mutations in the juxtamembrane (JM) or mutations in the NOTCH1 HD domain in combination with mutations in the NOTCH1 PEST domain or FBXW7.

Good outcome for T-ALL patients lacking *PTEN/AKT* and/or *NOTCH1/FBXW7* aberrations

In relation to outcome, relapse-free survival (RFS) and event-free survival (EFS) rates for *PTEN/AKT* mutant patients did not differ compared to wild-type patients (**Figures S6A-B**). In contrast to previous observations^{25,26}, no differences in outcome for *PTEN*-deleted patients versus other patients were observed nor for patients having mono-allelic versus bi-allelic *PTEN* mutations (data not shown). As the *PTEN/AKT* wild-type patient group is enriched for patients that harbor *NOTCH1*-activating mutations, which were previously associated with a trend towards poor outcome¹⁴, we compared CIR and EFS rates for patients with *PTEN/AKT* aberrations and/or *NOTCH1*-activating mutations versus patients lacking these mutations (wild-type patients). Wild-type patients had a significantly lower 5-yr CIR rate (8%) compared to *PTEN/AKT* and/or *NOTCH1*-activated patients (35%) in a stratified analysis in our cohorts (**Figure 3A and S6B** $p=0.005$). Only 2 out of 36 wild-type patients relapsed versus 33 out of 105 patients that had *NOTCH1*-activating and/or *PTEN/AKT* mutations (**Table S6** $p=0.002$). The 5-yr EFS rate for wild-type patients was $75\pm 7.7\%$ versus $60\pm 5.0\%$ for *NOTCH1/FBXW7* and/or *PTEN/AKT* mutant patients (**Figure 3B** $p=0.15$), due to a relatively high number of toxic deaths or secondary malignancies in the wild-type patient group (**Table S6** $p=0.03$; **Figure S6B**). We further investigated clinical and molecular-genetic parameters with 5-years relapse-free survival (RFS) rates (**Table S7**). We found improved 5-yr RFS rates for male patients ($p=0.01$), but inferior RFS rates for *TLX3*-rearranged T-ALL ($p=0.04$) as well as for patients having *PTEN/AKT* and/or *NOTCH1* activating mutations ($p=0.005$). Multivariate analysis demonstrated that male gender and *PTEN/AKT/NOTCH1/FBXW7* mutations remained independent predictors for improved or worse outcome, respectively (**Table S8**).

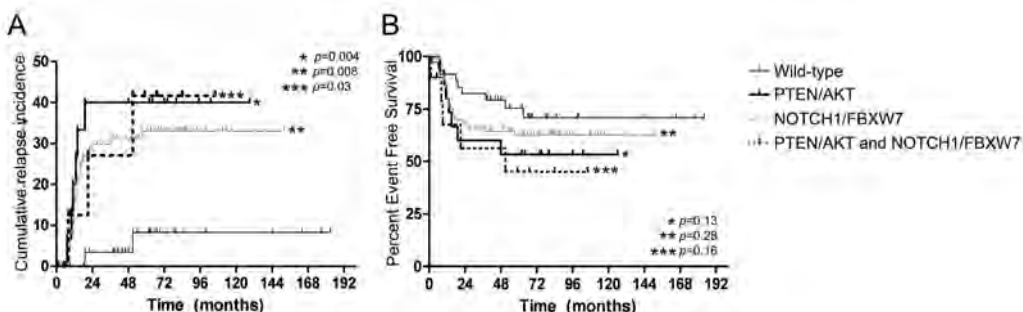


Figure 3 | T-ALL patients without *PTEN/AKT* and/or *NOTCH1*-activating mutations have a good outcome. Cumulative incidence of relapse (CIR) (A) and event-free survival (EFS) for DCOG and COALL pediatric T-ALL patients. Different patients groups are indicated in the legend. Log-rank p -values in a stratified analysis for different DCOG and COALL mutation groups relative to *PTEN/AKT* and *NOTCH1/FBXW7* non-mutated patients (i.e. wild-type patients) have been indicated.

DISCUSSION

Eighteen percent of the patients have aberrations that affect the PI3K/AKT pathway in our pediatric T-ALL patients cohort ($n=146$). *PTEN* aberrations were identified in $\sim 16\%$, whereas

AKT mutations were observed in ~2% of T-ALL patients. In other studies, *PTEN* mutations were identified in 5-27% of patients^{10,19,24-26}. Gutierrez et al (2009) identified *PTEN/AKT* mutations in ~48% of the patients ($n=44$)²⁶, which is considerably higher compared to our study.

Major *PTEN* inactivation mechanisms are nonsense mutations and deletions. We identified defective splicing as an alternative mechanism to reduce *PTEN* expression in 2% of T-ALL patients. No mutations in donor/acceptor sites or closely flanking intronic sequences of the exons involved were identified, but we cannot exclude that intronic mutations at greater distance from these donor/acceptor sites are present that affect *PTEN*-splicing. Splice-defective patients did not express full-length *PTEN* transcript, indicating that both *PTEN* alleles were inactivated. Alternative splice isoforms of *PTEN* have been described before in Cowden Syndrome (CS), sporadic breast cancer or Bannayan-Riley-Ruvalcaba syndrome (BRRS), and were shown to alter full-length *PTEN* expression levels⁴⁵. Two *PTEN* wild-type T-ALL patients completely lacked *PTEN* protein. Although *PTEN* promoter mutations have been described for patients with CS and autism spectrum disorders^{46,47} and *PTEN* promoter hypermethylation was described for endometrial cancer, sporadic breast cancer and T-ALL³⁷⁻³⁹, evidence for promoter mutations or promoter hypermethylation was not identified in our T-ALL patient series, so additional mechanisms to inactivate *PTEN* may exist in T-ALL. We cannot exclude that these mechanisms involve microRNAs, including miR-19b or miR-20a⁴⁸. Also, a regulatory role for the *PTEN* pseudogene *PTENP1* on *PTEN* expression have been identified before with *PTENP1* acting as a decoy transcript that bind miR-19b and miR-20a, resulting in elevated *PTEN* levels⁴⁸. Other miRNAs have been identified that regulate *PTEN* expression⁸.

Mono-allelic inactivation of *PTEN* in cancer led to the hypothesis that *PTEN* is a haploinsufficient tumor suppressor gene⁴⁹. We have identified *PTEN* aberrations in a single allele in approximately one third of *PTEN*-mutated T-ALL patients, and these patients expressed lower *PTEN* protein levels compared to wild-type patients, in concordance with previous findings²⁴. These expression levels were still significantly higher compared to patients with bi-allelic *PTEN* mutations/deletions. Thus, mono-allelic loss of *PTEN* may be sufficient to provide a proliferation advantage in T-ALL, but an oncogenic pressure remains ongoing to inactivate the second functional *PTEN* allele. This notion is further substantiated by subclonal *PTEN* deletions in two T-ALL patients that already had one dysfunctional *PTEN* allele.

Inactivation of *PTEN* results in ectopic activation of *AKT*^{19,24}. However, using RPMA, we did not find different phospho-*AKT* levels or phosphorylation of downstream *AKT* targets in *PTEN/AKT* patients compared to patients lacking *PTEN/AKT* aberrations, and differences were also not observed between *PTEN/AKT* mutant cell lines and wild-type lines. It may be that differences in phosphorylation levels for *AKT* and downstream targets between *PTEN/AKT* mutant patients and wild-type patients are subtle and difficult to be accessed on primary patient material by RPMA or that *AKT* may also be regulated through other oncogenic pathways. In this respect, activation of the *AKT* pathway has been identified in over 75 percent of T-ALL cases⁵⁰, which is well above the incidence of *PTEN/AKT* aberrations (this study). In T-ALL, activation of *AKT* has been described downstream of *NOTCH1*⁴¹, and *AKT* may be activated upon transcriptional

repression of PTEN by the NOTCH1-activated transcriptional repressor HES1²⁴. So AKT activation as consequence of *PTEN/AKT* mutations or through NOTCH1-activating mechanisms could explain the lower frequency of *PTEN/AKT* mutations in patients that have NOTCH1-activating mutations in our cohort. Furthermore, the 9 out of 10 *PTEN/AKT*-mutated patients that had NOTCH1-activating mutations only had weakly NOTCH1-activating mutations (i.e. *NOTCH1*-HD or PEST domain mutations or *FBXW7* mutations)⁴², pointing to a common downstream target and therefore eliminating the necessity to accumulate both *PTEN/AKT* and strong NOTCH1-activating mutations. Also in the study of Medyouf et al (2010), 4 of the 6 primary T-ALL samples with PTEN inactivating mutation were also NOTCH1 mutated and only carried weakly activating PEST domain mutations⁵¹. Consequently, ICN, MYC (another NOTCH1 target gene) and the indirectly NOTCH1 activator MUSASHI1/2 are expressed at lower levels in *PTEN/AKT*-mutated patients. Although *PTEN/AKT* mutations and NOTCH1-activating mutations may both converge on the activation of AKT, the association of *PTEN/AKT* mutations with *TAL/LMO*-rearranged patients (this study) and NOTCH1-activating mutations that are especially predominant in *TLX3*-rearranged patients¹⁴ also imply that both oncogenic pathways may activate different routes within different T-ALL subtypes.

The lower frequency of combined *PTEN/AKT* and NOTCH1-activating mutations may further explain cellular insensitivity of *PTEN/AKT* mutant cases towards γ -secretase inhibitors (GSI)²⁴. Our data show that most PTEN-inactivating mutations occur independently from NOTCH1-activating mutations, implying that *PTEN/AKT*-mutant leukemic cells are not sensitive towards GSIs rather than PTEN aberrations would provoke γ -secretase resistant²⁴. In this respect, we demonstrated that various T-ALL cell lines that have *PTEN* mutations (SKW3, SUPT1, LOUCY and KE37) respond to γ -secretase inhibitors. Our findings are in concordance to one previous study which showed that *PTEN* negative primary T-ALL cells or NOTCH1-induced T-ALL cells in mice on a *Pten* null background are equally sensitivity to γ -secretase inhibitors than primary T-ALL cells or NOTCH-induced tumors with unaffected PTEN loci, respectively⁵¹.

In the study of Gutierrez et al (2009), *PTEN/AKT* patients did not predict for event-free survival, but *PTEN* deletions seemed to be associated with early treatment failure²⁶. Jotta et al (2010) demonstrated poor overall survival rates for *PTEN*-mutated high-risk patients²⁵. In this last study, a trend towards poor outcome was related to the presence of mono-allelic or bi-allelic *PTEN* mutations/deletions. We could not confirm this, as most of our patients demonstrated bi-allelic inactivation of PTEN through additional mechanisms, such as alternative splicing that have thus far not been investigated in T-ALL. Distinguishing patients groups in our cohort based on the presence or absence of *PTEN/AKT* and *NOTCH1/FBXW7* mutations revealed that patients with *PTEN/AKT* mutations fared as poorly as patients with *NOTCH1/FBXW7* mutations or both. The patients without *PTEN/AKT* and *NOTCH1/FBXW7* mutations had a good outcome, and almost no relapses were observed for these patients.

In conclusion, missense or nonsense mutations or deletions affecting the *PTEN* gene occur in 13 percent of pediatric T-ALL patients, and may result in the activation of the AKT pathway. The AKT E17K activating mutation was observed in ~2% of T-ALL patients. Defective *PTEN* splicing is an

additional *PTEN*-inactivating event, but so far the underlying mechanism is poorly understood. *PTEN/AKT* mutations are predominantly associated with *TAL/LMO*-rearranged T-ALL, with most *PTEN/AKT*-mutated patients lacking *NOTCH1*-activating mutations. T-ALL patients that lack *PTEN/AKT* and *NOTCH1/FBXW7* mutations demonstrated a good overall outcome.

AUTHORSHIPS AND DISCLOSURES

L.Z. designed experiments, performed research and wrote manuscript, M.J.V. performed research and wrote manuscript, V.C. performed RPMA analysis, J.B.-G. performed *PTEN* mutation analysis and FISH, C.K. performed MSP, PCRs, cell cycle analyses and FISH, W.K.S. performed *PTEN* mutation analysis and prepared samples for RPMA analysis, E.S., A.J.P.V, W.K. and M.H. provided patient samples and clinical and immunophenotypic data, E.P. supervised study, and wrote manuscript, R.P. designed and supervised study and wrote manuscript, J.P.P.M. was principal investigator, designed and supervised the study, and wrote manuscript. None of the authors had competing financial interest.

4

ACKNOWLEDGEMENTS

The authors would like to thank M.W. Sahebali for sequencing experiments. This work was supported by the The Children Cancer Free Foundation (Stichting Kinderen Kankervrij (KiKa)) and the Erasmus University Trustfonds foundation.

REFERENCES

1. Pui CH, Evans WE. Treatment of acute lymphoblastic leukemia. *N Engl J Med.* 2006;354:166-178.
2. Ferrando AA, Neuberg DS, Staunton J, et al. Gene expression signatures define novel oncogenic pathways in T cell acute lymphoblastic leukemia. *Cancer Cell.* 2002;1:75-87.
3. Soulier J, Clappier E, Cayuela JM, et al. HOXA genes are included in genetic and biologic networks defining human acute T-cell leukemia (T-ALL). *Blood.* 2005;106:274-286.
4. Van Vlierberghe P, van Grotel M, Tchinda J, et al. The recurrent SET-NUP214 fusion as a new HOXA activation mechanism in pediatric T-cell acute lymphoblastic leukemia. *Blood.* 2008;111:4668-4680.
5. Homminga I, Pieters R, Langerak AW, et al. Integrated Transcript and Genome Analyses Reveal NKX2-1 and MEF2C as Potential Oncogenes in T Cell Acute Lymphoblastic Leukemia. *Cancer Cell*;19:484-497.
6. Meijerink JP. Genetic rearrangements in relation to immunophenotype and outcome in T-cell acute lymphoblastic leukaemia. *Best Pract Res Clin Haematol.* 2010;23:307-318.
7. Mullighan CG. Mutations of NOTCH1, FBXW7, and prognosis in T-lineage acute lymphoblastic leukemia. *Haematologica.* 2009;94:1338-1340.
8. Clappier E, Collette S, Grardel N, et al. NOTCH1 and FBXW7 mutations have a favorable impact on early response to treatment, but not on outcome, in children with T-cell acute lymphoblastic leukemia (T-ALL) treated on EORTC trials 58881 and 58951. *Leukemia.* 2010;24:2023-2031.
9. Kox C, Zimmermann M, Stanulla M, et al. The favorable effect of activating NOTCH1 receptor mutations on long-term outcome in T-ALL patients treated on the ALL-BFM 2000 protocol can be separated from FBXW7 loss of function. *Leukemia.* 2010;24:2005-2013.
10. Larson Gedman A, Chen Q, Kugel Desmoulin S, et al. The impact of NOTCH1, FBW7 and PTEN mutations on prognosis and downstream signaling in pediatric T-cell acute lymphoblastic leukemia: a report from the Children's Oncology Group. *Leukemia.* 2009;23:1417-1425.
11. Park MJ, Taki T, Oda M, et al. FBXW7 and NOTCH1 mutations in childhood T cell acute lymphoblastic leukaemia and T cell non-Hodgkin lymphoma. *Br J Haematol.* 2009;145:198-206.
12. van Grotel M, Meijerink JP, van Wering ER, et al. Prognostic significance of molecular-cytogenetic abnormalities in pediatric T-ALL is not explained by immunophenotypic differences. *Leukemia.* 2008;22:124-131.
13. Weng AP, Ferrando AA, Lee W, et al. Activating mutations of NOTCH1 in human T cell acute lymphoblastic leukemia. *Science.* 2004;306:269-271.
14. Zuurbier L, Homminga I, Calvert V, et al. NOTCH1 and/or FBXW7 mutations predict for initial good prednisone response but not for improved outcome in pediatric T-cell acute lymphoblastic leukemia patients treated on DCOG or COALL protocols. *Leukemia.* 2010;24:2014-2022.
15. Aster JC, Pear WS, Blacklow SC. Notch signaling in leukemia. *Annu Rev Pathol.* 2008;3:587-613.
16. Asnafi V, Buzyn A, Le Noir S, et al. NOTCH1/FBXW7 mutation identifies a large subgroup with favorable outcome in adult T-cell acute lymphoblastic leukemia (T-ALL): a Group for Research on Adult Acute Lymphoblastic Leukemia (GRAALL) study. *Blood.* 2009;113:3918-3924.
17. Breit S, Stanulla M, Flohr T, et al. Activating NOTCH1 mutations predict favorable early treatment response and long-term outcome in childhood precursor T-cell lymphoblastic leukemia. *Blood.* 2006;108:1151-1157.
18. Zhu YM, Zhao WL, Fu JF, et al. NOTCH1 mutations in T-cell acute lymphoblastic leukemia: prognostic significance and implication in multifactorial leukemogenesis. *Clin Cancer Res.* 2006;12:3043-3049.
19. Maser RS, Choudhury B, Campbell PJ, et al. Chromosomally unstable mouse tumours have genomic alterations similar to diverse human cancers. *Nature.* 2007;447:966-971.
20. Mullighan CG, Goorha S, Radtke I, et al. Genome-wide analysis of genetic alterations in acute

- lymphoblastic leukaemia. *Nature*. 2007;446:758-764.
21. Shan X, Czar MJ, Bunnell SC, et al. Deficiency of PTEN in Jurkat T cells causes constitutive localization of Itk to the plasma membrane and hyperresponsiveness to CD3 stimulation. *Mol Cell Biol*. 2000;20:6945-6957.
 22. Sakai A, Thieblemont C, Wellmann A, Jaffe ES, Raffeld M. PTEN gene alterations in lymphoid neoplasms. *Blood*. 1998;92:3410-3415.
 23. Gronbaek K, Zeuthen J, Guldborg P, Ralfkiaer E, Hou-Jensen K. Alterations of the MMAC1/PTEN gene in lymphoid malignancies. *Blood*. 1998;91:4388-4390.
 24. Palomero T, Sulis ML, Cortina M, et al. Mutational loss of PTEN induces resistance to NOTCH1 inhibition in T-cell leukemia. *Nat Med*. 2007;13:1203-1210.
 25. Jotta PY, Ganazza MA, Silva A, et al. Negative prognostic impact of PTEN mutation in pediatric T-cell acute lymphoblastic leukemia. *Leukemia*. 2010;24:239-242.
 26. Gutierrez A, Sanda T, Grebliunaite R, et al. High frequency of PTEN, PI3K, and AKT abnormalities in T-cell acute lymphoblastic leukemia. *Blood*. 2009;114:647-650.
 27. Leslie NR, Downes CP. PTEN function: how normal cells control it and tumour cells lose it. *Biochem J*. 2004;382:1-11.
 28. Maehama T. PTEN: its deregulation and tumorigenesis. *Biol Pharm Bull*. 2007;30:1624-1627.
 29. Kamps WA, Bokkerink JP, Hahlen K, et al. Intensive treatment of children with acute lymphoblastic leukemia according to ALL-BFM-86 without cranial radiotherapy: results of Dutch Childhood Leukemia Study Group Protocol ALL-7 (1988-1991). *Blood*. 1999;94:1226-1236.
 30. Kamps WA, Bokkerink JP, Hakvoort-Cammel FG, et al. BFM-oriented treatment for children with acute lymphoblastic leukemia without cranial irradiation and treatment reduction for standard risk patients: results of DCLSG protocol ALL-8 (1991-1996). *Leukemia*. 2002;16:1099-1111.
 31. Veerman AJ, Kamps WA, van den Berg H, et al. Dexamethasone-based therapy for childhood acute lymphoblastic leukaemia: results of the prospective Dutch Childhood Oncology Group (DCOG) protocol ALL-9 (1997-2004). *Lancet Oncol*. 2009;10:957-966.
 32. Van Vlierberghe P, van Grotel M, Beverloo HB, et al. The cryptic chromosomal deletion del(11)(p12p13) as a new activation mechanism of LMO2 in pediatric T-cell acute lymphoblastic leukemia. *Blood*. 2006;108:3520-3529.
 33. van Grotel M, Meijerink JP, Beverloo HB, et al. The outcome of molecular-cytogenetic subgroups in pediatric T-cell acute lymphoblastic leukemia: a retrospective study of patients treated according to DCOG or COALL protocols. *Haematologica*. 2006;91:1212-1221.
 34. Paweletz CP, Charboneau L, Bichsel VE, et al. Reverse phase protein microarrays which capture disease progression show activation of pro-survival pathways at the cancer invasion front. *Oncogene*. 2001;20:1981-1989.
 35. Petricoin EF, 3rd, Espina V, Araujo RP, et al. Phosphoprotein pathway mapping: Akt/mammalian target of rapamycin activation is negatively associated with childhood rhabdomyosarcoma survival. *Cancer Res*. 2007;67:3431-3440.
 36. Han SY, Kato H, Kato S, et al. Functional evaluation of PTEN missense mutations using in vitro phosphoinositide phosphatase assay. *Cancer Res*. 2000;60:3147-3151.
 37. Roman-Gomez J, Jimenez-Velasco A, Agirre X, et al. Lack of CpG island methylator phenotype defines a clinical subtype of T-cell acute lymphoblastic leukemia associated with good prognosis. *J Clin Oncol*. 2005;23:7043-7049.
 38. Sadeq V, Isar N, Manoochehr T. Association of sporadic breast cancer with PTEN/MMAC1/TEP1 promoter hypermethylation. *Med Oncol*. 2011;28:420-423.
 39. Salvesen HB, Stefansson I, Kretzschmar EI, et al. Significance of PTEN alterations in endometrial carcinoma: a population-based study of mutations, promoter methylation and PTEN protein

- expression. *Int J Oncol*. 2004;25:1615-1623.
40. Carpten JD, Faber AL, Horn C, et al. A transforming mutation in the pleckstrin homology domain of AKT1 in cancer. *Nature*. 2007;448:439-444.
 41. Chan SM, Weng AP, Tibshirani R, Aster JC, Utz PJ. Notch signals positively regulate activity of the mTOR pathway in T-cell acute lymphoblastic leukemia. *Blood*. 2007;110:278-286.
 42. Chiang MY, Xu L, Shestova O, et al. Leukemia-associated NOTCH1 alleles are weak tumor initiators but accelerate K-ras-initiated leukemia. *J Clin Invest*. 2008;118:3181-3194.
 43. Weng AP, Millholland JM, Yashiro-Ohtani Y, et al. c-Myc is an important direct target of Notch1 in T-cell acute lymphoblastic leukemia/lymphoma. *Genes Dev*. 2006;20:2096-2109.
 44. Imai T, Tokunaga A, Yoshida T, et al. The neural RNA-binding protein Musashi1 translationally regulates mammalian numb gene expression by interacting with its mRNA. *Mol Cell Biol*. 2001;21:3888-3900.
 45. Agrawal S, Eng C. Differential expression of novel naturally occurring splice variants of PTEN and their functional consequences in Cowden syndrome and sporadic breast cancer. *Hum Mol Genet*. 2006;15:777-787.
 46. Teresi RE, Zbuk KM, Pezzolesi MG, Waite KA, Eng C. Cowden syndrome-affected patients with PTEN promoter mutations demonstrate abnormal protein translation. *Am J Hum Genet*. 2007;81:756-767.
 47. Buxbaum JD, Cai G, Chaste P, et al. Mutation screening of the PTEN gene in patients with autism spectrum disorders and macrocephaly. *Am J Med Genet B Neuropsychiatr Genet*. 2007;144B:484-491.
 48. Polisenio L, Salmena L, Zhang J, et al. A coding-independent function of gene and pseudogene mRNAs regulates tumour biology. *Nature*. 2010;465:1033-1038.
 49. Salmena L, Carracedo A, Pandolfi PP. Tenets of PTEN tumor suppression. *Cell*. 2008;133:403-414.
 50. Silva A, Yunes JA, Cardoso BA, et al. PTEN posttranslational inactivation and hyperactivation of the PI3K/Akt pathway sustain primary T cell leukemia viability. *The Journal of clinical investigation*. 2008;118:3762-3774.
 51. Medyouf H, Gao X, Armstrong F, et al. Acute T-cell leukemias remain dependent on Notch signaling despite PTEN and INK4A/ARF loss. *Blood*. 2010;115:1175-1184.

SUPPLEMENTARY DATA

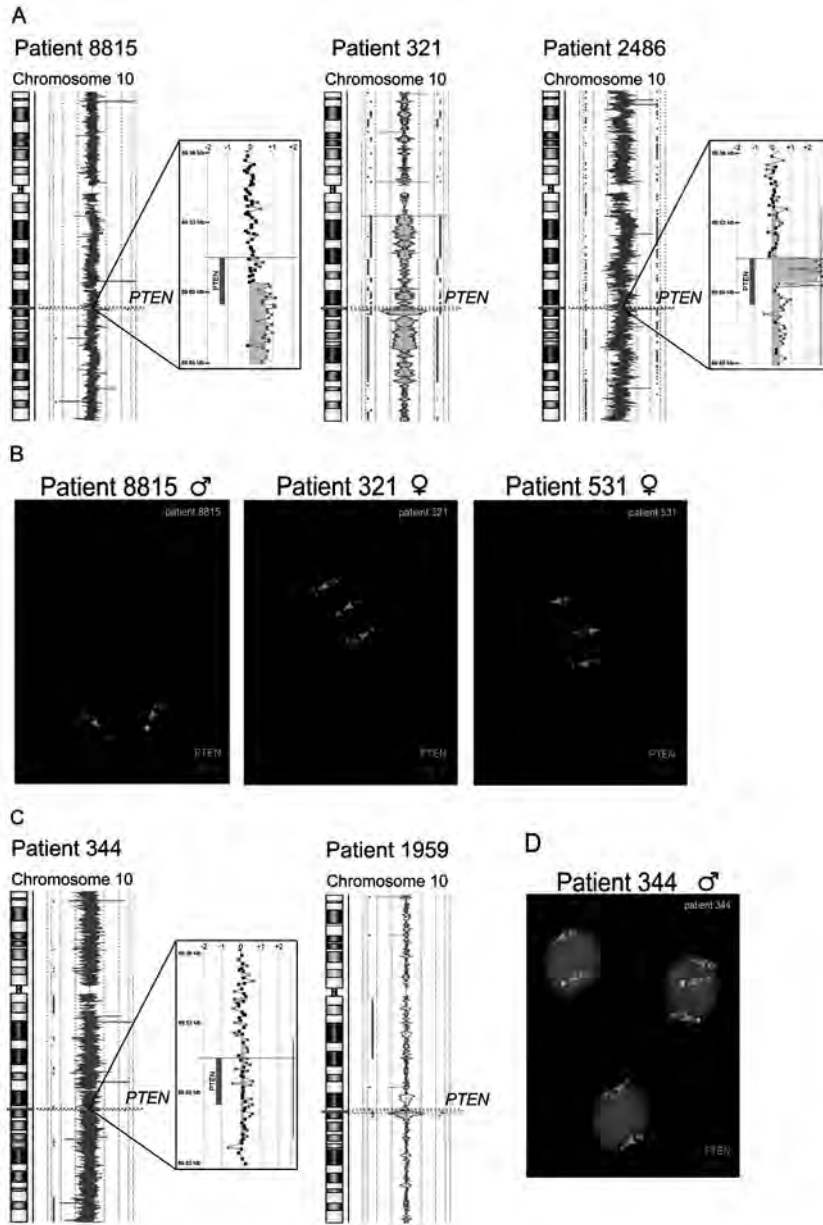


Figure S1 | *PTEN* deletions in T-ALL patients detected by array CGH and FISH analysis. (A) Array CGH and (B) FISH results of T-ALL patients with a clonal *PTEN* deletion. (C) Array CGH and (D) FISH results of patients with a subclonal *PTEN* deletion.

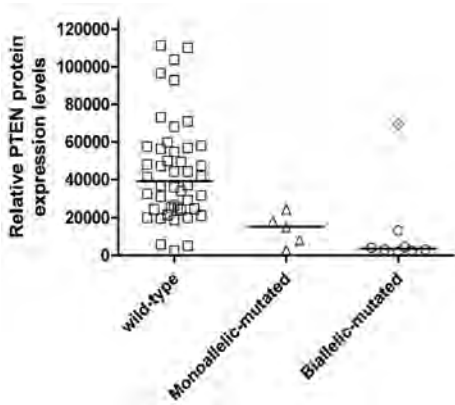


Figure S2 | PTEN protein expression levels in *PTEN* wild-type patients, *PTEN* monoallelic and biallelic-mutated T-ALL patients.

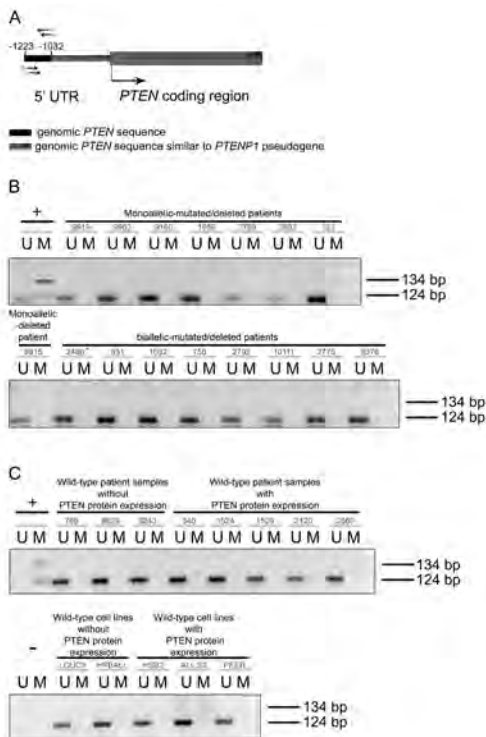


Figure S3 | **Methylation-specific PCR of the *PTEN* promoter region in T-ALL patients.** (A) Schematic overview of *PTEN* promoter area depicting overlapping sequences between the *PTEN* gene and the *PTENP1* pseudogene in gray and the unique *PTEN* sequence in black. Primers used for methylation-specific PCR are indicated by arrows where M indicates primers used for the amplification of methylated DNA and U indicates primers used for the amplification of unmethylated DNA. -1223 and -1032 indicate the numbers of base pairs before the *PTEN* start site. (B) PCR results of methylation-specific PCR in mono-allelic and bi-allelic mutated/deleted patients and (C) in *PTEN* wild-type patients and cell lines with and without *PTEN* expression. + indicates the the positive control. U shows the PCR result for unmethylated DNA (124bp) and M for methylated.

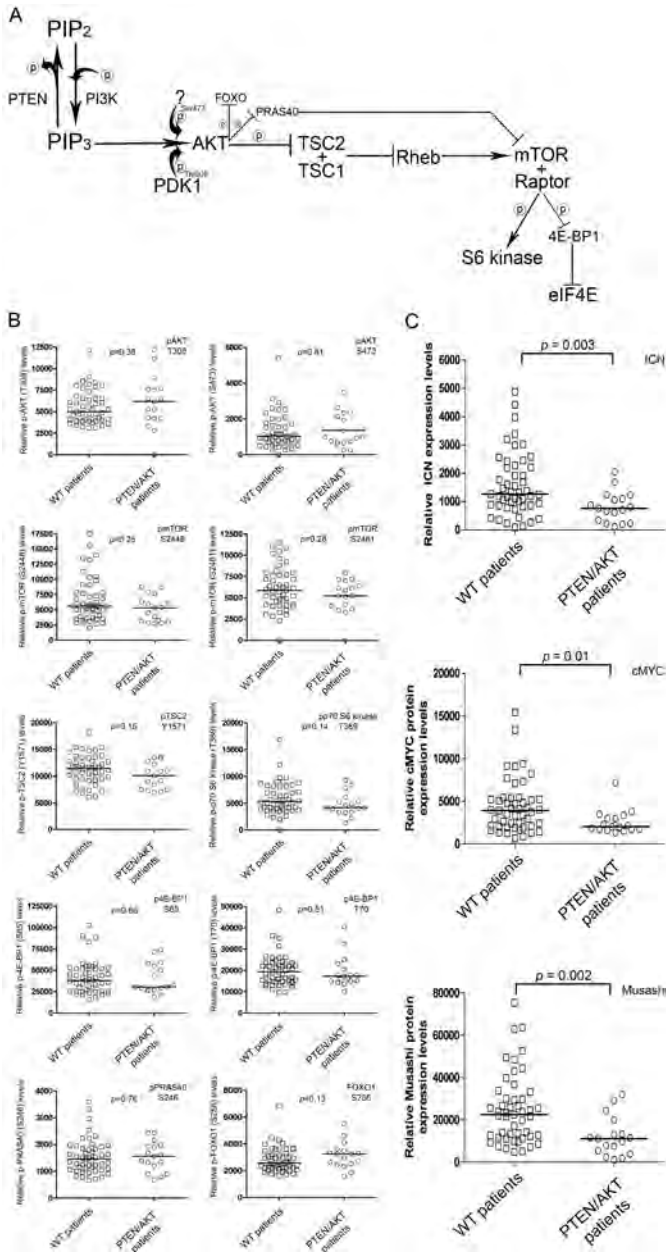


Figure S4 | Total and phosphorylated levels of PTEN/AKT and NOTCH pathways mediators in T-ALL. (A) Schematic overview of AKT and its potential downstream signaling partners. (B) The expression of phosphorylated AKT (T308 and S473) levels as well as the activation status of potential downstream signaling components in PTEN/AKT mutant versus PTEN/AKT non-mutated (wild-type) patients, analyzed by reverse-phase protein microarray. Potential downstream targets include mTOR (S2448 and S2481), p70 S6 kinase (T389), 4E-BP1 (S65 and T70), TSC2 (Y1571), PRAS40 (S246), and FOXO1 (S256). The p-value for each comparison is indicated. (C) The expression of intracellular NOTCH1 (ICN), the NOTCH1 target molecule cMYC, and the indirect NOTCH1 activator MUSASHI1/2 (MSI1/2), in PTEN/AKT mutant and PTEN/AKT non-mutated T-ALL patient samples. The p-value for each comparison is indicated.

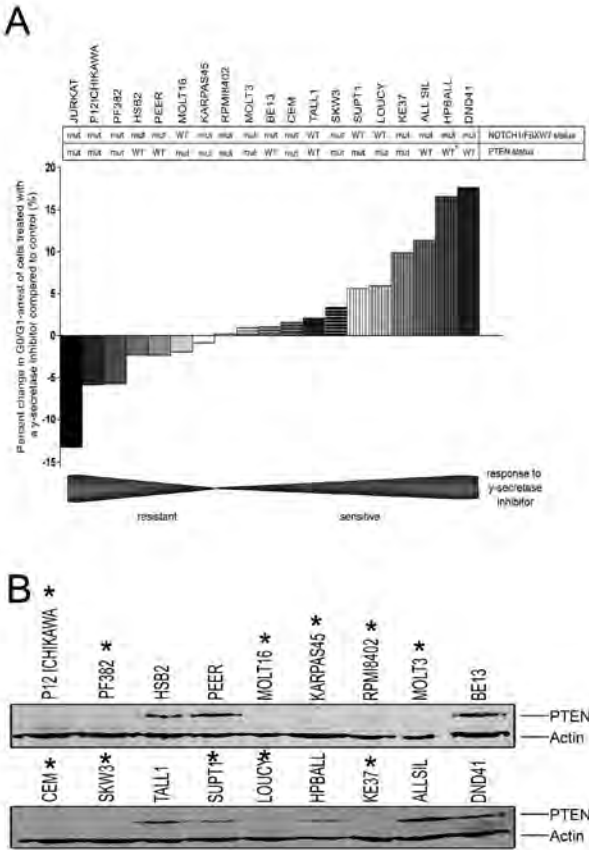


Figure S5 | *PTEN* mutations are not necessarily related with resistance towards the γ -secretase inhibitor compound E. (A) Response of indicated T-ALL cell lines towards the γ -secretase inhibitor compound E, measured by G0/G1-arrest following 96 h of γ -secretase inhibitor treatment relative to DMSO-treated control cells. Cell lines that do not undergo G0/G1-arrest are indicated as resistant cell lines, whereas cell lines that do undergo G0/G1-arrest following incubation with compound E are indicated as sensitive. *Cell lines with reduced PTEN expression through mutations, deletions or aberrant splicing. *PTEN* and *NOTCH1/FBXW7* mutational status. Genetic aberrations in the HPBALL cell line that result in low or loss of PTEN protein levels have not been identified. (B) Western blot analysis of PTEN protein levels. Cell lines have been ordered based on their compound E resistance with most resistant cell lines at the upper left corner to most sensitive cell lines in the lower right corner. β -actin is used as loading control.

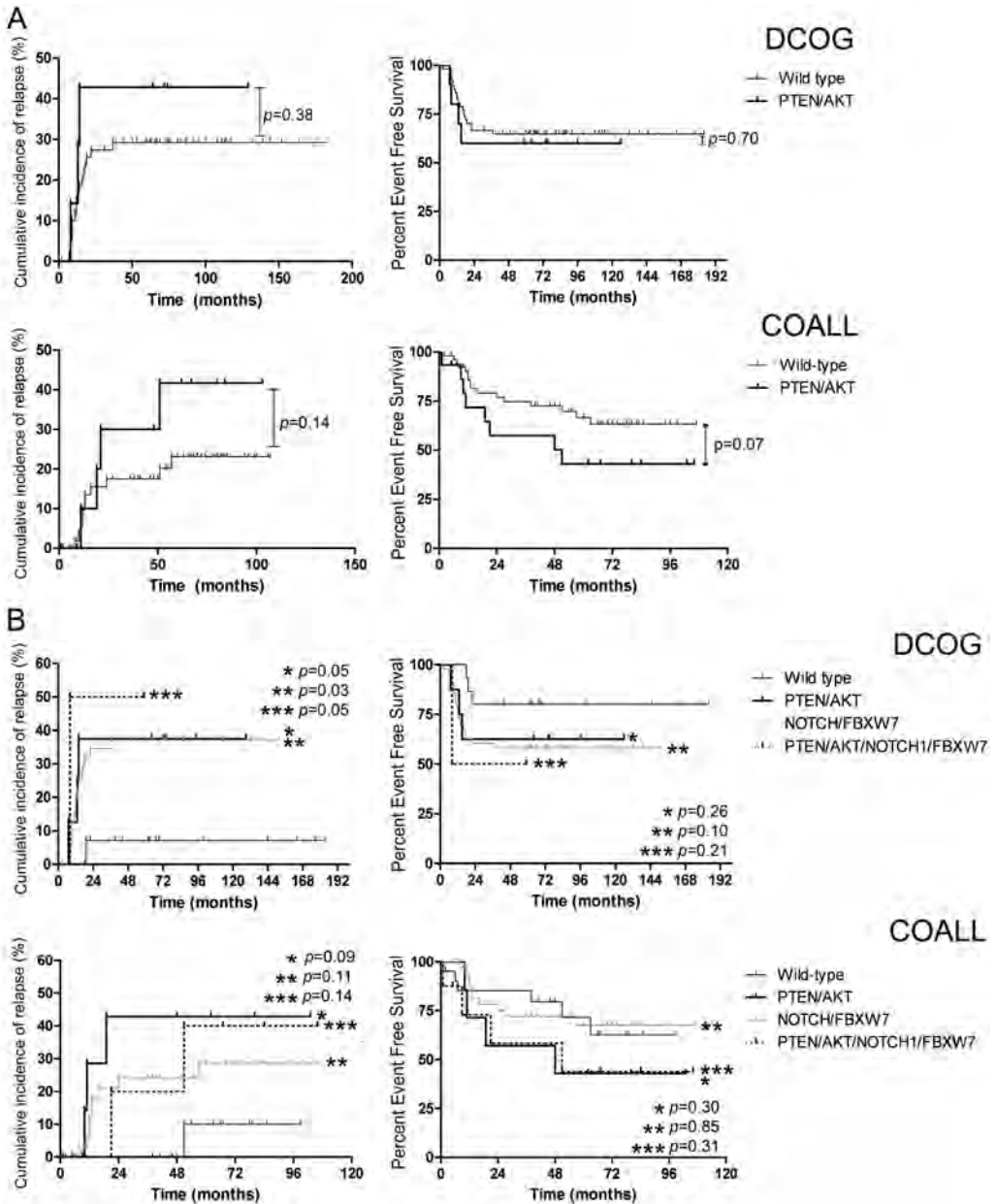


Figure S6 | Survival curves of T-ALL patients in both cohorts separately. (A) Relapse free survival and event free survival of *PTEN/AKT* wild-type (gray line) and mutant patients (black line) in DCOG and COALL cohorts. (B) Relapse free survival and event free survival of *PTEN/AKT* and *NOTCH1/FBXW7* wild-type patients (dark gray line), *PTEN/AKT* mutant (black line), *NOTCH1/FBXW7* mutant (light gray line) and of patients with *PTEN/AKT* as well as *NOTCH1/FBXW7* mutations (dotted black line) in DCOG and COALL cohorts.

4

Exon	Primer Sequence Forward	Primer sequence Reverse	Product (Bp)
PTEN exon 1	5'-AGCTTCTGCATCTCTCTC-3'	5'-TTTCGCATCCGCTACTC-3'	203
PTEN exon 2	5'-ACATTGACCACCTTTTATTACTC-3'	5'-GGTAAGCCAAAAATGATTATAG-3'	368
PTEN exon 3	5'-ATGTGTGGCTTTTGTGTGT-3'	5'-GCTCTTGGACTTCTTGACTTA-3'	229
PTEN exon 4	5'-TCAGGCAATGTTTGTAGTATT-3'	5'-ATCGGGTTTAAGTTATACAACATA-3'	175
PTEN exon 5	5'-TTGTATGCAACATTTCTAAAGTT-3'	5'-ATCTGTTTTCCAATAAATTCTCA-3'	393
PTEN exon 6	5'-ACGACCCAGTTACCATAGC-3'	5'-TAGCCCAATGAGTTGAACA-3'	405
PTEN exon 7	5'-AATCGTTTTTGGACAGTTTGGAC-3'	5'-TCACCAATGCCAGAGTAAG-5'	378
PTEN exon 8	5'-GATTGCCTTATAATAGTCTTTGTG-3'	5'-TTTTTGGACGCTGTGTACATT-3'	594
PTEN exon 9	5'-GCCTCTTAAAGATCATGTTTG-3'	5'-GGTCCATTTTCAGTTTATCA-3'	399
PTEN cDNA PCR I	5'-TCCATCTGCAGAAAGAAG-3'	5'-CAGATGATTCTTAAACAGGTAGC-3'	639
PTEN cDNA PCR II	5'-AGAGCGCTATGTGTATTAT-3'	5'-GTCCATTTTCAGTTTATCAAG-3'	764
PTEN USP	5'-TTTTGAGGTGGTTTGGGTTTTGGT-3'	5'-ACACAATCACATCCCAACACCA-3'	124
PTEN MSP	5'-TTTTTTTTCGGTTTTTCGAGGC-3'	5'-CAATCGCGTCCCAACGCCG-3'	134
PTEN promoter	5'-CCTGCATTTCCCTCTACA-3'	5'-GCTGCACGGTTAGAAAAG-3'	801
AKT1 exon 4	5'-CAGGGCCGTTTCTGTC-3'	5'-CCAGCCAGTGCTTGT-3'	434
PI3K p110 exon 10	5'-GTTGGCTAACTCAGCAGTTAC-3'	5'-TGTGCCAACTACCAATGTAGTA-3'	605
PI3K p85 exon 12+13	5'-CTGGAAACCATAGTGAACT-3'	5'-ATGGCACTGAGTTTATACATTTTC-3'	573

Table S1 | Primers used for PCR amplification of *PTEN*, *AKT* and *PI3K*.

Gene	Aberration	RQ-PCR primer/probe	FISH type	BAC clones	Refs
<i>TAL1</i>	del(1)(p32) or t(1;14)(p32;q11) or t(1;7)(p32;q34)	FW 5'-CGC TCC TAC CCT GCA AAC A-3' RV 5'-CCG AGG AAG AGG ATG CAC A-3' 5'-(FAM)-ACC TCA GCT CCG CGG AAG TTG C-(TAMRA)-3'	Fusion	Dako	Gabert et al., Leukemia 2003
<i>LMO2</i>	del(11)(p12p13)		Split	RP11-646J21 (telomeric) RP11-98C11 (telomeric) RP11-603J2 (telomeric) RP11-36H11 (centromeric) RP11-769M16 (centromeric) RP11-465C16 (centromeric)	Van Vlierbergh et al., Blood 2006
irs that were significantly associated with good or					
<i>LMO2</i>	t(11;14)(p13;q11) or t(7;11)(q34;p13)		Fusion	RP11-646J21 RP11-98C11	Van Vlierbergh et al., Blood 2006
<i>CALM-AF10</i>	t(10;14)(p13;q14)	FW 5'-TTA ACT GGG GGA TCT AAC TG-3' 5' transcript RV 5'-GCT GCT TTG CTT TCT CTT C-3' 3' transcript RV 5'-CCC TCT GAC CCT CTA GCT TC-3' 5'-(FAM)-CTT GGA ATG CCG CAA CAA TG-(TAMRA)-3'	Split Fusion	RP11-29E15 (centromeric <i>CALM</i>) RP11-12D16 (telomeric <i>CALM</i>) RP11-12D16 (telomeric <i>CALM</i>) RP11-399C16 (centromeric <i>AF10</i>)	Van Grotel et al., Haematologica 2006 Van Grotel et al., Haematologica 2006
<i>TLX1</i>	t(10;14)(q24;q11) or t(7;10)(q34;q24)	FW 5'-CTC ACT GGC CTC ACC TT-3' RV 5'-CTG TGC CAG GCT CTT CT-3' 5'-(FAM)-CCT TCA CAC GCC TGC AGA TC-(TAMRA)-3'	Split	Dako	
<i>TLX3</i>	t(5;14)(q35;q32) #	FW 5'-TCT GCG AGC TGG AAA A-3' RV 5'-GAT GGA GTC GTT GAG GC-3' 5'-(FAM)-CAA AAA CCG GAG GAC CAA GT-(TAMRA)-3'	Split	Dako	
<i>MLL</i>	11q23 rearrangements		Split	Dako	
<i>SET-NUP214</i>	del(9)(q34)	FW 5'-TTC CCG ATA TGG ATG ATG-3' RV 5'-CTT TGG GCA AGG ATT TG-3'			Van Vlierbergh et al., Blood 2006
<i>GAPDH</i>		FW 5'-GTC GGA GTC AAC GGA TT-3' RV 5'-AAG CTT CCC GTT CTC AG-3' 5'-(FAM)-TCA ACT ACA TGG TTT ACA TGT TCC AA-(TAMRA)-3'			Stam et al., Blood 2003

Table S2 | RQ-PCR primer and probes and FISH BAC-clones. Primer and probe combinations to identify the *SIL-TAL1* deletion, *CALM-AF10* 5' or 3' fusion transcripts, *TLX1* transcripts, *TLX3* transcripts, or the *SET-NUP214* gene fusion by RQ-PCR analysis. For the detection of mRNA transcripts, *GAPDH* is used as normalization control. BAC clones for the various FISH analyses to identify *TAL1* rearrangements (including the *SIL-TAL1* deletion) the *LMO2* deletion or translocation variants, the *CALM-AF10* translocation, *TLX1* translocations, the *TLX3* translocation and #other *TLX3* translocation or *MLL* rearrangements.

Patient	PTEN mutation		affected exon(s)	PTEN deletion	PTEN splicing	PTEN protein	AKT mutation	NOTCH/FBXW7 mutation
	Allele A	Allele B						
335	R129G	T231fsX24	ex5 & ex7	WT/WT	ND	+	WT	WT
344	F144fsX37	R232fsX23	ex5 & ex7	subclonal	ND	absent	ND	PEST
531*	P246fsX11	-	ex7	del/WT	ND	absent	WT	WT
750	D235fsX9	P245fsX12	ex7	ND	ND	absent	WT	PEST
1032	R232fsX13	Q244fsX8	ex7	WT/WT	ND	absent	WT	WT
1959	R129fsX4/P245fsX3	WT/-	ex5 & ex7	subclonal	ND	ND	WT	WT
2759	R232*	WT	ex7	WT/WT	ND	ND	WT	WT
2775	R233fsX10	P245fsX9	ex7	WT/WT	ND	ND	WT	HD/FBXW7
2792	R232fsX10	P243fsX18	ex7	WT/WT	ND	ND	WT	WT
9160	C249fsX10	WT	ex7	WT/WT	WT	absent	WT	WT
9376	R232fsX10	P245fsX14	ex7	WT/WT	ND	absent	WT	FBXW7
9577	L180fsX2	I305fsX7	ex6 & ex8	WT/WT	ND	absent	WT	HD
9919	T231fsX12	WT	ex7	WT/WT	ND	absent	WT	HD/FBXW7
9963	T276A	WT	ex8	WT/WT	WT	absent	WT	WT
10111	C104fsX2	K236fsX5	ex5 & ex7	WT/WT	ND	absent	WT	WT
2852	P245fsX3	WT	ex7	del/WT	altered/WT	ND	WT	WT
321	WT	-	-	del/WT	WT	absent	WT	PEST
2486	-	-	-	del/del	ND	absent	WT	WT
8815	WT	-	-	del/WT	altered	absent	WT	WT
9243	WT	WT	-	WT/WT	altered	absent	WT	WT
769	WT	WT	-	WT/WT	WT	absent	WT	FBXW7
8629	WT	WT	-	WT/WT	WT	absent	WT	HD
2781	WT	WT	-	WT/WT	ND	ND	E17K	WT
2787	WT	WT	-	ND	ND	ND	E17K	WT
3028	WT	WT	-	ND	ND	ND	E17K	FBXW7

Table S3 | PTEN and AKT aberrations in pediatric T-ALL. Homozygous mutations are marked by an asterisk; ND: not done; WT: wild-type; Del: deletion. NOTCH1-activating mutations are indicated as heterodimerization domain (HD) or proline, glutamic acid, serine, and threonine rich domain (PEST) mutations or mutations that occur in the E3-ubiquitin ligase *FBXW7* gene.

Patient	PTEN mutation		affected exon(s)	PTEN splicing	PTEN deletion	PTEN protein	AKT mutation	NOTCH/FBXW7 mutation	PTEN reference
	Allele A	Allele B							
JURKAT	P245fsX9	WT	ex7	ND	ND	ND	ND	JM/FBXW7	new
MOLT16	P245fsX12	P245fsX12	ex7	ND	ND	absent	ND	WT	new
MOLT3	D267fsX?	WT	ex8	ND	ND	absent	ND	HD/PEST	23
PF382	V84fsX?	WT	ex4	ND	ND	absent	ND	HD/PEST	23
CEM	Y28fsX?	WT	ex2	ND	ND	absent	ND	HD/FBXW7	22,23
P12ichikawa	W274X	WT	ex8	ND	ND	absent	ND	FBXW7	22,23
KARPAS45	R334*	WT	ex7	ND	ND	absent	ND	HD/FBXW7	22
RPM18402	K236fsX?	R159S	ex7	ND	ND	low present	ND	FBXW7	22,23
SUPT1	R172C	WT	ex6	ND	del/WT/WT/WT	low present	ND	WT	new
LOUCY	WT	WT	-	altered	del/WT	absent	ND	WT	22+confirmed
SKW3	ND	WT	-	ND	del/WT	absent	ND	PEST	ND
KE37	WT	WT	-	no transcript	del/WT/del/WT	absent	ND	PEST	22
HPBALL	WT	WT	-	WT	WT/WT	low present	ND	HD/PEST	22,23
HSB2	WT	WT	-	no transcript	WT/WT	+	ND	HD/FBXW7	new
PEER	WT	WT	-	ND	ND	+	ND	HD/FBXW7	new
ALLSIL	WT	WT	-	ND	ND	+	ND	HD/PEST	23
DND41	WT	WT	-	ND	ND	+	ND	HD/PEST	22,23
TALL1	WT	WT	-	ND	ND	+	ND	WT	18+confirmed
BE13	WT	WT	-	ND	ND	+	ND	HD/FBXW7	18+confirmed

Table S4 | PTEN genetics of T-ALL cell lines.

Table S5 | Patients’ characteristics and mutation overview for 146 pediatric T-ALL patients.
Available on request.

4

	<i>PTEN/AKT+NOTCH/FBXW7</i> aberration				
	WT		Mut		<i>p</i>
Total number of patients (<i>n</i> =141)	36		105		
Male	24		73		0,75
Female	12		32		
Median age (range)	7.1 (1.1-16.7)		7.6 (1.3-17.8)		0.05 □
Median WBC (range)	125 (2.0-649.0)		124 (3.0-900.0)		0.61 □
Events (<i>n</i> =49)	WT <i>n</i> (%)		Mut <i>n</i> (%)		<i>p</i>
	9		40		
relapse (%)	2	(22%)	33	(83%)	0.002 †
toxic death/2nd malignancy (%)	4/3	(78%)	4/3	(17%)	0,03
Immunophenotypic (<i>n</i> =138)	WT <i>n</i> (%)		Mut <i>n</i> (%)		<i>p</i>
Pre-T/Pro-T +	9	(23%)	30	(77%)	0,61
Cortical T +	12	(21%)	46	(79%)	0,20
Mature T +	15	(37%)	26	(63%)	0,06

Table S6 | Clinical and immunophenotypic data of *PTEN/AKT* and *NOTCH1/FBXW7*-mutated versus wild-type patients. Significant P values are indicated in bold. All P values were calculated using Pearson's chi2 test, unless indicated; WT: wild-type; Mut, mutant; P: P value; Median age indicated in years; □ Mann-Whitney-U test; WBC: white blood cell count; white blood cell counts are indicated as number of blasts (x109/L); †Fisher's exact test.

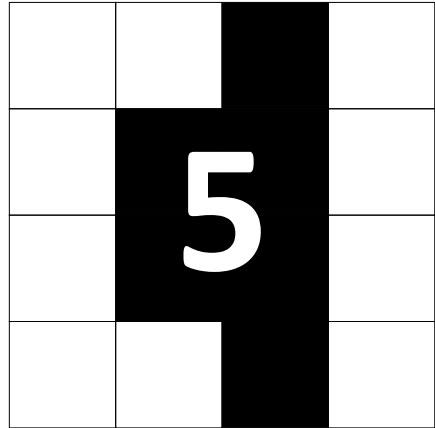
Clinical (<i>n</i> =146)	DCOG		COALL		Overall stratified analysis	
	5-yrs RFS (% ± SD)	<i>P</i>	5-yrs RFS (% ± SD)	<i>P</i>	5-yrs RFS (% ± SD)	<i>P</i>
male (<i>n</i> =100) vs female (<i>n</i> =46)	84 ± 8 vs 66 ± 7	0.19	91 ± 6 vs 62 ± 9	0,03	88 ± 5 vs 65 ± 5	0,01
age <10 (<i>n</i> =96) vs ≥10 yrs (<i>n</i> =50)	62 ± 11 vs 74 ± 6	0.53	82 ± 8 vs 69 ± 8	0.31	74 ± 7 vs 72 ± 5	0,81
WBC <50 (<i>n</i> =31) vs ≥50 *10 ⁹ /liter (<i>n</i> =114)	69 ± 6 vs 80 ± 13	0.4	70 ± 7 vs 84 ± 10	0.13	70 ± 5 vs 83 ± 8	0,09
Cytogenetics (<i>n</i> =146)						
TAL1 + (<i>n</i> =27) vs TAL1 - (<i>n</i> =119)	92 ± 7 vs 66 ± 6	0.07	62 ± 15 vs 76 ± 6	0.27	79 ± 9 vs 71 ± 5	0.47
LMO2 + (<i>n</i> =14) vs LMO2 - (<i>n</i> =132)	57 ± 19 vs 73 ± 6	0.43	75 ± 22 vs 74 ± 6	0.73	64 ± 15 vs 74 ± 4	0.70
TLX3 + (<i>n</i> =29) vs TLX3 - (<i>n</i> =117)	57 ± 12 vs 75 ± 6	0.11	54 ± 17 vs 78 ± 6	0.17	56 ± 10 vs 77 ± 4	0,04
TLX1 + (<i>n</i> =8) vs TLX1 - (<i>n</i> =138)	80 ± 18 vs 70 ± 6	0.54	73 ± 6 vs 100 ± 0	0.46	86 ± 13 vs 72 ± 4	0,37
HOXA + (<i>n</i> =13) vs HOXA - (<i>n</i> =133)	40 ± 23 vs 74 ± 6	0.15	83 ± 15 vs 73 ± 6	0.62	64 ± 15 vs 74 ± 4	0,53
□ MEF2C+ (<i>n</i> =6) vs MEF2C - (<i>n</i> =140)	73 ± 6 vs 71 ± 6	0.56	80 ± 18 vs 100 ± 0	0.85	83 ± 15 vs 72 ± 4	0,65
□ NKX2-1+ (<i>n</i> =7) vs NKX2-1 - (<i>n</i> =139)	100 ± 0 vs 70 ± 6	0.40	100 ± 0 vs 71 ± 7	0.20	100 ± 0 vs 71 ± 4	0.13
† unknowns (<i>n</i> =42) vs knowns (<i>n</i> =104)	75 ± 10 vs 70 ± 7	0.81	78 ± 10 vs 73 ± 7	0.88	77 ± 7 vs 71 ± 5	0.78
Gene expression clusters (<i>n</i> =117) ‡						
TAL/LMO + (<i>n</i> =53) vs TAL/LMO - (<i>n</i> =64)	73 ± 10 vs 67 ± 10	0.70	69 ± 10 vs 79 ± 7	0.36	71 ± 7 vs 75 ± 6	0.70
TLX + (<i>n</i> =30) vs TLX - (<i>n</i> =87)	60 ± 14 vs 74 ± 8	0.25	65 ± 13 vs 79 ± 6	0.36	63 ± 9 vs 77 ± 5	0.15
Proliferative + (<i>n</i> =19) vs Proliferative - (<i>n</i> =98)	83 ± 15 vs 68 ± 8	0.40	89 ± 11 vs 73 ± 7	0.40	87 ± 9 vs 71 ± 5	0,20
Immature(ETP)ALL + (<i>n</i> =15) vs Immature(ETP)ALL - (<i>n</i> =102)	50 ± 35 vs 70 ± 7	0.97	91 ± 9 vs 72 ± 7	0.23	85 ± 10 vs 71 ± 5	0,32
Type B mutations						
<i>PTEN/AKT</i> mutant (<i>n</i> =25) vs wild-type (<i>n</i> =117)	60 ± 16 vs 71 ± 6	0.38	57 ± 15 vs 78 ± 6	0.14	59 ± 11 vs 75 ± 4	0,09
<i>NOTCH1/FBXW7</i> mutant (<i>n</i> =90) vs wild-type (<i>n</i> =51)	62 ± 8 vs 82 ± 8	0.10	70 ± 8 vs 80 ± 9	0.41	66 ± 5 vs 81 ± 6	0,08
<i>PTEN/AKT/NOTCH1/FBXW7</i> mutant (<i>n</i> =105) vs wild-type (<i>n</i> =36)	62 ± 7 vs 93 ± 7	0,03	68 ± 7 vs 90 ± 10	0.07	65 ± 5 vs 92 ± 6	0,005
<i>PHF6</i> mutant (<i>n</i> =12) vs wild-type (<i>n</i> =51)	73 ± 13 vs 67 ± 7	0.69	ND	ND	ND	ND
<i>WT1</i> mutant (<i>n</i> =17) vs wild-type (<i>n</i> =129)	63 ± 17 vs 72 ± 6	0.47	49 ± 23 vs 77 ± 6	0.21	59 ± 13 vs 75 ± 4	0.17
Del 9p21 (<i>n</i> =88) vs wild-type (<i>n</i> =25)	72 ± 7 vs 63 ± 17	0.67	68 ± 8 vs 94 ± 6	0.06	70 ± 5 vs 84 ± 7	0.24

Table S7 | Significant log rank P values for DCOG or COALL cohort analyses are indicated in bold; RFS: relapse free survival; SD: standard deviation; P: P value; WBC: white blood cell count; □ Different genetic aberrations have been identified that all result in the activation of the *MEF2C* or *NKX2-1/NKX2-2* oncogenes that define novel genetic T-ALL subtypes; † All patients who have one of the above described cytogenetic aberrations (known) versus all patients without any of these above described aberrations (unknown); ‡ 113 out of 117 T-ALL patients included in the gene expression profiling study had a known *PTEN* and *AKT* mutation status. T-ALL patients were assigned to the *TAL/LMO* group based on the presence of *TAL1* or *LMO2* rearrangements or by having a *TAL/LMO* expression signature.

	Univariate analyses using Cox regression model			
	<i>n</i>	Hazard ratio	95% confidence interval	<i>P</i>
male vs female	146	0,3	0.122 - 0.820	0,02
<i>TLX3</i>	146	2,1	1.030 - 4.339	0,04
<i>PTEN/AKT/NOTCH1/FBXW7</i>	141	6,1	1.456 - 25.310	0,01
	Multivariate analyses using Cox regression model			
	<i>n</i>	Hazard ratio	95% confidence interval	<i>P</i>
male vs female	146	0,37	0.141 - 0.959	0,04
<i>TLX3</i>	146	1,7	0.843 - 3.629	0,13
<i>PTEN/AKT/NOTCH1/FBXW7</i>	141	5,6	1.341 - 23.437	0,02

Table S8 | NOTCH1-activating and PTEN/AKT mutations predict for poor outcome in pediatric T-ALL. Univariate and multivariate Cox's regression analyzes using relapse free survival for various parameters that were significantly associated with good or poor relapse free survival.

CHAPTER



***PTEN* micro-deletions in T-cell acute lymphoblastic leukemia are caused by illegitimate RAG-mediated recombination events**

Rui D. Mendes^{1,9}, Leonor M. Sarmiento^{2,9}, Kirsten Canté-Barrett¹, Linda Zuurbier¹, Jessica G.C.A.M. Buijs-Gladdines¹, Vanda Póvoa², Willem K. Smits¹, Miguel Abecasis³, J. Andres Yunes⁴, Edwin Sonneveld⁵, Martin A. Horstmann^{6,7}, Rob Pieters^{1,8}, João T. Barata^{2,10} and Jules P.P. Meijerink^{1,10}

¹Department of Pediatric Oncology/Hematology, Erasmus MC Rotterdam-Sophia Children's Hospital, Rotterdam, the Netherlands; ²Instituto de Medicina Molecular, Faculdade de Medicina da Universidade de Lisboa, Lisboa, Portugal; ³Cardiologia Pediátrica Medico Cirúrgica, Hospital Sta. Cruz, Lisboa, Portugal; ⁴Centro Infantil Boldrini, Campinas, SP, Brazil; ⁵Dutch Childhood Oncology Group (DCOG), the Hague, the Netherlands; ⁶German Cooperative Study Group for Childhood Acute Lymphoblastic Leukemia (COALL), Hamburg, Germany; ⁷Research Institute Children's Cancer Center Hamburg, Clinic of Pediatric Hematology and Oncology, University Medical Center Hamburg-Eppendorf, Hamburg, Germany; ⁸Princess Maxima Center for Pediatric Oncology, Utrecht, Netherlands

⁹These authors are co-first authors; ¹⁰These authors contributed equally to this work

Blood 2014: Epub ahead of print

ABSTRACT

PTEN inactivating mutations and/or deletions is an independent risk factor for relapse just like NOTCH-activating mutations or male gender for T-cell acute lymphoblastic leukemia (T-ALL) patients treated on DCOG or COALL protocols. Some monoallelic mutated or *PTEN* wild-type patients lack *PTEN* protein, implying that additional *PTEN* inactivation mechanisms exist. We show that *PTEN* is inactivated by small deletions affecting a few exons only in 8% of pediatric T-ALL patients. These micro-deletions were clonal in 3% and sub-clonal in 5% of patients. Conserved deletion breakpoints are flanked by cryptic RAG-recombination signal sequences (cRSS) and frequently have non-template derived nucleotides inserted in between breakpoints, implying that micro-deletions are the result of illegitimate RAG recombination activity. Identified cRSSs drive RAG-dependent recombination in a reporter system as efficiently as *bona fide* RSSs that flank gene segments of the T-cell receptor locus. Remarkably, equivalent micro-deletions were also detected in thymocytes of healthy individuals. Similar to other *PTEN* aberrations, micro-deletions strongly associate with the TALLMO-subtype characterized by *TAL1* or *LMO2* rearrangements. Primary and secondary xenotransplantation of *TAL1*-rearranged leukemia allowed development of leukemic subclones with newly acquired *PTEN* micro-deletions. Ongoing RAG activity may therefore actively contribute to the acquisition of pre-leukemic hits, clonal diversification and disease progression.

INTRODUCTION

T-cell acute lymphoblastic leukemia (T-ALL) is an aggressive leukemia caused by the malignant transformation of T-cell precursors in the thymus. T-ALL represents 10-15% of pediatric acute leukemias. Despite major therapeutic improvements due to treatment intensification and refined risk-adapted stratification during the past decade, ~30% of T-ALL cases relapse with very poor prognosis.¹

T-cell transformation is characterized by aberrant expression of oncogenic transcription factors combined with inactivation of tumor suppressor genes (e.g. *PTEN*, *CDKN2A*) and/or activation of the NOTCH1 pathway.² The ectopic expression of oncogenes is typically caused by chromosomal rearrangements—the so-called type A hits—that place T-ALL oncogenes under the control of strong T-cell specific promoters or enhancer elements.^{3,4} In many cases, the analysis of translocation breakpoint regions revealed illegitimate V(D)J recombination to be involved in this process, through the binding of the recombination activating gene (RAG)-1/2 proteins to conserved DNA sequences that resemble authentic recombination signal sequences (RSS).⁵ These recurrent chromosomal rearrangements activate several oncogenes, such as *TAL1*, *LMO2*, *TLX3*, *TLX1* or *NKX2-1/NKX2-2*, which are believed to represent the clonal drivers that occur in a nearly mutually exclusive pattern.^{2,6}

Besides the type A mutations, recurrent genetic aberrations that affect cell viability and/or proliferation—the so-called type B hits—are found in nearly all T-ALL genetic subgroups. Type B mutations include NOTCH1-activating mutations affecting *NOTCH1* and *FBXW7* that are found in over 60% of pediatric T-ALL patients (⁷⁻¹¹; reviewed in ¹²), as well as less frequent events such as *IL7R* mutations in around 10% of T-ALL cases.^{13,14} In addition, mutations in the phosphatase and tensin homolog (*PTEN*) tumor suppressor gene have been associated with poor prognosis,¹⁵⁻¹⁸ resulting in overactive PI3K–AKT signaling that drives enhanced cell proliferation and cell metabolism, and impairs apoptosis.^{16,19,20} *PTEN* is considered to be a haploinsufficient tumor suppressor gene, because *PTEN* dose determines cancer susceptibility.²¹⁻²³ The majority of *PTEN* aberrations in T-ALL are deletions affecting the entire *PTEN* locus or mutations that truncate the membrane binding C2-domain.^{15,18}

In our previous studies, we detected *PTEN* aberrations in 13-20% of T-ALL patients ^{18,24} and revealed that those mutations are especially associated with *TAL* or *LMO* rearrangements and nearly absent in *TLX3*-rearranged T-ALL.¹⁸ In general, *PTEN* mutated T-ALL appears to be devoid of NOTCH1-activating mutations.¹⁸ Interestingly, we did not observe differential *AKT* activation when comparing *PTEN* mutant/deleted with wild-type patient samples, indicating that other mechanisms may influence the PI3K–AKT pathway. In this respect, non-deletional posttranslational inactivation of *PTEN*,²⁴ rare mutations in *PIK3CA* (encoding PI3K) and *AKT* themselves ¹⁶, or PI3K–AKT pathway activation downstream of activated NOTCH1 have been described.¹⁵ However, none of these mechanisms explain the absence of *PTEN* protein in some T-ALL patient samples that have retained at least one *PTEN* wild-type allele.¹⁸

In this study, we have used multiplex ligation-dependent probe amplification (MLPA) to

investigate copy-number variations among *PTEN* exons to detect potential additional *PTEN* deletions. We identified *PTEN* micro-deletions in T-ALL patient samples and we provide evidence that these are driven by illegitimate RAG-mediated recombination events.

MATERIALS AND METHODS

Samples

A total of 146 primary pediatric T-ALL patient samples were enrolled in the Dutch Childhood Oncology Group (DCOG) protocols ($n=72$)²⁵⁻²⁷ or the German Co-Operative Study Group for Childhood Acute Lymphoblastic Leukemia study (COALL-97) ($n=74$) were included in this study.²⁸ The patients' parents or legal guardians provided informed consent to use leftover diagnostic material for research in accordance with the Institutional Review Board of the ErasmusMC (Rotterdam, the Netherlands), the Ethics Committee of the City of Hamburg, Germany, and the Declaration of Helsinki. Leukemia cells were harvested and enriched from blood or bone marrow samples as described previously,²⁹ all containing >90% of leukemic cells.

Normal thymocytes were isolated from thymic tissue obtained from children undergoing cardiac surgery at the Hospital Sta. Cruz, Centro Hospitalar de Lisboa Ocidental (Lisboa, Portugal) as described.^{24,30} Informed consent and approval by the local ethical committee were obtained in accordance with the Declaration of Helsinki.

Multiplex ligation-dependent probe amplification (MLPA) reaction

For MLPA analysis, the SALSA MLPA kit (MRC-Holland, Amsterdam, the Netherlands) was used in combination with the P200-A1 Human DNA reference-1 probemix kit (MRC-Holland). Two synthetic left and right hybridization probe oligonucleotide (LPO and RPO) pairs were designed per exon for all 9 exons of *PTEN*. Probe pairs were designed according to the manufacturer guidelines, and obtained from IDT (Coralville, USA). Probe pairs were combined into a probemix with a concentration of 4nM per oligonucleotide (**Table S1**). Reactions were carried out in a model 2320 thermocycler (Applied Biosystems, Bleiswijk, the Netherlands). MLPA fragment analysis was performed using GeneMarker V1.85 (Softgenetics, State College, PA, USA).

Breakpoint Mapping and PCR-based screening

To map breakpoints for *PTEN* exons 2-3 and 4-5 deletions, multiple forward or reverse primers were designed for *PTEN* introns 1, 3 and 5 (**Table S2** and **S3**). Specific primers (**Table S4**) were selected for *PTEN* exon 2-3 and 4-5 breakpoint screening. Positive reactions were directly sequenced for both strands or following cloning into the TOPO TA vector (Life Technologies). Sequence reactions were run on the 3130x capillary sequencer (Applied Biosystems) and analyzed using CLC Main Workbench software (Aarhus, Denmark).

Computational detection of putative RAG recombination signal sequences

The human *PTEN* gene (ENSG00000171862) was screened for the presence of cryptic RAG recombination signal sequences (cRSS) using the PERL software algorithms developed by Cowell *et al.*³¹ Mouse 12- and 23-RSSs (n=356) from all TCR and Ig loci were used for modeling. Both the program and 12-/23-RSSs were available at <http://www.duke.edu/~lgcowell/>. The program computes RSS information content (RIC) scores for 12-spacer RSSs (i.e. 28-bp sequences comprising the heptamer, a 12-bp spacer and the nonamer sequences: RIC12) or 23-spacer RSSs (i.e. 39-bp sequences comprising the heptamer, a 23-bp spacer and the nonamer sequences: RIC23) to predict cryptic RSSs (cRSS) based on a comparison to the RIC score for actual immunoglobulin and T-cell receptor RSS. RSSs that potentially function within the range of actual antigen receptor loci RSSs are predicted to score above the -38,81 as RIC12 and -58,45 as RIC23 thresholds. RSSs that potentially function within the range predicted for degenerated RSSs, i.e. the so-called cryptic RSSs (cRSS), score below these thresholds but above the background (e.g. the mean of RIC scores determined for non-RSS DNA sequences: -60,07 for RIC12 and -77,76 for RIC23) as previously described.³¹

Generation of GFPi-*PTEN* cRSS reporter constructs and recombination assay

To measure efficiencies of predicted cRSSs in mediating recombination of GFPi-mRFP reporter constructs, PCR amplified *PTEN* cRSS1-4 or defined RSS control sequences were cloned into this reporter construct as previously described.³² Predicted *PTEN* cRSS1-4 or control RSSs were tested in combination with a consensus 12 or 23 RSS (**Figure 3B**). All RSS or cRSS used in the GFPi-mRFP constructs are summarized in Table S5.

Recombination assays were carried out as described,³² with minor adaptations. Briefly, HEK293T cells grown in standard culture conditions were seeded at 2×10^5 cells per well in 12-well plates. After 24h, cells were transfected with a transfection mix that contains 5 μ L of Lipofectamine 2000 (Invitrogen, Carlsbad, CA, USA), 300 μ L of Optimem (Gibco, Life Technologies, Paisley, UK), 0.8 μ g of CMV-RAG1,³² 0.7 μ g of CMV-RAG2,³² and 2.5 μ g of a GFPi-mRFP construct variant. Medium was replaced 16h after transfection. Cells were harvested at 48h following transfection, and analyzed by flow cytometry for GFP and RFP fluorescence using a FACSAria III (BD Bioscience, Madrid, Spain). Data analysis was performed using the FlowJo software (TreeStar Inc., Ashland, OR).

Xenotransplantation

NOD-SCID-IL2R γ^{null} (NSG) mice were bred and housed under specific pathogen free (SPF) conditions at the Experimental Animal Facility of ErasmusMC. All experiments have been approved by the committee on animal welfare of ErasmusMC and are in compliance with Dutch legislation. Sets of 6–10 week old mice were intravenously injected with $1-5 \times 10^6$ human bone marrow leukemic cells. Upon signs of illness, mice were euthanized and leukemic cells were collected from the different organs. Likewise, primary transplanted leukemic cells from bone marrow, thymus or spleen were retransplanted.

Statistics

Statistics was performed using IBM SPSS Statistics 21 software (IBM, Armonk, NY, USA). The Pearson's Chi-square was used to test statistical significant differences for nominal distributed data, the Fisher's exact test in tests where the number of patients tested in individual groups was lower than five and the Mann-Whitney-U test for continuously distributed data. Data were considered significant when $p \leq 0.05$ (two-sided). Differences in relapse-free survival were tested by using the log-rank test. Proportional risk for relapse was done by univariate and multivariate Cox regression analysis. The recombination efficiencies of cRSSs were compared using a one-way ANOVA with the Bonferroni's multiple comparison post-test and significant differences were considered when $p \leq 0.05$.

RESULTS

Identification of *PTEN* micro-deletions

In our previous study, we identified various T-ALL primary patient samples that lack *PTEN* protein expression and seemed *PTEN* wild-type or that contained an inactivating mutation or *PTEN* deletion in only one allele (summarized in **Table 1**).¹⁸ To identify additional *PTEN* inactivating mechanisms, we performed MLPA analysis to screen for potential micro-deletions affecting single or a few *PTEN* exons that had been missed by array-CGH and FISH analyses. We analyzed 146 T-ALL patient samples for copy-number alterations in any of all 9 coding exons. Heterozygous micro-deletions were detected in 3 T-ALL patients (**Figure 1A**), encompassing exons 2 and 3 in 2 patients (#21, #11) and exons 4 and 5 in another patient (#20). Accordingly, 2 out of the 3 patients (#11, #20) demonstrated defective *PTEN*-splicing with previously unknown underlying genetic aberrancies.¹⁸ A fourth patient (#12) was identified with a homozygous deletion of exons 2 and 3 that was confirmed by high-resolution array-CGH analysis (**Figure 1A, B**).

In order to clone the breakpoint regions of these micro-deletions, a PCR-based strategy was designed for introns 1 and 3 (patients #21, #11 and #12) and intron 3 and 5 (patient #20) (**Figure 2A, B**), and resulting positive reactions were cloned and sequenced. These analyses predicted micro-deletions of ~65Kb that encompassed exons 2-3 and of ~11Kb that encompassed exons 4-5 (**Figure 2B**). The homozygously deleted patient (#12) revealed different breakpoints that point to independent deletion events for each allele, with insertion of random bases in between breakpoints for one allele (**Figure 2B**). Breakpoints for the exon 2-3 micro-deletion in patient #21 were identical to breakpoints of one allele of patient #12 and also lacked insertion of random bases. T-ALL patient #11 had a similar exon 2-3 deletion that shared the identical breakpoint in intron 3 but had an alternate breakpoint in intron 1 (**Figure 2A-C**). Breakpoints for the fourth T-ALL patient #20 with a micro-deletion that affected exons 4 and 5 were located in introns 3 and 5 (**Figure 2B**). All three types of micro-deletions result in out-of-frame *PTEN* transcripts (**Figure 2C**).

Patient	PTEN mutation		PTEN Deletion (FISH/Array-CGH)	PTEN Deletion (MLPA)	Genomic breakpoint PCR	Aberrant transcript	PTEN protein	Cytogenetic aberration	NOTCH/FBXW7 mutation
	Allele A	Allele B							
Clonal inactivation of 2 alleles									
1	R129G	T231fsX24	-	-	-	ND	Mutant	LMO3	-
2	F144fsX37	R232fsX23	Subcl Del	-	-	ND	Absent	LMO2	PEST
3	P246fsX11	-	Het Del	Het Del exons 2-	-	ND	Absent	SIL-TAL1	-
4	D235fsX9	P245fsX12	ND	ND	-	ND	Absent	CALM-AF10	PEST
5	R232fsX13	G244fsX8	-	-	-	ND	Absent	Unknown	-
6	R233fsX10	P245fsX9	-	-	-	ND	ND	Unknown	FBXW7
7	R232fsX10	P243fsX18	-	-	-	ND	ND	TLX1	-
8	R232fsX10	P245fsX14	-	-	-	ND	Absent	LMO2	FBXW7
9	L180fsX2	1305fsX7	-	-	Intron 1-3 Del (type II; Subcl)	ND	Absent	NKX2-5	HD
10	C104fsX2	K236fsX5	-	-	-	ND	Absent	SIL-TAL1	-
11	P245fsX3	-	ND	Het Del exons 2-	Intron 1-3 Del (type II, Clonal)	in1/2-ex4	ND	MYC	-
12	-	-	Hom Del/FISH negative	Hom Del exons	2 Intron 1-3 Del variants (type I, Clonal)	in1/2-ex4	Absent	SIL-TAL1	-
Clonal inactivation of 1 allele									
13	R129fsX4/P245fsX3	-	Subcl Del	Het Del exons 1-	-	ND	ND	Unknown	-
14	R232(STOP)	-	-	-	-	-	ND	SIL-TAL1	-
15	C249fsX10	-	-	-	Intron 1-3 Del (type I; Subcl)	-	Absent	Unknown	-
16	T231fsX14	-	-	-	-	-	Absent	NKX2-1	HD/FBXW7
17	T276A	-	-	-	Intron 1-3 Del (type I; Subcl)	-	-	Unknown	-
18	-	-	Het Del	Het Del exons 1-	Intron 1-3 Del (type I; Subcl)	WT	Absent	Unknown	PEST
19	-	-	Het Del	Het Del exons 3-	Intron 1-3 Del (type I; Subcl)	Altered	Absent	SIL-TAL1	-
20	-	-	-	Het Del exons 4-	Intron 3-5 Del (type III, Clonal) / Intron 1-3 Del (type I; Subcl)	ex3-ex6	Absent	SIL-TAL1	-
21	-	-	ND	Het Del exons 1-	Intron 1-3 Del (type I, Clonal)	in1/2-ex4	ND	SIL-TAL1	HD
22	-	-	Het Del	Het Del exons 2-	-	ND	ND	Unknown	-
Subclonal inactivating event only									
23	R232fsX (Subcl)	-	-	-	-	-	ND	SIL-TAL1	-
24	-	-	-	-	Intron 1-3 Del (type I; Subcl)	-	ND	ND	HD/PEST
25	-	-	ND	-	Intron 1-3 Del (type I; Subcl)	-	ND	SIL-TAL1	-
26	-	-	-	-	Intron 1-3 Del (type I; Subcl)	-	ND	Unknown	-
Others									
27	-	-	-	-	-	-	Absent	TAL2	FBXW7
28	-	-	-	-	-	-	Absent	TAL1	HD

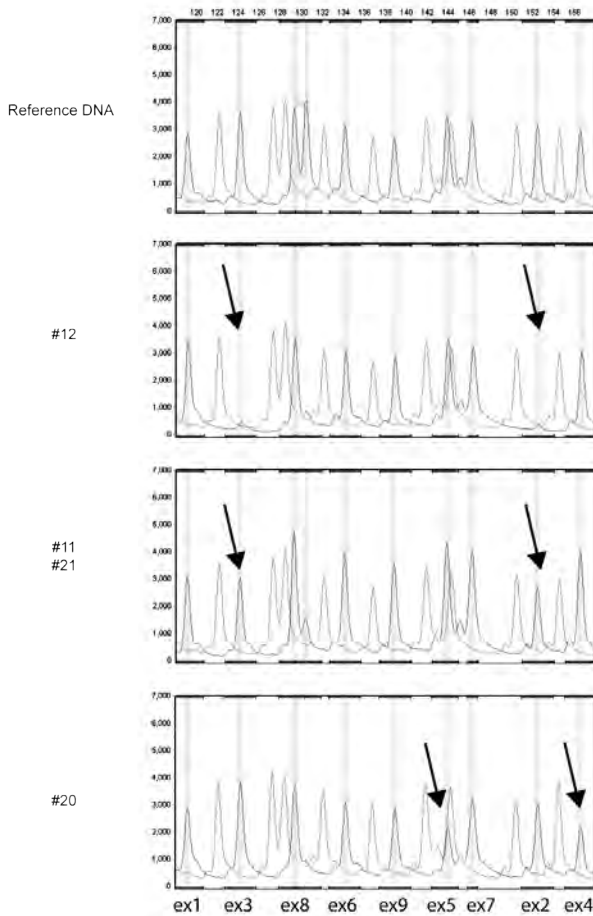
Table 1 | *PTEN* genetics of T-ALL patients. *PTEN* frameshift mutations are indicated with the number of encoded amino acids in the alternative reading frame. *PTEN* deletion status was determined by fluorescent in situ hybridization (FISH), array-comparative genomic hybridization (array-CGH) and/or multiplex ligation-dependent probe amplification (MLPA). Introns harboring the genomic breakpoints of *PTEN* deletions and/or micro-deletions have been indicated. Exons for alternative spliced *PTEN* transcripts are indicated. Abbreviations: Del, deletion; FS, frameshift; HD, *NOTCH1* heterodimerization domain mutation; Het, heterozygous; Hom, homozygous; PEST, *NOTCH1* mutation in the proline, glutamine, serine and threonine-rich C-terminal region; Subcl, subclonal.

5

	Univariate analyses using Cox regression model			
	<i>n</i>	Hazard ratio	95% confidence interval	<i>P</i>
Male gender	146	3.278	1.267-8.486	0.014
TLX3	146	2.044	1- 4.175	0.05
NOTCH1/FBXW7	141	2.077	0.946-4.560	0.068
§PTEN/AKT aberrations	142	1.675	0.787-3.567	0.18
	Multivariate analyses using Cox regression model			
	<i>n</i>	Hazard ratio	95% confidence interval	<i>P</i>
Male gender	141	2.910	1.117 – 7.577	0.029
TLX3	141	2.018	0.921 – 4.424	0.079
NOTCH-activating	141	2.588	1.083 – 6.183	0.032
§PTEN/AKT aberrations	141	3.407	1.254-7.400	0.014

Table 2 | NOTCH1-activating and *PTEN/AKT* mutations predict for poor outcome in pediatric T-ALL treated on DCOG ALL7/8/9 or COALL-97/03 protocols. Univariate and multivariate Cox regression analyses stratified for DCOG or COALL treatment protocols using relapse-free survival for various parameters that were significantly associated with poor relapse-free survival (see supplementary table S7). §Includes T-ALL patients that do not express *PTEN* protein while lacking *PTEN* aberrations, but does not include patient samples with *PTEN* aberrations only on the subclonal level.

A



B

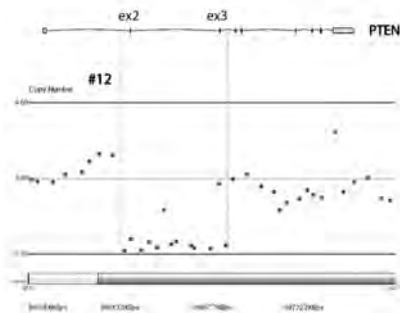
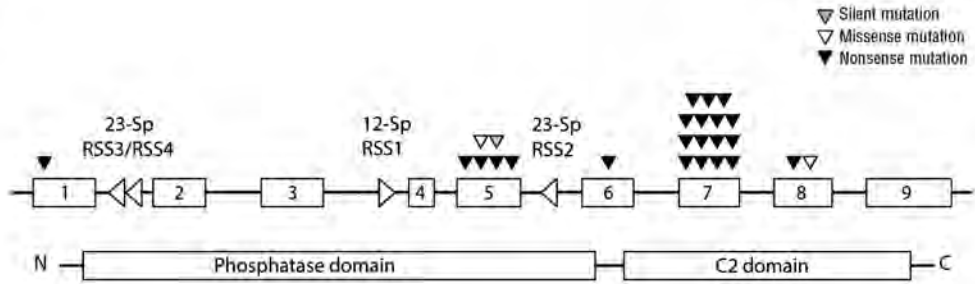


Figure 1 | Identification of *PTEN* micro-deletions in T-ALL patients. (A) MLPA electropherograms of normal reference DNA and representative examples of T-ALL patients with heterozygous or homozygous *PTEN* micro-deletions affecting exons 2-3 or a heterozygous deletion of exons 4-5. Fluorescence intensities of amplified PCR products for specific *PTEN* exons are shown. PCR product sizes are shown at the top. Each arrow points to a homo- or heterozygously deleted exon. (B) Array-CGH plot exhibiting the homozygous *PTEN* exon 2-3 micro-deletion in one T-ALL patient sample.

A



B

Type-I DNA breakpoints

Patient	brk intr 1	n-bases	brk intr 3	Clonality status
WT	TCAT <u>ATATTTTGT (23) TAGGGTG</u> <u>cRSS1</u>	NNNNNNNN (65Kb) NNNNNNNN	<u>CACAGAT (12) ACATAAACA</u> <u>cRSS1</u>	CCCC
21	TCAT <u>ATATTTTGT (23) TAGGGTG</u>		CACAGAT (12) ACATAAACA	CCCC Clonal
12	TCAT <u>ATATTTTGT (23) TAGGGTG</u>		CACAGAT (12) ACATAAACA	CCCC Clonal
12	TCAT <u>ATATTTTGT (23) TAGGGTG</u>	GACTGAACCTCT	----GAT (12) ACATAAACA	CCCC Clonal
24	TCAT <u>ATATTTTGT (23) TAGGGTG</u>	TAGGGGAG	CACAGAT (12) ACATAAACA	CCCC Subclonal
25	TCAT <u>ATATTTTGT (23) TAGGGTG</u>	ATCCC	CACAGAT (12) ACATAAACA	CCCC Subclonal
19	TCAT <u>ATATTTTGT (23) TAGGGTG</u>	GTCCA	CACAGAT (12) ACATAAACA	CCCC Subclonal
15	TCAT <u>ATATTTTGT (23) TAGGGTG</u>	GAT	CACAGAT (12) ACATAAACA	CCCC Subclonal
20	TCAT <u>ATATTTTGT (23) TAGGGTG</u>		CACAGAT (12) ACATAAACA	CCCC Subclonal
17	TCAT <u>ATATTTTGT (23) TAGGGTG</u>		CACAGAT (12) ACATAAACA	CCCC Subclonal
26	TCAT <u>ATATTTTGT (23) TAGGGT-</u>	TCA	CACAGAT (12) ACATAAACA	CCCC Subclonal

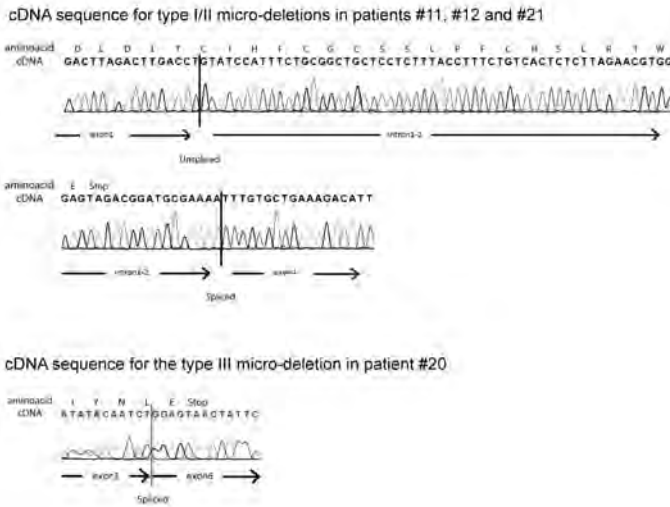
Type-II DNA breakpoints

Patient	brk intr 1	n-bases	brk intr 3	Clonality status
WT	TCCA <u>GCTTTAGAT (23) TACAGTG</u> <u>cRSS4</u>	NNNNNNNN (65Kb) NNNNNNNN	<u>CACAGAT (12) ACATAAACA</u> <u>cRSS1</u>	CCCC
11	TCCA <u>GCTTTAGAT (23) TACAGTG</u>	GCCCTCG	---AGAT (12) ACATAAACA	CCCC Clonal
9	TCCA <u>GCTTTAGAT (23) TACAGTG</u>	GGTTT	CACAGAT (12) ACATAAACA	CCCC Subclonal

Type-III DNA breakpoints

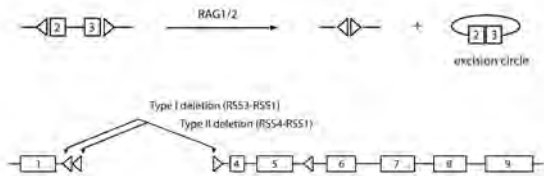
Patient	brk intr 3	n-bases	brk intr 5	Clonality status
WT	GTAG <u>CACAGAT (12) ACATAAACA</u> <u>cRSS1</u>	NNNNN (11Kb) NNNNNNN	<u>TGTTCTCAA (23) TACTGTG</u> <u>cRSS2</u>	TAAACCCCTAACTTTAG
20	GTAG -----	AATTCGGGTCTGCCAG	-----	TTAG Clonal

C



D

Signal joint formation in exon 2-3 micro-deletions



Coding joint formation in exon 4-5 micro-deletion

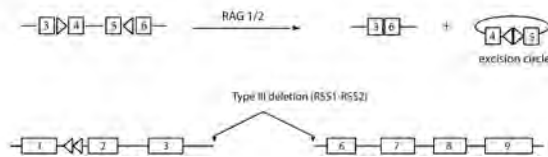


Figure 2 | Breakpoints of *PTEN* micro-deletions. (A) Schematic representation of the *PTEN* gene. Missense mutations are represented by open triangles above the exons, whereas a silent mutation is presented as a filled grey triangle as shown before¹⁸. Nonsense insertion/deletion mutations are indicated by a filled black triangle. Left or right-pointing open triangles in introns 1, 3 and 5 represent cRSSs. (B) Sequences of cloned intron 1-3 type I and type II breakpoints and the intron 3-5 type III breakpoint for T-ALL patients with *PTEN* micro-deletions. Cryptic recombination signal sequences (cRSS) are indicated by a box with the canonic CAC trinucleotide sequences or the corresponding GTG nucleotides in heptamer sequences indicated in bold and underlined. Insertion of non-template, random nucleotides are shown in bold. (C) Examples of sequence traces of cDNA resulting from type I, II and III micro-deletions. (D) Involvement of specific cRSSs in illegitimate RAG-mediated recombination events resulting in types I and II micro-deletions (signal joint) and aberrant *PTEN* splice variant or the type III with the aberrant exon 4-5 micro-deletion *PTEN* transcript (coding joint).

As MLPA does not allow for sensitive detection of subclones with micro-deletions, we performed PCR analysis to screen the T-ALL cohort for similar micro-deletions. Seven additional patients were identified with deletions affecting exons 2-3 that were similar to the breakpoints as observed in patients #21 and #12 (**Figure 2B**). Based on the conservation of breakpoints, this micro-deletion was denoted as a type I micro-deletion. One additional patient was identified with breakpoints similar to patient #11, therefore this deletion was denoted as a type II micro-deletion. The deletion affecting exons 4 and 5 as identified in patient #20 was accordingly denoted as a type III micro-deletion. These deletions had not been detected before by array-CGH, FISH or MLPA analyses. One patient sample (#20) had already been identified by MLPA as having a clonal micro-deletion affecting exons 4 and 5, but also contained a subclonal type I micro-deletion in exons 2 and 3 as detected by PCR (**Figure 2B** and **Table 1**). In another case (#19), array-CGH had revealed a heterozygous *PTEN* deletion of exons 3-9, but now PCR also revealed a subclonal type I exon 2-3 micro-deletion (**Table 1**). Sequencing of the breakpoints in these additional T-ALL cases revealed that five out of the seven type I deletions and the type II deletion involved the insertion of unique, random nucleotide sequences, thereby excluding false positives due to PCR contamination. Notably, the PCR product for these patient samples as visualized by gel electrophoresis was much weaker than those for the 4 patient samples with clonal micro-deletions (data not shown). This strongly indicates that these deletions must be present on the subclonal level and therefore only detectable by specific PCRs. Overall, we have identified *PTEN* micro-deletions in 11 out of 146 T-ALL patients (8%), comprising a total of 13 deletional events. Only 4 patients presented these mutations at the clonal level.

The *PTEN* breakpoints are flanked by cryptic RAG recombination signal sequences

The conservation of breakpoints among patient samples and the inclusion of non-template derived nucleotides by terminal deoxynucleotidyltransferase (TdT)³³ in most breakpoint regions pointed to a RAG-mediated deletion mechanism. We then searched for the presence of cryptic RAG recombination signal sequences (cRSS) that could function as putative RAG-mediated recombination signals, such as the RSS involved in T- or B-cell receptor gene segment rearrangements.³⁴ Analysis of sequences directly flanking the breakpoints immediately revealed typical CAC canonic trinucleotides (**Figure 2B** and **Table S5**), which is a hallmark of the heptamer sequences of RSSs. The search for nearby nonamer sequences with A-nucleotide enrichment revealed a putative 12-spacer cRSS in intron 3 with a 5' to 3' orientation (cRSS1). A 23-spacer RSS was identified that directly flanks the breakpoint in intron 5 (cRSS2), and two others were identified flanking both breakpoints in intron 1 (cRSS3 and cRSS4; **Figure 2A, B** and **Table S5**). All 23-spacer cRSSs (cRSS2, cRSS3 and cRSS4) are present in a 3' to 5' orientation with respect to the *PTEN* reading frame orientation, and are therefore correctly positioned to allow illegitimate RAG-mediated recombinations with cRSS1 (**Figure 2A, C**). In this scenario, RAG1/2 molecules bind a pair of 12- and 23-RSSs resulting in two DNA double-strand breaks adjacent to each heptamer. Most micro-deletion breakpoints are the consequence of heptamer-to-heptamer sequence fusions resembling signal joints of excision circles that are generated during normal T-

or B-cell receptor gene segment rearrangements (**Figure 2D**, top): Types I and II micro-deletions result from cleaved DNA sequences 3-prime of cRSS3 or cRSS4, respectively, that are fused to sequences 5-prime of cRSS1. This retains both cRSSs in the genomic sequences that flank the deletion breakpoints as depicted in Figure 2D. The type III deletion resembles a typical coding joint that results from cleaved DNA sequences 5-prime of cRSS1 that are fused to sequences 3-prime of cRSS2 resulting in the loss of cRSSs from the genomic sequence (**Figure 2D**, bottom). T- or B-cell receptor coding joints give rise to fused gene segments with potential exonuclease processing of both ends and incorporation of random nucleotides whereby directly flanking RSSs and intervening DNA sequences are lost as excision circles. For the type III deletion of patient #20 (**Figure 2B**), this led to the fusion of sequences 5-prime of cRSS1 to sequences of 3-prime of cRSS2 with loss of 14 nucleotides and incorporation of 17 GC-rich N-nucleotides.

Cryptic RSS prediction using the Positional Information Algorithm

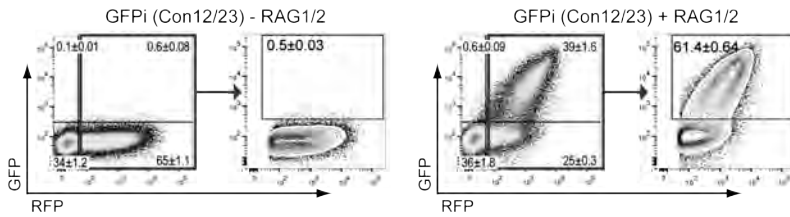
To further characterize these cRSSs and estimate their recombination potential, we scanned the human *PTEN* locus using the Positional Information Algorithm designed by Cowell and colleagues³¹ that calculates RSS Information Content (RIC) score.³¹ Cryptic RSSs with RIC scores close to RIC score threshold levels that discriminate bona-fide functional RSSs flanking gene segments of antigen receptor loci from cRSSs (i.e. -38.81 for 12-spacer RSSs and -58.45 for 23-RSSs) were further investigated.³¹ This search in the *PTEN* locus predicted a 12-spacer cRSS1 with a strong RIC score of -34.23 as well as 23-spacer cRSS2 (-55.59) and cRSS3 (-59.78) with RIC scores that were close to the threshold levels separating RSSs from cRSSs. A 23-spacer cRSS4 was predicted with a RIC score of -75.59 that is barely above the mean background RIC score value for 39-nucleotide non-RSS DNA sequences (-77.76). Thus, the obtained RIC scores for cRSS1, cRSS2 and cRSS3 strongly support *PTEN* micro-deletions as RAG-mediated recombination events with similar recombination potential to that of bona-fide RSSs flanking immunoglobulin V(D)J gene segments.

Cryptic RSS1-4 support RAG-mediated recombination *in vitro*

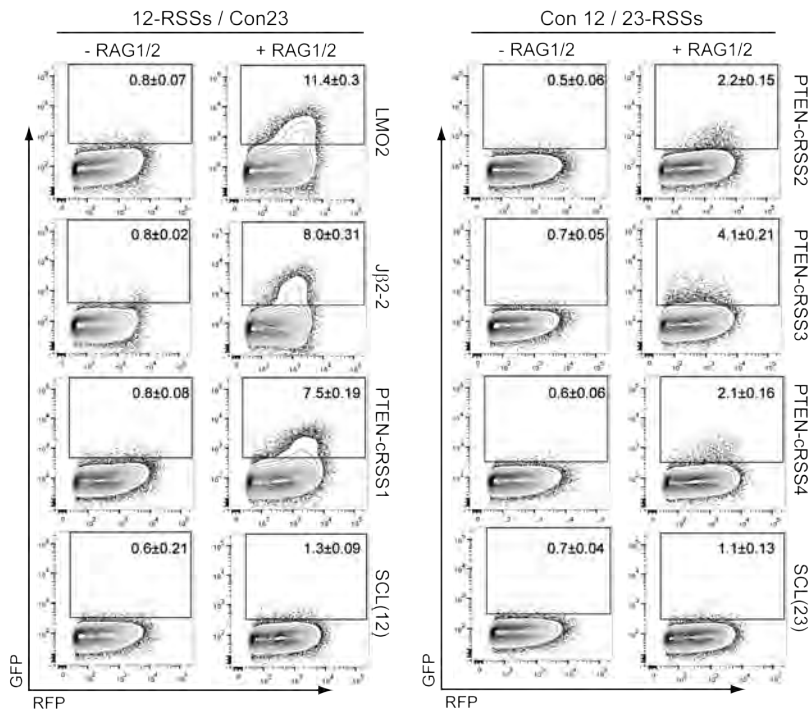
We then tested whether the predicted cRSS1-4 could functionally mediate RAG recombination events. We used the GFPi-mRFP RAG reporter construct³² (**Figure 3A**), in which the 12-spacer cRSS1 was cloned in combination with a consensus 23-spacer RSS. Also, the 23-spacer RSSs (cRSS2, cRSS3 and cRSS4) were cloned in combination with a consensus 12-spacer RSS. RAG-mediated recombination activities were tested in HEK293T cells. Recombination efficiency of each variant GFPi-cRSS-mRFP construct was measured by flow cytometry as the frequency of GFP-positive (recombination-positive) cells within the population of RFP-positive (transfected) cells (**Figure 3A**). Indeed, all four *PTEN* cRSSs were able to mediate RAG-dependent recombination of the GFPi substrate (Figure 3B). Recombination efficiencies were $7.5 \pm 0.19\%$ for cRSS1 (**Figure 2B**, left panel), $2.2 \pm 0.15\%$ for cRSS2, $4.1 \pm 0.21\%$ for cRSS3 and $2.1 \pm 0.16\%$ for cRSS4 (right panel). For comparison, the putative 12-spacer cRSS SCL(12)³² or the 23-spacer cRSS SCL(23)³⁵ from the human *SCL* gene yielded $1.3 \pm 0.09\%$ and $1.1 \pm 0.13\%$ of GFP-positive cells, respectively. Both of

A

GFPi (MSCV-GFPinverted-IRES-RFP)



B



C

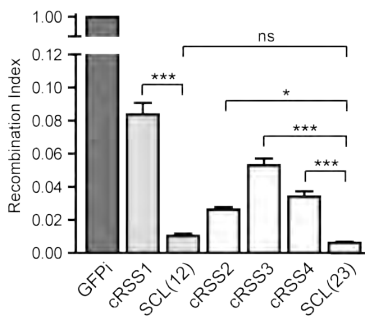


Figure 3 | Intronic *PTEN* cryptic RSS mediate RAG recombination events. (A) Upper panel: Linear representation of the GFPi reporter construct that results in the inversion of GFP coding sequence during RAG-mediated recombination, and consequent GFP expression. The inverted GFP sequence (light green box) is flanked by a proximal 12-spacer RSS (light grey triangle) and a distal 23-spacer RSS (dark grey triangle) followed by the IRES-RFP as transfection control reporter (red box). GFP positivity is a measure for recombination potential. Lower panel: Control *in vitro* RAG recombination assay; flow cytometry analysis of HEK293T cells transiently transfected with either an irrelevant, mock vector (in the absence of RAG1/2 expression vectors; negative control) or the GFPi-reporter construct containing the consensus 12- and 23-RSS in the presence of RAG1/2 expression vectors.³² The flow cytometry plots show the expression of GFP and RFP within gated live cells defined by FSC and SSC parameters (not shown) and the values represent the percentage of each cell population in the quadrants. The gate used to discriminate RFP-positive from RFP-negative cells is depicted by a red square and used for the contour plot analysis. The efficiency of recombination is indicated as the percentage of GFP-positive (recombination positive) cells within the RFP-positive (transfected) population. (B) Flow cytometry analysis of HEK293T cells transiently transfected with the GFPi variant constructs containing specific 12-spacer cRSS (LMO2, SCL/TAL1, *PTEN*-cRSS1 or the J β 2.2-RSS) site combined with the consensus 23-spacer RSS (left panel). The GFPi variant constructs containing the consensus 12-RSS³² was combined with 23-spacer *PTEN* cRSS2, cRSS3, cRSS4 or the control SCL/TAL1 23-spacer cRSS version (right panel). The human LMO2 12-spacer cRSS and the mouse J β 2.2 *bona fide* RSS were used to establish the range of recombination activities for low-efficiency RSSs as measured by the GFPi reporter assay. The 12- and 23-spacer versions of the human SCL/TAL1 cRSS were used to define the lower limit of detection of cRSS function in this reporter assay. Average percentage \pm SD of GFP⁺ cells in the RFP⁺ population are derived from 4-5 independent experiments. (C) Recombination index was determined by normalizing the recombination efficiencies of each indicated reporter to that of GFPi Con12/23 and recombination efficiencies were calculated subtracting the GFP background of each respective unrecombined control. Values represent the mean \pm SEM of 3 independent experiments with 3 replicates per condition; * $p < 0.05$; ** $p < 0.01$ and *** $p < 0.0001$.

these SCL cRSSs were used as references for the lower limit of detection in the GFPi-mRFP RAG reporter assay, as these do not give rise to distinct GFP-positive cell populations in the reporter assay. In contrast, the 12-spacer RSS that flanks the J β 2-2 gene segment of the mouse *TCRB* locus yielded $8.0 \pm 0.31\%$ of GFP-positive cells. Also, the 12-spacer cRSS that is involved in recurrent LMO2 translocations in T-ALL⁵ yielded $11.4 \pm 0.30\%$ of GFP-positive cells. These reporters highlight the capability of the recombination assay to measure low-efficiency RSS and cRSS activities. Despite the low frequencies of recombination, cRSS2-4 reporters give rise to distinct populations of GFP-positive cells (**Figure 3B**), in contrast to SCL(12) and SCL(23) cRSSs. Moreover, the efficiencies of recombination of *PTEN* cRSS1-4 differed significantly from the those of SCL(12) or SCL(23) cRSSs (**Figure 3C**). These results strongly support the involvement of predicted cRSS1-4 in *PTEN* micro-deletions in illegitimate RAG-mediated recombination events. Additionally, the recombination potential of these cRSSs are in line with the observed frequencies of type I micro-deletions (cRSS3-cRSS1) versus type II (cRSS4-cRSS1) and type III (cRSS1-cRSS2) micro-deletions in T-ALL patients (**Figure 2B**).

RAG-mediated *PTEN* deletions in xenografted human T-ALL cells

Subclonal micro-deletions in *PTEN*, even in patients that already had undergone clonal inactivating events affecting one allele, strongly imply that acquisition of micro-deletions is an ongoing phenomenon in T-ALL leading to clonal diversity.³⁶ To test this, we performed primary and secondary xenotransplantation experiments into NSG mice (**Figure 4A**) using TAL1-rearranged T-ALL blasts from patient (#24) at diagnosis that had a subclonal micro-deletion (**Figure 4B**). Several months post-transplantation, mice developed overt leukemia. Primary (X1)

and secondary (X2) xenotransplanted material was then analyzed for the presence of *PTEN* micro-deletions in bone marrow, thymus, spleen and liver biopsies. Using MLPA analysis, no *PTEN* micro-deletions were detected (data not shown), indicating that the subclonal *PTEN* micro-deletion in the diagnostic patient material had not been clonally selected following xenotransplantation. Three distinct, subclonal *PTEN* micro-deletions were detected by PCR in thymocyte and liver biopsies: One (X1-24 thymus-1) was identical to the micro-deletion as originally identified in this patient (**Figure 4B**), whereas 2 novel micro-deletions were detected suggesting that these had occurred upon serial retransplantation.

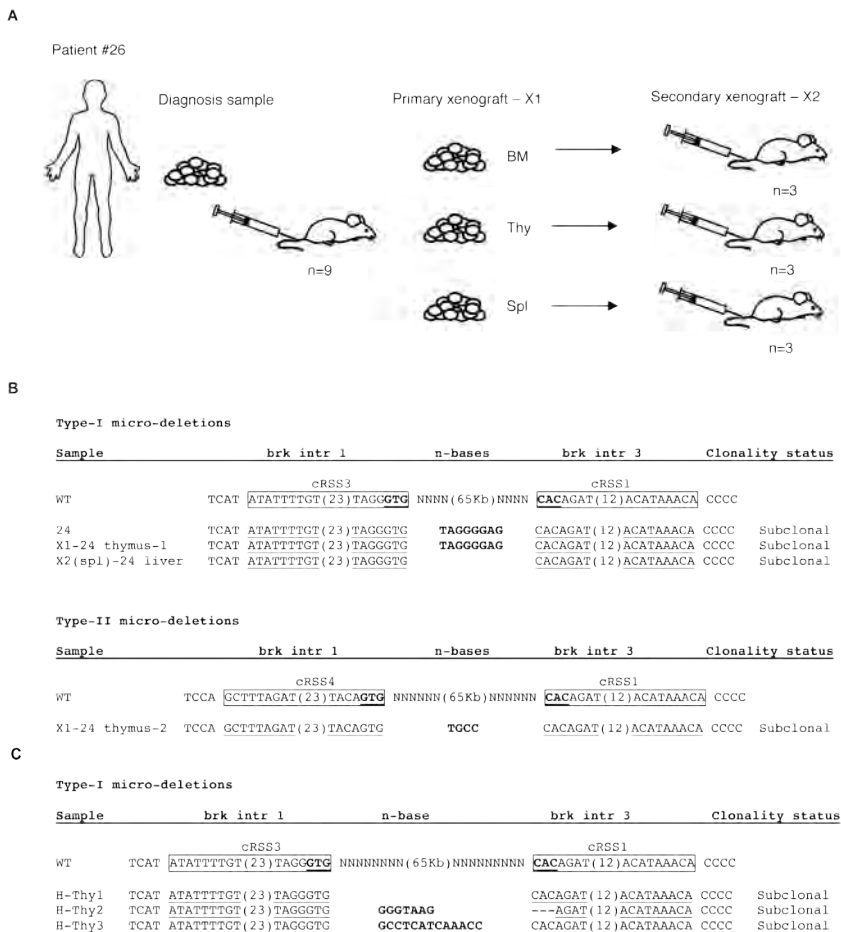


Figure 4 | *PTEN* micro-deletions in xenotransplants of a T-ALL primary patient sample and in human thymocytes from healthy individuals. (A) Schematic representation of the xenotransplantation strategy. Several months post-transplant of the patient's (#24) leukemic cells into immunodeficient NSG mice (n=9), we collected cells from bone marrow (BM), thymus (Thy), spleen (Spl) and liver. Primary (X1) and secondary (X2) xenotransplanted material was then analyzed for the presence of any of the three different *PTEN* micro-deletions. (B) Breakpoint sequences of *PTEN* micro-deletions as detected in samples from primary (X1) and secondary (X2) xenotransplanted mice. Canonic CAC trinucleotide sequences or the corresponding GTG nucleotides in heptamer sequences are indicated in bold and underlined. (C) Sequences of the breakpoints for *PTEN* type I micro-deletions as identified in thymocytes of healthy individuals (H-Thy1 – H-Thy3).

***PTEN* deletions are associated with *TALLMO* T-ALL patients**

PTEN aberrations have been associated with a low incidence of NOTCH1-activating mutations, but with a high incidence of rearrangements in *TAL1*- and/or *LMO2*-related oncogenes.¹⁸ We now extend these findings, totaling 26 out of 146 T-ALL patients (18%) that have *PTEN* aberrations including point, missense or nonsense mutations, entire locus deletions and/or micro-deletions at the clonal or subclonal level as summarized in **Table 1**. Twelve patients had clonally inactivated *PTEN* on both alleles and 10 patients on one allele. Evidence for subclonal *PTEN* aberrations was found in 11 patients, seven of whom also had clonally inactivated *PTEN* at least in one allele. The other four patients had either a subclonal missense mutation (patient #23) or subclonal micro-deletions (3 patients) only. Still, for 8 T-ALL patients for whom protein data were available, absence of *PTEN* protein could not be solely explained by the genetic aberrations found, suggesting that additional *PTEN* inactivating mechanisms await identification. Overall, our previously observed association with *TAL* or *LMO*-rearranged leukemia¹⁸ became considerably more significant ($p=0.003$; **Table S6**). Also, the significance levels for absence of these mutations in *TLX3*-rearranged T-ALL ($p=0.002$; **Table S6**) and reduced overlap with NOTCH1-activating mutations were further strengthened ($p=0.001$, **Table S6**).

***PTEN* aberrations and outcome**

We then investigated the relationship of *PTEN/AKT* aberrations with outcome. Our results do not support observations³⁶ that *PTEN*-inactivated T-ALL subclones become selected during disease progression giving rise to relapse. Therefore, we regarded T-ALL patients with subclonal *PTEN* aberrations as wild type patients in outcome analyses. *PTEN/AKT* aberrant T-ALL patients, including those patients without *PTEN* protein expression, were not significantly associated with poor outcome in both treatment cohorts (5yrs RFS for *PTEN/AKT* mutant patients is $64\pm 15\%$ versus $70\pm 6\%$ for wild type patients on DCOG protocols and $57\pm 15\%$ versus $76\pm 6\%$ for patients on COALL protocols). This is due to the fact that *PTEN/AKT* mutations and NOTCH-activating mutations predominantly behave as mutually exclusive mutations. In addition, NOTCH-activating mutations have a strong trend towards poor outcome (5yrs RFS for NOTCH-activated patients is $62\pm 8\%$ versus $82\pm 8\%$ for wild type patients on DCOG protocols and $68\pm 8\%$ versus $80\pm 9\%$ for patients on COALL protocols, (stratified $p=0.06$ (for protocol); and supplementary Table S7).³⁷ However, if NOTCH-activated and *PTEN/AKT* mutated T-ALL patients are being compared to wild type patients, wild type patients demonstrate significantly fewer relapses (stratified $p=0.04$; **Figure 5**), albeit having more frequent events including toxic deaths and secondary malignancies.¹⁸ Using the Cox regression proportional hazard method, NOTCH-activating and *PTEN/AKT* mutations were investigated along with male gender and the presence of *TLX3* rearrangements that are negatively related with poor outcome (Supplementary **Table S7** and **Table 2**). Even though both NOTCH1-activating mutations and *PTEN/AKT* mutations did not significantly predict for increased risk for relapse in univariate analyses, both were identified as strong, independent risk factors along with male gender in a multivariate analysis (**Table 2**).

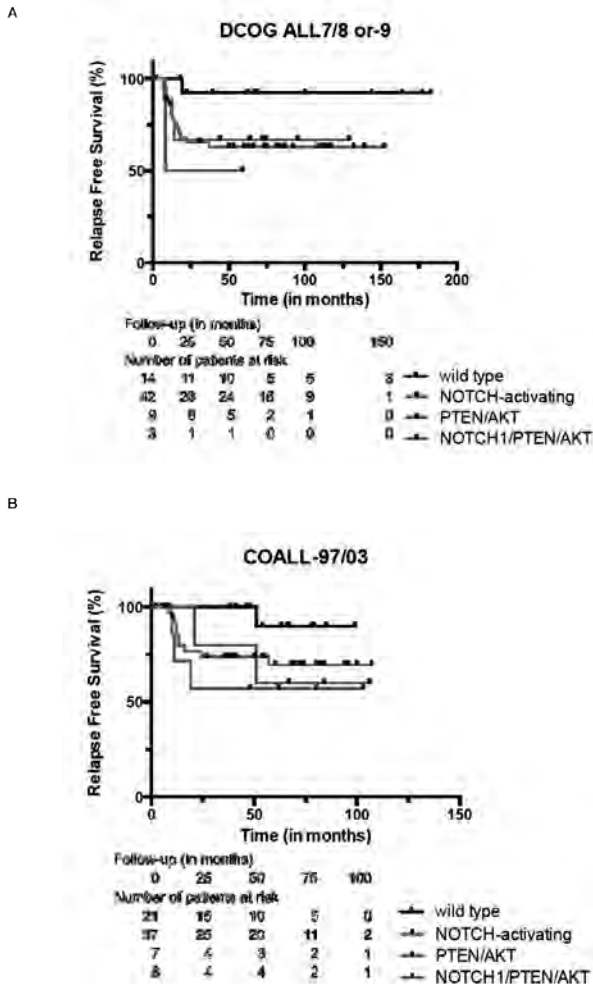


Figure 5 | T-ALL patients lacking *PTEN/AKT* mutations and NOTCH-activating mutations have a good outcome. Relapse free survival curves (RFS) for T-ALL patients treated on (A) Dutch DCOG ALL7/8 or 9 protocols or (B) German COALL-97/03 protocols. Green line; NOTCH-activating mutations including mutations in *NOTCH* and *FBXW7*, red line; *PTEN*-inactivating or *AKT*-activating mutations, blue line; NOTCH-activating mutations and *PTEN*-inactivating or *AKT*-activating mutations combined, black line; wild type for *NOTCH/FBXW7* and *PTEN/AKT*. Tick-marks in figures refer to patients that are lost from further follow-up. The numbers of patients included at various time points in these studies have been shown.

Illegitimate RAG-mediated *PTEN* micro-deletions in healthy human thymocytes

The presence of recombination-prone cRSSs in *PTEN* intron sequences led us to speculate that micro-deletions may occur in healthy thymocytes. Screening DNAs that were isolated from thymocytes of non-leukemic children for the presence of *PTEN* micro-deletions by PCR revealed evidence for subclonal type I deletions in 3 out of 11 (27%) thymocyte biopsies. Two of those micro-deletions had unique random nucleotide sequences inserted in between the breakpoints (**Figure 4C**), ruling out false PCR positivity due to contamination. Thus, RAG-mediated *PTEN* micro-deletions are not exclusive to T-ALL, but also occur during normal T-cell development.

DISCUSSION

PTEN has been identified as a haploinsufficient tumor suppressor gene,²¹⁻²³ for which gene mutations and/or deletions have been associated with poor outcome in T-ALL in various^{17,18,38,39} but not all studies.^{16,40} For T-ALL patients treated on DCOG ALL-7/8/9 or COALL97/03 treatment protocols, we demonstrate that clonal PTEN inactivating aberrations or loss of PTEN protein is an independent factor that predicts for relapse just like NOTCH-activating mutations and male gender. About half of the T-ALL patients that retained one wild type allele do not express PTEN protein. This indicates that additional genetic, epigenetic or post-translational inactivating events are expected. In this study, we have identified recurrent inactivating *PTEN* micro-deletions in T-ALL patients due to illegitimate RAG-mediated recombination events, mediated through cryptic RSSs (cRSSs). Taking into account all point, missense or nonsense mutations as well as deletions including micro-deletions, 18% of T-ALL patients in our patient cohort harbor PTEN inactivating aberrations.

Increasing evidence suggests that cRSSs can participate in oncogenic mechanisms, including chromosomal translocations in lymphoma, B-ALL^{41,42} and T-ALL^{4,43,44}, such as *SIL-TAL1* gene fusions and *HPRT* deletions. Different chromosomal translocation mechanisms have been described as a consequence of erroneous rearrangements between cRSS that flank oncogenes with RSS-sequences of T-cell receptor gene segments. Alternatively, broken DNA strands near oncogenes become mistakenly fused through a non-cRSS mechanism to T-cell receptor gene during V(D) J-assembly (reviewed in⁴⁵). Other illegitimate, cRSS-driven coding-joint recombination events may cause intrachromosomal deletions such as described for *IKZF1*,^{46,47} *ERG1*,⁴⁸ *BTG1*,⁴⁹ and *CDKN2A/B*⁵⁰⁻⁵² in humans and *Notch1*^{53,54} and *Bcl11b*⁵⁵ in mice.

PTEN micro-deletions occur as a consequence of aberrant RAG-mediated recombination events. This is supported by the fact that the breakpoints are flanked by cRSSs, which contain heptamer and nonamer sequences that are separated by 12 or 23 nucleotide spacers. Three out of the four identified cRSSs have high RIC scores.⁵⁶ In recombination assays, 12- or 23-nucleotide spacers cRSS1-4 facilitate recombinations when combined with 23- or 12-nucleotide spacers consensus RSSs, respectively.⁵⁷ Efficiencies for those recombinations equals those of functional RSSs that flank gene segments of immunoglobulin or TCR genes when tested in this system.³² The frequencies of different types of micro-deletions matches with the efficiency levels of cRSSs in the recombination assay with cRSS1 and cRSS3 being responsible for the type I micro-deletion in 10 out of 13 micro-deletion events.

Four out of 12 (33%) signal joint-related type I and II micro-deletions have perfect heptamer-to-heptamer fusions that lack incorporation of random nucleotides just like signal-joints of excision circles as generated during IgH or TCR assembly processes. The other 8 signal junctions (67%) represented atypical joints that incorporated 3 to 13 random GC-rich N-nucleotides. Twenty to thirty percent of V(D)J-associated signal junctions in mouse lymphocytes represent atypical joints,⁵⁸ and the T-cell receptor-mediated translocation breakpoint as observed in the SUP-T1 T-ALL cell line is a comparable atypical signal junction.⁵⁹ Three out of these 8 atypical

signal joints (patient #12, #26 and #11) also demonstrated evidence for exonuclease processing of signal ends (Figure 2B). Arnal and co-workers proposed that non-canonic heptamer sequence variations may destabilize the RAG post-cleavage complex that make coding-ends and signal-ends available for alternative joining mechanisms.⁶⁰ Such a mechanism could also result in a RAG-mediated open-and-shut joint recombination,^{61,62} which includes RAG cleavage adjacent to a cRSS heptamer, processing of the open coding-end by exonuclease activity and insertion of random nucleotides by TdT that is followed by re-ligation of the previously adjacent coding and signal ends. This may explain at least one rare T-ALL case with a mutation affecting the start codon of *PTEN*.²⁴ This mutation is flanked by a 12-spacer cRSS with a strong RIC score of -45.48 (Sarmiento et al, unpublished results). It resulted in a deletion of 13 nucleotides including the ATG start codon with the insertion of 15 random nucleotides. This cRSS allowed RAG-mediated recombinations equal to the efficiency ($2.5 \pm 0.13\%$) of the mouse IgH locus VH/87 RSS that rarely undergoes recombination *in-vitro*.⁶³ However, no other T-ALL patient in our current series was identified with an equivalent mutation at this position, indicating that aberrant open-and-shut recombinations at this position are rare. For missense in/del mutations in exon 7 of *PTEN*,^{15,17,18,24} no cRSS sequences could be identified by the positional information algorithm indicating that these mutations are generated by means of other mechanisms.

The identification of subclonal *PTEN* micro-deletions—as well as entire *PTEN* locus deletions¹⁸—indicates that RAG activity may be ongoing in (at least part of) the leukemic cell population. This may explain clonal diversity and selection that results in disease progression and relapse. This latter is also supported by *in-vitro* recombination assays using T-ALL cell lines, and demonstrate that about one percent of leukemic cells or less will undergo recombinations of the reporter construct within a one week time-frame.³² Since intraclonal heterogeneity at diagnosis and clonal evolution at relapse are known to occur in ALL,^{48,64-67} we checked whether *PTEN* micro-deletions present in a minor leukemic clone at presentation of disease could become clonally selected following xenograft transplantation such as previously demonstrated for *PTEN*-inactivated T-ALL blasts by means of lentiviral shRNA transfer³⁶ or gain of *BTG1* micro-deletions at relapse of B-ALL patients.⁴⁹ In contrast to the study of Clappier et al.,³⁶ we did not observe preferential selection of leukemic cells with *PTEN* micro-deletions to near clonal levels following xenotransplantation. This could be explained by the preferential outgrowth of other leukemic subclones with certain mutations that are specifically advantageous for engraftment in mice over leukemic subclones having *PTEN* micro-deletions. Furthermore, additional and new illegitimate RAG-mediated *PTEN* micro-deletions were detected that had not been found in the primary leukemic patient cells possibly as consequence of ongoing RAG activity. However, at present we cannot formally rule out that subclonal selection of a leukemic subpopulation with a novel *PTEN* micro-deletion occurred from a PCR-undetectable subclone that was already present at diagnosis. In addition, one patient had a subclonal missense mutation, indicating that there is an ongoing pressure on TALLMO-dysregulated leukemic cells to inactivate remaining wild-type *PTEN* alleles. RAG activity also results in *PTEN* micro-deletions in developing thymocytes of healthy individuals. These rearrangements may facilitate a pre-malignant condition from which

leukemia can develop. Likewise, Marlunescu *et al*⁵ described two mechanisms of illegitimate V(D)J chromosomal rearrangement that were found in healthy children, i.e. the D δ 2/LMO2 recombination in the t(11;14)(p13;q11) and the TAL2/TCR β translocation t(7;9)(q34;q32)⁶⁸ that are known to represent driving oncogenic lesions in T-ALL.

Overall, our discovery of *PTEN* micro-deletions has reinforced the fact that *PTEN* aberrations are especially abundant in *TAL*- or *LMO*-rearranged leukemia but not in *TLX3*-rearranged patients,¹⁸ as previously observed for adult T-ALL patient series³⁹. *PTEN* abnormalities seem to be associated with a reduced incidence of *NOTCH1*-activating mutations. The TALLMO subtype represents an immunophenotypically mature subtype of arrested leukemic cells in T-ALL, in which ongoing RAG-activity creates an opportunistic and extended time window for cRSS-mediated illegitimate recombination events. These may provoke disease progression and relapse in leukemia patients, adding a new level of complexity that should be addressed in the development of future antileukemic strategies for ALL. Taking into account all currently known *PTEN* inactivation mechanisms (*PTEN* mutations, entire locus deletions and *PTEN* micro-deletions), some seemingly wild type T-ALL patients still lack *PTEN* protein expression indicating that other *PTEN* inactivation mechanisms await identification.

AUTHORSHIPS AND DISCLOSURES

Contribution: R.D.M., L.M.S., J.T.B. and J.P.P.M. designed the study and wrote the manuscript; R.D.M., W.K.S., L.Z. and J.G.C.A.M.B.-G. performed the MLPA analyses, breakpoint mapping and PCR-based screening of *PTEN* micro-deletions; J.A.Y. performed the computational detection of putative RAG recombination signal sequences; L.M.S. and V.P. were responsible for generation of GFPi-*PTEN* cRSS reporter constructs and recombination assays; K.C.-B. and W.K.S. performed the xenotransplantation experiments; J.P.P.M. performed the statistic analyses of the data; M.A., E.S., M.H. collected and provided patient samples and their characteristics; R.D.M., L.M.S., K.C.-B., R.P., J.T.B., J.P.P.M. analyzed and interpreted data; and all authors read, revised, and approved the paper. Conflict-of-interest disclosure: no competing financial interests.

ACKNOWLEDGEMENTS

The authors would like to thank Gustavo G.L. Costa and Izabella A.P. Neshich for help with computational detection of cRSSs. RM, KCB and LZ were financed by the Stichting Kinderen Kankervrij (Grant no. KiKa 2007-12, KiKa 2008-29 and KiKa 2013-116). LMS received a postdoctoral fellowship from Fundação para a Ciência e a Tecnologia (FTC). This work was supported by grants PTDC/SAU-ONC/113202/2009 from FCT (to JTB), and FAPESP 08/10034-1.

REFERENCES

1. Pui CH, Evans WE. Treatment of acute lymphoblastic leukemia. *N Engl J Med.* 2006;354:166-178.
2. Meijerink JP. Genetic rearrangements in relation to immunophenotype and outcome in T-cell acute lymphoblastic leukaemia. *Best Pract Res Clin Haematol.* 2010;23:307-318.
3. Dik WA, Nadel B, Przybylski GK, et al. Different chromosomal breakpoints impact the level of LMO2 expression in T-ALL. *Blood.* 2007;110:388-392.
4. Le Noir S, Ben Abdelali R, Lelorch M, et al. Extensive molecular mapping of TCRalpha/delta- and TCRbeta-involved chromosomal translocations reveals distinct mechanisms of oncogene activation in T-ALL. *Blood.* 2012;120:3298-3309.
5. Marculescu R, Le T, Simon P, Jaeger U, Nadel B. V(D)J-mediated translocations in lymphoid neoplasms: a functional assessment of genomic instability by cryptic sites. *J Exp Med.* 2002;195:85-98.
6. Homminga I, Pieters R, Langerak AW, et al. Integrated transcript and genome analyses reveal NKX2-1 and MEF2C as potential oncogenes in T cell acute lymphoblastic leukemia. *Cancer Cell.* 2011;19:484-497.
7. Weng AP, Ferrando AA, Lee W, et al. Activating mutations of NOTCH1 in human T cell acute lymphoblastic leukemia. *Science.* 2004;306:269-271.
8. Sulis ML, Williams O, Palomero T, et al. NOTCH1 extracellular juxtamembrane expansion mutations in T-ALL. *Blood.* 2008;112:733-740.
9. Malyukova A, Dohda T, von der Lehr N, et al. The tumor suppressor gene hCDC4 is frequently mutated in human T-cell acute lymphoblastic leukemia with functional consequences for Notch signaling. *Cancer Res.* 2007;67:5611-5616.
10. O'Neil J, Grim J, Strack P, et al. FBW7 mutations in leukemic cells mediate NOTCH pathway activation and resistance to gamma-secretase inhibitors. *J Exp Med.* 2007;204:1813-1824.
11. Thompson BJ, Buonamici S, Sulis ML, et al. The SCFFBW7 ubiquitin ligase complex as a tumor suppressor in T cell leukemia. *J Exp Med.* 2007;204:1825-1835.
12. Ferrando AA. The role of NOTCH1 signaling in T-ALL. *Hematology Am Soc Hematol Educ Program.* 2009:353-361.
13. Shochat C, Tal N, Bandapalli OR, et al. Gain-of-function mutations in interleukin-7 receptor-alpha (IL7R) in childhood acute lymphoblastic leukemias. *J Exp Med.* 2011;208:901-908.
14. Zenatti PP, Ribeiro D, Li W, et al. Oncogenic IL7R gain-of-function mutations in childhood T-cell acute lymphoblastic leukemia. *Nat Genet.* 2011;43:932-939.
15. Palomero T, Sulis ML, Cortina M, et al. Mutational loss of PTEN induces resistance to NOTCH1 inhibition in T-cell leukemia. *Nat Med.* 2007;13:1203-1210.
16. Gutierrez A, Sanda T, Grebliunaite R, et al. High frequency of PTEN, PI3K, and AKT abnormalities in T-cell acute lymphoblastic leukemia. *Blood.* 2009;114:647-650.
17. Jotta PY, Ganazza MA, Silva A, et al. Negative prognostic impact of PTEN mutation in pediatric T-cell acute lymphoblastic leukemia. *Leukemia.* 2010;24:239-242.
18. Zuurbier L, Petricoin EF, Vuerhard MJ, et al. The significance of PTEN and AKT aberrations in pediatric T-cell acute lymphoblastic leukemia. *Haematologica.* 2012.
19. Palomero T, Dominguez M, Ferrando AA. The role of the PTEN/AKT Pathway in NOTCH1-induced leukemia. *Cell Cycle.* 2008;7:965-970.
20. Maser RS, Choudhury B, Campbell PJ, et al. Chromosomally unstable mouse tumours have genomic alterations similar to diverse human cancers. *Nature.* 2007;447:966-971.
21. Alimonti A, Carracedo A, Clohessy JG, et al. Subtle variations in Pten dose determine cancer susceptibility. *Nat Genet.* 2010;42:454-458.

22. Correia NC, Girio A, Antunes I, Martins LR, Barata JT. The multiple layers of non-genetic regulation of PTEN tumour suppressor activity. *Eur J Cancer*. 2014;50:216-225.
23. Berger AH, Knudson AG, Pandolfi PP. A continuum model for tumour suppression. *Nature*. 2011;476:163-169.
24. Silva A, Yunes JA, Cardoso BA, et al. PTEN posttranslational inactivation and hyperactivation of the PI3K/Akt pathway sustain primary T cell leukemia viability. *The Journal of clinical investigation*. 2008;118:3762-3774.
25. Kamps WA, Bokkerink JP, Hahlen K, et al. Intensive treatment of children with acute lymphoblastic leukemia according to ALL-BFM-86 without cranial radiotherapy: results of Dutch Childhood Leukemia Study Group Protocol ALL-7 (1988-1991). *Blood*. 1999;94:1226-1236.
26. Kamps WA, Bokkerink JP, Hakvoort-Cammel FG, et al. BFM-oriented treatment for children with acute lymphoblastic leukemia without cranial irradiation and treatment reduction for standard risk patients: results of DCLSG protocol ALL-8 (1991-1996). *Leukemia*. 2002;16:1099-1111.
27. Veerman AJ, Kamps WA, van den Berg H, et al. Dexamethasone-based therapy for childhood acute lymphoblastic leukaemia: results of the prospective Dutch Childhood Oncology Group (DCOG) protocol ALL-9 (1997-2004). *Lancet Oncol*. 2009;10:957-966.
28. Escherich G, Horstmann MA, Zimmermann M, Janka-Schaub GE. Cooperative study group for childhood acute lymphoblastic leukaemia (COALL): long-term results of trials 82,85,89,92 and 97. *Leukemia*. 2010;24:298-308.
29. van Grotel M, Meijerink JP, van Wering ER, et al. Prognostic significance of molecular-cytogenetic abnormalities in pediatric T-ALL is not explained by immunophenotypic differences. *Leukemia*. 2008;22:124-131.
30. Barata JT, Silva A, Abecasis M, et al. Molecular and functional evidence for activity of murine IL-7 on human lymphocytes. *Exp Hematol*. 2006;34:1133-1142.
31. Cowell LG, Davila M, Kepler TB, Kelsoe G. Identification and utilization of arbitrary correlations in models of recombination signal sequences. *Genome Biol*. 2002;3:RESEARCH0072.
32. Trancoso I, Bonnet M, Gardner R, et al. A Novel Quantitative Fluorescent Reporter Assay for RAG Targets and RAG Activity. *Front Immunol*. 2013;4:110.
33. Gellert M. V(D)J RECOMBINATION: RAG PROTEINS, REPAIR FACTORS, AND REGULATION*. *Annual Review of Biochemistry*. 2002;71:101-132.
34. Lewis SM, Agard E, Suh S, Czyzyk L. Cryptic signals and the fidelity of V(D)J joining. *Mol Cell Biol*. 1997;17:3125-3136.
35. Raghavan SC, Kirsch IR, Lieber MR. Analysis of the V(D)J Recombination Efficiency at Lymphoid Chromosomal Translocation Breakpoints. *Journal of Biological Chemistry*. 2001;276:29126-29133.
36. Clappier E, Gerby B, Sigaux F, et al. Clonal selection in xenografted human T cell acute lymphoblastic leukemia recapitulates gain of malignancy at relapse. *J Exp Med*. 2011;208:653-661.
37. Zuurbier L, Homminga I, Calvert V, et al. NOTCH1 and/or FBXW7 mutations predict for initial good prednisone response but not for improved outcome in pediatric T-cell acute lymphoblastic leukemia patients treated on DCOG or COALL protocols. *Leukemia*. 2010;24:2014-2022.
38. Bandapalli OR, Zimmermann M, Kox C, et al. NOTCH1 activation clinically antagonizes the unfavorable effect of PTEN inactivation in BFM-treated children with precursor T-cell acute lymphoblastic leukemia. *Haematologica*. 2013;98:928-936.
39. Trinquand A, Tanguy-Schmidt A, Ben Abdelali R, et al. Toward a NOTCH1/FBXW7/RAS/PTEN-based oncogenetic risk classification of adult T-cell acute lymphoblastic leukemia: a Group for Research in Adult Acute Lymphoblastic Leukemia study. *J Clin Oncol*. 2013;31:4333-4342.
40. Larson Gedman A, Chen Q, Kugel Desmoulin S, et al. The impact of NOTCH1, FBW7 and PTEN mutations on prognosis and downstream signaling in pediatric T-cell acute lymphoblastic leukemia: a report from

- the Children's Oncology Group. *Leukemia*. 2009;23:1417-1425.
41. Marculescu R, Le T, Bocskor S, et al. Alternative end-joining in follicular lymphomas' t(14;18) translocation. *Leukemia*. 2002;16:120-126.
 42. Papaemmanuil E, Rapado I, Li Y, et al. RAG-mediated recombination is the predominant driver of oncogenic rearrangement in ETV6-RUNX1 acute lymphoblastic leukemia. *Nat Genet*. 2014.
 43. Aplan PD, Lombardi DP, Ginsberg AM, et al. Disruption of the human SCL locus by "illegitimate" V-(D)-J recombinase activity. *Science*. 1990;250:1426-1429.
 44. Larmonie NS, Dik WA, Meijerink JP, et al. Breakpoint sites disclose the role of the V(D)J recombination machinery in the formation of T-cell receptor (TCR) and non-TCR associated aberrations in T-cell acute lymphoblastic leukemia. *Haematologica*. 2013;98:1173-1184.
 45. Radich J, Sala O. The Biology of Adult Acute Lymphoblastic Leukemia. In: Advani AS, Lazarus HM, eds. *Adult Acute Lymphocytic Leukemia: Humana Press*; 2011:25-44.
 46. Mullighan CG, Miller CB, Radtke I, et al. BCR-ABL1 lymphoblastic leukaemia is characterized by the deletion of Ikaros. *Nature*. 2008;453:110-114.
 47. Iacobucci I, Storlazzi CT, Cilloni D, et al. Identification and molecular characterization of recurrent genomic deletions on 7p12 in the IKZF1 gene in a large cohort of BCR-ABL1-positive acute lymphoblastic leukemia patients: on behalf of Gruppo Italiano Malattie Ematologiche dell'Adulto Acute Leukemia Working Party (GIMEMA AL WP). *Blood*. 2009;114:2159-2167.
 48. Clappier E, Auclerc MF, Rapon J, et al. An intragenic ERG deletion (ERG) is a marker of an oncogenic subtype of B-cell precursor acute lymphoblastic leukemia with a favorable outcome despite frequent IKZF1 deletions. *Leukemia*. 2013.
 49. Waanders E, Scheijen B, van der Meer LT, et al. The origin and nature of tightly clustered BTG1 deletions in precursor B-cell acute lymphoblastic leukemia support a model of multiclonal evolution. *PLoS Genet*. 2012;8:e1002533.
 50. Raschke S, Balz V, Efferth T, Schulz WA, Florl AR. Homozygous deletions of CDKN2A caused by alternative mechanisms in various human cancer cell lines. *Genes Chromosomes Cancer*. 2005;42:58-67.
 51. Novara F, Beri S, Bernardo ME, et al. Different molecular mechanisms causing 9p21 deletions in acute lymphoblastic leukemia of childhood. *Hum Genet*. 2009;126:511-520.
 52. Kitagawa Y, Inoue K, Sasaki S, et al. Prevalent involvement of illegitimate V(D)J recombination in chromosome 9p21 deletions in lymphoid leukemia. *J Biol Chem*. 2002;277:46289-46297.
 53. Ashworth TD, Pear WS, Chiang MY, et al. Deletion-based mechanisms of Notch1 activation in T-ALL: key roles for RAG recombinase and a conserved internal translational start site in Notch1. *Blood*. 2010;116:5455-5464.
 54. Tsuji H, Ishii-Ohba H, Katsube T, et al. Involvement of illegitimate V(D)J recombination or microhomology-mediated nonhomologous end-joining in the formation of intragenic deletions of the Notch1 gene in mouse thymic lymphomas. *Cancer Res*. 2004;64:8882-8890.
 55. Sakata J, Inoue J, Ohi H, et al. Involvement of V(D)J recombinase in the generation of intragenic deletions in the Rit1/Bcl11b tumor suppressor gene in gamma-ray-induced thymic lymphomas and in normal thymus of the mouse. *Carcinogenesis*. 2004;25:1069-1075.
 56. Cowell LG, Davila M, Yang K, Kepler TB, Kelsoe G. Prospective estimation of recombination signal efficiency and identification of functional cryptic signals in the genome by statistical modeling. *J Exp Med*. 2003;197:207-220.
 57. Grawunder U, Harfst E. How to make ends meet in V(D)J recombination. *Curr Opin Immunol*. 2001;13:186-194.
 58. Lee J, Desiderio S. Cyclin A/CDK2 regulates V(D)J recombination by coordinating RAG-2 accumulation and DNA repair. *Immunity*. 1999;11:771-781.
 59. Baer R, Forster A, Rabbitts TH. The mechanism of chromosome 14 inversion in a human T cell

- lymphoma. *Cell*. 1987;50:97-105.
60. Arnal SM, Holub AJ, Salus SS, Roth DB. Non-consensus heptamer sequences destabilize the RAG post-cleavage complex, making ends available to alternative DNA repair pathways. *Nucleic Acids Res*. 2010;38:2944-2954.
 61. Lewis SM, Hesse JE, Mizuuchi K, Gellert M. Novel strand exchanges in V(D)J recombination. *Cell*. 1988;55:1099-1107.
 62. Elliott JF, Rock EP, Patten PA, Davis MM, Chien YH. The adult T-cell receptor delta-chain is diverse and distinct from that of fetal thymocytes. *Nature*. 1988;331:627-631.
 63. Davila M, Liu F, Cowell LG, et al. Multiple, conserved cryptic recombination signals in VH gene segments: detection of cleavage products only in pro B cells. *J Exp Med*. 2007;204:3195-3208.
 64. Anderson K, Lutz C, van Delft FW, et al. Genetic variegation of clonal architecture and propagating cells in leukaemia. *Nature*. 2011;469:356-361.
 65. Mullighan CG, Phillips LA, Su X, et al. Genomic analysis of the clonal origins of relapsed acute lymphoblastic leukemia. *Science*. 2008;322:1377-1380.
 66. Yang JJ, Bhojwani D, Yang W, et al. Genome-wide copy number profiling reveals molecular evolution from diagnosis to relapse in childhood acute lymphoblastic leukemia. *Blood*. 2008;112:4178-4183.
 67. Kuster L, Grausenburger R, Fuka G, et al. ETV6/RUNX1-positive relapses evolve from an ancestral clone and frequently acquire deletions of genes implicated in glucocorticoid signaling. *Blood*. 2011;117:2658-2667.
 68. Marculescu R, Vanura K, Le T, et al. Distinct t(7;9)(q34;q32) breakpoints in healthy individuals and individuals with T-ALL. *Nat Genet*. 2003;33:342-344.

SUPPLEMENTARY DATA

<i>PTEN</i> exon	LPO GGGTCCCTAAGGGTTGGA	RPO TCTAGATTGGATCTGCTGGCAC
3	GGGTTCCCTAAGGGTTGGACCATACAGATACAACTGTGATGATGTTTCTATTGTATGCT	GCAAAATCTCTAAACAACACTTAAAGTGAAGTATCTGCTGTTAGAGTGAGGATTTATCTTTATTCTAGATTGGATCTGCTGGCAC
8	GGGTTCCCTAAGGGTTGGACATTGCAAGTAGAGGCTGCAGATAATGACAAAGAA	TATCTAGTACTTAAACAAAATGATCTGCAAAAGCAATAAAGCAAAAGCCACCGGATACAGATTTATTCTAGATTGGATCTGCTGGCAC
4 rev	GGGTTCCCTAAGGGTTGGATGCTCAATGCTTCCAGCACAATAAAGAAAAGTT	TAAAAGGTATAAAGTATCTTTGGCAGCTAGGAAGAAAAAAGTCAATATCTTTATTCTTACTAGATTGGATCTGCTGGCAC
9	GGGTTCCCTAAGGGTTGGAGTGAAGTCATATTTGGGGTTTCTATTTAAATTTCTTT	CTCTAGGTGAAGCTGACTTCACAAAACAGTAGAGGAGCCCTCATATTTATTCTTACTTTATTCTAGATTGGATCTGCTGGCAC
1	GGGTTCCCTAAGGGTTGGATCAAGTCAGAGCCATTTCCATCTGCGAGAAGAA	GGCCCCCAGCAGGAGCTCTGCCATCTCTCCCTCTTTTCTCAGGATTTATTCTTACTTTATTCTAGATTGGATCTGCTGGCAC
6	GGGTTCCCTAAGGGTTGGACAGAGCAGAGGCGTATGTGATTTATAGTCACTGT	TAAAGAACTCTGAGTATAGACCAGTGGCAGCTGTTGTTCAATTTATTCTTACTTTATTCTAGATTGGATCTGCTGGCAC
5	GGGTTCCCTAAGGGTTGGATGCGAGAGGAGCGACTGCTGTATGATA	FTGCAATTATTTACTCGGGGCAATTTTAAAGGACAGAGGCAATTTATTATTCTTACTTCTAGATTGGATCTGCTGGCAC
7	GGGTTCCCTAAGGGTTGGATCTGCAATTCAGAGCCACACAGCGGAA	BAGAAGTCTGATCTTGGATTCGCCAGCGGCTACTGATTTATTATTCTTCTAGATTGGATCTGCTGGCAC
4 rev	GGGTTCCCTAAGGGTTGGATCTCTCACTGATAATCTGGATGACTCATTATTGTATGA	CAGTAAGATACAGTCTATCGGGTTAAGTATACAACATAGTACAGTACTTACACCATTTATCTTCTAGATTGGATCTGCTGGCAC
2	GGGTTCCCTAAGGGTTGGACAGTGTATTGCTGCATATTCAGATTTCTTCCCTAAAGTACTCAG	ATATTTATCCAACATATTGCTATGGGATTTCTGCAAGAGACTGTTTATTATTCTAGATTGGATCTGCTGGCAC
7	GGGTTCCCTAAGGGTTGGATCTTCCACAAAGAAACAGATGCTAAAAGGTTT	GTACTTTTCTTCTGGGGAATATCCAAAATAGGACAGATAAAAGTTTATCCCTACAATTTCTAGATTGGATCTGCTGGCAC
5	GGGTTCCCTAAGGGTTGGATGGGGAAGTAAAGACAGAGACAAAAGTAAAGTT	ATTTTTTGATGTTTTCTTCCCTCTCGGATGAGAAATTTATGGAAATTTATTATTCTTCTAGATTGGATCTGCTGGCAC
9 rev	GGGTTCCCTAAGGGTTGGACAGTATAGGATAAACAAGTGTGCTCAGAAAAGAAATGTTC	CTATAAGCTGTAATCGACCAATGCTTATGCCATTATTTATTATTCTTCTAGATTGGATCTGCTGGCAC
6 rev	GGGTTCCCTAAGGGTTGGAAAGATGAGAATTCAGGACTTACTGCAAGT	TCCGCCACTGAACATTGGAAAGTTTCAACATCATCTGTGAAAGTTTATTATTATTCTTCTAGATTGGATCTGCTGGCAC
8	GGGTTCCCTAAGGGTTGGACATTTGTGGGGTTGGTACTGTATGTA	TGTGATGTGTTTAATCTAGGATACAGCTGATGAGAACTTGGATTTATTATTCTTCTAGATTGGATCTGCTGGCAC
3	GGGTTCCCTAAGGGTTGGATGCAGAGATGATGTTACTGATCTGCTT	AAATGACTTGGCATCTACCCATATTGGAGCCATAACCCGTGGTATTATTCTTCTAGATTGGATCTGCTGGCAC
1	GGGTTCCCTAAGGGTTGGATCCAGGACTACACTGGGATGCTAGTAGA	GCCTCGGCTGGGACTCTGCTCCACCCAGACTACTTATTCTAGATTGGATCTGCTGGCAC

Table S1 | Design of LPO and RPO *PTEN* hybridization probes for MLPA amplification.

Primer sequence Forward/Reverse	Primers position (GRCh37)
FW: 5'-CGAGGGGCATCAGCTA-3'	Chr:10 89.624.110-89.624.125
FW: 5'-TCTGGGAGACAGATTTCTTTTC-3'	Chr:10 89.626.319-89.626.339
FW: 5'-TTGGGTAAACAAACAGTTCAG-3'	Chr:10 89.628.198-89.628.219
FW: 5'-TTGGGCCATGTTAGGATT-3'	Chr:10 89.630.012-89.630.029
FW: 5'-TTGGGGATGTCATTAAGC-3'	Chr:10 89.631.816-89.631.834
FW: 5'-TTGGCTGATTGTGAAAGTGT-3'	Chr:10 89.633.635-89.633.654
FW: 5'-TTCCCAAATGAGGTAAAATG-3'	Chr:10 89.635.523-89.635.543
FW: 5'-CCAAGCAATGCAGACTTACT-3'	Chr:10 89.637.291-89.637.310
FW: 5'-AGGCTTGAGCAGTTGTAGATAG-3'	Chr:10 89.639.040-89.639.061
FW: 5'-GGCTGCATTAATTTGATCTGTA-3'	Chr:10 89.640.922-89.640.943
FW: 5'-CCAGGCAGCTTCAGACT-3'	Chr:10 89.642.530-89.642.547
FW: 5'-GTTCCCAAATCTAAAACAGAGAC-3'	Chr:10 89.644.400-89.644.422
FW: 5'-GCCAGCTGAATTTACTTTAATG-3'	Chr:10 89.646.287-89.646.308
FW: 5'-CCCCCTTTTCTCTATCATGT-3'	Chr:10 89.648.219-89.648.239
FW: 5'-CTGGCTTGTGAAGAGAGAAT-3'	Chr:10 89.649.821-89.649.841
FW: 5'-CTGGGCAACATGATGAAA-3'	Chr:10 89.651.378-89.651.395
FW: 5'-GGGCATTGGATTAGGTCA-3'	Chr:10 89.652.427-89.652.444
FW: 5'-TTGGGGTTTTGTTTTGATTT-3'	Chr:10 89.653.486-89.653.505
RV: 5'-TGGGCAGTCCCTAAAACACTCT-3'	Chr:10 89.655.808-89.655.789
RV: 5'-CCCCATCTGTAATAAGGAGAAG-3'	Chr:10 89.657.310-89.657.290
RV: 5'-TCCCCTACTTCTCAGGATC-3'	Chr:10 89.659.092-89.659.073
RV: 5'-GGCGGTGTCATAATGTCTT-3'	Chr:10 89.690.830-89.690.812

Table S2 | Primers used for *PTEN* exon 2_3 breakpoint mapping.

5

Primer sequence Forward/Reverse	Primers position (GRCh37)
FW: 5'-CAAACGATAAAAACCATTACAAG-3'	Chr:10 89.685.281-89.685.303
FW: 5'-TCCGACAGATTTCATGTTACTT-3'	Chr:10 89.685.510-89.685.530
FW: 5'-AGCCDACCATCCACTG-3'	Chr:10 89.687.368-89.687.383
FW: 5'-AATGCTGGCTTTGACTGAA-3'	Chr:10 89.688.968-89.688.986
FW: 5'-GGAAGCACGTGAATTTACAGTA-3'	Chr:10 89.690.506-89.690.527
RV: 5'-GGAGGGAGGAACACAAGAT-3'	Chr:10 89.693.370-89.693.352
RV: 5'-GAAGCAGAAAGAAAATGATGAA-3'	Chr:10 89.695.389-89.695.369
RV: 5'-CAGGGATAAAGAAGCTAAGAACA-3'	Chr:10 89.697.244-89.697.222
RV: 5'-CGCTTCAACTCAGGACCTA-3'	Chr:10 89.699.184-89.699.166
RV: 5'-TCCGACTGCACGTAATTATC-3'	Chr:10 89.701.201-89.701.182
RV: 5'-CTGCATGATTTTCATCACTGTC-3'	Chr:10 89.703.130-89.703.110
RV: 5'-CCCCTCTGTCAAACCAAT-3'	Chr:10 89.705.100-89.705.083
RV: 5'-AGGGCTTCTCGTCAACAG-3'	Chr:10 89.706.988-89.706.971
RV: 5'-TTGGGAGGCTCACATGTA-3'	Chr:10 89.708.947-89.708.930
RV: 5'-GCGCGTGTGATGTGTA-3'	Chr:10 89.710.642-89.710.626
RV: 5'-GCTGCCACGTCTTATCACT-3'	Chr:10 89.712.480-89.712.462

Table S3 | Primers used for *PTEN* exon 4_5 breakpoint mapping.

Screening breakpoint <i>PTEN</i> deletion (DNA/cDNA)	Primer sequence Forward/Reverse	Primers position (GRCh37)
Exon 2_3: DNA	FW: 5'-GCTGCTCCTCTTTACCTTTC-3' or FW: 5'-GGCTGCTCCTCTTTACCTT-3'	Chr:10 89.624.321-89.624.340 Chr:10 89.624.320-89.624.338
	RV: 5'-ATCCCAAAAGTTCAAACATC-3' or RV: 5'-AGCAAATCCTGATCTGAAGTAAT-3'	Chr:10 89.689.878-89.689.858 Chr:10 89.689.797-89.689.819
	FW: 5'-CGAGGGGCATCAGCTA-3' or FW: 5'-CCGTTTTTAGGTTTCAGGTC-3'	Chr:10 89.624.110-89.624.125 Chr:10 89.625.248-89.625.267
Exon 2_3: cDNA	RV: 5'-GGCGGTGTCATAATGTCTT-3' or RV: 5'-AGCAAATCCTGATCTGAAGTAAT-3'	Chr:10 89.690.830-89.690.812 Chr:10 89.689.797-89.689.819
	FW: 5'-GAAACCAATGGATTGTAGTTTATT-3' or RV: 5'-TCCGACTGCACGTAATTATC-3'	Chr:10 89.689.486-89.689.509 Chr:10 89.701.201-89.701.182
Exon 4_5: DNA	FW: 5'-GAAACCAATGGATTGTAGTTTATT-3' or RV: 5'-TCCGACTGCACGTAATTATC-3'	Chr:10 89.689.486-89.689.509 Chr:10 89.701.201-89.701.182
Exon 4-5: cDNA	FW: 5'-AAGCATAAAAACCATTACAAGAT-3' or RV: 5'-CAGTGCCACTGGTCTATAATC-3'	Chr:10 89.685.283-89.685.305 Chr:10 89.711.961-89.711.941

Table S4 | Specific primers to screen for *PTEN* exon 2_3 and 4_5 breakpoints.

12-spacer RSS	heptamer	12-spacer	nonamer	RIC*
Consensus 12-sp ¹	CACAGTG	CTACAGACTGGA	ACAAAAACC	
Human <i>PTEN</i> cRSS1	CACAGAT	AAATATACTTTT	ACATAAACA	-34.2
Human <i>PTEN</i> exon 1	CAAAGAG	ATCGTTAGCAGA	AACAAAAGG	-45.48
Human SCL12 ^{1,2}	CACAGCC	TCGCGCATTCT	GTATATTGC	
Human LMO2 ^{1,2}	CACAGTA	TTGTCTTACCCA	GCAATAATT	
Mouse J β 2-2 ^{1,3}	CACAGTC	GTCGAAATGCTG	GCACAAACC	
Mouse VH/87 IgH ⁴	CACTATT	AGGATCAATCCT	TCAAATCCA	
23-spacer RSS	heptamer	23-spacer	nonamer	RIC*
Consensus 23-sp ¹	CACAGTG	CTACAGCTCCACTGTCTACTGGA	ACAAAAACC	
Human <i>PTEN</i> cRSS2	CACAGTA	TTTCACTTCTATGAAACTAATTA	TTGAGAACA	-55.59
Human <i>PTEN</i> cRSS3	CACCCTA	GGTTGAATACACAGAAAGGAAAC	ACAAAATAT	-59.78
Human <i>PTEN</i> cRSS4	CACTGTA	TGAAAAAAGCTAACATACCTACA	ATCTAAAGC	-75.59
Human SCL 23 ²	CACAGCC	TCGCGCATTCTGTATATTGCGT	AAGGAAAAG	

*RIC scores are only stated for newly identified cRSS in *PTEN*.

References:

1. Trancoso I, Bonnet M, Gardner R, et al. A Novel Quantitative Fluorescent Reporter Assay for RAG Targets and RAG Activity. *Front Immunol.* 2013;4:110.
2. Raghavan SC, Kirsch IR, Lieber MR. Analysis of the V(D)J Recombination Efficiency at Lymphoid Chromosomal Translocation Breakpoints. *Journal of Biological Chemistry.* 2001;276:29126-29133.
3. Cowell LG, Davila M, Yang K, Kepler TB, Kelsoe G. Prospective estimation of recombination signal efficiency and identification of functional cryptic signals in the genome by statistical modeling. *J Exp Med.* 2003;197:207-220.
4. Davila M, Liu F, Cowell LG, et al. Multiple, conserved cryptic recombination signals in VH gene segments: detection of cleavage products only in pro B cells. *J Exp Med.* 2007;204:3195-3208.

Table S5 | RSSs tested with the GFPi reporter construct.

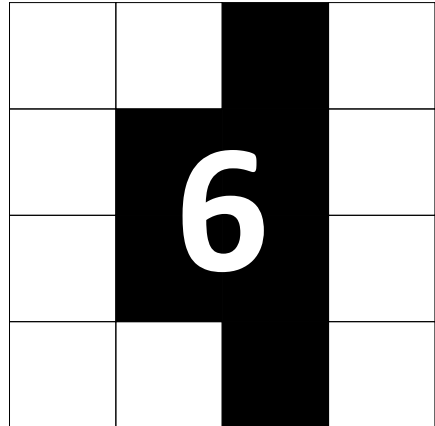
Clinical (<i>n</i> =142)	<i>PTEN</i> mutation/deletion		<i>p</i> -value
	WT	Mut	
Gender			0.91
Male (<i>n</i> =97)	79	18	
Female (<i>n</i> =45)	37	8	
Median age (range)	7.9(1.3-17.8)	4.7 (1.1-15.9)	0.03*
Median WBC (range)	119.2 (2.0-900.0)	134 (5.0-600.0)	0.14*
Cytogenetics (<i>n</i> =142)	WT n(%)	Mut n(%)	<i>p</i> -value [^]
<i>TAL</i>-related § (<i>n</i> =29)	18 (60%)	11 (40%)	0.002
<i>LMO</i>-related § (<i>n</i> =19)	16 (84%)	3 (16%)	1#
<i>TLX3</i>+ (<i>n</i> =28)	28 (100%)	0 (0%)	0.002#
<i>TLX1</i>+ (<i>n</i> =7)	6 (86%)	1 (14%)	1#
<i>HOXA</i>+ (<i>n</i> =13)	13 (100%)	0 (0%)	0.13#
Unknown (<i>n</i> =48)	37 (77%)	11 (23%)	0.31
Unsupervised clusters (<i>n</i> =113)	WT n(%)	Mut n(%)	<i>p</i> -value [^]
<i>TAL/LMO</i>+ (<i>n</i> =51)	35 (69%)	16 (31%)	0.003#
Proliferative (<i>n</i> =19)	16 (84%)	3 (16%)	1#
Immature (<i>n</i> =15)	13 (87%)	2 (13%)	0.73#
<i>TLX</i> (<i>n</i> =28)	28 (100%)	0 (0%)	0.002#
NOTCH1/FBXW7 status (<i>n</i> =141)	WT n(%)	Mut n(%)	<i>p</i> -value [^]
wild-type (<i>n</i> =51)	34 (66%)	17 (34%)	0.001
mutant (<i>n</i> =90)	81 (90%)	9 (10%)	

Table S6 | Overall clinical and molecular cytogenetics of *PTEN*-mutated patients versus wild-type patients. [^], statistical analysis of the prevalence of *PTEN* aberrations within specific genetic T-ALL subgroups, as indicated, compared to other all other T-ALL subgroups combined. Abbreviations: Mut, mutant; WT, wild-type; WBC, white blood cell count. Significant *p*-values are indicated in bold. All *p*-values were calculated by using Pearson's Chi-square test, unless indicated; *Mann-Whitney U test, #Fisher's exact test. §Two T-ALL cases have *TAL2* and *LMO1* or *TAL1* and *LMO2* rearrangements; The *TAL/LMO* group consists of *TAL1* and/or *LMO2* rearranged patients and patients lacking these aberrations but that have an identical or *TAL/LMO*-like gene expression profile.

Clinical (n=146)	DCOG		COALL		Overall stratified analysis	
	5-yrs RFS (% ± SD)	P	5-yrs RFS (% ± SD)	P	5-yrs RFS (% ± SD)	P
male (n=100) vs female (n=46)	66 ± 7 vs 84 ± 8	0.19	61 ± 9 vs 91 ± 6	0.02	65 ± 5 vs 88 ± 5	0.009
age ≥ 10 yrs (n=50) vs age < 10 yrs (n=96)	62 ± 11 vs 74 ± 6	0.53	79 ± 9 vs 69 ± 8	0.51	72 ± 7 vs 72 ± 5	0.99
WBC *10 ⁹ leukocytes/liter ≥ 50 (n=114) vs WBC < 50 (n=31)	69 ± 6 vs 80 ± 13	0.4	68 ± 7 vs 84 ± 10	0.11	69 ± 5 vs 83 ± 8	0.08
† Driving oncogenic type A mutations/rearrangements (n=146)						
TAL1, TAL2 or LYL1 (n=30) vs other (n=116)	93 ± 6 vs 65 ± 6	0.04	66 ± 14 vs 74 ± 7	0.49	81 ± 8 vs 71 ± 5	0.25
LMO1, LMO2 or LMO3 (n=19) vs other (n=127)	50 ± 16 vs 75 ± 6	0.09	75 ± 22 vs 72 ± 6	0.67	59 ± 13 vs 74 ± 4	0.29
TLX3 (n=29) vs other (n=117)	57 ± 12 vs 75 ± 6	0.11	54 ± 17 vs 76 ± 6	0.22	56 ± 10 vs 76 ± 4	0.04
TLX1 (n=8) vs other (n=138)	80 ± 18 vs 70 ± 6	0.54	100 vs 72 ± 6	0.45	86 ± 13 vs 71 ± 4	0.36
§HOXA-activated (n=13) vs other (n=133)	40 ± 22 vs 74 ± 6	0.15	71 ± 17 vs 72 ± 6	0.82	58 ± 14 vs 74 ± 4	0.26
§MEF2C-activated (n=6) vs other (n=140)	100 vs 71 ± 6	0.56	80 ± 18 vs 72 ± 6	0.80	83 ± 15 vs 72 ± 4	0.62
NKX2-1/NKX2-2 (n=7) vs other (n=139)	100 vs 70 ± 6	0.40	100 vs 70 ± 7	0.19	100 vs 71 ± 4	0.12
‡ Unsupervised gene expression clusters (n=117)						
TAL/LMO cluster (n=53) vs other (n=64)	73 ± 10 vs 67 ± 10	0.70	69 ± 10 vs 77 ± 7	0.49	71 ± 7 vs 73 ± 6	0.81
TLX cluster (n=30) vs other (n=87)	60 ± 14 vs 74 ± 8	0.25	65 ± 13 vs 77 ± 6	0.45	63 ± 9 vs 76 ± 5	0.18
Proliferative cluster (n=19) vs other (n=98)	83 ± 15 vs 68 ± 8	0.39	82 ± 12 vs 73 ± 7	0.70	82 ± 10 vs 71 ± 5	0.39
Immature cluster (n=15) vs other (n=102)	50 ± 35 vs 70 ± 7	0.97	91 ± 9 vs 70 ± 7	0.18	85 ± 10 vs 71 ± 5	0.28
Type B mutations						
PTEN/AKT mutant/no PTEN protein (n=31) vs other (n=111)	64 ± 15 vs 70 ± 6	0.54	57 ± 15 vs 76 ± 6	0.19	60 ± 10 vs 74 ± 4	0.17
NOTCH1/FBXW7 mutant (n=90) vs other (n=51)	62 ± 8 vs 82 ± 8	0.10	68 ± 8 vs 80 ± 9	0.33	65 ± 5 vs 81 ± 6	0.06
PTEN/AKT/NOTCH1/FBXW7 mutant/no PTEN protein (n=109) vs other (n=32)	63 ± 7 vs 92 ± 7	0.04	66 ± 7 vs 90 ± 10	0.06	65 ± 5 vs 92 ± 6	0.005
WT1 mutant (n=17) vs other (n=129)	63 ± 17 vs 72 ± 6	0.47	46 ± 22 vs 76 ± 6	0.16	57 ± 13 vs 74 ± 4	0.14
Del 9p21 (n=116) vs other (n=25)	70 ± 6 vs 75 ± 13	0.66	64 ± 8 vs 94 ± 6	0.03	68 ± 5 vs 86 ± 6	0.07

Table S7 | 5-years relapse free survival of patient groups based on clinical, (cyto)genetic or biological characteristics. Significant log-rank p-values for DCOG or COALL cohort analyses are indicated in bold; RFS, Relapse free survival; SD, standard deviation; P, p-value; WBC, white blood cell count; †All patients having one of the specified cytogenetic aberrations are being compared to patients lacking those specific aberrations (indicated as “other”); §Different genetic aberrations have been identified that activate *HOXA* or *MEF2C* oncogenes in specific genetic subtypes of T-ALL patients (Meijerink JP. Best Pract Res Clin Haematol, 2010; Homminga I. et al., Cancer Cell 2011); ‡Unsupervised clusters as defined in Homminga I. et al., Cancer Cell 2011. §The *del9p21* status was determined by multiplex ligation-dependent probe amplification (MLPA) analysis for *p15/CDKN2B* and *p16/CDKN2A* loci as designed by MRC-Holland, Amsterdam, the Netherlands. ||*PTEN* status does not include patient samples having *PTEN* mutations or deletions on the subclonal level.

CHAPTER



Mutually Exclusive Mutations in the IL7-Receptor Signaling Pathway in T-Cell Acute Lymphoblastic Leukemia Respond to Combined Inhibition of MEK/ERK and PI3K/AKT/mTOR Pathways

Kirsten Canté-Barrett¹, Linda Zuurbier¹, Jessica G.C.A.M. Buijs-Gladdines¹, Willem K. Smits¹, Maartje J. Vuerhard¹, Clarissa Kooi¹, Mahban Irandoust¹, Dirk Geerts¹, Edwin Sonneveld², Martin Horstmann^{3,4}, Rob Pieters^{1,5}, and Jules P.P. Meijerink¹

¹Department of Pediatric Oncology/Hematology, Erasmus MC Rotterdam-Sophia Children's Hospital, Rotterdam, the Netherlands; ²Dutch Childhood Oncology Group (DCOG), the Hague, the Netherlands; ³German Cooperative Study Group for Childhood Acute Lymphoblastic Leukemia (COALL), Hamburg, Germany; ⁴Research Institute Children's Cancer Center Hamburg, Clinic of Pediatric Hematology and Oncology, University Medical Center Hamburg-Eppendorf, Hamburg, Germany; ⁵Princess Máxima Center of Pediatric Oncology, Utrecht, the Netherlands.

ABSTRACT

The JAK-STAT, RAS-MEK-ERK and PI3K-AKT-mTOR pathways are important for growth and survival signaling pathways in many cell types, and are frequently mutated in cancer. In leukemic cells, recurrent somatic mutations in *JAK*, *RAS* and *AKT* genes result in uncontrolled proliferation. In the present study of 146 sequenced pediatric T-cell acute lymphoblastic leukemia (T-ALL) patients, 64 harbor mutations in *JAK1*, *JAK3*, *N-RAS*, *K-RAS*, *NF1*, *AKT*, *PTEN* or in *IL7Ra*, activating all three pathways. No mutations were identified in *JAK2* and *TYK2*. Strikingly, these mutations occur in a predominantly mutually exclusive fashion, suggesting they share aberrant activation of similar downstream targets. We adapted the Ba/F3 IL3-dependent cell line to express many of these mutated genes in a doxycycline-inducible manner and found that expression of these mutations—in contrast to expression of the wild type genes—render Ba/F3 cells IL3-independent. Additionally, the IL7Ra- and JAK-mutated Ba/F3 cells are sensitive to JAK inhibition by Ruxolitinib or JAK inhibitor I, but relatively resistant to downstream RAS-MEK-ERK or PI3K-AKT-mTOR inhibition, indicating that inhibition of one of these downstream pathways is insufficient. This result can be explained by our observation that inhibition of just one pathway triggers enhanced signaling of the other pathway. We therefore tested combinations of inhibitors for the ability to completely block the IL7R signaling pathway irrespective of the level of activation by specific mutations. The combination of the MEK inhibitor CI-1040 with the PI3K inhibitor Ly294002 proved most efficient in blocking signaling in IL7Ra- or JAK1-mutated Ba/F3 lines as exemplified by the complete absence of p70-S6Kinase phosphorylation that is downstream of both pathways. Since most leukemias depend on one or both pathways, combined MEK and PI3K inhibition should be investigated further and considered a therapeutic option in addition to current treatment protocols.

INTRODUCTION

During the last two decades, T-ALL has been extensively typed for recurrent chromosomal rearrangements and mutations¹⁻³. Distinct T-ALL subtypes have been identified that are characterized by specific driving oncogenic lesions—i.e. the so-called type A mutations—that facilitate differentiation arrests at specific T-cell developmental stages⁴⁻⁷. Type A mutations are accompanied by type B mutations^{6,8} that disturb a multitude of cellular processes such as cell cycle, apoptosis, ubiquitin-mediated proteolysis, or kinase activity by activating pathways including NOTCH1^{9,10}, N/K-RAS¹¹⁻¹⁴, JAK-STAT^{3,15}, PTEN-PI3K-AKT^{10,16}.

Mutations in *interleukin-7 receptor alpha chain (IL7Ra)* have recently been identified as an additional type B mutation in approximately 9% of pediatric T-ALL patients^{17,18}. Activating *IL7Ra* mutations generate a cysteine residue in the juxta-membrane-transmembrane domain of the receptor that facilitates formation of intermolecular disulfide bonds, homodimerization, and IL7-independent signaling of the mutant IL7Ra^{17,18}. IL7R signaling results in the phosphorylation and activation of STAT5, JAK1 and PI3K-AKT and provides a proliferation and survival advantage in T-cell development and T-ALL¹⁸⁻²⁰. Survival of normal developing thymocytes depends on the IL7R-mediated induction of anti-apoptotic BCL2²¹⁻²³. Signaling through the intact heterodimeric IL7 receptor α - with common γ -chain is required for normal thymocytes development beyond the early double-negative 2 (DN2) stage^{24,25}. The *IL7Ra* gene is one of many transcriptional targets of NOTCH1; its expression can be regulated by interaction of NOTCH1 with a distal *IL7Ra* enhancer²⁶⁻²⁸. When expressed, the IL7R is activated by interaction with its ligand IL7 and recruits Janus kinases (JAK1 and JAK3) and STAT5^{29,30}. In malignant T-cells, IL7-dependent survival and cell cycle progression primarily act via the downstream PI3K-AKT pathway that not only induces *BCL2* expression, but also down-regulates the cell cycle inhibitor p27^{KIP1}^{31,32}. Additionally, IL7-induced lymphomas in mice depend on STAT5³³ and ectopic STAT5 expression in transgenic mice or in bone marrow transplantation assays is sufficient to induce thymic T-cell lymphomas^{34,35}. Recently, activating *STAT5B* mutations have been identified in human T-ALL³⁶⁻³⁸.

Mutations in *JAK1* have been found in 4-27% of T-ALL patients^{3,15,39,40}. Even though they have been detected in AML, pre-B-ALL and solid tumors, *JAK1* mutations are most frequent in T-ALL^{15,39-42}. Activating *JAK1* mutations induce IL3-independent growth of Ba/F3 cells and activate downstream AKT and ERK^{15,42}. Similar to the *JAK2_V617F* mutation in myeloid disorders⁴³⁻⁴⁸, *JAK1* mutant molecules need the FERM domain to interact with interleukin homodimers or heterodimers to initiate ligand-independent activation of STAT proteins^{49,50}. The gene encoding the non-receptor type protein tyrosine phosphatase 2 (*PTPN2*), an important negative regulator of JAK1, is deleted in 6% of (predominantly *TLX1*-rearranged) T-ALL patients^{51,52}. *PTPN2* deletion is associated with activation of both wild type and mutant JAK1 and decreases the sensitivity of mutant JAK1-transformed Ba/F3 cells to the JAK inhibitor I⁵².

In contrast to other hematological malignancies^{41,53}, *JAK2* mutations have not been found in T-ALL. Several *JAK2* fusion products exist in a variety of hematological disorders (reviewed in⁵³). Of these fusions, the *ETV6-JAK2* fusion product is associated with T-ALL⁵⁴. This raises the

possibility that *JAK2* fusion products can act as oncogenes and contribute to the pathogenesis of T-ALL, as was demonstrated in *ETV6-JAK2* transgenic mice⁵⁵.

JAK3 is activated by interacting with the common γ -chain of several interleukin heterodimeric receptors⁵⁶, has an important role in lymphoid development, and was found mutated in adult T-cell leukemia/lymphoma and acute megakaryoblastic leukemia (AMKL) (reviewed in ^{53,57}). Even though it was discovered in AMKL, the *JAK3_A572V* pseudo-kinase domain mutant causes lymphoproliferative disease in mice, activates STAT5, AKT and ERK and induces ligand-independent growth when transfected in Ba/F3 cells^{58,59}. Interestingly, both *JAK3_A572V* and *JAK3_A573V* mutations were found in natural killer/T-cell lymphoma⁶⁰, while the *JAK3_A573V* and two other *JAK3* mutations (*JAK3_R657Q* and *JAK3_M511I*) have recently also been found in T-ALL patients^{3,61}.

In addition to *IL7Ra* and *JAK* mutations^{3,15,17,18}, previous studies reported other mutated signaling molecules in T-ALL that normally act in response to IL7 signaling including *N/K-RAS*¹²⁻¹⁴, *NF1*¹¹, *PTEN*, *PI3K*, *AKT*^{10,16,62}. Here, we set out to uncover the degree to which all of these mutations of *IL7Ra* and its downstream signaling molecules co-occur in T-ALL and the degree to which they can activate (independent of ligand stimulation) the different signal-transduction pathways JAK-STAT, RAS-MEK-ERK and PI3K-AKT-mTOR. We tested clinically relevant inhibitors for their ability to block activation of these pathways and found that combined inhibition of MEK and PI3K/AKT abolishes all activation of downstream signaling molecules.

MATERIALS AND METHODS

Patient samples

In this study, 146 primary pediatric T-ALL patient samples were included. The patients' parents or legal guardians provided informed consent to use leftover diagnostic material for research in accordance with the Institutional Review Board of the Erasmus MC Rotterdam and the Declaration of Helsinki. Leukemia cells were harvested from blood or bone marrow samples and enriched to a purity of at least 90%.

Detection of mutations

Hotspot areas of *N-RAS* and *K-RAS* (exons 2 and 3), the FERM domain (exons 3-9), pseudokinase domain (exons 12-18) and kinase domain (exons 19-25) of *JAK1*, the pseudokinase (exons 12-19) and kinase domain (exons 20-25) of *JAK2*, the SH2 domain (exon 11), pseudokinase (exons 12-17) and kinase domain (exons 18-24) of *JAK3*, and the complete *TYK2* gene (exon 1-23) were sequenced. PCR reactions were performed using 25-50ng genomic DNA, 300nM primers, 200 μ M dNTPs, 2mM MgCl₂, 1.25 units of *ampliTaq* gold (Applied Biosystems) in 1x PCR buffer II (Applied Biosystems) in a volume of 50 μ l. PCR products were purified with the Millipore Vacuum Manifold filter system (Millipore) and sequenced (BigDye Terminator v3.1 Cycle sequencing Kit, Applied Biosystems) on the ABI PRISM 3130 DNA Analyzer (Applied Biosystems).

Ba/F3 transfectants

Gateway multi-site recombination (Invitrogen) was used to simultaneously clone multiple DNA fragments (**Supplementary Figure S1A**) into our Gateway-adapted pcDNA3.1 destination vector that contains either a SV40-driven neomycin or puromycin cassette. Ba/F3 cells were transfected by electroporation and transfected cells were enriched to >95% purity using the CD271 (LNGFR) MicroBead kit and magnetic separation (MiltenyiBiotec). Single-cell clones were grown after plating the enriched cells at 0.5 cells/well in 96-well plates.

Doxycycline-dependent induction of mutant genes in Ba/F3 cells

We developed a doxycycline-inducible system in the murine Ba/F3 cell line that normally depends on IL3 for survival and proliferation (**Supplementary Figure S1**). IL3 withdrawal was done regularly to ensure that all selected Ba/F3 clones remain IL3-dependent. Doxycycline-induced expression of the mutant gene was done for 24 hours after which IL3-independent proliferation and activation of signaling molecules was tested for each of the lines.

Inhibitors

IC50 values for each of the inhibitors were determined using the following concentration ranges: 0.5 nM-2 μ M for JAK inh 1 (Merck #420099), 0.5 nM-5 μ M for Ruxolitinib (SelleckChem#S1378), 0.2-50 μ M for Pimozide (Sigma-Aldrich #P1793), 0.2-16.7 μ M for Ly294002 (Cell Signaling #9901), 0.06-5 μ M for MK-2206 (SelleckChem#S1078), 0.4 nM-4 μ M for Rapamycin (SelleckChem#S1039), and 0.5-125 μ M for CI-1040 (Axon Medchem #Axon 1368).

Antibodies

Antibodies used for western blots: phospho-AKT S473 (#9271), phospho-ERK1/2 (#4370), phospho-JAK1 (#3331), phospho-MEK1/2 (#9154), phospho-mTOR(#2971), phospho-p70S6Kinase (#9204), phospho-STAT1 (#9167), phospho-STAT3 (#9145), phospho-STAT5 (#9351), phospho-TYK2 (#9321), DYKDDDDK (#2368) (Cell Signaling Technology), CD127(IL7Ra) (R&D systems #MAB306), RAS (Millipore #05-516) and β -actin (Sigma #2547). CD127-FITC (#130-094-888) and CD271(LNGFR)-APC (#130-091-884, both from Miltenyi Biotec) were used for flow cytometry.

Statistics

Statistics were performed using SPSS 15.0 software. Pearson's Chi-square test was performed to test statistical significant differences in the distribution of nominal data. If the number of patients tested in individual groups was lower than five, Fisher's exact test was used instead. Statistical significance for continuous distributed data was tested using the Mann-Whitney-U test. Data were considered significant when $p < 0.05$ (two-sided).

RESULTS AND DISCUSSION

Identification of *JAK1*, *JAK3*, *N-RAS* and *K-RAS* mutations in T-ALL

IL7R mutations were previously identified in 9% of pediatric T-ALL cases¹⁸. In addition, mutations affecting all three of the following pathways occur in T-ALL: JAK-STAT, RAS-MEK-ERK and PI3K-AKT-mTOR^{3,10-16,62}. Since these pathways are downstream of *IL7R* signaling, we questioned whether these mutations occur in a mutually exclusive manner in T-ALL. We screened 146 pediatric T-ALL patient samples for mutations in the Janus kinase gene family, as well as for mutations in *N-RAS* and *K-RAS*. While we did not detect any mutations in *JAK2* or *TYK2*, several T-ALL patient samples revealed *JAK1*, *JAK3*, *N-RAS* or *K-RAS* mutations (**Table 1**). Out of 146 samples, 10 harbor *JAK1* and/or *JAK3* mutations, 2 of which have both a *JAK1* and a *JAK3* mutation. Out of 146 samples, 15 have *N-RAS* or *K-RAS* mutations. *NF1* negatively regulates RAS signaling and is deleted in 3 instances¹¹. From the 18 cases in which RAS signaling is enhanced by an *N/K-RAS* mutation or *NF1* deletion, only 3 co-occur with *JAK* mutations, and one with an *IL7Ra* mutation. Except for this co-occurrence with one *N-RAS* mutation, *IL7Ra* mutations do not co-occur with *JAK*, *RAS*, *PTEN* and *AKT* mutations. Previously described inactivating *PTEN* and activating *AKT* mutations⁶² also occur in a mutually exclusive manner with *IL7Ra* and *JAK* mutations, and rarely occur together with *N-RAS* or *K-RAS* mutations (**Table 1**). Together, the results summarized in **Table 1** reveal that activating mutations in JAK-STAT, RAS-MEK-ERK and PI3K-PTEN-AKT-mTOR pathways downstream of *IL7R* signaling are essentially mutually exclusive in T-ALL. Furthermore, *IL7Ra* mutations predominantly fall in the TLX subgroup; one has a gene expression profile (GEP) of the TALLMO subgroup whereas no *IL7Ra* mutations were detected in the proliferative or ETP-ALL subgroups (**Supplementary Table S1**). *JAK* mutations are associated with a GEP cluster other than the TALLMO group and *RAS* or *NF1* mutations frequently occur in ETP-ALL (**Supplementary Table S1**³). Combined, the *IL7R* pathway mutations *IL7Ra*, *JAK* and *RAS* tend to correlate with the TLX and ETP-ALL GEP clusters, which consist of TCRgd lineage (TLX3) and immature (ETP-ALL) arrested T-ALL cells. The *IL7Ra*, *JAK* and *RAS* mutated cases frequently also contain *NOTCH1/FBXW7* mutations (**Table 1**). Indeed, RAS-activating and (weak) NOTCH-activating mutations cooperate in T-ALL; Notch1-activating mutations are acquired in a majority of oncogenic K-RAS or RASGRP1-induced mouse models of T-ALL⁶³⁻⁶⁵. In contrast, *PTEN/AKT* mutated cases do not frequently contain *NOTCH1/FBXW7* mutations (**Table 1**). This concurs with our previous findings that *PTEN/AKT* mutations predominantly associate with the TALLMO subgroup and are mostly mutually exclusive with NOTCH-activating mutations^{62,66}.

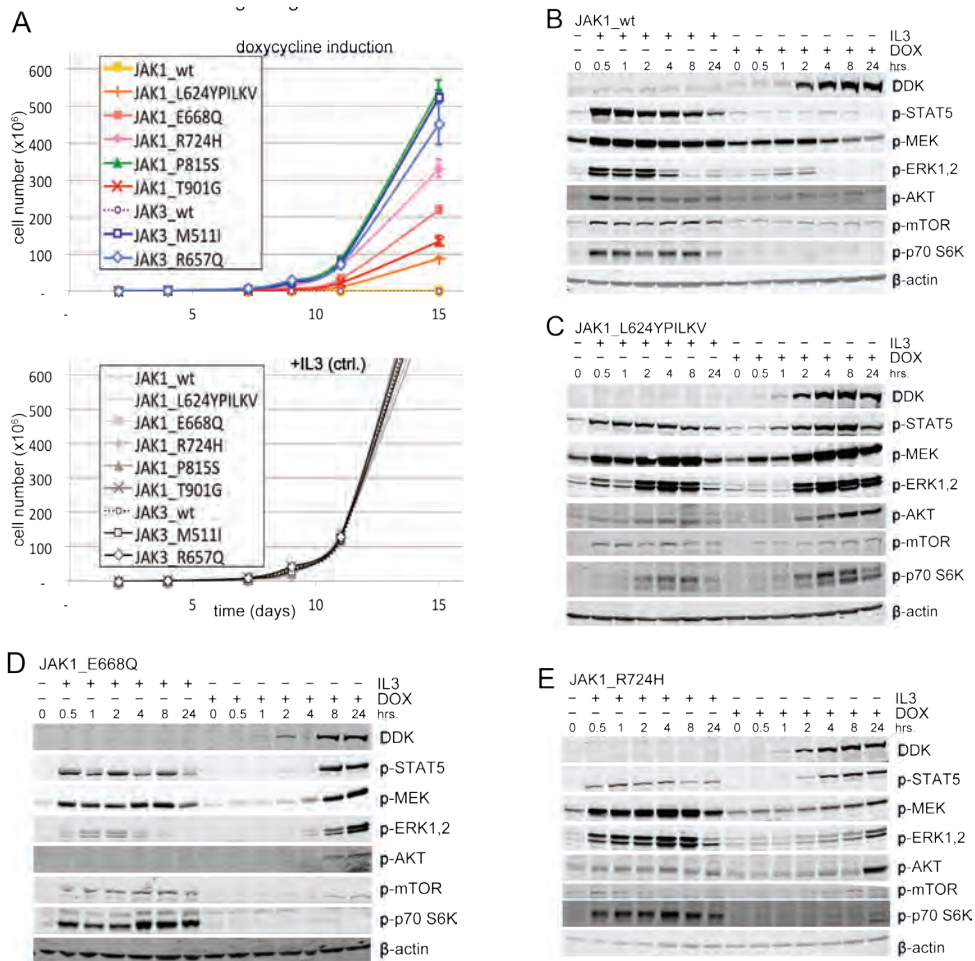
Transforming capacities of *JAK1* and *JAK3* mutants

IL7 signaling is important for survival and growth of developing T-cells and activates the JAK-STAT and PI3K-AKT-mTOR pathways^{19,29,30,32,67}. Because we determined that both *IL7Ra* mutations and mutations in *JAK1/3*, *N/K-RAS*, *PTEN* and *AKT* that are in pathways downstream of *IL7R* signaling occur in a mutually exclusive manner, we next explored whether these mutations could function in a similar way. In order to test this, we cloned and transfected several constructs containing the

oncogene	GEP Cluster	IL7R	JAK1	JAK3	N-RAS	K-RAS	NF1	PTEN	AKT	NOTCH/FBXW7
		non-cysteine mutations								
MLL	nd	V253WN	-	-	-	-		-	-	-
	ETP-ALL	V253GPSL	-	-	-	-		-	-	PEST
		cysteine mutations								
TLX3	nd	IL241-242CLEG	-	-	-	-		-	-	HD/PEST
TLX3	TLX	PILLT240-244RFCPH	-	-	-	-		-	-	HD
TLX3	TLX	PILLTIS240-246LKC	-	-	-	-		-	-	-
TLX3	TLX	LLT242-244HFPNCGP	-	-	G12D	-		-	-	HD
HOXA	TLX	L243RLECV	-	-	-	-		-	-	PEST
HOXA	nd	LL242-L243FPHQHC	-	-	-	-		-	-	FBXW7
SET-NUP214	TLX	LLTIS242-246PQGCG	-	-	-	-		-	-	HD/FBXW7
	nd	PIL240-242QSPSC	-	-	-	-		-	-	HD
	TLX	LT243-244LMCPT	-	-	-	-		-	-	JM
	TALLMO	PILLTIS240-S246LQSC	-	-	-	-		-	-	-
TLX3	TLX	-	E668Q	-	nd	nd	Del/333dupA	-	-	HD/FBXW7
LYL1/LMO2	TALLMO	-	L624YPILKV	-	-	-		-	-	JM/PEST
	Proliferative	-	V427M	-	-	-		-	-	HD/PEST
CALM-AF10	nd	-	P815S	-	-	-		-	-	HD/PEST
RUNX1-AFF3	ETP-ALL	-	T901G	M511I	-	-		-	-	PEST
	ETP-ALL	-	R724H	M511I	G12D	-		-	-	PEST
	ETP-ALL	-	-	M511I	nd	nd	Del/-	-	-	PEST
TLX3	TLX	-	-	M511I	-	-		-	-	JM
CALM-AF10	TLX	-	-	R657Q	-	-		-	-	HD/PEST
TLX3	TLX	-	-	R657Q	nd	nd		-	-	ND
TLX3	TLX	-	-	-	G12D	-		-	-	-
TLX3	TLX	-	-	-	G12V	-		-	-	HD
TLX3	nd	-	-	-	G12C	-		-	-	HD/FBXW7
TLX3	nd	-	-	-	G13V	-		-	-	HD/FBXW7
CALM-AF10	ETP-ALL	-	-	-	G12D	-		-	-	-
SIL-TAL1	nd	-	-	-	G13C	-		Mut/Del	-	-
NKX2-5	ETP-ALL	-	-	-	G13D	-		Mut/Mut/Subcl. Del	-	HD
	TALLMO	-	-	-	G12R	-		-	-	FBXW7
TAL2	TALLMO	-	-	-	G12D	-		no protein	-	FBXW7
LMO2	TALLMO	-	-	-	G12D	-		-	-	-
TLX3	TLX	-	-	-	Q61R	-		-	-	HD/FBXW7
MEF2C	ETP-ALL	-	-	-	Q61L	-		-	-	HD/PEST
CALM-AF10	ETP-ALL	-	-	-	nd	nd	Del/3734DelCnsGGTTTATGGTTT	-	-	-
	nd	-	-	-	G12D	-		-	-	HD
SIL-TAL1	TALLMO	-	-	-	-	-		Subcl. Del/-	-	HD/PEST
SIL-TAL1	TALLMO	-	-	-	-	-		Mut/Mut	-	-
SIL-TAL1	TALLMO	-	-	-	-	-		Del/-	-	HD
SIL-TAL1	TALLMO	-	-	-	-	-		Subcl. Del/-	-	-
SIL-TAL1	TALLMO	-	-	-	-	-		Subcl. Mut/-	-	-
SIL-TAL1	TALLMO	-	-	-	-	-		Del/Del	-	-
SIL-TAL1	TALLMO	-	-	-	-	-		Del/Subcl. Del	-	-
SIL-TAL1	TALLMO	-	-	-	-	-		Del/Subcl. Del	-	-
SIL-TAL1	TALLMO	-	-	-	-	-		Mut/Mut	-	-
LMO3	TALLMO	-	-	-	-	-		Mut/Mut	-	-
LMO2	TALLMO	-	-	-	-	-		Mut/Mut	-	FBXW7
	TALLMO	-	-	-	-	-		Mut/Mut	-	HD
	TALLMO	-	-	-	-	-		Mut/Mut	-	-
	TALLMO	-	-	-	-	-		Subcl. Del/-	-	-
	TALLMO	-	-	-	-	-		Mut/Subcl. Del	-	-
	TALLMO	-	-	-	-	-		Mut/Subcl. Del	-	-
NKX2-1	Proliferative	-	-	-	-	-		Mut/-	-	HD/FBXW7
TAL1	Proliferative	-	-	-	-	-		no protein	-	HD
SIL-TAL1	Proliferative	-	-	-	-	-		Mut/Mut	-	-
SIL-TAL1	Proliferative	-	-	-	nd	-		Mut/Mut	-	PEST
	ETP-ALL	-	-	-	-	nd		Del/-	-	PEST
MYC	nd	-	-	-	-	-		Mut/Del	-	-
LMO2	nd	-	-	-	-	-		Mut/Mut/Subcl. Del	-	PEST
	nd	-	-	-	-	-		Del/-	-	-
	nd	-	-	-	-	-		Mut/Del	-	-
TLX1	Proliferative	-	-	-	-	-		-	E17K	-
TLX3	Proliferative	-	-	-	-	-		-	E17K	FBXW7
LMO1	TALLMO	-	-	-	-	-		-	E17K	-

Table 1 | From a cohort of 146 screened pediatric T-ALL patients, 64 are listed with mutations in at least one of the following genes: *IL7Ra*, *JAK1*, *JAK3*, *N-RAS*, *K-RAS*, *NF1*, *PTEN* and *AKT*. The *NOTCH/FBXW7* mutational status is listed in the last column. The column ‘oncogene’ lists the driving oncogene or translocation based on the known genetic aberration. GEP cluster: unsupervised clustering groups the patients based on gene expression profile similarity. ND: not done; -: tested negative.

truncated NGFR reporter (LNGFR) and (wild-type or mutant) gene with a C-terminal DDK (Flag) tag (JAK and AKT constructs) or without a tag (IL7Ra and N-RAS constructs) into Ba/F3 cells (**Supplementary Figure S1A, B**). All Ba/F3 lines express LNGFR (**Supplementary Figure S1C**). Upon addition of doxycycline, the wild type and mutant genes are induced as measured by DDK expression (western blot, **Supplementary Figure S1D**) and IL7Ra/CD127 or RAS expression (flow cytometry; **Supplementary Figure S1C, E**). We tested whether each of these stable Ba/F3 lines could support cell proliferation in the absence of IL3 when induced with doxycycline. All JAK mutants support IL3-independent proliferation (**Figure 1A**) and activation of certain signal transduction pathways, whereas expression of wild-type JAK1 or JAK3 does not (**Figure 1B-G** and **Supplementary Figure S2**). Activation of doxycycline-induced signaling pathways was usually 2-4 hours delayed when compared to IL3 induction (after which signaling is detectable virtually immediately). This delay is due to the time needed to express the mutant protein after addition of doxycycline (**Figure 1B-G** and **Supplementary Figure S2**).



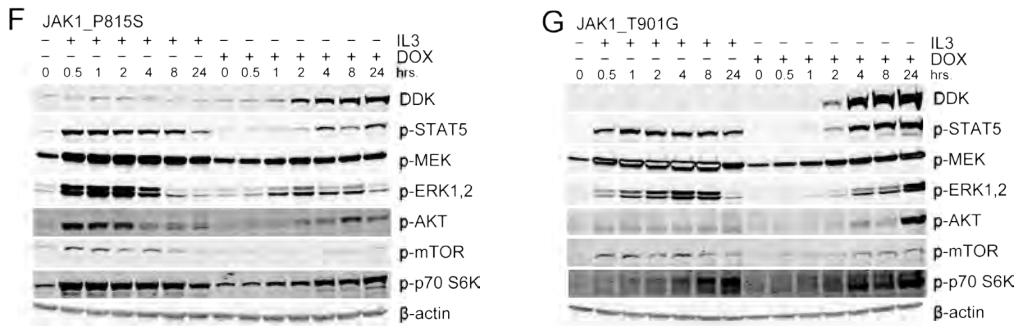


Figure 1 | *JAK1* and *JAK3* mutations promote IL3-independent proliferation and *JAK1* mutants activate downstream signaling. **A.** Survival curves of Ba/F3 lines with different *JAK1* or *JAK3* constructs after induction by doxycycline (top) or in the presence of IL3 (control; bottom). The cultures were each initiated with 2×10^5 cells at day 0 after extensive washing. **B-G.** Western blot analyses of DDK and multiple phospho-proteins of lysates from a time-series after stimulation with IL3 or induction of the mutant construct by doxycycline (DOX) of Ba/F3 lines containing *JAK1*_wt (**B**), *JAK1*_L624YPIIKV (**C**), *JAK1*_E668Q (**D**), *JAK1*_R724H (**E**), *JAK1*_P815S (**F**), and *JAK1*_T901G (**G**). Levels of b-actin were used as total protein loading controls.

The cysteine-mutated IL7Ra line results in ligand-independent downstream signaling and cell proliferation

IL7R mutations were previously identified in 9% of pediatric T-ALL cases, most of which result in the introduction of a cysteine amino acid that facilitates receptor homodimerization and ligand-independent activation¹⁸. We explored activation of JAK-STAT, RAS-MEK-ERK, and PI3K-AKT-mTOR signal transduction pathways upon expression of *IL7Ra*_wt, a non-cysteine mutant *IL7Ra*_V253GPSL (also designated as *IL7Ra*_GPSL) and a cysteine mutant *IL7Ra*_PILLT240-244RFCPH (also designated as *IL7Ra*_RFCPH). The *IL7Ra*_RFCPH mutant, but not the *IL7Ra*_wt and GPSL mutant line, supports IL3-independent proliferation (**Supplementary Figure S3A**). When IL7 was added instead of IL3, the *IL7Ra*_wt and *IL7Ra*_GPSL lines also supported cell proliferation, indicating that the *IL7R* pathway is functionally intact and actively signaling when stimulated (**Supplementary Figure S3A**). The IL7-dependent proliferation of all three *IL7Ra* lines and the IL3- and IL7-independent proliferation of only the *IL7Ra*_RFCPH cysteine mutant line is supported by activated downstream signaling as evident from the expression of key phosphorylated molecules in the JAK-STAT, RAS-MEK-ERK and PI3K-AKT-mTOR pathways (**Supplementary Figure S3B-D**). In addition, these data clearly demonstrate that apart from the JAK-STAT and PI3K-AKT-mTOR pathways, *IL7R* signaling also results in the activation of the RAS-MEK-ERK pathway.

While the cysteine mutant *IL7Ra*_RFCPH supports IL7-independent proliferation and activation of downstream signaling molecules (**Supplementary Figure S3A, D**), there is currently no evidence from these *in vitro* studies that the non-cysteine mutant (*IL7Ra*_GPSL) has any transforming capacities. Because *IL7Ra*_GPSL supports Ba/F3 growth in the presence of IL7, it is possible that this mutation leads to a selective advantage in the context of IL7 signaling in leukemia patients. The cysteine mutation in the transmembrane region of the IL7 receptor—that is lacking in the *IL7Ra*_GPSL mutant but present in most other *IL7Ra* mutations—allows

cysteine-cysteine bonds and homodimerization of the receptor (**Supplementary Figure S4**), which results in IL7-independent signaling^{17,18}.

Transforming capacities of AKT and N-RAS mutants

Similar to the IL7Ra and JAK mutant lines, both AKT_E17K and N-RAS_G12D mutations (but not the wild-type molecules) result in IL3-independent growth and activation of downstream signal transduction (**Supplementary Figure S5**). The AKT_E17K mutant induces proliferation, but at a lower rate than the JAK and IL7Ra mutants. The N-RAS_G12D mutant does not provide a growth advantage right after doxycycline induction, but starts proliferating after approximately 7 days. The proliferation rate after 7 days, however, is comparable to that of the JAK and IL7Ra mutants (**Supplementary Figure S5A**).

Different mutants result in different activation of signal-transduction pathways

After 24 hours of doxycycline induction the signaling pathways seem maximally active and thus this time-point was taken to compare signaling between the different mutant lines. Even though the JAK1, JAK3 and IL7Ra mutants all give rise to a growth advantage, not all downstream signaling molecules are activated to the same extent (**Figure 2**). For example, the JAK1_R724H and JAK1_T901G mutant lines display stronger signaling than the JAK3 mutants as determined by the expression of phospho-STAT proteins, p-MEK, p-AKT and p-S6Kinase (**Figure 2**).

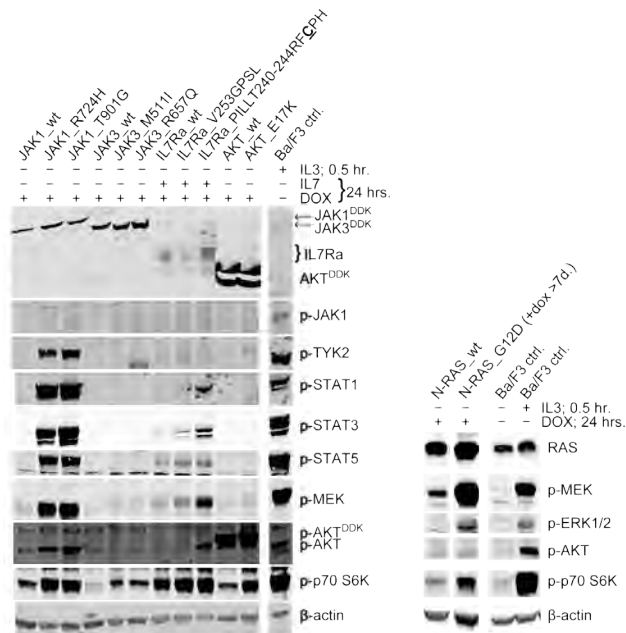


Figure 2 | Differential activation of downstream signaling by *IL7Ra*, *JAK1*, and *JAK3* mutants. Western blot analysis of several phospho-proteins to indicate the relative signal transduction strength between different wild type and mutant Ba/F3 lines after 24 hours of induction with doxycycline.

Remarkably, these JAK1 mutants also cause TYK2 phosphorylation. The AKT, JAK1 and IL7Ra mutants have comparable p-S6Kinase activation as a final read-out of pathway activation, but the IL7Ra lines do not yield similarly high levels of p-STAT, p-MEK and p-AKT compared to the JAK1 mutants. Furthermore, the IL7Ra cysteine mutant RFCPH signals somewhat stronger than the non-cysteine mutant IL7Ra_GPSL (**Figure 2**). *IL7Ra* mutations that result in IL7Ra homodimers due to cysteine bonds enhance JAK1 activation but not JAK3¹⁸. A possible explanation is that mutant IL7Ra homodimerization occurs at the expense of heterodimerization with the common γ -chain that is normally required for binding and activation of JAK3^{56,68}. While the JAK3 mutant lines result in very robust IL3-independent growth (**Figure 1A**), the phosphorylated signaling molecules are very weak in comparison to the JAK1 and IL7Ra mutants (**Figure 2**). We speculate that activation of the RAS-MEK-ERK pathway by JAK3 remains dependent on the presence of the IL7R when JAK3 is mutated, whereas signaling of mutant JAK1 could have become independent of receptor binding.

IL7R pathway inhibitors affect the transforming capacities of the different mutants

Because the growth curves and downstream signaling of the different mutant lines are not identical, it is plausible that responses to the inhibitors of different downstream signaling molecules in the IL7R pathway also differ. Multiple Ba/F3 lines were subjected to a concentration range of several inhibitors (**Figure 3A**) and cell growth was tested in an MTT assay to address differences in sensitivity. Ba/F3 lines without doxycycline-induction of the transgene and in the presence of IL3 (as indicated by the solid black symbols (**Figure 3**) behave like the non-manipulated parental Ba/F3 cell line and are resistant to all inhibitors except Ruxolitinib (**Figure 3C**) and the RAS inhibitor Tipifarnib (not shown). Despite the fact that Ba/F3 cells are somewhat sensitive to the JAK inhibitor Ruxolitinib in the presence of IL3 signaling, Ba/F3 lines that are induced to express IL7Ra, JAK1 and JAK3 mutant versions (that grow independently of IL3) are extremely sensitive to Ruxolitinib (red symbols, **Figure 3C**). On the other hand, Ba/F3 lines that depend only on active AKT or N-RAS signaling are completely unaffected by JAK inhibition (**Figure 3C**). Ruxolitinib inhibits constitutively active JAK1 and JAK3 signaling as well as signaling from the upstream IL7Ra mutants, but not the downstream AKT or RAS signaling, indicating the specificity of this JAK inhibitor.

Experiments with the JAK inhibitor 1 show a similar pattern (**Figure 3B**), although not all lines are sensitized to the same extent: IL7Ra RFCPH and JAK3_R657Q seem less sensitive to JAK inhibitor 1 when compared to the non-induced (+IL3) controls. Except for a moderate effect on JAK1 mutants, the STAT5 inhibitor Pimozide has no effect on the mutant lines (**Figure 3D**), suggesting additional pathways activated by IL7R signaling are involved. Indeed, the PI3K inhibitor Ly294002 results in less growth of the JAK1, JAK3 and AKT mutant lines, but not of the IL7Ra lines (**Figure 3E**). The AKT and mTOR inhibitors affect only the mutant AKT lines effectively (**Figure 3F-G**). MEK inhibition slows growth of the mutant N-RAS lines, and the JAK lines to varying degrees, but has no effect on the IL7Ra and mutant AKT lines (**Figure 3H**).

Combined, these data indicate that inhibiting JAK can be effective in targeting leukemic cells

harboring activating mutations in *IL7Ra*, *JAK1* and *JAK3*. However, leukemic cells with mutations in any molecules downstream of or parallel to this pathway (*PI3K*, *PTEN*, *AKT*, *N-RAS*, *K-RAS*, *NF1*) will grow independent of inhibition of upstream signaling.

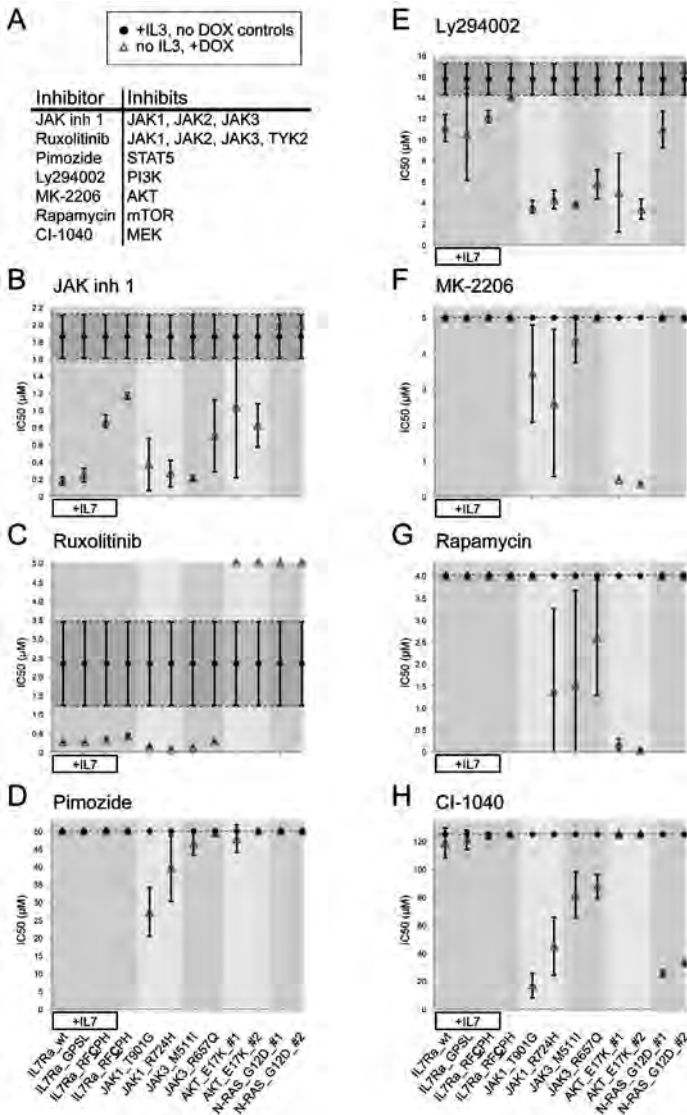
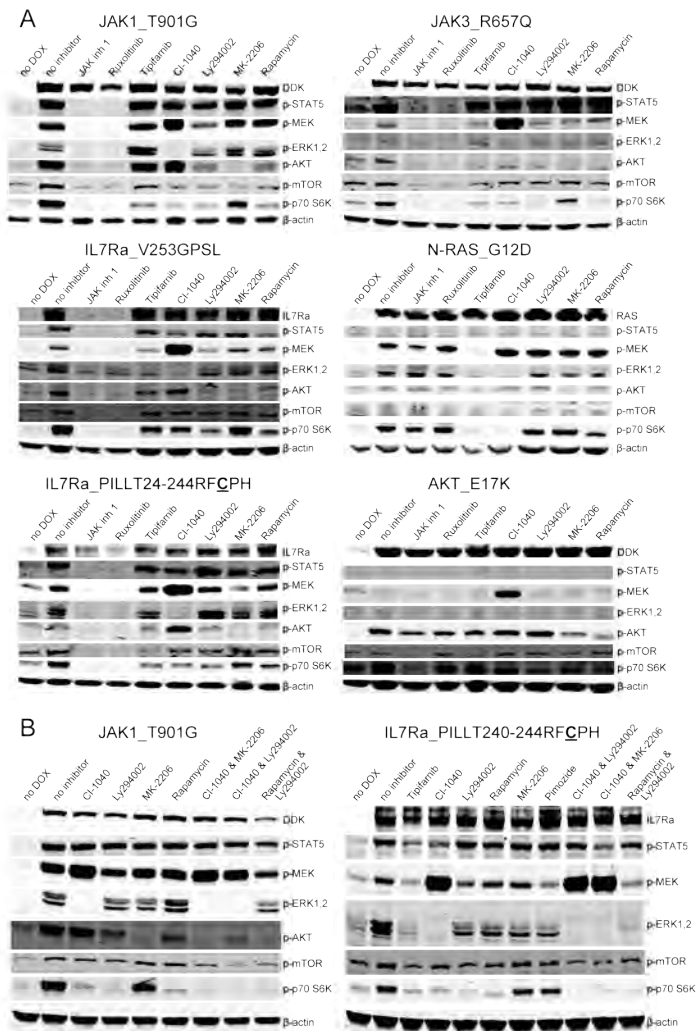


Figure 3 | Sensitivity levels of *IL7Ra*, *JAK*, *AKT*, and *RAS* mutant lines to various *JAK*, *PI3K*-*AKT*, and *RAS*-*MEK* pathway inhibitors. A. Inhibitors that were tested in MTT assays. B-H. Summary of the IC₅₀ values obtained for each of the indicated Ba/F3 lines in the presence of IL3 (control, indicated by the average of all Ba/F3 lines; solid black circles) or after doxycycline-induction of the (mutant) protein in the absence of IL3 (open red triangles). The maximum used concentrations of the inhibitors were 2 μM for JAK inh 1 (B), 5 μM for Ruxolitinib (C), 50 μM for Pimozide (D), 16.7 μM for Ly294002 (E), 5 μM for MK-2206 (F), 4 μM for Rapamycin (G), and 125 μM for CI-1040 (H); points that reach the maximum value represent a completely resistant condition for which an IC₅₀ could not be determined. Varying sensitivity of control Ba/F3 cells to JAK inh 1, Ruxolitinib, and Ly294002 is indicated by the darker shaded area between dashed lines (B, C, E).

Inhibiting PI3K-AKT or RAS-MEK-ERK signaling cross-activates the other pathway

In addition to reducing the cell proliferation (**Figure 3**), the use of single JAK inhibitors JAK inh I or Ruxolitinib effectively prevents phosphorylation of downstream molecules in IL7Ra mutant and JAK mutant Ba/F3 lines (**Figure 4A**). In line with inhibition of IL7Ra proximal signaling, downstream mutant RAS and AKT are insensitive to these JAK inhibitors, but do respond to their specific inhibitors. For example, Tipifarnib and CI-1040 (inhibition of RAS and MEK, respectively) block signaling by the N-RAS_G12D mutant as demonstrated by the lack of phosphorylated p70S6K (**Figure 4A**). Inhibitors of PI3K pathway molecules Ly294002, MK-2206 and Rapamycin effectively inhibit growth (**Figure 3**) and p-p70 S6K (**Figure 4A**) of the AKT_E17K, but not the N-RAS_G12D mutant. Exposure of IL7Ra or JAK mutants to any of the single agents Ly294002, MK-2206, Rapamycin or CI-1040 only has a partial effect (JAK mutants) or no effect (IL7Ra lines) on reducing proliferation (**Figure 3E-H**) and a partial effect on reduction of p-p70 S6K (**Figure 4A**).



C

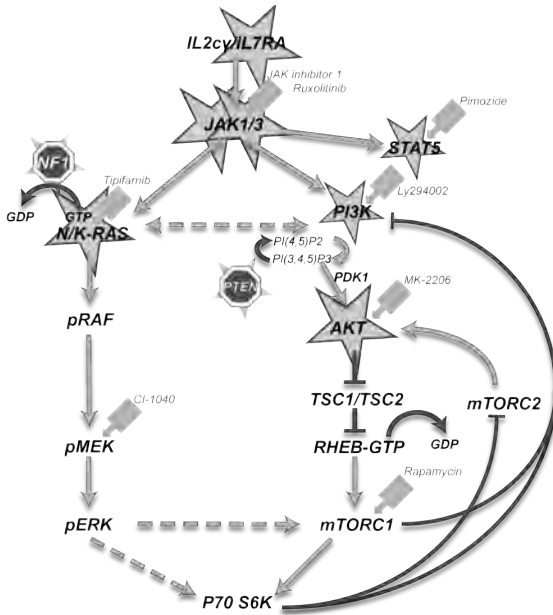


Figure 4 | Effect of the (combinations of) specific inhibitors on downstream signaling induced by the IL7Ra, JAK, AKT, and RAS mutants. A. Western blot analysis of phospho-proteins of doxycycline-induced mutant Ba/F3 lines (6 hours after IL3 deprivation) in the presence of several pathway inhibitors (24 hours). The following concentrations of inhibitors were used: JAK inh 1 (1 μ M), Ruxolitinib (1 μ M), Tipifarnib (10 μ M, RAS inhibitor), CI-1040 (10 μ M), Ly294002 (10 μ M), MK-2206 (2 μ M), Rapamycin (1 μ M). **B.** The combination of the MEK inhibitor CI-1040 with either Ly294002 (PI3K) or MK-2206 (AKT), and the combination of mTOR and PI3K inhibitors Rapamycin and Ly294002 was used in two mutant lines: JAK1_T901G and IL7Ra_PILLT240-244R/FCPH. **C.** Schematic representation of signaling pathways with activating (blue stars) and inactivating (stop signs) mutated molecules found in T-ALL and the corresponding inhibitors (red font). Green arrows indicate activation, red lines inhibition.

The data suggest that IL7R signals through an alternate pathway than RAS-MEK-ERK and PI3K-AKT-mTOR, or that the IL7Ra lines enhance activation of one pathway when the other pathway is blocked. Some evidence points to the latter mechanism. In the JAK1 and IL7Ra lines, the p-AKT levels in the presence of the MEK inhibitor CI-1040 are as high as or higher than in control cells without any inhibitor (**Figure 4A**), suggesting the AKT pathway is preferred when the MEK-ERK pathway is blocked. RAS can signal to PI3K⁶⁹, and may do so in an enhanced manner in tumors that depend on this signaling for survival and in which the MEK-ERK pathway is blocked or in which a potential negative feedback loop is circumvented.

Combined inhibition of PI3K and MEK results in complete loss of downstream signaling

To test whether the RAS-MEK-ERK and PI3K-AKT-mTOR pathways are both important for the signaling capabilities of the Ba/F3 mutant lines, we analyzed the effect of an AKT- or PI3K inhibitor in combination with a MEK inhibitor in comparison to the effect of the single agents. Many cancers depend on these important pathways and combining MEK and PI3K inhibitors has been suggested to be effective in several cancer types⁷⁰⁻⁷². We tested activation of signaling

molecules in the presence of the following combinations of inhibitors: CI-1040 (MEK) with Ly294002 (PI3K), CI-1040 (MEK) with MK-2206 (AKT), and Rapamycin (mTOR) with Ly294002 (PI3K) (**Figure 4B**). All three combinations of inhibitors lead to significant reduction of p-p70S6K in the JAK1_T901G as well as the IL7Ra_RFPCPH mutant line as compared to the inhibition by each of the individual agents (**Figure 4B**). The most potent combination tested here is the CI-1040 and Ly294002, resulting in complete absence of p-p70 S6K (**Figure 4B**) and suggesting a synergistic mechanism. In addition to inhibiting both arms of signal transduction at the levels of MEK and PI3K simultaneously (**Figure 4C**), this combination of inhibitors also prevents any potential activation by cross-signaling between RAS and PI3Kinase⁶⁹, by the PI3K-dependent feedback loop from mTORC1 to ERK activation⁷³, or potential other cross-signaling events between these pathways⁷⁴.

Many leukemias depend on one or more of the central JAK-STAT, RAS-MEK-ERK and PI3K-AKT-mTOR growth and survival signaling pathways. In T-ALL, somatic mutations in genes of these pathways are acquired across different oncogene-driven subtypes, can be subclonal and/or arise at relapse, and are mostly mutually exclusive. Multiple inhibitors of the MEK and PI3K pathways are available, some of which are used clinically. Inhibiting both pathways simultaneously has a synergistic effect on blocking downstream signal transduction and also targets potential subclones. Therefore, combined MEK and PI3K pathway inhibition should be considered as a therapeutic option in addition to current treatment protocols.

REFERENCES

1. Meijerink JP. Genetic rearrangements in relation to immunophenotype and outcome in T-cell acute lymphoblastic leukaemia. *Best Pract Res Clin Haematol.* 2010;23:307-318.
2. Van Vlierberghe P, Ferrando A. The molecular basis of T cell acute lymphoblastic leukemia. *J Clin Invest.* 2012;122:3398-3406.
3. Zhang J, Ding L, Holmfeldt L, et al. The genetic basis of early T-cell precursor acute lymphoblastic leukaemia. *Nature.* 2012;481:157-163.
4. Ferrando AA, Neuberg DS, Staunton J, et al. Gene expression signatures define novel oncogenic pathways in T cell acute lymphoblastic leukemia. *Cancer Cell.* 2002;1:75-87.
5. Soulier J, Clappier E, Cayuela JM, et al. HOXA genes are included in genetic and biologic networks defining human acute T-cell leukemia (T-ALL). *Blood.* 2005;106:274-286.
6. Van Vlierberghe P, van Grotel M, Tchinda J, et al. The recurrent SET-NUP214 fusion as a new HOXA activation mechanism in pediatric T-cell acute lymphoblastic leukemia. *Blood.* 2008;111:4668-4680.
7. Homminga I, Pieters R, Langerak AW, et al. Integrated transcript and genome analyses reveal NKX2-1 and MEF2C as potential oncogenes in T cell acute lymphoblastic leukemia. *Cancer Cell.* 2011;19:484-497.
8. Meijerink JP, den Boer ML, Pieters R. New genetic abnormalities and treatment response in acute lymphoblastic leukemia. *Semin Hematol.* 2009;46:16-23.
9. Weng AP, Ferrando AA, Lee W, et al. Activating mutations of NOTCH1 in human T cell acute lymphoblastic leukemia. *Science.* 2004;306:269-271.
10. Palomero T, Dominguez M, Ferrando AA. The role of the PTEN/AKT Pathway in NOTCH1-induced leukemia. *Cell Cycle.* 2008;7:965-970.
11. Balgobind BV, Van Vlierberghe P, van den Ouweland AM, et al. Leukemia-associated NF1 inactivation in patients with pediatric T-ALL and AML lacking evidence for neurofibromatosis. *Blood.* 2008;111:4322-4328.
12. Kawamura M, Ohnishi H, Guo SX, et al. Alterations of the p53, p21, p16, p15 and RAS genes in childhood T-cell acute lymphoblastic leukemia. *Leuk Res.* 1999;23:115-126.
13. von Lintig FC, Huvar I, Law P, et al. Ras activation in normal white blood cells and childhood acute lymphoblastic leukemia. *Clin Cancer Res.* 2000;6:1804-1810.
14. Yokota S, Nakao M, Horiike S, et al. Mutational analysis of the N-ras gene in acute lymphoblastic leukemia: a study of 125 Japanese pediatric cases. *Int J Hematol.* 1998;67:379-387.
15. Flex E, Petrangeli V, Stella L, et al. Somatically acquired JAK1 mutations in adult acute lymphoblastic leukemia. *J Exp Med.* 2008;205:751-758.
16. Gutierrez A, Sanda T, Grebliunaite R, et al. High frequency of PTEN, PI3K, and AKT abnormalities in T-cell acute lymphoblastic leukemia. *Blood.* 2009;114:647-650.
17. Shochat C, Tal N, Bandapalli OR, et al. Gain-of-function mutations in interleukin-7 receptor-alpha (IL7R) in childhood acute lymphoblastic leukemias. *J Exp Med.* 2011;208:901-908.
18. Zenatti PP, Ribeiro D, Li W, et al. Oncogenic IL7R gain-of-function mutations in childhood T-cell acute lymphoblastic leukemia. *Nat Genet.* 2011;43:932-939.
19. Laouar Y, Crispe IN, Flavell RA. Overexpression of IL-7R alpha provides a competitive advantage during early T-cell development. *Blood.* 2004;103:1985-1994.
20. Rich BE, Campos-Torres J, Tepper RI, Moreadith RW, Leder P. Cutaneous lymphoproliferation and lymphomas in interleukin 7 transgenic mice. *J Exp Med.* 1993;177:305-316.
21. Akashi K, Kondo M, von Freeden-Jeffry U, Murray R, Weissman IL. Bcl-2 rescues T lymphopoiesis in interleukin-7 receptor-deficient mice. *Cell.* 1997;89:1033-1041.

22. Maraskovsky E, O'Reilly LA, Teepe M, et al. Bcl-2 can rescue T lymphocyte development in interleukin-7 receptor-deficient mice but not in mutant rag-1^{-/-} mice. *Cell*. 1997;89:1011-1019.
23. von Freeden-Jeffry U, Solvason N, Howard M, Murray R. The earliest T lineage-committed cells depend on IL-7 for Bcl-2 expression and normal cell cycle progression. *Immunity*. 1997;7:147-154.
24. Peschon JJ, Morrissey PJ, Grabstein KH, et al. Early lymphocyte expansion is severely impaired in interleukin 7 receptor-deficient mice. *J Exp Med*. 1994;180:1955-1960.
25. Cao X, Shores EW, Hu-Li J, et al. Defective lymphoid development in mice lacking expression of the common cytokine receptor gamma chain. *Immunity*. 1995;2:223-238.
26. Gonzalez-Garcia S, Garcia-Peydro M, Martin-Gayo E, et al. CSL-MAML-dependent Notch1 signaling controls T lineage-specific IL-7R{alpha} gene expression in early human thymopoiesis and leukemia. *J Exp Med*. 2009;206:779-791.
27. Wang H, Zang C, Taing L, et al. NOTCH1-RBPJ complexes drive target gene expression through dynamic interactions with superenhancers. *Proc Natl Acad Sci U S A*. 2014;111:705-710.
28. Wang H, Zou J, Zhao B, et al. Genome-wide analysis reveals conserved and divergent features of Notch1/RBPJ binding in human and murine T-lymphoblastic leukemia cells. *Proc Natl Acad Sci U S A*. 2011;108:14908-14913.
29. Foxwell BM, Beadling C, Guschin D, Kerr I, Cantrell D. Interleukin-7 can induce the activation of Jak 1, Jak 3 and STAT 5 proteins in murine T cells. *Eur J Immunol*. 1995;25:3041-3046.
30. Jiang Q, Li WQ, Aiello FB, et al. Cell biology of IL-7, a key lymphotrophin. *Cytokine Growth Factor Rev*. 2005;16:513-533.
31. Barata JT, Cardoso AA, Nadler LM, Boussiotis VA. Interleukin-7 promotes survival and cell cycle progression of T-cell acute lymphoblastic leukemia cells by down-regulating the cyclin-dependent kinase inhibitor p27(kip1). *Blood*. 2001;98:1524-1531.
32. Barata JT, Silva A, Brandao JG, et al. Activation of PI3K is indispensable for interleukin 7-mediated viability, proliferation, glucose use, and growth of T cell acute lymphoblastic leukemia cells. *J Exp Med*. 2004;200:659-669.
33. Abraham N, Ma MC, Snow JW, et al. Haploinsufficiency identifies STAT5 as a modifier of IL-7-induced lymphomas. *Oncogene*. 2005;24:5252-5257.
34. Kelly JA, Spolski R, Kovanen PE, et al. Stat5 synergizes with T cell receptor/antigen stimulation in the development of lymphoblastic lymphoma. *J Exp Med*. 2003;198:79-89.
35. Moriggl R, Sexl V, Kenner L, et al. Stat5 tetramer formation is associated with leukemogenesis. *Cancer Cell*. 2005;7:87-99.
36. Atak ZK, Gianfelici V, Hulselmans G, et al. Comprehensive analysis of transcriptome variation uncovers known and novel driver events in T-cell acute lymphoblastic leukemia. *PLoS Genet*. 2013;9:e1003997.
37. Kontro M, Kuusanmaki H, Eldfors S, et al. Novel activating STAT5B mutations as putative drivers of T-cell acute lymphoblastic leukemia. *Leukemia*. 2014.
38. Bandapalli OR, Schuessele S, Kunz JB, et al. The activating STAT5B N642H mutation is a common abnormality in pediatric T-cell acute lymphoblastic leukemia and confers a higher risk of relapse. *Haematologica*. 2014.
39. Asnafi V, Le Noir S, Lhermitte L, et al. JAK1 mutations are not frequent events in adult T-ALL: a GRAALL study. *Br J Haematol*. 2010;148:178-179.
40. Jeong EG, Kim MS, Nam HK, et al. Somatic mutations of JAK1 and JAK3 in acute leukemias and solid cancers. *Clin Cancer Res*. 2008;14:3716-3721.
41. Mullighan CG, Zhang J, Harvey RC, et al. JAK mutations in high-risk childhood acute lymphoblastic leukemia. *Proc Natl Acad Sci U S A*. 2009;106:9414-9418.
42. Xiang Z, Zhao Y, Mitaksov V, et al. Identification of somatic JAK1 mutations in patients with acute myeloid leukemia. *Blood*. 2008;111:4809-4812.

43. Baxter EJ, Scott LM, Campbell PJ, et al. Acquired mutation of the tyrosine kinase JAK2 in human myeloproliferative disorders. *Lancet*. 2005;365:1054-1061.
44. James C, Ugo V, Le Couedic JP, et al. A unique clonal JAK2 mutation leading to constitutive signalling causes polycythaemia vera. *Nature*. 2005;434:1144-1148.
45. Kralovics R, Passamonti F, Buser AS, et al. A gain-of-function mutation of JAK2 in myeloproliferative disorders. *N Engl J Med*. 2005;352:1779-1790.
46. Levine RL, Wadleigh M, Coombs J, et al. Activating mutation in the tyrosine kinase JAK2 in polycythemia vera, essential thrombocythemia, and myeloid metaplasia with myelofibrosis. *Cancer Cell*. 2005;7:387-397.
47. Zhao R, Xing S, Li Z, et al. Identification of an acquired JAK2 mutation in polycythemia vera. *J Biol Chem*. 2005;280:22788-22792.
48. Lu X, Huang LJ, Lodish HF. Dimerization by a cytokine receptor is necessary for constitutive activation of JAK2V617F. *J Biol Chem*. 2008;283:5258-5266.
49. Gordon GM, Lambert QT, Daniel KG, Reuther GW. Transforming JAK1 mutations exhibit differential signalling, FERM domain requirements and growth responses to interferon-gamma. *Biochem J*. 2010;432:255-265.
50. Hornakova T, Staerk J, Royer Y, et al. Acute lymphoblastic leukemia-associated JAK1 mutants activate the Janus kinase/STAT pathway via interleukin-9 receptor alpha homodimers. *J Biol Chem*. 2009;284:6773-6781.
51. Kleppe M, Lahortiga I, El Chaar T, et al. Deletion of the protein tyrosine phosphatase gene PTPN2 in T-cell acute lymphoblastic leukemia. *Nat Genet*. 2010;42:530-535.
52. Kleppe M, Soulier J, Asnafi V, et al. PTPN2 negatively regulates oncogenic JAK1 in T-cell acute lymphoblastic leukemia. *Blood*. 2011;117:7090-7098.
53. Vainchenker W, Constantinescu SN. JAK/STAT signaling in hematological malignancies. *Oncogene*. 2013;32:2601-2613.
54. Lacronique V, Boureux A, Valle VD, et al. A TEL-JAK2 fusion protein with constitutive kinase activity in human leukemia. *Science*. 1997;278:1309-1312.
55. Carron C, Cormier F, Janin A, et al. TEL-JAK2 transgenic mice develop T-cell leukemia. *Blood*. 2000;95:3891-3899.
56. Witthuhn BA, Silvennoinen O, Miura O, et al. Involvement of the Jak-3 Janus kinase in signalling by interleukins 2 and 4 in lymphoid and myeloid cells. *Nature*. 1994;370:153-157.
57. Cornejo MG, Boggon TJ, Mercher T. JAK3: a two-faced player in hematological disorders. *Int J Biochem Cell Biol*. 2009;41:2376-2379.
58. Cornejo MG, Kharas MG, Werneck MB, et al. Constitutive JAK3 activation induces lymphoproliferative syndromes in murine bone marrow transplantation models. *Blood*. 2009;113:2746-2754.
59. Walters DK, Mercher T, Gu TL, et al. Activating alleles of JAK3 in acute megakaryoblastic leukemia. *Cancer Cell*. 2006;10:65-75.
60. Koo GC, Tan SY, Tang T, et al. Janus kinase 3-activating mutations identified in natural killer/T-cell lymphoma. *Cancer Discov*. 2012;2:591-597.
61. Bains T, Heinrich MC, Loriaux MM, et al. Newly described activating JAK3 mutations in T-cell acute lymphoblastic leukemia. *Leukemia*. 2012;26:2144-2146.
62. Zuurbier L, Petricoin EF, 3rd, Vuerhard MJ, et al. The significance of PTEN and AKT aberrations in pediatric T-cell acute lymphoblastic leukemia. *Haematologica*. 2012;97:1405-1413.
63. Chiang MY, Xu L, Shestova O, et al. Leukemia-associated NOTCH1 alleles are weak tumor initiators but accelerate K-ras-initiated leukemia. *J Clin Invest*. 2008;118:3181-3194.
64. Kindler T, Cornejo MG, Scholl C, et al. K-RasG12D-induced T-cell lymphoblastic lymphoma/leukemias harbor Notch1 mutations and are sensitive to gamma-secretase inhibitors. *Blood*. 2008;112:3373-

3382.

65. Oki T, Kitaura J, Watanabe-Okochi N, et al. Aberrant expression of RasGRP1 cooperates with gain-of-function NOTCH1 mutations in T-cell leukemogenesis. *Leukemia*. 2012;26:1038-1045.
66. Mendes RD, Sarmiento LM, Cante-Barrett K, et al. PTEN micro-deletions in T-cell acute lymphoblastic leukemia are caused by illegitimate RAG-mediated recombination events. *Blood*. 2014.
67. Fry TJ, Mackall CL. The many faces of IL-7: from lymphopoiesis to peripheral T cell maintenance. *J Immunol*. 2005;174:6571-6576.
68. Bousiotis VA, Barber DL, Nakarai T, et al. Prevention of T cell anergy by signaling through the gamma c chain of the IL-2 receptor. *Science*. 1994;266:1039-1042.
69. Castellano E, Downward J. RAS Interaction with PI3K: More Than Just Another Effector Pathway. *Genes Cancer*. 2011;2:261-274.
70. Guenther MK, Graab U, Fulda S. Synthetic lethal interaction between PI3K/Akt/mTOR and Ras/MEK/ERK pathway inhibition in rhabdomyosarcoma. *Cancer Lett*. 2013;337:200-209.
71. Chappell WH, Steelman LS, Long JM, et al. Ras/Raf/MEK/ERK and PI3K/PTEN/Akt/mTOR inhibitors: rationale and importance to inhibiting these pathways in human health. *Oncotarget*. 2011;2:135-164.
72. Engelman JA, Chen L, Tan X, et al. Effective use of PI3K and MEK inhibitors to treat mutant Kras G12D and PIK3CA H1047R murine lung cancers. *Nat Med*. 2008;14:1351-1356.
73. Carracedo A, Ma L, Teruya-Feldstein J, et al. Inhibition of mTORC1 leads to MAPK pathway activation through a PI3K-dependent feedback loop in human cancer. *J Clin Invest*. 2008;118:3065-3074.
74. Aksamitiene E, Kiyatkin A, Kholodenko BN. Cross-talk between mitogenic Ras/MAPK and survival PI3K/Akt pathways: a fine balance. *Biochem Soc Trans*. 2012;40:139-146.

SUPPLEMENTARY DATA

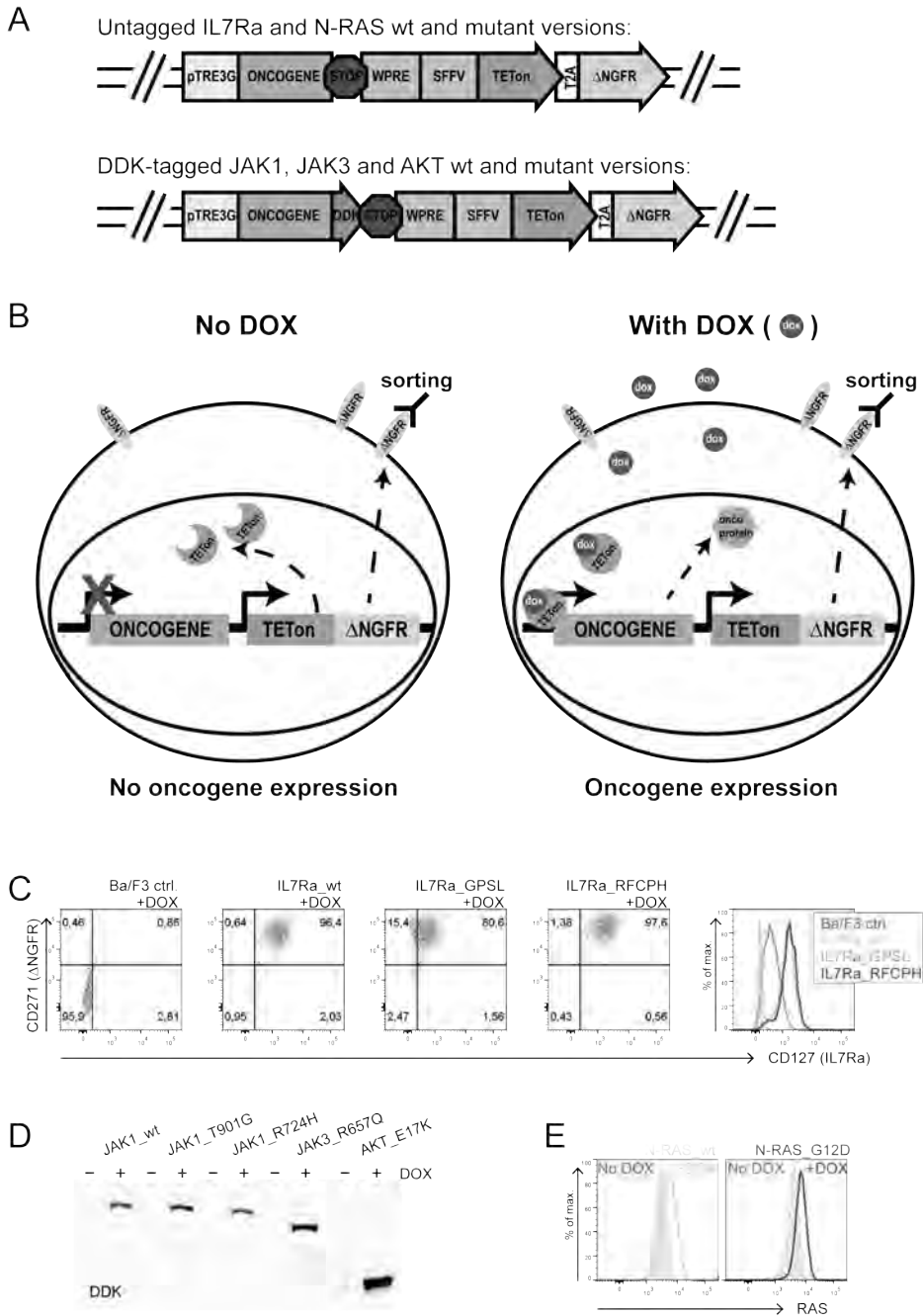


Figure S1 | Schematic representation of the mutant constructs and doxycycline-inducible Ba/F3 clones.

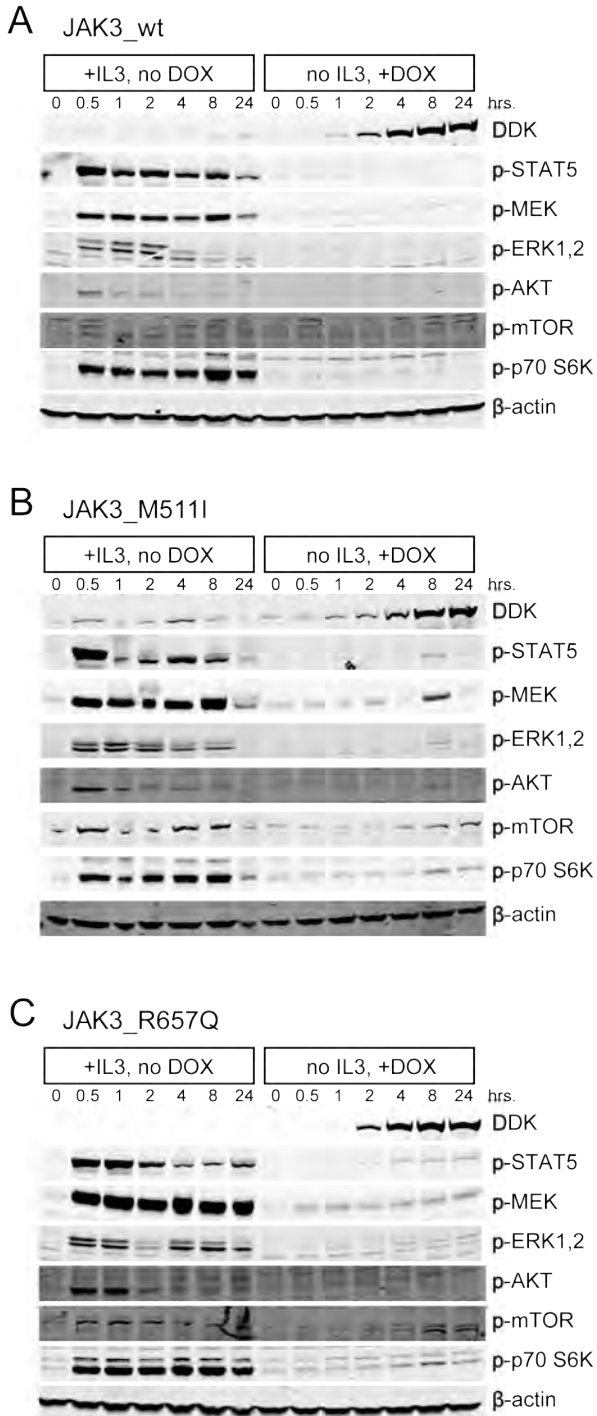


Figure S2 | JAK3 mutations activate downstream signaling.

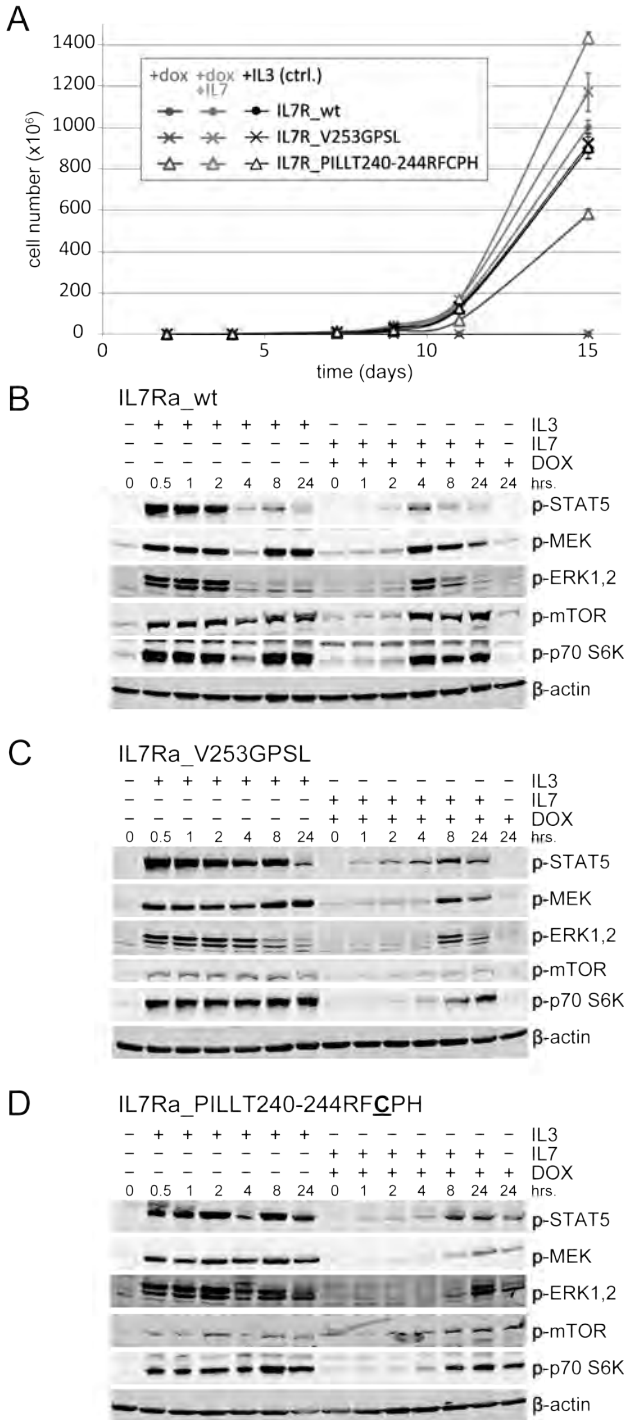


Figure S3 | The IL7Ra cysteine-mutant harbors autonomous transforming capacity and activates downstream signaling.

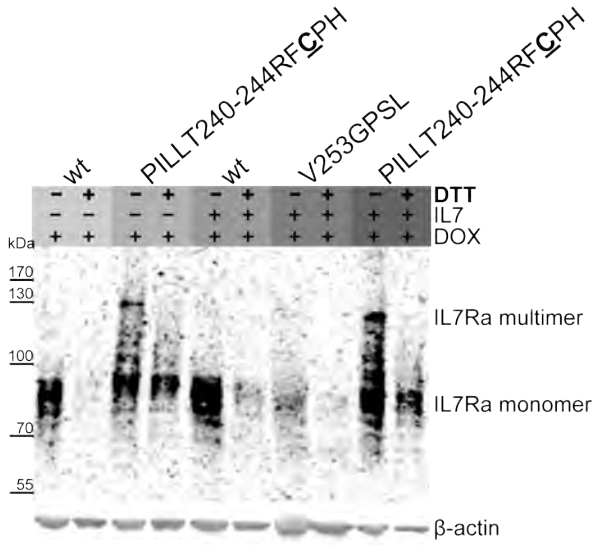


Figure S4 | The IL7R a cysteine-mutant results in higher-order multimer formation.

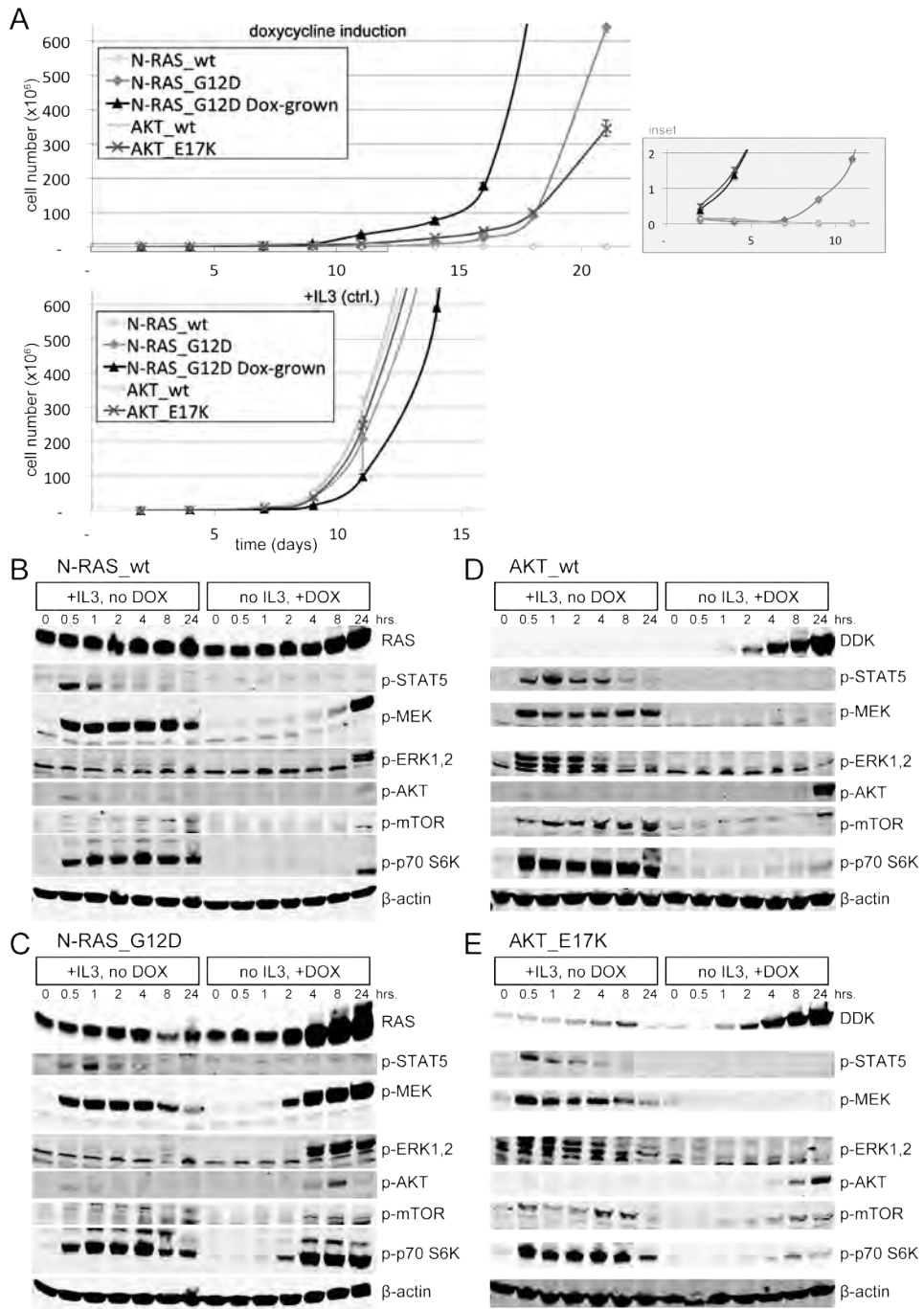
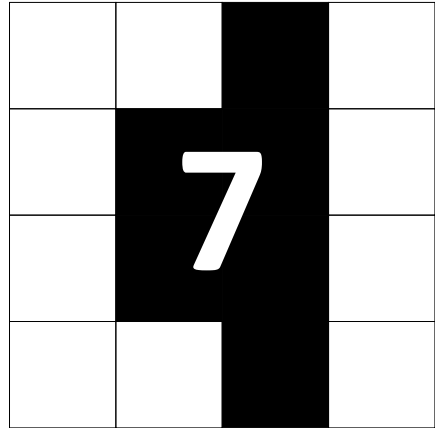


Figure S5 | *N-RAS* and *AKT* mutations activate downstream signaling.

Unsupervised GEP clusters	IL7Ra		JAK1/3		NF1, N/K-RAS	
	mutations (n=7)	p-value	mutations (n=9)	p-value	mutations (n=14)	p-value
TALLMO (n=53)	1.9%	0.13	1.9%	0.039*	6.3%	0.08
TLX (n=30)	20%	0.001*	13.3%	0.23	18.5%	0.35
Proliferative (n=19)	0%	0.60	5.3%	1	0%	0.12
ETP-ALL/immature (n=15)	0%	0.59	20%	0.09	46.2%	0.002*
Total (n=117)	6.0%		7.7%		12.0%	

Table S1 | Co-occurrence of *IL7Ra*, *JAK1/3* and *NF1*, *N/K-RAS* mutations with unsupervised gene expression profile (GEP) clusters.

CHAPTER



Immature *MEF2C*-dysregulated T-cell leukemia patients have an early T-cell precursor acute lymphoblastic leukemia gene signature and typically have non-rearranged T-cell receptors

Linda Zuurbier¹, Alejandro Gutierrez^{2,3}, Charles G. Mulighan⁴, Kirsten Canté-Barrett¹, A. Olivier Gevaert⁵, Johan de Rooi^{6,7}, Yunlei Li¹, Willem K. Smits¹, Jessica G.C.A.M. Buijs-Gladdines¹, Edwin Sonneveld⁸, A. Thomas Look^{2,3}, Martin Horstmann^{9,10}, Rob Pieters^{1,8}, and Jules P.P. Meijerink¹

¹*Department of Pediatric Oncology/Hematology, Erasmus MC Rotterdam-Sophia Children's Hospital, Rotterdam, the Netherlands;*

²*Department of Pediatric Oncology, Dana-Farber Cancer Institute, Boston, MA, USA;*

³*Division of Hematology/Oncology, Children's Hospital, Boston, MA, USA;*

⁴*Department of Pathology, St Jude Children's Research Hospital, Memphis, TN, USA;*

⁵*Center for Cancer Systems Biology (CCSB) & Department of Radiology, Stanford University School of Medicine, Stanford, CA, USA;*

⁶*Department of Biostatistics, Erasmus MC Rotterdam, Rotterdam, the Netherlands;*

⁷*Department of Bioinformatics, Erasmus MC Rotterdam, Rotterdam, the Netherlands;*

⁸*Dutch Childhood Oncology Group (DCOG), the Hague, the Netherlands;*

⁹*German Cooperative Study Group for Childhood Acute Lymphoblastic Leukemia (COALL), Hamburg, Germany;*

¹⁰*Research Institute Children's Cancer Center Hamburg, Clinic of Pediatric Hematology and Oncology, University Medical Center Hamburg-Eppendorf, Hamburg, Germany*

ABSTRACT

Three distinct immature T-cell acute lymphoblastic leukemia entities have been described including cases that express an early T-cell precursor immunophenotype or expression profile, immature *MEF2C*-dysregulated T-cell acute lymphoblastic leukemia cluster cases based on gene expression analysis (immature cluster) and cases that retain non-rearranged *TRG@* loci. Early T-cell precursor acute lymphoblastic leukemia cases exclusively overlap with immature cluster samples based on the expression of early T-cell precursor acute lymphoblastic leukemia signature genes, indicating that both are featuring a single disease entity. Patients lacking *TRG@* rearrangements represent only 40% of immature cluster cases, but no further evidence was found to suggest that cases with absence of bi-allelic *TRG@* deletions reflect a distinct and even more immature disease entity. Immature cluster/early T-cell precursor acute lymphoblastic leukemia cases are strongly enriched for genes expressed in hematopoietic stem cells as well as genes expressed in normal early thymocyte progenitor or double negative-2A T-cell subsets. Identification of early T-cell precursor acute lymphoblastic leukemia cases solely by defined immunophenotypic criteria strongly underestimates the number of cases that have a corresponding gene signature. However, early T-cell precursor acute lymphoblastic leukemia samples correlate best with a CD1 negative, CD4 and CD8 double negative immunophenotype with expression of CD34 and/or myeloid markers CD13 or CD33. Unlike various other studies, immature cluster/early T-cell precursor acute lymphoblastic leukemia patients treated on the COALL-97 protocol did not have an overall inferior outcome, and demonstrated equal sensitivity levels to most conventional therapeutic drugs compared to other pediatric T-cell acute lymphoblastic leukemia patients.

INTRODUCTION

During normal T-cell development, early T-cell precursors (ETPs) migrate to the thymus to differentiate into mature T-cells.^{1,2} T-cell acute lymphoblastic leukemias (T-ALL) represent malignant counterparts of thymocytes that have arrested at specific developmental stages that are coupled to specific patterns of T-cell receptor rearrangements.³ Developmental arrest seems dependent on the presence of so-called “type A mutations”, which activate either T-ALL oncogenes such as *TAL1*, *LMO2*, *TLX3*, *TLX1*, *NKX2-1/NKX2-2* or fusion proteins that activate *HOXA* genes.⁴⁻⁶ For TLX oncoproteins, it has recently been found that these can directly interfere with *TRA@* rearrangements by binding to ETS1 on the E α enhancer resulting in a block of active transcription, histone modification-dependent chromatin opening and rearrangements resulting in a developmental arrest.⁷

Various studies have identified T-ALL entities that arrest at an extremely immature developmental stage. Using transcriptome analysis, it was first described as the *LYL1* subgroup based on the appreciation of high *LYL1* expression.⁸ Three years later, the immature subgroup was also identified by unsupervised cluster analysis and that expressed a early thymocyte profile.⁹ Coustan-Smith and co-workers identified the ETP-ALL subtype that is characterized by a distinct ETP gene-expression profile and immunophenotype.^{10,11} Using unsupervised transcriptome analysis, we described in 2011 that immature T-ALL cluster patients are characterized by rearrangements of either *MEF2C* or *MEF2C*-regulating transcription factors.⁶ Another immature T-ALL entity was described in 2010 that is characterized by absence of bi-allelic deletions of the T cell receptor gamma gene locus (*TRG@*)—and denoted as ABD cases—possibly representing early maturation arrest before the onset of T-cell receptor rearrangements.¹²

ETP-ALL as first described by Coustan-Smith and colleagues predicts poor outcome for patients treated on St. Jude (XIII, XIV and XV) or AIEOP ALL-2000 protocols.¹⁰ Although immature T-cell development arrest was identified as a poor prognostic factor for T-ALL before,¹³⁻¹⁸ that study identified a uniform entity that expresses a gene signature alike early thymic progenitor cells.^{10,11} In children, the incidence of ETP-ALL is approximately 13 percent of all T-ALL cases, but varies among different cohorts: St. Jude Children’s research Hospital study (17 ETP-ALL out of 135 T-ALL patients), AIEOP ALL-2000 study (13/100 cases), COG9404 and DFCl00-01 (14/40 cases), the Tokyo Children’s Cancer Study group L99-15 (5/91 cases) and Shanghai Children’s Medical Center study (12/72 cases).^{10,12,19,20} ETP-ALL patients—as predicted by the mouse ETP gene signature¹⁰—that were treated on Children’s Oncology Group Study (COG) P9404 or Dana-Farber Cancer Institute (DFCI) 00-01 protocols or ETP-ALL patients based on the ETP-ALL immunophenotype in the Japanese L99-15 study or the Shanghai study were also related with poor outcome.^{12,19,20} For adult T-ALL patients, the incidence of immunophenotypic ETP-ALL was 7.4% and was also associated with poor outcome for patients treated on German ALL multicenter study group (GMALL) protocols alike the inferior outcome for early T-ALL.²¹ Molecular analysis by whole-genome sequencing revealed that most ETP-ALL cases harbor loss-of-function alterations in regulators of hematopoietic and lymphoid development (*RUNX1*, *IKZF1*, *ETV6*, *GATA3* and

EP300) or in components of the polycomb repressor complex 2 (*PRC2*).¹¹ The gene-expression profile includes many genes that are expressed in both normal and malignant hematopoietic stem cells, suggesting that ETP-ALL represents an immature leukemia with stem cell and myeloid features.^{11,22} Accordingly, recurrent mutations in myeloid-specific oncogenes (e.g., *IDH1*, *IDH2*, *DNMT3A*, *FLT3*, *NRAS*), were identified in immature²² or ETP-ALL T-ALL patients while having a low incidence of NOTCH1-activating mutations.^{11,23} At this stage, it remains unknown whether ETP-ALL cases are related to the AML entity that has *C/EBPA* hypermethylation with expression of T-lineage markers and/or T-ALL mutations like *NOTCH1* mutations.^{24,25}

In the study of Gutierrez and co-workers, ABD T-ALL was associated with a poor response to induction chemotherapy, 5-year event-free survival and overall survival in pediatric T-ALL patients who were treated using the COG P9404 or DFCI 00-01 protocol.¹² Similar results were described for ABD T-ALL in children treated on Taiwanese TPOG-ALL-97/2002 protocols,²⁶ as well as for pediatric T-cell lymphoblastic lymphoma patients.²⁷

In the present study, we investigated the extent to which ETP-ALL, immature cluster T-ALL and ABD overlap by comparing gene expression and immunophenotypic profiles of the ETP-ALL and immature cluster cases and determining the ABD status of these cases. Our findings strongly suggest that—based on gene expression—ETP-ALL and immature cluster T-ALL represent a single entity in which ABD is a subgroup. Furthermore, classifying ETP-ALL cases purely based on the previously proposed ETP immunophenotype significantly underestimates the number of actual patients with an immature cluster/ETP-ALL gene expression profile.

MATERIALS AND METHODS

Patient samples

For this study, we used diagnostic samples from 117 patients for which gene expression data were available. These patients had enrolled in the Dutch Childhood Oncology Group (DCOG) ALL-7/8 ($n=19$)^{28,29} and ALL-9 ($n=26$) protocols,³⁰ together with 72 patients who were enrolled in the German Co-Operative Study Group for Childhood Acute Lymphoblastic Leukemia study (COALL-97).³¹ Seventeen COALL patients underwent bone marrow transplantation due to non-response to therapy at day 29. T-ALL was defined as being positive for TdT, CD2, cytoplasmic CD3 (CyCD3) and/or CD7. The median follow-up times for the DCOG and COALL patients were 63 and 52 months, respectively. Each patient's parents or legal guardian provided informed consent to use excess diagnostic material for research purposes as approved by the Institutional Review Board/Ethics committee of the Erasmus MC Rotterdam and in accordance to the Declaration of Helsinki. Leukemic cells were harvested from blood or bone marrow samples and enriched as described previously.³² Enriched samples contained >90% leukemic cells.

Fluorescent in-situ hybridization (FISH).

FISH analysis was performed on thawed cytospin

slide as described before.⁵ To identify rearrangements of the *LYL1* locus, we used homelabeled BAC clones RP11-352L7 and RP11-356L15 (BAC/PAC Resource Center, Children's Hospital, Oakland, USA).

Genomic DNA and RNA extraction and ABD status detection by quantitative PCR

Genomic DNA and RNA were isolated from $\geq 5 \times 10^6$ leukemic cells using TRIzol reagent (Invitrogen) according to the manufacturer's protocol, with minor modifications.³² DNA was stored at 4°C. For RNA isolation, an additional phenol-chloroform extraction was performed as a minor modification of the protocol, and RNA was precipitated with isopropanol together with 1 μ l (20 μ g/ml) glycogen (Roche, Almere, the Netherlands). After precipitation, the RNA pellets were dissolved in 20 μ l RNase-free TE buffer (10 mM Tris-HCl, 1 mM EDTA, pH 8.0), and the concentration was measured spectrophotometrically.³² The presence of absence of bi-allelic *TRG@* deletions (ABD) was determined using quantitative PCR, targeting the intron between TRGV11 and TRGJP1 as described previously.¹²

***In vitro* cytotoxicity assay**

In vitro cytotoxicities for leukemic cells towards serial dilutions of L-Asparaginase (0.003-10 IU/mL, Paronal, Christiaens, Breda, The Netherlands), prednisolone (0.08-250 μ g/mL, BUFA BV, Uitgeest, the Netherlands), vincristine (0.05-50 μ g/mL TEVA Pharma BV, Mijdrecht, The Netherlands), daunorubicin hydrochloride (0.002-2.0 μ g/mL, Ceubidine, Rhône-Poulenc Rorer, Amstelveen, The Netherlands) or cytarabine (0.002-2.5 μ g/mL, Cytosar, Pharmacia & Upjohn, Woerden, the Netherlands) were determined using the MTT assay.³³ Briefly, 1.6×10^5 leukemic cells (>90% purity as determined by morphological examination of May-Grunwald-Giemsa (Merck, Darmstadt, Germany) stained cytospin slides) were exposed to serial dilutions of chemotherapeutic drugs in duplicate in a final volume of 100 μ l culture media (RPMI 1640 (Life Technologies, Breda, The Netherlands) supplemented with 10% fetal calfs serum (Integro, Zaandam, The Netherlands), 5 μ g/mL transferrin, 5 ng/mL sodium selenite (ITS media supplement, Sigma-Aldrich, Zwijndrecht, The Netherlands), 100 IU/mL penicillin, 100 μ g/mL streptomycin, 0.125 μ g/mL fungizone (Life technologies)). Following 4 days of incubation in a humidified incubator at 37°C with 5% CO₂, 5 mg/mL MTT (3-[4,5- dimethyldiazol-2-yl]-2,5-diphenyltetrazoliumbromide, Sigma-Aldrich) was added and incubated for an additional 6 hrs at 37°C to facilitate reduction of MTT tetrazolium salt into formazan crystals by viable cells. Total formazan production was measured spectrophotometrically at 562 nm. For each patient sample, leukemic cells incubated in the absence of drugs was used as control, whereas the assay performed on pure media containing wells were used for background correction (blank values). Leukemic cells survival following exposure to each drug concentration was calculated for background corrected OD values using the formula: ((OD drug incubated wells / OD control wells) x 100%), and the LC50 drug concentrations, at which 50% of the leukemic cells die, were calculated.

Microarray expression analyses

RNA integrity testing, copy-DNA and copy-copy RNA (ccRNA) syntheses, washing, hybridization to Human Genome U133 plus 2.0 microarrays (Affymetrix, Santa Clara, CA), extraction of probe set intensities from CEL-files and normalization with RMA or VSN methods were performed as previously described.⁵ Geneset enrichment analysis (GSEA;³⁴) was performed on our Affymetrix U133 plus 2.0 microarray expression dataset for 117 T-ALL cases⁶ using 1000 random permutations. Enrichment scores and nominal p-values were obtained for up- or down-regulated probe sets among the TOP100, 200 or 500 most significantly, differentially expressed probesets for human ETP-ALL compared to other T-ALL cases.¹¹ Also up- or down-regulated genes or probesets for C/EBPA-mutated AML²⁵ and early T cell (MPP-ETP-DN2A) and committed T cell (DN2B-and later) subsets³⁵ were tested. ETP-ALL patients were identified by Prediction Analysis of Microarrays (PAM)³⁶ implemented in R using the human ETP-ALL probe set signature.¹¹ The classifier was built on the 100, 200 or 500 most significant probe sets from this ETP-ALL gene signature (**Supplementary Table S1**)¹¹ using class labels immature cluster ($n=15$) and non-immature cluster ($n=102$) in our gene expression cohort comprising 117 T-ALL patient samples. Patients with a cross-validated probability greater than 0.6 for being classified as immature were considered to be ETP-ALL patients. Microarray data are available at the gene expression omnibus (<http://www.ncbi.nlm.nih.gov/geo/>), accession GSE10609 and GSE26713. Differentially expressed genes between ETP-ALL cases with or without bi-allelic *TRG@* rearrangements (ABD versus non-ABD ETP-ALL) were obtained by regression analysis using the *limma* package in the R statistical software package. VSN- or RMA-normalized expression values for *MEF2C* (probe set 239966_at), *LMO1* (probe set 206718_at), *LMO2* (probe set 204249_s_at), *LYL1* (probe set 210044_s_at), *ERG1* (probeset 1563392_at) and *BAALC* (probe set 222780_s_at) were used to test for differential expression between the T-ALL groups (representative probe sets were used). Human hematopoietic progenitor signature genes (probesets) as established by Novershtern and coworkers³⁷ within the immature cluster gene signature were enriched using the Fisher's exact test. Differentially expressed genes between the immature cluster ($n=15$)⁶ versus other T-ALL cases ($n=102$) in our T-ALL microarray expression set were analyzed using the Wilcoxon statistical test and corrected for multiple testing error using the false discovery rate procedure as previously described³⁸ using the Bioconductor package Multitest. A total of 784 probe sets with an FDR p-value less than $p=0.01$ was selected as the Immature cluster expression signature gene set (**Supplementary Table S5**).

Statistics

Statistics were performed using the PASW Statistics 1 software program. The Pearson's Chi-square test was performed to test for statistically significant differences in the distribution of nominal data; if fewer than five patients were tested in the individual groups the Fisher's exact test was used instead (as indicated in the corresponding tables). Statistical significance for continuous distributed data was tested using the Mann-Whitney *U* test. Differences between patient populations with respect to relapse-free survival (RFS) and event-free survival (EFS)

were tested using the log-rank test. An event for EFS is defined as relapse, lack of response to induction therapy, death in remission due to toxicity, or the development of a secondary malignancy. Differences were considered to be significant when $p < 0.05$ (two-sided).

RESULTS

ETP-ALL, immature cluster (*MEF2C*), and ABD T-ALL patients

We investigated whether immature T-ALL cluster cases (15 cases) as previously identified using our unsupervised clustering approach⁶ displayed ETP-ALL or ABD immature features consistent with two previous studies.^{10,12} For this gene expression cohort comprised of 117 pediatric T-ALL patient samples, prediction analysis of microarrays (PAM) predicted immature cluster cases as ETP-ALL based on the 100, 200 or 500 most significant probe sets from the human ETP-ALL gene signature¹¹ (**Supplementary Table S1**). Most significant up- and down-regulated probe sets from the ETP-ALL gene signature are strongly enriched as assessed by GSEA analysis in immature cluster and non-immature cluster cases, respectively (**Supplementary Figure S1**). By using PAM analysis, 13 out of 15 immature cluster cases were consistently predicted as ETP-ALL based on these ETP-ALL probe sets, while none of the remaining 102 non-immature cluster cases were predicted ($p < 0.001$; **Supplementary Figure S2**). This implies that ETP-ALL and the immature cluster represent single or strongly overlapping T-ALL entities (**Table 1 and Supplementary Table S2**). Two out of 15 immature cluster cases were not predicted by the ETP-ALL gene signature. Seven patients (6%) were identified as ABD cases based on the preservation of non-rearranged *TRG@* loci as detected by RQ-PCR¹² (**Table 1**). Six of the seven ABD cases were immature cluster cases,⁶ and five out of these six also had an ETP signature (**Supplementary Figure S3**). Thus, approximately 40% (5/13 or 6/15) of immature cluster/ETP-ALL cases have retained non-rearranged *TRG@* loci.

Relation to immunophenotype

ETP-ALL cases were originally defined by the absence of both CD1 and CD8 (present in fewer than 5% of leukemic cells), absent or weak expression of CD5 (in $\leq 75\%$ of total cells or ≥ 10 -fold lower than in normal T-cells), or the expression of one or more of the markers CD117, CD34, HLA-DR, CD13, CD33, CD11b and CD65 (in $\geq 25\%$ of total cells).¹⁰ We next defined whether ETP-ALL gene signature positive cases met with the immunophenotypic criteria as originally proposed for ETP-ALL.¹⁰ In the present study, historic flow cytometry data were not obtained on the gated leukemic cell population and various markers were missing, so we used a simplified ETP-ALL immunophenotype as being CD1 negative, CD8 negative, weak CD5 ($\leq 75\%$) or CD5 negative with positive expression of CD34 or CD13/33.¹⁰ We identified only five samples out of the 111 patients for whom both immunophenotype and gene-expression data were available that had such an immunophenotype, and only three of these five cases expressed an ETP-ALL signature ($p = 0.01$, **Table 2**). Leaving out the CD5 marker led to the identification of 10 out of 13 ETP-

Patient	Study Group	unsupervised cluster n=15/117	ETP-ALL by PAM n=13/117	ABD status n=7/117	ETP immunophenotype		Cytogenetic rearrangement (oncogene)	Follow-up/Event	Follow-up time (months)
					including CD5 (≤75%) n=11/117	excluding CD5 criteria n=11/117			
9194	COALL97	immature	ETP-ALL	one copy retained	yes	yes	<i>Inv(7) (HOXA)</i>	long-term survivor	96
572	ALL-9	immature	ETP-ALL	both copies retained	-	yes	<i>RUNX1-AFF3 (MEF2C)</i>	long-term survivor	63
1524	COALL97	immature	ETP-ALL	both copies retained	-	yes	<i>ETV6-NCOA2 (MEF2C)</i>	long-term survivor	54
1964	COALL97	immature	ETP-ALL	both copies retained	-	yes	<i>MEF2C</i>	long-term survivor	46
10030	COALL97	immature	ETP-ALL	both copies retained	NA	NA	unknown	long-term survivor	82
167	COALL97	immature	ETP-ALL	deleted	-	yes	unknown	long-term survivor	80
321	COALL97	immature	ETP-ALL	deleted	-	yes	unknown	toxicity of therapy	9
491	COALL97	immature	ETP-ALL	deleted	-	-	<i>MEF2C</i>	long-term survivor	72
2130	COALL97	immature	ETP-ALL	deleted	-	-	unknown	2nd malignancy	27
9577	COALL97	immature	ETP-ALL	deleted	-	-	<i>BCL11B-NKX2.5 (MEF2C)</i>	relapse	23
2736	ALL-9	immature	ETP-ALL	deleted	yes	yes	<i>CALM1AF10 (HOXA)</i>	relapse	19
1509	COALL97	immature	ETP-ALL	deleted	yes	yes	<i>CALM1AF10 (HOXA)</i>	long-term survivor	54
2703	ALL-9	immature	ETP-ALL	deleted	-	yes	unknown	2nd malignancy	18
2252	COALL97	immature	-	deleted	-	-	<i>BCL11B-PU.1 (MEF2C)</i>	long-term survivor	41
9105	COALL97	immature	-	one copy retained	-	-	<i>MYB</i>	toxicity after relapse (+glioblastoma)	76
221	COALL97	TAL/LMO	-	one copy retained	-	-	unknown	long-term survivor	78
2750	ALL-9	TLX	-	deleted	-	yes	<i>CALM1AF10 (HOXA)</i>	relapse	20
10111	COALL97	TAL/LMO	-	deleted	-	yes	<i>SIL-TAL (TAL1)</i>	long-term survivor	80
9858	COALL97	TLX	-	deleted	-	yes	<i>TLX3</i>	relapse CNS	26
720	ALL-9	TLX	-	deleted	-	yes	<i>TLX3</i>	long-term survivor	63
2780	ALL-8	TLX	-	deleted	-	yes	<i>TLX3</i>	long-term survivor	132
1753	COALL97	TAL/LMO	-	deleted	yes	yes	<i>SIL-TAL (TAL1)</i>	long-term survivor	85
585	COALL97	TLX	-	deleted	-	yes	<i>TLX3</i>	long-term survivor	70
9421	COALL97	TLX	-	deleted	yes	yes	<i>TLX3</i>	relapse	8
1032	COALL97	TAL/LMO	-	deleted	-	yes	unknown	long-term survivor	62
1632	COALL97	TAL/LMO	-	deleted	-	yes	unknown	relapse	12
9963	COALL97	TAL/LMO	-	deleted	-	yes	unknown	2nd malignancy	48

Table 1 | Characteristics of immature T-ALL, ETP-ALL (predicted ETP-ALL), ABD patients and patients that have an ETP-ALL immunophenotype. Immature, ETP-ALL, and ABD patients are depicted in bold. ETP-ALL, early T-cell precursor ALL; ABD, absence of bi-allelic deletions; For the chromosomal rearrangement analysis, one case has *TAL1* and *LMO2* translocations and one case has *TAL2* and *LMO1* translocations. Unsupervised subgroups have been published before;⁶ ETP-ALL immunophenotypes for DCOG and COALL cohort was based on <25% expression of CD1 and CD8, ≥25% expression of CD13, CD33 or CD34 with ≤75% CD5 expression.

Immunophenotypic markers	ETP-ALL GEP		p-value	Sensitivity	Specificity
	No	Yes			
CD34+ (n=111)					
yes	26	8	0,021	62%	73%
no	72	5			
CD33/CD13+ (n=111)					
yes	12	6	0,007#	46%	88%
no	86	7			
CD34/CD33/CD13+ (n=110)					
yes	35	10	0,007	77%	64%
no	62	3			
CD2+ (n=114)					
yes	83	9	0,27	69%	18%
no	18	4			
CD5-/CD5weak (n=115)					
yes	13	4	0,1	31%	87%
no	89	9			
CD1- (n=113)					
yes	51	11	0,011	92%	49%
no	50	1			
CD4- (n=115)					
yes	29	13	<0,001	100%	72%
no	73	0			
CD8- (n=115)					
yes	32	13	<0,001	100%	71%
no	70	0			
CD4/CD8 DN (n=115)					
yes	14	13	<0,001	100%	86%
no	88	0			
CD1-, CD8-, CD34/CD33/CD13+, CD5(≤75%) (n=111)					
ETP-ALL immunophenotype	2	3	0,01	22%	98%
no ETP-ALL immunophenotype	96	10			
CD1-, CD8-, CD34/CD33/CD13+ (n=111)					
yes	11	10	<0,001	77%	89%
no	87	3			
CD1-, CD4/CD8 DN, CD34/CD33/CD13+ (n=111)					
yes	6	10	<0,001	77%	94%
no	92	3			

Table 2 | Immunophenotypic markers predicting for immature T-ALL cases with an ETP-ALL gene expression profile. Expression of (combinations of) immunophenotypic markers for predicted ETP-ALL cases versus other T-ALL cases (all categories are also CD7+). GEP: gene expression profile. The number of patient samples with available marker information and significance levels have been indicated. #Log-rank p-value.

ALL but also identified 11 out of 98 T-ALL cases that lack an ETP-ALL gene expression signature ($p < 0.001$, **Table 2**).

We then investigated which other (combinations of) immunophenotypic markers could be defined that most strongly associates with cases expressing the ETP-ALL gene signature (**Table 2**). This analysis showed that these ETP-ALL cases strongly associated with absence of CD4 expression in addition to absence of CD8. Inclusion of absence of CD4 expression in addition to absence of expression of CD1 and CD8 but presence of expression of CD34 and/or CD13/33 markers (i.e. CD1-, CD4/CD8 DN, CD34/CD33/CD13+) predicted 10 out of 13 cases with an ETP-ALL gene signature compared to only 6 out of 98 T-ALL cases that lacked an ETP-ALL gene signature, resulting in 77% sensitivity and 94% specificity levels (**Table 2**). This immunophenotype also strongly associated with the immature cluster cases; 10 of the 15 immature cluster cases had this immunophenotype compared to only 6 of the 96 non-immature cluster cases ($p < 0.001$, sensitivity 67%, specificity 94%; **Supplementary Table S3**). Also, four out of seven ABD cases had such an immunophenotype compared to 12 out of 104 non-ABD patients ($p = 0.008$, **Supplementary Table S4**).

Clinical and molecular-genetic features

Predicted ETP-ALL patients did not associate with gender or age, but white blood cell (WBC) counts tended to be lower for both ETP-ALL cases and immature cluster cases, and were significantly lower for ABD cases (15×10^9 vs. 129×10^9 cells/L; $p = 0.002$; **Table 3, Supplementary Tables S3 and S4**). Predicted ETP-ALL patients lacked rearrangements in *TAL1*, *LMO2*, *TLX3*, *TLX1*, *MYB* or *NKX2-1/NKX2-2* genes (**Tables 1 and 3**). However, three of the 13 ETP-ALL cases had *HOXA*-dysregulating events.^{9,39} These same three cases also represent immature cluster cases and have an immature immunophenotype with expression of the myeloid marker CD33.⁶ *MEF2C*-dysregulating mechanisms—including *ETV6-NCOA2* (1 case), *RUNX1-AFF3* (1 case), *NKX2-5* (1 case) and *PU.1/SPI1* (1 case) translocations—or a *MEF2C* rearrangement (2 cases) were originally identified in six out of 15 immature cluster cases.⁶ Five of these six cases expressed the human ETP-ALL gene signature (**Tables 1 and 3**; $p < 0.001$). The *PU.1/SPI1* immature cluster case was the only *MEF2C*-dysregulated case that was not predicted by the human ETP-ALL gene signature. No genetic aberrations have been identified for 5 ETP-ALL cases yet. With respect to other recurrent T-ALL mutations, the incidences of NOTCH1-activating mutations (*NOTCH1/FBXW7*) and PTEN/AKT mutations in the immature cluster, ETP-ALL and ABD cases did not differ significantly from other T-ALL patients (**Table 3, Supplementary Tables S3 and S4**). Similar results were obtained with respect to *PHF6* and *WT1* mutations. *ETV6* and *RUNX1* mutations, as previously associated with early T-ALL²² or immunophenotypic ETP-ALL,¹¹ were only identified in two and one cases out of 71 COALL-97 T-ALL patients, respectively (data not shown), but none of these mutant cases expressed an ETP-ALL gene signature.

The ETP-ALL cases in our cohort were associated with high *MEF2C*, *LMO2* and *LYL1* expression levels (**Figure 1 (panels A, C and D)**; $p < 0.0001$, $p < 0.0001$ and $p = 0.0002$ respectively). *LMO2* and *LYL1* were previously identified as direct target genes for *MEF2C*.⁶ *MEF2C*-dysregulating events

	ETP-ALL PAM prediction				p-value	Bonferroni-Holm alpha
	No		Yes			
	n	(%) or range	n	(%) or range		
Total	104	(89%)	13	(11%)		
Clinical (n=117)						
Gender						
Male	76	(75%)	7	(54%)	0.02#	0.0036
Female	28	(25%)	6	(46%)		
Median age yrs (range)	7.8	(1.5-17.8)	10.8	(3.7-16.4)	0.19*	-
Median WBC x10⁹ cells/liter (range)	119	(2-900)	94	(2-435)	0.16*	-
Chromosomal rearrangements (n=117)						
<i>TAL1/2/LYL1</i> (n=27)	27	(27%)	0	(0%)	0.037	
<i>LMO1/2/3</i> (n=14)	14	(14%)	0	(0%)	0.36	
<i>TLX3</i> (n=22)	22	(22%)	0	(0%)	0.12	
<i>TLX1</i> (n=7)	7	(7%)	0	(0%)	1	
<i>HOXA</i> (n=10)	7	(7%)	3	(24%)	0.08	
<i>MEF2C</i> (n=6)	1	(1%)	5	(38%)	<0.001	0.0031
<i>NKX2-1/NKX2-2</i> (n=7)	7	(7%)	0	(0%)	1	
Unknown (n=26)	21	(21%)	5	(38%)	0.16	
Unsupervised T-ALL clusters (n=117)						
<i>TALLMO</i> (n=53)	53	(51%)	0	(0%)		
Proliferative (n=19)	19	(18%)	0	(0%)		
Immature (n=15)	2	(2%)	13	(100%)	<0.001	0.0031
<i>TLX</i> (n=30)	30	(29%)	0	(0%)		
NOTCH1/FBXW7 status (n=112)						
wild-type (n=42)	38	(38%)	4	(31%)	0.76	
mutant (n=70)	61	(62%)	9	(69%)		
PTEN/AKT status (n=113)						
wild-type (n=92)	81	(81%)	11	(85%)	1	
mutant (n=21)	19	(19%)	2	(15%)		
PHF6 status (n=41)						
wild-type (n=32)	29	(76%)	3	(100%)	1	
mutant (n=9)	9	(24%)	0	(0%)		
WT1 status (n=115)						
wild-type (n=101)	88	(86%)	13	(100%)	0.36	
mutant (n=14)	14	(14%)	0	(0%)		

Table 3 | Overall clinical, immunophenotypic and molecular cytogenetic properties of predicted ETP-ALL and non-ETP-ALL patients. Unsupervised clusters were based on gene-expression signatures mainly representing known cytogenetic subgroups,⁶ with the *TALLMO* cluster consisting of patients with a *TALLMO* gene signature, of which the various patients have a *TAL1*, *TAL2*, *LYL1* or *LMO1*, *LMO2* or *LMO3* rearrangement. Patients from the proliferative cluster are primarily characterized by an *NKX2-1/NKX2-2* or *TLX1* rearrangement. The immature cluster includes patients with high *MEF2C* expression and *MEF2C* dysregulating aberrations. The *TLX* cluster is comprised of patients who are predominantly characterized by having *HOXA* or *TLX3* rearrangements. Significant *p*-values are indicated in bold. The *p*-values were calculated using the Fisher’s exact test except as follows: *Mann-Whitney *U* test; #Pearson’s Chi-square test. ^The significance levels of ETP-ALL frequencies within the indicated cytogenetic subtypes were compared to all other subtypes. ETP, early T-cell precursor; WBC, white blood cell count; the Bonferroni-Holm significance level for multiple testing correction is indicated.

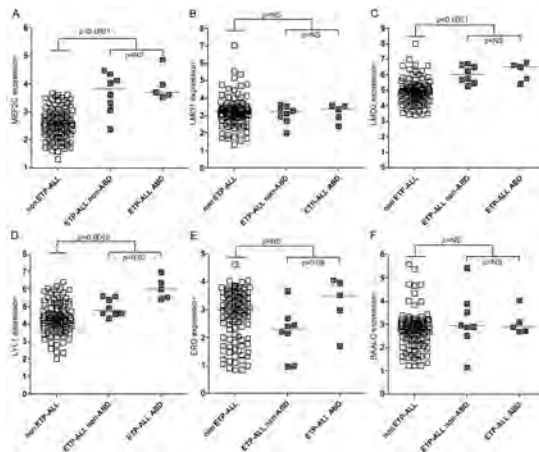


Figure 1 | ETP-ALL patients express high *MEF2C*, *LMO2* and *LYL1* levels but not *ERG* or *BAALC*. The expression of (A) *MEF2C* (probe set 239966_at), (B) *LMO1* (probe set 206718_at), (C) *LMO2* (probe set 204249_s_at), (D) *LYL1* (probe set 210044_s_at), (E) *ERG* (probe set 1563392_at), and (F) *BAALC* (probe set 222780_s_at) was based on VSN normalized microarray gene expression data for ETP-ALL (grey squares) and non-ETP-ALL cases (white squares). For the ETP-ALL subgroup, the ABD and non-ABD cases are indicated separately.

were identified in both ETP-ALL cases with and without ABD characteristics: three ABD ETP-ALL cases had *MEF2C*-dysregulating events compared to two non-ABD ETP-ALL cases (**Table 1**). Cytogenetic defects underlying the other two ETP-ALL cases with ABD-characteristics include a *HOXA* case due to an inversion on chromosome 7 and an unknown case. Two other ABD cases did not have an ETP-ALL profile: one had a MYB translocation and was identified as immature cluster case before whereas the other belonged to the TALLMO cluster for which the underlying genetic defect remains unknown (**Table 1 and Supplementary Table S4**). LIMMA (Linear Models for MicroArray data) analysis revealed that no genes were differentially expressed between the ABD and non-ABD ETP-ALL cases, suggesting that these cases likely represent a single disease entity. Although the expression of *LYL1* was higher in the ABD cases than in the non-ABD ETP-ALL cases, significance was lost following correction for multiple testing. *ERG1* or *BAALC* levels, previously linked to adult immature T-ALL/ETP-ALL and poor outcome in some^{40,41} but not all studies,⁴² were not significantly elevated in our pediatric ETP-ALL series.

Both pediatric and adult ETP-ALL cases are characterized by the expression of hematopoietic stem cell signature genes.^{11,22} ETP-ALL may therefore resemble a stem cell-like leukemia with myeloid and lymphoid features. Consistent with this hypothesis, the gene signature of our immature cluster⁶ (**Supplementary Table S5**) was significantly enriched for genes (probe sets) that are expressed in sorted hematopoietic stem cells, early erythroid precursor cells, and B-cell fractions as established by Novershtern and co-workers³⁷ (**Supplementary Table S6**). Remarkably, genes that are typically down-regulated during normal T-cell development were enriched in cases with the immature cluster signature. Also B-cell genes were significantly enriched possibly reflecting the early status of ETP-ALL as an entity that has not yet committed to T-cell development. This is further strengthened by strong enrichment of genes that are expressed in normal MMP-ETP-DN2A immature stages rather than genes from later T-cell development stages beyond DN2B (**Supplementary Figure S4A-B**). It was also reported that ETP-ALL cases express myeloid signature genes.^{11,22} We therefore tested whether ETP-ALL cases would be enriched for differentially expressed genes of AML cases with hypermethylation or mutation of *C/EBPA*. Although gene set enrichment (GSEA) results overall were not significant possibly due to the limited number of probe sets, most of these up- or down-regulated signature genes were strongly enriched in immature cluster/ETP-ALL cases (**Supplementary Figure S4C-D**). These data confirm that immature cluster/ETP-ALL is a stem cell-like leukemia that arises at the decision point between early myeloid and lymphoid development.

Relation to outcome

ETP-ALL has been associated with extremely poor outcome in several studies.^{10,12,19} Therefore, we investigated the outcome of immature cluster/ETP-ALL patients in the COALL-97 protocol: 72 out of the 117 patients for which gene expression signatures were available had been enrolled in the COALL-97 protocol, and these 72 included 11 of the 15 immature cluster patients and 10 of the 13 predicted ETP-ALL cases. Surprisingly, ETP-ALL patients were not significantly different than the other T-ALL patients with respect to relapse-free survival (5-year RFS was

89±11 vs. 71±7%, respectively; $p=0.31$) or event-free survival (5-year EFS was 70±15 vs. 61±7%, respectively; $p=0.66$) (**Figure 2**). Moreover, no differences were detected in the 5-year overall survival (OS) curves (not shown). Also with respect to the immature cluster cases, the ABD cases and the cases with an ETP-ALL immunophenotype as defined by our criteria, no differences in the RFS or EFS curves were identified (**Supplementary Figure S5A-C**). For ETP-ALL patients, high-dose cytarabine has been suggested to improve outcome of ETP-ALL patients.¹¹ As the COALL-97 protocol is a high-dose cytarabine-containing treatment, this may be one of the reasons for the relative good outcome of ETP-ALL and ABD patients in this study compared to other studies.^{10,12,19,26} However, we could not demonstrate differential sensitivity levels to various drugs including cytarabine for ETP-ALL patients in our *in vitro* cytotoxicity assay (**Supplementary Figure S6**).

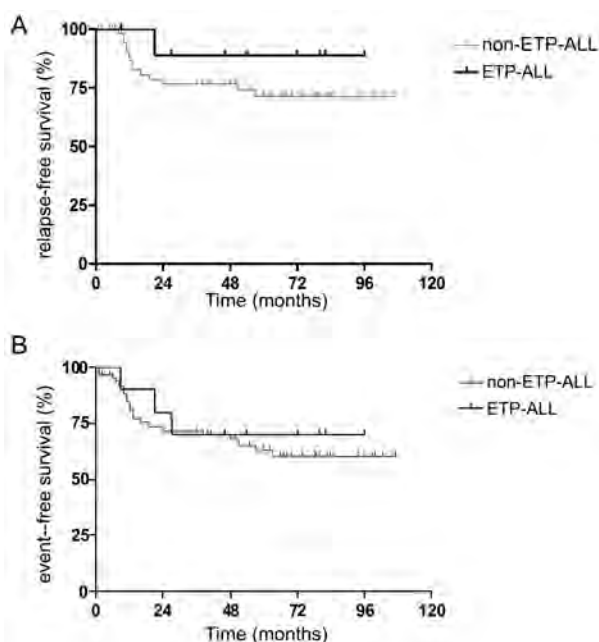


Figure 2 | ETP-ALL patients who were treated using the COALL-97 protocol were not associated with poor outcome. (A) Relapse-free survival (RFS) and **(B)** event-free survival (EFS) curves were generated for the COALL pediatric T-ALL patients. Shown are the RFS and EFS curves for ETP-ALL cases (black line) versus non ETP-ALL cases (grey line).⁶ Vertical tick marks represent individual cases for which no further follow-up data is available.

DISCUSSION

In this study, we found that 13 of our 15 previously reported immature cluster cases⁶ are consistently predicted by PAM based on the human ETP-ALL expression signature,^{10,11} strongly suggesting that ETP-ALL and immature cluster cases represent a single entity. Consistent with

previous observations,¹² we found that ABD T-ALL patients represent a subset of the immature cluster/ETP-ALL cases. Six out of 7 ABD patients belong to the immature cluster, where 5 out of 7 cases had an ETP-ALL signature. So, approximately 40% of immature cluster cases retains non-rearranged *TRG@* loci, and perhaps represents an even more immature entity among immature cluster/ETP-ALL cases. This entity may closely overlap with the FLT3 mutant adult ETP-ALL cases that fail to demonstrate monoclonal TCR rearrangements⁴³ in line with expected results for ABD ETP-ALL patients. Although we identified some genes using our microarray analysis that were differentially expressed between the ABD and non-ABD immature cluster/ETP-ALL cases (including higher levels of *LYL1* in ABD cases), none of these differences remained significant after correcting for multiple testing. The total number of ABD and non-ABD immature cluster/ETP-ALL patients in our cohort may have been insufficient to reveal subtle differences in gene expression levels. On the other hand, we did not detect differences in oncogenic rearrangement types between the ABD and non-ABD immature cluster/ETP-ALL cases. We also found that both ABD-ETP-ALL as well as non-ABD ETP-ALL entities are associated with *MEF2C*-dysregulating mechanisms and both entities lack *TAL1*, *TLX1* and *NKX2-1/NKX2-2* rearrangements that were previously associated with other T-ALL subgroups.⁶ A low white blood cell count was significantly associated with both the ETP-ALL and ABD cases. Taken together, based on expression profiles, genetic data and clinical findings, ABD and non-ABD ETP-ALL cases seem to reflect a single ETP-ALL entity. In line with others,^{11,22} immature cluster/ETP-ALL cases are enriched for stem-cell gene signatures. ETP-ALL cases are also strongly enriched for genes that are normally up-regulated in MMP-ETP-DN2A immature T-cell subsets, but do not express genes that are normally expressed in T-cell subsets beyond the DN2B stage.³⁵ Although overall enrichment results for AML with inactivated *C/EBPA* expression²⁵ were not significant, most of the up- or down-regulated signature genes for that AML cluster were concordantly up- or down-regulated in immature cluster/ETP-ALL cases. Lack of significance may be due to the limited size of the gene signatures. Alternatively, it may be due to the fact that this cluster contains 2 AML entities of which only *C/EBPA*-hypermethylated AML cases have T-ALL characteristics.²⁵ These data imply that immature cluster/ETP-ALL in *C/EBPA*-hypermethylated AML cases may be closely-related disease entities that needs further investigation. To date, exome sequencing of ETP-ALL patient samples has identified mutations in genes that regulate hematopoietic and lymphoid development, cytokine and/or Ras signaling pathways and the polycomb repressor complex 2 (PRC2) reflecting important chromatin-modifying enzymes and myeloid-leukemia associated oncogenes. In addition, the prevalence of NOTCH1-activating mutations is reduced in ETP-ALL patient samples.^{11,21-23}

Our immature cluster/ETP-ALL cases lack *PHF6* and *WT1* mutations, and no differences were observed with respect to the frequency of NOTCH1-activating mutations or PI3K/AKT-activating events between the immature cluster/ETP-ALL cases and the other T-ALL cases. The low incidence of *ETV6* and *RUNX1* mutations may reflect the lower incidence of mutations in children as compared to adult leukemia patients.⁴⁴ Although none of these mutations have previously been explicitly associated with outcome in our relatively limited number of patient

samples, additional mutation screens using an expanded series of patient samples are required to determine whether our immature cluster/ETP-ALL samples differ from the spectrum of mutations identified in the St. Jude's and COG patient samples.^{11,22} In contrast to adult T-ALL studies,⁴⁰⁻⁴² we did not observe low *ERG/BAALC* expression in our immature cluster/ETP-ALL samples in line with results for adult T-ALL patients that enrolled on GRAALL protocols.⁴²

With respect to our immature T-ALL cluster, we previously identified a variety of distinct genetic rearrangements that result in the activation of oncogenes (e.g., *NKX2-5*, *PU.1*, and *MEF2C*), *RUNX1*, or *ETV6* fusion products, all of which converge on the activation of *MEF2C*.⁶ Although *MEF2C* seems to be activated in multiple immature cluster/ETP-ALL samples for which the underlying genetic defect has not yet been identified, some cases had low levels of *MEF2C* expression, suggesting that alternate pathogenic pathways may also be affected in ETP-ALL. The expression of *LMO2* and *LYL1* was significantly elevated in immature cluster/ETP-ALL samples, and both of these genes were previously identified as direct target genes for *MEF2C*.⁶ Unlike previous findings,⁸ immature cluster/ETP-ALL patients lack *LYL1* rearrangements as assessed by FISH. The only *LYL1*-rearranged case in our cohort has a *TALLMO* gene signature, consistent with the high homology between *TAL1* and *LYL1* oncoproteins.⁴⁵

Coustan-Smith and colleagues originally described an ETP-ALL immunophenotype that was associated with T-ALL cases that were predicted by a mouse ETP-like signature.¹⁰ This immunophenotype includes multiple markers and may therefore be less useful for identifying ETP-ALL cases in retrospective studies for which in general relatively fewer parameters are available. With respect to our cohort, immunophenotypic parameters were measured on the bulk of mononuclear cells following Ficoll gradient centrifugation. The leukemic population may therefore be contaminated with low numbers of normal cells. We then set the positivity threshold for various markers to $\geq 25\%$. Using the immunophenotypic data, we characterized ETP-ALL cases by a simplified ETP-ALL immunophenotype that apart from expressing CD7 also expressed CD34 and/or myeloid markers CD13 and/or CD33, no or weak ($< 75\%$) expression of CD5 in the absence of CD1 and CD8. Only five out of 117 patients were identified in our study that met this criterion and only 3 of these samples had an ETP-ALL gene signature. In the study of Gutierrez *et al.*,¹² only one out of 14 cases as identified by the mouse ETP-like gene signature has such an ETP-ALL immunophenotype.¹⁰ Also in the original ETP-ALL study of Coustan-Smith and coworkers,¹⁰ only nine of the 14 initial cases that were identified using the mouse ETP gene signature had a bona fide ETP-ALL immunophenotype. In all of these instances the current ETP-ALL immunophenotype may severely underestimate the actual number of ETP-ALL cases that express an ETP-ALL gene signature. For our cohort, the CD34+ and/or CD13/33+, CD1- CD4- and CD8- immunophenotype in addition to CD7 positivity most closely associated with cases that expressed the human ETP-ALL gene signature, with a sensitivity level of 77% and a specificity level of 94%.

Predicted ETP-ALL patients based on the human ETP-ALL gene signature that were treated on the COALL-97 protocol did not show a worse outcome in comparison to non ETP-ALL patients in contrast to some other studies.^{10,19-21} We also did not observe a worse outcome for immature

cluster cases, ABD patients and immunophenotypic ETP-ALL patients (regardless of the inclusion of CD5 data). As ETP-ALL cases express human hematopoietic stem cell gene signatures and early myeloid-associated gene signatures,^{11,22} treatment with high-dose cytarabine as included in AML treatment protocols has been suggested to improve the outcome or to increase the cure rate of ETP-ALL patients.¹¹ High-dose cytarabine has been incorporated into the COALL-97 treatment protocol, and this may explain the relatively good outcome in contrast to various other studies.^{10,19-21} So far, *in vitro* cytotoxicity data for various conventional therapeutic drugs including cytarabine failed to reveal differences in sensitivity levels for immature cluster/ETP-ALL compared to other T-ALL patient samples.

In conclusion, the expression of the ETP-ALL gene signature and clustering in the immature T-ALL cluster (following unsupervised cluster analysis) are highly overlapping and point to a single ETP-ALL entity with respect to biology and genetics. We found no evidence to suggest that ABD and non-ABD cases reflect distinct entities among ETP-ALL cases. Different ETP-ALL patient populations may be identified based on immunophenotypic or gene expression data (ETP-ALL gene signature) and could explain differences in outcome between our and other studies. In this study, samples with an ETP-ALL gene signature correlated best with a CD34/13/33+, CD1- and CD4/CD8 double negative immunophenotype. ETP-ALL cases in the COALL-97 study did not associate with a poor outcome compared to other T-ALL cases. High-dose cytarabine as incorporated in the COALL-97 protocol may have improved the outcome for ETP-ALL patients. Limited numbers of ETP-ALL cases have been investigated in various studies so far. Better definitions for ETP-ALL based on immunophenotypic and gene expression data and clinical outcome require a systematic review as part of a large international meta-analysis.

AUTHORSHIPS AND DISCLOSURES

JM and RP designed the study, analyzed data and wrote manuscript. RP, ES and MH provided study center data and patient materials. LZ, KC-B, OG, JdR, YL, WKS, and JB-G performed research, analyzed data and wrote manuscript. AG, CGM, ES, MLB, ATL, MH analyzed data and wrote manuscript. ATL is consultant, advisor and stock owner of Oncomed.

ACKNOWLEDGEMENTS

This work was supported by the The Children Cancer Free Foundation (Stichting Kinderen Kankervrij (KiKa): project numbers KIKA2007-012 (LZ), KIKA2008-029 (KC-B and WKS)), and KIKA2010-82 (YL) and the Dutch Cancer Society Project number AMC2008-4265 (JB-G)).

REFERENCES

1. Kueh HY, Rothenberg EV. Regulatory gene network circuits underlying T cell development from multipotent progenitors. *Wiley Interdiscip Rev Syst Biol Med.* 2012;4:79-102.
2. Thompson PK, Zuniga-Pflucker JC. On becoming a T cell, a convergence of factors kick it up a Notch along the way. *Semin Immunol.* 2011;23:350-359.
3. Asnafi V, Beldjord K, Boulanger E, et al. Analysis of TCR, pT alpha, and RAG-1 in T-acute lymphoblastic leukemias improves understanding of early human T-lymphoid lineage commitment. *Blood.* 2003;101:2693-2703.
4. Meijerink JP. Genetic rearrangements in relation to immunophenotype and outcome in T-cell acute lymphoblastic leukaemia. *Best Pract Res Clin Haematol.* 2010;23:307-318.
5. Van Vlierberghe P, Pieters R, Beverloo HB, Meijerink JP. Molecular-genetic insights in paediatric T-cell acute lymphoblastic leukaemia. *Br J Haematol.* 2008;143:153-168.
6. Homminga I, Pieters R, Langerak AW, et al. Integrated transcript and genome analyses reveal NKX2-1 and MEF2C as potential oncogenes in T cell acute lymphoblastic leukemia. *Cancer Cell.* 2011;19:484-497.
7. Dadi S, Le Noir S, Payet-Bornet D, et al. TLX homeodomain oncogenes mediate T cell maturation arrest in T-ALL via interaction with ETS1 and suppression of TCRalpha gene expression. *Cancer Cell.* 2012;21:563-576.
8. Ferrando AA, Neuberg DS, Staunton J, et al. Gene expression signatures define novel oncogenic pathways in T cell acute lymphoblastic leukemia. *Cancer Cell.* 2002;1:75-87.
9. Soulier J, Clappier E, Cayuela JM, et al. HOXA genes are included in genetic and biologic networks defining human acute T-cell leukemia (T-ALL). *Blood.* 2005;106:274-286.
10. Coustan-Smith E, Mullighan CG, Onciu M, et al. Early T-cell precursor leukaemia: a subtype of very high-risk acute lymphoblastic leukaemia. *Lancet Oncol.* 2009;10:147-156.
11. Zhang J, Ding L, Holmfeldt L, et al. The genetic basis of early T-cell precursor acute lymphoblastic leukaemia. *Nature.* 2012;481:157-163.
12. Gutierrez A, Dahlberg SE, Neuberg DS, et al. Absence of Biallelic TCR{gamma} Deletion Predicts Early Treatment Failure in Pediatric T-Cell Acute Lymphoblastic Leukemia. *J Clin Oncol.* 2010;28:3816-3823.
13. Asnafi V, Buzyn A, Thomas X, et al. Impact of TCR status and genotype on outcome in adult T-cell acute lymphoblastic leukemia: a LALA-94 study. *Blood.* 2005;105:3072-3078.
14. Garand R, Voisin S, Papin S, et al. Characteristics of pro-T ALL subgroups: comparison with late T-ALL. *The Groupe d'Etude Immunologique des Leucemies. Leukemia.* 1993;7:161-167.
15. Marks DI, Paietta EM, Moorman AV, et al. T-cell acute lymphoblastic leukemia in adults: clinical features, immunophenotype, cytogenetics, and outcome from the large randomized prospective trial (UKALL XII/ECOG 2993). *Blood.* 2009;114:5136-5145.
16. Thiel E, Kranz BR, Raghavachar A, et al. Prethymic phenotype and genotype of pre-T (CD7+/ER-) cell leukemia and its clinical significance within adult acute lymphoblastic leukemia. *Blood.* 1989;73:1247-1258.
17. Uckun FM, Gaynon PS, Sensel MG, et al. Clinical features and treatment outcome of childhood T-lineage acute lymphoblastic leukemia according to the apparent maturational stage of T-lineage leukemic blasts: a Children's Cancer Group study. *J Clin Oncol.* 1997;15:2214-2221.
18. Vitale A, Guarini A, Ariola C, et al. Adult T-cell acute lymphoblastic leukemia: biologic profile at presentation and correlation with response to induction treatment in patients enrolled in the GIMEMA LAL 0496 protocol. *Blood.* 2006;107:473-479.
19. Inukai T, Kiyokawa N, Campana D, et al. Clinical significance of early T-cell precursor acute

- lymphoblastic leukaemia: results of the Tokyo Children's Cancer Study Group Study L99-15. *Br J Haematol.* 2012;156:358-365.
20. Ma M, Wang X, Tang J, et al. Early T-cell precursor leukemia: a subtype of high risk childhood acute lymphoblastic leukemia. *Front Med.* 2012;6:416-420.
 21. Neumann M, Heesch S, Gokbuget N, et al. Clinical and molecular characterization of early T-cell precursor leukemia: a high-risk subgroup in adult T-ALL with a high frequency of FLT3 mutations. *Blood Cancer J.* 2012;2:e55.
 22. Van Vlierberghe P, Ambesi-Impiombato A, Perez-Garcia A, et al. ETV6 mutations in early immature human T cell leukemias. *J Exp Med.* 2011;208:2571-2579.
 23. Neumann M, Heesch S, Schlee C, et al. Whole-exome sequencing in adult ETP-ALL reveals a high rate of DNMT3A mutations. *Blood.* 2013;121:4749-4752.
 24. Terriou L, Ben Abdelali R, Roumier C, et al. C/EBPA methylation is common in T-ALL but not in M0 AML. *Blood.* 2009;113:1864-1866; author reply 1866.
 25. Wouters BJ, Jorda MA, Keeshan K, et al. Distinct gene expression profiles of acute myeloid/T-lymphoid leukemia with silenced CEBPA and mutations in NOTCH1. *Blood.* 2007;110:3706-3714.
 26. Yang YL, Hsiao CC, Chen HY, et al. Absence of biallelic TCRgamma deletion predicts induction failure and poorer outcomes in childhood T-cell acute lymphoblastic leukemia. *Pediatr Blood Cancer.* 2012;58:846-851.
 27. Callens C, Baleyrier F, Lengline E, et al. Clinical impact of NOTCH1 and/or FBXW7 mutations, FLASH deletion, and TCR status in pediatric T-cell lymphoblastic lymphoma. *J Clin Oncol.* 2012;30:1966-1973.
 28. Kamps WA, Bokkerink JP, Hahlen K, et al. Intensive treatment of children with acute lymphoblastic leukemia according to ALL-BFM-86 without cranial radiotherapy: results of Dutch Childhood Leukemia Study Group Protocol ALL-7 (1988-1991). *Blood.* 1999;94:1226-1236.
 29. Kamps WA, Bokkerink JP, Hakvoort-Cammel FG, et al. BFM-oriented treatment for children with acute lymphoblastic leukemia without cranial irradiation and treatment reduction for standard risk patients: results of DCLSG protocol ALL-8 (1991-1996). *Leukemia.* 2002;16:1099-1111.
 30. Veerman AJ, Kamps WA, van den Berg H, et al. Dexamethasone-based therapy for childhood acute lymphoblastic leukaemia: results of the prospective Dutch Childhood Oncology Group (DCOG) protocol ALL-9 (1997-2004). *Lancet Oncol.* 2009;10:957-966.
 31. van Grotel M, Meijerink JP, van Wering ER, et al. Prognostic significance of molecular-cytogenetic abnormalities in pediatric T-ALL is not explained by immunophenotypic differences. *Leukemia.* 2008;22:124-131.
 32. Stam RW, den Boer ML, Meijerink JP, et al. Differential mRNA expression of Ara-C-metabolizing enzymes explains Ara-C sensitivity in MLL gene-rearranged infant acute lymphoblastic leukemia. *Blood.* 2003;101:1270-1276.
 33. Den Boer ML, Harms DO, Pieters R, et al. Patient stratification based on prednisolone-vincristine-asparaginase resistance profiles in children with acute lymphoblastic leukemia. *J Clin Oncol.* 2003;21:3262-3268.
 34. Subramanian A, Tamayo P, Mootha VK, et al. Gene set enrichment analysis: a knowledge-based approach for interpreting genome-wide expression profiles. *Proc Natl Acad Sci U S A.* 2005;102:15545-15550.
 35. Mingueneau M, Kreslavsky T, Gray D, et al. The transcriptional landscape of alphabeta T cell differentiation. *Nat Immunol.* 2013;14:619-632.
 36. Tibshirani R, Hastie T, Narasimhan B, Chu G. Diagnosis of multiple cancer types by shrunken centroids of gene expression. *Proc Natl Acad Sci U S A.* 2002;99:6567-6572.
 37. Novershtern N, Subramanian A, Lawton LN, et al. Densely interconnected transcriptional circuits

- control cell states in human hematopoiesis. *Cell*. 2011;144:296-309.
38. Hochberg Y, Benjamini Y. More powerful procedures for multiple significance testing. *Stat Med*. 1990;9:811-818.
 39. Bergeron J, Clappier E, Cauwelier B, et al. HOXA cluster deregulation in T-ALL associated with both a TCRD-HOXA and a CALM-AF10 chromosomal translocation. *Leukemia*. 2006;20:1184-1187.
 40. Baldus CD, Burmeister T, Martus P, et al. High expression of the ETS transcription factor ERG predicts adverse outcome in acute T-lymphoblastic leukemia in adults. *J Clin Oncol*. 2006;24:4714-4720.
 41. Baldus CD, Martus P, Burmeister T, et al. Low ERG and BAALC expression identifies a new subgroup of adult acute T-lymphoblastic leukemia with a highly favorable outcome. *J Clin Oncol*. 2007;25:3739-3745.
 42. Ben Abdelali R, Asnafi V, Leguay T, et al. Pediatric-inspired intensified therapy of adult T-ALL reveals the favorable outcome of NOTCH1/FBXW7 mutations, but not of low ERG/BAALC expression: a GRAALL study. *Blood*. 2011;118:5099-5107.
 43. Neumann M, Coskun E, Fransecky L, et al. FLT3 mutations in early T-cell precursor ALL characterize a stem cell like leukemia and imply the clinical use of tyrosine kinase inhibitors. *PLoS One*. 2013;8:e53190.
 44. Welch JS, Ley TJ, Link DC, et al. The origin and evolution of mutations in acute myeloid leukemia. *Cell*. 2012;150:264-278.
 45. Homminga I, Vuerhard MJ, Langerak AW, et al. Characterization of a pediatric T-cell acute lymphoblastic leukemia patient with simultaneous LYL1 and LMO2 rearrangements. *Haematologica*. 2012;97:258-261.

SUPPLEMENTARY DATA

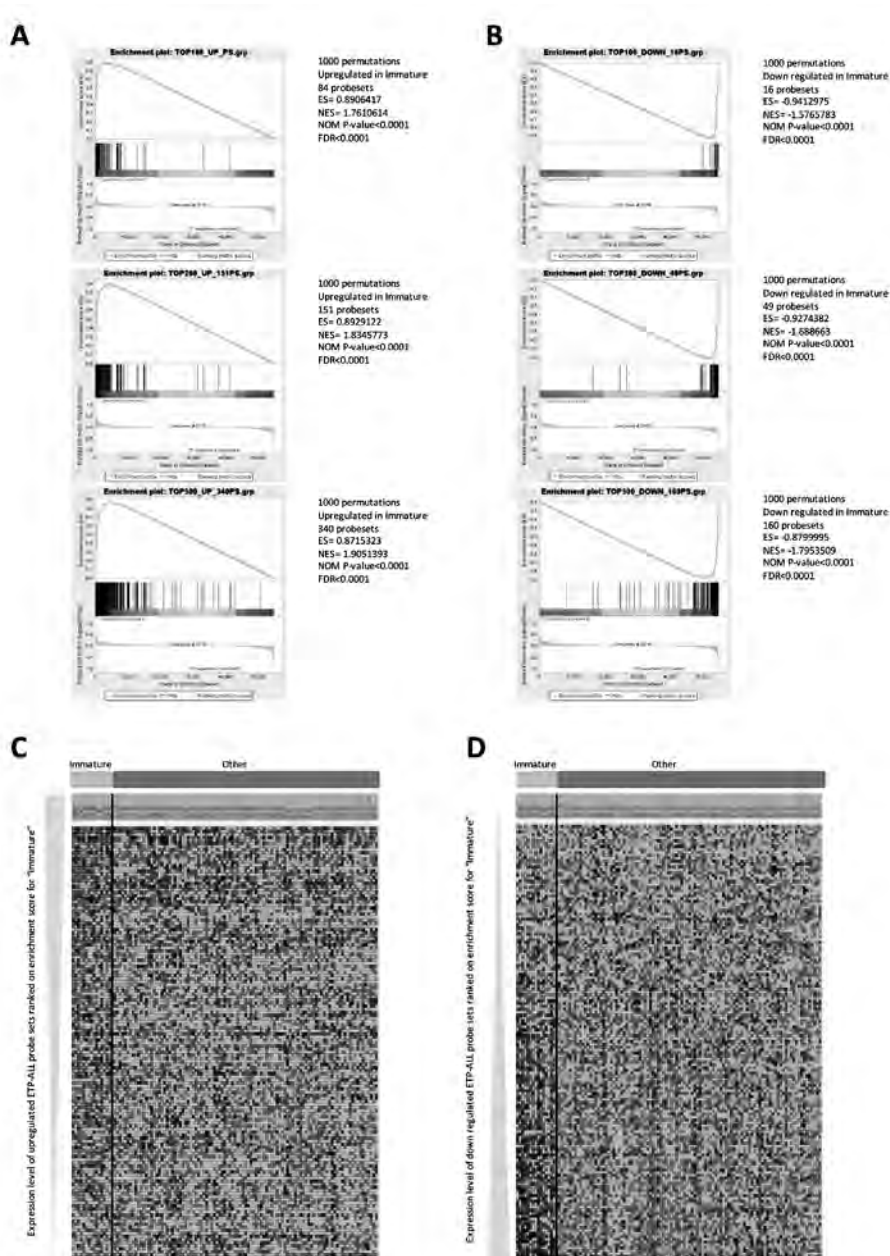


Figure S1 | ETP-ALL signature genes are enriched in the immature T-ALL cluster. Gene set enrichment analysis (GSEA) for (A) up- and (B) down-regulated probesets from the top100, 200 or 500 most significantly differentially expressed probesets from the human ETP-ALL gene signature (Zhang et al., nature 2012) for immature cluster versus other T-ALL patients. Significance levels for each analysis has been indicated. Heatmaps for (C) up- and (D) down-regulated probesets for immature cluster patients versus other T-ALL patients.

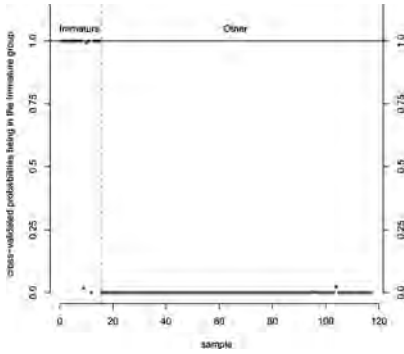


Figure S2 | PAM prediction of immature cluster cases versus non-immature cluster T-ALL patients based on the TOP100, 200 or 500 most significant probe sets from the human ETP-ALL gene signature (Zhang et al., Nature 2012). Only results for the TOP100 most significant ETP-ALL gene signature probe sets are shown predicting 13 out of 15 immature cluster cases while none of the 102 non-immature cluster cases on this probe selection ($p < 0.001$).

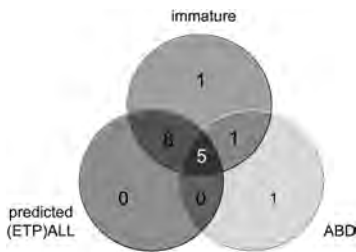


Figure S3 | **Overlap between the immature cluster, ETP-ALL and ABD characteristics in our pediatric T-ALL cohort.** The number of ETP-ALL positive patients in this Venn diagram is depicted by the gray sphere, the number of ABD patients is depicted by blue sphere, and the number of immature cluster patients is depicted by the dark blue sphere. This diagram is based on 117 T-ALL patients for whom gene expression array data were available.

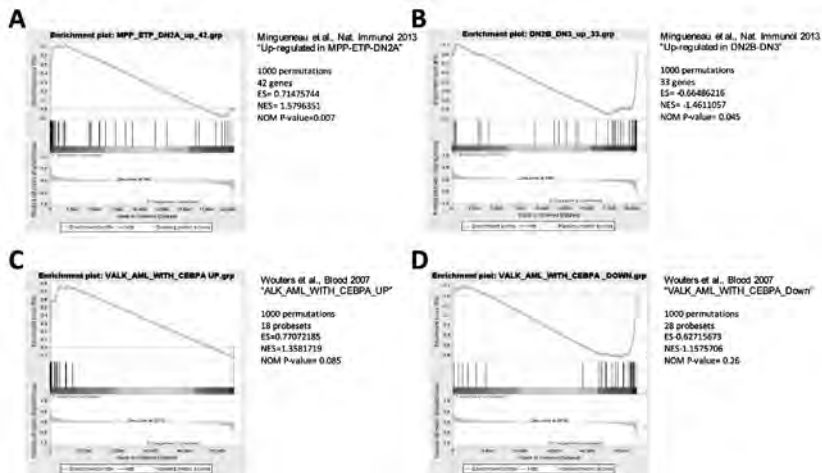


Figure S4 | **Immature cluster/ETP-ALL cases are enriched for early T-cell development signatures.** Enrichment of (A) MPP-ETP-DN2A or (B) post-DN2A T-cell signatures genes in immature cluster/ETP-ALL T-ALL cases. GSEA for (C) up- or (D) down-regulated genes of CEBPA-inactivated AML patient samples in immature cluster/ETP-ALL T-ALL cases.

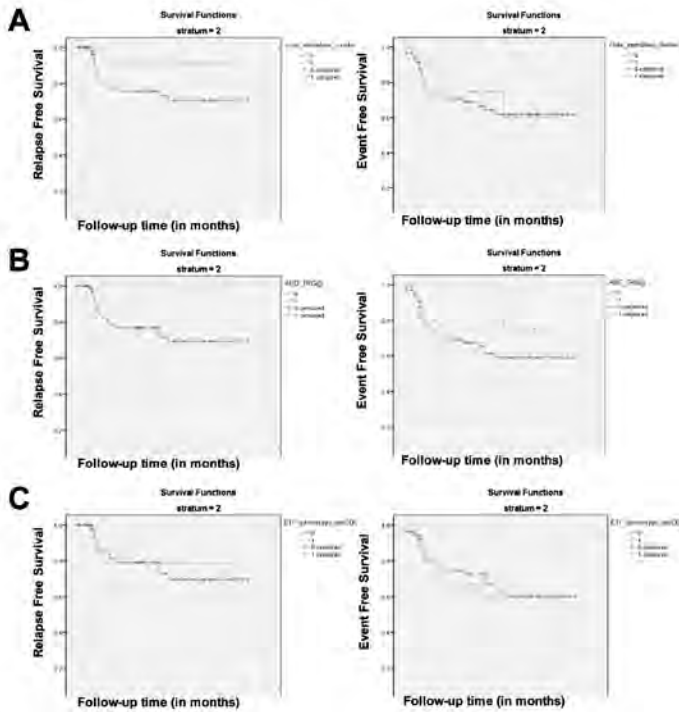


Figure S5 | Immature cluster T-ALL, ABD and immunophenotypic ETP-ALL patients treated on the COALL-97 protocol do not predict for poor outcome. Relapse free survival (RFS) and event free survival (EFS) curves for COALL-97 pediatric T-ALL patients. RFS and EFS curves (A) for immature cluster T-ALL cases upon unsupervised cluster (green line) versus other T-ALL cases (blue line), (B) for ABD T-ALL cases (green line) versus non-ABD cases (blue line), and (C) for ETP-ALL cases as identified upon immunophenotypic parameters (green line) compared to other T-ALL cases (blue line). Cases that are lost from further follow-up are represented by vertical tick marks.

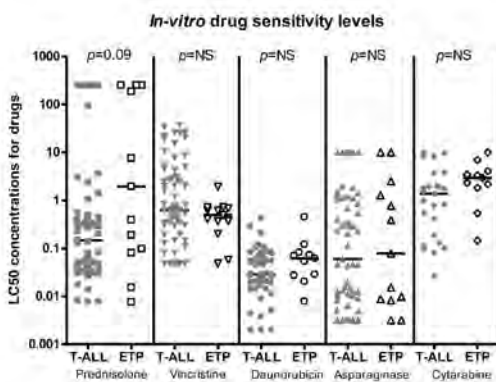


Figure S6 | In vitro sensitivity of Immature cluster/ETP-ALL leukemic cells towards chemotherapeutic agents. In vitro drug sensitivity levels towards prednisolone (squares), vincristine (downside-facing triangles), daunorubicin (circles), L-asparaginase (upside-facing triangles) and cytarabine (diamonds) were measured for leukemic cells of Immature cluster/ETP-ALL patients (open symbols) versus other T-ALL cases (closed gray symbols). The sensitivity level for each sample is indicated as the LC50 drug concentration that is lethal for 50 percent of the leukemic cells. Significance levels have been indicated. NS, not significant.

Table S1 | Available on request.

Patient	unsupervised cluster	ETP-ALL probability PAM top100 human GEP n=15/117	ETP-ALL probability PAM top200 human GEP n=13/117	ETP-ALL probability PAM top500 human GEP n=13/117	ETP-ALL summary PAM	ABD status n=7/117	simplified ETP-ALL immunophenotype			CD8 % positive	CD4 % positive	CD1 % positive	CD5 % positive	CD34 % positive	CD13 % positive	CD33 % positive
							including CD5 (≤75%)	excluding CD5 criteria	% positive							
9194	immature	1	1	1	ETP-ALL	one copy retained	-	yes	1	1	1	7	2	NA	40	
572	immature	1	1	1	ETP-ALL	both copies retained	-	yes	2	3	0	96	59	0	0	
1524	immature	1	1	1	ETP-ALL	both copies retained	-	yes	3	1	2	97	53	3	66	
1964	immature	1	1	1	ETP-ALL	both copies retained	-	yes	3	3	0	92	72	66	85	
10030	immature	1	1	1	ETP-ALL	both copies retained	NA	NA	1	1	NA	56	1	0	0	
167	immature	1	1	1	ETP-ALL	deleted	-	yes	16	2	14	90	45	0	0	
321	immature	1	1	1	ETP-ALL	deleted	-	yes	6	5	6	97	35	2	60	
491	immature	1	1	1	ETP-ALL	deleted	-	-	3	1	23	95	22	2	15	
2130	immature	1	1	1	ETP-ALL	deleted	-	yes	21	0	0	88	67	0	5	
9577	immature	1	1	1	ETP-ALL	deleted	-	yes	15	9	66	80	0	0	4	
2736	immature	1	1	1	ETP-ALL	deleted	yes	yes	1	1	0	2	69	2	44	
1509	immature	1	1	1	ETP-ALL	deleted	yes	yes	4	3	0	7	6	NA	39	
2703	immature	0.99	1	1	ETP-ALL	deleted	-	yes	1	0	8	92	79	3	0	
2252	immature	0.02	0	0	-	deleted	-	-	93	73	90	95	7	2	2	
9105	immature	0	0	0	-	one copy retained	-	-	53	68	7	83	0	0	0	
9012	TLX	0	0.36	1	-	deleted	-	-	3	13	10	96	ND	ND	ND	
9226	TAL/LMO	0	0	0	-	deleted	-	-	3	2	6	96	2	10	10	
9639	TLX	0	0	0	-	deleted	-	-	0	96	3	95	0	0	0	
9421	TLX	0.02	0.06	0.28	-	deleted	yes	yes	17	10	7	65	82	0	40	
231	TAL/LMO	0	0	0	-	one copy retained	-	-	83	43	60	80	95	3	5	
2750	TLX	0	0	0	-	deleted	-	yes	1	69	0	94	0	0	28	
10111	TAL/LMO	0	0	0	-	deleted	-	yes	3	2	1	95	79	1	4	
9858	TLX	0	0	0	-	deleted	-	yes	4	68	2	97	67	NA	4	
720	TLX	0	0	0	-	deleted	-	yes	0	83	11	96	39	0	0	
2780	TLX	0	0	0	-	deleted	yes	yes	7	57	6	70	7	28	28	
1753	TAL/LMO	0	0	0	-	deleted	yes	yes	6	6	4	90	49	0	0	
585	TLX	0	0	0	-	deleted	-	yes	17	17	17	86	86	16	20	
1032	TAL/LMO	0	0	0	-	deleted	-	yes	7	10	0	95	88	0	0	
1832	TAL/LMO	0	0	0	-	deleted	-	yes	9	31	22	94	53	15	5	
9963	TAL/LMO	0	0	0	-	deleted	-	yes	3	1	15	93	83	14	0	

Table S2 | Immunophenotype of the immature cluster, ETP-ALL, and ABD T-ALL patients and patients with an ETP immunophenotype.

	Immature Cluster					Bonferroni-Holm alpha
	-		+		p-value	
	n	(%) or range	n	(%) or range		
Total	102	(89%)	15	(11%)		
Clinical (n=117)						
Gender						
Male	75		8		0.13	
Female	27		7			
Median age yrs (range)	7.8	(1.5-17.8)	10.1	(3.1-16.4)	0.51*	-
Median WBC x10e9 cells/liter (range)	120	(2-900)	88	(2-435)	0.062*	-
ETP-immunophenotype: CD5 (≤75%) (n=111)						
ETP immunophenotype	2	(2%)	3	(20%)	0.017	0.0033
non ETP immunophenotype	94	(98%)	12	(80%)		
CD1-, CD4/CD8 DN, CD34/CD33/CD13+ (n=111)						
yes	6	(6%)	10	(67%)	<0.001	0.0029
no	90	(94%)	5	(33%)		
Chromosomal rearrangements (n=117)						
TAL1/2/LYL1 (n=27)	27	(26%)	0	(0%)	0.021	0.0036
LMO1/2/3 (n=14)	14	(14%)	0	(0%)	0.21	
TLX3 (n=22)	22	(22%)	0	(0%)	0.07	
TLX1 (n=7)	7	(7%)	0	(0%)	0.59	
HOXA (n=10)	7	(7%)	3	(20%)	0.12	
MEF2C (n=6)	0	(0%)	6	(40%)	<0.001	0.0029
NKX2-1/NKX2-2 (n=7)	7	(7%)	0	(0%)	0.59	
Unknown (n=26)	20	(19%)	6	(40%)	0.097	
NOTCH1/FBXW7 status (n=112)						
wild-type (n=42)	36	(37%)	6	(40%)	1#	
mutant (n=70)	61	(63%)	9	(60%)		
PTEN/AKT status (n=113)						
wild-type (n=92)	79	(81%)	13	(87%)	0.73	
mutant (n=21)	19	(19%)	2	(13%)		
PHF6 status (n=41)						
wild-type (n=32)	29	(76%)	3	(100%)	1	
mutant (n=9)	9	(24%)	0	(0%)		
WT1 status (n=115)						
wild-type (n=101)	86	(86%)	15	(100%)	0.21	
mutant (n=14)	14	(14%)	0	(0%)		

Table S3 | Overall clinical, immunophenotypic and molecular cytogenetic characteristics of the immature cluster (MEF2C) versus non-immature cluster T-ALL patients.

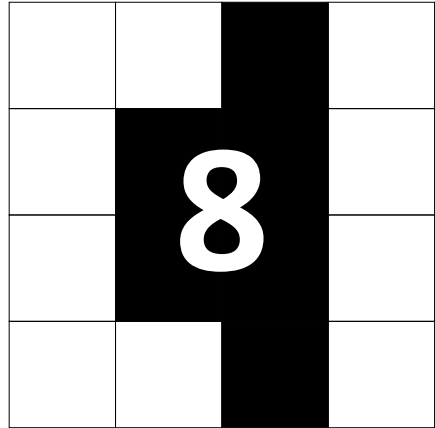
	ABD				p-value	Bonferroni-Holm alpha
	-		+			
	n	(%) or range	n	(%) or range		
Total	110	(89%)	7	(11%)		
Clinical (n=117)						
Gender						-
Male	81		3		0.1	
Female	29		4			
Median age yrs (range)	7.7	(1.5-17.8)	10.8	(5.4-16.1)	0.13*	-
Median WBC x10e9 cells/liter (range)	120	(2-900)	15	(2-248)	0.002*	0.003
ETP-immunophenotype: CD5 (≤75%) (n=111)						
ETP immunophenotype	3	(3%)	1	(14%)	0.23	
non ETP immunophenotype	101	(97%)	6	(86%)		
CD1-, CD4/CD8 DN, CD34/CD33/CD13+ (n=111)						
yes	12	(12%)	4	(57%)	0.008	0.0033
no	92	(88%)	3	(43%)		
Chromosomal rearrangements (n=117)						
TAL1/2/LYL1 (n=27)	27	(24%)	0	(0%)	0.2	
LMO1/2/3 (n=14)	14	(13%)	0	(11%)	0.6	
TLX3 (n=22)	22	(20%)	0	(0%)	0.35	
TLX1 (n=7)	7	(6%)	0	(0%)	1	
HOXA (n=10)	9	(8%)	1	(22%)	0.47	
MEF2C (n=6)	3	(2%)	3	(33%)	0.002	0.003
NKX2-1/NKX2-2 (n=7)	7	(6%)	0	(0%)	1	
Unknown (n=26)	23	(21%)	3	(33%)	0.18	
Unsupervised T-ALL clusters (n=116)						
TAL/LMO (n=53)	52	(48%)	1	(14%)		
Proliferative (n=19)	19	(17%)	0	(0%)		
Immature (n=15)	9	(8%)	6	(86%)	<0.001	0.0028
TLX (n=29)	29	(27%)	0	(0%)		
NOTCH1/FBXW7 status (n=112)						
wild-type (n=42)	39	(37%)	3	(43%)	1	
mutant (n=70)	66	(63%)	4	(57%)		
PTEN/AKT status (n=113)						
wild-type (n=95)	85	(80%)	7	(100%)	0.35	
mutant (n=18)	21	(20%)	0	(0%)		
PHF6 status (n=41)						
wild-type (n=32)	31	(78%)	1	(100%)	1	
mutant (n=9)	9	(22%)	0	(0%)		
WT1 status (n=115)						
wild-type (n=100)	93	(93%)	7	(100%)	0.59	
mutant (n=15)	15	(7%)	0	(0%)		

Table S4 | Overall clinical, immunophenotypic and molecular cytogenetic characteristics of ABD versus non-ABD T-ALL patients.

Table S5 | Gene signature of the immature cluster. Available on request.

Table S6 | Genes (probe sets) expressed in sorted hematopoietic cells, early erythroid precursor cells, and B-cell fractions established by Novershtern and co-workers. Available on request.

CHAPTER



Differential activation of pathways in genetic subgroups of T-cell acute lymphoblastic leukemia

**Linda Zuurbier¹, Emanuel F. Petricoin III^{2,3}, Valerie Calvert², Jessica G.C.A.M. Buijs-Gladdines¹,
Willem K. Smits¹, Edwin Sonneveld³, Rob Pieters^{1,4} and Jules P.P. Meijerink¹**

From the ¹Department of Pediatric Oncology/Hematology, Erasmus MC Rotterdam-Sophia Children's Hospital, Rotterdam, The Netherlands; ²Center for Applied Proteomics and Molecular Medicine, George Mason University, Manassas, VA, USA; ³NCI-FDA Clinical Proteomics Program, Food and Drug Administration, Bethesda, MD, USA; ⁴Princess Maxima Center for pediatric Oncology, Utrecht, The Netherlands.

ABSTRACT

Using an approach combining transcriptome data with proteome data that includes the activation state of molecules, we could identify pathways that seem inactive or active in T-ALL subgroups. Based on these data, TALLMO cluster patients seem to express molecules involved in T-cell receptor (TCR) signaling and metabolic glycolysis and lipid signaling. In TLX cluster patients a NOTCH1 pathway signature was observed independent of NOTCH genetic status. Proliferative cluster patients showed an active cell cycle signature, combined with a high expression of DNA repair genes but low p53 activity and circadian rhythm gene expression. In contrast, immature patients seem to express molecules involved in cell proliferation and migration at low levels. Furthermore, they had a low expression of TCR and high expression of B-cell receptor signaling genes. The alternative TGF-beta signaling via p38 MAPkinases may be important for MEF2C activation in immature patients. Regarding type B T-ALL mutation groups, NOTCH1-activated patients seem to have low and/or inactive PKC θ and p27 levels. This is in contrast to *PTEN*/*AKT*-mutated patients, whom seem to have high PKC θ levels. Moreover high expression of cell cycle and glycolysis genes were measured in these patients. WT1-inactivated patients had increased expression of gene involved in tRNA thiolation, which possibly reflects high levels of dominant negative WT1 transcripts. Also, WT1-inactivated patients seem to normally repress growth factor pathways, including TCR, cKIT and EGFR and JAK/STAT, AKT and mTOR.

INTRODUCTION

Pediatric T-cell acute lymphoblastic leukemia (T-ALL) accounts for 15% of all acute lymphocytic leukemia diagnosed in children. T-ALL is a high-risk disease,¹ and 20 percent of T-ALL patients relapse. Patients receive intensive chemotherapy which impedes further intensification of therapy.² Once relapsed, curative treatment options are limited and most relapsed patients ultimately die. To improve cure rates and to reduce treatment related toxicities, it is of utmost importance to understand pathogenic mechanisms of the disease and to develop new therapies for personalized medicine.

T-ALL is characterized by specific genetic alterations that have been categorized into type A and type B mutations^{3,4}. Type A mutations define at least 4 genetic subtypes that comprise *TAL1*, *LMO2*, *TLX3*, *TLX1* or *NKX2-1/NKX2-2* rearrangements or *HOXA*- or *MEF2C*-activating chromosomal and mutual exclusive rearrangements⁵⁻⁸ that drive specific gene expression signatures^{5,7,8}. Type B mutations are distributed across all T-ALL subgroups, including NOTCH1-activating mutations, mutations that drive the PTEN/AKT pathway, RAS mutations and others as reviewed elsewhere^{3,9}. Some aberrations have been linked with poor or good prognosis, but studies so far revealed that the prognostic significance of many markers were not consistent among studies impeding implementation for treatment stratification in current patient care³.

Gene expression profiling (GEP) combined with detailed molecular-cytogenetic analyses has improved understanding disease biology and discovering new patient groups. This identified various *TALLMO* cases with unknown abnormalities that had activating *LMO2* deletions, *TAL2*-, *LYL1*- or *LMO3*-rearrangements^{8,10,11} and two new genetic subtypes that comprise *MEF2C* or *NKX2-1/NKX2-2*-activating rearrangements. Unsupervised cluster analysis helped to distinguish 4 major T-ALL clusters, i.e. the *TALLMO*, *TLX*, proliferative and immature clusters⁶. Most *TAL*- or *LMO*-rearranged cases fell into the *TALLMO* cluster, whereas the proliferative cluster comprised mostly *NKX2-1* or *TLX1*-rearranged cases that all expressed CD1 and highly expressed cell-cycle regulating genes. The *TLX* cluster almost exclusively comprised *TLX3* or *HOXA*-rearranged cases whereas the immature cluster comprised all *MEF2C*-activated cases as consequence a variety of different oncogenic rearrangements. This immature cluster was recently proven to overlap with the early T-cell progenitor ALL (ETP-ALL)¹², an immature T-ALL entity that was associated with poor outcome in various studies¹³⁻¹⁵.

Oncogenic transcription factors transform cells by regulating the expression levels of downstream genes. As mRNA expression levels do not strictly recapitulate the proteomic fingerprint due to post-transcriptional and -translational mechanisms, we combined gene expression analyses with oncogene-related proteome signatures based on the activation status of various signal transduction pathway proteins, to study pathway analysis in T-ALL. This may help to distinguish drugable targets for future tailored treatment strategies, as well as to discover new diagnostic and prognostic biomarkers.

Using the reverse-phase protein array technique (RPMA) we previously showed that primary patient samples with *NOTCH1* and/or *FBXW7* mutations (*NOTCH1*-activated patients) have

increased cleaved (activated) intracellular NOTCH1 protein (ICN) expression compared to wild-type *NOTCH1/FBXW7* patients, as was only known for T-ALL cell lines¹⁶⁻¹⁹. *Chan et al* (2007) demonstrated that NOTCH1 was an important regulator of multiple mTOR signaling proteins in T-ALL cell lines, mediated by cMYC²⁰. Furthermore, using RPMA we also demonstrated that *PTEN*-mutated patient samples that lack PTEN protein expression were surprisingly not associated with increased AKT signaling activity as suggested in other studies²¹⁻²⁴. This indicated that, apart from PTEN mutations/deletions, other aberrations exist that also drive activation of AKT, including NOTCH1-activating mutations²⁴. *PTEN*-mutated patients expressed low levels of ICN, MYC and Musashi proteins that are indicative of decreased NOTCH1 signaling, in line with the reduced incidence of NOTCH-activating mutations in *PTEN*-mutated patient samples²³.

In the present study, we integrated transcriptome and proteome data to study pathway activation in T-ALL groups. We used global test analysis of gene expression data combined with RPMA-generated protein data describing the activation status of a selected panel of signal transduction molecules that may be dysregulated in pediatric T-ALL patients. To the best of our knowledge, broad screens on the activation status for such a panel of signal transduction components simultaneously and in combination with transcriptional analyses, have not been done before on primary T-ALL patient samples. We investigated differential expression of pathway and protein activation among T-ALL clusters, as well as among patient samples that presented with different type B mutations.

MATERIALS AND METHODS

Patient samples

A total of 117 primary pediatric T-ALL patients were included in this study. The patients' parents or legal guardians provided informed consent to use leftover diagnostic material for research in accordance with the Institutional Review Board of the Erasmus MC Rotterdam and the Declaration of Helsinki. Leukemia cells were harvested and enriched of blood or bone marrow samples as described before, with all samples containing >90% of leukemic cells²⁵. Clinical data were supplied by both study group centers.

Reverse Phase Protein Microarray analysis (RPMA)

Reverse phase protein microarray construction and analysis was performed essentially as previously described^{26,27}. To isolate proteins from 10×10^6 leukemic cells, lysis was performed in 20 μ L Tissue Protein Extraction Reagent (TPER, Pierce Biotechnology, Rockford, IL, USA) with 300 nM NaCl, 1 mM orthovanadate and protease inhibitors. Cells were incubated at 4°C for 20' and subsequently centrifuged at 10.000 rpm for 5' in an Eppendorf centrifuge. Supernatants were stored at -80°C prior to printing on the microarrays. Lysates were diluted to 1.0 mg/ml protein concentration and mixed 1:1 with 2x SDS Tris-glycine buffer (Invitrogen) containing 5% 2-mercaptoethanol (Sigma, Zwijndrecht, the Netherlands) (FC = 0.5 mg/ml). Lysates were

spotted at a concentration of 0.5 µg/µl (neat spot) and 0,125 µg/µl in duplicate with 350 micron pins on glass-backed nitrocellulose coated array slides (FAST slides, Whatman plc, Kent, UK) using an Aushon Biosystems 2470 (Aushon Biosystems, Billerica, MA, USA). To prevent bias through the composition of the array, patient samples of different clusters were randomly distributed over the RPMA array. Printed slides were stored at -20°C or directly used. The first of each 25 slides printed were subjected to Sypro Ruby Protein Blot staining (Invitrogen) to determine total protein amount. These slides were visualized on a NovaRay CCD fluorescent scanner (Alpha Innotech, San Leandro, CA, USA). The remaining slides were used for staining with a specific antibody. Prior to this, slides were incubated with 1x Reblot (Chemicon, Temecula, CA, USA) for 15' and subsequently washed with PBS twice. This was continued with a blocking procedure for 5 hrs using 1gr I-block (Applied Biosystems) diluted in 500mL PBS with 0,5% Tween-20. Slides were stained with an automated slide stainer (Dako) according to manufacturer's instructions using the Autostainer catalyzed signal amplification (CSA) kit (Dako). In each staining run, a negative control slide was stained with the secondary antibody only for background subtraction. Briefly, endogenous biotin was blocked for 10 minutes with the biotin blocking kit (Dako), followed by application of protein block for 5 minutes; primary antibodies were diluted in antibody diluent and incubated on slides for 30 minutes and biotinylated secondary antibodies were incubated for 15 minutes. Signal amplification involved incubation with a streptavidin-biotin-peroxidase complex provided in the CSA kit for 15 minutes, and amplification reagent (biotinyl-tyramide/hydrogen peroxide, streptavidin-peroxidase) for 15 minutes each. A signal is generated using streptavidin-conjugated IRDye680 (LI-COR Biosciences, Lincoln, NE, USA). Slides were allowed to air dry following development. Stained slides were scanned individually on the NovaRay scanner (Alpha Innotech) and files were saved in TIF format in Photoshop 7.0. All slides were subsequently analyzed with the MicroVigene v2.8.1.0 program (VigeneTech, Carlisle, MA, USA).

Genomic DNA extraction, PCR and sequencing

Genomic DNA isolation, PCR and sequencing analyses of the *NOTCH*, *FBXW7*, *PTEN*, *AKT*, *PIK3CA*, *PIK3RI*, and *WT1* genes were previously described^{19,23,28}.

Fluorescence in-situ hybridization analysis (FISH) and RQ-PCR

Rearrangements of the *TLX1*, *TLX3*, *TAL1*, *LMO2* and *MLL* loci were determined using fluorescence in-situ hybridization analysis (FISH)^{8,25,29}. *SET-NUP214* or *CALM-AF10* fusion products or expression levels of *SIL-TAL1*, *TLX1* or *TLX3* were detected by an RQ-PCR strategy^{8,25,29}.

Gene expression arrays

Gene expression arrays and analyses were done using Humane Genome U133 plus2.0 oligonucleotide microarrays (Affymetrix, Santa Clara, CA, USA), according to the procedure described before^{6,25}, and have been deposited at the GEO database (<http://www.ncbi.nlm.nih.gov/geo/>), accession GSE10609 and GSE26713).

Microarray-based comparative genome hybridization (array-CGH)

Array-CGH analysis was performed on the human genome CGH Microarray 44A ($n=4$), 105K ($n=2$), and 400K ($n=54$) (Agilent Technologies, Santa-Clara, CA, USA). These arrays harbor 60-mer oligo-nucleotide probes, spanning both coding and non-coding sequences. The procedure was done as described before⁸. Analyses were done using Agilent Genomic Workbench software v3.1.28.

Statistics

Statistics were performed using SPSS 18.0 software. Statistical significance for continuous distributed data was tested using the Mann-Whitney-U test. Data were considered significant when $p \leq 0.05$ (two-sided). The Bioconductor package Global test³⁰ on gene expression data was performed in R for pathway analysis and is based on the empirical Bayesian generalized linear model and determines whether a pre-specified group of genes is differentially expressed in relation to sample parameters. It does, however, not take into account whether genes are up- or downregulated. Correction for multiple testing (Benjamini and Hochberg's method) was applied and sampling analyses revealed a comparative P-value (< 0.05) and was done to exclude pathways which are coincidentally detected as being significantly differentially expressed. Using the Bioconductor package Pathview³¹ expression changes were imaged in KEGG images. When multiple genes were involved at one pathway node, the sum of all expression levels was taken. Probe sets linked to multiple genes were excluded. The probe set with the highest variance was used when multiple probe sets represented one gene, using the Bioconductor Genefilter package.

RESULTS

In this study, we investigated the activation status of cellular signaling pathways at transcriptional and protein level in specific T-ALL subgroups. We examined differential expression of pathways in various unsupervised T-ALL clusters as previously described⁶, i.e. the TALLMO, TLX, proliferative and immature/ETP-ALL cluster¹² (herein called immature). These clusters are almost exclusively associated with the presence of specific driving oncogenic transcription factor rearrangements⁶. Also, patients with various type B aberrations were investigated for differentially expressed pathways, including NOTCH1-activated patients (having *NOTCH1* and/or *FBXW7* mutations), *PTEN/AKT*-mutated patients (having silenced *PTEN* and/or *AKT* mutations) and *WT1*-inactivated patients (having *WT1* mutations or deletions)^{19,23,28}.

For analyses of gene expression data by microarray analysis, the global test analysis was performed in R, using KEGG pathway information including 229 KEGG cellular signaling pathway maps. Due to extensive crosstalk between pathways, many KEGG pathway maps contain overlapping molecules. In this study, 117 T-ALL patient samples were used of which 53 belongs to TALLMO, 30 to TLX, 19 to the proliferative and 15 to the immature cluster. Sixty-eight

patients have NOTCH1-activating mutations, whereas 20 are mutated in *PTEN* or *AKT* and 14 are WT1-inactivated. Significantly differentially expressed pathway maps identified in each group were categorized by body task according to supplied KEGG information; organismal system, environmental information processing, cellular processes and metabolism. The expression direction of each pathway was determined by imaging expression levels in KEGG maps using Pathview in R, which visualizes significant up-or downregulation of particular genes within a pathway. Only pathway maps showing a clear expression direction were further investigated and described (**Table 1 and 2**; marked in gray).

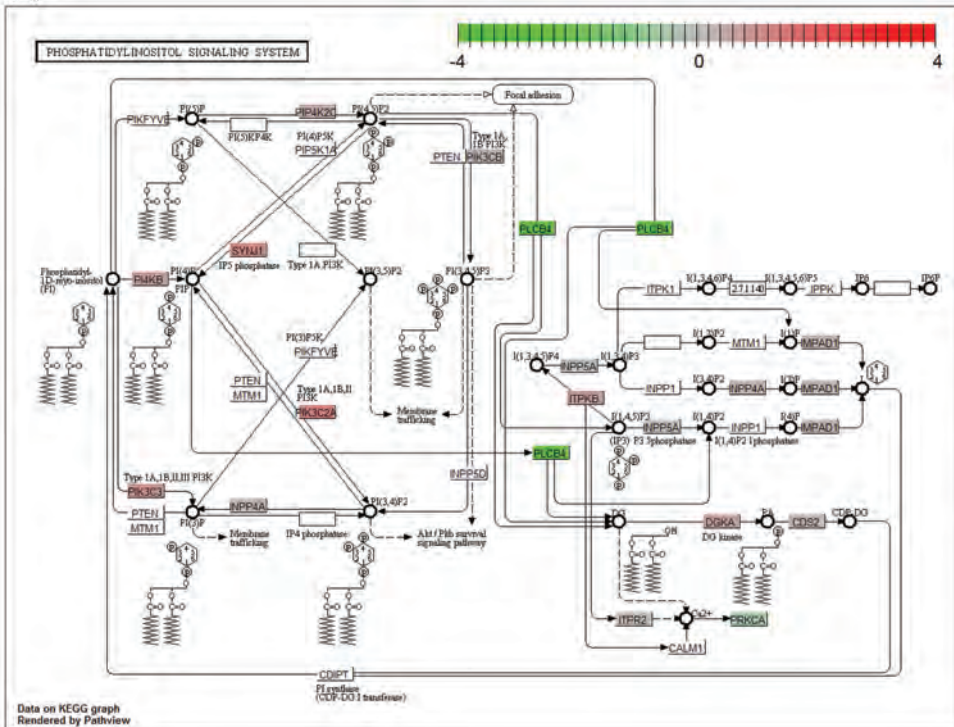
To determine total and phosphorylated protein levels of 91 selected signal transduction molecules, we used the reverse-phase protein microarray (RPMA) technique (see **Table S1**). This technique was applied on protein lysates of 66 primary T-ALL patients. Differential protein expression was examined using Mann-whitney U statistics between one and all other subgroups ($p \leq 0.05$, **Table 1 and 2**). Sixty-one out of the 66 patients had corresponding gene expression data. These included 25 TALLMO cluster patients, 14 TLX and 10 proliferative cluster and 12 immature cluster patients. It also included 38 NOTCH1-activated patients, 17 *PTEN/AKT*-mutated patients and 8 WT1-inactivated patients. Clinical and genetic patient data were available for all these patients (**Table S2**).

TALLMO cluster

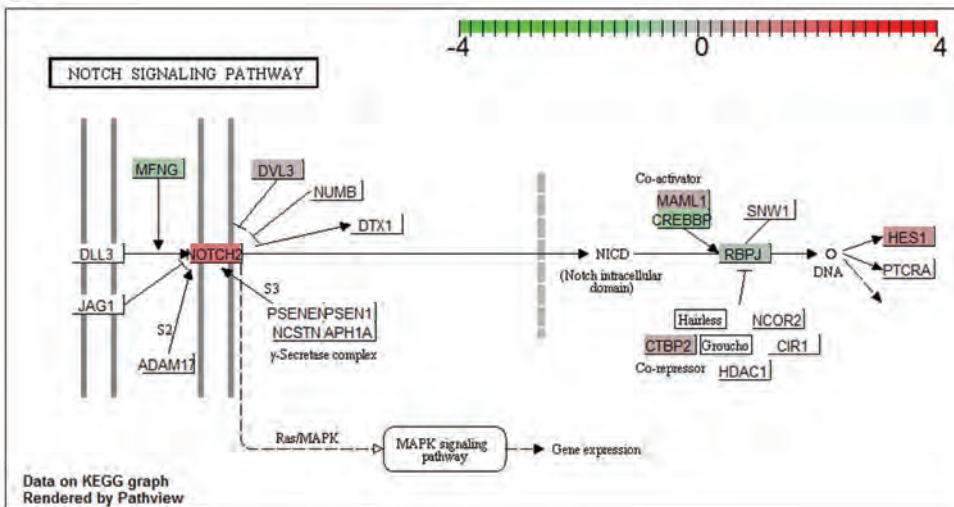
First, we examined transcriptionally differentially expressed KEGG pathways in TALLMO cluster patients ($n=53$) when compared to all other T-ALL patients (**Table 1**). We observe a clear differential expression pattern of the phosphatidylinositol signaling system, the inositol phosphate metabolism, glycerolipid metabolism, starch and sucrose metabolism, gap junctions and the T-cell receptor (TCR) signaling pathway in these patients (**Figure 1A and Figure S1A-E**). TALLMO patients seem to actively alter their phosphorylated phosphatidylinositols (PtdIns/PIP) status as well as these of the phosphorylated inositol (IP) derivatives (FDR $p=5.5 \cdot 10^{-11}$ respectively FDR $p=5.3 \cdot 10^{-11}$), which is mediated by various differentially expressed phosphatases and kinases including PTEN and PI3K isoforms. Both processes are important for membrane-trafficking and lipid signaling (second messengers) leading to cellular growth, migration, survival and differentiation. Downstream signaling can occur through the AKT/mTOR pathway, among others. Within the glycerolipid metabolism (FDR $p < 1 \cdot 10^{-12}$), we observe conversion of molecules mainly towards diacylglycerols (DAG) or its phosphorylated form phosphatidic acid (diacylglycerophospholipid). Both can function as second messengers within the PtdIns and IP metabolisms. Gene expression within the starch and sucrose metabolism points towards active glycolysis in TALLMO patients, meaning the generation of ATP molecules. Furthermore, the formation of gap junctions seems inactive in TALLMO patients (FDR $p=2.9 \cdot 10^{-10}$) indicating that intercellular channels essential for transendothelial migration of lymphocytes may not be actively formed. Interestingly, TALLMO cells appear to have a differential expression of genes encoding TCR signaling drivers (FDR $p=6.0 \cdot 10^{-11}$), which is indicated by high expression of e.g. multiple *TRA* (*TCR α*) and *TRB* (*TCR β*) variants, *LCK*, *CD40LG* (*CD40 ligand*), *LAT*, *CD28*, *NFATC1*,

Global test results	KEGG map	pathway	Class	P	Adjusted P	Comparative P	RPM results	P	expression	
TALLMO cluster (n=25)										
Organismal system										
04560	T cell receptor signaling pathway		Sign., Transduction	4.25E-12	6.02E-11	0.032	pGSK3 α	S21/9	0.004	high
04270	Vascular smooth muscle contraction		Circulatory system	2.79E-12	5.31E-11	0.032	GSK3 β	G27	0.016	high
04370	Salivary secretion		Digestive system	<1E-12	<1E-12	0.039	pPKC δ	T538	0.019	high
04372	Pancreatic secretion		Digestive system	<1E-12	<1E-12	0.032	pABL	T735	0.039	low
04374	Protein digestion and absorption		Digestive system	2.54E-12	5.31E-11	0.045	P13K	S217/221	0.019	low
04371	Gastric acid secretion		Digestive system	2.10E-11	2.53E-10	0.037	pMEK1/2	T187	0.030	low
04720	Long-term potentiation		Nervous system	1.48E-11	1.88E-10	0.025	pp27		0.030	low
Environmental Information Processing										
Phosphatidylinositol signaling system										
04070	Phosphatidylinositol signaling system		Sign., Transduction	3.20E-12	5.45E-11	0.031	CD44	S2481	0.039	low
Cellular processes										
04540	Gap junction		Cell communication	2.49E-11	2.85E-10	0.039	pMTOR	Y719	0.039	low
Metabolism										
00561	Glycerolipid metabolism		Lipid metabolism	<1E-12	<1E-12	0.036	pc-KIT	Y1571	0.041	low
00590	Arachidonic acid metabolism		Lipid metabolism	<1E-12	<1E-12	0.049	pp70 S6	T389	0.043	low
00500	Starch and sucrose metabolism		Carbohydrate metabolism	1.19E-12	3.89E-11	0.045	MYC		0.044	low
00562	Inositol phosphate metabolism		Carbohydrate metabolism	1.97E-12	5.31E-11	0.045			0.048	low
00512	Mucin type O-Glycan biosynthesis		Glycan biosynth + metab.	3.51E-12	5.45E-11	0.037				
00930	Retinol metabolism		Metab. cofactors + vitamins	6.14E-11	5.62E-10	0.015				
00750	Vitamin B6 metabolism		Metab. cofactors + vitamins	2.61E-08	8.29E-08	0.039				
TLX cluster (n=30)										
Organismal system										
04570	Leukocyte transendothelial migration		Immune system	1.84E-09	3.84E-08	0.034	pSMAD158	S/S, S/S, S/S	<0.001	high
04270	Vascular smooth muscle contraction		Circulatory system	3.97E-09	6.50E-08	0.046	pp70 S6	T389	0.003	high
04614	Renin-angiotensin system		Endocrine system	5.24E-09	7.50E-08	0.022	casease 3	cleaved Asp175	0.011	high
Environmental Information Processing										
Phosphatidylinositol signaling system										
04070	Phosphatidylinositol signaling system		Sign., Transduction	1.54E-11	1.78E-09	0.004	beta-catenin	T638/41	0.032	high
04060	Cytokine-cytokine receptor interaction		Sign., molecules + interaction	1.95E-10	5.59E-09	0.023	pPKC δ	Thr 505	0.038	high
04630	Jak-STAT signaling pathway		Sign., Transduction	5.93E-10	1.51E-08	0.032	pLCK		0.008	low
Cellular processes										
04115	p53 signaling pathway		Cell growth and death	2.83E-09	5.41E-08	0.031	p27	Y1020	0.016	low
04540	Gap junction		Cell communication	6.23E-09	8.39E-08	0.032	pSHP1		0.031	low
04330	Gap junction		Cell communication	8.52E-09	1.08E-07	0.055				
Genetic information processing										
Sulfur relay system										
04122	Sulfur relay system		Folding, sorting, degradation	3.91E-09	6.50E-08	0.033				
Metabolism										
00920	Sulfur metabolism		Energy metabolism	5.72E-11	3.37E-09	0.009				
00750	Vitamin B6 metabolism		Metab. cofactors + vitamins	5.89E-11	3.37E-09	0.009				
00532	Glycosaminoglycan biosynthesis - chondroitin sulfate / dermatan sulfate		Glycan biosynth + metab.	1.02E-10	4.60E-09	0.012				
00562	Inositol phosphate metabolism		Carbohydrate metabolism	1.60E-10	5.22E-09	0.030				
00930	Retinol metabolism		Metab. cofactors + vitamins	1.83E-09	3.84E-08	0.006				
Proliferative cluster (n=19)										
Organismal system										
04610	Complement and coagulation cascades		Immune system	6.36E-08	1.87E-06	0.012	pABL	T735	0.002	high
04914	Progesterone-mediated oocyte maturation		Endocrine system	9.68E-08	1.87E-06	0.009	plGF-1R/IRB	Y1135/36, Y1150/51	0.011	high
04910	Insulin signaling pathway		Endocrine system	1.27E-07	1.94E-06	0.017	pLCK	Thr505	0.020	high
04640	Hematopoietic cell lineage		Immune system	1.77E-07	2.39E-06	0.003	P13K		0.021	high
04710	Circadian rhythm		Environmental adaptation	2.79E-07	3.02E-06	0.009	pPKY2	Y402	0.028	high
04380	Osteoclast differentiation		Development	6.67E-07	4.13E-06	0.041	pPKC δ	T638/41	0.039	high
Environmental Information Processing										
Wnt signaling pathway										
04310	Wnt signaling pathway		Sign., Transduction	3.48E-08	1.87E-06	0.008	casease 3	cleaved Asp175	0.001	low
04514	Cell adhesion molecules (CAMs)		Sign., molecules + interaction	7.09E-08	1.87E-06	0.025	casease 3		0.044	low
04010	MAPK signaling pathway		Sign., Transduction	6.33E-07	4.13E-06	0.030	pBRAF	S445	0.044	low
Cellular processes										
04520	Adherens junction		Cell communication	3.52E-10	8.05E-08	0				
04115	p53 signaling pathway		Cell growth and death	3.70E-09	4.23E-07	0				
04110	Cell cycle		Cell growth and death	2.21E-08	1.69E-06	0				
04114	Oocyte meiosis		Cell growth and death	1.06E-07	1.87E-06	0.005				

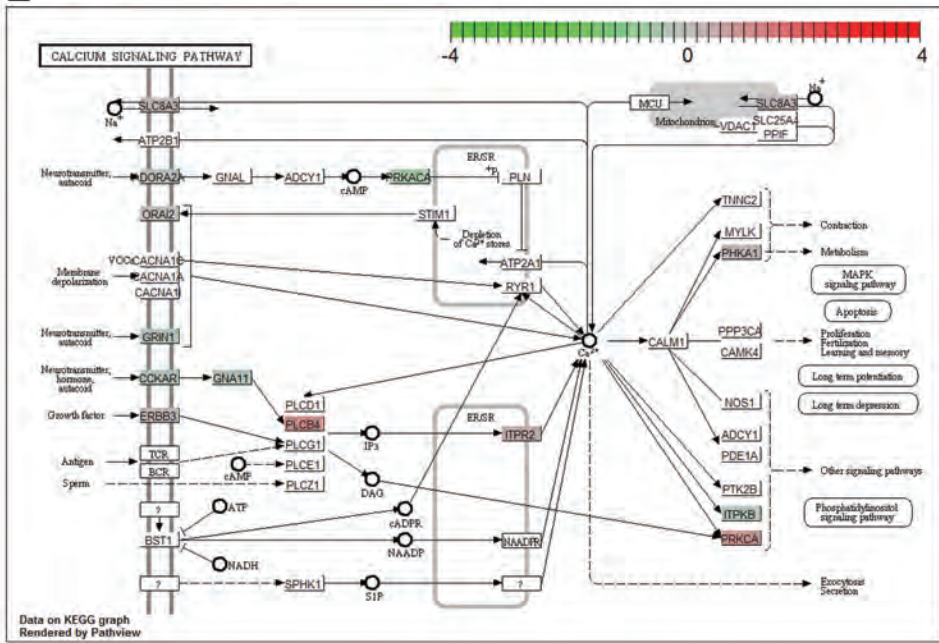
A



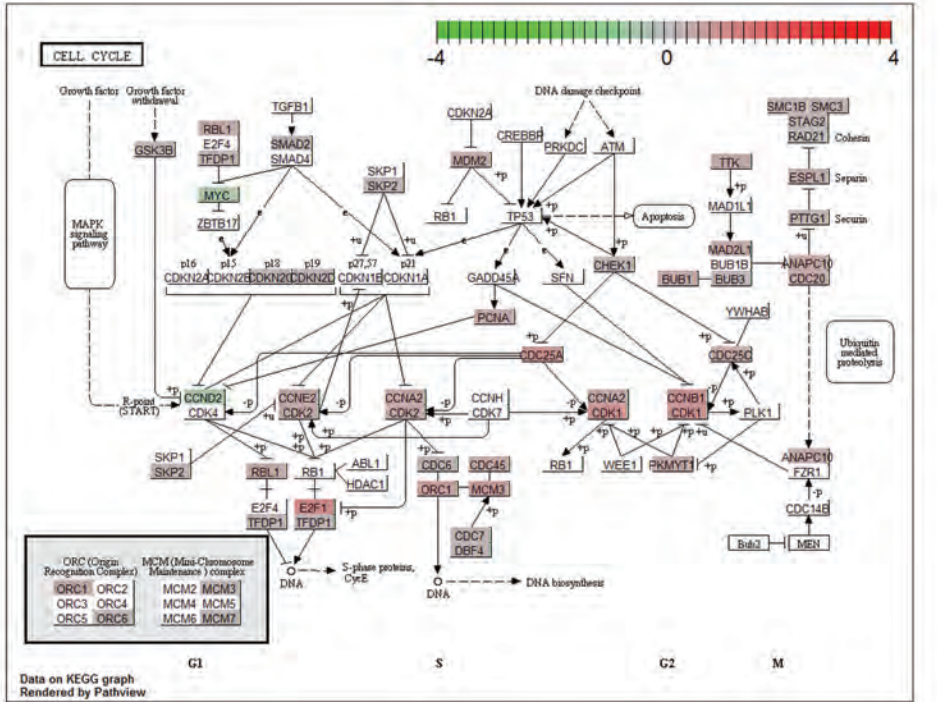
B



E



F



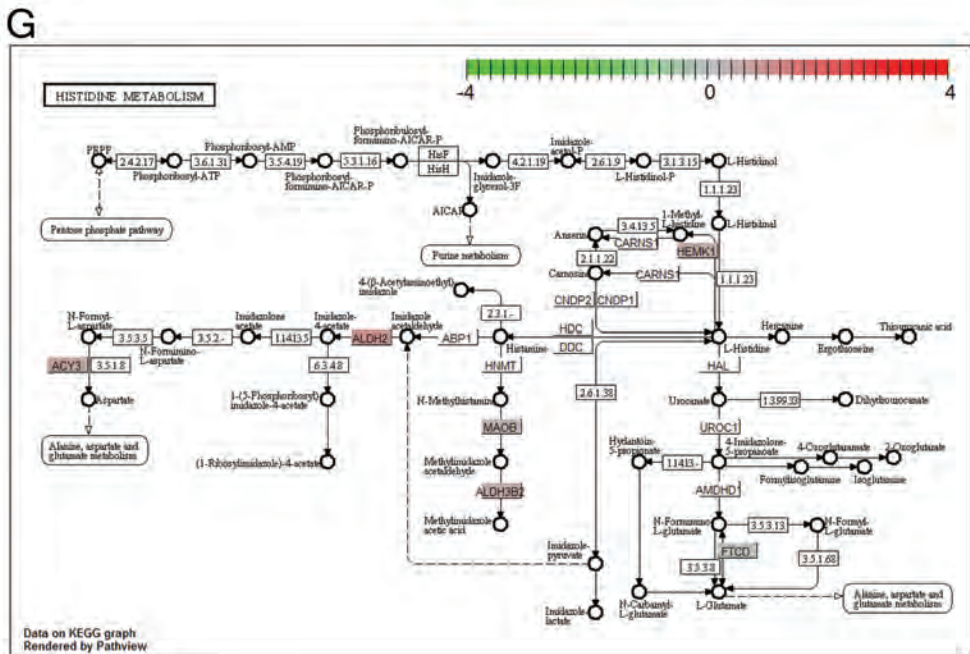


Figure 1 | A selection of differentially expressed KEGG pathway maps. Red indicates higher, green indicates lower expression of a particular gene compared to all other subgroups. (A) phosphatidylinositol signaling system in TALLMO patients, (B) NOTCH signaling in TLX patients, (C) circadian rhythm in proliferative patients, (D) MAPK signaling pathway in immature patients, (E) calcium signaling pathway in NOTCH1-activated patients, (F) cell cycle in *PTEN/**AKT*-mutated patients and (G) histidine metabolism in WT1-inactivated patients.

ZAP70, *VAV1*, *CD3D* (*CD3δ*), *CD247* (*CD3ζ*), *CD3G* (*CD3γ*) and *FYN* genes and a low expression of *TCRA/D* ($\alpha\delta$) loci (data not shown).

Proteome analyses revealed 15 proteins that were differentially expressed in TALLMO patients ($n=25$, **Table 1**). The transcriptional activities regarding active glycolysis seem to be reflected by abundant expression of total GSK3 β ($p=0.02$) and inactive phosphorylated GSK3 β proteins in TALLMO samples compared to all other clusters ($p=0.004$) (**Figure 2**). GSK3 β is inactive when phosphorylated at Ser9, prevents glycogen storage and has a function within Wnt signaling. GSK3 β /phosphorylated-GSK3 $\alpha\beta$ ratios are similar in TALLMO and all other patients, suggesting that effectively more non-phosphorylated/active GSK3 is present in TALLMO patients. In support of this notion, based on two *GSK3B* gene expression array probe sets that had above-background levels, *GSK3B* RNA levels are slightly increased in TALLMO patients (data not shown). In addition, a strong correlation is observed between total GSK3 β protein level and phosphorylated GSK3 $\alpha\beta$ ($R^2=0.804$). This indicates that *GSK3B* transcription is relatively equal to phosphorylation in these patients and implies GSK3 $\alpha\beta$ phosphorylation is not enhanced in these patients, but more likely, *GSK3B* transcription is enhanced. Whereas high numbers of various (other) PI3K subunits were just described to be observed at transcriptional level, protein levels of the regulatory PI3K

class I α -subunit (p85 class I regulatory subunit) appear low in this T-ALL subgroup (**Figure 2**, $p=0.019$). Also PI3K-downstream effectors like AKT-mTOR, seem inactive (**Figure 2**) as observed by low levels of phospho-TSC2 ($p=0.04$), phospho-mTOR ($p=0.04$) and phospho-p70 S6 kinase (RPS6KB1; $p=0.04$). Levels of the cell cycle inhibitor protein p27 (CDKN1B; $p=0.02$) are high but predominantly present in their non-phosphorylated, active form (**Figure 2**, $p=0.03$). Among others, transcription of *p27* can be initiated by Forkhead transcription factors (downstream AKT) but also HES1 (downstream NOTCH1) and kinases that can phosphorylate p27, including AKT. The cHER2 receptor ($p=0.03$), that partially fulfills an mTOR-like function upon HER2 expression, is also expressed at low levels in TALLMO cluster patients. Furthermore, the novel isoform PKC θ that is important for TCR signaling is highly expressed ($p=0.04$) and corresponds to a high expression of TCR signaling genes in this group. Also, phospho-ABL ($p=0.003$), phospho-MEK1/2 ($p=0.03$), receptor tyrosine kinase phospho-c-KIT ($p=0.04$), cell migratory protein CD44 ($p=0.04$) and MYC (**Figure 2**, $p=0.05$) are expressed at significantly lower levels in this cluster.

TLX cluster

Differential transcriptional expression analysis of KEGG pathways within the TLX T-ALL cluster patients ($n=30$) compared to all other T-ALL patients (**Table 1**) points towards a high gene expression signature of the NOTCH1 pathway (**Figure 1B**, FDR $p=1.1*10^{-7}$). As this cluster predominantly consists of *TLX3*-rearranged patients, this validates our previous finding of a higher incidence of NOTCH1-activating mutations within *TLX3*-rearranged patients¹⁹. However interestingly, NOTCH1 signature genes seem also highly expressed in NOTCH1 wild-type TLX cluster patients (**Figure 3**). Furthermore, in contrast to TALLMO cluster patients TLX cluster patients may have an active PtdIns signaling system and IP metabolism (**Figure S2A,B**, FDR $p=1.8*10^{-9}$ and FDR $p=5.2*10^{-9}$ respectively). Signaling for leukocyte transendothelial migration seems shut-off in TLX cluster patients (**Figure S2A, C**, FDR $p=3.8*10^{-8}$) and many cytokine receptors are significantly differently expressed (**Figure S2D**, FDR $p=5.6*10^{-9}$). Among these are reduced expression levels of *IL4* and *IL4R* genes and a high expression of *PDGF* family members and ligands.

Ten proteins were differentially expressed in the TLX cluster ($n=14$) compared to all other T-ALL patients. The TLX cluster shows significant enrichment of NOTCH1 signaling proteins Musashi (MSI1/2; $p<0.001$) as well as the downstream target MYC ($p=0.02$) (**Table 1, Figure 2**) which validates our global test result. TLX cluster patients do not seem to express the cell cycle inhibitor p27 of which transcription can be regulated by NOTCH1 target HES1 as well as by Forkhead transcription factors (**Figure 2**, CDKN1B; $p=0.016$). The phosphatase phospho-SHIP1 seems not expressed (INPP5D; $p=0.031$). SHIP1 is involved in PIP and IP signaling which appear not to be active in TLX patients. Furthermore, this cluster highly expresses the calcium-sensitive kinase phospho-PKC α/β (**Figure 2**, $p=0.038$), β -catenin that is important for migration but also for transcriptional activation of the Wnt signaling (**Figure 2**, $p=0.03$), the mTOR target phospho-p70 S6 kinase (**Figure 2**, RPS6KB1; $p=0.003$), phospho-SMAD1/5/8 (**Figure 2**, $p<0.001$), and cleaved pro-apoptotic caspase 3 (**Figure 2**, $p=0.011$) but low levels of the TCR protein phospho-LCK ($p=0.008$).

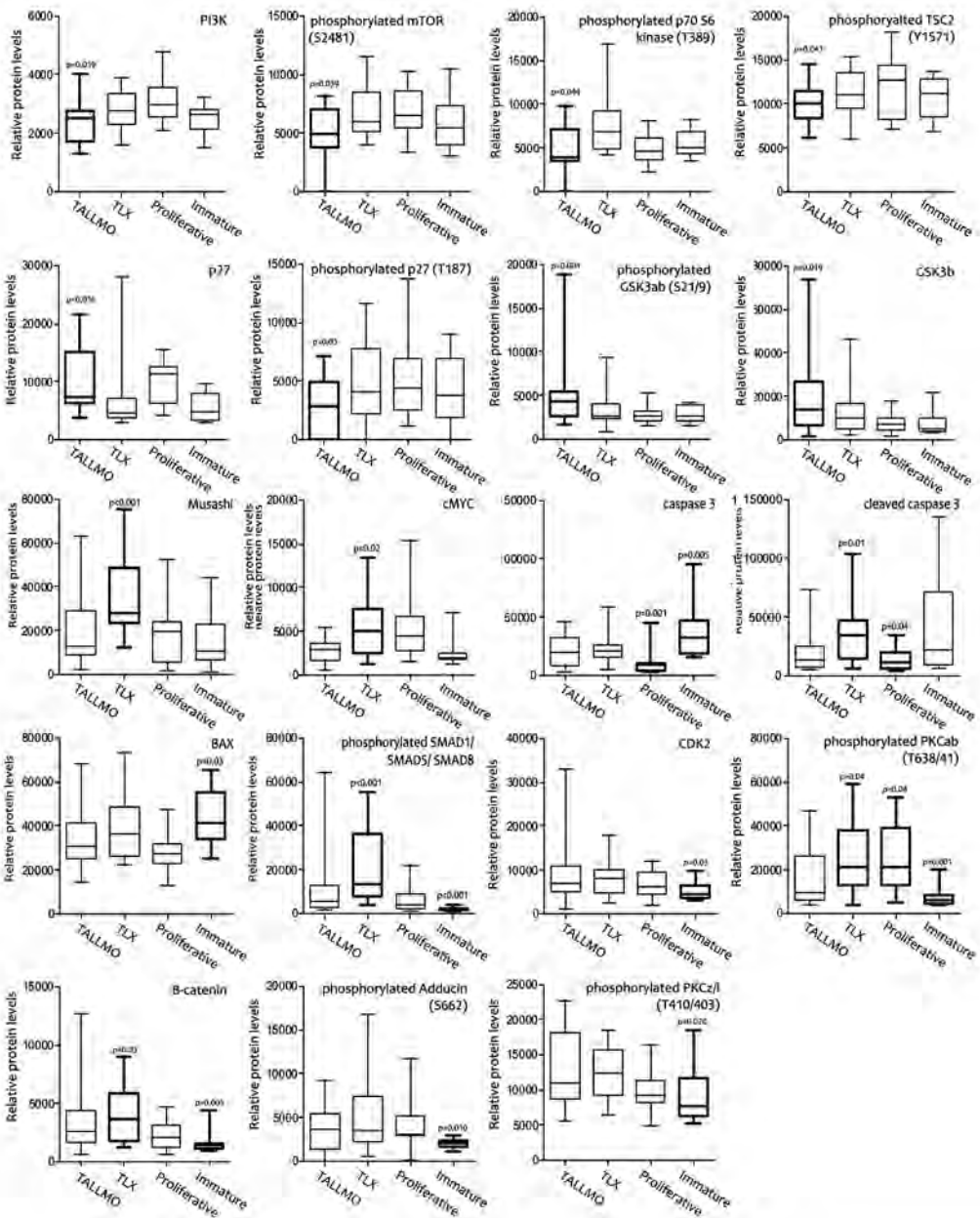


Figure 2 | Protein expression levels of proteins that are differentially expressed in TALLMO, TLX, proliferative or immature patient clusters. Differential expression of a selection of proteins in TALLMO cluster patients, TLX cluster patients, proliferative and TLX or immature cluster patients and immature cluster patients. P-value is calculated by Mann-whitney U, in which expression levels of specific molecules in one cluster are compared to these of all other subtypes together. Expression levels are depicted by boxplots showing the distribution of values with standard deviations. Median expression is shown by a bar. Bold boxplots represent the distribution of expression values that are significantly different compared to all others together.

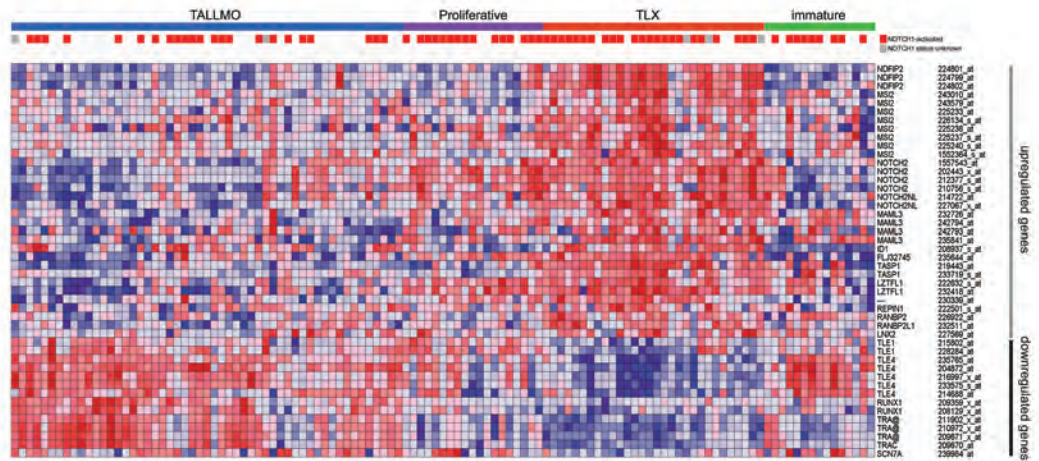


Figure 3 | High activation of the NOTCH1 pathway genes in patients of the TLX cluster. Heatmap for selected genes that belong to the NOTCH1 pathway that are differentially expressed (FDR $p < 0.05$) between *NOTCH1/FBXW7* wild-type versus NOTCH1-activated patients as previously identified¹⁹. Each row represents a gene and each column represent a patient. Unsupervised T-ALL clusters⁶ are depicted at the top of the heatmap. The *NOTCH1/FBXW7* mutational status is depicted for each patient, in which NOTCH1-activated patients are in red. The mutational status for patients indicated by a gray bar has not been determined.

Proliferative cluster

We described before that the proliferative cluster ($n=19$) is associated with a high expression of genes involved in the cell cycle and spindle assembly⁶. Indeed, our global test result shows cell cycle and DNA replication (**Table 1 and Figure S3A,B**, FDR $p=1.7 \times 10^{-6}$ and FDR $p=4.0 \times 10^{-6}$ respectively) as one of the top pathways differentially and highly expressed in this cluster compared to all other clusters. This was supported by an increased gene expression of those involved in the production of the one carbon pool by folate and folate biosynthesis, as well as of purine and pyrimidine metabolism (**Figure S3C-F**, FDR $p=1.9 \times 10^{-6}$, FDR $p=3.6 \times 10^{-6}$, FDR $p=2.1 \times 10^{-6}$ and FDR $p=2.5 \times 10^{-6}$ respectively). Differentially expressed pathways also include those that involve the same genes, like spindle assembly processes (**Figure S3G,H**, progesterone-mediated oocyte maturation, FDR $p=1.9 \times 10^{-6}$ and oocyte meiosis, FDR $p=1.9 \times 10^{-6}$). Furthermore, there seem to be active amino acid conversions along with decreased breakdown of amino acids through the urea cycle (arginine and proline metabolism, FDR $p=1.9 \times 10^{-6}$), possibly to save nitrogen groups for the synthesis of purines. A high expression of cell cycle genes seems to be accompanied by an increase in DNA repair genes which is reflected by the differential high expression of genes involved in homologous recombination, nucleotide excision repair, mismatch repair, base excision repair and the p53 pathway (**Figure S3K-N**, FDR $p=1.9 \times 10^{-6}$, FDR $p=4.1 \times 10^{-6}$, FDR $p=4.1 \times 10^{-6}$, FDR $p=4.1 \times 10^{-6}$ and FDR $p=4.2 \times 10^{-7}$ respectively). *CHEK2* and the *TP53* gene itself are highly expressed, but most of p53's target genes are expressed on a low level. In addition, *CDK4* and *CDK2* genes that are normally suppressed by p53 effectors are elevated in this cluster and support the high expression cell cycle genes. Our data points towards inactivation of the biological rhythm that coordinates cell cycle activity (**Figure 1C**, circadian rhythm, FDR $p=3.0 \times 10^{-6}$). Generation of ATP seems to

be reflected by high expression of genes that are involved the intra-mitochondrial export of freshly produced proteins but not of these produced in the endoplasmic reticulum (protein export **Figure S3O**, FDR $p=6.2*10^{-6}$). Mitochondrial genes mainly encode proteins involved in the aerobic mitochondrial energy metabolism. Also genes resulting in fatty acid degradation from ketone bodies that can serve as fuel supply are highly expressed in this cluster (**Figure S3P**, FDR $p=9.8*10^{-6}$). Regarding signal transduction pathways, there is a very low expression of MAPK pathway genes involved in classical or p38/Jnk branches (**Figure S3Q**, FDR $p=4.1*10^{-6}$), normally resulting in proliferation, differentiation or apoptosis of cells. Also the canonical Wnt signaling pathway responsible for cell cycle activity seems inactive. In contrast, the Wnt/ Ca^{2+} pathway that can regulate transcription through the NFAT transcription factor and thereby cellular activation seems active (**Figure S3R**, FDR $p=1.9*10^{-6}$). Surprisingly, genes of the AKT/mTOR pathway are low expressed in this cluster (Insulin signaling pathway, **Figure S3S**, FDR $p=1.9*10^{-6}$), which is one of the major routes of protein translation. Expression of genes involved in cell adhesions are low expressed (adherens junction **Figure S3T**, FDR $p=8.1*10^{-8}$), except for *ACTN1* which is essential for cytokinesis. Moreover membrane-bound adhesion molecules that can regulate immune responses are low expressed including *ICOS*, *HLA-A*, *CD34*, *F11R*, *CD6*, *PVRL2* and *ITGB7* (cell adhesion molecules **Figure S3U**, FDR $p=1.9*10^{-6}$). This did not include the T-cell marker and TCR co-receptor *CD8*, which can bind major histocompatibility complex I (MHC I) and is highly expressed. Furthermore, genes regulating osteoclast differentiation are expressed at low levels (**Figure S3V**, FDR $p=4.1*10^{-6}$).

On the protein level, 11 proteins were differentially expressed in these patients ($n=10$). A high expression of cell cycle players in these patients is also observed on protein level as patients demonstrate higher levels of various kinases including the cell cycle protein phospho-ABL ($p=0.002$), phospho-cKIT ($p=0.01$), phospho-LCK ($p=0.02$), PI3K (**Figure 2**, $p=0.02$), phospho-PYK2 ($p=0.03$) and phospho-PKCb (**Figure 2**, $p=0.04$) (**Table 1**). Also MYC levels are high in this cluster (**Figure 2**, $p=0.05$). The membrane receptor phospho-IGF-1R/Rb ($p=0.02$) is also highly expressed, and low levels of pro-apoptotic proteins caspase 3 ($p=0.001$) and cleaved caspase 3 are observed ($p=0.04$) (**Figure 2**). Caspase 3 can be activated by p53, among others, upon irreparable DNA damage. This is in line with our global test results that points towards a low p53 activity. Phosphorylated B-RAF, a member of the MAPK pathway, is low expressed in this cluster ($p=0.04$), which correlates with the low expression of MAPK genes that we observe in these patients.

Immature cluster

Immature cluster patients ($n=15$) express high levels of genes involved in the B-cell receptor (BCR) signaling pathway (**Table 1 and Figure S4A,B**, BCR signaling, FDR $p=8.9*10^{-9}$ and FcεRI signaling pathway, FDR $p=4.1*10^{-8}$). In contrast, genes encoding key proteins of the TCR signaling are not expressed in these patients (**Figure S4C**, FDR $p=2.5*10^{-7}$). This is in line with the immature early T-cell progenitor state of this T-ALL subtype¹². This is also reflected by the low expression of T-cell markers but expression of myeloid markers (**Figure S4D**, hematopoietic cell lineage,

FDR $p=5.5 \times 10^{-7}$). Whereas proliferative patients seem to have an elevated expression of cell cycle genes, immature patients do not (**Figure S4E-G**, cell cycle, FDR $p=1.3 \times 10^{-6}$, progesterone-mediated oocyte maturation, FDR $p=6.0 \times 10^{-7}$ and oocyte meiosis, FDR $p=4.0 \times 10^{-7}$). This inactive proliferative stage is further supported by a low expression of some genes of the RNA degradation machinery and various metabolisms including ketone bodies synthesis and degradation, N-glycan biosynthesis for protein folding, butanoate and purine metabolisms (**Figure S4G-L**, FDR $p=2.6 \times 10^{-8}$, FDR $p=6.6 \times 10^{-9}$, FDR $p=8.8 \times 10^{-9}$, FDR $p=9.2 \times 10^{-7}$ and FDR $p=9.3 \times 10^{-7}$ respectively). Interestingly, tight and adherens junctions seem not expressed (**Figure S4M,N**, FDR $p=3.6 \times 10^{-9}$ and FDR $p=6.6 \times 10^{-9}$ respectively). These are normally formed during cell migration. In contrast, the map of actin cytoskeleton regulation illustrates that focal adhesions seem to be formed in immature cluster patients (regulation of actin cytoskeleton, **Figure S4O**, FDR $p=1.9 \times 10^{-7}$). These normally link lymphocytes to the extracellular matrix to transmit signals. In addition to this notion, we observe a low expression of enzymes involved in dephosphorylation and thereby inactivation of sphingolipids (**Figure S4P**, FDR $p=3.3 \times 10^{-7}$). Like focal adhesions, these are important for outside-inwards signaling and consequential regulation of intracellular cascades. Differential expression of genes involved in TGF-beta (TGFB) signaling (**Figure S4Q**, FDR $p=2.1 \times 10^{-8}$) point to inactivity of canonical cascades despite the fact that TGFB and TGFB receptors are actively transcribed. The MAPK signaling pathway is an alternative potential TGFB downstream pathway involving MAPK12 (p38, **Figure 1D**, FDR $p=1.9 \times 10^{-7}$) and seems active, which may explain MEF2C activation in this cluster. Furthermore genes involved in the JNK-axis including MAPK9 (JNK2) and downstream Jun transcription factor seem to have a low transcriptional expression. Jun is an anti-apoptotic and cell cycle promoting protein.

At the protein level, 17 proteins were differential expressed in immature cluster patients ($n=12$); inactivity of the canonical TGFB/BMP signaling observed at the transcriptional level is confirmed by low expression of phosphorylated SMAD1/5/8 proteins ($p<0.001$, **Figure 2**). Similar, the low adhesion gene expression signature is supported by low phosphorylated adducin levels (**Figure 2**, ADD1-3; $p=0.01$) and β -catenin (**Figure 2**, CTNNB1; $p=0.005$). Interestingly, the presence of pro-apoptotic molecules caspase 3 and BAX (**Figure 2**, $p=0.005$ and $p=0.04$ respectively) and the low levels of the cell cycle proteins CDK2 and MYC (**Figure 2**, $p=0.03$ and $p=0.04$ respectively) confirm the low proliferative activity of T-ALL cells in this immature cluster. This is also supported by a low expression on the cell cycle inhibitor p27 (**Figure 2**, CDKN1B; $p=0.02$). Phospho-SAPK/JNK ($p=0.008$) proteins are observed at low levels, which coincide with the global test result showing low activity of JNK2 and subsequent Jun and suggesting a low anti-apoptotic and low cell cycle activities. Furthermore, many other proteins are low expressed which may support the low proliferative activity, including phospho-PKC ζ/λ (**Figure 2**, PRKCZ/I $p=0.024$) and phospho-PKC $\alpha\beta$ (**Figure 2**, PRKCA/PRKCB), calcium-dependent phospholipid binding protein annexin A1 (ANXA1; $p=0.03$) and various AKT pathway molecules including phospho-SHIP1 (INPPD5; $p=0.02$), phospho-PDK1 ($p=0.04$), phospho-4E-BP1 (EIF4EBP1; $p=0.04$) and transcription factors phospho-FOXO3 ($p=0.04$) and phospho-CREB (**Figure 2**, $p=0.01$) of which the latter can also signal downstream of the p38 MAPK.

NOTCH1-activating mutations

As expected, global test analysis of NOTCH1-activated patients ($n=68$) compared to *NOTCH1/FBXW7* wild-type patients demonstrated that the NOTCH1 pathway is markedly induced in patients with NOTCH1-activating mutations (FDR $p=7.2*10^{-4}$, **Table 2 and Figure S5A**). High differential expression of genes that are involved in the calcium signaling pathway (**Figure 1E**, FDR $p=2.3*10^{-2}$) suggests active release of calcium through ERBB4, PLCB4 and ITPR2 and subsequent PKC alpha activation. This activation pattern was also visible in the phosphatidylinositol signaling system KEGG map (**Figure S5B**, FDR $p=1.3*10^{-2}$), however this map also depicts a low expression of genes of the connected PIP/IP3 lipid signaling cascades. Interestingly, NOTCH1-activated patients have a very low expression of cell membrane proteins that are involved in immunity, including HLA proteins (cell adhesion molecules map **Figure S5C**, FDR $p=1.6*10^{-2}$). Also molecules involved in phagosome and endocytosis processes seem to be low expressed (**Figure S5D-F**, FDR $p=2.0*10^{-2}$ and FDR $p=3.1*10^{-2}$ respectively and natural killer cell-mediated cytotoxicity map FDR $p=1.6*10^{-2}$). These processes are normally involved in antigen presentation on the cell surface. Furthermore, myeloid/platelet-cell membrane markers are expressed at low levels (hematopoietic cell lineage **Figure S5G**, FDR $p=1.3*10^{-2}$) whereas T-cell maturity markers CD4 and CD8 are abundantly expressed. Also, genes involved in cell migration are expressed at low levels (leukocyte transendothelial migration **Figure S5H**, FDR $p=2.3*10^{-2}$).

In addition to protein expression data we described before¹⁹, we observe high levels of activated PKC α/β (**Figure 4A**, PRKCA/B; $p=0.001$) and the calcium-dependent phospholipid-binding protein annexin A1 (ANXA1; $p=0.04$; **Figure 4A**) in NOTCH1-activated patients ($n=38$) compared to *NOTCH1/FBXW7* wild-types patients (**Table 2**). This supports our global test results that indicate a high expression of calcium signaling genes. In contrast, low activity of the calcium-independent PKC θ isoform was measured (**Figure 4A**, PRKCQ; $p=0.04$). We also observe a low expression of the cell cycle inhibitor p27 (**Figure 4A**, CDKN1B; $p=0.03$), and residual p27 seems to be predominantly present in its inactive, phosphorylated state in these patients (**Figure 4A**, $p=0.03$).

PTEN/AKT mutations

Regarding *PTEN/AKT*-mutated patients ($n=20$), global testing supports low NOTCH1 pathway activation in these patients as we observed before at protein level (FDR $p=4.8*10^{-2}$, **Table 2 and Figure S6A**). This finding nicely matches our previously observations in which we noticed that NOTCH1-activating mutations and *PTEN/AKT* mutations hardly co-express²³. Data support a high expression of genes of the TCR signaling but a low expression of these of the B-cell receptor signaling in *PTEN/AKT*-mutated patients (**Figure S6B,C**, FDR $p=7.2*10^{-2}$ and FDR $p=4.8*10^{-2}$ respectively). Many genes encoding differentiation markers of all blood lineages and many cytokine and cytokine-receptors are differentially expressed (**Figure S6D,E**, hematopoietic cell lineage map FDR $p=7.2*10^{-2}$ and cytokine-cytokine receptor interaction FDR $p=5.7*10^{-2}$ respectively). These include high expression of pro-inflammatory *IL2*, *IL4*, *IL9* and *IL17* receptors and *CXCR4* but low expression of B-cell-specific cytokines *IL6* and *CXCR5*. Data indicates an active

Global test results		KEGG map		pathway	Class	P	Adjusted P	Comparative P	RPMA results		P	expression
NOTCH1-activating mutations (n=68)		NOTCH1-activating mutations (n=38)							Protein	specific residue		
Organismal system												
04730	Long-term depression				Nervous system	2.75E-05	2.46E-03	0	pPKC α	T638/41	0.001	high
04610	Complement and coagulation cascades				Immune system	3.15E-04	1.29E-02	0.003	ICN	V1744	0.004	high
04971	Gastric acid secretion				Digestive system	4.05E-04	1.29E-02	0.002	pp27	T187	0.029	high
04614	Renin-angiotensin system				Endocrine system	4.79E-04	1.29E-02	0.007	AmexinA1		0.044	high
04720	Long-term potentiation				Nervous system	4.80E-04	1.29E-02	0	p27		0.025	low
04640	Hematopoietic cell lineage				Immune system	6.32E-04	1.29E-02	0	pPKC β	T538	0.042	low
04970	Salivary secretion				Digestive system	8.43E-04	1.48E-02	0.006				
04270	Vascular smooth muscle contraction				Circulatory system	9.02E-04	1.48E-02	0				
04662	B cell receptor signaling pathway				Immune system	1.39E-03	1.58E-02	0.016				
04650	Natural killer cell mediated cytotoxicity				Immune system	1.45E-03	1.58E-02	0.006				
04320	Dorso-ventral axis formation				Development	1.58E-03	1.64E-02	0.032				
04977	Vitamin digestion and absorption				Digestive system	1.71E-03	1.70E-02	0.027				
04972	Pancreatic secretion				Digestive system	1.82E-03	1.70E-02	0.020				
04912	GnRH signaling pathway				Endocrine system	2.29E-03	1.82E-02	0.011				
04916	Melanogenesis				Endocrine system	2.68E-03	1.89E-02	0.019				
04974	Protein digestion and absorption				Digestive system	2.95E-03	1.89E-02	0.045				
04670	Leukocyte transendothelial migration				Immune system	3.64E-03	2.25E-02	0.041				
Environmental Information Processing												
04330	Notch signaling pathway				Sign. Transduction	3.16E-06	7.23E-04	0				
04070	Phosphatidylinositol signaling system				Sign. Transduction	6.75E-04	1.29E-02	0.002				
04514	Cell adhesion molecules (CAMs)				Sign. molecules + interaction	1.28E-03	1.58E-02	0.002				
04370	VEGF signaling pathway				Sign. Transduction	3.29E-03	2.15E-02	0.034				
04020	Calcium signaling pathway				Sign. Transduction	4.08E-03	2.34E-02	0.028				
Cellular Processes												
04540	Gap junction				Cell communication	1.81E-04	1.04E-02	0.001				
04145	Phagosome				Transport and catabolism	2.92E-03	1.99E-02	0.011				
04144	Endocytosis				Transport and catabolism	6.43E-03	3.07E-02	0.027				
Metabolism												
00512	Mucin type O-Glycan biosynthesis				Glycan biosynth. + metab.	6.17E-04	1.29E-02	0.017				
00053	Ascorbate and aldarate metabolism				Carbohydrate metabolism	1.32E-03	1.58E-02	0.020				
00532	Glycosaminoglycan biosynthesis - chondroitin sulfate / dermatan sulfate				Glycan biosynth. + metab.	2.73E-03	1.99E-02	0.039				
00780	Biotin metabolism				Metab. cofactors + vitamins	1.41E-02	5.47E-02	0.048				
PTEN/AKT mutations (n=20)												
Organismal system												
04914	Progesterone-mediated oocyte maturation				Endocrine system	1.17E-03	4.76E-02	0	pPKC β	T538	0.011	high
04662	B cell receptor signaling pathway				Immune system	1.84E-03	4.76E-02	0.004	PTEN	S380	-0.001	low
04650	Natural killer cell mediated cytotoxicity				Immune system	2.23E-03	4.76E-02	0.001	pPTEN		-0.001	low
04614	Renin-angiotensin system				Endocrine system	2.36E-03	4.76E-02	0.014	Musashi		0.002	low
04974	Protein digestion and absorption				Digestive system	4.49E-03	5.61E-02	0.027	ICN	V1744	0.003	low
04270	Vascular smooth muscle contraction				Circulatory system	4.73E-03	5.61E-02	0.016	pSMAD1/58	S/S, S/S, S/S	0.004	low
04730	Long-term depression				Nervous system	4.90E-03	5.61E-02	0.015	pPKC α	T638/41	0.006	low
04664	Fc epsilon RI signaling pathway				Immune system	5.92E-03	5.65E-02	0.038	MVC		0.013	low
04640	Hematopoietic cell lineage				Immune system	8.86E-03	7.23E-02	0.040	Amexin A1		0.026	low
04660	T cell receptor signaling pathway				Immune system	1.01E-02	7.23E-02	0.043	pp27	T187	0.038	low
Environmental Information Processing												
04330	Notch signaling pathway				Sign. Transduction	8.26E-04	4.76E-02	0.001				
04630	Jak-STAT signaling pathway				Sign. Transduction	1.38E-03	4.76E-02	0.002				
04350	TGF-beta signaling pathway				Sign. Transduction	2.55E-03	4.76E-02	0.009				
04060	Cytokine-cytokine receptor interaction				Sign. molecules + interaction	5.86E-03	5.65E-02	0.019				

cell proliferation signature (**Figure 1F and S6F-J**, cell cycle FDR $p=5.3 \times 10^{-2}$, p53 signaling pathway FDR $p=4.8 \times 10^{-2}$, oocyte meiosis FDR $p=4.8 \times 10^{-2}$, progesterone-mediated oocyte maturation, FDR $p=4.8 \times 10^{-2}$, pyrimidine metabolism FDR $p=8.4 \times 10^{-2}$ and base excision repair FDR $p=7.2 \times 10^{-2}$). Genes of the fructose and mannose metabolism point towards glycogen breakdown for energy supply (**Figure S6I**, FDR $p=4.8 \times 10^{-2}$). Genes of the bone morphogenic pathway (BMP) including receptor-regulated *SMAD1*, *SMAD5* or *SMAD8* and consequent *ID1* transcription are not expressed whereas these of the *ACVR2B* and *TGFBR* downstream routes including receptor-regulated *SMAD2* or *SMAD3* are expressed (**Figure S6L**, FDR $p=4.8 \times 10^{-2}$).

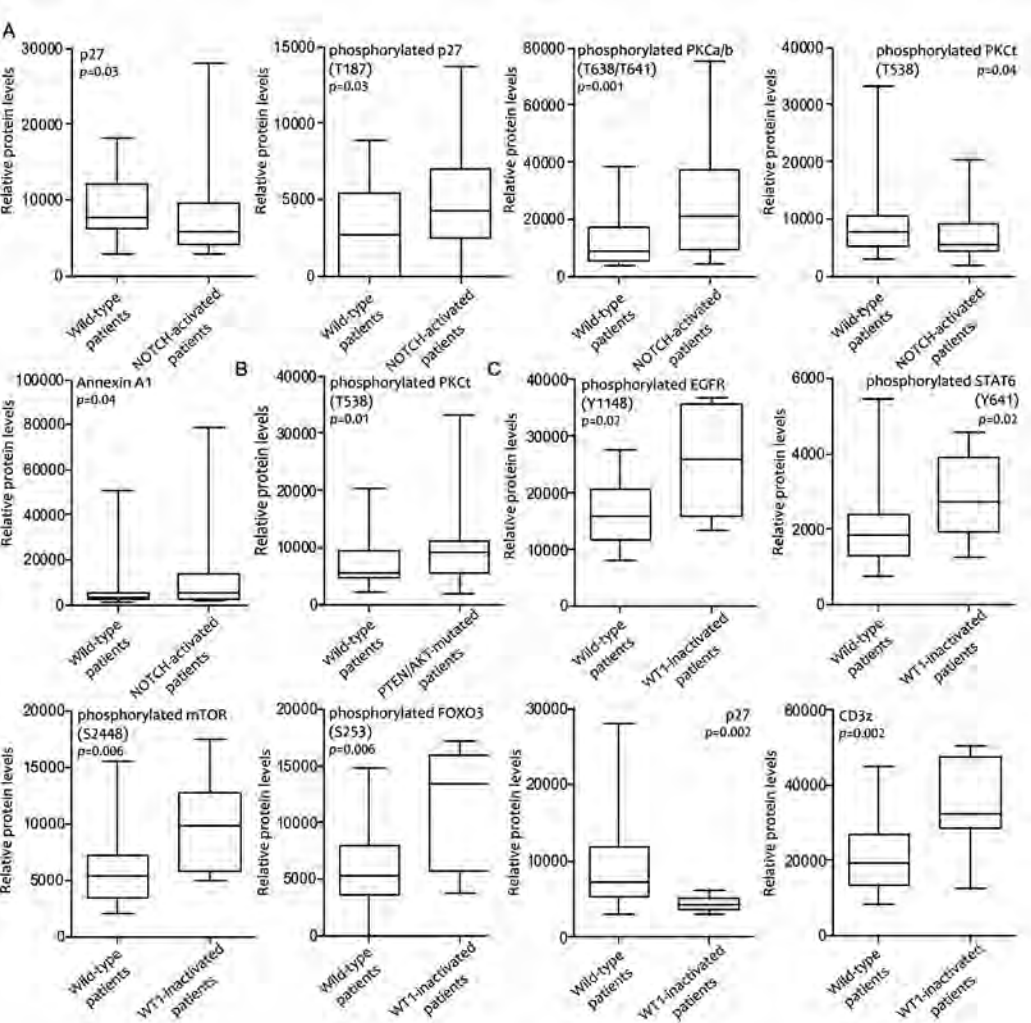


Figure 4 | Significant differentially expressed proteins in type B T-ALL subgroups. P-value is calculated by Mann-Whitney U. Expression levels are depicted by box plots showing the distribution of values with standard deviations. Median expression is shown by a bar. (A) NOTCH1-activated (*NOTCH1* and/or *FBXW7*-mutated), (B) *PTEN/AKT*-mutated, (C) *WT1*-inactivated patients.

Members and transcriptional targets of the JAK/STAT pathway *PIM1*, *CISH*, *MYC*, *CCND1* and *SPRED1* are not actively transcribed in *PTEN/AKT*-mutated patients (**Figure S6M**, FDR $p=4.8*10^{-2}$). Expression levels of TGF β and JAK/STAT pathway molecules may explain low MYC levels in these patients²³.

Regarding expression levels of proteins in *PTEN/AKT*-mutated patients ($n=17$), 10 were differentially expressed of which 5 were described by us before²³. Due to the near mutual exclusiveness of NOTCH1-activating and *PTEN/AKT* mutations in our cohort²³ and only 19 out of the 66 patients were genetically wild-type for both abnormalities, various proteins were expressed in *PTEN/AKT*-mutated and NOTCH1-activating patients in this manner. This includes calcium-dependent annexin A1 (*ANXA1*; $p=0.03$) and PKC α/β (*PRKCA*; $p=0.006$) that are expressed at low levels in *PTEN/AKT*-mutated patients. In contrast, they have high levels of phospho-PKC θ (*PRKCG*; $p=0.01$) (**Figure 4B and Table 2**). In line of an active cell cycle gene signature, we measured low p27 levels and its phosphorylated inactive form (*CDKN1B*; $p=0.04$), which coincides with low *p27* gene expression levels (data not shown). Also, BMP-regulated SMAD1/5/8 proteins are expressed at low levels, as observed on transcript level.

WT1-inactivating mutations

Differential expression of genes in *WT1*-inactivated patients ($n=14$) compared to all other T-ALL patients (**Table 2**) points to calcium release through phospholipase C and ITPR1, which correlates with a high expression of downstream *PRKCA* (protein kinase C alpha) (**Figure S7A**, FDR $p=2.0*10^{-2}$). In line with this, there is a high expression of genes involved in IP4 to IP3 to IP2 and IP conversions which are important in calcium signaling, but not of those converting from IP to IP4. Also genes regulating PIP conversions seem to be expressed at low levels (inositol metabolism **Figure S7B,C**, FDR $p=1.7*10^{-2}$ and phosphatidylinositol signaling system, FDR $p=1.5*10^{-2}$). Surprisingly, genes involved in the formation of stress fibers (leukocyte transendothelial migration **Figure S7D,E**, FDR $p=2.0*10^{-2}$ and vascular smooth muscle contraction, FDR $p=1.8*10^{-2}$) are abundantly found leukemic cells of *WT1*-mutated patients, although these processes normally occur in endothelial cells. Expression of genes involved in the histidine metabolism support degradation of L-histidine and histamine in these patients (**Figure 1G**, FDR $p=2.0*10^{-2}$). Histidine can be converted to aspartate, which is a precursor of lysine. During this reaction glutamate is released. Genes of the sulfur relay system are highly expressed (**Figure S7F**, FDR $p=2.0*10^{-2}$) and may indicate high levels of thiolation of tRNA's which is important for efficient translation of genes enriched for lysine, glutamine and glutamate codons.

Out of the 91 measured proteins, 32 were differentially expressed in *WT1*-mutated T-ALL patients compared to all other patients ($n=8$, **Table 2**). These patients have high levels of membrane receptors phospho-ckIT ($p=0.005$) and phospho-EGFR (**Figure 4C**, $p=0.02$) as well as further downstream effectors including phospho-JAK1 ($p=0.03$), phospho-STAT3 ($p=0.05$), phospho-STAT5 ($p=0.005$) and phospho-STAT6 (**Figure 4C**, $p=0.02$). Also the AKT/MTOR pathway seems activated which is indicated by high levels of inactive phospho-TSC2 ($p=0.04$), phospho-mTOR on residues S2448 (**Figure 4C**, $p=0.006$) and S2481 ($p=0.02$) and high expression of the

protein translation downstream target phospho-4EBP1 ($p=0.03$), as well as phospho-FOXO3 (**Figure 4C**, $p=0.006$) and phospho-FOXO1/O3 ($p=0.009$) suppression of their downstream target p27 (**Figure 4C**, $p=0.002$). We also observe abundant expression of various T-cell receptor (TCR) signaling components including CD3 ζ (**Figure 4C**, $p=0.002$) and its interacting partner phospho-ZAP70/phospho SYK ($p=0.01$), phospho-SYK ($p=0.005$), phospho-PKC α/β ($p=0.007$), phospho-PYK2 ($p=0.01$), phospho-SHC ($p=0.02$), phospho-PKC δ (PRKCD; $p=0.04$) and phospho-FYN ($p=0.05$), as well as high expression of PI3K ($p=0.02$) and RAS ($p=0.05$) (**Table 2**).

DISCUSSION

By combining gene expression and protein data, we analyzed differentially expressed pathways in T-ALL pediatric patient subgroups at the transcriptome and proteome level. The main results are shown in **table 3**. In TALLMO cluster patients, we measured high transcript levels of genes and proteins involved in metabolic processes. First, this includes these involved in the prevention of glucose to glycogen conversion (GSK3) and these involved in active glycolysis in which ATP molecules are produced. A second glycolysis-connected metabolism seems to be relatively active in these patients; *de novo* fatty acid synthesis (lipogenesis). During aerobic glycolysis acetyl-CoA can be provided for the *de novo* lipogenesis when glucose levels are excessive. It is known that many cancer cells are highly dependent on *de novo* lipogenesis for their proliferation and survival and many enzymes regulating these mechanisms are upregulated in many cancers^{32,33}. Increased lipogenesis in TALLMO patients is indicated by a high expression of genes encoding enzymes that can convert phosphorylated phosphatidylinositols (PtdIns/PIP) and inositol (IP) lipids. Signaling through PtdIns and IP are important for membrane-trafficking and cell and lipid signaling (second messengers, eg. diacylglycerol and calcium) leading to cellular growth, migration, survival and differentiation. Although one downstream signaling cascade is the AKT/mTOR pathway, we did not observe AKT/mTOR pathway activation in TALLMO patients. Lipogenic and glycolytic enzymes are promising targets for therapy as they can be remarkably active in cancer cells in contrast to normal cells. Inhibitory substances are currently under extensive research as anti-cancer agents in general³⁴. This is similar for GSK3 inhibitors which, based on this data, might be very effective in TALLMO cells. Remarkably, in our cohort this cluster contains the most loss of function mutations in *PTEN*²³. *PTEN* is a phosphatase also involved in these metabolic systems and can confer PtdIns(3,4,5)P³ (PIP₃) into PtdIns(4,5)P² (PIP₂) as well as PtdIns(3,4)P² into PtdIns(4)P (PIP) and PtdIns(3)P into PI. Regarding *PTEN* mutations in T-ALL, literature predominantly focusses on PIP₃ and subsequent downstream AKT/mTOR activation²⁴ which we did also not observe for these patients in our cohorts²³. However, based on these data one might suggest that one of the mechanisms that contribute to the oncogenic effects of *PTEN* mutations is through other than PIP₃ PtdIns and IP lipids, which seem to be particularly important in TALLMO patients. Alternatively, high expression of enzymes involved in the IP metabolism can be a bystander result of active T-cell receptor (TCR) signaling in TALLMO cluster patients, eg. via the high expression of TCR-downstream Ca²⁺-independent PKC θ proteins which can activate

the PLC γ /Ca²⁺/IP route. Active TCR signaling may reflect the maturation status of the TALLMO subtype as immunophenotypically being the most mature T-ALL entity³⁵. These data suggest that neither TALLMO nor *PTEN/AKT*-mutated patients will benefit from PI3K/mTOR inhibitors.

Based on these data, it seems that NOTCH1 signaling is important in TLX patients. Whereas the frequency of NOTCH1-activating mutations is enriched in TLX patients, a NOTCH1 signature was observed in all TLX patients independent of NOTCH genetic status. This suggests addition to NOTCH signaling in TLX cluster patients. The TLX cluster comprised predominantly *TLX3*- and *HOXA*-rearranged patients. Direct relations between HOX family members and NOTCH1 signaling are described and may be partially responsible for the increased NOTCH activity in this cluster. First, this concerns a relation between HOXA and MSI (Musashi; an indirect NOTCH activator) expression. A putative HOXA9 transcription factor binding site is known for the *MSI2* gene and the fusion protein NUP98-HOXA9 is able to induce *MSI2* expression³⁶. On the other hand, MSI is able to induce HOXA9 and HOXA10 expression³⁷. These data suggest a possible interplay between HOXA transcription factors and MSI. Second, the NOTCH1 downstream gene *taspace 1*¹⁹ is essential for MLL-cleavage that can regulate HOX gene expression³⁸. Based on this data, this second largest pediatric T-ALL cluster might be very well treatable with gamma-secretase inhibitors (GSI), independently of NOTCH1 genetic status. GSIs are currently being intensively investigated as therapeutic approach in T-ALL^{39,40}, and high *MSI2* expression has already been identified by Palomero et al., to be related to GSI sensitivity in cell lines²⁴.

The proliferative cluster comprises patients that are predominantly characterized by *NKX2-1*, *NKX2-2* or *TLX1* translocations and has been associated with expression of genes involved in cell cycle regulation⁶. We now confirmed this by the global test analysis that showed a high expression of genes regulating the cell cycle, DNA repair and replication and ATP-generating metabolisms. In addition, this was indicated by a high expression of active (cell cycle) kinases and MYC as shown on protein level. Although high p53 transcript levels were observed, downstream pathway molecules were expressed at low levels and suggest a low p53 activity. p53 becomes activated upon cellular stress. Its activity can change rapidly and largely depends on alterations in the p53 protein and to a minor extend, relieve of translational repression. For example, upon stress signals p53 stability, change of p53 cellular localization, blockage of the p53 transactivation domain or enhancement of p53 DNA-binding capacity can occur⁴¹. A possible low functional activity of p53 can be due to interference with these mechanisms. For example, inactivating *p53* or *ATM* kinase mutations (both found in ~5% of pediatric T-ALL patients) as well as *PTEN/AKT* mutations (~5-63% of pediatric T-ALL patients) can reduce p53 activity through different mechanisms and might have an important function in proliferative cluster patients^{23,42,43}. Interestingly, we observed that T-cells of the proliferative cluster expressed genes involved in the circadian rhythm at very low levels. This is an important regulator of the cell cycle, DNA damage responses, senescence and metabolism and dysregulation is linked with cancer. Restoring it would be a potential for therapy, though the exact regulatory mechanisms are still unclear⁴⁴.

The early T-cell maturity state of immature patients that resemble early T-cell precursor (ETP)

ALL patients, was confirmed by a significantly low expression of key T-cell receptor pathway genes along with a high expression of B-cell receptor (BCR) pathway genes as well as the expression of myeloid surface markers. This is in line with our previous report in which we recently showed that our ETP-ALL cohort is enriched for genes expressed in hematopoietic stem cells, early erythroid precursor cells, T-cell and B-cell sorted fractions (established by Novershtern and co-workers) and also enrichment of B-cell-related genes, using gene set enrichment analysis¹². We now also show that this immature state seems to be reflected by an inactive proliferative and migratory behavior as samples expressed cell cycle genes and various proteins at very low levels -as reported before⁶-, as well as these of genes involved in spindle assembly and RNA degradation and junction formation. Pro-apoptotic proteins BAX and caspase 3 were highly expressed compared to all other clusters indicating that apoptotic thresholds may be relatively high in these patients and may be exploited in treatment strategy for this high-risk cluster. Interestingly, the canonical TGF-beta signaling pathways seem inactive in these patients, despite a high expression of TGF-beta ligands and TGF-beta receptor. We suggest alternative TGF-beta signaling is very important in immature patients through downstream MAPKs (p38 MAPKs) that may result in ectopic MEF2C levels. MEF2C is a well known transcription factor downstream of p38 MAPkinases which can also be activated through the BCR signaling, also active in immature patients⁴⁵.

NOTCH1-activated patients were characterized by differential expression of hematopoietic cell lineage markers, indicated by a high expression of both CD4/CD8 T-cell maturity markers. This probably reflects the intermediate/cortical T-cell differentiation stage which was immunophenotypically shown by us before¹⁹. Remarkably, NOTCH1-activated patients had a very low expression of genes encoding major histocompatibility complexes (MHC) and other genes involved in phagosome and endocytosis processes, indicating a possible mechanism of the cancerous cells to evade the immune system. Furthermore, NOTCH1-activated patient samples seem to carry low levels of p27 proteins, which is in line with previous studies that reported cell cycle inhibitor p27 as being a target of the HES-1 repressor^{46,47}, one of the most important NOTCH1 downstream target genes. Second, HES1 can transcriptionally alter *PTEN* levels. PTEN regulates AKT activity that can in turn, repress p27 activity either by direct phosphorylation or transcription via Forkhead transcription factors⁴⁸. Third, residual p27 levels are almost entirely phosphorylated and therefore inactive in NOTCH1-activated patients. NOTCH1 also upregulates SKP2 directly⁴⁶, that is responsible for the recognition of phosphorylated p27 at Thr187, and thereby targets p27 for ubiquitination-dependent protein degradation. It is also shown that *p27* gene expression is increased after GSI treatment that inhibits NOTCH signaling²⁰. Furthermore, we suggest a role for calcium and calcium-dependent processes in NOTCH1-activated patients, involving PKC α and annexin A1. Interestingly, NOTCH1-activated patients had low levels of PKC θ , a protein which is very recently described as being indirectly downregulated by NOTCH1; PKC θ expression is correlated with high levels of reactive oxygen species (ROS) and thereby decreases activity of leukemia-initiating cells (LIC's)⁴⁹. PKC θ is induced by RUNX1 that is repressed by RUNX3, which is a direct NOTCH1 target. It is suggested that patients with low PKC θ activity will

have a poor outcome⁴⁹. In previous studies we showed a poor outcome for NOTCH1-activated patients¹⁹ so it should be investigated whether direct targeting of PKC θ may be a therapeutic option for T-ALL.

High levels of PKC θ are detected in *PTEN/AKT*-mutated patients. In addition to low ICN (activated-NOTCH) levels in *PTEN/AKT*-mutated patients, high PKC θ levels can be as a consequence of an increased expression of TCR signaling genes. In addition to decreased LIC activity as a result of high PKC θ levels, Silva et al. described that high ROS levels abolish PTEN function as alternative mechanism for genetic inactivation²². Interestingly, *PTEN/AKT*-mutated patients also have a very high expression of genes involved in cell cycle and spindle formation, which is accompanied by a high expression of genes involved in active glycogenolysis to supply ATP (glycogen degradation). Like TALLMO cluster patients that are enriched for *PTEN/AKT* mutations in our cohorts, it might be worthwhile to verify whether these patients are sensitive for inhibitors of glycolysis.

Concerning pathway activation in *WT1*-mutated patients we observed expression of genes involved in calcium release and subsequent activated pathways. Also glutamate production seemed to be increased in *WT1*-mutated patients as well as thiolation of tRNA's which is important for efficient translation of genes enriched for glutamate, among others. Interestingly, *WT1* is one of such glutamate-rich genes implying the translation of truncated *WT1* proteins may be very active and might act in a dominant negative fashion. Protein data showed that *WT1*-mutated patients have a very active protein signature compared to all other T-ALL samples. *WT1* is suggested to participate in the RNA splicing process of genes and is a transcription factor acting as a haploinsufficient tumor suppressor gene in T-ALL, though the transcriptional targets of *WT1* are largely unknown. Literature suggest its role in growth factor receptor inhibition by transcriptional repression⁵⁰⁻⁵³. Nonsense and missense mutations or deletions in the *WT1* gene effect the DNA-binding domain of *WT1*, and are expected to thereby disable its DNA binding activity and thereby disability transcriptional repression^{28,54-59}. It should be investigated whether this may explain high expression of activated receptors cKIT and EGFR and subsequent active AKT and JAK/STAT signaling pathways. In addition, downstream TCR proteins were highly expressed in their active form. This supports the suggestion for a role of *WT1* in growth factor inhibition, which function is diminished upon *WT1* loss. Kinase inhibitors are under extensive development and might be very well useful in proliferative patients, *WT1*-mutated patients or patients with high TCR signaling, e.g. sunitinib which targets c-kit among other kinases, bosutinib which can inhibit src kinases or dasatinib which targets the TCR and downstream src kinases.

Taken together, these data confirm and suggest specific pathway activation in T-ALL in various genetic subgroups, possibly as a direct or indirect result of genetic changes. Therefore, these data provides targets of therapeutic approach in specific T-ALL subgroups which should be further investigated.

T-ALL subtype	pathway	therapeutic option
TALLMO	glycolysis lipogenesis TCR signaling	glycolytic enzyme inhibitors & GSK3 inhibitors lipogenic enzyme inhibitors kinase inhibitors
TLX	NOTCH signaling	NOTCH inhibitors, e.g. GSI's
Proliferative	cell cycle regulation circadian rhythm	chemotherapy, CDK inhibitors restoration through e.g. demethylating agents
Immature	TCR signaling BCR signaling myeloid surface markers cell cycle regulation cell adhesion TGFb signaling	kinase inhibitors chemotherapy, CDK inhibitors MAPK inhibitor
NOTCH1-activated	NOTCH signaling immune recognition p27 calcium signaling	NOTCH inhibitors, e.g. GSI's calcium blockers
PTEN/AKT-mutated	PKCt cell cycle regulation glycogenolysis	PKCt inhibitors (none FDA-approved yet) chemotherapy, CDK inhibitors glycolytic enzyme inhibitors
WT1-inactivated	calcium signaling glutamate production growth factor receptor pathways	calcium blockers kinase inhibitors

Table 3 | Main results of this study. Deregulated pathways and therapeutic possibilities that should be further investigated in TALLMO, TLX, Proliferative and immature cluster patients, NOTCH1-activated, *PTEN/AKT*-mutated and WT1-inactivated patients.

AUTHORSHIPS AND DISCLOSURES

L.Z. designed experiments, performed research and wrote manuscript, E.P. supervised study, and wrote manuscript, V.C. performed RPMA analysis, J.B.-G. prepared samples, W.K.S prepared samples, E.S provided patient samples and clinical and immunophenotypic data, R.P. designed and supervised study and wrote manuscript, J.P.P.M. was principal investigator, designed and supervised the study, and wrote manuscript. None of the authors had competing financial interest.

ACKNOWLEDGEMENTS

This work was supported by The Children Cancer Free Foundation (Stichting Kinderen Kankervrij (KiKa) grant 2007-012) (L.Z.) and grant 2008-029 (W.K.S.)) and the Dutch Cancer Society (grant AMC2008-4265 (JB-G)) and the Erasmus University Trustfonds foundation.

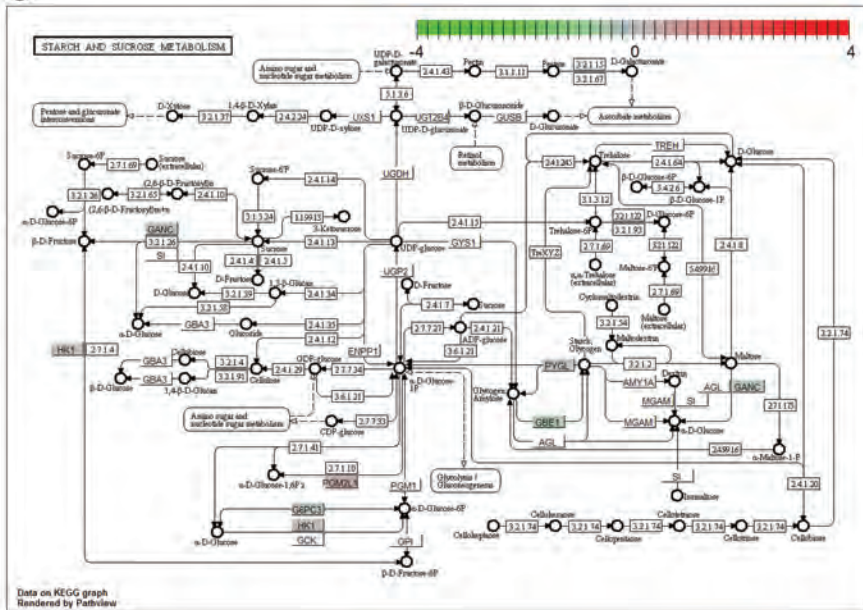
REFERENCES

1. Pui CH, Evans WE. Treatment of acute lymphoblastic leukemia. *N Engl J Med.* 2006;354:166-178.
2. Veerman AJ, Kamps WA, van den Berg H, et al. Dexamethasone-based therapy for childhood acute lymphoblastic leukaemia: results of the prospective Dutch Childhood Oncology Group (DCOG) protocol ALL-9 (1997-2004). *Lancet Oncol.* 2009;10:957-966.
3. Meijerink JP. Genetic rearrangements in relation to immunophenotype and outcome in T-cell acute lymphoblastic leukaemia. *Best Pract Res Clin Haematol*;23:307-318.
4. Van Vlierberghe P, Ferrando A. The molecular basis of T-cell acute lymphoblastic leukemia. *J Clin Invest*;122:3398-3406.
5. Ferrando AA, Neuberg DS, Staunton J, et al. Gene expression signatures define novel oncogenic pathways in T-cell acute lymphoblastic leukemia. *Cancer Cell.* 2002;1:75-87.
6. Homminga I, Pieters R, Langerak AW, et al. Integrated transcript and genome analyses reveal NKX2-1 and MEF2C as potential oncogenes in T-cell acute lymphoblastic leukemia. *Cancer Cell*;19:484-497.
7. Soulier J, Clappier E, Cayuela JM, et al. HOXA genes are included in genetic and biologic networks defining human acute T-cell leukemia (T-ALL). *Blood.* 2005;106:274-286.
8. Van Vlierberghe P, van Grotel M, Tchinda J, et al. The recurrent SET-NUP214 fusion as a new HOXA activation mechanism in pediatric T-cell acute lymphoblastic leukemia. *Blood.* 2008;111:4668-4680.
9. Van Vlierberghe P, Pieters R, Beverloo HB, Meijerink JP. Molecular-genetic insights in paediatric T-cell acute lymphoblastic leukaemia. *Br J Haematol.* 2008;143:153-168.
10. Homminga I, Vuerhard MJ, Langerak AW, et al. Characterization of a pediatric T-cell acute lymphoblastic leukemia patient with simultaneous LYL1 and LMO2 rearrangements. *Haematologica*;97:258-261.
11. Simonis M, Klous P, Homminga I, et al. High-resolution identification of balanced and complex chromosomal rearrangements by 4C technology. *Nat Methods.* 2009;6:837-842.
12. Zuurbier L, Gutierrez A, Mullighan CG, et al. Immature MEF2C-dysregulated T-cell leukemia patients have an early T-cell precursor acute lymphoblastic leukemia gene signature and typically have non-rearranged T-cell receptors. *Haematologica*;99:94-102.
13. Coustan-Smith E, Mullighan CG, Onciu M, et al. Early T-cell precursor leukaemia: a subtype of very high-risk acute lymphoblastic leukaemia. *Lancet Oncol.* 2009;10:147-156.
14. Gutierrez A, Dahlberg SE, Neuberg DS, et al. Absence of biallelic TCRgamma deletion predicts early treatment failure in pediatric T-cell acute lymphoblastic leukemia. *J Clin Oncol*;28:3816-3823.
15. Inukai T, Kiyokawa N, Campana D, et al. Clinical significance of early T-cell precursor acute lymphoblastic leukaemia: results of the Tokyo Children's Cancer Study Group Study L99-15. *Br J Haematol*;156:358-365.
16. Chiang MY, Xu L, Shestova O, et al. Leukemia-associated NOTCH1 alleles are weak tumor initiators but accelerate K-ras-initiated leukemia. *J Clin Invest.* 2008;118:3181-3194.
17. Sulis ML, Williams O, Palomero T, et al. NOTCH1 extracellular juxtamembrane expansion mutations in T-ALL. *Blood.* 2008;112:733-740.
18. Weng AP, Ferrando AA, Lee W, et al. Activating mutations of NOTCH1 in human T-cell acute lymphoblastic leukemia. *Science.* 2004;306:269-271.
19. Zuurbier L, Homminga I, Calvert V, et al. NOTCH1 and/or FBXW7 mutations predict for initial good prednisone response but not for improved outcome in pediatric T-cell acute lymphoblastic leukemia patients treated on DCOG or COALL protocols. *Leukemia*;24:2014-2022.
20. Chan SM, Weng AP, Tibshirani R, Aster JC, Utz PJ. Notch signals positively regulate activity of the mTOR pathway in T-cell acute lymphoblastic leukemia. *Blood.* 2007;110:278-286.
21. Maser RS, Choudhury B, Campbell PJ, et al. Chromosomally unstable mouse tumours have genomic

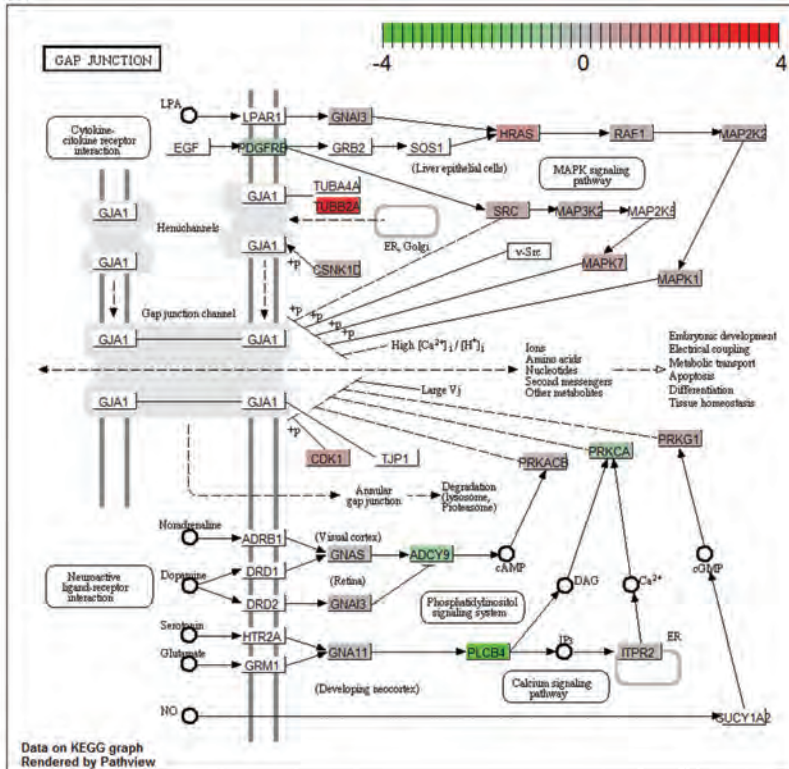
- alterations similar to diverse human cancers. *Nature*. 2007;447:966-971.
22. Silva A, Yunes JA, Cardoso BA, et al. PTEN posttranslational inactivation and hyperactivation of the PI3K/Akt pathway sustain primary T-cell leukemia viability. *J Clin Invest*. 2008;118:3762-3774.
 23. Zuurbier L, Petricoin EF, 3rd, Vuerhard MJ, et al. The significance of PTEN and AKT aberrations in pediatric T-cell acute lymphoblastic leukemia. *Haematologica*;97:1405-1413.
 24. Palomero T, Sulis ML, Cortina M, et al. Mutational loss of PTEN induces resistance to NOTCH1 inhibition in T-cell leukemia. *Nat Med*. 2007;13:1203-1210.
 25. Van Vlierberghe P, van Grotel M, Beverloo HB, et al. The cryptic chromosomal deletion del(11)(p12p13) as a new activation mechanism of LMO2 in pediatric T-cell acute lymphoblastic leukemia. *Blood*. 2006;108:3520-3529.
 26. Paweletz CP, Charboneau L, Bichsel VE, et al. Reverse phase protein microarrays which capture disease progression show activation of pro-survival pathways at the cancer invasion front. *Oncogene*. 2001;20:1981-1989.
 27. Petricoin EF, 3rd, Espina V, Araujo RP, et al. Phosphoprotein pathway mapping: Akt/mammalian target of rapamycin activation is negatively associated with childhood rhabdomyosarcoma survival. *Cancer Res*. 2007;67:3431-3440.
 28. Tosello V, Mansour MR, Barnes K, et al. WT1 mutations in T-ALL. *Blood*. 2009;114:1038-1045.
 29. van Grotel M, Meijerink JP, Beverloo HB, et al. The outcome of molecular-cytogenetic subgroups in pediatric T-cell acute lymphoblastic leukemia: a retrospective study of patients treated according to DCOG or COALL protocols. *Haematologica*. 2006;91:1212-1221.
 30. Goeman JJ, van de Geer SA, de Kort F, van Houwelingen HC. A global test for groups of genes: testing association with a clinical outcome. *Bioinformatics*. 2004;20:93-99.
 31. Luo W, Brouwer C. Pathview: an R/Bioconductor package for pathway-based data integration and visualization. *Bioinformatics*;29:1830-1831.
 32. Menendez JA, Lupu R. Fatty acid synthase and the lipogenic phenotype in cancer pathogenesis. *Nat Rev Cancer*. 2007;7:763-777.
 33. Tennant DA, Duran RV, Gottlieb E. Targeting metabolic transformation for cancer therapy. *Nat Rev Cancer*;10:267-277.
 34. Pelicano H, Martin DS, Xu RH, Huang P. Glycolysis inhibition for anticancer treatment. *Oncogene*. 2006;25:4633-4646.
 35. van Grotel M, Meijerink JP, van Wering ER, et al. Prognostic significance of molecular-cytogenetic abnormalities in pediatric T-ALL is not explained by immunophenotypic differences. *Leukemia*. 2008;22:124-131.
 36. Ito T, Kwon HY, Zimdahl B, et al. Regulation of myeloid leukaemia by the cell-fate determinant Musashi. *Nature*;466:765-768.
 37. Hope KJ, Cellot S, Ting SB, et al. An RNAi screen identifies Msi2 and Prox1 as having opposite roles in the regulation of hematopoietic stem cell activity. *Cell Stem Cell*;7:101-113.
 38. Hsieh JJ, Cheng EH, Korsmeyer SJ. Taspase1: a threonine aspartase required for cleavage of MLL and proper HOX gene expression. *Cell*. 2003;115:293-303.
 39. Real PJ, Tosello V, Palomero T, et al. Gamma-secretase inhibitors reverse glucocorticoid resistance in T-cell acute lymphoblastic leukemia. *Nat Med*. 2009;15:50-58.
 40. O'Neil J, Grim J, Strack P, et al. FBW7 mutations in leukemic cells mediate NOTCH pathway activation and resistance to gamma-secretase inhibitors. *J Exp Med*. 2007;204:1813-1824.
 41. Ryan KM, Phillips AC, Vousden KH. Regulation and function of the p53 tumor suppressor protein. *Curr Opin Cell Biol*. 2001;13:332-337.
 42. Hof J, Krentz S, van Schewick C, et al. Mutations and deletions of the TP53 gene predict nonresponse to treatment and poor outcome in first relapse of childhood acute lymphoblastic leukemia. *J Clin*

- Oncol;29:3185-3193.
43. Liberzon E, Avigad S, Stark B, et al. Germ-line ATM gene alterations are associated with susceptibility to sporadic T-cell acute lymphoblastic leukemia in children. *Genes Chromosomes Cancer*. 2004;39:161-166.
 44. Savvidis C, Koutsilieris M. Circadian rhythm disruption in cancer biology. *Mol Med*;18:1249-1260.
 45. Khiem D, Cyster JG, Schwarz JJ, Black BL. A p38 MAPK-MEF2C pathway regulates B-cell proliferation. *Proc Natl Acad Sci U S A*. 2008;105:17067-17072.
 46. Dohda T, Maljukova A, Liu L, et al. Notch signaling induces SKP2 expression and promotes reduction of p27Kip1 in T-cell acute lymphoblastic leukemia cell lines. *Exp Cell Res*. 2007;313:3141-3152.
 47. Rao SS, O'Neil J, Liberator CD, et al. Inhibition of NOTCH signaling by gamma secretase inhibitor engages the RB pathway and elicits cell cycle exit in T-cell acute lymphoblastic leukemia cells. *Cancer Res*. 2009;69:3060-3068.
 48. Medema RH, Kops GJ, Bos JL, Burgering BM. AFX-like Forkhead transcription factors mediate cell-cycle regulation by Ras and PKB through p27kip1. *Nature*. 2000;404:782-787.
 49. Giambra V, Jenkins CR, Wang H, et al. NOTCH1 promotes T-cell leukemia-initiating activity by RUNX-mediated regulation of PKC-theta and reactive oxygen species. *Nat Med*;18:1693-1698.
 50. Englert C, Hou X, Maheswaran S, et al. WT1 suppresses synthesis of the epidermal growth factor receptor and induces apoptosis. *Embo J*. 1995;14:4662-4675.
 51. Graham K, Li W, Williams BR, Fraizer G. Vascular endothelial growth factor (VEGF) is suppressed in WT1-transfected LNCaP cells. *Gene Expr*. 2006;13:1-14.
 52. Idelman G, Glaser T, Roberts CT, Jr, Werner H. WT1-p53 interactions in insulin-like growth factor-1 receptor gene regulation. *J Biol Chem*. 2003;278:3474-3482.
 53. Roberts CT, Jr. Control of insulin-like growth factor (IGF) action by regulation of IGF-I receptor expression. *Endocr J*. 1996;43 Suppl:S49-55.
 54. English MA, Licht JD. Tumor-associated WT1 missense mutants indicate that transcriptional activation by WT1 is critical for growth control. *J Biol Chem*. 1999;274:13258-13263.
 55. Little M, Holmes G, Bickmore W, et al. DNA binding capacity of the WT1 protein is abolished by Denys-Drash syndrome WT1 point mutations. *Hum Mol Genet*. 1995;4:351-358.
 56. Englert C, Vidal M, Maheswaran S, et al. Truncated WT1 mutants alter the subnuclear localization of the wild-type protein. *Proc Natl Acad Sci U S A*. 1995;92:11960-11964.
 57. Borel F, Barilla KC, Hamilton TB, Iskandar M, Romaniuk PJ. Effects of Denys-Drash syndrome point mutations on the DNA binding activity of the Wilms' tumor suppressor protein WT1. *Biochemistry*. 1996;35:12070-12076.
 58. King-Underwood L, Pritchard-Jones K. Wilms' tumor (WT1) gene mutations occur mainly in acute myeloid leukemia and may confer drug resistance. *Blood*. 1998;91:2961-2968.
 59. Renneville A, Kaltenbach S, Clappier E, et al. Wilms tumor 1 (WT1) gene mutations in pediatric T-cell malignancies. *Leukemia*;24:476-480.

C



D



E

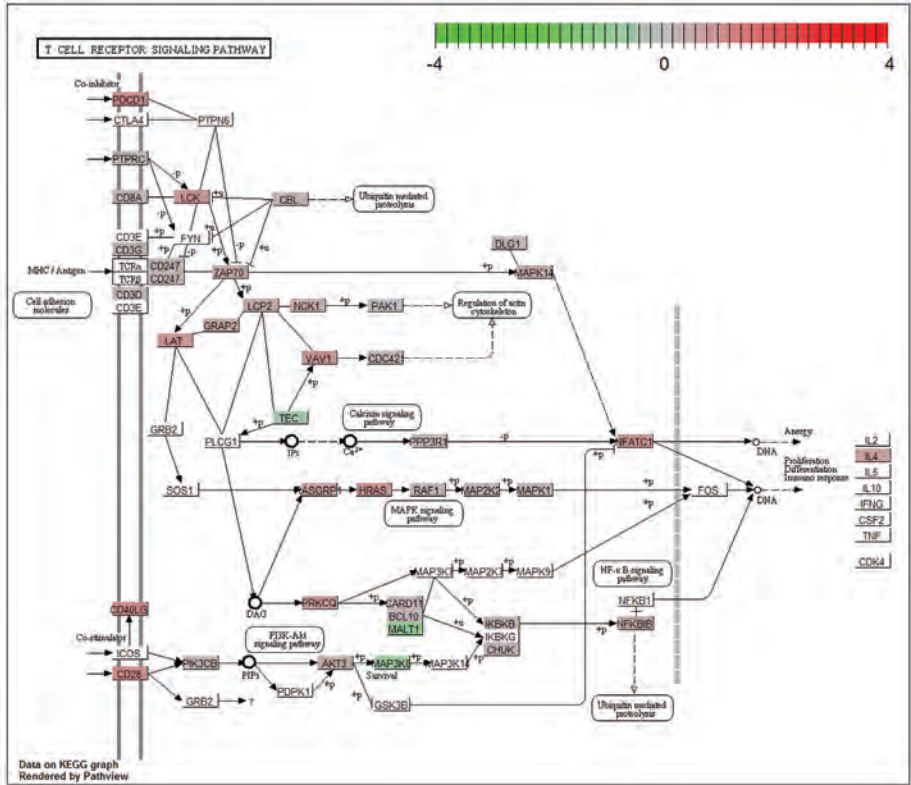
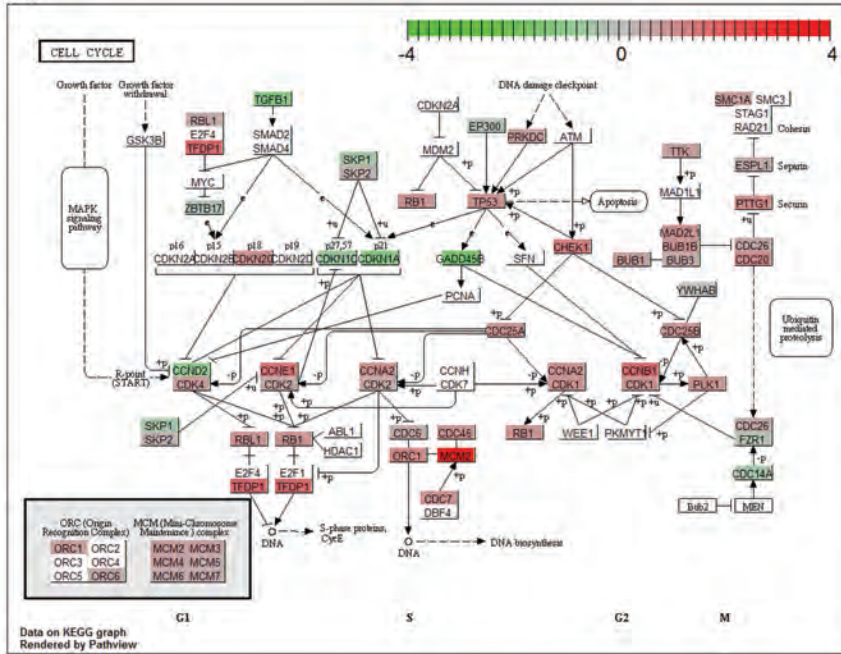
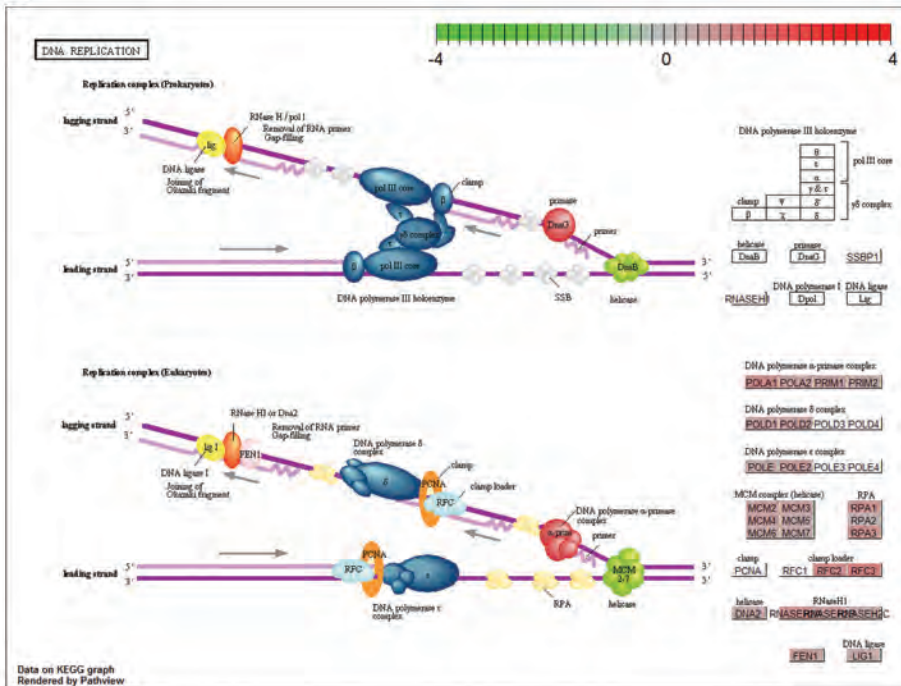


Figure S1 | Differentially expressed KEGG pathway maps of TALLMO cluster patients. (A) inositol phosphate metabolism, (B) glycerolipid metabolism, (C) starch and sucrose metabolism, (D) gap junction and (E) T-cell receptor signaling pathway.

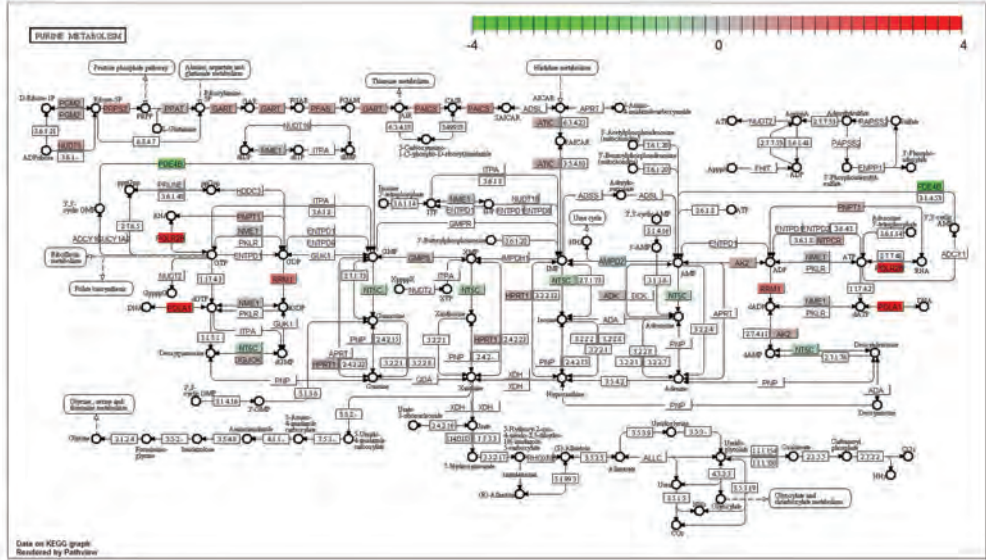
A



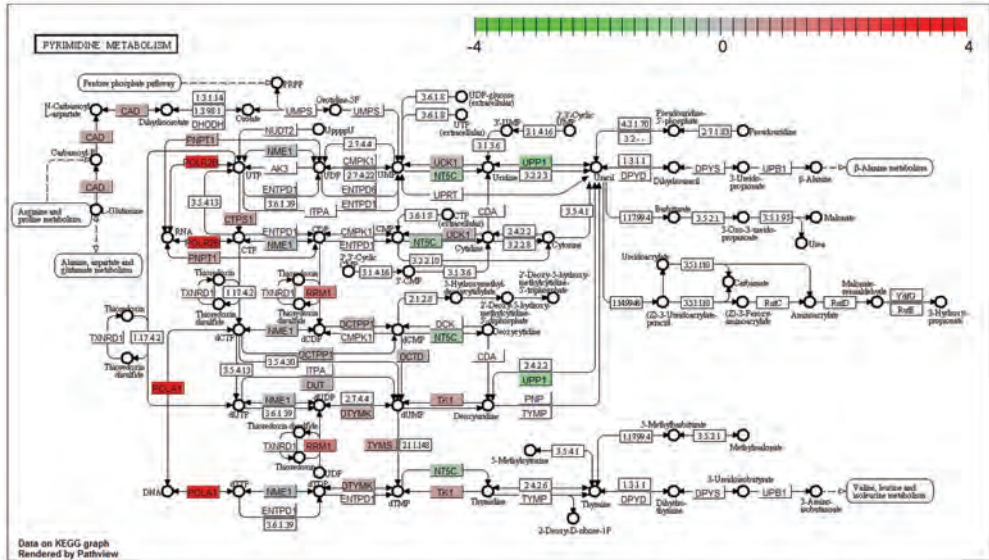
B



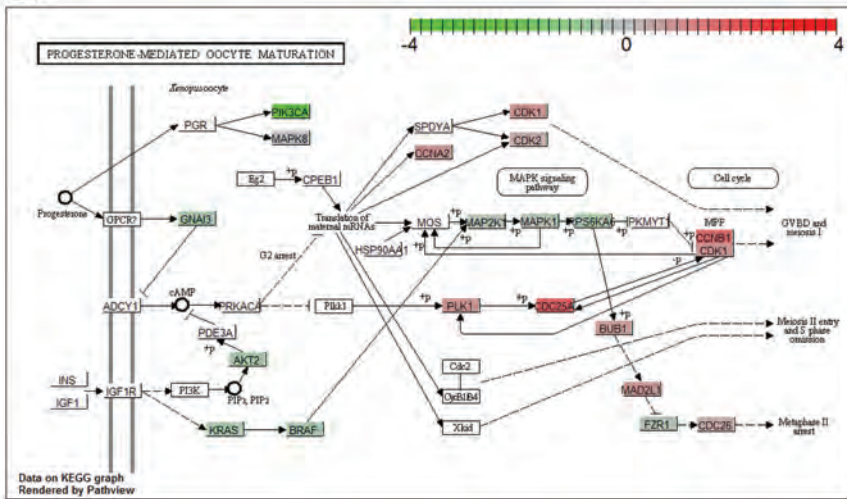
E



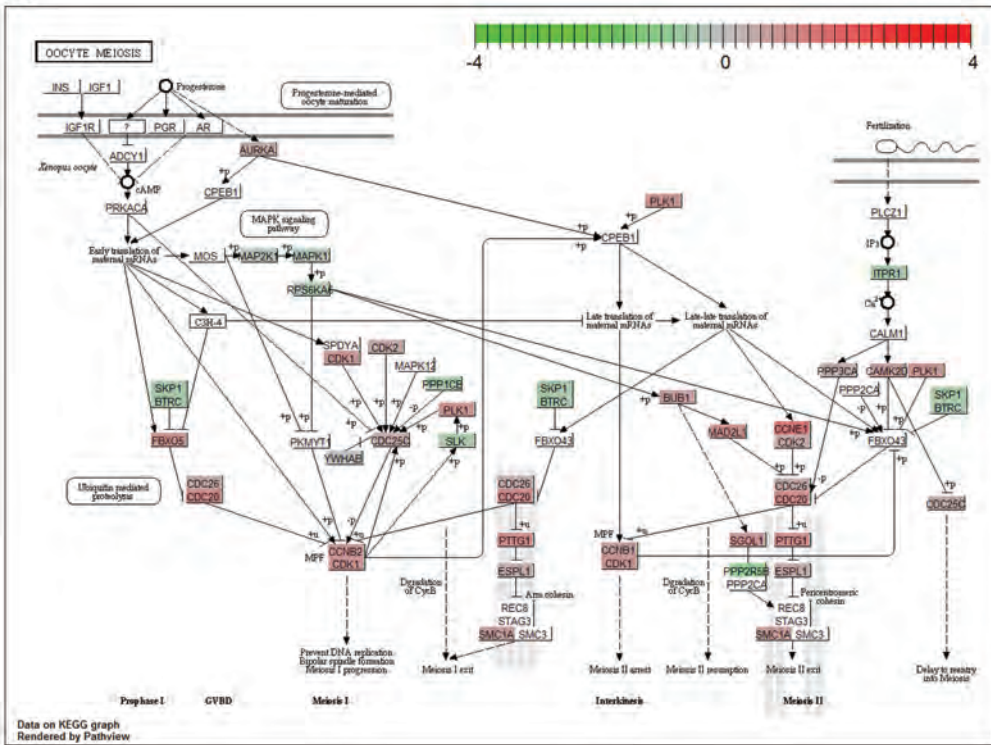
F

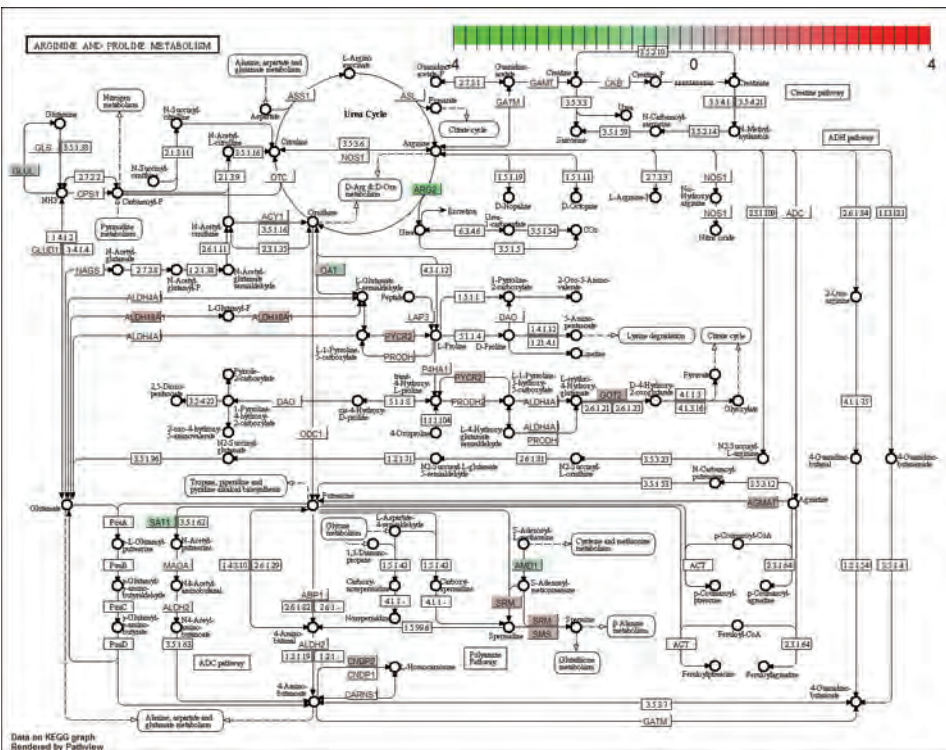
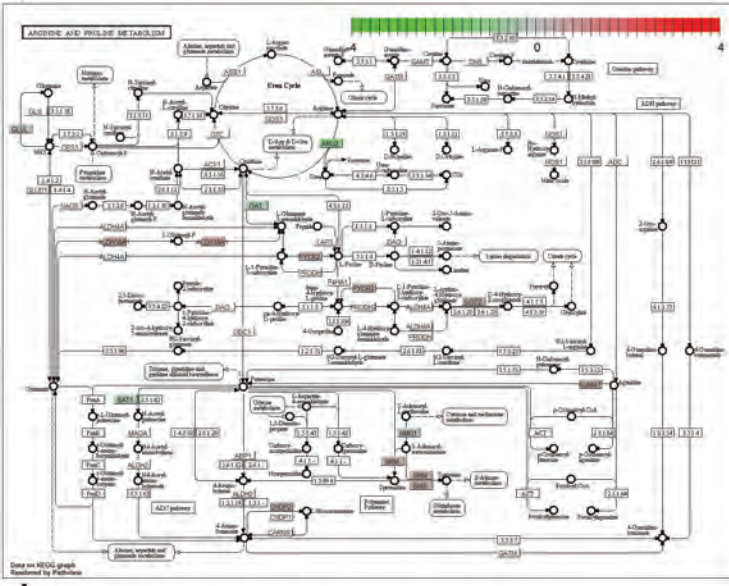


G

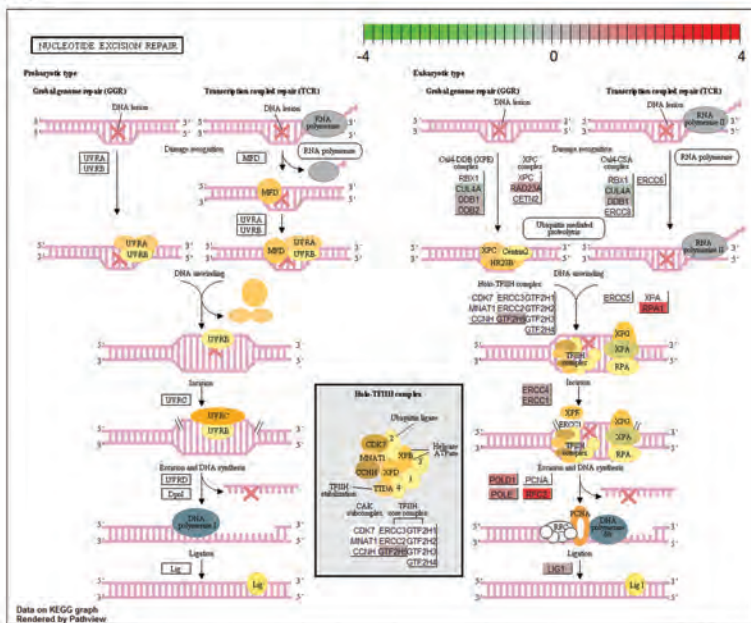


H

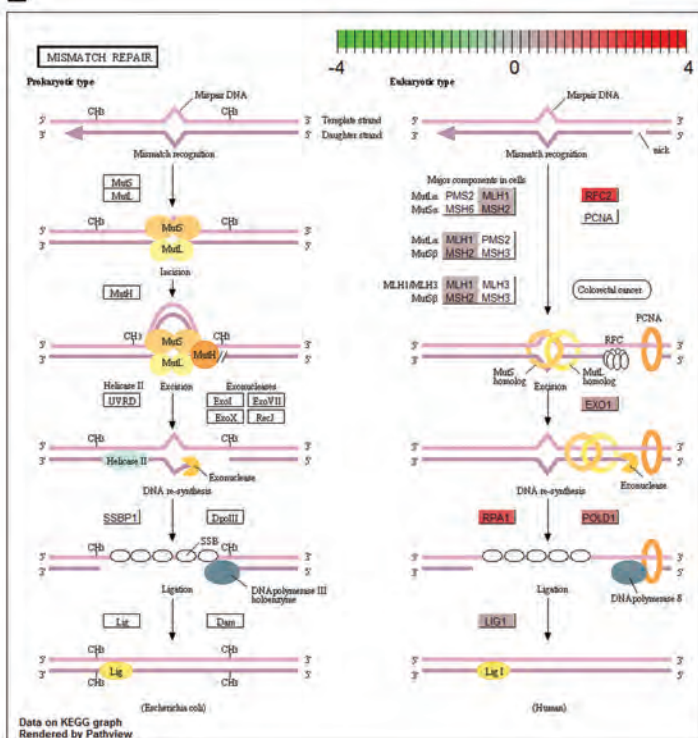




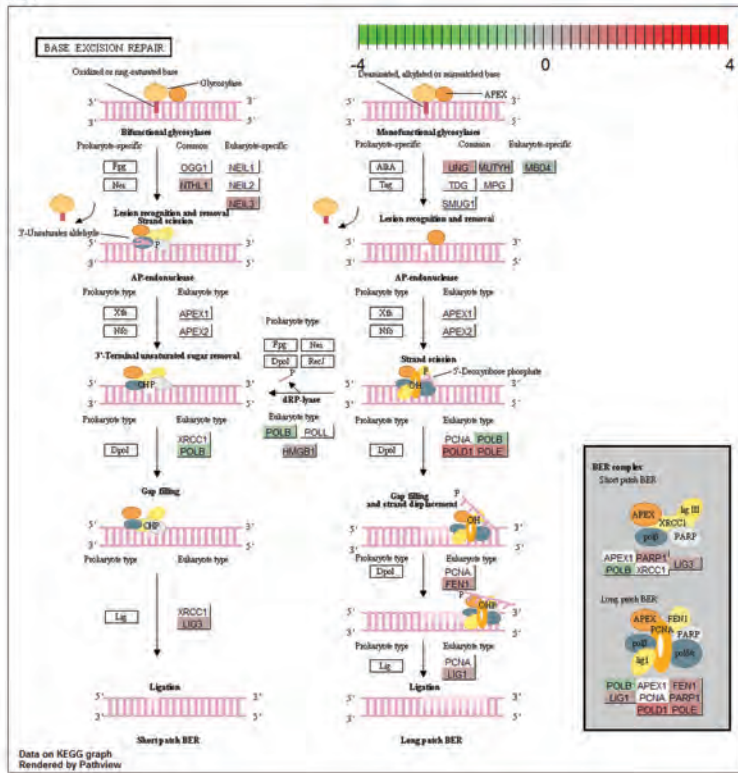
K



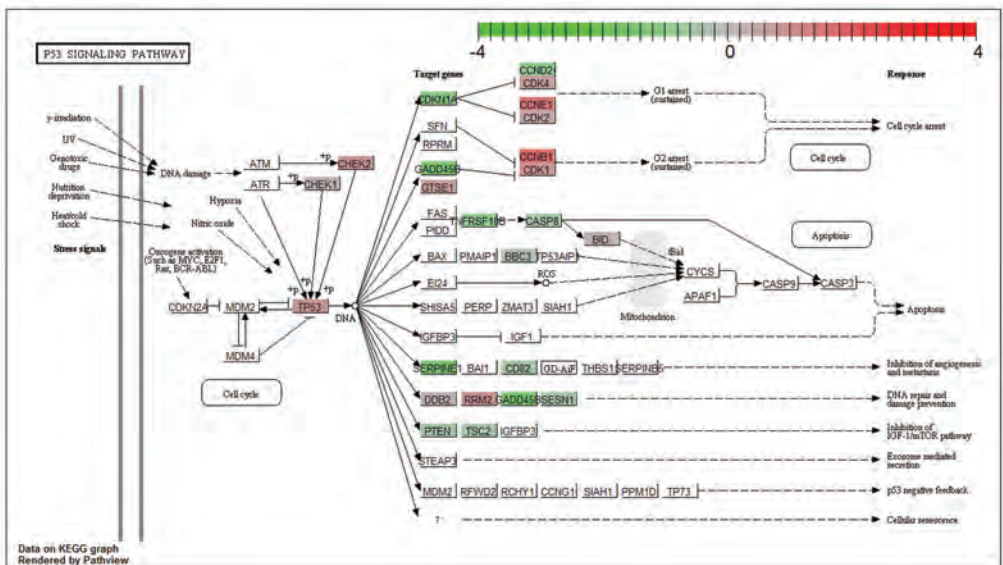
L



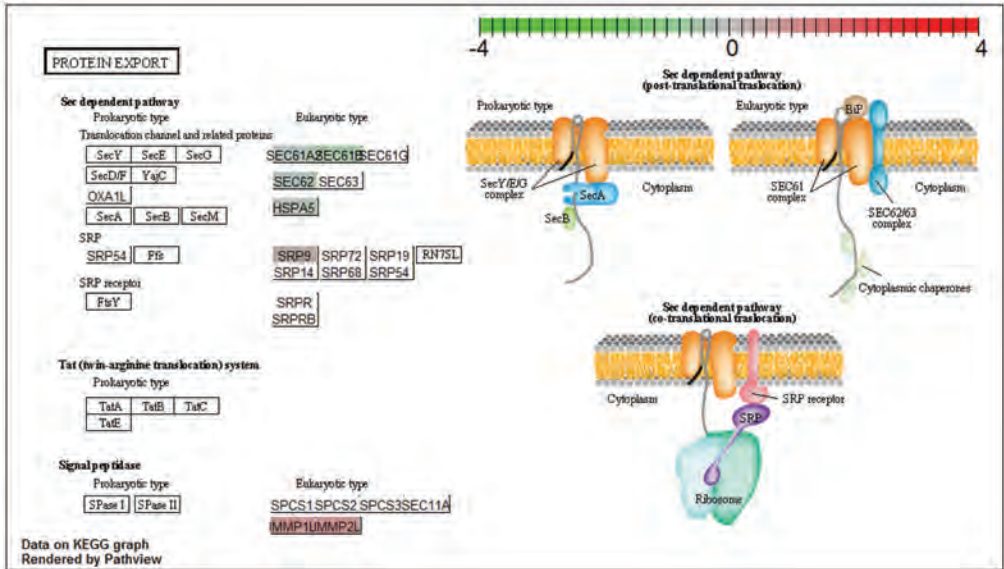
M



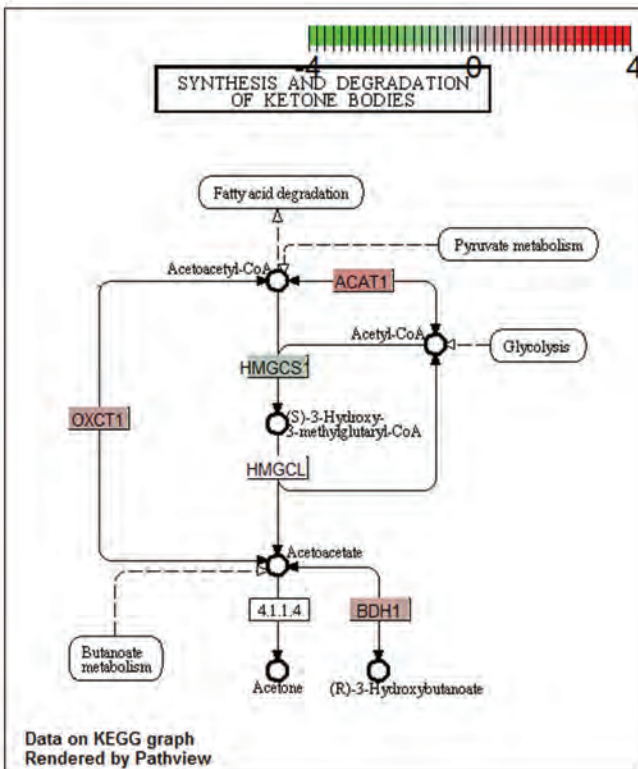
N



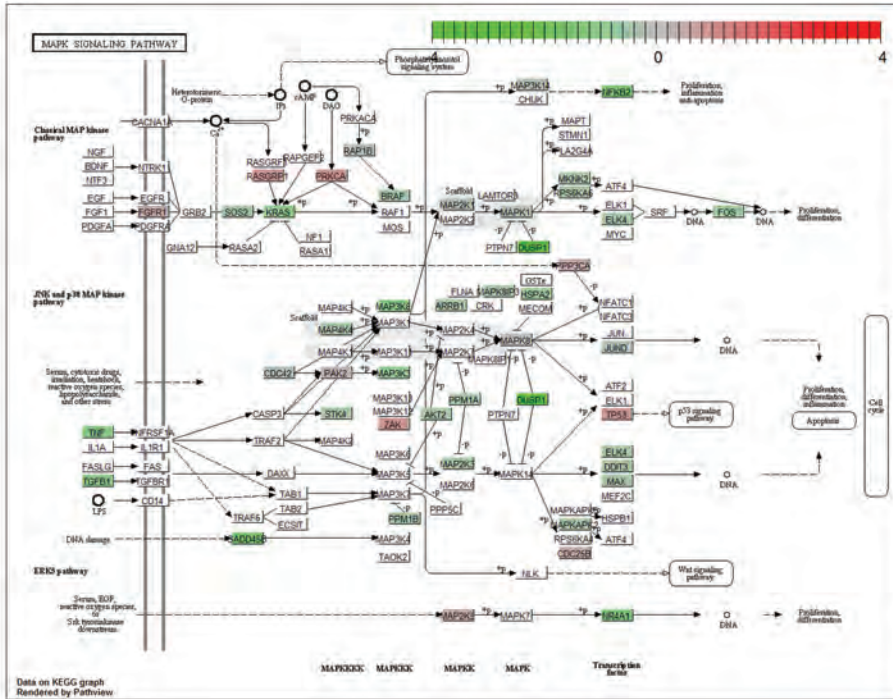
O



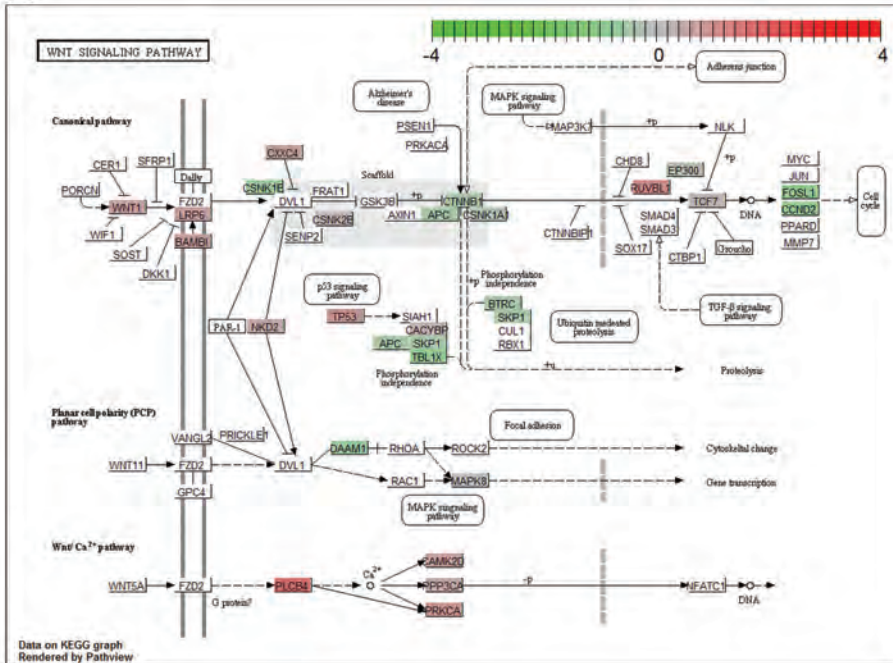
P



Q

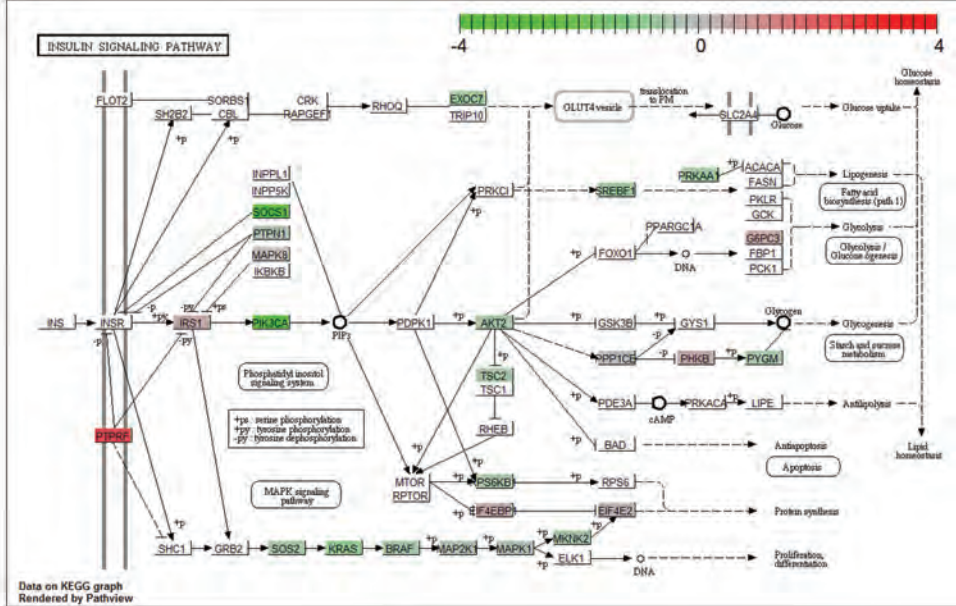


R

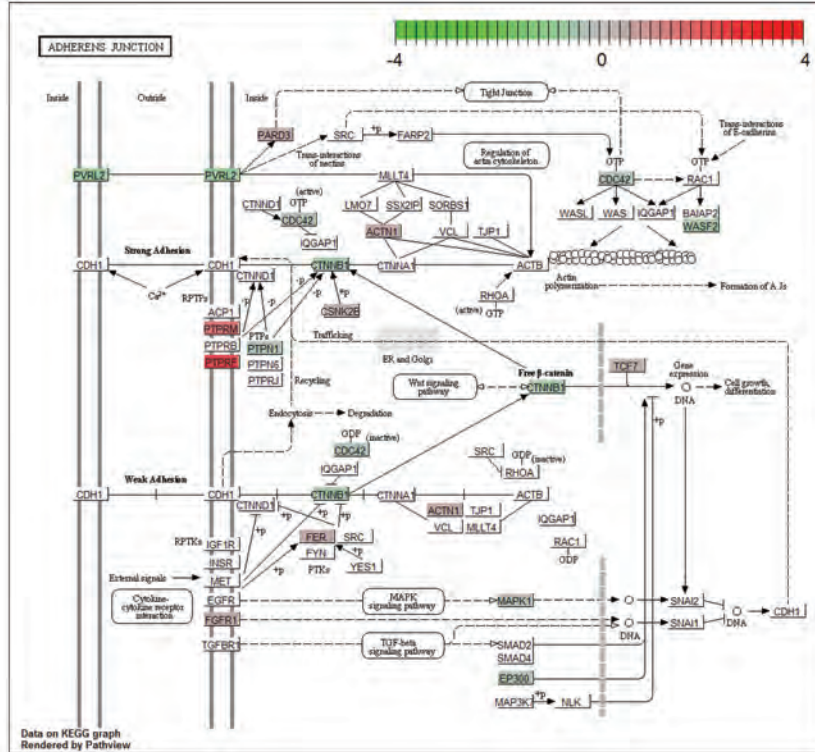


8

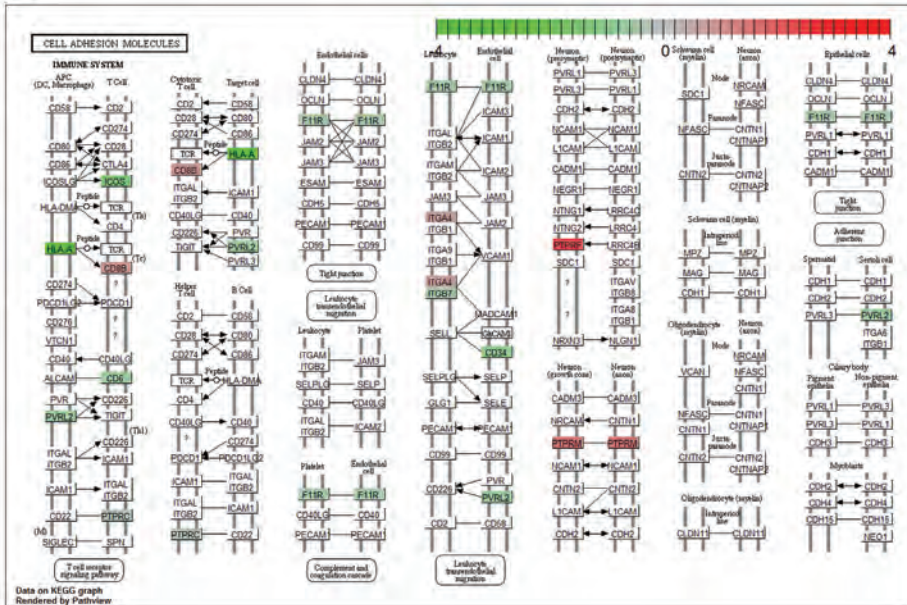
S



T



U



V

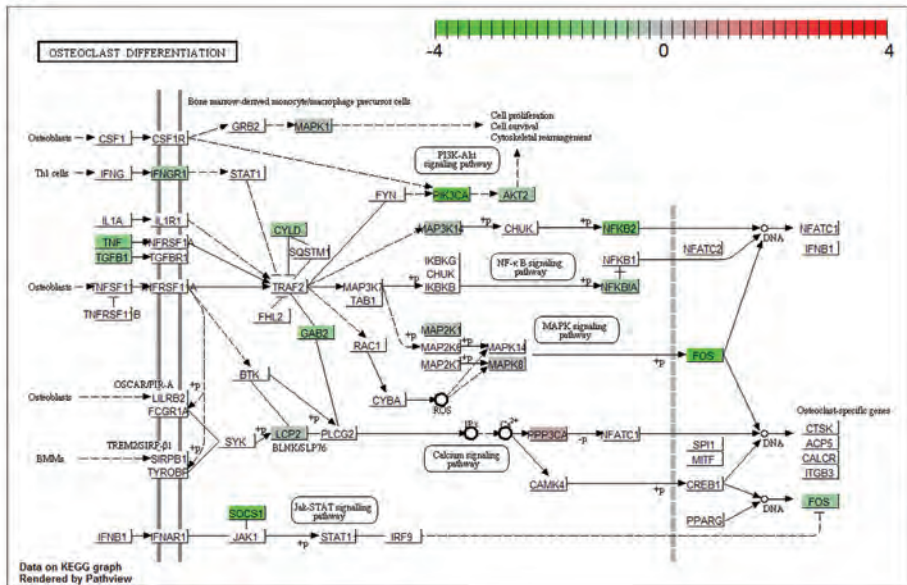
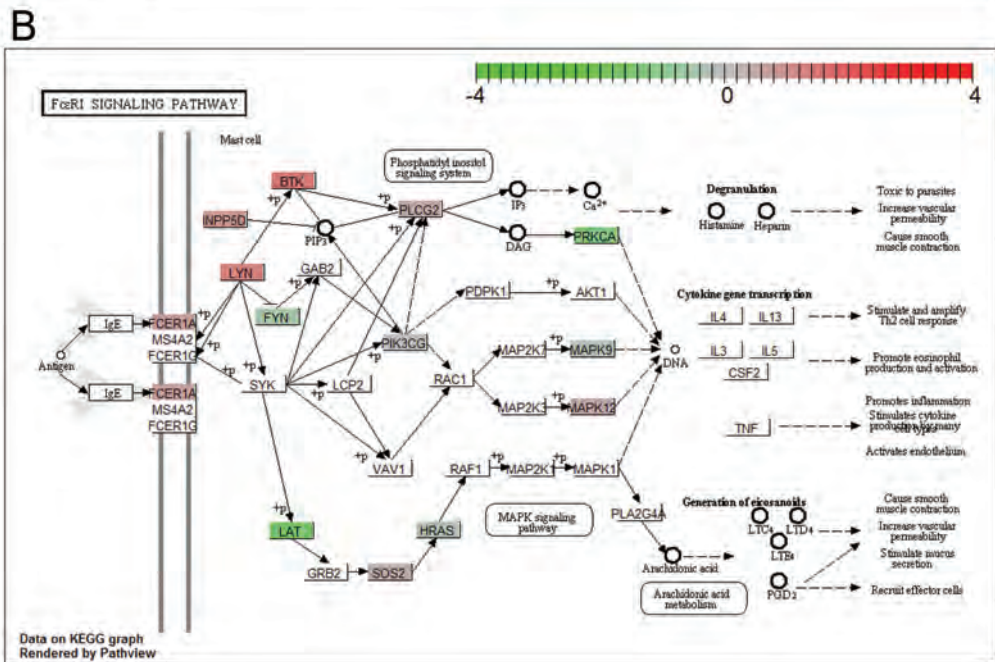
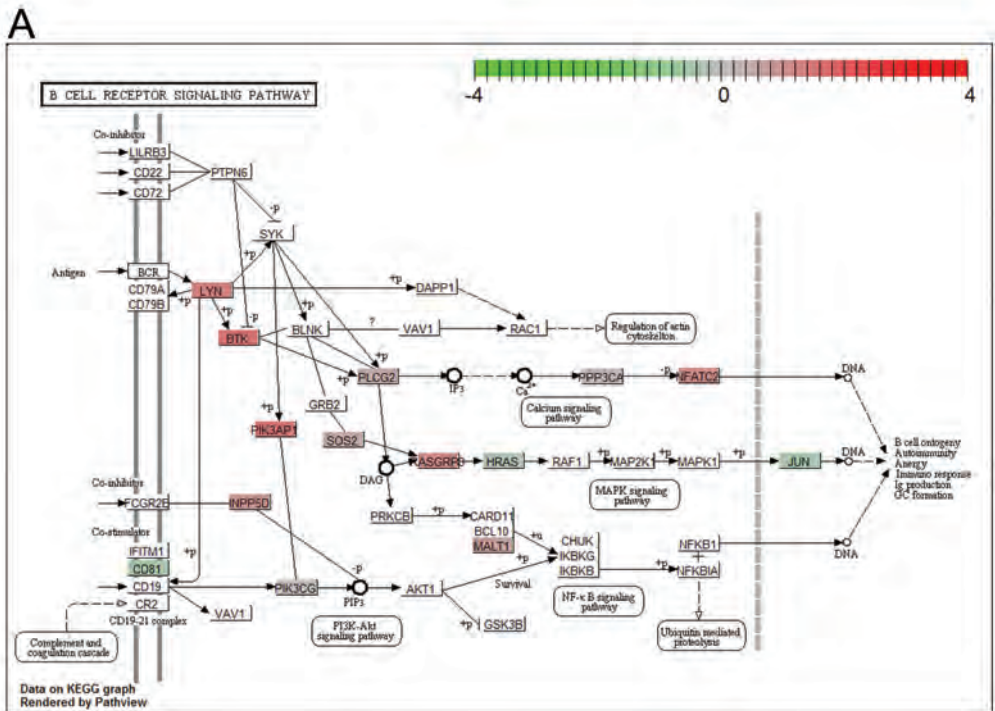
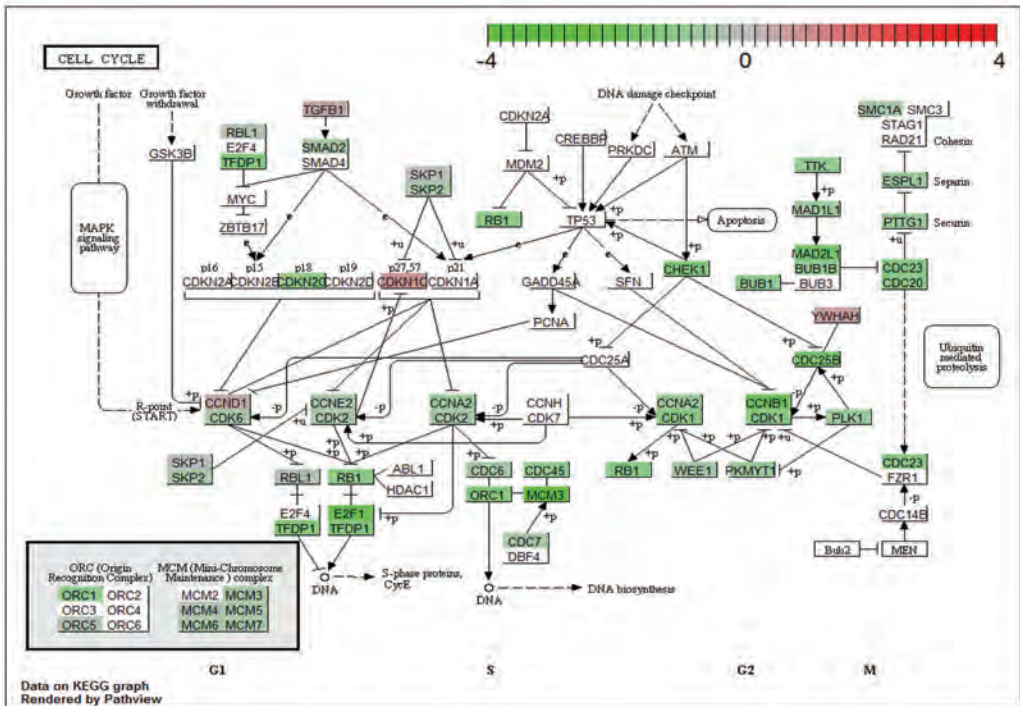


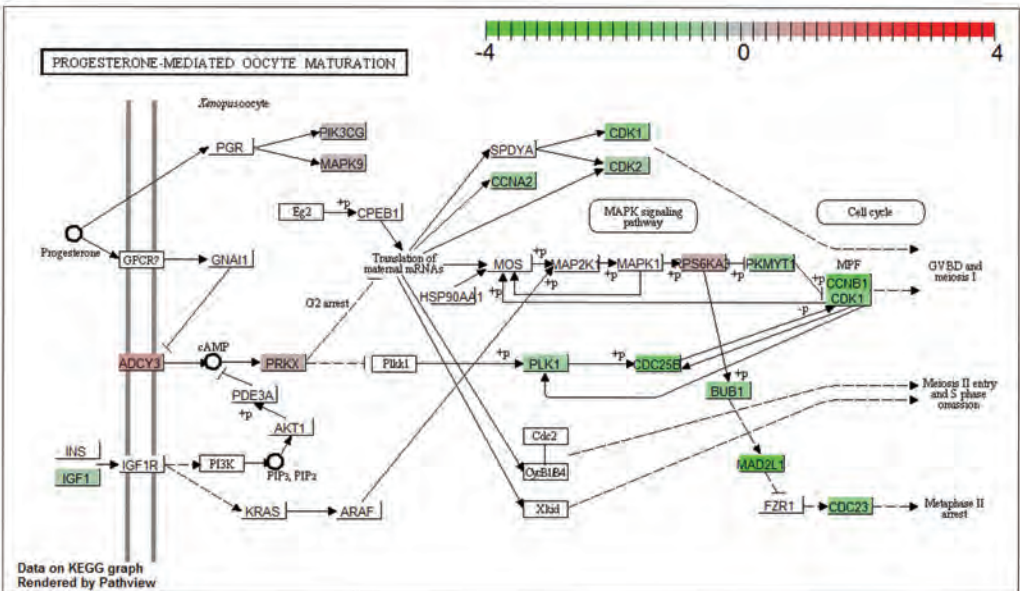
Figure S3 | Differentially expressed KEGG pathway maps of proliferative cluster patients. (A) cell cycle, (B) DNA replication, (C) one carbon pool by folate, (D) folate biosynthesis, (E) purine metabolism, (F) pyrimidine metabolism, (G) progesterone-mediated oocyte maturation, (H) oocyte meiosis, (K) nucleotide excision repair, (L) mismatch repair, (M) base excision repair, (N) p53 signaling pathway, (O) protein export, (P) synthesis and degradation of ketone bodies, (Q) MAPK signaling pathway, (R) Wnt signaling pathway, (S) insulin signaling pathway, (T) adherens junction, (U) cell adhesion molecules, (V) osteoclast differentiation.



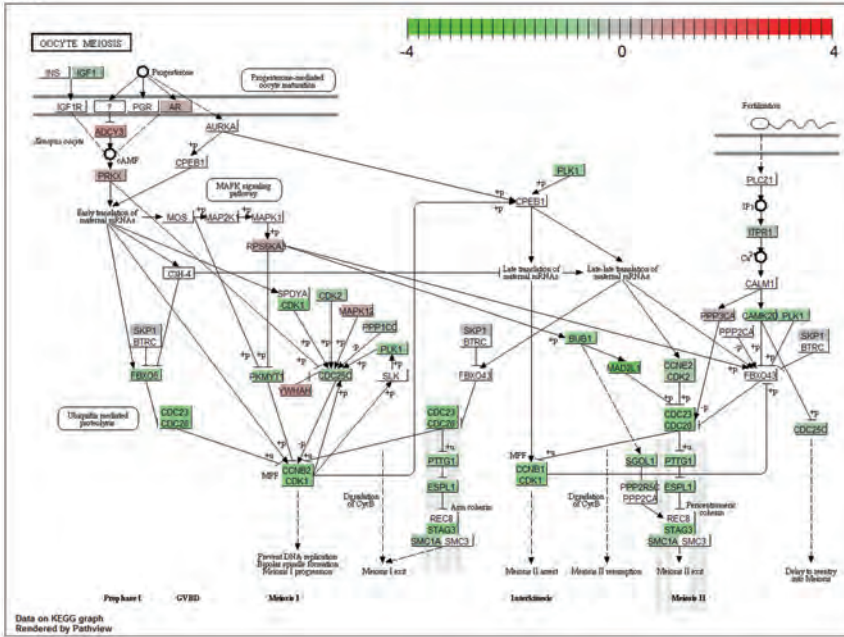
E



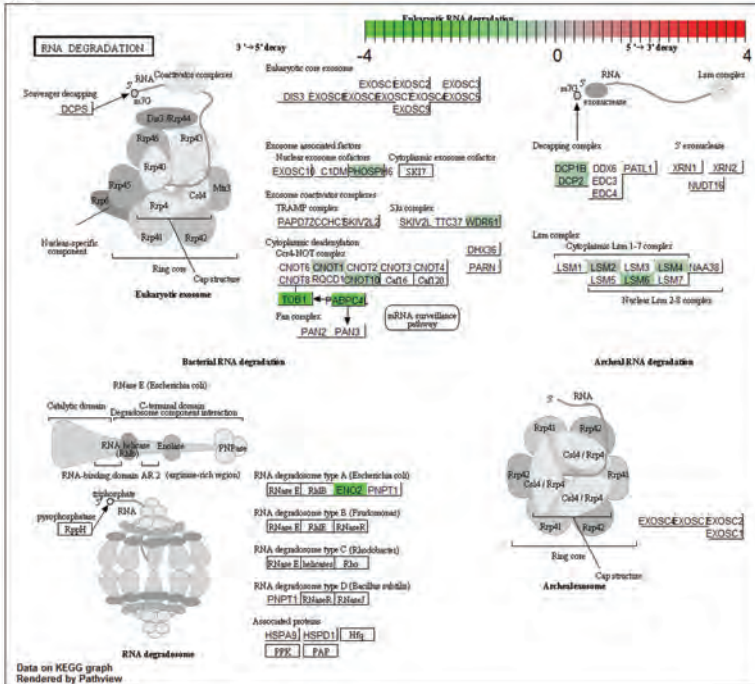
F

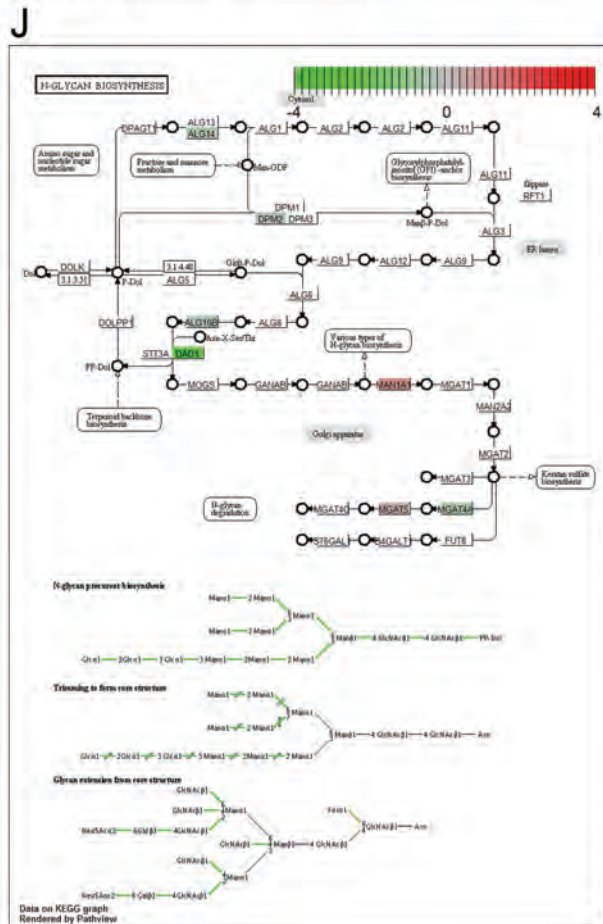
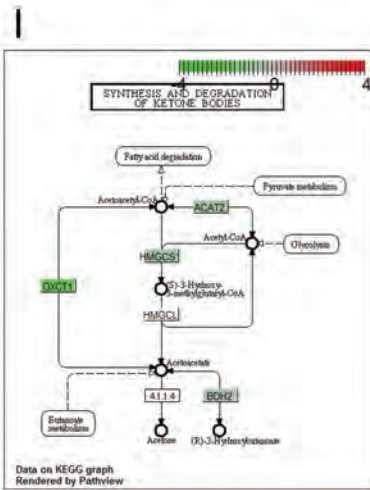


G

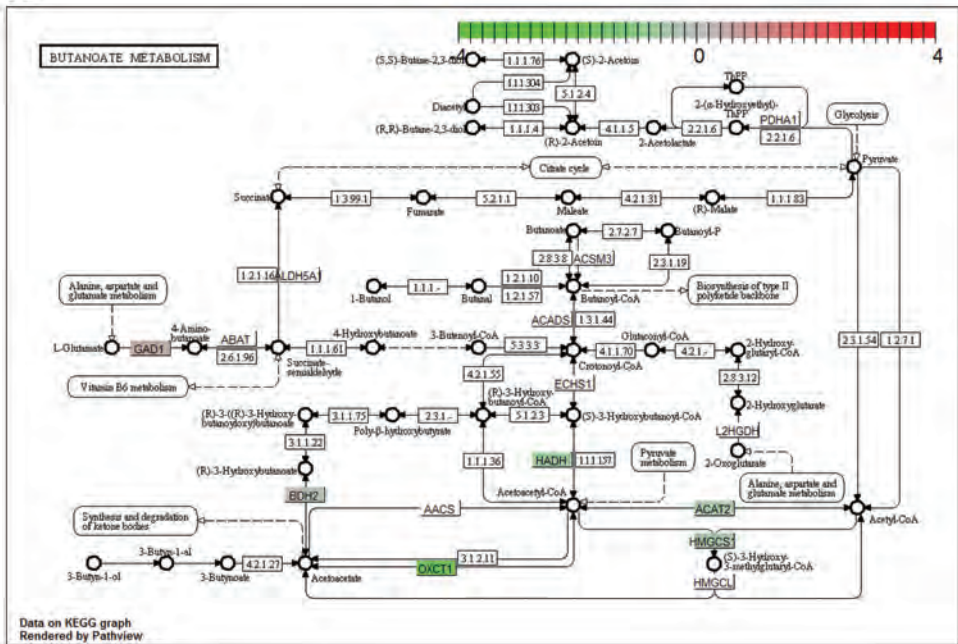


H

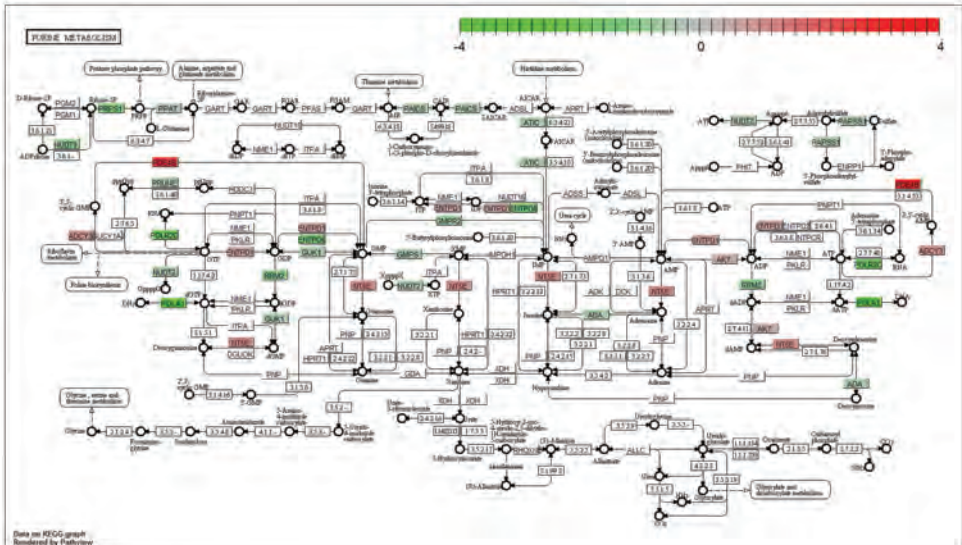




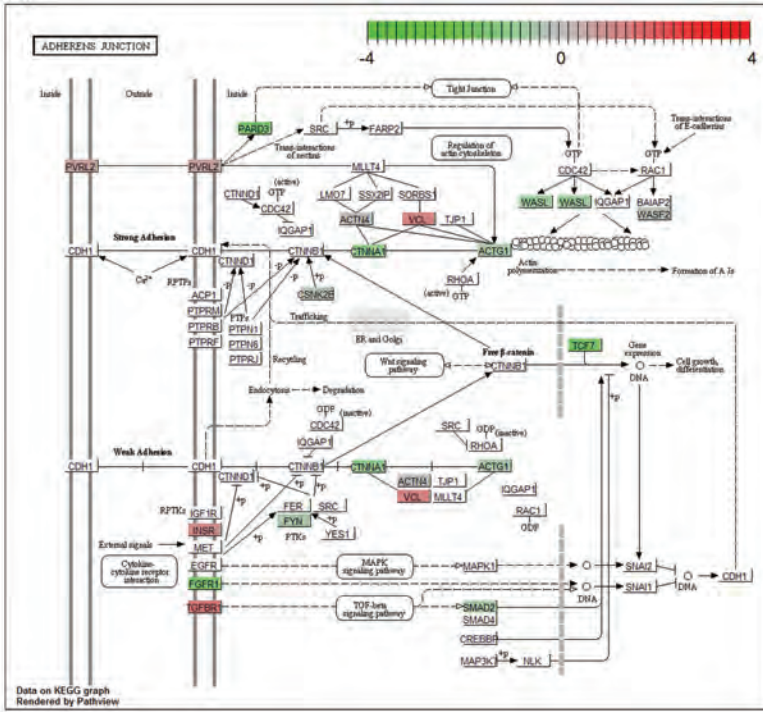
K



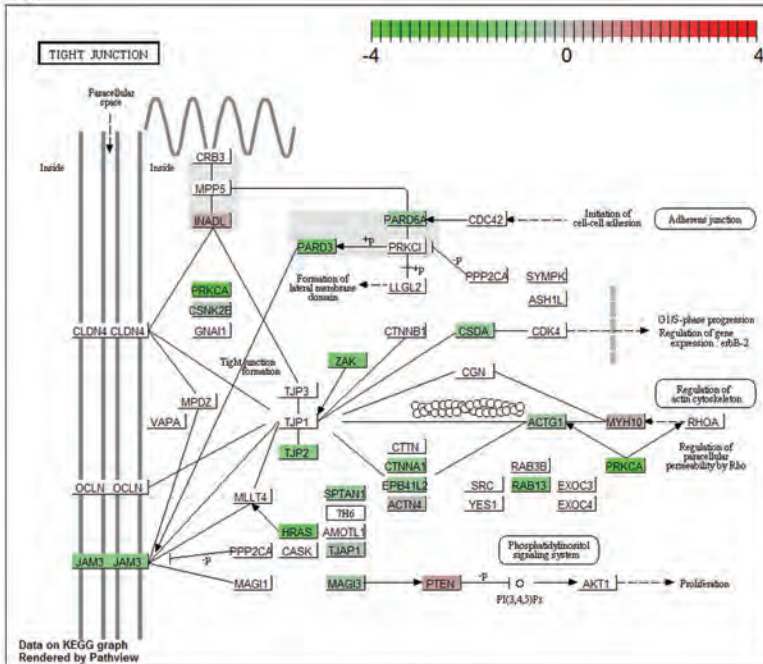
L

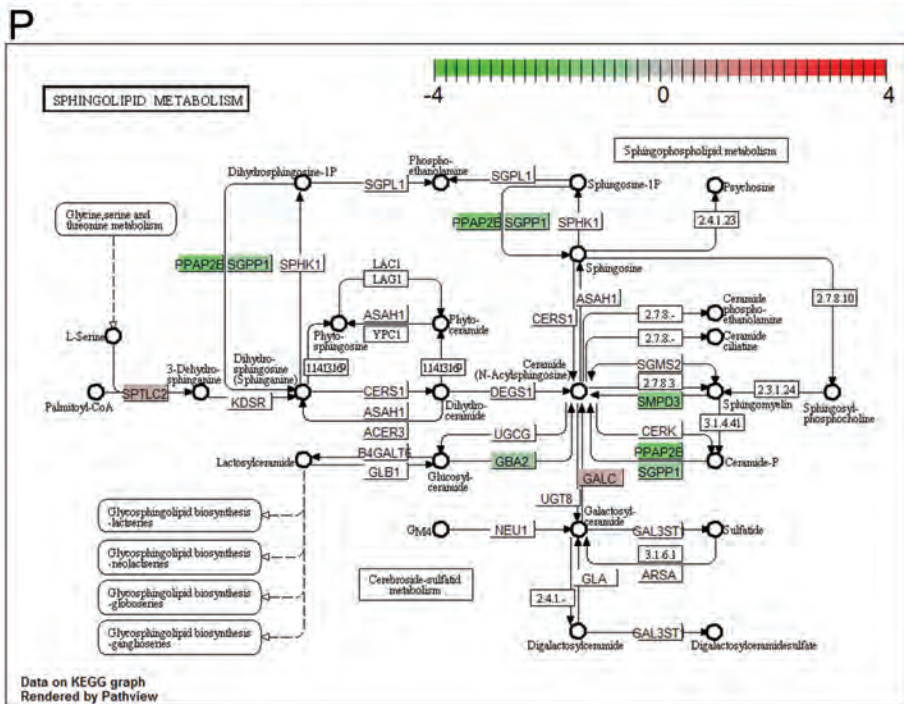
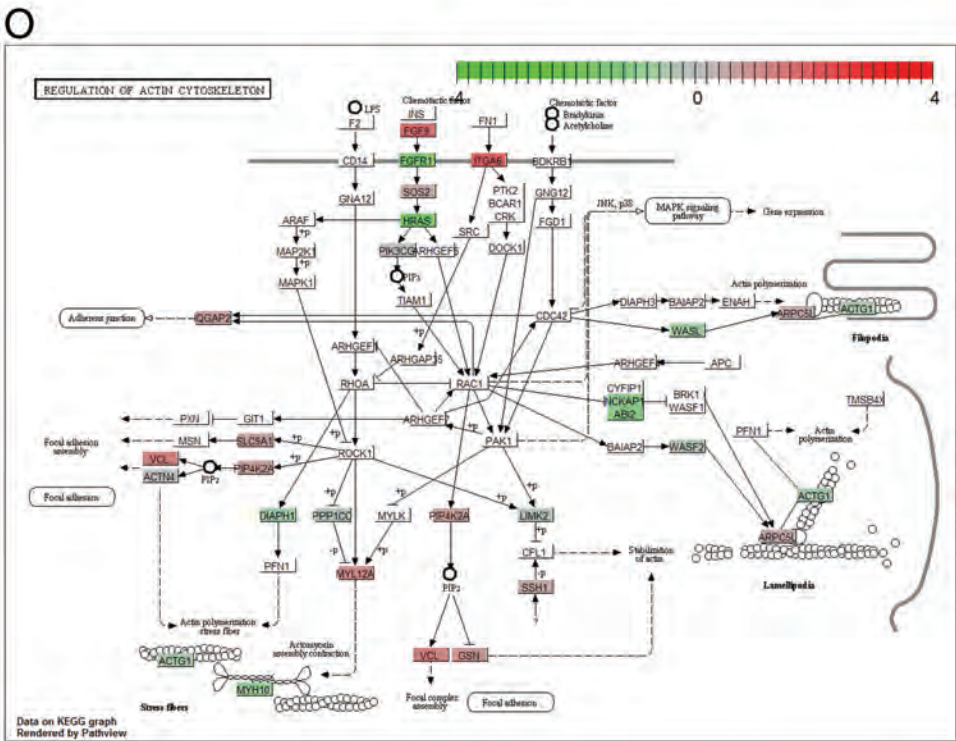


M



N





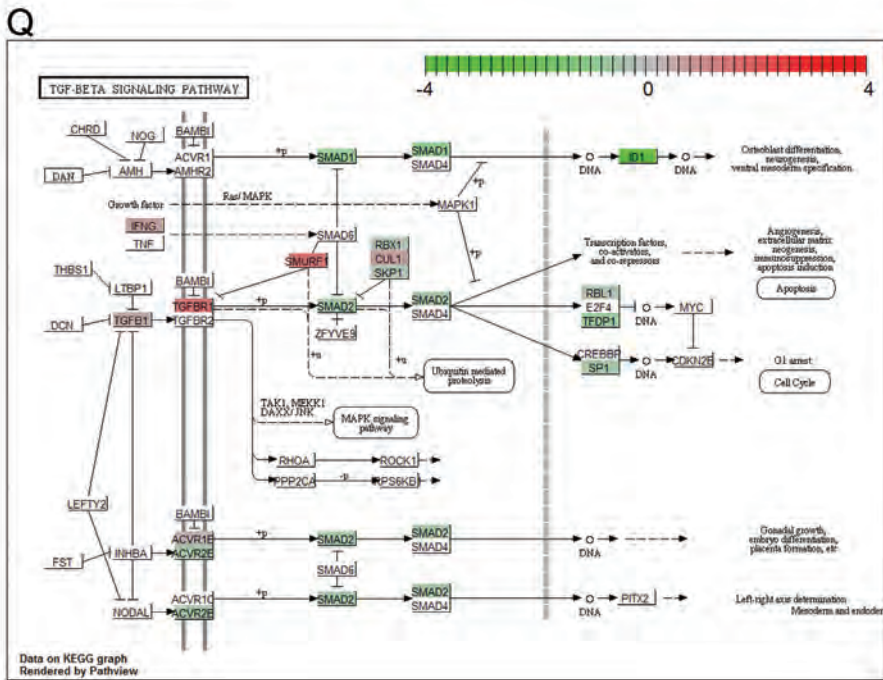
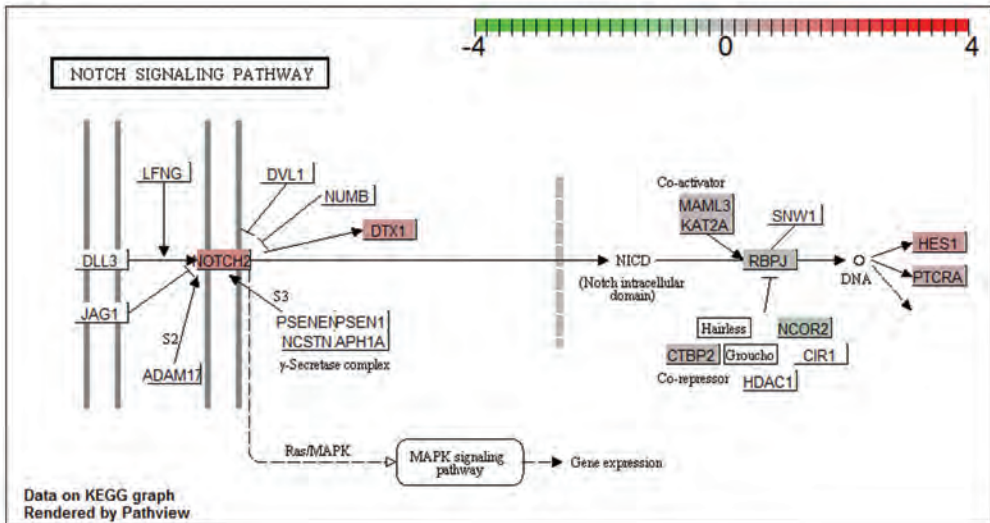
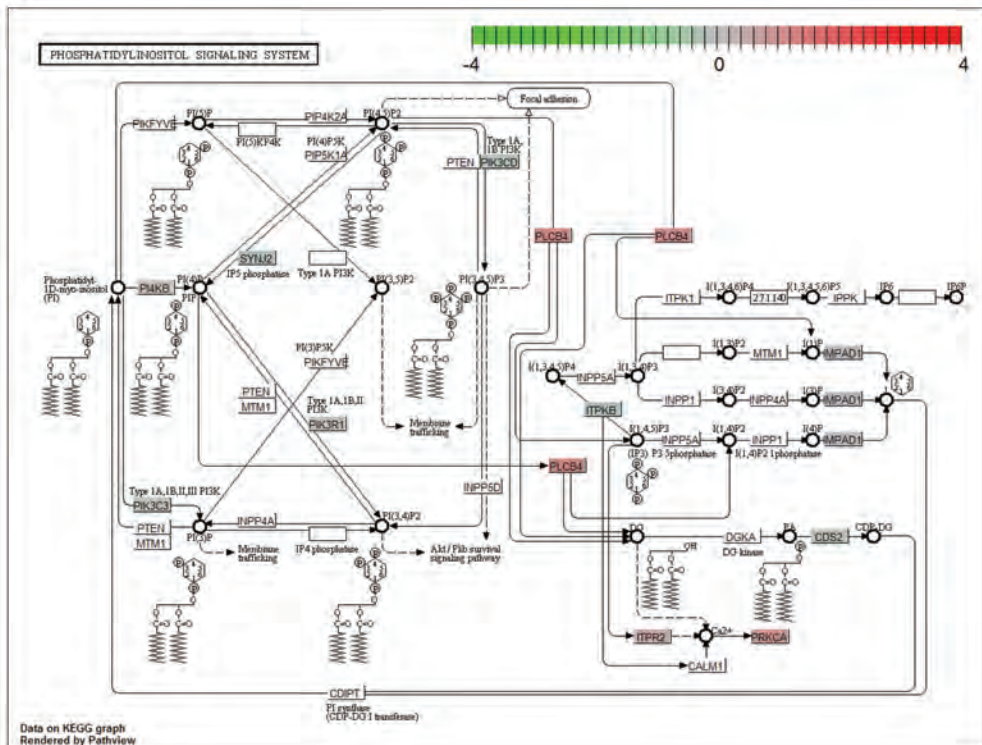


Figure S4 | Differentially expressed KEGG pathway map of immature cluster patients. (A) B-cell receptor signaling pathway, (B) FcεRI signaling pathway, (C) T-cell receptor signaling pathway, (D) hematopoietic cell lineage, (E) cell cycle, (F) progesterone-mediated oocyte maturation, (G) oocyte meiosis, (G) RNA degradation, (I) synthesis and degradation of ketone bodies, (J) N-glycan biosynthesis, (K) butanoate metabolism, (L) purine metabolism, (M) adherens junction, (N) tight junction, (O) regulation of actin cytoskeleton, (P) sphingolipid metabolism, (Q) TGF beta signaling pathway.

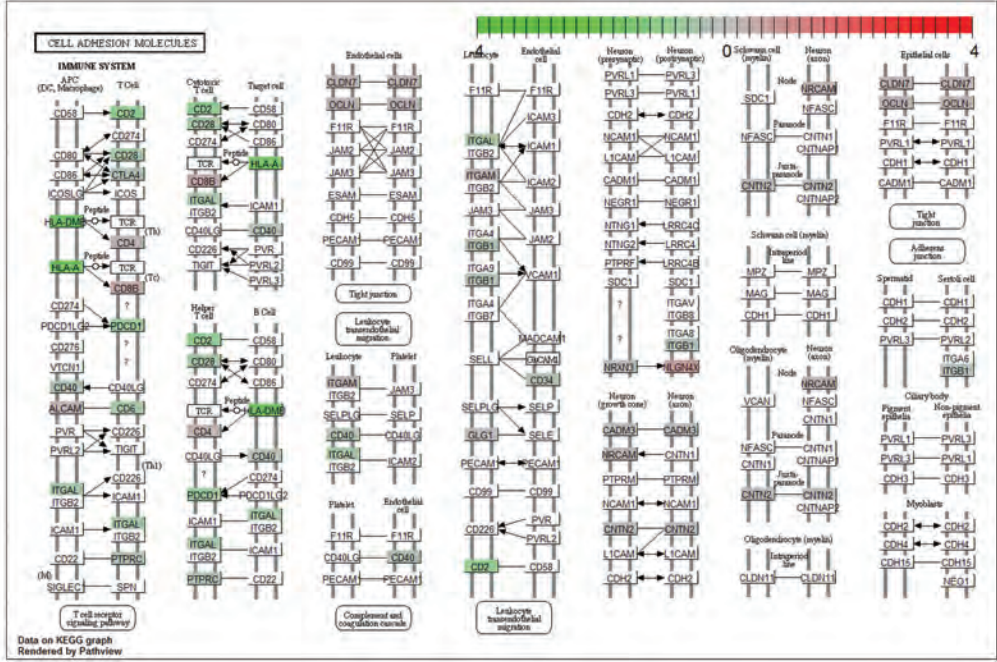
A



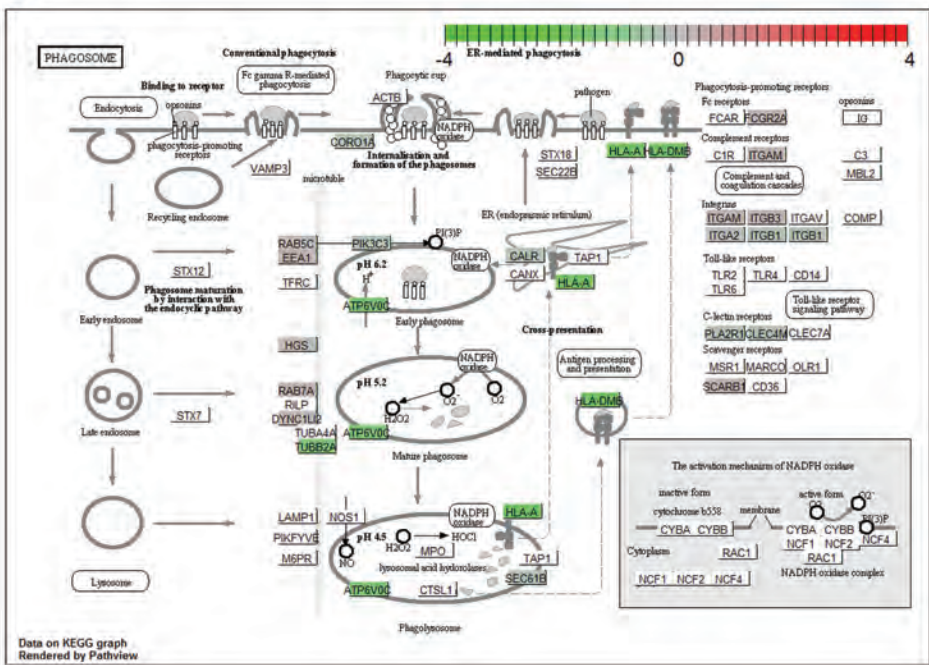
B



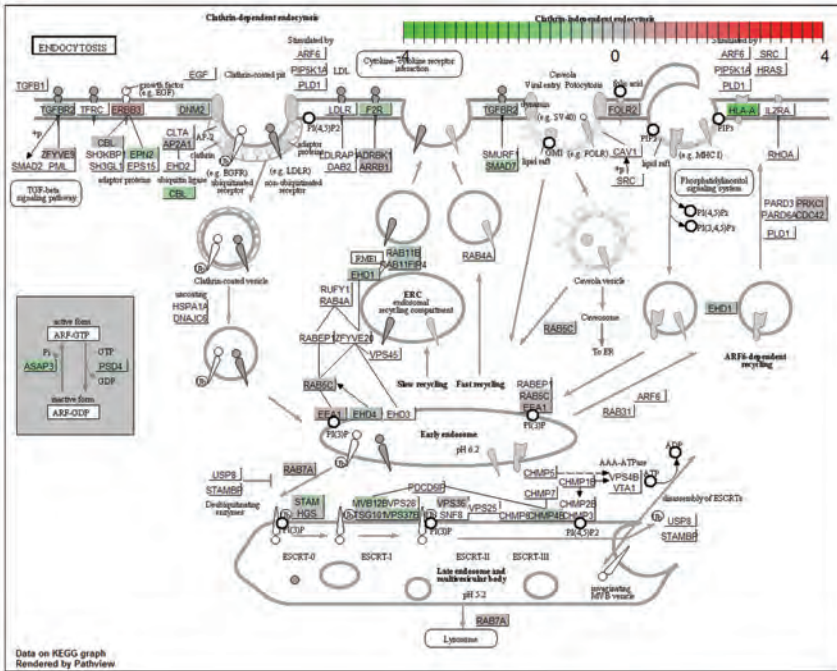
C



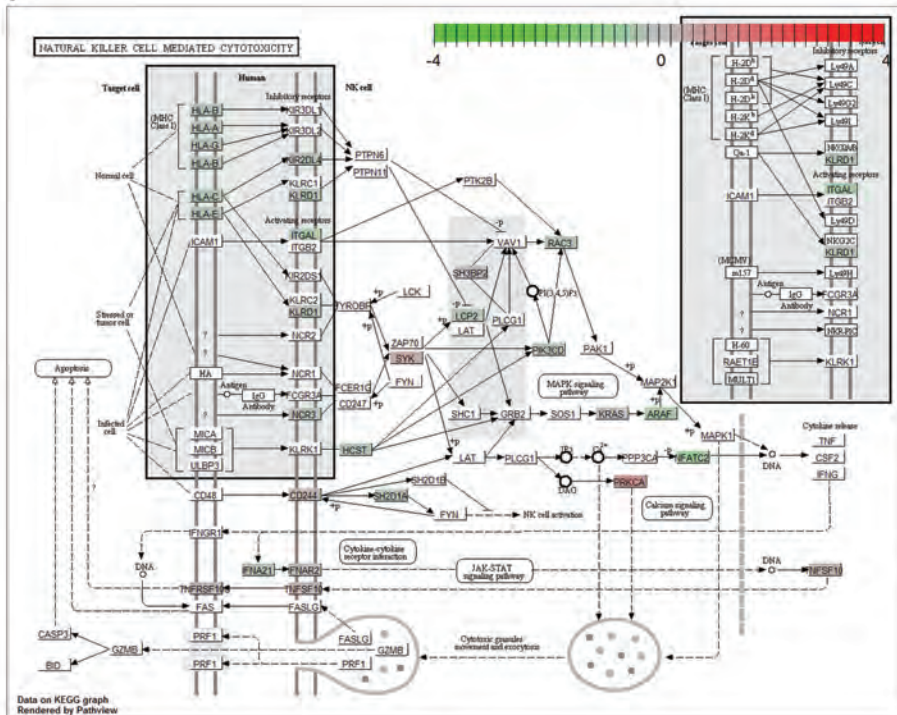
D



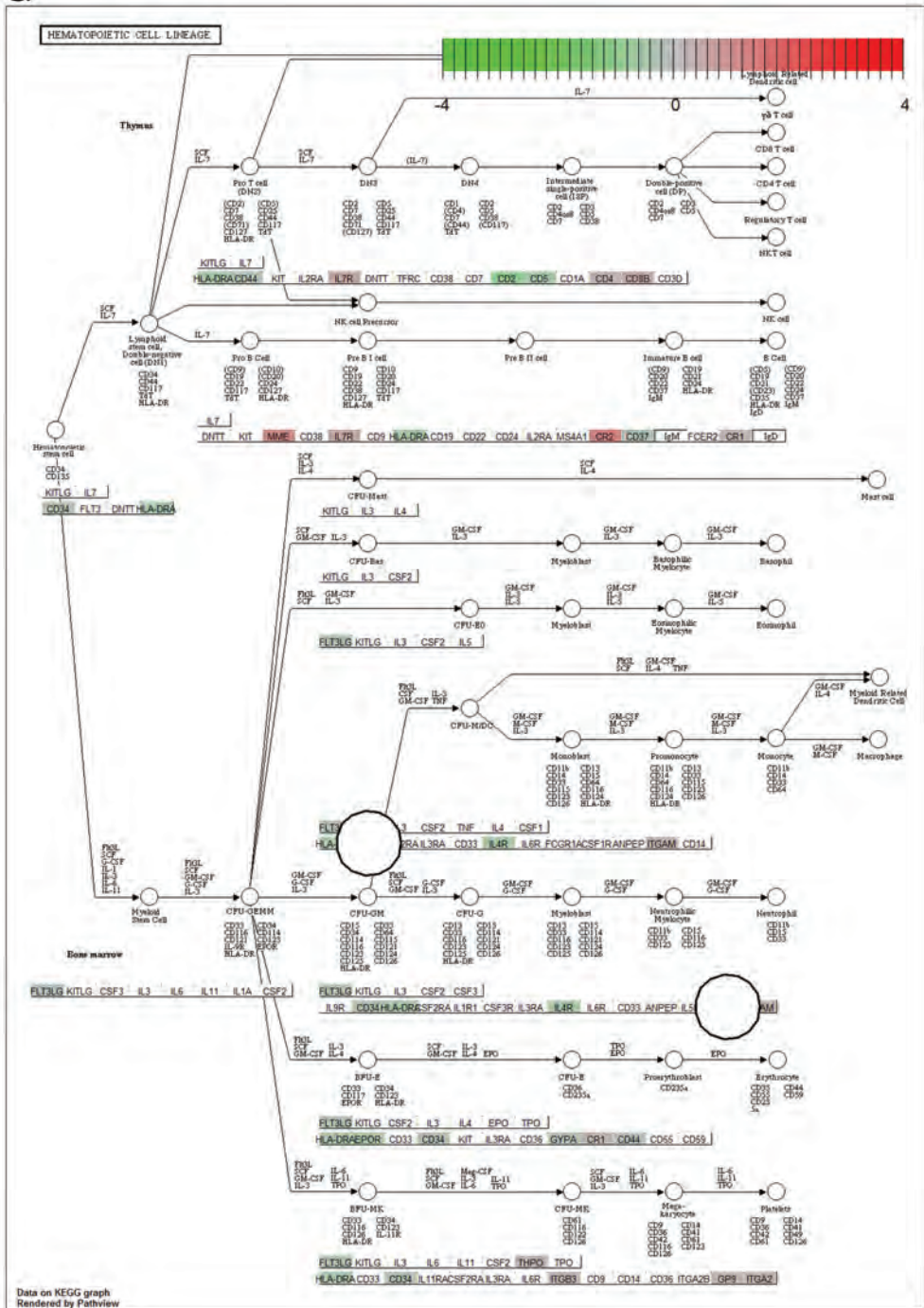
E



F



G



Data on KEGG graph
Rendered by Pathview

H

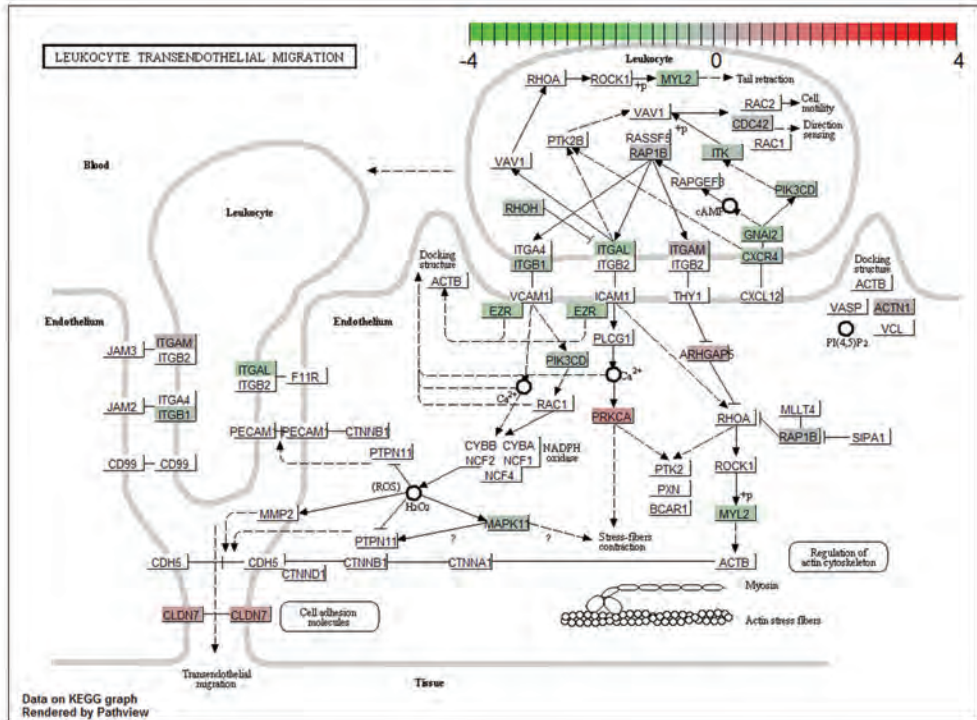
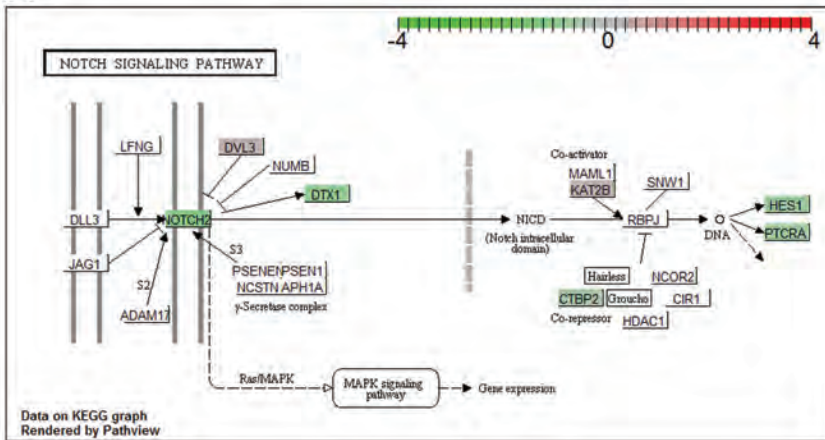
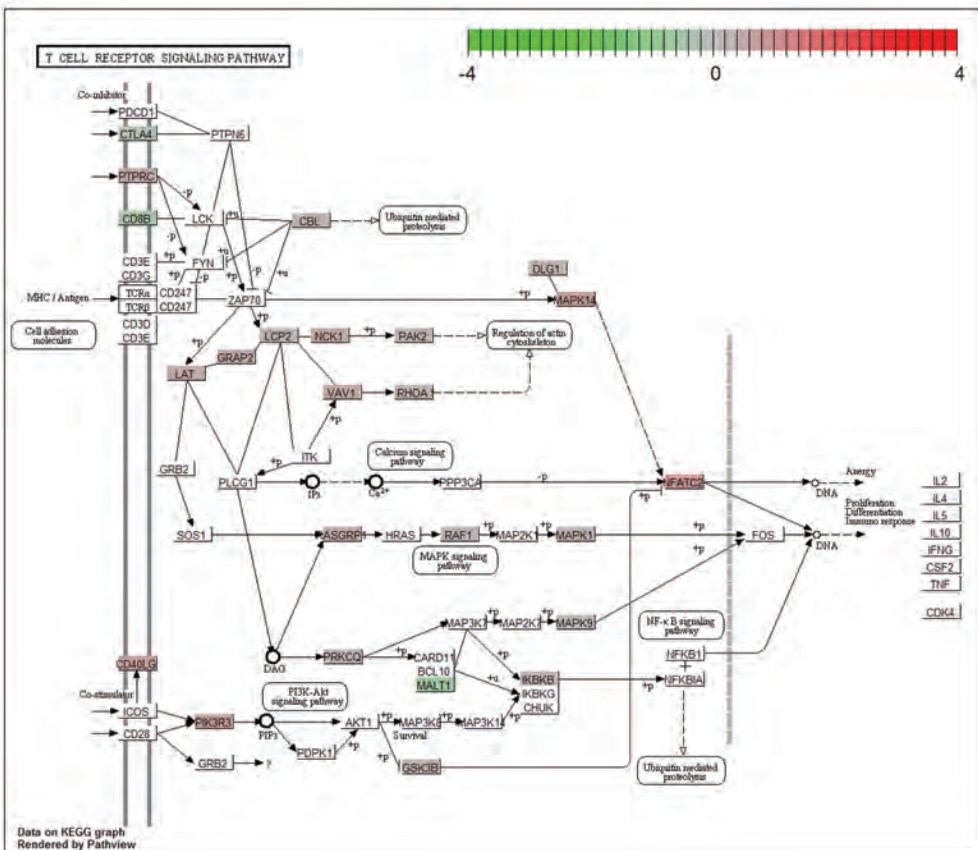


Figure S5 | Differentially expressed KEGG pathway map of NOTCH1-activated patients. (A) NOTCH signaling pathway, (B) phosphatidylinositol signaling system, (C) cell adhesion molecules, (D) phagosome, (E) endocytosis, (F) natural killer cell mediated cytotoxicity, (G) hematopoietic cell lineage, (H) leukocyte transendothelial migration.

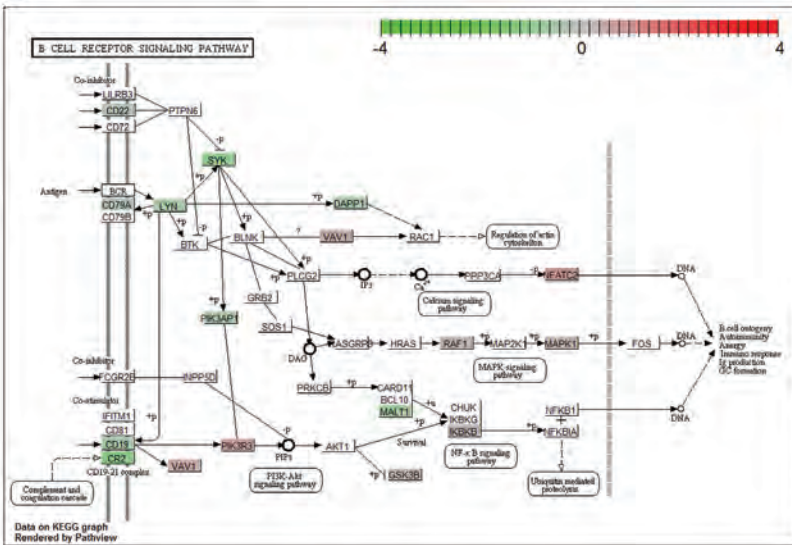
A



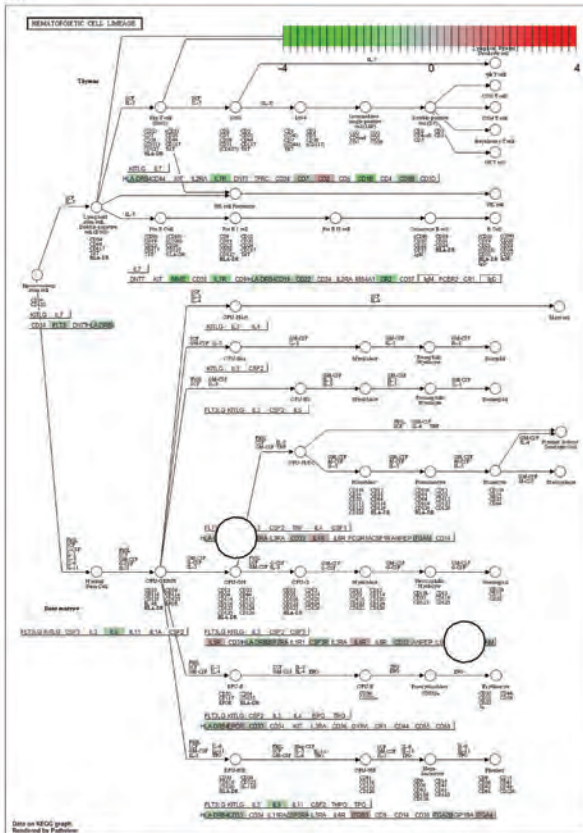
B



C

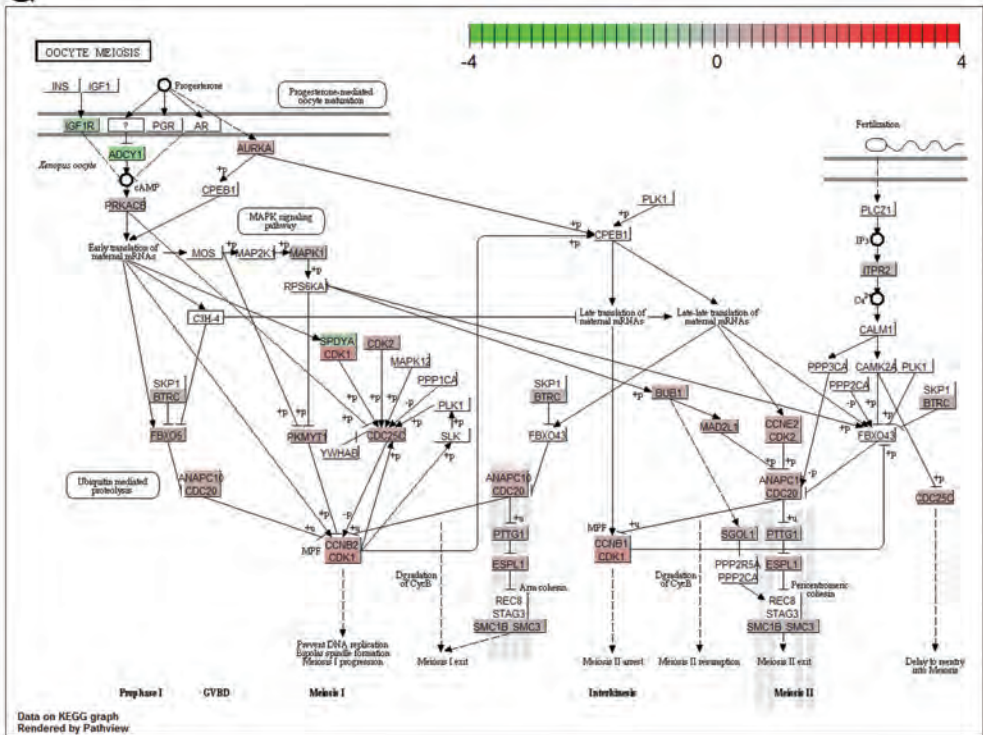


D

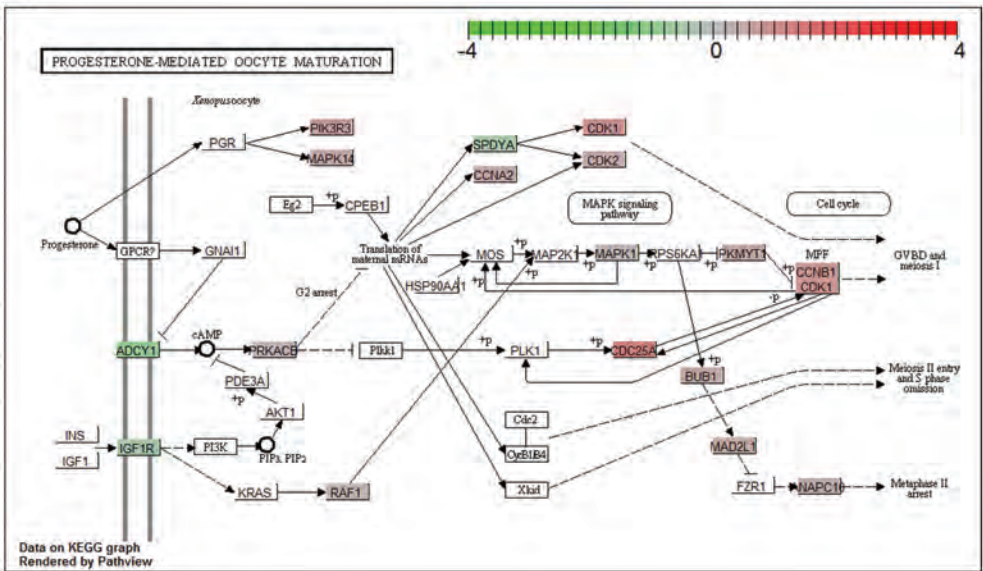


8

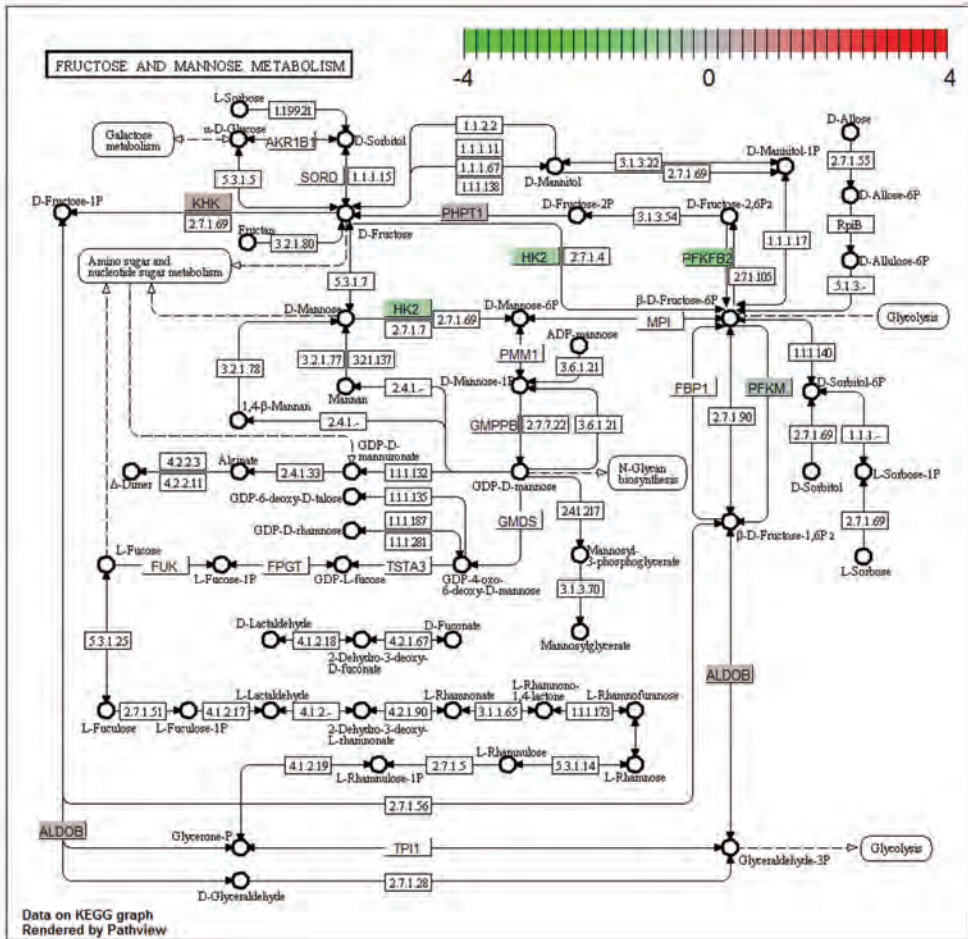
G



H



K



8

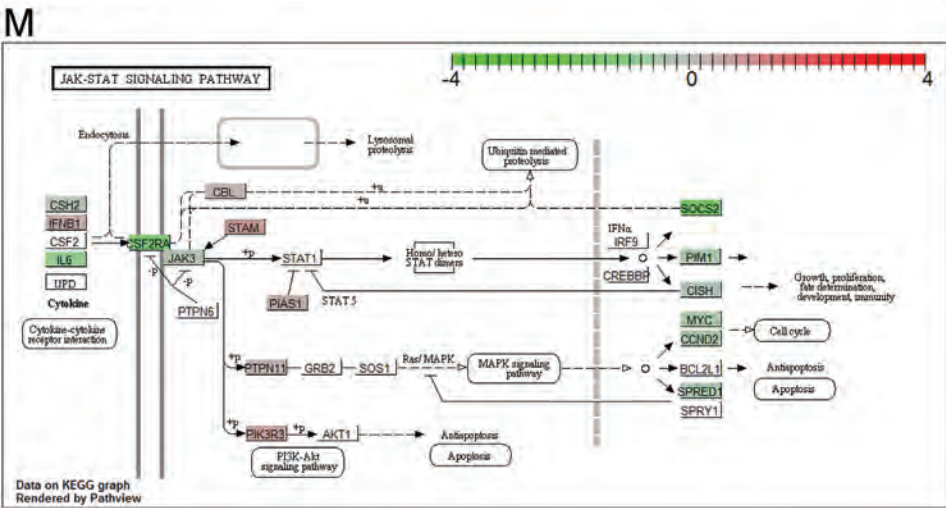
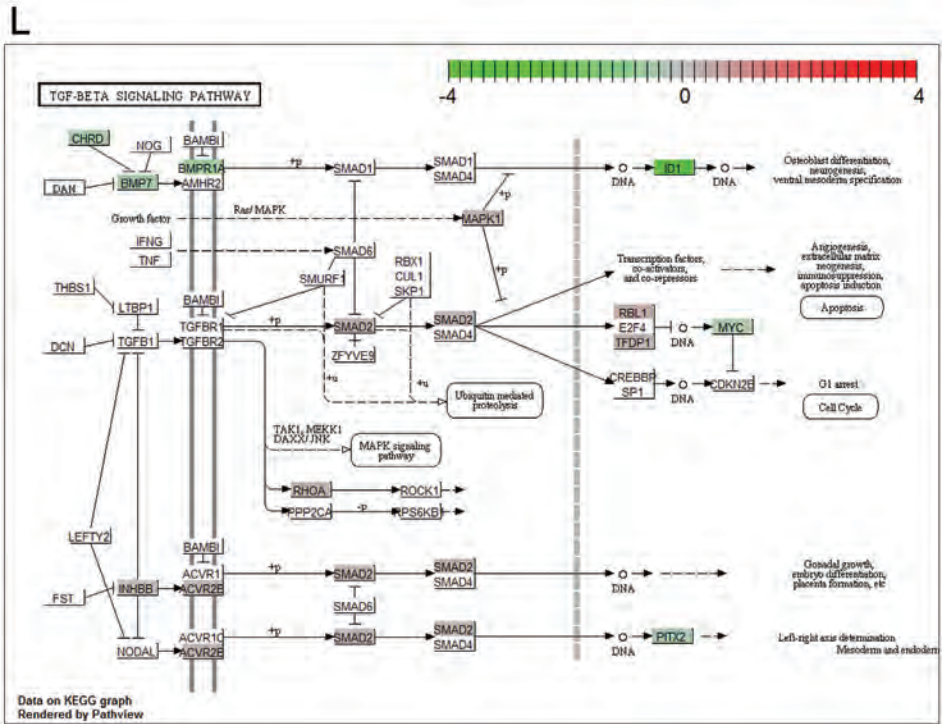
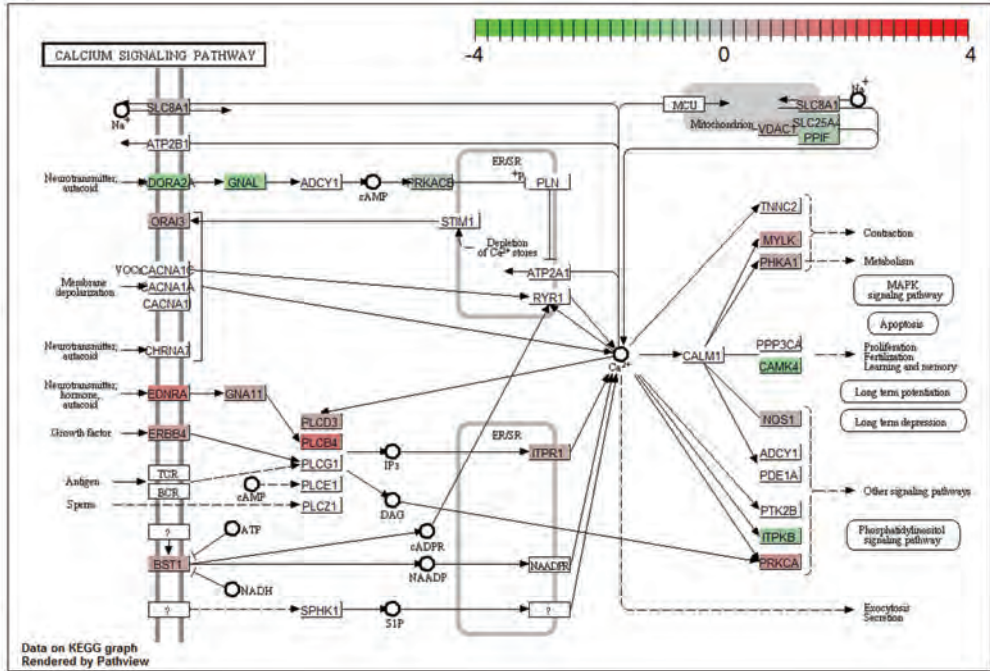
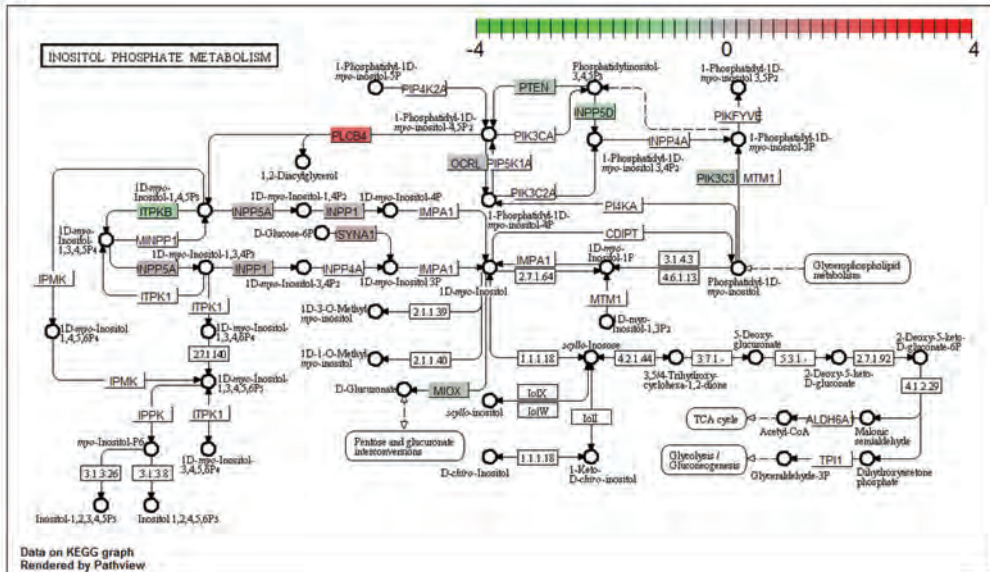


Figure S6 | Differentially expressed KEGG pathway maps of PTEN/AKT-mutated patients. (A) NOTCH signaling, (B) T-cell receptor signaling, (C) B-cell receptor signaling, (D) hematopoietic cell lineage, (E) cytokine cytokine receptor interaction, (F) p53 signaling pathway, (G) oocyte meiosis, (H) progesterone-mediated oocyte maturation, (I) pyrimidine metabolism, (J) base excision repair, (K) fructose and mannose metabolism, (L) TGF beta signaling pathway, (M) JAK-STAT signaling pathway.

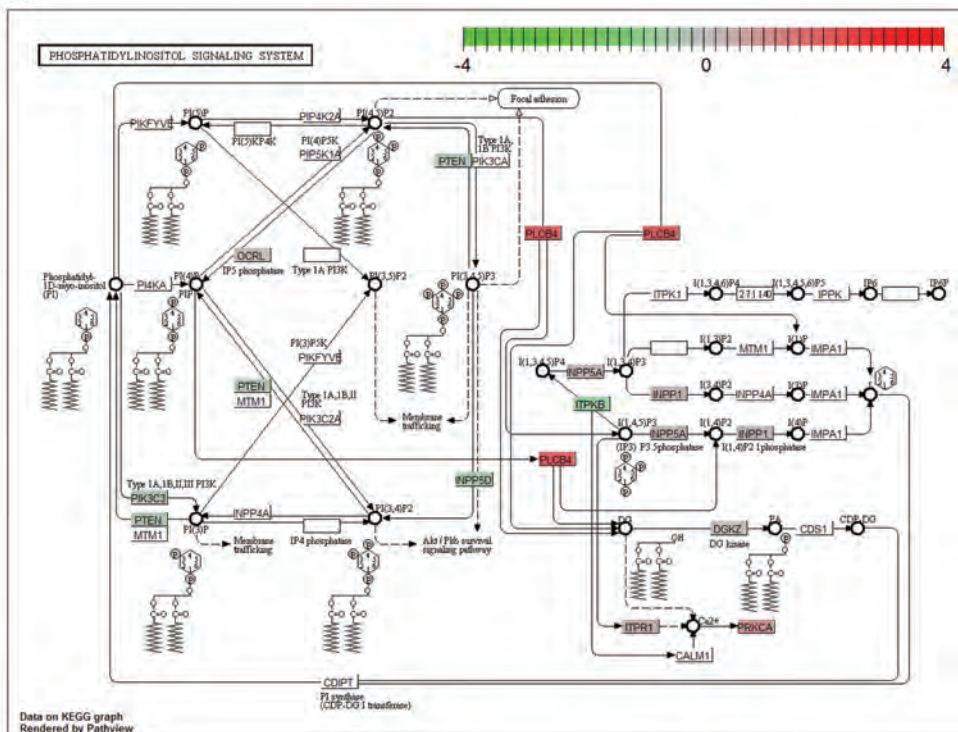
A



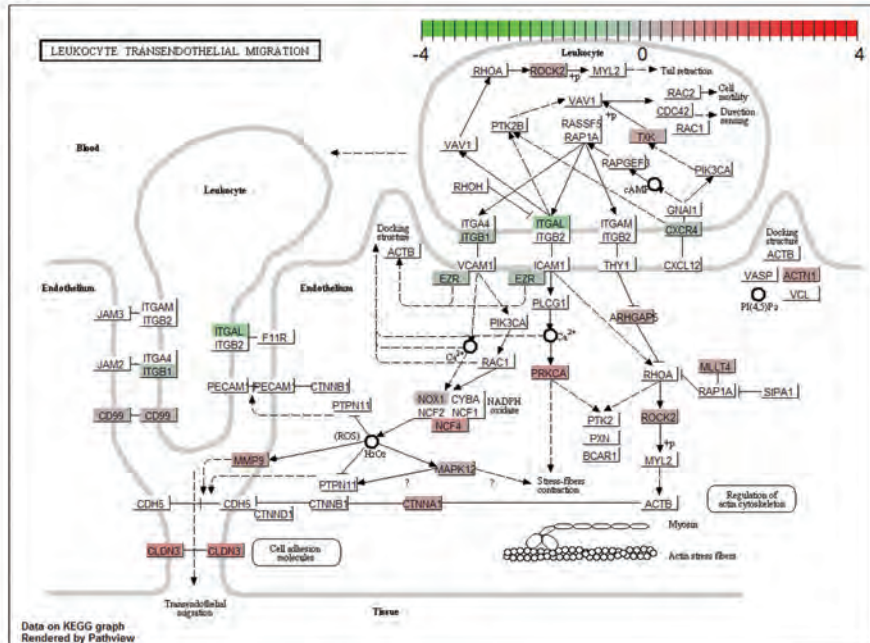
B



C



D



Protein	clonality	clone	host	company	cat. #
phospho 4E-BP1 (S65)	polyclonal	-	rabbit	cell signaling	9451
phospho 4EBP1 (T70)	polyclonal	-	rabbit	cell signaling	9455
phospho c-ABL (T735)	polyclonal	-	rabbit	cell signaling	2864
phospho ACCL (S79)	polyclonal	-	rabbit	cell signaling	3661
phospho Adducin (S662)	polyclonal	-	rabbit	upstate	06-820
phospho AKT (T308)	polyclonal	-	rabbit	cell signaling	9275
phospho AKT (S473)	polyclonal	-	rabbit	cell signaling	9271
phospho AMPKa (S485)	polyclonal	-	rabbit	cell signaling	4184
phospho AMPKb (S108)	polyclonal	-	rabbit	cell signaling	4181
Annexin A1	monoclonal	29	mouse	BD	610066
BAD	polyclonal	-	rabbit	cell signaling	9292
phospho BAD (S155)	polyclonal	-	rabbit	cell signaling	9297
BAX	polyclonal	-	rabbit	cell signaling	2772
phospho BCL2 (T56)	polyclonal	-	rabbit	cell signaling	2875
phospho BCL2 (S70)	monoclonal	5H2	rabbit	cell signaling	2827
BCL-XL	polyclonal	-	rabbit	cell signaling	2762
Calcineurin A	monoclonal	EP1669Y	rabbit	Abcam	Ab52761
β -Catenin	polyclonal	-	rabbit	cell signaling	9562
CD3e	polyclonal	-	rabbit	Abcam	Ab5690
CD3z	monoclonal	1D4	mouse	BD	556336
CD44	monoclonal	156-3C11	mouse	cell signaling	3570
CD45	monoclonal	69	mouse	BD	610265
CDK2	monoclonal	78B2	rabbit	cell signaling	2546
caspase 3	polyclonal	-	rabbit	cell signaling	9662
cleaved caspase 3	monoclonal	Asp175	rabbit	cell signaling	9661
phospho CREB (S133)	polyclonal	-	rabbit	cell signaling	9191
E2A	monoclonal	G98-271	mouse	BD	554199
phospho EGFR (Y1148)	polyclonal	-	rabbit	Biosource/Invitrogen	44-792
phospho Elk (S383)	polyclonal	-	rabbit	cell signaling	9181
phospho ERK1/2 (T204/Y202)	polyclonal	-	rabbit	cell signaling	9101
phospho FADD (S194)	polyclonal	-	rabbit	cell signaling	2781
phospho FKHR/FOXO1 (S256)	polyclonal	-	rabbit	cell signaling	9461
phospho FKHR/FOXO3 (S253)	polyclonal	-	rabbit	upstate	06-953
FKHR/FKHRL1 (T24/T32)	polyclonal	-	rabbit	cell signaling	9464
phospho Fyn (T12)	polyclonal	-	rabbit	Santa-cruz	sc-16848
phospho GSK3 α / β S21/9	polyclonal	-	rabbit	cell signaling	9331
GSK3b	polyclonal	-	rabbit	cell signaling	9332
c-HER2	polyclonal	-	rabbit	cell signaling	2242
phospho IGF-1R (Y1135/36)/IR (Y1150/51)	monoclonal	19H7	rabbit	cell signaling	3024
Ikaros	polyclonal	-	rabbit	Abcam	ab26083
IkBa	polyclonal	-	rabbit	cell signaling	9242
phospho IkBa (S32-S36)	polyclonal	-	Mouse	BD	551818
IRF-4	polyclonal	-	rabbit	cell signaling	4948
phospho JAK1 (Y1022-1023)	polyclonal	-	rabbit	cell signaling	3331
phospho c-kit (Y719)	polyclonal	-	rabbit	cell signaling	3391 ¹
phospho LCK (Y505)	polyclonal	-	rabbit	Biosource/Invitrogen	44-850
phospho MARCKS (S152-156)	polyclonal	-	rabbit	cell signaling	2741
phospho MEK1/2 S217/221	polyclonal	-	rabbit	cell signaling	9121
phospho mTOR (S2481)	polyclonal	-	rabbit	cell signaling	2974
phospho mTOR (S2448)	polyclonal	-	rabbit	cell signaling	2971
Musashi	polyclonal	-	rabbit	cell signaling	2154
c-MYC	polyclonal	-	rabbit	cell signaling	9402
NFAT2C	monoclonal	2A4	mouse	Abnova	H00004773-M01A
phospho NFkB p65 (S536)	polyclonal	-	rabbit	cell signaling	3031
phospho eNOS-peNOSII (S116)	polyclonal	-	rabbit	Upstate	07-357
Notch1 cleaved V1744	polyclonal	-	rabbit	cell signaling	2421
p27/kip	monoclonal	57	mouse	BD	610241
phospho p27 (T187)	polyclonal	-	rabbit	Zyemed	71-7700
phospho p38 (T180-Y182)	polyclonal	-	rabbit	cell signaling	9211
phospho p70 S6 kinase (T389)	polyclonal	-	rabbit	cell signaling	9205
phospho PDK1 (S241)	polyclonal	-	rabbit	cell signaling	3061
PI3K, α subunit	monoclonal	4	mouse	BD	610045
phospho PKA C (T197)	polyclonal	-	rabbit	cell signaling	4781
phospho PKC α / β (T638/41)	polyclonal	-	rabbit	cell signaling	9375
phospho PKC δ (T505)	polyclonal	-	rabbit	cell signaling	9374
phospho PKC θ (T538)	polyclonal	-	rabbit	cell signaling	9377
phospho PKC ζ (T410/403)	polyclonal	-	rabbit	cell signaling	9378
phospho PLCy (Y783)	polyclonal	-	rabbit	cell signaling	2821
phospho PRAS40 (T246)	polyclonal	-	rabbit	Biosource/Invitrogen	44-1100
PTEN	polyclonal	-	rabbit	cell signaling	9552
phospho PTEN (S380)	polyclonal	-	rabbit	cell signaling	9551
PU.1	polyclonal	-	rabbit	cell signaling	2266
phospho PYK2 (Y402)	polyclonal	-	rabbit	cell signaling	3291
phospho B-Raf (S445)	polyclonal	-	rabbit	cell signaling	2696

RAS	monoclonal	RAS10	mouse	Millipore	05-516
phospho SAPK/JNK (T183/Y185)	polyclonal	-	rabbit	cell signaling	9251
phospho SHC (Y317)	polyclonal	-	rabbit	upstate	07-206
phospho SHIP1 (Y1020)	polyclonal	-	rabbit	cell signaling	3941
phospho Smad1 (S/S)/Smad5 (S/S)/Smad8 (S/S)	polyclonal	-	rabbit	cell signaling	9511
phospho SMAD2 (S465/467)	polyclonal	-	rabbit	cell signaling	3101
c-SRC	polyclonal	-	rabbit	Santa Cruz	sc-18
phospho SRC (Y527)	polyclonal	-	rabbit	cell signaling	2105
phospho STAT1 (Y701)	polyclonal	-	rabbit	upstate	07-307
phospho STAT3 (S727)	polyclonal	-	rabbit	cell signaling	9134
phospho STAT5 (Y694)	polyclonal	-	rabbit	cell signaling	9351
phospho STAT6 (Y641)	polyclonal	-	rabbit	cell signaling	9361
phospho SYK (Y525-Y526)	polyclonal	-	rabbit	cell signaling	2711
phospho TSC2 (Y1571)	polyclonal	-	rabbit	cell signaling	3614
phospho TYK2 (Y1054-1055)	polyclonal	-	rabbit	cell signaling	9321
XIAP	polyclonal	-	rabbit	cell signaling	2042
phospho ZAP70/SYK (Y319/352)	polyclonal	-	rabbit	cell signaling	2701

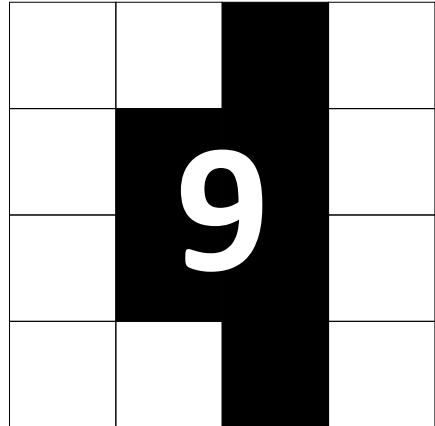
Table S1 | Antibodies used for Reverse-phase protein microarrays (RPMA).

Patient	Patient	GEP data	RPMA	Cluster	Cytogenetics	NOTCH1-activated	PTEN/AKT	WT1
1	1960	1	NA	TALLMO	SIL-TAL1	unknown	unknown	WT
2	1753	2	1	TALLMO	SIL-TAL1	WT	WT	WT
3	1815	3	2	TALLMO	unknown	MUT	WT	WT
4	9027	4	NA	TALLMO	unknown	MUT	WT	WT
5	9928	5	3	TALLMO	LMO2	MUT	WT	WT
6	2120	6	4	TALLMO	TAL1	WT	WT	WT
7	9226	7	5	TALLMO	unknown	WT	WT	WT
8	9376	8	6	TALLMO	LMO2	MUT	MUT	WT
9	1032	9	7	TALLMO	unknown	WT	MUT	WT
10	10111	10	8	TALLMO	SIL-TAL1	WT	MUT	WT
11	9963	11	9	TALLMO	unknown	WT	MUT	WT
12	8815	12	10	TALLMO	SIL-TAL1	WT	MUT	WT
13	2787	13	NA	TALLMO	LMO1	WT	MUT	WT
14	335	14	11	TALLMO	LMO3	WT	MUT	WT
15	2775	15	NA	TALLMO	unknown	MUT	MUT	WT
16	1842	16	NA	TALLMO	SIL-TAL1	WT	WT	WT
17	9160	17	12	TALLMO	unknown	WT	MUT	WT
18	258	18	13	TALLMO	SIL-TAL1	MUT	WT	WT
19	9243	19	14	TALLMO	SIL-TAL1	WT	MUT	WT
20	9323	20	15	TALLMO	TAL1	MUT	WT	WT
21	2760	21	NA	TALLMO	SIL-TAL1	WT	WT	WT
22	2789	22	NA	TALLMO	LMO2	MUT	WT	WT
23	2774	23	NA	TALLMO	SIL-TAL1	MUT	WT	WT
24	2788	24	NA	TALLMO	TAL1	MUT	WT	WT
25	2844	25	NA	TALLMO	SIL-TAL1	MUT	MUT	WT
26	1632	26	NA	TALLMO	unknown	MUT	WT	WT
27	9083	27	16	TALLMO	SIL-TAL1	WT	WT	WT
28	2117	28	NA	TALLMO	TAL2/LMO1	MUT	WT	WT
29	2720	29	NA	TALLMO	TAL1	MUT	WT	WT
30	1949	30	NA	TALLMO	SIL-TAL1	MUT	WT	WT
31	2759	31	NA	TALLMO	SIL-TAL1	WT	MUT	WT
32	2649	32	NA	TALLMO	MYC	WT	WT	WT
33	1941	33	NA	TALLMO	SIL-TAL1	WT	WT	WT
34	1950	34	NA	TALLMO	LMO2	MUT	WT	WT
35	2641	35	NA	TALLMO	NKX2-1	unknown	unknown	MUT
36	2782	36	NA	TALLMO	unknown	MUT	WT	WT
37	2794	37	17	TALLMO	unknown	WT	WT	WT
38	704	38	NA	TALLMO	LYL1(Irene)	MUT	WT	WT
39	9827	39	18	TALLMO	unknown	WT	WT	WT
40	10110	40	19	TALLMO	LMO2	MUT	WT	WT
41	2322	41	20	TALLMO	LMO2	MUT	WT	WT
42	3037	42	NA	TALLMO	SIL-TAL1	WT	WT	WT
43	492	43	NA	TALLMO	LMO2	WT	WT	WT
44	1132	44	21	TALLMO	LMO2	WT	WT	WT
45	2805	45	NA	TALLMO	unknown	WT	WT	WT
46	230	46	NA	TALLMO	unknown	WT	WT	WT
47	2436	47	22	TALLMO	unknown	WT	WT	MUT
48	2486	48	23	TALLMO	SIL-TAL1	WT	MUT	WT
49	768	49	24	TALLMO	TAL2	MUT	MUT	WT
50	9938	50	25	TALLMO	LMO2	MUT	WT	WT
51	2722	51	NA	TALLMO	TAL1	MUT	WT	WT
52	1948	52	NA	TALLMO	unknown	WT	WT	WT
53	2846	53	NA	TALLMO	LMO2	WT	WT	WT
54	2113	54	NA	CL-P	unknown	MUT	WT	WT
55	2792	55	NA	CL-P	TLX1	WT	MUT	WT
56	9919	56	26	CL-P	NKX2.1	MUT	MUT	WT
57	9989	57	NA	CL-P	NKX2.1	MUT	WT	WT
58	9696	58	27	CL-P	unknown	MUT	WT	WT
59	2669	59	28	CL-P	SIL-TAL1/LMO2	MUT	WT	WT
60	750	60	29	CL-P	SIL-TAL1	MUT	MUT	WT
61	8628	61	30	CL-P	TAL1	MUT	MUT	WT
62	2737	62	NA	CL-P	TLX1	MUT	WT	WT
63	2229	63	31	CL-P	TLX1	MUT	WT	WT
64	2781	64	NA	CL-P	TLX1	WT	MUT	MUT
65	10138	65	32	CL-P	NKX2-2	WT	WT	WT
66	1446	66	33	CL-P	NKX2.1	MUT	WT	WT
67	9247	67	34	CL-P	NKX2.1	MUT	WT	WT
68	2702	68	NA	CL-P	NKX2.1	MUT	WT	WT
69	914	69	35	CL-P	MYB	WT	WT	WT
70	3044	70	36	CL-P	CALMAF10	MUT	WT	WT
71	2691	71	37	CL-P	TLX3	MUT	WT	MUT
72	3028	72	NA	CL-P	TLX3	MUT	MUT	MUT

73	8639	73	NA	TLX	SETNUP214	MUT	WT	WT
74	1113	74	NA	TLX	SETNUP214	MUT	WT	WT
75	2911	75	38	TLX	Inv(7)	MUT	WT	MUT
76	1570	76	39	TLX	HOXA	MUT	WT	WT
77	8577	77	40	TLX	SETNUP214	MUT	WT	MUT
78	222	78	NA	TLX	TLX3	MUT	WT	MUT
79	2757	79	NA	TLX	TLX3	MUT	WT	WT
80	634	80	41	TLX	TLX3	WT	WT	WT
81	2723	81	NA	TLX	TLX3	MUT	WT	MUT
82	2780	82	NA	TLX	TLX3	MUT	WT	WT
83	1179	83	42	TLX	TLX3	MUT	WT	WT
84	749	84	43	TLX	TLX3	WT	WT	WT
85	1946	85	NA	TLX	TLX3	MUT	WT	MUT
86	720	86	44	TLX	TLX3	MUT	WT	MUT
87	9421	87	45	TLX	TLX3	MUT	WT	MUT
88	378	88	46	TLX	TLX3	MUT	WT	WT
89	9858	89	47	TLX	TLX3	MUT	WT	MUT
90	2750	90	NA	TLX	CALMAF10	MUT	WT	WT
91	1944	91	NA	TLX	TLX1	MUT	WT	WT
92	1955	92	NA	TLX	TLX1	MUT	unknown	WT
93	2772	93	NA	TLX	TLX3	MUT	WT	WT
94	2650	94	NA	TLX	TLX3	MUT	WT	WT
95	1954	95	NA	TLX	TLX3	unknown	unknown	WT
96	9757	96	48	TLX	TLX3	MUT	WT	WT
97	759	97	49	TLX	TLX1	WT	WT	WT
98	9012	98	50	TLX	TLX3	WT	WT	WT
99	1701	99	NA	TLX	TLX2	MUT	WT	WT
100	2509	100	NA	TLX	TLX3	MUT	WT	WT
101	585	101	51	TLX	TLX3	MUT	WT	MUT
102	9830	102	NA	TLX	TLX3	unknown	WT	WT
103	2703	103	NA	Immat	unknown	WT	WT	WT
104	2130	104	NA	Immat	unknown	MUT	WT	WT
105	2252	105	52	Immat	PU.1	WT	WT	WT
106	572	106	53	Immat	RUNX1AFF3	MUT	WT	WT
107	9194	107	NA	Immat	HOXA	MUT	WT	WT
108	321	108	54	Immat	unknown	MUT	MUT	WT
109	491	109	55	Immat	MEF2C	MUT	WT	WT
110	10030	110	NA	Immat	unknown	MUT	WT	WT
111	1964	111	56	Immat	MEF2C	WT	WT	WT
112	1524	112	57	Immat	ETV6NCOA2	MUT	WT	WT
113	167	113	58	Immat	unknown	MUT	WT	WT
114	1509	114	59	Immat	CALMAF10	WT	WT	WT
115	2736	115	NA	Immat	CALMAF10	WT	WT	WT
116	9577	116	60	Immat	NKX2-5	MUT	MUT	WT
117	9105	117	61	Immat	MYB	WT	WT	WT
118	531	NA	62	ND	SIL-TAL1	WT	MUT	WT
119	419	NA	63	ND	TLX1	MUT	WT	WT
120	540	NA	64	ND	MLL	WT	WT	WT
121	344	NA	65	ND	LMO2	MUT	MUT	WT
122	2460	NA	66	ND	unknown	MUT	WT	WT

Table S2 | Characteristics of patients used for gene expression arrays and reverse phase microarrays.

CHAPTER



Summary

Future prospective
Nederlandse samenvatting

SUMMARY

T cell acute lymphoblastic leukemia (T-ALL) is a very heterogeneous disease involving a spectrum of genetic events resulting in the uncontrolled expansion of immature T-lymphocytes (blasts). This multicomination of genetic events seems different in each patient. Two types of mutations occur in T-ALL which we categorized as type A mutations and type B mutations¹. Type A mutations are characterized as clonal chromosomal rearrangements that activate oncogenes mainly involved in cell differentiation. Ectopic expression of the oncogenes provoke a specific T cell developmental block and accompanying gene expression profile. Four expression clusters have been identified so far, ie. the TALLMO, TLX, proliferative and immature/ETP-ALL (early thymic progenitor ALL) clusters. In general, type B mutations occur in any of the identified T-ALL clusters, although some may have preferences for particular subtypes. Type B mutations affect molecules that participate in classical signal transduction pathways like NOTCH or PI3K/AKT signaling, cell cycle of cytokine receptors^{1,2}.

Associations of particular mutations with T cell phenotype or with additional mutations have been noticed³, however, the biological rationale behind this is still not clear. An explanation for the association of mutations with a T cell phenotype is that the activity of a gene can vary between T cell development stages under normal circumstances. It may therefore be more prone to mutate during the stage in which it is active (open chromatin). Alternatively, mutations (or their counterpart) are potential oncogenic at one particular development stage only. An explanation for the co-expression of particular mutations may be the additive/synergistic oncogenic potential of some combinations. Another reason may be that a cell needs guaranty that a particular mechanism is dysregulated, in terms of oncogenic addiction, and therefore multiple hits interfering with one mechanism may be present. Gaining knowledge regarding these topics is hampered by the fact that T-ALL involves many genetic alterations and many are still undiscovered. This comes along with the drawback that a leukemic cell can have many mutations but only a few have the potential to alter cell proliferation or self-renewal activity (driver mutations) and others are present but lack oncogenic capacity (passenger mutations)⁴.

Currently, the survival rate of children with T-ALL is around 80% for patients treated on one of the latest treatment protocols, e.g. the ALL10 protocol⁵. Twenty percent of patients relapse. Outcome for relapsed patients is extremely poor due to acquired therapy resistance, resulting in death for most relapsed patients. T-ALL treatment is based on combinational chemotherapy⁶. As children are still in development late side-effects can have a major impact. For this reason, the reduction of side-effects in children is very important which can be achieved by treatment stratification. Based on current protocols many patients may receive super-or suboptimal therapy. High doses of drugs are already given to high-risk patients and improvement of treatment now requires targeted therapy. This therapy should, in most optimal situation, be directed to driving oncogenic aberrations.

To answer questions above and to improve treatment stratification, we aimed to map the most frequent aberrations in a cohort of 146 pediatric T-ALL patients treated according to DCOG ALL7/8/9 or COALL-97 protocols to determine the heterogeneous landscape of alterations in children with T-ALL. Furthermore, we have correlated specific features with survival of patients. In addition, we extended our genetic analyses by examining pathway expression at transcriptional and translational level that are changed as a consequence of different genetic aberrations that occur in T-ALL patients.

Chapter 2 provides an overview of our current understanding of genetic aberrations in T-ALL. This includes type A aberrations, but focuses more on the different pathways that are most likely to be dysregulated as a consequence of type B aberrations.

In our study NOTCH1-activating type B mutations were first mapped (**chapter 3**), which activate the NOTCH pathway and is the most recurrently mutated pathway in T-ALL found so far. Sixty-three percent of patients in our cohorts have NOTCH1-activating mutations. Most other studies have screened for NOTCH1-activating mutations in mutational hotspots. We screened almost the entire gene except for the EGF-repeats and the LNR domain of the *NOTCH1* gene, as well as a large part of the *FBXW7* gene. *FBXW7* can target NOTCH1 for proteosomal degradation. Our study confirmed that most *NOTCH1* mutations are present in the heterodimerization and juxtamembrane domain as well as in the *FBXW7*-targeted PEST domain of NOTCH1. Mutations are rare in the ANK, TAD and RAM domains^{7,8}, and none were found in our cohort. New mutations in the *FBXW7* gene were revealed, of which most were at the far C-terminal end of the gene. We observed a negative association of NOTCH1-activating mutations and *TAL1* or *LMO2* family members. As most of these patients are arrested at a late T cell developmental stage, NOTCH1-activating mutations were also negatively associated with the presence of mature T cell markers. Mutations were also positively associated with *TLX3* rearrangements. Patients with NOTCH1-activating mutations expressed a clear distinct NOTCH1-activated RNA signature, that included some known NOTCH1-regulated genes. This signature can contribute to the biological understanding of NOTCH1 activity which is important for specific therapeutic development. For the first time in patient samples we revealed that mutated patients have, as was already hypothesized based on cell line data, increased activated NOTCH1 (ICN) protein levels. Interestingly, when patients were subdivided based on weak or strong NOTCH1-activating mutations, as previously documented in *in vitro* and *in vivo* models⁹, ICN was indeed expressed at lower levels in patients presenting with weak NOTCH1-activating mutations compared to patients with strong NOTCH1-activating mutations. This pattern was similar at gene expression level. An additional ten patients showed either high ICN levels or its target genes and seem to lack NOTCH1-activating mutations or *NOTCH1* translocations. This indicates the presence of additional, yet unidentified genomic alterations may be present in a minor part of patients presumably in the *NOTCH1* EGF or LNR repeats, remaining sequences of the *FBXW7* gene or in other NOTCH1-regulating genes. This means not all NOTCH1-activated patients are identified

yet. Patients with NOTCH1-activating mutations have poor relapse-free survival rates in our cohorts, but strikingly, have a better initial prednisone response *in vitro*. The clinical impact of NOTCH1 mutations and prognosis is inconsistent among study cohorts. These discrepancies might be created by several factors; the existence of different treatment protocols and outcome parameters used, yet unidentified NOTCH1-activating mutations and differences in distribution of weak and strong NOTCH1-activating mutations which may be different entities with a distinct treatment response. Indeed, we noticed different survival rates between these (weak and strong) patient groups in DCOG cohort patients, however this could not be confirmed in COALL cohort patients.

A relation between NOTCH1 and PTEN expression was described by Palomero et al.¹⁰, who described PTEN as being a downstream NOTCH1 target via HES1 and leading to AKT activation. As a proper GSI response required low or normal AKT levels, loss of the AKT inhibitor PTEN was believed to result in GSI resistance. To investigate the role of PTEN in T-ALL and its relation to NOTCH1 and potential therapeutic inhibition, our cohort was screened for *PTEN*, *PIK3CA* (PI3K isoform), *PIK3RI* (PI3K isoform) and *AKT1* type B genetic aberrations (**chapter 4**). During this screen, we identified a new mechanism for PTEN-silencing in pediatric T-ALL in a minor part of patients, which involved aberrant *PTEN*-splicing that resulted in absence of PTEN protein. Taken all patients with identified aberrations (*PTEN* mutations/deletions, *AKT1* mutations and loss of PTEN protein due to incorrect splicing or yet unidentified mechanisms) together, 13% of patients have *PTEN/AKT* mutations. All patients with nonsense mutations or deletions of *PTEN* did have low or no PTEN protein expression, depending on the mono-allelic or bi-allelic mutation status. Total absence of PTEN in some mono-allelic mutated patients suggest for alternative yet unidentified inactivation of PTEN. No differences in the levels of activated downstream proteins involved in AKT-mTOR pathway, or other AKT downstream proteins (PRAS40 and forkhead transcription factors) were measured in *PTEN/AKT*-mutated patients compared to wild-type patients. In contrast to what we expected based on the data from the Palomero study¹⁰, *PTEN/AKT* mutations were negatively associated with NOTCH1-activating mutations. Some *PTEN/AKT*-mutated patients had only weak NOTCH1-activating mutations. Patients with *PTEN/AKT* mutations had significantly low levels of NOTCH1 pathway proteins MYC and musashi. *PTEN/AKT* mutations were predominantly present in TALLMO patients and were associated with a mature T cell development stage. TLX patients were remarkably devoid of *PTEN/AKT* mutations, a pattern that seemed nearly reciprocal to NOTCH1-activating mutations. *PTEN/AKT* mutations were not associated with outcome per se. Nevertheless, taken poor prognostic NOTCH1-activating mutations into account as their presence negatively correlates with *PTEN/AKT* mutations, we observed good survival rates for *NOTCH1/FBXW7/PTEN/AKT* wild-type patients and poor survival rates for NOTCH1 activating and/or *PTEN/AKT*-mutated patients.

We further investigated *PTEN* splice defects in **chapter 5**. There we found evidence that these splice variants were due to micro-deletions affecting one or a few exons. Deletions were flanked by conserved immunoglobulin recombination signals and contained insertion of random nucleotides. This suggested that these deletions were a consequence of aberrant RAG-mediated

recombination events.

Screening of type B mutations was extended by the examination of *IL7Rα*, *JAK* and *RAS* mutations in **chapter 6**. We did not detect any *JAK2* or *TYK2* mutations. *IL7Rα* mutations in our cohort have been reported before¹¹ and were detected in 8% of the patients. *N-RAS/K-RAS* mutations were detected in 10% and *JAK1* and/or *JAK3* mutations in 7% of patients. Strikingly, except for one case, *IL7Rα* mutations were devoid of any other of these mutations. Also *PTEN/AKT* mutations did not co-occur together with *JAK* mutations and seldomly with *RAS* mutations. All *JAK* mutants that we tested had transformation capacity, as they showed IL3-independent growth in Ba/F3 cell lines. Wild-type *JAK1* or *JAK3* did not. Also *AKT* and *N-RAS* mutations induced IL3-independent growth. Protein analysis revealed increased expression of phosphorylated JAK-STAT, RAS-MEK-ERK and *PTEN/AKT* pathway proteins in *IL7Rα*-mutated patients. Interestingly, different *IL7Rα* and *JAK1* mutants did not activate similar downstream molecules to the same extent, however they all resulted in comparable elevated p70 S6 kinase activity. Also, *JAK3* mutants resulted in very robust IL3-independent growth compared to *IL7Rα* and *JAK1* mutants, although downstream phosphorylated signaling molecules were relatively weakly expressed. *IL7Rα* and *JAK1/3* but not *N-RAS* and *AKT* mutant cell lines were sensitive to the *JAK* inhibitor Ruxolitinib, which was accompanied by reduced downstream signaling molecules in *IL7Rα* and *JAK1/3*-mutated lines but not in *N-RAS* and *AKT*-mutated lines. Downstream STAT5 inhibitor did only moderately reduce growth of *JAK1* mutant lines but not in *IL7Rα* mutant lines, suggesting that *IL7Rα* mutants can signal through an alternative pathway, eg. RAS-ERK-MEK or PI3K/AKT. *JAK1/3* mutants but not *IL7Rα* mutants were sensitive to the PI3K/AKT-blocking agent LY294002. Combined RAS-MEK-ERK and PI3K/AKT pathway inhibitors in a *JAK1* and *IL7Rα* mutant line, significantly reduced phosphorylated signaling compared to single agent treatment. The insensitivity for single LY294002 treatment but sensitivity for LY294002 treatment combined with RAS-ERK-MEK inhibition suggests that the IL7R can signal through both pathways, but activates the RAS-MEK-ERK pathway for sustained survival when the PI3K/AKT pathway is blocked and vice versa.

Our group recently described a new cluster of patients based on unsupervised gene expression cluster analysis which have been associated with genetic aberrations that activate MEF2C¹². This group of patients is a very immature T-ALL phenotype with frequent co-expression of myeloid markers and herein called immature cluster. Two studies have been published that described a comparable group of patients; one T-ALL entity denoted as early T cell precursor (ETP) ALL which was identified using cluster analysis based on a previously established early T cell precursor (ETP) mouse RNA expression profile¹³. ETP-ALL is described as being an immature leukemia with stem cell and myeloid features with mutations in genes involved in hematopoietic and lymphoid development as well as in myeloid-specific oncogenes. Another early T-ALL entity was identified by lack of the TCRγδ (TRG@) gene and were denoted as ABD patients¹⁴. In **chapter 7**, we investigated the overlap of these different features in our T-ALL cohort. Our described immature cluster patients strongly resemble ETP-ALL patients based on the conservation of a human ETP-ALL gene expression profile (13 of our 15 immature patients were also ETP-ALL).

About half of our immature T-ALL cluster patients had no TCR $\gamma\delta$ deletions, indicating that ABD may represent a subtype within immature/ETP-ALL patients. We further observed that our immature cluster patients could not be predicted by the originally proposed immunophenotype for ETP-ALL patients. We proposed an alternative immunophenotype that correlated with our ETP-ALL patients. Our patients were associated with absence of CD1 and CD8 expression but also absence of CD4 expression, but with frequent expression of CD34 and/or CD13 or CD33. The stem cell-like phenotype of immature/ETP-ALL patients based on gene set enrichment analyses of gene expression microarray data was confirmed. In contrast to what has been described for ETP-ALL patients, immature/ETP-ALL patients treated on the COALL97/03 protocol did not have very poor survival rates and had equal sensitivity *in vitro* to various chemotherapeutic agents compared to other T-ALL patients. Based on the first described ETP-ALL study and two others that followed, it had been proposed to intensify treatment for these patients in the clinic as soon as possible. Our data point to more careful further evaluation of the prognostic significance of immature/ETP-ALL patients first. A trend for lower responsiveness of immature T-ALL/ETP-ALL patients to steroid treatment was observed. Our patients had received higher doses of cytarabine compared to other studies. We therefore suggest to evaluate the cytarabine dose for these patients that might explain the higher survival rates we observed for immature/ETP-ALL patients compared to other studies.

The consequences of all different genetic hits on pathway level are largely unknown. Therefore, in **chapter 8** we investigated differential pathway expression in T-ALL patient groups that reflect type A mutations or T-ALL patient groups based on type B mutations, using whole genomic transcriptome data and proteome data. In TALLMO patients, we observed a high expression of genes and proteins of T cell receptor (TCR) signaling and of metabolic glycolysis and lipid signaling, including GSK3. This suggests that these processes are important for cell function in these patients and therefore, it would be worthwhile to test the effect of kinase inhibitors, glycolysis and lipid inhibitors or specific GSK3 inhibitors in TALLMO patient samples. TLX cluster patient samples were clearly associated with NOTCH1 signaling. This extended our previous observations from chapter 3 that pointed to a very high NOTCH1-activating mutation rate which predominantly involved strong NOTCH1-activating mutations in *TLX3* patients. Besides this notion, NOTCH signaling was also observed in some NOTCH1 wild-type patients. This supports the idea of existing yet unidentified genetic aberrations that activate the NOTCH1 pathway (chapter 3) or suggest addiction to NOTCH1 signaling within this patient group, which is mediated by HOX-regulated NOTCH signaling. It would be very interesting to consider the *TLX3* T-ALL group for therapeutic NOTCH1 inhibition. Proliferative cluster patients had a high expression of genes involved in circadian rhythm. Restoring it would be a potential for therapy. The very high proliferative activity and DNA damage response in this cluster¹² was confirmed in this study. We measured high levels of p53 gene transcripts but a low expression of downstream genes/proteins, what might suggest low function activity of p53 through interference with p53 stability, localization, transactivation or DNA-binding capacity in this group. In addition to conventional chemotherapy, kinase inhibitors should be carefully studied as a potential therapeutic option for

these patients. This analysis showed that immature cases have a very low TCR signaling but very high B cell receptor signaling. Expression of cell adherence molecules is low. These observations may reflect the very early T cell arrest of this leukemia. Interestingly, these cells seem relatively proliferative and migratory inactive. We observed an interesting link between *MEF2C* and the *p38 MAPK* which seems very promising for further investigation. According to type B mutations, we confirmed the importance of the tumor suppressor gene p27 downstream of NOTCH1^{15,16} and observed low levels of PKC θ . PKC θ is a protein very recently described as being indirectly downregulated through NOTCH1 via RUNX3 and RUNX1¹⁷. In contrast, PKC θ levels were high in *PTEN/AKT*-mutated patients that are mostly devoid of NOTCH1-activating mutations or bear only weakly-activating mutations (chapter 4). These patients also had high expression levels of TCR genes and a very active proliferative signature. This makes also this group attractive for kinase inhibitors. *WT1*-inactivated patients showed very high levels of growth factor receptors and downstream signaling. As the functional role of *WT1* in T-ALL is unknown, the role of WT1 in translational repression of growth factors is an interesting mechanism to investigate, as well as the sensitivity of WT1-inactivated patient cells to well-known growth factor inhibitors.

FUTURE PROSPECTIVE

T-ALL is characterized by a variety of rearrangements and gene mutations, making a uniform targeted therapeutic approach difficult for this disease. Each patient displays a different mutation pattern and may therefore have a different response to therapy. To improve the survival rates of children with T-ALL and to decrease the severity of (long-term) side-effects, we aim for a better stratification of patients based on molecular-cytogenetic data and the development of targeted therapy.

Progression of T-ALL research with new tools

Major steps have been made due to new analytical techniques that continue to be developed in the near future, and that may help us to clarify disease biology and develop better treatment strategies. For example, next generation sequencing (NGS) in which whole patient genomes are screened is more and more being applied, enabling investigators to obtain a full spectrum of genetic aberrations that are present in each patient. Furthermore, data on relatively newly discovered transcriptional mechanisms including epigenetic modifications like DNA methylation and gene expression regulation by miRNA's, will further complete and complicate the picture. Bioinformatic tools will become more applicable and understandable, making it easier to integrate and interpret all data. These new techniques and data analyses tools enable researchers to obtain a more complete, and profound overview of oncogenic mechanisms. For example, novel NOTCH1-activating mutations may be identified with these tools in the future, that may clarify observed differences in the prognostic significance of NOTCH1-activating mutations among study cohorts. Also, other new genetic aberrations can now be easily identified and help to improve patient stratification. Information about downstream effects at the protein level is needed to provide more knowledge about interactions of activated pathways, which may reveal potential druggable targets or disease biomarkers. New techniques like the reverse-phase protein microarray (RPMA) provide accessibility to measure and understand these data as they include less experimental bias and more endpoints in one assay compared to conventional techniques like western blotting. Our studies already showed the advance of proteomic studies by identifying an additional mechanism of PTEN-silencing as well as by revealing the possibility for presence of novel NOTCH1-activating mutations. Techniques like NGS and RPMA can also be used when rather limited amounts of patient materials are available which is often a weakness of older techniques. High-throughput screens to identify druggable targets have also become a useful tool, for example siRNA libraries can identify expression of pivotal genes for tumorigenesis or disease resistance by silencing.

NOTCH1 and PTEN in T-ALL

An interesting topic in pediatric T-ALL is the relation between aberrant NOTCH1 and PTEN signaling. In 2007, *Palomero et al.* reported a direct mechanistic association between NOTCH1 and PTEN in T-ALL¹⁰. They suggested that PTEN is a downstream target of NOTCH1 via HES1,

resulting in AKT upregulation. As a consequence, *PTEN/AKT* mutations would provoke resistance to gamma-secretase inhibitors (GSIs) as these mutations result in continuously NOTCH1 downstream signaling independent of NOTCH1 activity. We doubt the clinical relevance of this proposed mechanism as we showed these two classes of mutations are almost never co-expressed in the same leukemic clone. In fact, NOTCH1-activating mutations and *PTEN/AKT* mutations seem to have a nearly reciprocal pattern. As a consequence, GSI resistance in *PTEN/AKT*-mutated patients may be due to the wild-type *NOTCH1/FBXW7* genotype of these cells which are less sensitive for GSIs, rather than due to interference with downstream NOTCH1 signaling. The inverse correlation of both mutations in one leukemic clone can be due to their association with different T cell development stages or type A mutations or due to the participation of both proteins in the same signaling pathway, as proposed¹⁰. In the latter situation, mutations in both genes might not have an additive effect concerning strong NOTCH1-activating mutations. However, weak NOTCH1-activating mutations may not be potent enough for proper AKT activation. Therefore, additional *PTEN/AKT* mutations may have benefits in weak NOTCH1-activated patients by provoking adequate AKT activation. If NOTCH1-activating mutations indeed result in PTEN inhibition and subsequent AKT activation, this may explain the equal levels of AKT and downstream AKT proteins between *PTEN/AKT*-mutated and *PTEN/AKT* wild-type (but predominantly NOTCH1-activated) patients. Our studies focuses on differences between groups and might therefore not identify important mechanisms in groups with similar pathway activation. Instead, more attention should be drawn to the similarities between the NOTCH1 and PTEN/AKT pathway in future studies.

NOTCH1 and patient outcome

Various studies have investigated the role of the NOTCH pathway for prognosis prediction of pediatric T-ALL patients, but the overall conclusion is unclear. Whereas some studies reported good survival rates for *NOTCH1*-mutated patients, other studies, among ours, reported similar or poor survival rates between mutated and *NOTCH1* wild-type patients^{3,7,8,18-24}. This variation between studies is probably due to the widespread role of the NOTCH pathway, the high rate of different and probably yet undiscovered mutations and the variety in treatment protocols around the world. In addition, interpretation is hampered as different studies use different outcome parameters, like minimal residual disease, *in vitro* therapy response, relapse-free, event-free or overall survival rates. Moreover, mutational screening is often incomplete thereby introducing extra bias. In this light, is of utmost important that clinical and research-based studies become more generalized. Furthermore, it is important to take additional aberrations into account when performing analyses as T-ALL turns out to be more a heterogeneous disease than originally thought.

Future therapy

The NOTCH and PTEN/AKT pathway would be attractive therapeutic targets, although more pathways as described above should be considered for therapeutic targeting. So far, none of

the targeted agents reached the clinic for T-ALL patients. A major drawback so far is that these agents are not effective enough as they block only one pathway and a cancer cell may simply escape by gaining additional mutations in different pathways to sustain its oncogenic potential. To overcome this problem, research is more focused now on combinational therapies targeting several key nodes of one or multiple pathways. GSIs are promising agents to treat patients that have active NOTCH signaling. Unfortunately, a first clinical trial with GSIs was hampered by extensive gastro-intestinal toxicity provoked by this compound and had to be retracted²⁵. Still, GSIs are of clinical interest as it may exert synergistic cytotoxic effects in lower doses when combined with other drugs. For example, GSIs were able to restore glucocorticoid-sensitivity in a glucocorticoid resistant T-ALL mouse model, while glucocorticoids prevent the GSI induced gastro-intestinal toxicity²⁶. GSIs have further been demonstrated to enhance the cytotoxic effects of dexamethasone *in vitro*²⁷. Furthermore, various GSI compounds are now under extensive development to overcome drug toxicity^{28,29}. Since the PI3K/AKT and NOTCH1 pathway might intertwine it is postulated that a combination of inhibitors targeting both pathways would be effective. Indeed, Rapamycin is shown to work additionally with NOTCH inhibitors in mice and also *Chan et al* and *Sanda et al* observed synergism between NOTCH1 and mTOR inhibitors or PI3K inhibitors in T-ALL cells *in vitro*^{30,31}. This indicates combinational therapies have significant potential for future treatment of T-ALL.

REFERENCES

1. Van Vlierberghe P, Pieters R, Beverloo HB, Meijerink JP. Molecular-genetic insights in paediatric T-cell acute lymphoblastic leukaemia. *Br J Haematol.* 2008;143:153-168.
2. Meijerink JP. Genetic rearrangements in relation to immunophenotype and outcome in T-cell acute lymphoblastic leukaemia. *Best Pract Res Clin Haematol*;23:307-318.
3. van Grotel M, Meijerink JP, van Wering ER, et al. Prognostic significance of molecular-cytogenetic abnormalities in pediatric T-ALL is not explained by immunophenotypic differences. *Leukemia.* 2008;22:124-131.
4. Bozic I, Antal T, Ohtsuki H, et al. Accumulation of driver and passenger mutations during tumor progression. *Proc Natl Acad Sci U S A*;107:18545-18550.
5. van Litsenburg RR, Uyl-de Groot CA, Raat H, Kaspers GJ, Gemke RJ. Cost-effectiveness of treatment of childhood acute lymphoblastic leukemia with chemotherapy only: the influence of new medication and diagnostic technology. *Pediatr Blood Cancer*;57:1005-1010.
6. Pui CH, Robison LL, Look AT. Acute lymphoblastic leukaemia. *Lancet.* 2008;371:1030-1043.
7. Park MJ, Taki T, Oda M, et al. FBXW7 and NOTCH1 mutations in childhood T cell acute lymphoblastic leukaemia and T cell non-Hodgkin lymphoma. *Br J Haematol.* 2009;145:198-206.
8. Zhu YM, Zhao WL, Fu JF, et al. NOTCH1 mutations in T-cell acute lymphoblastic leukemia: prognostic significance and implication in multifactorial leukemogenesis. *Clin Cancer Res.* 2006;12:3043-3049.
9. Chiang MY, Xu L, Shestova O, et al. Leukemia-associated NOTCH1 alleles are weak tumor initiators but accelerate K-ras-initiated leukemia. *J Clin Invest.* 2008;118:3181-3194.
10. Palomero T, Sulis ML, Cortina M, et al. Mutational loss of PTEN induces resistance to NOTCH1 inhibition in T-cell leukemia. *Nat Med.* 2007;13:1203-1210.
11. Zenatti PP, Ribeiro D, Li W, et al. Oncogenic IL7R gain-of-function mutations in childhood T-cell acute lymphoblastic leukemia. *Nat Genet*;43:932-939.
12. Homminga I, Pieters R, Langerak AW, et al. Integrated transcript and genome analyses reveal NKX2-1 and MEF2C as potential oncogenes in T cell acute lymphoblastic leukemia. *Cancer Cell*;19:484-497.
13. Coustan-Smith E, Mullighan CG, Onciu M, et al. Early T-cell precursor leukaemia: a subtype of very high-risk acute lymphoblastic leukaemia. *Lancet Oncol.* 2009;10:147-156.
14. Gutierrez A, Dahlberg SE, Neuberger DS, et al. Absence of biallelic TCRgamma deletion predicts early treatment failure in pediatric T-cell acute lymphoblastic leukemia. *J Clin Oncol*;28:3816-3823.
15. Dohda T, Maljukova A, Liu L, et al. Notch signaling induces SKP2 expression and promotes reduction of p27Kip1 in T-cell acute lymphoblastic leukemia cell lines. *Exp Cell Res.* 2007;313:3141-3152.
16. Rao SS, O'Neil J, Liberator CD, et al. Inhibition of NOTCH signaling by gamma secretase inhibitor engages the RB pathway and elicits cell cycle exit in T-cell acute lymphoblastic leukemia cells. *Cancer Res.* 2009;69:3060-3068.
17. Giambra V, Jenkins CR, Wang H, et al. NOTCH1 promotes T cell leukemia-initiating activity by RUNX-mediated regulation of PKC-theta and reactive oxygen species. *Nat Med*;18:1693-1698.
18. Breit S, Stanulla M, Flohr T, et al. Activating NOTCH1 mutations predict favorable early treatment response and long-term outcome in childhood precursor T-cell lymphoblastic leukemia. *Blood.* 2006;108:1151-1157.
19. Clappier E, Collette S, Grardel N, et al. NOTCH1 and FBXW7 mutations have a favorable impact on early response to treatment, but not on outcome, in children with T-cell acute lymphoblastic leukemia (T-ALL) treated on EORTC trials 58881 and 58951. *Leukemia.* 2010;24:2023-2031.
20. Kox C, Zimmermann M, Stanulla M, et al. The favorable effect of activating NOTCH1 receptor mutations on long-term outcome in T-ALL patients treated on the ALL-BFM 2000 protocol can be separated from

- FBXW7 loss of function. *Leukemia*. 2010;24:2005-2013.
21. Larson Gedman A, Chen Q, Kugel Desmoulin S, et al. The impact of NOTCH1, FBW7 and PTEN mutations on prognosis and downstream signaling in pediatric T-cell acute lymphoblastic leukemia: a report from the Children's Oncology Group. *Leukemia*. 2009;23:1417-1425.
 22. Zuurbier L, Homminga I, Calvert V, et al. NOTCH1 and/or FBXW7 mutations predict for initial good prednisone response but not for improved outcome in pediatric T-cell acute lymphoblastic leukemia patients treated on DCOG or COALL protocols. *Leukemia*. 2010;24:2014-2022.
 23. Jenkinson S, Koo K, Mansour MR, et al. Impact of NOTCH1/FBXW7 mutations on outcome in pediatric T-cell acute lymphoblastic leukemia patients treated on the MRC UKALL 2003 trial. *Leukemia*;27:41-47.
 24. Mansur MB, Hassan R, Barbosa TC, et al. Impact of complex NOTCH1 mutations on survival in paediatric T-cell leukaemia. *BMC Cancer*;12:9.
 25. van Es JH, van Gijn ME, Riccio O, et al. Notch/gamma-secretase inhibition turns proliferative cells in intestinal crypts and adenomas into goblet cells. *Nature*. 2005;435:959-963.
 26. Real PJ, Tosello V, Palomero T, et al. Gamma-secretase inhibitors reverse glucocorticoid resistance in T cell acute lymphoblastic leukemia. *Nat Med*. 2009;15:50-58.
 27. De Keersmaecker K, Lahortiga I, Mentens N, et al. In vitro validation of gamma-secretase inhibitors alone or in combination with other anti-cancer drugs for the treatment of T-cell acute lymphoblastic leukemia. *Haematologica*. 2008;93:533-542.
 28. Augelli-Szafran CE, Wei HX, Lu D, et al. Discovery of notch-sparing gamma-secretase inhibitors. *Curr Alzheimer Res*;7:207-209.
 29. Krop I, Demuth T, Guthrie T, et al. Phase I pharmacologic and pharmacodynamic study of the gamma secretase (Notch) inhibitor MK-0752 in adult patients with advanced solid tumors. *J Clin Oncol*;30:2307-2313.
 30. Chan S. Targeting the mammalian target of rapamycin (mTOR): a new approach to treating cancer. *Br J Cancer*. 2004;91:1420-1424.
 31. Sanda T, Li X, Gutierrez A, et al. Interconnecting molecular pathways in the pathogenesis and drug sensitivity of T-cell acute lymphoblastic leukemia. *Blood*. 2010;115:1735-1745.

NEDERLANDSE SAMENVATTING

T cel acute lymfatische leukemie (T-ALL) wordt gekarakteriseerd door veel verschillende genetische afwijkingen. Deze afwijkingen leiden tot ongecontroleerde celdeling van onrijpe lymfocyten (blasten). Een blast cel van een patiënt met T-ALL heeft meerdere genetische afwijkingen. Iedere patiënt heeft een andere combinatie van genetische afwijkingen. Bij T-ALL komen twee verschillende mutaties voor, welke wij type A en type B mutaties hebben genoemd. Type A mutaties zijn chromosomale herschikkingen welke oncogenen activeren die voornamelijk betrokken zijn cel differentiatie. Abnormale activatie van deze oncogenen zorgt voor een cel differentiatie blokkade en wordt gekenmerkt door een specifiek genexpressie profiel. Tot nu toe zijn vier gen expressie clusters geïdentificeerd; TALLMO, TLX, proliferatief en immatuur/ETP ALL cluster. Over het algemeen komen type B mutaties in ieder cluster voor, hoewel sommige wel voorkeur hebben voor een specifiek cluster. Type B mutaties komen voor in genen die betrokken zijn bij de signalering binnen en buiten een cel, zoals bijvoorbeeld de PI3K/AKT, NOTCH signalering of de cel cyclus.

Er zijn associaties gezien tussen mutaties en het T cel fenotype en tussen mutaties onderling. Een echte verklaring hiervoor is nog niet ontdekt.

Een verklaring voor de associatie van mutaties met T cel fenotype zou kunnen zijn dat onder normale omstandigheden, de activiteit van een gen verschilt tussen de verschillende T cel ontwikkeling stadia. Een gen is veel vatbaarder voor mutaties wanneer het actief is en het chromatine open gevouwen is. Een alternatief is dat een eiwit (of het eiwit waarmee het samenwerkt) alleen oncogene potentie heeft in een bepaald T cel ontwikkeling stadium.

Een verklaring voor het feit dat er combinaties van mutaties zijn die vaak binnen een patiënt voorkomen, zou kunnen zijn omdat bepaalde mutaties samen additief of synergistisch werken. Dit zou ook kunnen zijn omdat een cel zogenoemde "oncogene verslaving" heeft. Dit houdt in dat de cel meerdere punten van een signalerings route muteert, om er zeker van te zijn dat deze aangedaan is. Daardoor zijn er meerdere mutaties die interfereren met een mechanisme. Omdat T-ALL veroorzaakt wordt door veel genetische mutaties en doordat er nog steeds velen niet zijn ontdekt, is het moeilijk om een goede verklaring te vinden. Daar komt bij dat een cel ook veel mutaties heeft die geen invloed hebben op het gedrag en overleving van de cel (passerende mutaties) en dat er slechts een paar oncogene zijn (driver mutaties).

Met een van de recentste behandelprotocollen (ALL-10) is de overleving van kinderen met T-ALL 80%. Twintig procent van de kinderen krijgt een terugval. Overlevingscijfers van deze kinderen zijn erg laag, omdat ze vaak resistent zijn geworden voor de behandeling en daardoor niet goed zijn te behandelen en overlijden. Voor deze patiënten is het cruciaal effectievere behandeling te ontwikkelen. De behandeling van T-ALL is gebaseerd op om een combinatie van chemotherapie. Omdat kinderen nog volop in ontwikkeling en groei zijn, kunnen late bijwerkingen van medicatie grote invloed hebben. Daarom is het bij kinderen heel belangrijk om deze bijwerkingen te

verminderen. Het is daarvoor van belang dat patiënten, therapie “op maat” krijgen. Daarvoor is het identificeren van patiëntengroepen met overeenkomstige eigenschappen belangrijk. Met het huidige behandelprotocol krijgen patiënten suboptimale of superoptimale behandeling. Hoog-risico patiënten krijgen al een hoge dosis chemotherapie en verbetering van behandeling moet bereikt worden door kinderen een specifiekere behandeling te geven. Het meest ideale zou zijn wanneer deze behandeling specifiek gericht is tegen oncogenen.

Om bovenstaande vragen te beantwoorden, hebben wij van iedere patiënt in kaart gebracht welke combinaties van mutaties zij hebben. We hebben dit gedaan in een cohort van 146 patiënten welke behandeld zijn met het DCOG ALL7/8/9 protocol of COALL-97 protocol. Deze mutaties en andere patiënten eigenschappen hebben we gecorreleerd aan overlevingscijfers. Daarnaast hebben we op transcriptie- en translatie-niveau gekeken, welke veranderingen er zijn opgetreden in T-ALL patiënten met bepaalde mutaties.

In **hoofdstuk 2** is een overzicht van mutaties beschreven, die tot dusver bekend zijn in T-ALL. Dit bevat type A mutaties, maar is meer gespitst op type B mutaties en het (mogelijk) signaleringspad dat als gevolg van deze mutatie aangetast is in activiteit.

We zijn begonnen met het identificeren van NOTCH1-activerende mutaties binnen het cohort (**hoofdstuk 3**). Deze mutaties activeren de NOTCH1 signalering en is een van de meest voorkomende mutaties in kinderen met T-ALL. Drieënzestig procent van de kinderen heeft een NOTCH1-activerende mutatie. De meest beschreven studies dusver, hebben alleen gekeken naar mutaties in genetische hotspots. Wij hebben behalve het EGF- en LNR-domein van *NOTCH1*, bijna het hele *NOTCH1* gen en *FBXW7* gen gescreend. *FBXW7* is een eiwit dat er voor kan zorgen dat NOTCH1 wordt afgebroken in het proteosoom. Onze studie bevestigt dat *NOTCH1* mutaties voornamelijk voorkomen in het heterodimerisatie domein, juxtamembraan domein en het PEST domein waaraan *FBXW7* kan binden, zoals eerder in de literatuur beschreven. Mutaties zijn zeldzaam in het ANK, TAD en RAM domein van NOTCH1 en ook wij vonden geen mutaties hierin. Wij hebben nieuwe mutaties in *FBXW7* ontdekt en de meeste mutaties waren aanwezig in het C-terminale einde van het gen. Wij zagen een negatieve associatie tussen NOTCH1-activerende mutaties en afwijkingen in het *TAL1* en/of *LMO2* gen. *TAL1/LMO2* patiënten hebben vaak een matuur T cel fenotype waardoor NOTCH1-activerende mutaties ook negatief geassocieerd waren met de aanwezigheid van mature T cel markers. NOTCH1-activerende mutaties waren positief geassocieerd met *TLX3* herschikkingen. Patiënten met NOTCH1-activerende mutaties hadden een specifiek RNA expressie signatuur welke bekende genen bevat die door NOTCH1 worden gereguleerd. Dit signatuur kan bijdragen aan de begrijpbaarheid van de werking van NOTCH1, wat belangrijk is voor het ontwikkelen van geneesmiddelen die zich specifiek richten op NOTCH1. Wij hebben voor het eerst in patiënten samples aangetoond dat ook de actieve NOTCH1 eiwitvorm verhoogd is in gemuteerde patiënten. Dit was al eerder gehypothetiseerd op basis van data welke waren gegenereerd in cellijnen. Wanneer we patiënten indeelden op zwakke en sterke NOTCH1-activerende mutaties, gebaseerd op een eerdere publicatie

waarin *in vitro* en *in vivo* experimenten werden beschreven, zagen we dat patiënten met een zwakke NOTCH1-activerende mutatie verhoogd actief NOTCH1 eiwit hadden ten opzichte van NOTCH1/FBXW7 wild-type patiënten, en dat deze nog hoger was in patiënten met sterke NOTCH1-activerende mutaties. Gelijke resultaten zagen we op RNA expressie niveau. Ook tien wild-type patiënten lieten een hoge expressie van het actieve NOTCH1 eiwit zien, dan wel zijn target genen op RNA niveau. Echter deze patiënten hadden geen mutaties in de gescreende NOTCH1/FBXW7 domeinen of NOTCH1 translocaties. Dit suggereert dat deze patiënten mutaties hebben in het EGF- of LNR-domein van NOTCH1, in de delen van FBXW7 die niet gescreend zijn of in andere genen die NOTCH1 reguleren. Dit betekent dat niet alle NOTCH1-geactiveerde patiënten nog geïdentificeerd zijn. In deze cohorten hebben NOTCH1-geactiveerde patiënten vaak een terugval, maar reageren ze goed op prednisonbehandeling in een *in vitro* setting. De relatie tussen NOTCH1-activerende mutaties en de prognose van patiënten is vaak inconsistent tussen verschillende beschreven studiegroepen. Dit kan verklaard worden door verschillende factoren; er zijn verschillende behandelprotocollen en parameters voor overleving gebruikt in de verschillende studies, nog niet alle NOTCH1-activerende mutaties zijn ontdekt wat de screening onvolledig maakt en de distributie van zwakke en sterke NOTCH1-activerende mutaties kan verschillen tussen studiegroepen. In onze studie hebben wij aangetoond dat beide type mutaties geassocieerd zijn met andere overlevingscijfers binnen het DCOG cohort, maar niet het COALL cohort.

Palomero en collega's beschreef dat er een correlatie bestaat tussen NOTCH1 en PTEN expressie, waarbij PTEN een target van NOTCH1 zou zijn via HES1. Een goede response van de NOTCH1 γ -secretase inhibitor zou alleen mogelijk zijn wanneer er lage of normale AKT concentraties aanwezig zouden zijn. Een mutatie in PTEN zou leiden tot hoge AKT concentraties wat daardoor zou leiden tot resistentie voor γ -secretase inhibitors. Om de rol van PTEN in T-ALL en zijn relatie met NOTCH en γ -secretase inhibitors te onderzoeken, hebben wij onze cohorten gescreend op de aanwezigheid van PTEN, PIK3CA (PI3K isoform), PIK3RI (PI3K isoform) and AKT1 mutaties (**hoofdstuk 4**). Hierbij hebben wij bij een klein aantal patiënten een nieuw mechanisme van PTEN inactivatie als gevolg van defecte PTEN splicing ontdekt, wat resulteert in de afwezigheid van PTEN eiwit. Dertien procent van de kinderen heeft een afwijking in PTEN, PIK3RI of AKT1 (PTEN/AKT mutaties). Alle patiënten met een nonsense mutatie of deletie hadden geen of laag PTEN eiwit expressie, wat gecorreleerd was aan een mono-allelische of bi-allelische PTEN mutatie status. Afwezige PTEN eiwitexpressie in enkele mono-allelisch gemuteerde patiënten suggereert dat er meer PTEN-inactiverende mutaties zijn. We zagen geen verschil in eiwit expressie van de AKT-mTOR of andere downstream AKT eiwitten (zoals PRAS40 of forkhead transcriptiefactoren) tussen wild-type en PTEN/AKT gemuteerde patiënten. In tegenstelling tot onze verwachtingen gebaseerd op de Palomero studie, waren PTEN/AKT mutaties negatief geassocieerd met NOTCH1-activerende mutaties. Wanneer patiënten met een PTEN/AKT mutatie ook een NOTCH1-activerende mutatie hadden, was dit een zwakke NOTCH1-activerende mutatie. PTEN/AKT gemuteerde patiënten hadden een lage expressie van MYC en musashi eiwitten, welke betrokken zijn bij de NOTCH1 signalering. PTEN/AKT mutaties waren voornamelijk aanwezig in

patiënten met een TALLMO herschikking en hadden vaak expressie van mature T cel markers. Patiënten met een TLX herschikking hadden nagenoeg geen additionele *PTEN/AKT* mutatie. Dit patroon lijkt tegenovergesteld aan dat van NOTCH1-activerende mutaties. Op zichzelf zijn *PTEN/AKT* mutaties niet geassocieerd met overleving in dit cohort. Echter, wanneer we rekening houden met de negatieve associatie van *PTEN/AKT* mutaties en NOTCH1-activerende mutaties welke juist gecorreleerd zijn aan overleving, zien we dat *NOTCH1/FBXW7/PTEN/AKT* wild-type patiënten een goede overleving hebben en NOTCH1 activerend en/of *PTEN/AKT*-gemuteerde patiënten een slechte.

PTEN splice-defecten hebben we verder onderzocht in **hoofdstuk 5**. Hierbij hebben we ontdekt dat deze splice-defecten het gevolg waren van microdeleties in een of meerdere exonen. Deleties waren omgeven door immunoglobuline recombinatie signalen en bevatte inserties van random nucleotiden. Dit suggereert dat deze deleties als gevolg van abnormale RAG combinatie events zijn ontstaan.

In **hoofdstuk 6** werd het screenen van type B mutaties verder uitgebreid, met het identificeren van mutaties in de *IL7R* (*IL7* receptor), *JAK* en *RAS* genen. We vonden geen mutaties in *JAK2* en *TYK2*. De mutaties die in het *IL7R α* gen waren gedetecteerd, zijn al eerder gerapporteerd en kwamen voor in 8% van de kinderen met T-ALL. *N-RAS/K-RAS* mutaties werden gevonden in 10% van de patiënten en *JAK1* en/of *JAK3* mutaties in 7%. Opvallend was dat *IL7R α* mutaties, met uitzondering van 1 patiënt, nooit samen voorkwamen met een van de andere mutaties. Ook *PTEN/AKT* mutaties kwamen nooit tegelijk voor met *JAK* of *RAS* mutaties. Alle *JAK* mutaties die we hebben getest, waren in staat om een cel te transformeren. Hiervoor werden IL3-afhankelijke Ba/F3 cellijnen gebruikt. Wildtype *JAK1* en *JAK3* cellijnen konden dit niet. Ook *AKT* en *N-RAS* mutaties zorgden voor IL3-onafhankelijke groei. In *IL7R α* -gemuteerde patiënten zagen we op eiwitniveau een verhoogde fosforylatie van eiwitten die een rol spelen in de JAK-STAT, RAS-MEK-ERK of *PTEN/AKT* signaalpaden. Echter activeerden de verschillende *IL7R α* en *JAK1* mutanten niet dezelfde downstream eiwitten en in gelijke mate, maar hadden ze wel allemaal evenveel downstream p70 S6 kinase activiteit. Wat we ook zagen, was dat *JAK3* mutanten een erg robuuste versnelling in IL3-onafhankelijk groei lieten zien, vergeleken met *IL7R α* en *JAK1* mutanten, maar dat ze in vergelijking weinig verhoging van downstream gefosforyleerde eiwitten hadden. *IL7R α* en *JAK1/3*, maar niet *N-RAS* en *AKT* mutanten, waren gevoelig voor de JAK inhibitor Ruxolitinib. Ook hadden de gevoelige lijnen na behandeling een verlaagde expressie van downstream signaleringseiwitten, maar de ongevoelige lijnen niet. Inhibitie van STAT5, een downstream eiwit, zorgde voor matige reductie van groei in *JAK1* mutante lijnen maar niet in *IL7R α* mutanten lijnen. Dit suggereert dat *IL7R α* mutanten ook via andere downstream paden signaleren dan STAT5, zoals bijvoorbeeld het RAS-ERK-MEK of PI3K/AKT signaalpad. *JAK1/3* mutanten waren in tegenstelling tot *IL7R α* mutanten, gevoelig voor de PI3K/AKT inhibitor LY294002. Wanneer inhibitie van het PI3K/AKT pad in een *JAK1* of *IL7R α* mutante cellijn gecombineerd werd met inhibitie van het RAS-MEK-ERK pad, observeerden we een lagere expressie van downstream signaleringseiwitten dan wanneer de lijnen met 1 inhibitor werden behandeld. De ongevoeligheid voor de LY294002 inhibitor in combinatie met de extreme gevoeligheid voor een tweetal van PI3K/AKT en RAS-

MEK-ERK inhibitors suggereert dan de IL7R via beide signaalpaden kan signaleren, maar dat deze signaleert via het RAS-MEK-ERK pad wanneer het PI3K/AKT pad wordt geblokkeerd en andersom.

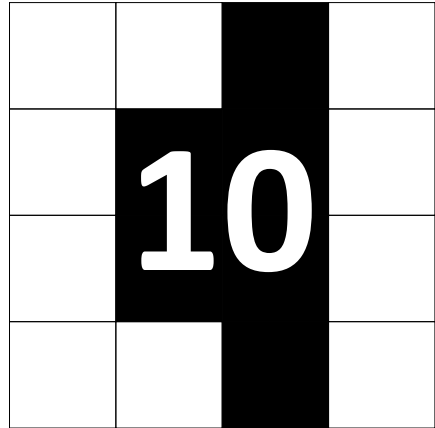
Onze onderzoeksgroep heeft recentelijk een nieuw patiëntencluster in T-ALL beschreven, welke gebaseerd is op genexpressie data en geassocieerd is met genetische afwijkingen die *MEF2C* activeren. Deze groep patiënten heeft een zeer immatuur T cel fenotype en brengt vaak myeloïde markers tot expressie. Daarom wordt deze groep het immature cluster genoemd. Twee andere studies beschreven een soortgelijke patiëntengroep: vroege voorloper T-ALL welke geïdentificeerd is op basis van het genexpressie profiel dat overeenkomt met het genexpressie profiel van muizen met vroege voorloper T-ALL. Vroege voorloper T-ALL is beschreven als een immature leukemie, welke eigenschappen heeft die overeenkomstig zijn met stamcellen en myeloïde cellen. Deze groep is geassocieerd met mutaties die de hematopoietische, lymfatische alsmede myeloïde celrijping verstoren. Een andere groep patiënten werd gekarakteriseerd door een deletie in het TCR $\gamma\delta$ (TRG@) gen. Deze patiënten worden ABD patiënten genoemd en worden ook geassocieerd met immature T-ALL. We hebben de overlap van deze drie immature patiëntengroepen binnen ons T-ALL cohort bestudeerd in **hoofdstuk 7**. Hierbij zagen we dat het genexpressie profiel van onze immature cluster patiënten sterk overeen kwam met dit van de vroege voorloper T-ALL patiënten (13 van de 15 immature patiënten werden ingedeeld als vroege voorloper T-ALL patiënten). Ongeveer de helft van de immature patiënten had geen TCR $\gamma\delta$ deletie, wat suggereert dat ABD een subtype binnen de immature/vroege voorloper T-ALL patiënten is. We merkten ook dat onze immature cluster patiënten niet konden worden geïdentificeerd op basis van het voorgestelde gepubliceerde immunofenotype dat bij vroege voorloper T-ALL patiënten hoort. Daarom hebben we een andere immunofenotype voorgesteld, dat wel karakteristiek is voor onze immature cluster patiënten; onze patiënten waren geassocieerd met de afwezigheid van CD1 en CD8 expressie, maar ook van CD4, en hadden frequent expressie van CD34 en/of CD13 of CD33. Met behulp van GSEA (Gene Set Enrichment Analysis; verrijking voor bekende genensets) op onze genexpressie data, konden we bevestigen dat deze patiënten een stamcel-achtig fenotype hebben. In tegenstelling tot wat eerder beschreven was, waren COALL97/03 patiënten niet gecorreleerd met een slechte overleving en hebben deze *in vitro* eenzelfde gevoeligheid voor chemotherapeutische middelen, dan andere T-ALL patiënten. In de eerdere publikatie over vroege voorloper T-ALL, alsmede in twee andere publikaties, was voorgesteld om vroege voorloper T-ALL patiënten zo snel mogelijk te behandelen volgens een intensief behandelprotocol. Onze data geeft aan om hier beter naar te kijken. We zagen wel een trend voor lagere gevoeligheid voor steroïden in immature patiënten. Vergeleken met andere behandelprotocollen, bevat het COALL97/03 protocol een hoge concentratie cytarabine. Deze hogere dosis verklaart mogelijk de betere overlevingscijfers van immature patiënten in ons cohort. Daarom stellen we voor om goed te kijken naar het effect van cytarabine in immature patiënten.

De gevolgen op eiwitniveau van genetische afwijkingen in T-ALL is grotendeels onbekend. Om dit te onderzoeken hebben we in **hoofdstuk 8** de differentiële expressie van signaleringspaden

op genexpressie- en eiwitniveau bestudeert in patiëntengroepen die type A mutaties reflecteren en in patiëntengroepen gebaseerd op type B mutaties. TALLMO patiënten hadden een hoge expressie van genen en eiwitten die betrokken zijn bij de T cel receptor (TCR) signalering, metabole glycolyse en vetzuur signaleringspaden waarbij onder andere GSK3 betrokken is. Dit geeft aan dat deze processen mogelijk belangrijk zijn voor celoverleving van deze patiënten. Daarom is het de moeite waard om het effect van remmers van deze processen, in deze patiënten te testen. Dit zijn bijvoorbeeld kinase inhibitors, glycolyse of vetzuur inhibitors of specifieke GSK3 inhibitors. TLX patiënten waren duidelijk geassocieerd met een actieve NOTCH signalering. Dit versterkt onze eerdere observatie in hoofdstuk 3, waarin we een positieve associatie van (voornamelijk sterke) NOTCH1-activerende mutaties met *TLX3* hergeschikte patiënten zagen. Activatie van NOTCH signalering zagen we ook in enkele wild-type patiënten. Dit kan komen door, zoals eerder gesuggereerd in hoofdstuk 3, de aanwezigheid van nog onbekende NOTCH1-activerende mutaties of komt door een verslaving aan actieve NOTCH signalering, mogelijk gedreven door HOX. Het is zeer interessant om te kijken of de TLX groep ook zeer gevoelig is voor NOTCH inhiberende γ -secretase remmers, welke gebruikt kunnen worden in therapeutische setting. Proliferatieve patiënten hadden een hoge expressie van genen die betrokken zijn bij de regulatie van de biologische klok. Herstel van deze verstoring zou een goede therapeutische mogelijkheid zijn voor deze patiënten. De hele hoge proliferatieve activiteit en DNA schade response die eerder geobserveerd zijn in deze patiënten, zagen we ook in deze studie. Ook zagen we een hoge expressie van *p53* transcripten maar een lage expressie van downstream *p53* genen en eiwitten. Dit suggereert dat de activiteit van *p53* heel laag is doordat er bijvoorbeeld verstoring is in de stabiliteit, localisatie, transactivatie of DNA bindingscapaciteit van *p53* in deze groep patiënten. Naast conventionele chemotherapie, zou er gekeken moeten worden naar de effectiviteit van kinase remmers als mogelijke behandelmethode in proliferatieve patiënten. Immature cluster patiënten lijken een erg lage activiteit van T cel signalering en een erg hoge activiteit van B cel signalering te hebben. Expressie van cel adhesie moleculen in deze groep is laag. Deze observaties zijn mogelijk een weerspiegeling van de erg vroeg T cel differentiatie stop van deze leukemie. Opvallend is dat deze cellen weinig proliferatie en migratie lijken te vertonen. We vonden een erg interessante link tussen MEF2C en *p38* MAPkinase, dat waardevol kan zijn voor verder onderzoek. Wat betreft type B mutaties, bevestigden we dat *p27* belangrijk is downstream van NOTCH en dat deze patiënten een lage expressie hebben van *PKC θ* . Recentelijk is beschreven dat *PKC θ* via *RUNX3* en *RUNX1* een indirect target van NOTCH1 is. In tegenstelling tot lage *PKC θ* concentraties in NOTCH1-geactiveerde patiënten, zagen we een hoge expressie van dit eiwit in *PTEN/AKT* gemuteerde patiënten. Deze patiënten hebben nauwelijks NOTCH1-activerende mutaties en als ze mutaties hebben, dan zijn deze zwak (hoofdstuk 4). *PTEN/AKT* gemuteerde patiënten lijken ook een actieve TCR signalering te hebben en erg proliferatief te zijn. Dit maakt deze groep daarom ook aantrekkelijk voor kinase inhibitors. Ingeactiveerde WT1 patiënten hadden een hoge concentratie van groeireceptoren en downstream signalering. De rol van WT1 in translationele inhibitie van groeireceptoren en de gevoeligheid van therapeutische remmers van groeifactoren in deze patiënten, is erg interessant om te onderzoeken omdat de

functie van WT1 in T-ALL nog grotendeels onbekend is.

CHAPTER



About the author

LIST OF PUBLICATIONS

Mendes RD*, Sarmiento LM*, Canté-Barrett K, **Zuurbier L**, Buijs-Gladdines JG, Póvoa V, Smits WK, Abecasis M, Yunes JA, Sonneveld E, Horstmann MA, Pieters R, Barata JT, Meijerink JP. PTEN micro-deletions in T-cell acute lymphoblastic leukemia are caused by illegitimate RAG-mediated recombination events. *Blood*. 2014 Jun 5. (Impact factor 2013 9.060)

* *shared first authorship*

Zuurbier L, Gutierrez A, Mullighan CG, Canté-Barrett K, Gevaert AO, de Rooi J, Li Y, Smits WK, Buijs-Gladdines JG, Sonneveld E, Look AT, Horstmann M, Pieters R, Meijerink JP. Immature MEF2C-dysregulated T-cell leukemia patients have an early T-cell precursor acute lymphoblastic leukemia gene signature and typically have non-rearranged T-cell receptors. *Haematologica*. 2014 Jan. (impact factor 2013 5.9)

Zuurbier L, Petricoin EF 3rd, Vuerhard MJ, Calvert V, Kooi C, Buijs-Gladdines JG, Smits WK, Sonneveld E, Veerman AJ, Kamps WA, Horstmann M, Pieters R, Meijerink JP. The significance of PTEN and AKT aberrations in pediatric T-cell acute lymphoblastic leukemia. *Haematologica*. 2012 Sep. (impact factor 5.9)

Zenatti PP, Ribeiro D, Li W, **Zuurbier L**, Silva MC, Paganin M, Tritapoe J, Hixon JA, Silveira AB, Cardoso BA, Sarmiento LM, Correia N, Toribio ML, Kobarg J, Horstmann M, Pieters R, Brandalise SR, Ferrando AA, Meijerink JP, Durum SK, Yunes JA, Barata JT. Oncogenic IL7R gain-of-function mutations in childhood T-cell acute lymphoblastic leukemia. *Nat Genet*. 2011 Sep. (impact factor 36.377)

Zuurbier L, Homminga I, Calvert V, te Winkel ML, Buijs-Gladdines JG, Kooi C, Smits WK, Sonneveld E, Veerman AJ, Kamps WA, Horstmann M, Petricoin EF 3rd, Pieters R, Meijerink JP. NOTCH1 and/or FBXW7 mutations predict for initial good prednisone response but not for improved outcome in pediatric T-cell acute lymphoblastic leukemia patients treated on DCOG or COALL protocols. *Leukemia*. 2010 Dec. (impact factor 8.966)

Van Vlierberghe P, Palomero T, Khiabani H, Van der Meulen J, Castillo M, Van Roy N, De Moerloose B, Philippé J, González-García S, Toribio ML, Taghon T, **Zuurbier L**, Cauwelier B, Harrison CJ, Schwab C, Pisecker M, Strehl S, Langerak AW, Gecz J, Sonneveld E, Pieters R, Paietta E, Rowe JM, Wiernik PH, Benoit Y, Soulier J, Poppe B, Yao X, Cordon-Cardo C, Meijerink J, Rabadan R, Speleman F, Ferrando A. PHF6 mutations in T-cell acute lymphoblastic leukemia. *Nat Genet*. 2010 Apr. (impact factor 36.377)

Sulis ML, Williams O, Palomero T, Tosello V, Pallikuppam S, Real PJ, Barnes K, **Zuurbier L**, Meijerink JP, Ferrando AA. NOTCH1 extracellular juxtamembrane expansion mutations in T-ALL. *Blood*.

2008 Aug. (impact factor 10.432)

Van Vlierberghe P, Homminga I, **Zuurbier L**, Gladdines-Buijs J, van Wering ER, Horstmann M, Beverloo HB, Pieters R, Meijerink JP. Cooperative genetic defects in TLX3 rearranged pediatric T-ALL. *Leukemia*. 2008 Apr. (impact factor 8.634)

Adema AD, **Zuurbier L**, Floor K, Hubeek I, Kaspers GJ, Albertoni F, Peters GJ. Cellular resistance against troxacitabine in human cell lines and pediatric patient acute myeloid leukemia blast cells. *Nucleosides Nucleotides Nucleic Acids*. 2006. (impact factor 0.784)

CURRICULUM VITAE

Linda Zuurbier werd op 21 mei 1983 geboren te Niedorp en behaalde in 2000 haar HAVO diploma aan het GSG (BAC) in Schagen. In ditzelfde jaar is zij in Alkmaar, de Hoger Laboratorium Opleiding (HLO) begonnen, richting medische biologie, waarvan ze in 2004 haar Bachelor diploma haalde. Tijdens deze opleiding heeft Linda een stage onderzoek van negen maanden aan de Vrije Universiteit Medisch Centrum (VUmc) gedaan, waarbij zij studie deed naar het werkingsmechanisme van het chemotherapeutica Troxacitibine (afdeling Medische Oncologie). Direct na het behalen van haar bachelor diploma, is zij de Master Oncology gestart aan het VUmc. Tijdens deze Master heeft zij twee stages gedaan. Een was aan het Nederlands Kanker Instituut (afdeling Tumor Biologie), waar zij heeft gekeken naar het antisense RNA van de *p53* en *cycline D1* genen. De andere stage was in de UK bij het Wellcome Trust Centre for Cell Biology te Edinburgh, waar zij eiwitten onderzocht die mogelijk aan condensin, een mitose-eiwit, binden. In 2006 behaalde Linda haar Master of Science. Voordat zij aan haar PhD begon, heeft zij om werkervaring op te doen, zes maanden als analist binnen de diagnostiek van de klinische genetica aan het VUmc gewerkt. Haar promotieonderzoek is gestart in 2007 aan het Erasmus Medisch Centrum/Sophia kindziekenhuis te Rotterdam, op de afdeling Kinderoncologie/hematologie, onder leiding van Prof. Rob Pieters en Dr. Jules Meijerink. Gedurende deze promotietijd heeft zij onderzoek gedaan naar genetische afwijkingen bij kinderen met T cel acute lymfatische leukemie (T-ALL), zoals beschreven in dit proefschrift. Voor dit onderzoek heeft zij zes maanden in Amerika gewoond, om de eiwitexpressie van T-ALL patiënten te meten en analyseren met behulp van de reverse-phase protein microarray techniek (RPMA). Dit is uitgevoerd op het lab van Prof. Petricoin aan de George Mason University (GMU) te Manassas. Vanaf 2012 tot heden, werkt Linda als post doc bij een start-up biotechnologie bedrijf, genaamd SomantiX BV, te Amsterdam. Hier identificeert zij tumorendotheel-specifieke markers en de functionele effecten na modulatie van marker expressie, met als doel om angiogenese remmers te ontwikkelen. Zij woont momenteel in Santpoort-Zuid, is getrouwd met Mark Opdam waarmee zij een zoontje heeft (Tamo, 1 jaar).

PHD PORTFOLIO

Name PhD student: Lidwina (Linda) C. Zuurbier, MSc

Erasmus MC department: Pediatric Oncology/Hematology

Research school: Molecular Medicine

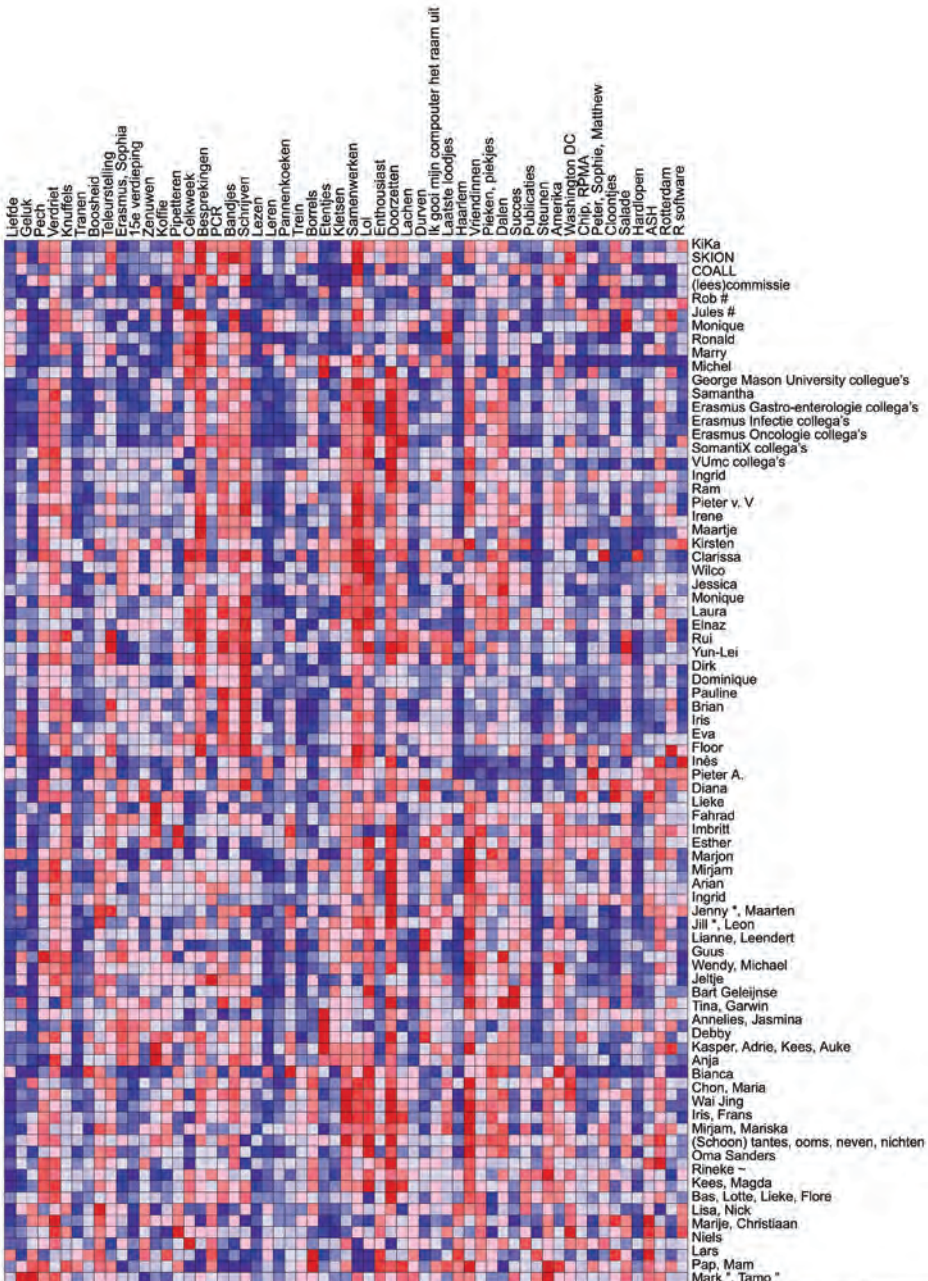
PhD period: June 2007 – June 2011

Promotor: Prof. Dr. Rob Pieters

Supervisor: Dr. Jules P.P. Meijerink

PhD training	Year	ECTS
General Courses		
- Biomedical English Writing and Communication		4
- Classical methods for data-analysis (CC02)		5.7
Seminars		
- Annual Molecular Medicine Day	2007-2011	1.2
- Research meetings dept of pediatrics and pediatric oncology Attendance and presentations	2007-2011	4
International and National Conferences and Presentations		
- European Hematology Association (EHA), London, UK Poster presentation	2011	1.6
- Dutch Hematology Congress, Papendal, The Netherlands, Oral presentation	2011	2
- European Hematology Association (EHA), Mandelieu, France Oral presentation	2010	2
- American Association of Hematology (ASH), Orlando, USA Poster presentation	2010	1.6
- Annual Molecular Medicine Day, Rotterdam, The Netherlands Poster presentation	2010	1.6
- American Association of Hematology (ASH), New Orleans, USA Poster presentation	2009	1.6
- Annual pediatric research meeting, Rotterdam, The Netherlands Poster presentation	2009	1.6
- American Association of Hematology (ASH), San Francisco, USA Poster presentation	2008	1.6
Other		
- Six months lab experience at the George Mason University (GMU), Manassas, USA, Centre for applied proteomics and molecular medicine, Prof. E. Petricoin	2008	
- European Hematology Association (EHA) Travel grant	2011	
- American Society of Hematology (ASH) Travel grant	2010	
Teaching		
- Supervision of Wasiem Sahebali, student of AVANS Hogeschool Breda. Nine months intern ship "NOTCH1 and PTEN in T-ALL" (final year Bachelor's)	2009	10
- Supervision of Samantha Nedermeijer, 4 th year medical student of ErasmusMc, 4 months investigating SHIP1 mutations in T-ALL		10
Total		48.5

DANKWOORD



Dankwoord. Iedereen, heel erg bedankt bij het tot stand brengen van mijn proefschrift! Deze heatmap geeft emoties en waardering weer, tijdens het behalen van mijn proefschrift. Rood betekent aanwezig, blauw betekent niet aanwezig. De kleurindeling is blind gerandomiseerd en de map is hiërarchisch geclusterd. Rijen; zonder jullie had ik het nooit gered! Bedankt!! Kolommen; emoties & karakteristieken van mijn promotie.

Speciale dank gaat uit naar mijn promotor en co-promoter; bedankt voor jullie begeleiding, input, kennis, discussies, enthousiasme en humor.

* Paranimfen, rotsen in de branding, oud collega's en vriendinnen, lief en leed delen we; bedankt!

- Lieve schoonmama, bedankt voor u vertrouwen, steun en positiviteit tijdens dit project. Ik mis u ontzettend.

* Mark & Tamo, mijn grote liefdes. Ik hou ontzettend van jullie!!!

